The University of Adelaide
Department of Geology and Geophysics

QUANTIFICATION OF EXHUMATION IN THE COOPER-EROMANGA BASINS, AUSTRALIA

Angelos Mavromatidis

June 1997

A thesis submitted to the University of Adelaide
in fulfilment of the requirements for the degree of
Doctor of Philosophy

CONTENTS

CHAPTER 3: RESULTS OF COMPACTION-BASED ANALYSIS OF EXHUMATION

CHAPTER 4: QUANTIFYING EXHUMATION USING VITRINITE REFLECTANCE

CHAPTER 5: EVIDENCE OF EXHUMATION FROM APATITE FISSION TRACK ANALYSIS AND FLUID INCLUSION HOMOGENIZATION TEMPERATURES

CHAPTER 6: COMPARISON OF EXHUMATION RESULTS FROM THE DIFFERENT METHODS AND INFERRED BURIAL/EXHUMATION HISTORIES FOR THE COOPER-EROMANGA BASINS

CHAPTER 7: STRUCTURAL FRAMEWORK AND TECTONIC MECHANISMS OF UPLIFT AND EROSION

LIST OF FIGURES

LIST OF TABLES

ABSTRACT

Exhumation in the Cooper-Eromanga Basins of South Australia and Queensland has been quantified using the compaction methodology. The standard method of estimating exhumation based on the degree of overcompaction of a single shale unit has been modified, and twelve units, predominantly shales ranging in age from Cretaceous to Permian have been analysed, and the results from different units crossplotted. Furthermore, not only sonic log data, but also data from the other porosity logs (density and neutron) and the adjusted sonic log have been used to quantify exhumation. However, values from the sonic log data are considered the most reliable.

The results of the compaction analysis reveal that Late Cretaceous - Tertiary exhumation increases eastwards from the Patchawarra Trough, through the Gidgealpa-Merrimelia-Innamincka Trend and Nappamerri Trough into the Queensland sector of the basins. Maxima of approximately 1 km of Late Cretaceous - Tertiary exhumation occur north of the Jackson-Naccowlah area and near the north-eastern boundary of South Australia in the Morney and Curalle domes. In many wells the Permo-Triassic section of the Cooper Basin is more overcompacted than the Mesozoic section of the overlying Eromanga Basin. In such areas maximum burial-depth of the Cooper Basin sequence is believed to have been attained in Late Triassic - Early Jurassic times, prior to the deposition of the Eromanga Basin, and not to have been subsequently re-attained.

Vitrinite reflectance data were also modelled in order to investigate exhumation in the Cooper-Eromanga Basins. However, without independent information on the thermal history of the area, vitrinite reflectance data cannot uniquely reveal exhumation magnitudes, because any excess of reflectance above that consistent with current temperatures can be explored by a combination of higher palaeogeothermal gradients and/or exhumation from greater burial-depth. Nonetheless, vitrinite reflectance data do seem to require a relatively recent increase in geothermal gradients in the basins, and higher geothermal gradients during the deposition of the Cooper Basin sequence. Exhumation magnitudes indicated by such a geothermal gradient history are largely consistent with those derived from the compaction methodology.

Exhumation results based on apatite fission track analysis and fluid inclusion homogenization temperatures have also been compiled and although of limited coverage, these results are also broadly consistent with those based on compaction analysis.

Seismic reflection profiles indicate the compressive nature of the structural style associated with the major uplift events in the Cooper-Eromanga Basins. While a number of mechanisms may have driven regional Late Cretaceous - Tertiary exhumation, the two-layer lithospheric compression model is considered as the most complete explanation of uplift.

The study has major implications for hydrocarbon exploration in the basins. Regarding maturation levels, predicted maturation of source rocks will be greater for any given geothermal history if Late Cretaceous - Tertiary exhumation is incorporated in maturation modelling. Perhaps even more importantly, the excess of exhumation of the Cooper Basin sequence over the Eromanga Basin sequence suggests that Cooper Basin source rocks in some areas are unlikely to charge Eromanga Basin reservoirs because hydrocarbons would have been expelled from these source rocks in Late Triassic - Early Jurassic times, prior to the deposition of the Eromanga Basin.

The study has also implications for depth-conversion of seismic two-way-times because it helps quantify the (high) velocity anomalies associated with overcompaction. Exhumation values from this study can also be used to improve porosity predictions of reservoir units in undrilled targets.

STATEMENT

This thesis contains no material which has been accepted for the award of any other degree or diploma in any university or other tertiary institution and, to the best of my knowledge and belief, contains no material previously published or written by another person, except where due reference has been made in the text.

If accepted for the award of the degree and, if applicable, I consent to the thesis being made available for photocopying and loan.

June 1997

ACKNOWLEDGEMENTS

This work was carried out while I was in receipt of an OPRS (Overseas Postgraduate Research Scholarship) award from the Australian Government and a scholarship from the University of Adelaide. I am grateful to my supervisor Dr. Richard Hillis who provided me constant support and encouragement to continue my studies during difficult times. It was he who first suggested applying the revised overcompaction technique using well log data from the Cooper-Eromanga Basins. I am grateful to my supervisor for his friendly guidance throughout my entire residence in Australia. I am also indebted for his careful and detailed corrections of drafts of this thesis. He also provided generous support for me to attend seminars and conferences, from which I gained useful information for my study.

I would like to thank Associate Prof. David McKirdy for his critical review of the vitrinite reflectance chapter. I am also indebted to Dr. Peter Tingate for reviewing the AFTA chapter and for his interest, encouragement and the discussions of the techniques and his invitation to give a seminar at the NCPGG (National Centre of Petroleum Geology & Geophysics) regarding the results of this thesis. Thanks to Prof. Reza Harami for his interest, comments and discussions on the project. I wish to extend my appreciation to fellow postgraduate student Rob Menpes for his discussions and assistance throughout the project. I would like to thank Ms Vivien Hope who as a university officer was always friendly and positive to my enquires. I wish to acknowledge Mr Tony Hill for his interest in the work, and his invitation to present the results of my research at MESA (Mines & Energy South Australia).

I am grateful to Santos Ltd. for access to their well log data and the computing facilities. More specifically, I wish to thank David Warner for discussions with his colleagues regarding the importance of the project and its implications for Santos' Ltd. exploration. I am grateful to David Hudson, Grant Jacquier and Paul Siffleet for the support in the use of software at Santos Ltd. Without these computer facilities, it would have been impossible to fulfil the aims of my study. Maris Zwigulis is also thanked for his 'curiosity' in discussing different aspects of this thesis during my research period.

I would like to acknowledge the moral support from my family in Greece. Despite not having seen them, during my studies in Australia, which made my and their life more difficult, they always encouraged me to continue and try to expand my knowledge. Last but certainly not least, I express many thanks to my partner Stephanie Eleftheriou for her moral and financial support. Her support was beyond thanks.

This thesis, particularly the well log, vitrinite reflectance and AFTA data, and seismic sections are published with the permission of the Santos Ltd. and the Cooper-Eromanga joint venture partners.

1. INTRODUCTION

1.1 Project Rationale

The subsidence history of sedimentary basins is expressed by, and can be relatively easily reconstructed from the preserved stratigraphic sequence. Uplift events, above sedimentary base level are expressed only by hiatuses or unconformities. Hence quantifying the exhumation associated with uplift is intrinsically more problematic than quantifying the burial associated with subsidence.

Exhumation is of particular significance in petroliferous basins. In exhumed basins, exhumation from maximum burial-depth influences multiple problems pertaining to hydrocarbon exploration in basins. The generation of hydrocarbons and migration occurs not with in the present structural framework of the basin, but within a framework modified by subsequent exhumation. Hence, if the magnitude of exhumation is quantified it can be used to better predict source rock maturity and to reconstruct basin morphology at the time of hydrocarbon migration and hence elucidate pre-exhumation migration pathways. Additionally, porosities and seismic velocities in the basin are generally attained at burial-depths greater than that presently observed. Prediction of these parameters should incorporate the (quantified) effects of exhumation from maximum burial-depth. Beyond its significance to petroleum exploration, quantifying exhumation is critical to investigating the dynamic driving forces of basin uplift events.

The Cooper-Eromanga Basins of South Australia and Queensland are not at their maximum burial-depth due to Late Cretaceous - Tertiary and Late Triassic - Early Jurassic exhumation (Section 1.2). The aim of this thesis is to determine the magnitudes of exhumation and to consider the implications for petroleum exploration and basin tectonics.

All methods of estimating exhumation utilise rock properties which are affected by, and retain a memory of, burial in excess of that presently observed. The main tool used for estimating the exhumation in this thesis is analysis of the degree of overcompaction of rock units. Compaction trends will be analysed using data from the porosity logs (sonic, density and neutron) and check-shot (or well velocity) surveys.

Significantly, this thesis analyses the degree of overcompaction not of a single rock unit, but rather of multiple units covering the complete stratigraphic range of the Cooper-Eromanga Basins. This analysis of multiple units allows exhumation to be quantified with more confidence than does analysis of a single unit and also allows estimates of the timing of exhumation to be made. In addition to utilizing compaction state to quantify exhumation, the available vitrinite reflectance data have been modelled. Data from apatite fission track analysis and fluid inclusion homogenization temperatures have also been compiled in order that exhumation in the Cooper-Eromanga Basins may be analysed from the perspective of as many different rock properties as possible.

1.2 The Cooper-Eromanga Basins

The Cooper and Eromanga Basins are Australia's largest onshore petroleum province, and are located in central and eastern Australia (Figure 1.1). The Eromanga Basin is the larger of the two and completely overlies the Cooper Basin. The Eromanga Basin extends over approximately 1,000,000 km^2 in the states of Queensland, New South Wales, South Australia and the extreme southeastern tip of the Northern Territory (Moore, 1986). The underlying north-easterly oriented Cooper Basin occupies about 153,000 km^2 in north-eastern of South Australia and south-western Queensland (Stanmore, 1989), and is located beneath the approximate centre of the Eromanga Basin.

The Eromanga Basin is a major Jurassic-Cretaceous depocentre hosting not only petroleum, but also the aquifers of the Great Artesian Basin. The Cooper Basin is one of several pre-Jurassic

sedimentary basins that underlie portions of the Eromanga Basin. To the northeast of the Cooper is the Carboniferous-Triassic Galilee Basin. Two other Carboniferous-Permian basins, the Pedirka and Simpson Desert Basins, are located to the west of the Cooper Basin. Older Paleozoic and Devonian Basins also underlie portions of the Eromanga and Cooper Basins (Vine, 1976) (Figure 1.2).

The sediments of the Cooper Basin were deposited during Late Carboniferous-Permian and Triassic times in predominantly fluvial and lacustrine environments (Battersby, 1976; Thornton, 1979). After the deposition of the Cooper Basin, in Late Triassic - Early Jurassic times, an exhumational event took place which resulted in the basin wide Nappamerri unconformity (Figure 1.3). Subsequently, the Eromanga Basin sediments were deposited in Jurassic and Cretaceous times in mainly fluvial-lacustrine and shallow marine environments (Bowering, 1982). After the deposition of the Eromanga Basin, major sedimentation ceased and over the last 90 Myr the basin has been characterized by periods of exhumation and minor sedimentation (Figure 1.3). The current stratigraphic nomenclature is shown in Figure 1.4. For a more detailed stratigraphic description of the basins the reader is referred to Petroleum Management Associates (1986).

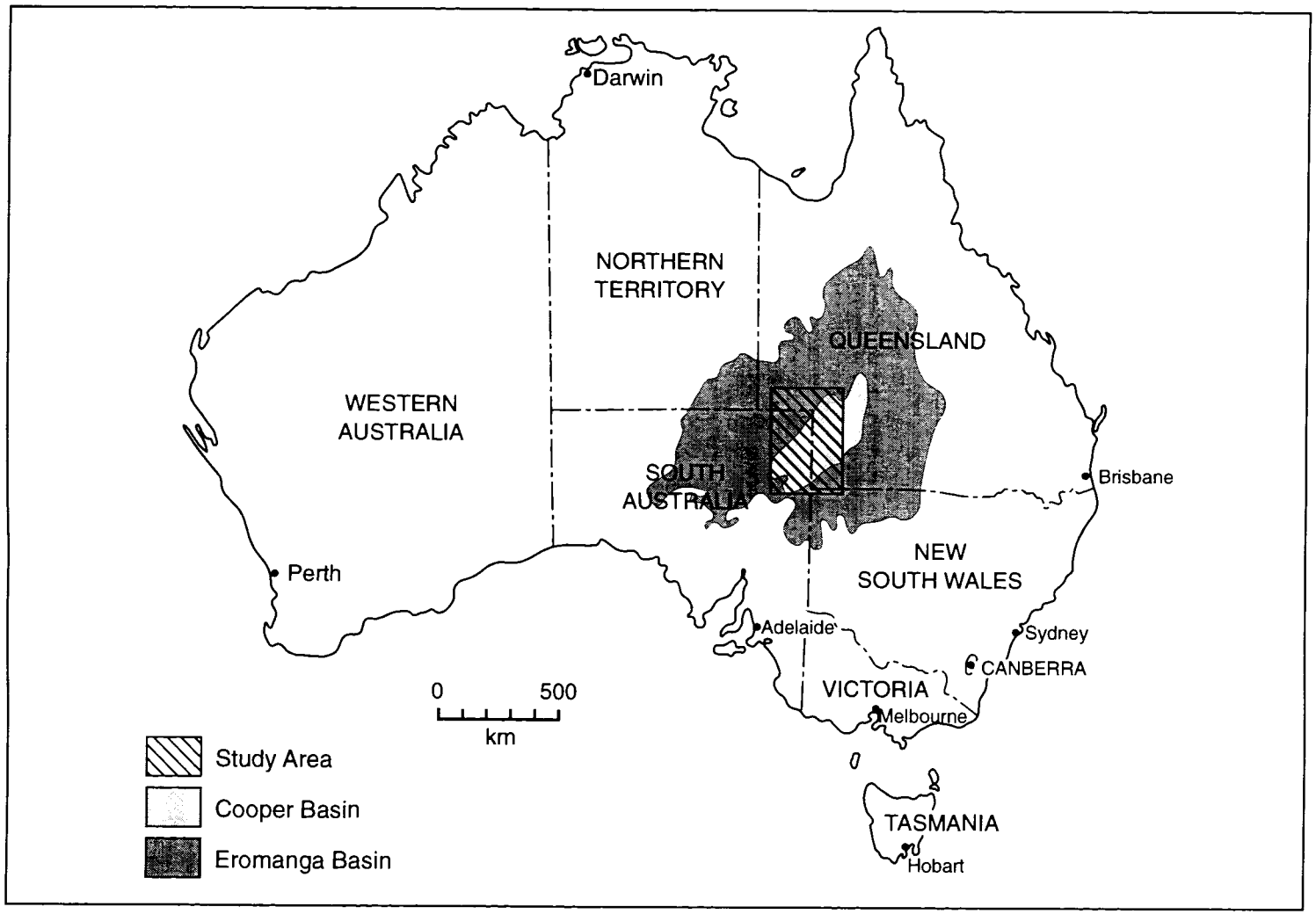

Figure 1.1. Location of the Cooper-Eromanga Basins on the Australian continent.

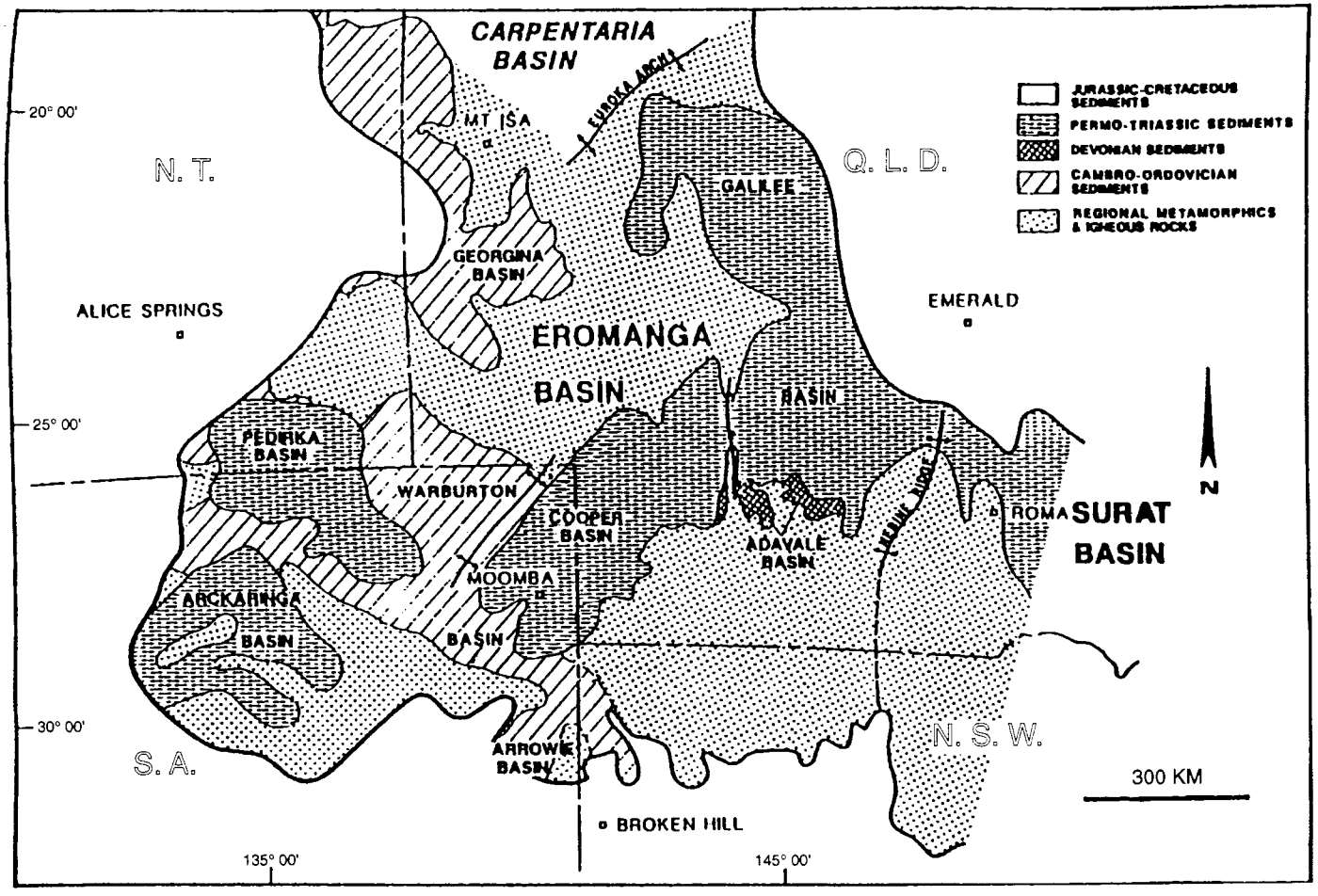

Figure 1.2. Geological setting of the Cooper-Eromanga Basins (after Wecker, 1989).

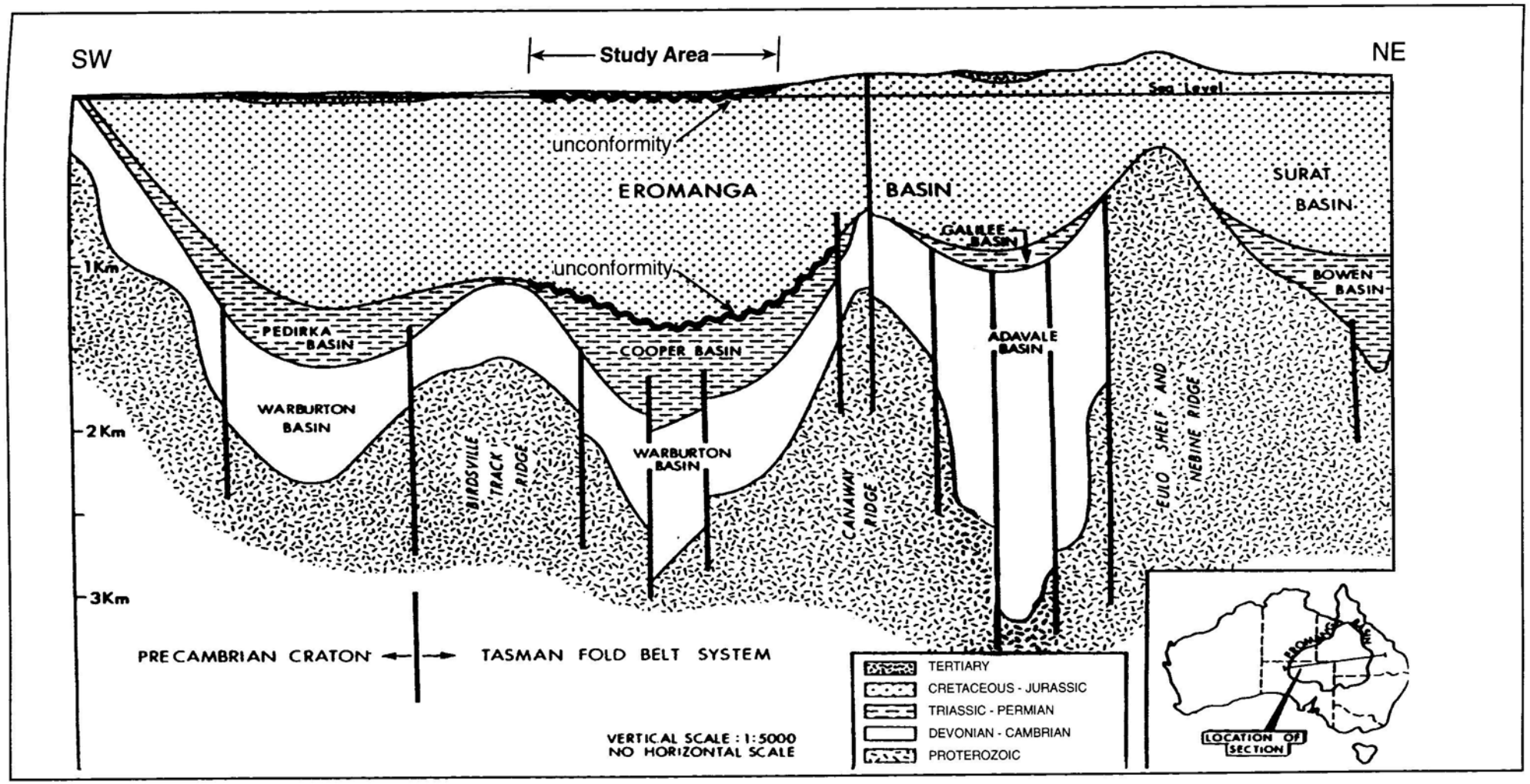

Figure 1.3. Diagrammatic cross section showing basin relationships. Cooper and Eromanga Basin unconformities are also shown (modified after Petroleum Management Associates, 1986).

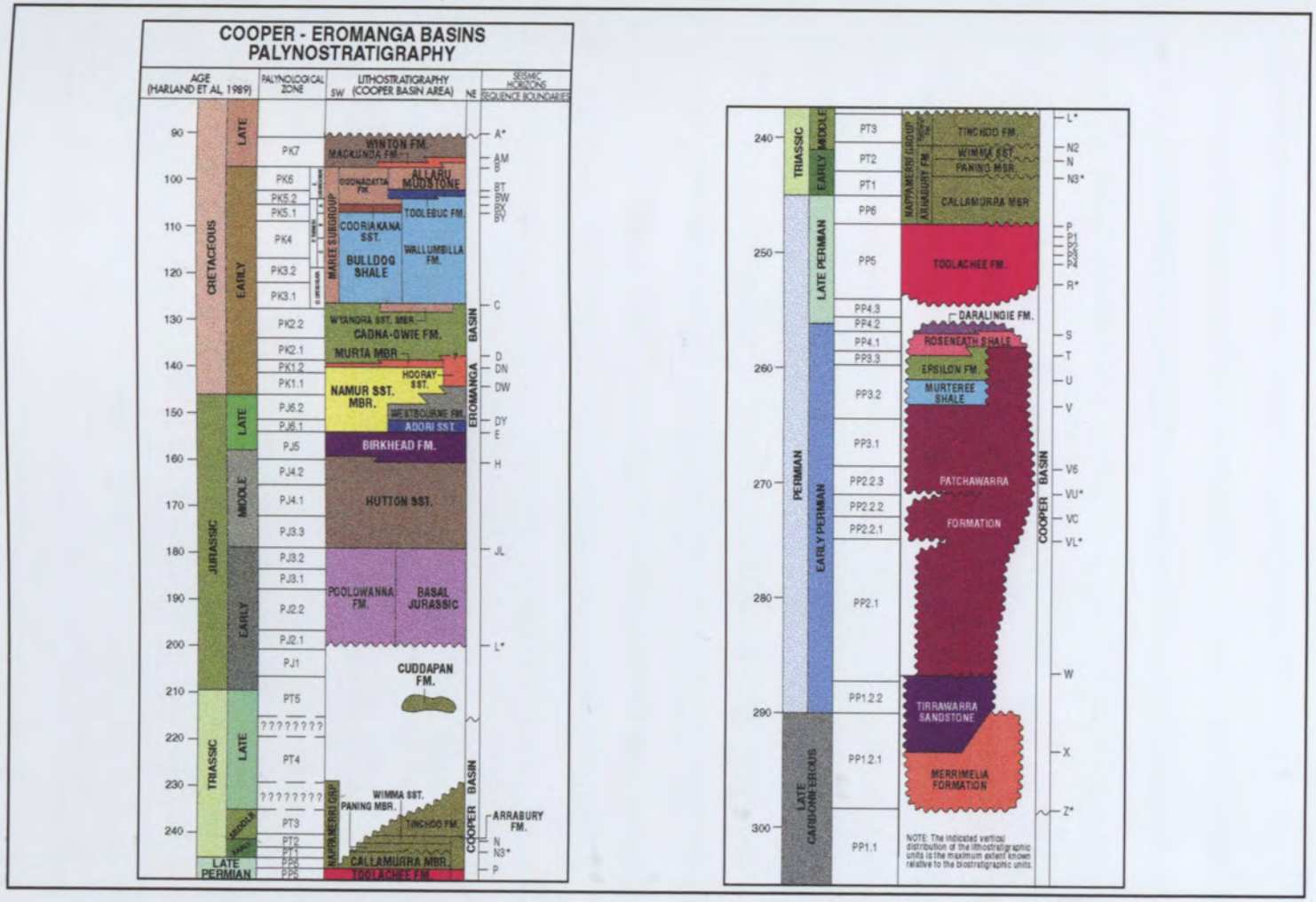

Figure 1.4. Cooper-Eromanga Basins palynostratigraphic nomenclature. (FM = Formation, GRP = Group, MBR = Member, SST = Sandstone) (modified after Santos, 1992).

1.3 Thesis Organization

Chapter 2 discusses the basis of the compaction methodology, including principles of sedimentary rock porosity and compaction. The use of other lithologies, in addition to shales, and the use of multiple logs and multiple stratigraphic units in compaction-based quantification of exhumation is also discussed. After the theoretical basis of the compaction analysis is discussed, the stratigraphic units and the principles of how to determine the normal compaction relations, ie. those unaffected by exhumation are presented. Chapter 3 presents and discusses the results of compaction analysis.

Chapter 4 deals with the estimation of exhumation in the Cooper-Eromanga Basins using the vitrinite reflectance method. Chapter 5 reviews evidence of exhumation and palaeo-thermal history in the Cooper-Eromanga Basins based on previous apatite fission track analysis (AFTA) and fluid inclusion homogenization temperatures.

Chapter 6 compares the estimates of exhumation based on compaction analysis, vitrinite reflectance, AFTA and fluid inclusion homogenization temperatures. Porosity-depth relations in the Cooper-Eromanga Basins are determined and the results are synthesised to determine the burial/exhumation history of representative wells. Chapter 7 shows the nature of the structural style associated with the exhumational events using seismic reflection profiles and discusses the possible tectonic driving mechanisms which may be responsible for the uplift and exhumation. Chapter 8 addresses the implications of burial/exhumation for source rock maturity, velocity/depth conversion and reservoir porosity. Finally, Chapter 9 summarises the results of the project.

2. QUANTIFYING EXHUMATION USING THE COMPACTION METHODOLOGY

2.1 Introduction

As discussed in the first chapter, the rocks of Cooper-Eromanga Basins have been exhumed from maximum burial-depth by Late Triassic - Early Jurassic and Late Cretaceous - Tertiary exhumation. The degree of compaction (as witnessed by porosities, densities, and seismic velocities) of the rocks in these basins was attained at burial-depths greater than that presently observed. The compaction methodology attempts to quantify the magnitude of exhumation by analysing the amount of overcompaction of the rocks.

As discussed later in this chapter, shale velocity has been widely taken as a reliable indicator of compaction state. Hence, shale velocities have been used to estimate exhumation in:

- north-western Germany (Jankowsky, 1962);
- United Kingdom, Southern North Sea (Marie, 1975);
- southwestern part of Western Canada Basin (Magara, 1976);
- Gulf Coast (Lang, 1978);
- Taranaki Basin, New Zealand (Wells, 1990);
- Eromanga Basin (Rodgers *et al.*, 1991);
- Beaufort-Mackenzie Basin, northern Canada (Issler, 1992);
- Barents Sea, Denmark (Nyland *et al.*, 1992; Skagen, 1992); and
- Danish Central Trough, North Sea (Japsen, 1993).

This study expands the standard shale velocity approach to compaction-based studies of exhumation. Firstly, all the porosity logs (sonic, density and neutron), and the velocity survey (check-shot) data, have been used. Secondly, multiple stratigraphic units (seven in the Eromanga Basin and five in the Cooper Basin), instead of a single shale unit, have been

analysed. After a brief discussion of porosity and compaction, this chapter discusses the use of multiple logs and multiple stratigraphic units in compaction-based quantification of exhumation. The results of this approach are presented in Chapter 3.

2.2 Porosity

Porosity (ϕ) is defined as the ratio of the void space (V_{void}) inside the rock, generally filled by liquids or gases, to the total or bulk volume (V_{tot}) of the rock:

$$\phi = \frac{V_{void}}{V_{tot}} . \tag{2.1}$$

The complement of the pore space is referred to as 'matrix', 'framework' or 'solidity'. There are a number of different kinds of porosity and their definitions, as applied in the ensuing discussion, need to be clarified.

Absolute (or total) porosity encompasses both interconnected and isolated pores. Effective (or productive) porosity encompasses only the interconnected part of absolute porosity.

Primary porosity originates during clastic sedimentation due to void spaces between grains. Secondary porosity is generated during diagenesis by such processes as fracturing and chemical dissolution.

Intergranular porosity consists of the void spaces between grains. Intragranular porosity occurs inside grains, and in the case of clay minerals is also referred to as interlayer porosity due to its position between sheets or layers of silicate minerals.

2.3 Compaction of Sedimentary Rocks: The Role of Burial-Depth

Compaction of sedimentary rocks is the reduction in their volume with burial. It is analysed through measurements of change in porosity, the only 'strain' parameter which can be readily measured. Three main mechanisms cause compaction, and burial-depth has a major control on all three processes (Figure 2.1). Mechanical rearrangement occurs dominantly in unconsolidated sediments under the effect of sedimentary loading, and involves the movement of matrix grains such that primary porosity is reduced. Mechanical deformation which becomes important with increasing burial-depth/overburden pressure (Figure 2.1) involves the strain and fracturing of matrix grains, again acting to reduce porosity. Finally, and dominating at greater burial-depth still, chemical processes such as pressure solution of matrix grains and reprecipitation of cements in pore spaces act to compact sedimentary rocks (Figure 2.1).

Whereas mechanical processes are clearly burial-depth controlled through overburden pressure, chemical processes are strongly controlled by other parameters such as the chemical stability of matrix grains. Furthermore, processes responsible for the creation of secondary porosity such as dolomitization, and feldspar dissolution, are not burial-depth controlled.

It is an assumption of the compaction-based method of determining exhumation that burial-depth, at the formational and regional scale, exerts the primary control on compaction. This assumption will be justified by the consistent apparent exhumation results derived from different stratigraphic units (Chapter 3).

2.4 Porosity Logs in Compaction Studies

The sonic, density and neutron logs are collectively known as the porosity logs because their response is strongly controlled by the amount of porosity, as opposed to the resistivity and electromagnetic propagation logs, the response of which is strongly controlled by the nature of

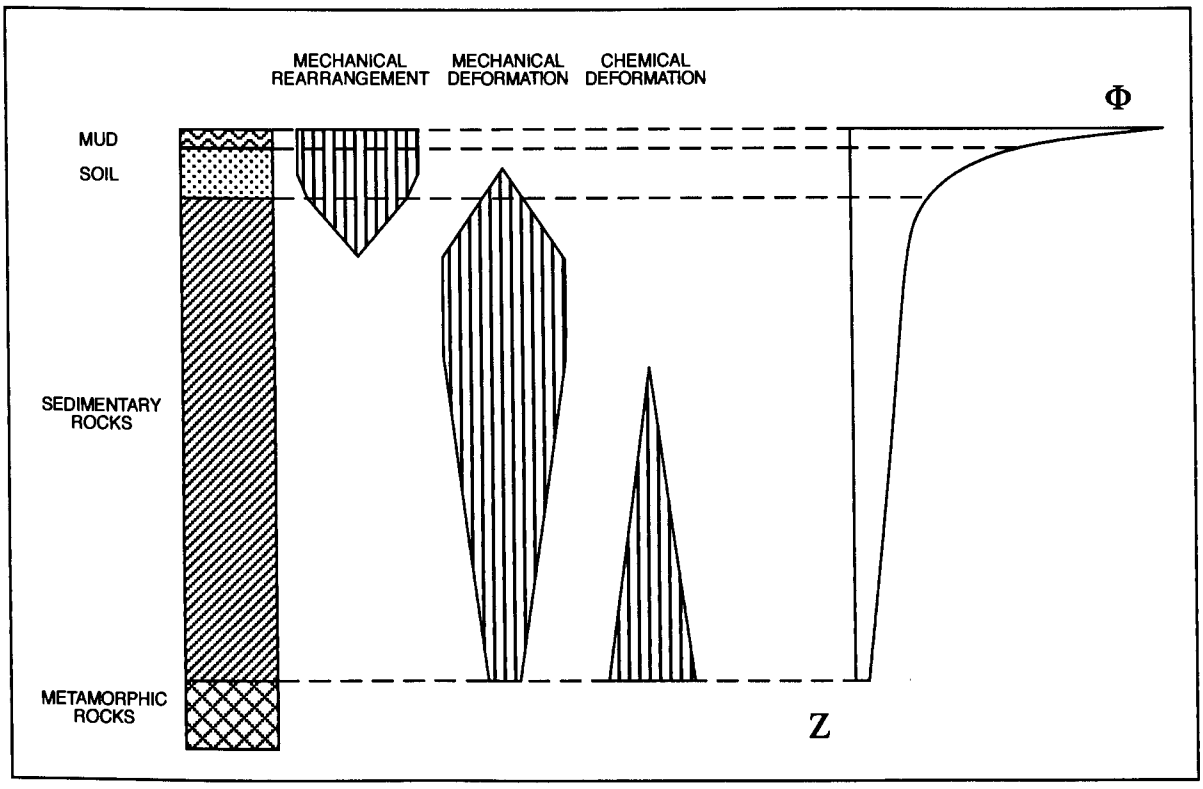

Figure 2.1. The four horizons in a sedimentary basin as defined by the principal mechanisms of compaction and porosity loss. The sedimentary column on the left is divided with depth as a function of the mechanical behaviour of the sediments. Sedimentary rocks from top to bottom: (1) a liquid zone zone made up of muds, (2) sediments that behave like soils, (3) sedimentary rocks *sensu stricto* and (4) metamorphic rocks. The Φ(Z) curve shows that most of the reduction of porosity takes place in the two upper horizons. The mechanical rearrangement of grains is responsible for most of the porosity reduction in the top two horizons of the sedimentary columns. Mechanical deformations may be elastic, plastic or breaking. Chemical deformations include diagenetic transformations as well as pressure-dissolution phenomena. The relative importance of those mechanisms in the way sediments evolve in time (or during burial) varies as a function of the nature of the grains making up the sediments (after Schneider *et al.*, 1994).

the fluids filling the pores (Schlumberger, 1989). Since porosity describes compaction state, the porosity logs are all appropriate indicators of compaction, and hence are appropriate for quantifying exhumation from compaction. Furthermore, they are routinely run in exploration wells and hence widely available.

The following discussion provides a simplified outline of the operating principles of the tools, details of which can be found in the large literature on the subject (eg. Serra, 1984;

Desbrandes, 1985; Schlumberger, 1989; Rider, 1991). The discussion highlights the use of the porosity logs in describing compaction, rather than with respect to hydrocarbon exploration and production-related issues. Together with the porosity logs, seismic check-shot (velocity survey) data were also used for exhumation estimates, and the procedures for these are also briefly discussed.

2.4.1 Sonic Log

Sonic logs measure the shortest time for a sound pulse to travel through the formation. The sound pulse travels through a mixture of fast matrix grains and slow formation fluids in the pore spaces. Hence the higher the porosity the slower the sound travels through the formation as a whole. Schlumberger's BHC (borehole compensated sonic) sonic log, with which sonic measurements were made in the data analysed has a depth of investigation of between 12 cm and 100 cm, decreasing with increasing velocity.

Since the sonic log measures the shortest time for an acoustic sound to travel through the formation, it circumvents any fracture or vugular porosity. Porosity of this type is generally secondary porosity and may constitute a significant part of the total porosity. Although the primary porosity is strongly controlled by burial-depth related processes, secondary porosity development is largely depth-independent, as discussed in Sections 2.2 and 2.3. The insensitiveness of the sonic log to secondary porosity can be a serious drawback in estimating hydrocarbon reservoir porosity, but here, where log measurements are being used to investigate maximum burial-depth and exhumation, it is considered advantageous. Indeed, the values of exhumation based on the sonic log are considered more reliable than these based on the other porosity logs (Chapter 3).

Due to computing costs the sonic and the other log data were smoothed and resampled to every 5 ft, from the original 0.5 ft sampling of the data. This smoothing and resampling has no

significant effect on the final results because we are considering the average compaction state of formation-scale stratigraphic units.

2.4.2 Seismic Check-Shot Velocities Survey and the Adjusted Sonic Log

The check-shot (or well velocity) survey is undertaken to facilitate tieing of reflections mapped on seismic data to geological horizons in the well. A shot is fired at the surface and the travel time to a number of geophones (mainly tops and bases of economically significant stratigraphic units in the Cooper-Eromanga Basins) in the well is recorded. One-way times to the geophones, thus to known depths in the well, are calculated with a geometric correction applied for any offset between the shot and the well. An adjusted sonic log can be calculated by combining the check-shot results with the sonic log. The adjusted sonic log has the high resolution of the sonic log, but velocities are corrected for 'drift' between the sonic log and the check-shot survey velocities. Drift is principally due to dispersion of velocities between the high frequency (20-40 kHz) of the sonic log and the lower frequency (5-50 Hz) of the seismic pulse (Goetz *et al.*, 1979; Hsu *et al.*, 1992).

Adjusted sonic logs were calculated where check-shot surveys were available (ie. 186 of the 206 wells analysed) using the subroutine 'Geophysics-Welltie' in MINCOM'S GEOLOG (1989) software package. This subroutine adjusts the sonic time log to compensate for drift, creating the adjusted sonic log, and so ties the sonic logs to the check-shot data. The drift corrected sonic is hereafter referred to as the adjusted sonic log (Δt_{adj}).

Despite calculating adjusted sonic logs as described above, the raw sonic log data were still also used to determine the compaction because:

- If dispersion is the main cause of sonic log drift in Cooper-Eromanga surveys, then uncorrected sonic log data are satisfactory for the purposes of this study,
- Velocity survey data are not available to drift-corrected the sonic log data in 20 of the wells analysed.

2.4.3 Density Log

Density logs measure the electron density of the formations. The density tool bombards the formation with medium-energy gamma rays and measures their attenuation between the tool source and detectors. The attenuation (Compton scattering) is a function of the number of electrons that the formation contains (electron density) which in turn is closely related to its bulk density. A number of borehole environmental corrections, including borehole size need to be applied to the density log measurements. Schlumberger's FDC (formation density compensated) log, with which density measurements were made in the logs analysed, has a depth of investigation of the order of 13 cm, decrasing with increasing density.

The density tool sees bulk density, ie. the average density both of the grains forming the rock, and the fluids enclosed in the interstitial pores, and as such compaction estimates based thereon include both primary and secondary porosity.

2.4.4 Neutron Log

The neutron log measures the hydrogen ion concentration of the formation. High-energy (fast) neutrons are emitted from a radioactive source in the tool. These neutrons collide with nuclei of the formations comprising the wellbore walls. With each collision, the neutron loses some of its energy. The greatest energy loss occurs when the neutron strikes a nucleus of equal mass, ie. a hydrogen nucleus. Thus, the slowing of neutrons depends largely on the amount of hydrogen in the formation. Low energy neutrons then diffuse randomly, until they are captured by the nuclei of atoms such as chlorine, hydrogen, or silicon. The capturing nucleus becomes strongly excited and emits a high-energy gamma-ray of capture. Depending on the type of neutron tool, either the gamma rays of capture or the slowed neutrons themselves are counted by a detector in the tool. Thus a measure of the hydrogen index of the formation is obtained, which is converted directly to neutron porosity units. As with the density log, a number of borehole environmental corrections, including borehole size need to be applied to the

neutron log measurements. Schlumberger's CNL (compensated neutron log) log, with which neutron log measurements were made in the data analysed has a depth of investigation of the order of 15-25 cm, increasing with decreasing porosity.

Since the neutron log is sensitive to all hydrogen nuclei, it responds to absolute, water-filled porosity, including water bound either within the molecule or absorbed between clay mineral layers. Hence when shales are present the effective porosity cannot be calculated without corrections. Like the density log, the neutron log will see secondary porosity.

2.4.5 Determining Porosity from the Porosity Logs

Porosity (ϕ) describes the degree of a rock's compaction, hence it is appropriate for use in estimating maximum burial-depths/exhumation. However, the porosity log data, not porosity itself, are used to estimate exhumation, hence the link between porosity (ϕ) and the values recorded by the porosity logs (Δt, ρ_b, ϕ_N) is critical.

Porosity calculation from the sonic log: Wyllie *et al.* (1956) proposed a linear *time-average* relationship between porosity (ϕ) and interval transit time (Δt):

$$\phi = \frac{\Delta t - \Delta t_{ma}}{\Delta t_f - \Delta t_{ma}}, \qquad (2.2)$$

where, ϕ = porosity;

Δt = interval transit time measured by sonic log;

Δt_f = transit time of the saturating fluid; and

Δt_{ma} = transit time of matrix material.

Equation (2.2) is the most widely quoted relation for porosity estimation using the sonic log. The equation states that the transit time measured by the tool is the sum of the time spent in the solid matrix and the time in the fluid. However, the Wyllie's *et al.* (1956) equation is not reliable in unconsolidated, high porosity formations (Sarmiento, 1961), or in very low porosity formations (Raymer *et al.*, 1980).

More recently Raiga-Clemenceau *et al.* (1988) proposed the *acoustic formation factor equation:*

$$\phi = 1 - \left(\frac{\Delta t_{ma}}{\Delta t} \right)^{1/x}, \tag{2.3}$$

where, ϕ = porosity;

Δt = interval transit time measured by sonic log;

Δt_{ma} = transit time of matrix material; and

x = exponent specific to the matrix lithology.

Raiga-Clemenceau *et al.* (1988) argue that this relation is reliable over a wider porosity range than Wyllie's *et al.* (1956) equation.

Porosity calculation from the density log: If we know the grain (matrix) density and the fluid density, we can determine porosity from bulk density:

$$\rho_b = \phi \rho_f + (1-\phi) \rho_{ma}$$

$$\Rightarrow \phi = \frac{\rho_{ma} - \rho_b}{\rho_{ma} - \rho_f}, \tag{2.4}$$

where, ϕ = porosity;

ρ_{ma} = matrix (grain) density;

ρ_f = fluid density; and

ρ_b = bulk density measured by the tool.

Determination of porosity from the neutron log: The neutron log tool directly measures the amount of hydrogen present in the formation. This is converted directly to (neutron) porosity following an API calibration (Schlumberger, 1989). Hence, neutron logs are scaled in (neutron) porosity units.

The determination of porosity in shaly units where the properties of the clay mineral matrix themselves change with depth is a major subject in its own right and is discussed for example by Asquith (1990). Crossplots, for example of the density and neutron log are often used to correct for non-effective porosity in shaly units.

In this study no attempt is made to convert interval transit time, bulk density, and neutron porosity values to porosity. The values are themselves taken to directly represent compaction (hence porosity). However, the above discussion highlights that each log sees porosity and hence compaction in a different way, particularly in the presence of shales, and this must be borne in mind when interpreting the results.

2.5 Use of Multiple Stratigraphic Units in Compaction Based Analysis of Exhumation

2.5.1 Use of Shales in Compaction-Based Analysis of Exhumation

It is has been widely demonstrated that shales show the most predictable and directly burial-depth controlled compaction (ie. porosity/depth) trends (Figure 2.2). Hence, their degree of compaction has been used as 'tool' for estimating exhumation in many parts of the world

(Section 2.1). On Figure 2.2 it can be seen clearly the rate of porosity decrease with increasing burial depth.

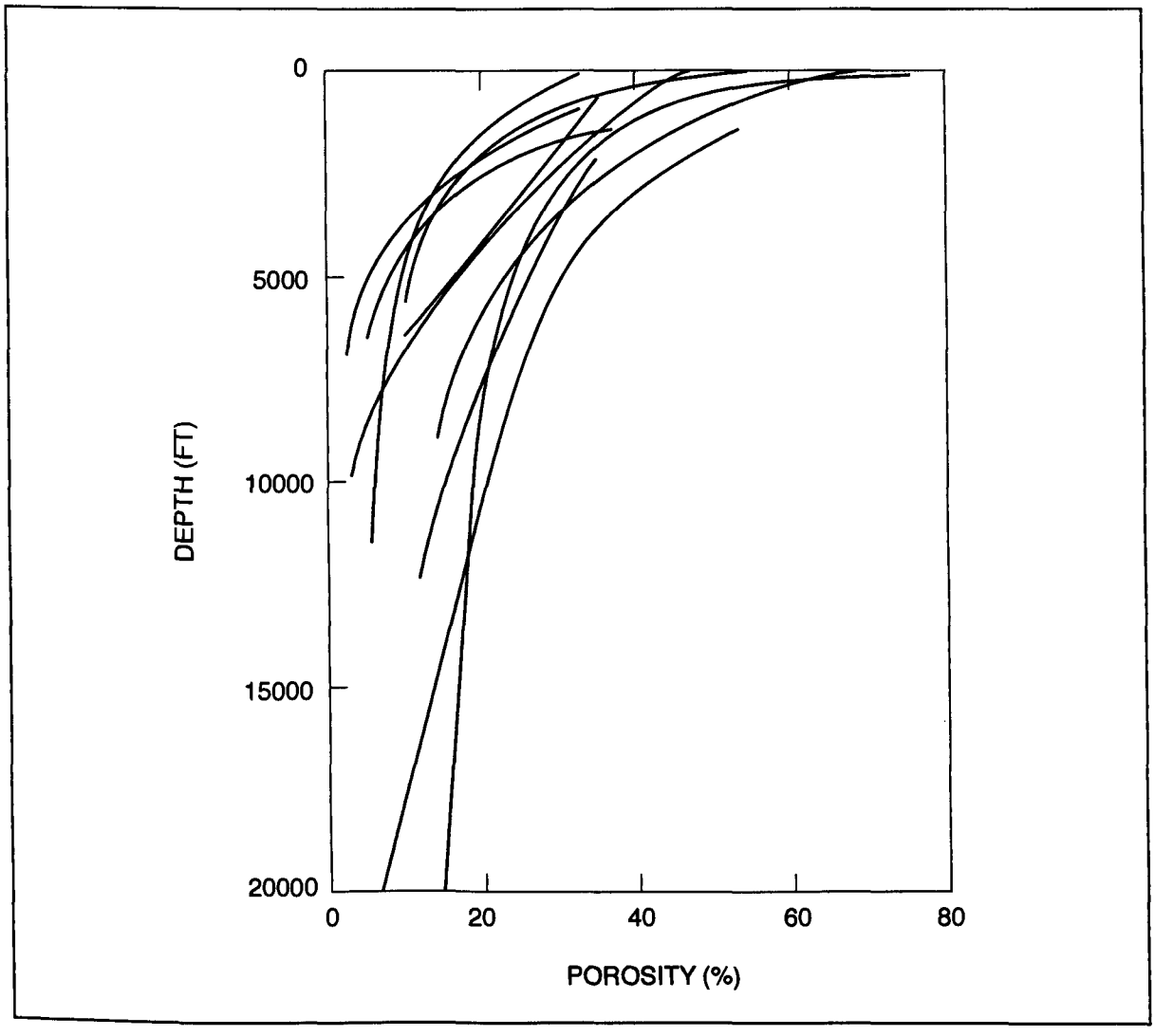

Figure 2.2. Relationship between porosity and depth of burial for shales and argillaceous sediments in different parts of the world. Shale porosity decreases with increasing burial-depth (after Rieke and Chilingarian, 1974).

2.5.2 Other Lithologies in Compaction-Based Analysis of Exhumation

Lithologies other than shales have not been widely used in compaction-based quantification of exhumation because non-burial-depth controlled processes, such as early cementation (at relatively shallow depths), can be responsible for porosity reduction. Furthermore, secondary

porosity generation can lead to an increase of porosity with burial-depth. However, mechanical and chemical compaction is strongly influenced by burial-depth in non-shale lithologies (Selley, 1978; Houseknecht, 1987; Dutton *et al.*, 1992; Dutton, 1993; Figure 2.3). Hence other lithologies merit consideration for use as records of maximum burial-depth.

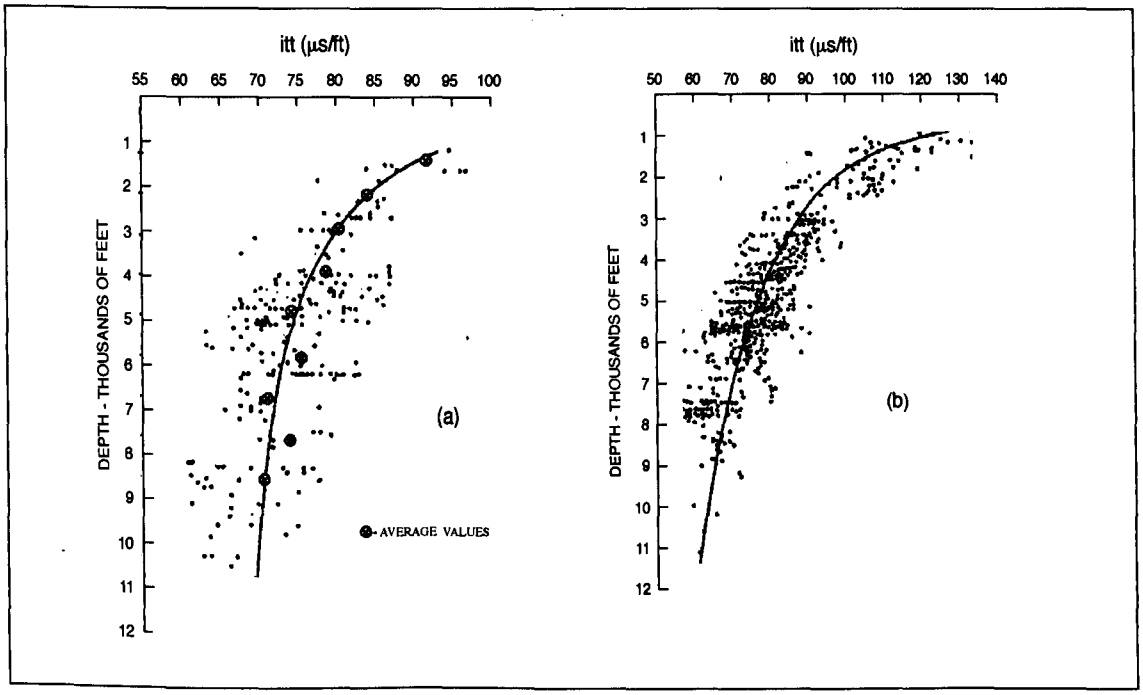

Figure 2.3. Effect of depth on interval transit time (itt) of (a) Mid-Continent Palaeozoic sandtones and (b) Lower Tertiary and Cretaceous sandstones (after Sarmienzo, 1961).

Bulat and Stoker (1987) used interval velocities to calculate uplift from different stratigraphic intervals in the United Kingdom Southern North Sea. The units they analysed were:

- Tertiary and Quaternary clays and sands;
- Upper Cretaceous chalks;
- Lower Cretaceous and Jurassic shales;
- Early Triassic sandstones;
- Early Triassic shales;
- Early - Late Triassic shales and evaporites;
- Early Permian sandstones and shales with evaporites;
- Carboniferous sands, shales and coals.

Although not statistically analysed by Bulat and Stoker (1987), the results from different units show broad agreement. Furthermore, they argue that results from a single stratigraphic unit need to be treated with caution.

Hillis (1992a) used the carbonate Oliver and Barracouta Formations to estimate exhumation in the Timor Sea. Despite the potential importance of cementation processes not controlled by burial-depth in carbonates, particularly in the near-surface, the Oliver Formation of the Timor Sea shows a clear increase in compaction (as witnessed by sonic velocity) with depth (Figure 2.4). Given the normal compaction trend defined by all the other wells, the Ashmore Reef well appears to have been exhumed from maximum burial-depth. However, one would not, in general, expect carbonates to show such a strong burial-depth controlled compaction trend. There are no significant thicknesses of carbonates in the Cooper-Eromanga Basins.

Hillis *et al.* (1994) analysed sonic velocity data in the Cretaceous Chalk and Kimmeridge Clay of the Inner Moray Firth, United Kingdom. The results were statistically consistent, suggesting that if, as widely accepted, burial-depth is the primary control on compaction of the Kimmeridge Clay, it is also the primary control on Chalk compaction. Hillis (1991) had previously shown that compaction within the United Kingdom chalk is strongly burial-depth controlled.

Menpes and Hillis (1995) used sonic velocities from chalks, shaly sandstones and shales to quantify erosion in the Celtic Sea/South-Western Approaches, offshore south-western United Kingdom. Apparent exhumation values from these stratigraphic units were statistically similar. It seems unlikely that burial-depth independent sedimentological and/or diagenetic processes could be responsible for similar amounts of overcompaction in the chalks, shaly sandstones, and shales analysed.

Hillis (1994; 1995a; b) estimated the Tertiary exhumation in the Southern North Sea using sonic velocities from chalks, sandstones and shales. Once again the consistency of results

from carbonate and clastic units indicates that overcompaction in the units analysed reflects previously greater burial-depth, rather than sedimentological and/or diagenetic processes.

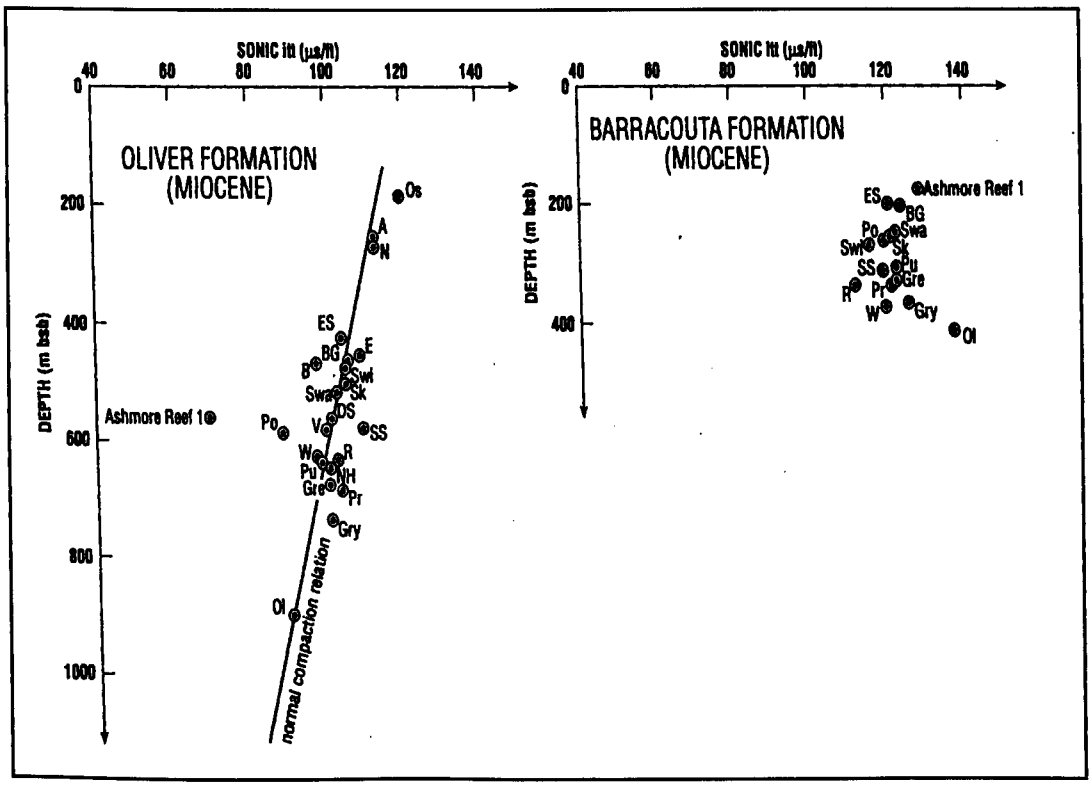

Figure 2.4. Mean interval transit time (itt)/midpoint depth data for the Oliver and Barracouta Formations of the Timor Sea. Note that the itt data for the Oliver Formation for all wells except Ashmore Reef-1 define a normal compaction trend, and that all the data from the Barracouta Formation are consistent. It is inferred that the Oliver Formation at Ashmore Reef-1 was exhumed from maximum burial-depth during the time gap encompassed by an unconformity between the Oliver and Barracouta Formations. Bsb: below sea bed (after Hillis, 1992).

It seems unlikely that burial-depth independent sedimentological and/or diagenetic processes could be responsible for similar amounts of overcompaction in the various lithologies in these examples. Burial at depth greater than currently observed is the most likely cause of consistent overcompaction (anomalously high velocities) in the units analysed. It is suggested that, at a formational and regional scale, burial-depth is the primary control on compaction in the units analysed. Hence the use of carefully selected lithologies other than shale in compaction-based estimates of exhumation is justified. Indeed, as discussed in the next section, results from multiple lithologies may be of critical importance.

2.5.3 Importance of Multiple Units in Compaction-Based Analysis of Exhumation

The use of multiple lithologies in the compaction-based analysis of maximum burial-depth has several advantages. Firstly, often no single stratigraphic unit is encountered in all the wells in an area of study. Secondly, assuming exhumation post-dated the youngest unit analysed, all the stratigraphic units in the same well should yield the same magnitude of exhumation. Hence by using the mean value from several stratigraphic units in the same well, the anomalous influence of any burial-depth-independent, sedimentological and/or diagenetic processes, that may affect the compaction state of a particular unit in the well, is lessened. Furthermore, if a younger unit exhibits no exhumation (ie. is everywhere at maximum burial-depth), or exhumation less than an older unit, and an older unit has been exhumed, the timing of exhumation may be constrained. For example, Hillis (1992a) showed that exhumation in the Timor Sea post-dated an overcompacted Miocene unit and pre-dated a normally compacted Pliocene-Recent unit (Figure 2.4).

Figure 2.5a shows a theoretical burial/exhumation history plot for wells in a basin in which has experienced two periods of exhumation, both followed by further burial. Units A and B, which predate the first event, yield higher apparent exhumation estimates than Units C and D (Figure 2.5b). Units A and B exhibit the same amount of apparent exhumation, as do Units C and D (Figure 2.5c). It is expected, that there is more scatter in real data, however, this example illustrates the potential of the analysis of multiple stratigraphic units for determining the age of exhumation.

Given the success of non-shale lithologies in predicting exhumation, and the importance of analysing multiple units, this study uses 12 different stratigraphic units to determine exhumation in Cooper-Eromanga Basins.

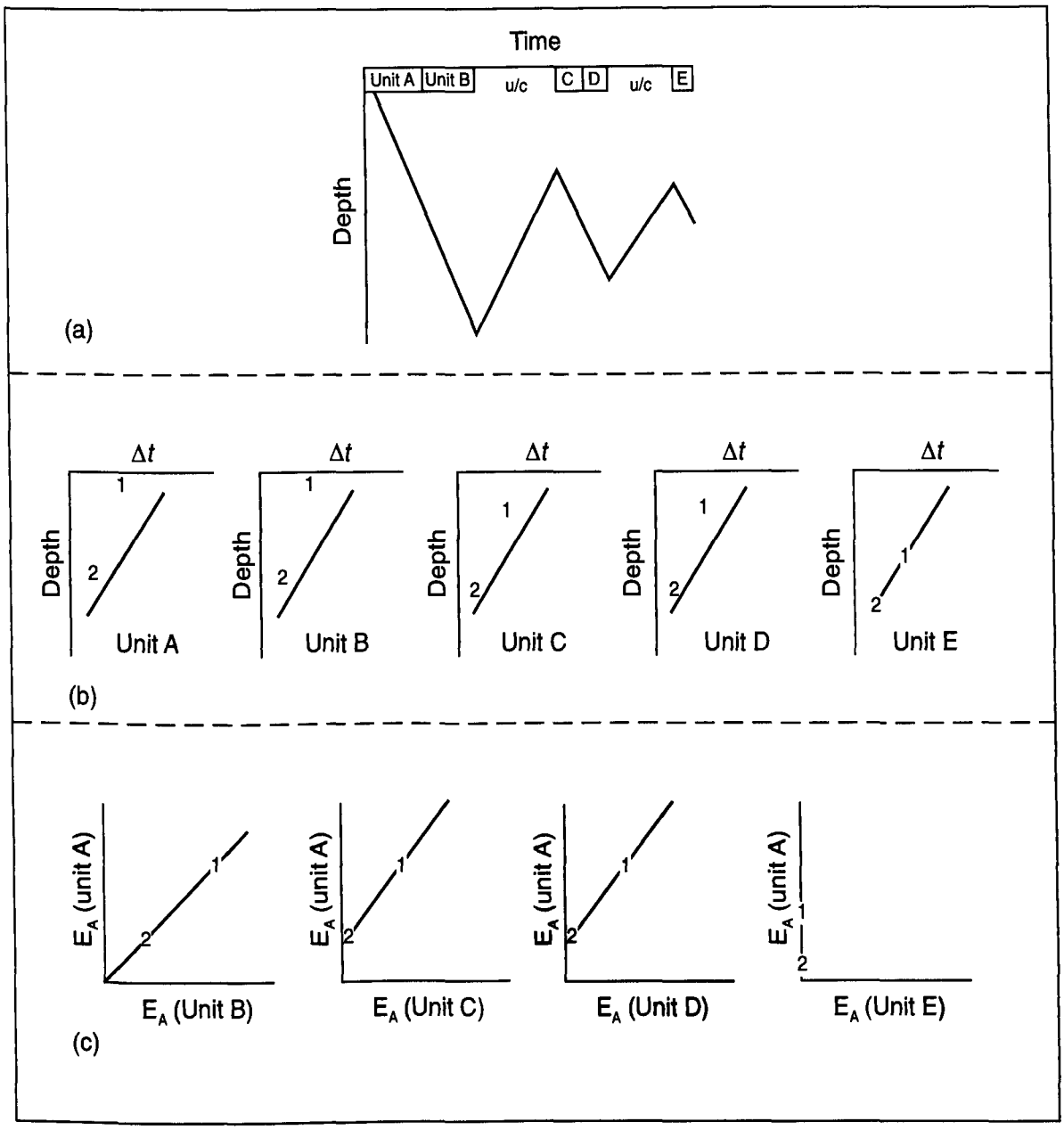

Figure 2.5. (a) Theoretical basin burial history plot for a basin which has undergone two distinct exhumation events, both followed by further burial. (b) Units A and B exhibit greater apparent exhumation than Units C and D, which in turn exhibit greater apparent exhumation than Unit E, which is normally compacted. (c) Unit A and B yield the same apparent exhumation values, as do Units C and D. Unit B exhibits greater apparent exhumation than Unit C, and Unit D exhibits greater apparent exhumation than Unit E. 1 and 2 are two theoretical wells from the basin which have undergone the same burial history, but exhibit different magnitudes of apparent exhumation.

2.6 Quantifying Exhumation

2.6.1 Quantification of Apparent Exhumation

The reduction of porosity of shales, sandstones, siltstones and lithological combinations thereof with increasing burial-depth is a largely non-reversible process. Because depth-controlled compaction is largely irreversible, units that are shallower than their greatest burial depth will be overcompacted, with respect to their present burial depth. The units analysed are assumed to follow a normal compaction (ie. porosity, velocity, density, etc.) trend with burial, and compaction is assumed not to be reversed by subsequent exhumation.

With these assumptions the amount of elevation of exhumed sedimentary rocks above their maximum burial-depth, termed 'apparent exhumation', is given by the displacement, along the depth axis, of the observed compaction trend from the normal, undisturbed trend (Figure 2.6). Figure 2.6 shows the evolution of the sonic log, of a unit, in a well during initial burial (A), subsequent exhumation (B), and post-exhumational burial (C, D, and E). The amount of apparent exhumation (E_A) of the well B is the vertical displacement, along the depth axis, between its itt/depth trend and that of the normal compaction relationship in well A: 500 m in this case. This can be estimated graphically, however, in practice, it was determined numerically using the simple equation:

$$E_A = 1/m(\Delta t_u - \Delta t_r) - d_u + d_r \ , \qquad (2.5)$$

where, m = gradient of the normal compaction relationship;

Δt_u = mean interval transit time of the well under consideration;

Δt_r = mean interval transit time of the reference well;

d_u = midpoint depth of the unit in the well under consideration; and

d_r = midpoint depth of the unit in the reference well.

The above equation (2.5) is also used for the estimation of apparent exhumation from the adjusted sonic, density and neutron logs where instead of Δt_u and Δt_r, is used Δt_{adju} and Δt_{adjr}, ρ_{bu} and ρ_{br}, and ϕ_{Nu} and ϕ_{Nr}, were used as appropriate.

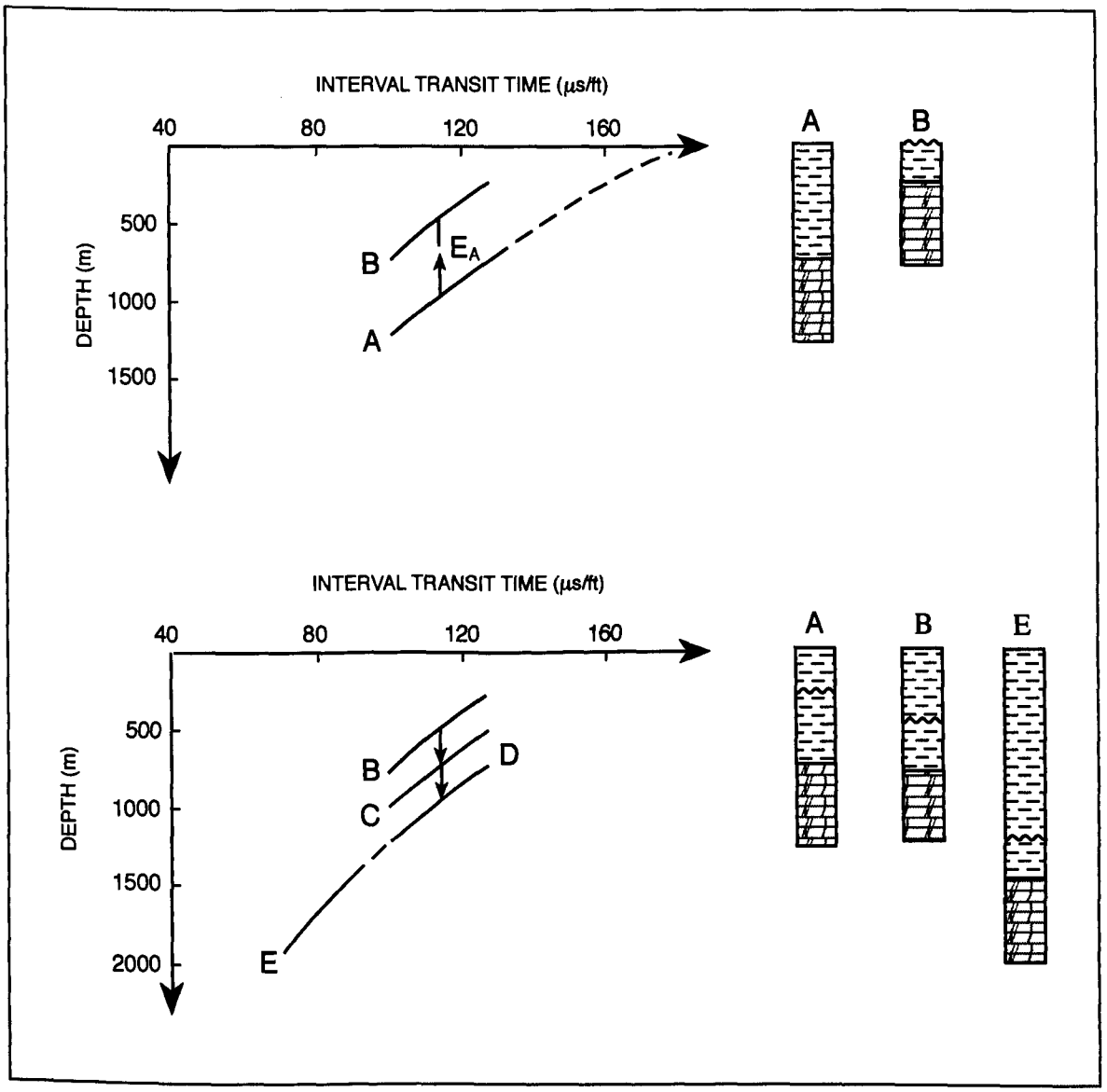

Figure 2.6. Interval transit time evolution during burial (A), subsequent uplift and exhumation (B), and post-exhumational burial (C, D and E). The apparent exhumation (E_A) is the amount of exhumation not reversed by subsequent burial (ie. height above maximum burial depth) (after Hillis, 1991).

2.6.2 Apparent Exhumation, Exhumation and Maximum Burial-Depth

The quantity (E_A) is referred to as apparent exhumation because it is exhumation not reversed by subsequent burial. It is not necessarily the same as the amount of exhumation that occurred at the time the rocks were being elevated. If there is no post-exhumational burial, then apparent exhumation is the true exhumation magnitude. However, if renewed burial follows exhumation, the magnitude of apparent exhumation determined from the porosity log data is reduced by the amount of that subsequent burial (Figure 2.6, well C). Once the unit again reaches its maximum burial-depth (Figure 2.6, well D), it is normally compacted, and no evidence of the previous exhumational phase can be detected by this method. Overburden weight following exhumation does not cause any further porosity loss until the formation re-attains its previous maximum burial-depth. In general, total exhumation at the time the rocks were being elevated (E_T) is the sum of apparent exhumation (E_A) and post-exhumational burial (B_E):

$$E_T = E_A + B_E . \tag{2.6}$$

In Figure 2.6, well C exhibits apparent exhumation of 250 m. It is necessary to add 250 m of post-exhumational burial to the 250 m of the apparent exhumation in order to obtain the total exhumation of 500 m. In well D, the formation has returned to its previous burial-depth of well A, and there is no remaining sonic log anomaly. If the post-exhumational burial continues beyond well D, the formation will once again begin to follow its normal compaction trend as shown by well E.

Maximum burial-depth (B_T) is constrained by the apparent exhumation (E_A) and not the amount of exhumation at the time the rocks were being exhumed (E_T). It is given by the sum of the present burial-depth (B_P) and apparent exhumation (E_A):

$$B_T = E_A + B_P. \tag{2.7}$$

Figure 2.7 further illustrates the relationships between apparent exhumation (E_A), total exhumation (E_T), post-exhumational burial (B_E), present burial-depth (B_P) and maximum burial-depth (B_T) with regard to wells A and C in Figure 2.6.

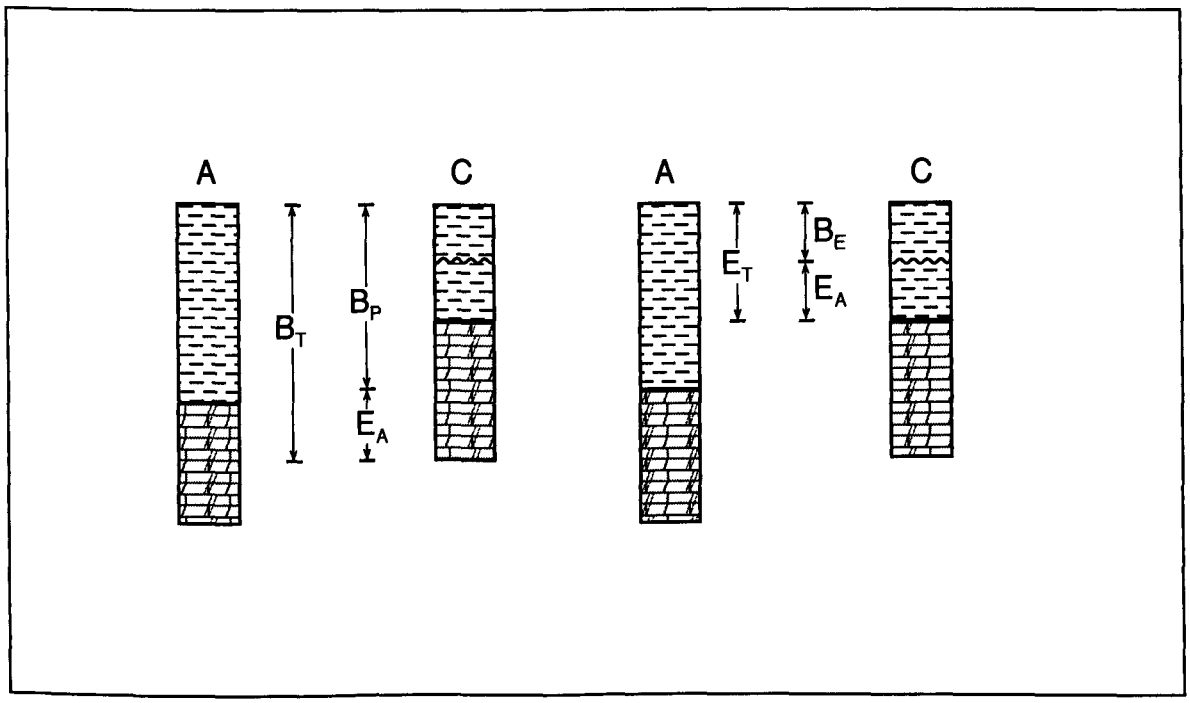

Figure 2.7. Relationship between apparent exhumation (E_A), present burial-depth (B_P), maximum burial-depth (B_T), post-exhumational burial (B_E), and exhumation at the time of denudation (E_T), for wells A and C of Figure 2.6. Well A is prior to exhumation, well C post-dates exhumation and post-exhumational burial (after Menpes and Hillis, 1995).

2.6.3 Uplift, Erosion and Exhumation

Confusion exists in published literature regarding different measures of uplift and their respective reference frames (England and Molnar, 1990; Brown, 1991; Riis and Jensen, 1992). For principally tectonic/geodynamic reasons, displacement of the earth's surface with respect to the geoid (surface uplift), displacement of rocks with respect to the geoid (uplift of rocks), and displacement of rocks with respect to the surface (exhumation) should be distinguished. Although all three quantities are related *(surface uplift = uplift of rock - exhumation)* they cannot be equal, unless all are zero (England and Molnar, 1990; Riis and Jensen, 1992). It is

important to distinguish these different quantities because only surface uplift requires work against gravity, and hence a tectonic driving force. Uplift of rock or exhumation, although significant with regard to geohistory modelling, may be caused solely by changes in sedimentary or erosional base level (eg. sea-level). Analysis of porosity log data as presented in this thesis quantifies the displacement of rocks with respect to the surface. Although previous authors (Bulat and Stoker, 1987; Hillis, 1991) have used the term 'uplift' to describe this quantity, the term 'exhumation' is now preferred following the definitions of England and Molnar (1990). The term 'erosion' is avoided because this refers not only to the process of elevating rocks with respect to the surface, but also to the removal and transport of weathered material. Only removed rocks are eroded, however, the entire rock column is exhumed as a result of erosion.

2.7 Selection of Stratigraphic Units for Compaction-Based Analysis of Exhumation

2.7.1 General Principles

Stratigraphically-equivalent units that exhibit a vertically- and laterally-consistent relation between depth and compaction are required to determine maximum burial-depth. The units should show little bulk lateral facies variation, in order to satisfy the assumption that their compaction trends are laterally consistent. Cooper-Eromanga lithologies are dominantly clastic, with relatively few carbonate or evaporite sequences. Given that shales in particular, and clastics in general are more likely to show a consistent relationship between depth and compaction than carbonate and/or evaporite sequences, it is relatively easy to select multiple units from the Cooper-Eromanga for compaction-based analysis of maximum burial-depth (Figure 2.8). The seven units selected for analysis from the Eromanga Basin were the: Winton Formation, Oodnadatta Formation/Allaru Mudstone, Wallumbilla Formation/Bulldog Shale, Cadna-owie Formation, Birkhead Formation and Hutton Sandstone. The five units selected for

analysis from the Cooper Basin were the: Nappamerri Group, Toolachee Formation, Roseneath Shale, Murteree Shale and Patchawarra Formation.

The tops and the bases of the units analysed were consistently picked from vertically compressed plots (1:5500 scale) of the sonic and gamma-ray logs (Figure 2.8). The compressed plots facilitate the picking of tops and bases which, for consistency within this study, were frequently slightly modified from those on operators' composite logs (Figure 2.9). The top of the Winton Formation, the youngest unit analysed, was often picked below the operators' pick because the quality of the logs in the first few metres (at the top of the shallowest logging run) was inappropriate for estimating exhumation (Figure 2.9).

Coals in the Toolachee and Patchawarra Formations presented a significant problem. Cooper Basin coals have an anomalously low natural gamma intensity and low seismic velocity (high slowness) compared to interbeded shales and sandstones. The laterally variable amount of low velocity (and low density, high neutron porosity) coal strongly influences the average velocity (density and neutron porosity) in the Toolachee and Patchawarra Formations. The thickest possible sections of the Toolachee and Patchawarra Formations free of coal were thus used in the analysis (Figure 2.9). Coal-free sections were picked by excluding units with low gamma ray and high sonic interval transit times (more than 95 μs/ft). In some wells, coal-free sections could not be picked.

Only relatively thick units are considered to give reliable results in compaction-based analysis of exhumation, and the following units were excluded because they were too thin to be reliable: the Coorikiana Sandstone, the Toolebuc Formation, the Wyandra Sandstone Member, the Murta Member, and the Adori Sandstone (in the Eromanga Basin) and the Daralingie Formation, Tirrawarra Sandstone, and the Merrimellia Group (in the Cooper Basin). If less than 40 m of a unit is present, that unit was not analysed because relatively condensed sequences of a given unit are likely to have anomalous porosity/compaction characteristics.

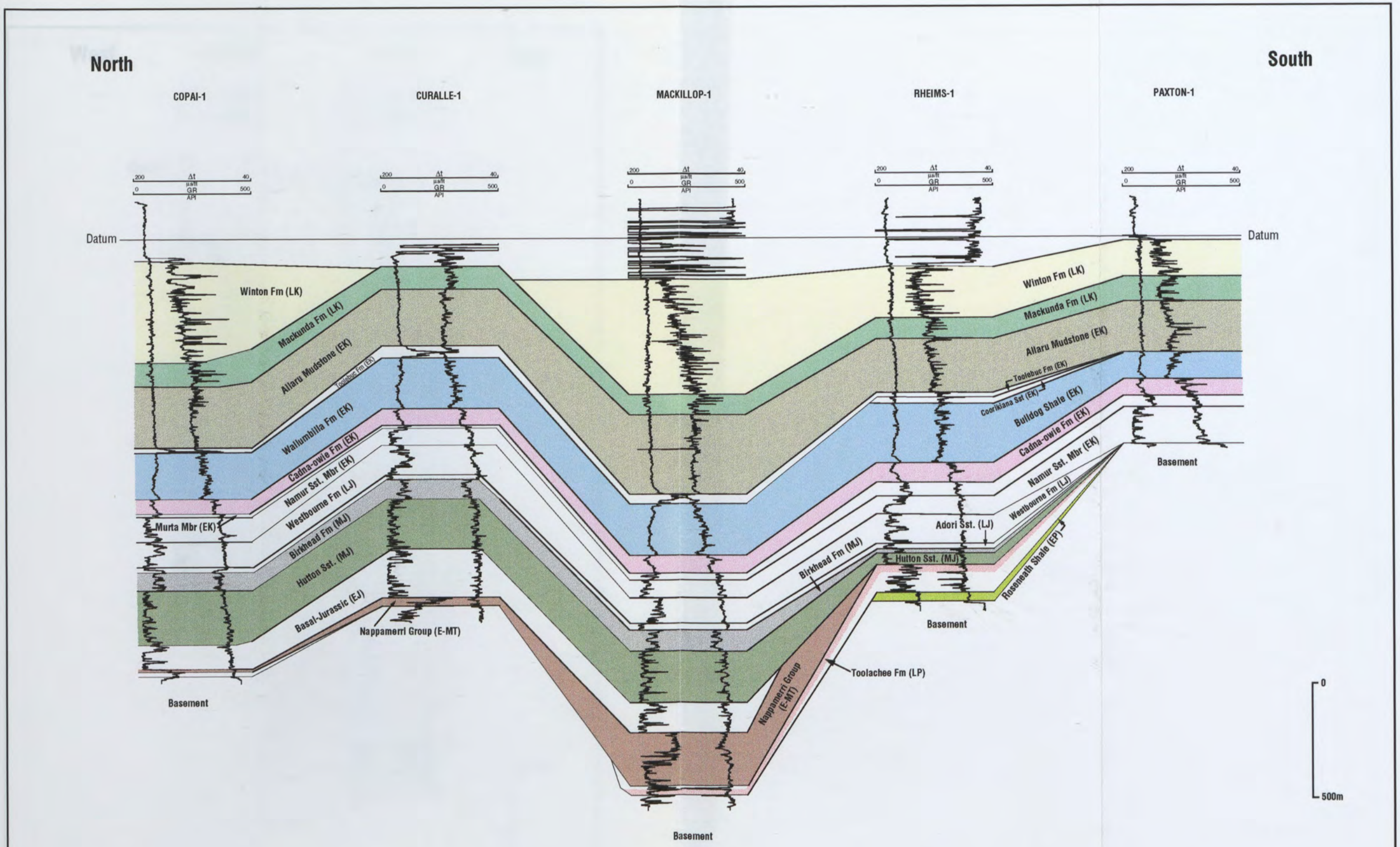

Figure 2.8a. Correlation of gamma ray (GR) (left trace) and sonic transit time (Δt) (right trace) logs for wells in the Cooper-Eromanga Basins. The staratigraphic units analysed are marked by different colours. Reference datum is the mean sea level (0 metres). The section line is shown on Figure 2.8d. (LK, Late Cretaceous: EK, Early Cretaceous: LJ, Late Jurassic: MJ, Middle Jurassic: EJ, Early Jurassic: E-MT, Early -Middle Triassic: LP, Late Permian: EP, Early Permian).

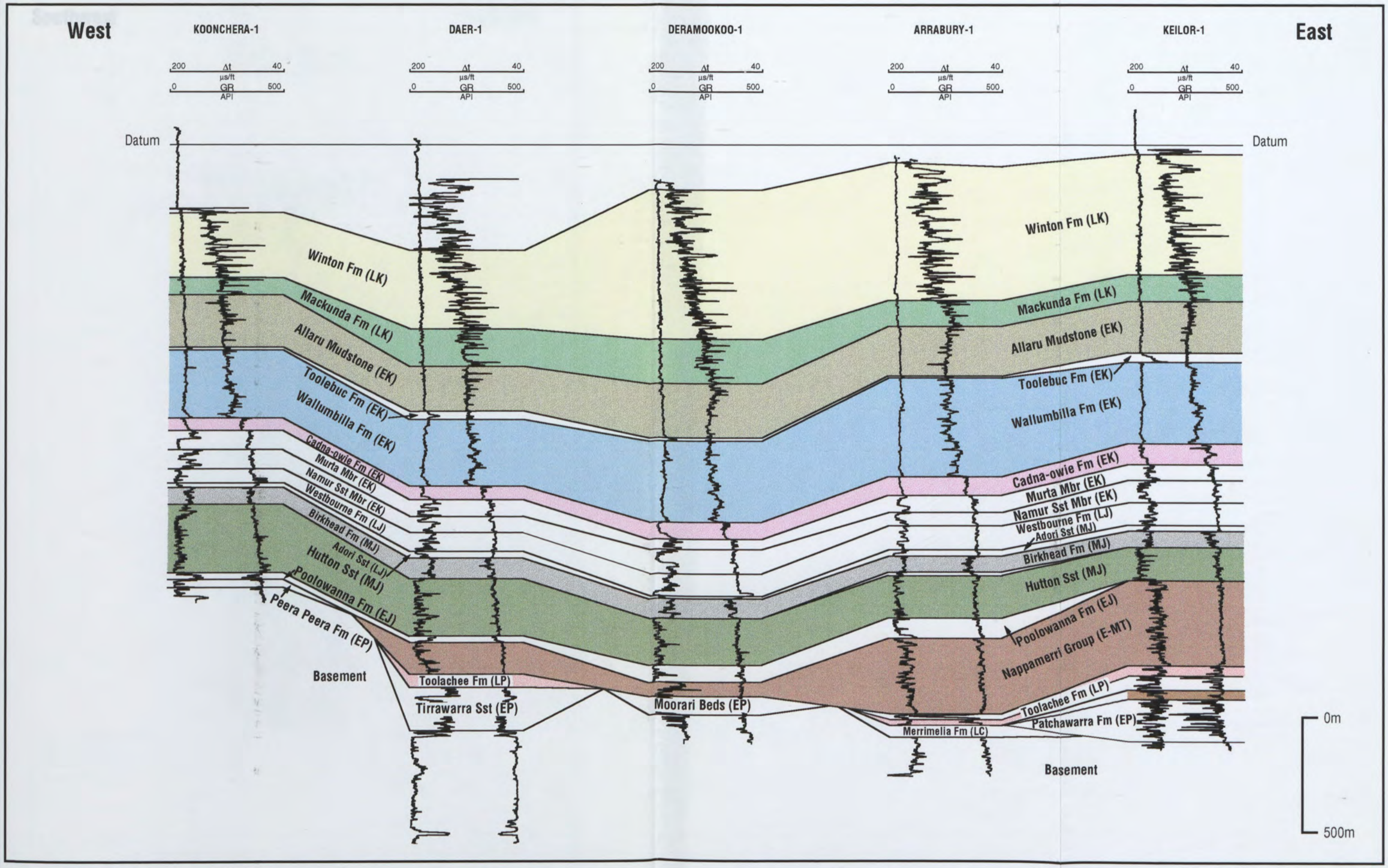

Figure 2.8b. Correlation of gamma ray (GR) (left trace) and sonic transit time (Δt) (right trace) logs for wells in the Cooper-Eromanga Basins. The stratigraphic units analysed are marked by different colours. Reference datum is the mean sea level (0 metres). The section line is shown on Figure 2.8d. (LK, Late Cretaceous; EK, Early Cretaceous; LJ, Late Jurassic; MJ, Middle Jurassic; EJ, Early Jurassic; E-MT, Early-Middle Triassic; LP, Late Permian; EP, Early Permian; LC, Late Carboniferous).

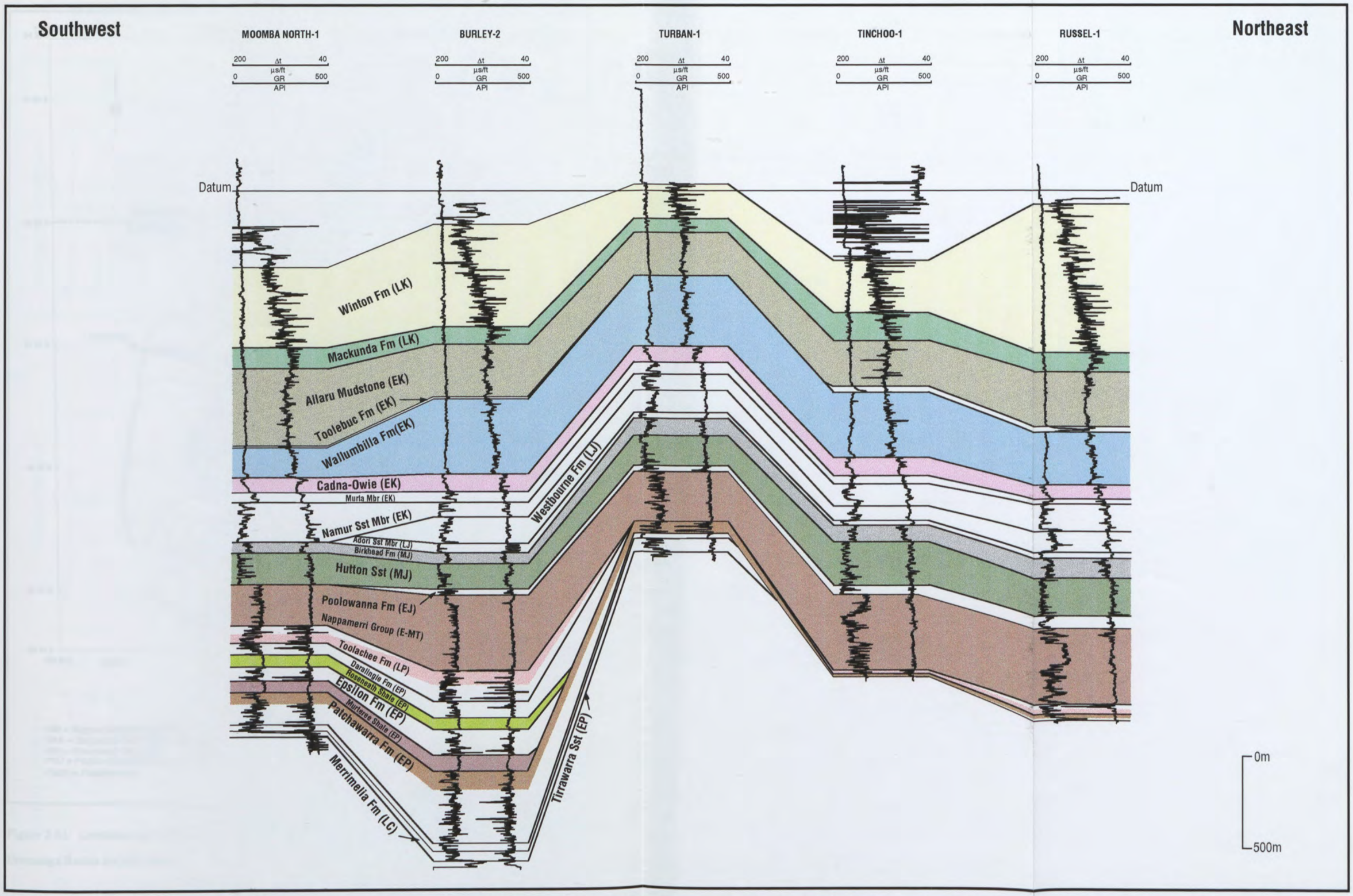

Figure 2.8c. Correlation of gamma ray (GR) (left trace) and sonic transit time (Δt) logs for wells in the Cooper-Eromanga Basins. The stratigraphic units analysed are marked by different colours. Reference datum is the mean sea level (0 metres). The section line is shown on Figure 2.8d. (LK, Late Cretaceous; EK, Early Cretaceous; LJ, Late Jurassic; MJ, Middle Jurassic; EJ, Early Jurassic; E-MT, Early-Middle Triassic; LP, Late Permian; EP, Early Permian; LC, Late Carboniferous).

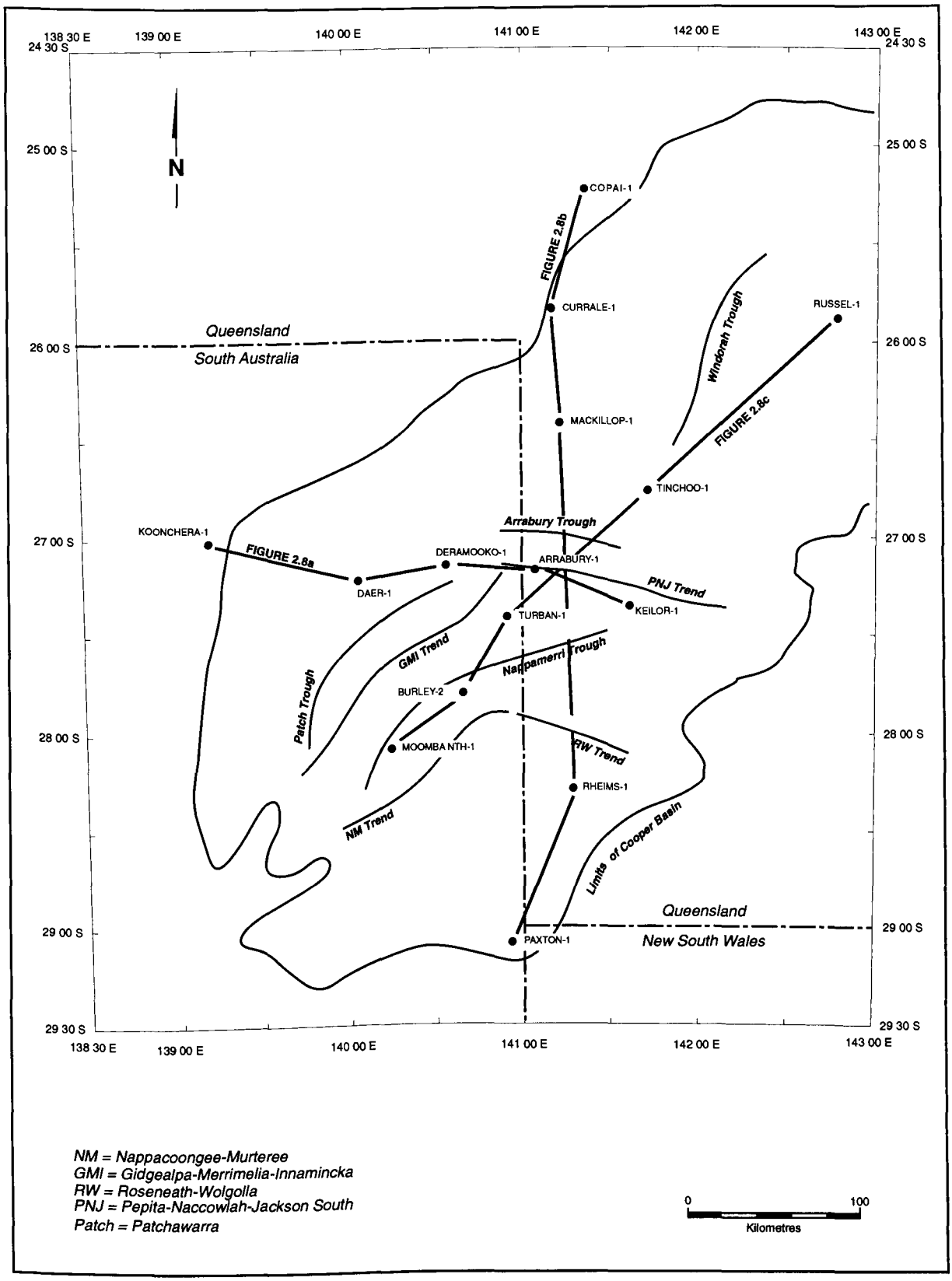

Figure 2.8d. Location map for the section lines of Figures 2.8a. - 2.8c. Major tectonic elements of the Cooper-Eromanga Basins are also shown.

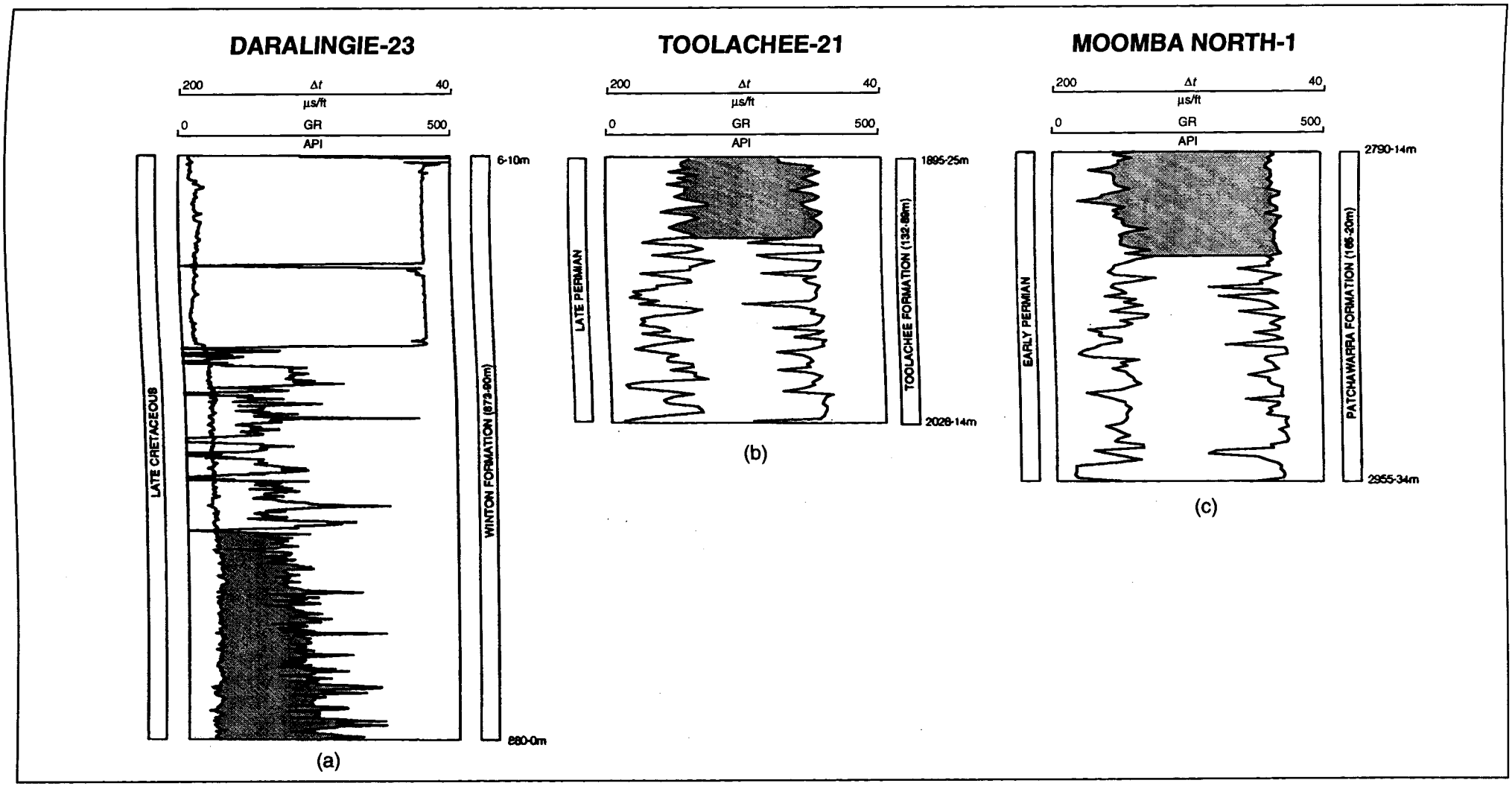

Figure 2.9. Modification of tops and bases from those on operators logs for the (a) Winton Formation, (b) Toolachee Formation, and (c) Patchawarra Formation. The part of each formation used in compaction analysis is shown in grey colour. See text for further discussion.

All log displays and subsequent calculations were undertaken using the MINCOM'S GEOLOG (1989) software package. Care was taken to edit out spurious data due for example to erroneous scale changes, cycle skipping effects and hole size effects on the density and neutron logs.

2.7.2 Summary of the Units Analysed

The stratigraphic units analysed, are briefly summarised below, following the description of Petroleum Management Associates (1986), except for the Nappamerri Group which follows the description of Powis (1989).

Eromanga Basin: Cretaceous

Winton Formation: The Late Albian to Cenomanian Winton Formation consists of low energy meandering fluvial to marshy grey shales and siltstones with sandstone and coal interbeds. The formation occurs as outcrop, or near surface subcrop over much of southwestern Queensland and extends into South Australia and the Northern Territory, reaching a maximum thickness of over 900 m in each of the Nappamerri, Patchawarra, Poolowanna, and Windorah Troughs.

Mackunda Formation: The Late Albian Mackunda Formation is a marginal marine sequence consisting of siltstone, calcareous sandstone and shale. The formation represents a transition of paralic sedimentation between the marine Allaru Mudstone and the non-marine Winton Formation. The Mackunda Formation averages about 60 m thickness in the central Eromanga Basin and 120 m in the southwestern part of the study area, although it can be as 275 m thick outside of the study area.

Oodnadatta Formation: The Oodnadatta Formation consists predominantly of shale and siltstone with minor calcareous sandstone and rare limestone beds. The formation is considered to be Early to Late Albian in age and believed to have been deposited under low energy shallow marine conditions. The formation reaches a maximum thickness of approximately 300 m but is not as extensive as the Allaru Mudstone, and confined to the southern and southwest parts of the study area.

Allaru Mudstone: The Albian Allaru Mudstone consists mainly of grey mudstone with thin interbeds of calcareous siltstone and minor very fine grained sandstone. The sequence was deposited in an apparently shallow, quiet water marine environment. Its differentiation from the lithological similar and laterally equivalent Oodnadatta Formation is based entirely on the presence of the underlying Toolebuc Formation. The Allaru and Oodnadatta Formations were grouped together in this analysis.

Wallumbilla Formation: The Aptian to Albian in Wallumbilla Formation consists of grey siltstone and mudstone with minor interbeds of fine sandstone. The formation appears to have been deposited in a shallow, epicontinental marine paralic environment. The unit varies considerably in thickness, which has a maximum in the southwest of approximately 500 m.

Bulldog Shale: The Bulldog Shale is lithological similar to the laterally equivalent Wallumbilla Formation and the two formations were grouped together in this analysis.

Cadna-owie Formation: The Neocomian to Early Aptian Cadna-owie Formation reflects the transition from terrestrial deposition of sediments, which persisted through the Permo-Triassic and Jurassic, of the Cooper-Eromanga Basins to marine deposition, which prevailed throughout much of the Cretaceous. The formation is widespread, ranging in thickness from about 40 m to over 90 m. Mudstones are an important, but usually minor facies in the lowermost part of the formation. The lower part of the formation consists predominantly of fine to medium grained quartzose sandstone with siltstone especially towards the base. The lower part of the formation appears to have been deposited under paralic conditions. The top of the Cadna-owie Formation is characterised by a distinctive marker bed across much of the Eromanga Basin. This distinctive unit, which is up to 25 m thick is characterised by an anomalously high gamma-ray response and low sonic velocity.

Eromanga Basin: Jurassic

Birkhead Formation: The Mid - Late Jurassic Birkhead Formation consists of shallow lacustrine, swamp, bog and fluvial sediments, which contrast with the massive, high energy braided stream sediments which comprise most of the underlying Hutton Sandstone. The formation consists of shales, siltstones and rare fine grained sandstones. Coal in the Birkhead Formation is widespread but does not constitute a major lithology. The thickness of the Formation is typicaly approximately 95 m.

Hutton Sandstone: The Early-Mid Jurassic Hutton Sandstone consists of very fine to conglomeratic quartzose sand, moderately to well consolidated with a clay matrix. Minor constituents of the sandstones include finely disseminated carbonaceous and micaceous detritals and potash feldspars. Minor siltstone and shale layers occur throughout the Hutton Sandstone, usually at the top of fining upwards sequences that represent individual episodes. In the Nappamerri Trough, shale is present at the base of the Hutton Sandstone. As with the Basal Jurassic, the depocentre of the Hutton Sandstone is in the axis of the Windorah Trough, where up to 200 m of Hutton Sandstone are present.

Cooper Basin: Triassic

Nappamerri Group: According to Powis' (1989) subdivision of the Nappamerri Group, it comprises from the base, the Early Triassic Arrabury Formation, the Middle Triassic Tinchoo Formation and the Late Triassic Cuddapan Formation. The Group consists of interbedded shales, sandstones and siltstones. The shale and siltstone is varicoloured, dolomitic and in part carbonaceous. The group was deposited in a continental fluviatile and lacustrine environment. The section is in excess of 400 m in the northern Cooper Basin. There is a considerable thinning of the Group over the Gidgealpa-Merrimelia-Innamincka trend.

Cooper Basin: Permian

Toolachee Formation: The Toolachee Formation consists of equal proportions of sandstone, shale, and coal. In general the formation comprises an upper unit of predominantly carbonaceous shale with interbedded sandstones and coals and a lower unit of predominantly sandstone. The formation reaches a maximum thickness in the Patchawarra Trough of only 100 m but exceeds 250 m in the Nappamerri and Tenappera Troughs. The formation is absent over severe structural highs, such as the Gidgealpa-Merrimelia-Innamincka anticline trend and the Nappacoongee-Murteree High. Sediments were deposited in an extensive floodplain environment.

Roseneath Shale: The Roseneath Shale is a sequence of dark grey carbonaceous siltstone and minor sandstone. It has a maximum thickness of 88 m at Toolachee East. The shale was deposited in one large lake which transgressed from the east.

Murteree Shale: The Murteree Shale comprises a uniform suite of dark carbonaceous and in part slightly micaceous shales with minor amounts of interbedded siltstones and fine-grained sandstones. The thickest section of the formation is 75 m and occurs in the Nappamerri Trough area. The Murteree Shale was deposited in thick non-marine lacustrine environment.

Patchawarra Formation: The Patchawarra Formation is the thickest formation of the Cooper Basin. The thickest Patchawarra Formation is 600 m and occurs in the Patchawarra Trough area. The formation is present over much of the Cooper Basin. It consists of a sequence of sandstones, shales, siltstones and coals which were deposited in channels, point bars overbank and backswamp environments of a meandering fluvial system.

2.8 Normal Compaction Relationships

2.8.1 General Principles

Since apparent exhumation is given by the displacement, on the depth axis, of a given porosity log/depth point from the normal porosity log/depth relation (ie. that unaffected by exhumation), *the crux of apparent determination lies in the selection of the normal porosity log/depth relation.*

The problem of determining a true normal compaction trend and the parameters involved them have been widely discussed (Marie, 1975; Magara, 1976; Bulat and Stoker, 1987; Hillis, 1991; 1995a; b). The following principles follow those of Magara (1976), Bulat and Stoker, (1987) and Hillis (1995a; b) (Figure 2.10).

The form (linear, exponential etc.) of the normal compaction relation should be dictated by the porosity/depth curve because petrophysical properties such as velocity and density decrease with burial-depth due to their dependence on porosity. Bulat and Stoker (1987) combined the standard exponential porosity/depth relation (eg. Sclater and Christie, 1980) with Wyllie *et al.*'s (1956) time average relation (equation 2.2) to obtain the relation between velocity (v) and burial-depth (d):

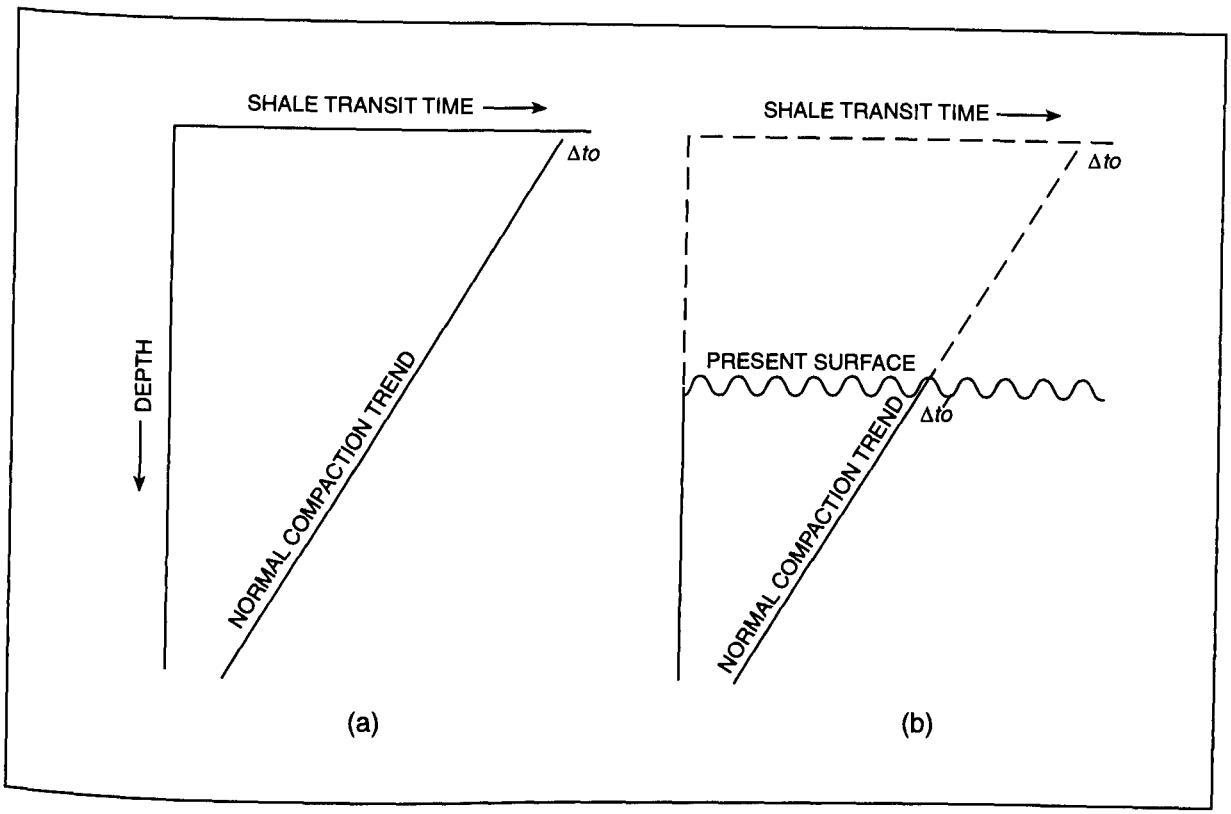

Figure 2.10a. Schematic diagrams showing the normal compaction trends of shale transit time-depth plots where there was no exhumation (A) and where there was exhumation (B). In case (B), the surface transit time value Δt_b for the case of no exhumation. If the normal compaction trend is further extrapolated to Δt_o, the original surface of the sedimentary section can be determined. The distance between the exhumation surface (the present surface in this case) and the level at which the extrapolated level value equals Δt_o is the approximate thickness of the sedimentary rocks removed by exhumation (modified after Magara, 1976).

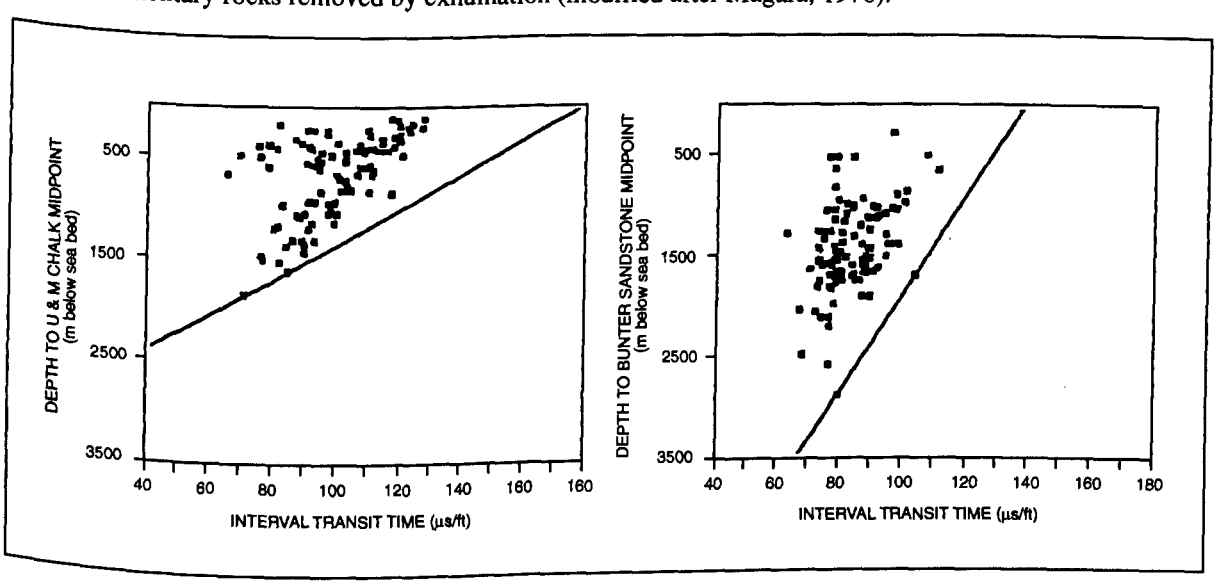

Figure 2.10b. Definition of the normal compaction relationship for two stratigraphic units in the UK Southern North Sea. For a linear decrease of Δt with depth, any two wells that can be linked by a straight line that has no points falling to its right, less compacted side, may define normal compaction (after Hillis, 1995a).

$$\frac{1}{v} = a + b\exp(\frac{-d}{c}) \ , \qquad (2.8)$$

where a, b, and c are constants (Figure 2.11). This relation is close to linear for the burial-depths under consideration, hence the normal compaction relation was taken to be linear in form (cf. Bulat and Stoker, 1987).

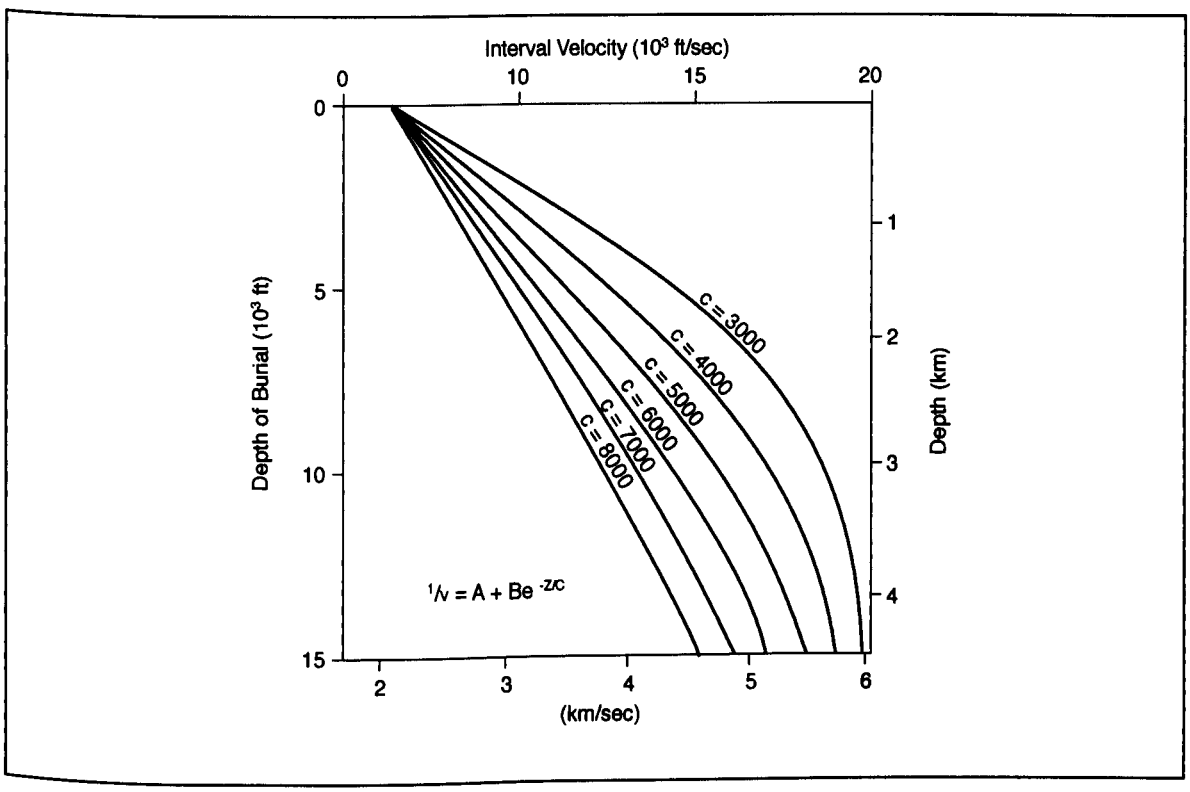

Figure 2.11. Theoretically derived plots of depth of burial against interval velocity for various values of the decay constant, c. Even with very rapid rates of compaction, the function approximates to a straight line for depths of burial less than 7000'. Normal compaction curves have been assumed to be linear for the purposes of this study (after Bulat and Stoker, 1987).

Published results for compaction curves support the linear velocity/depth function, and the assumption that linearity is valid over a large range of depths (Perrier and Quiblier, 1974; Wells, 1990; Issler, 1992; Japsen, 1993; Hillis, 1993; 1994; 1995a; b) (Figure 2.12). As shown in Section 2.4.5 Wyllie *et al.*'s (1956) equation for determing porosity from the sonic log (equation 2.2) has the same form as the relation for determing porosity from the density log (equation 2.4), hence equation 2.8 and the assumption of linearity is also considered

appropriate for the density log. The linear trend is assumed to be suitable for neutron porosity log.

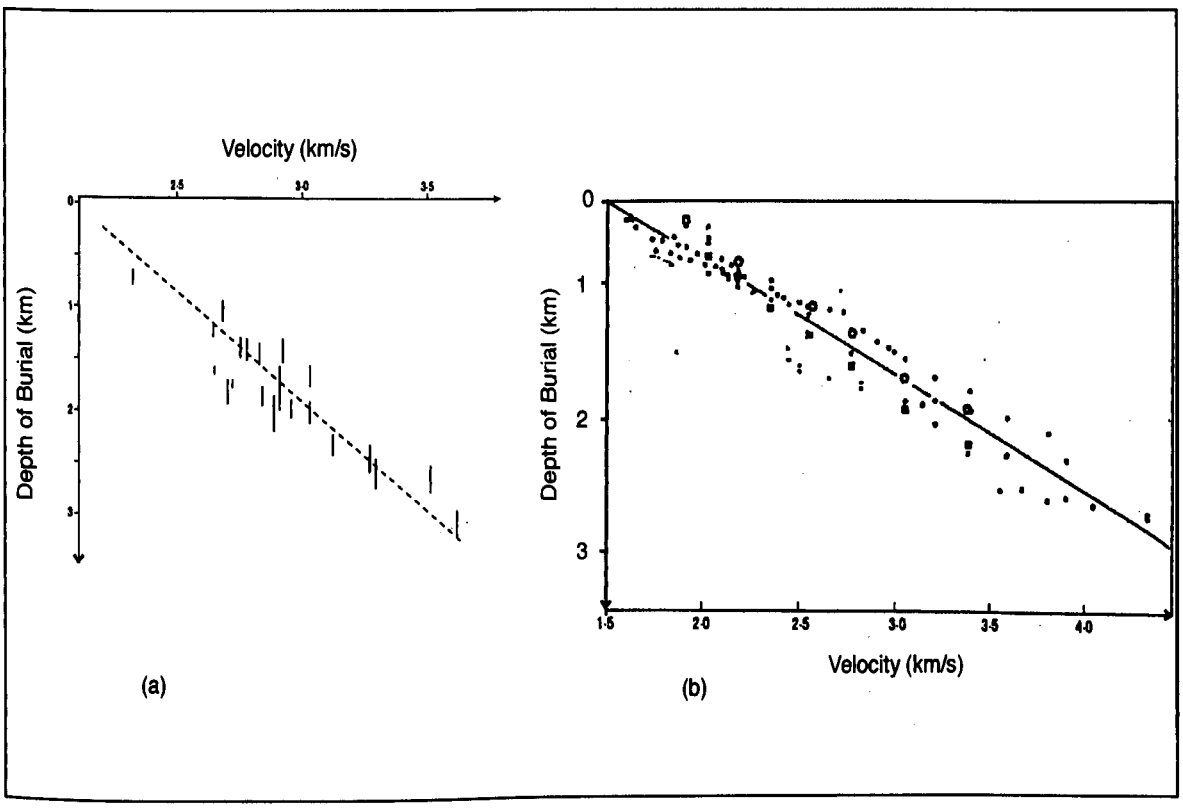

Figure 2.12. Plots of sonic velocity (km/s) versus depth of burial from (a) 30 wells in northern Denmark (modified from Japsen, 1993); and (b) five New Zealand Wells (modified from Wells, 1990). Both plots show a linear increase in velocity with increasing depth.

In an area subject to exhumation, the wells with the highest porosity (ie. highest Δt , highest Δt_{adj}, highest ϕ_N, and lowest ρ_b) for their given burial-depth should be taken to be normally compacted, provided that their relatively high porosity is not due to phenomena that may inhibit normal compaction (such as overpressure or hydrocarbon-filled porosity). For a linear decrease of Δt, Δt_{adj}, ϕ_N with depth, and linear increase of ρ_b with depth, the two wells that can be linked by a straight line that has no points falling to its less compacted side, define normal compaction. These are termed the *reference wells* (Figure 2.13). It must be assumed that the reference wells defining the normal compaction relation are at maximum burial-depth, and have not themselves been exhumed. In the event that the reference wells have been

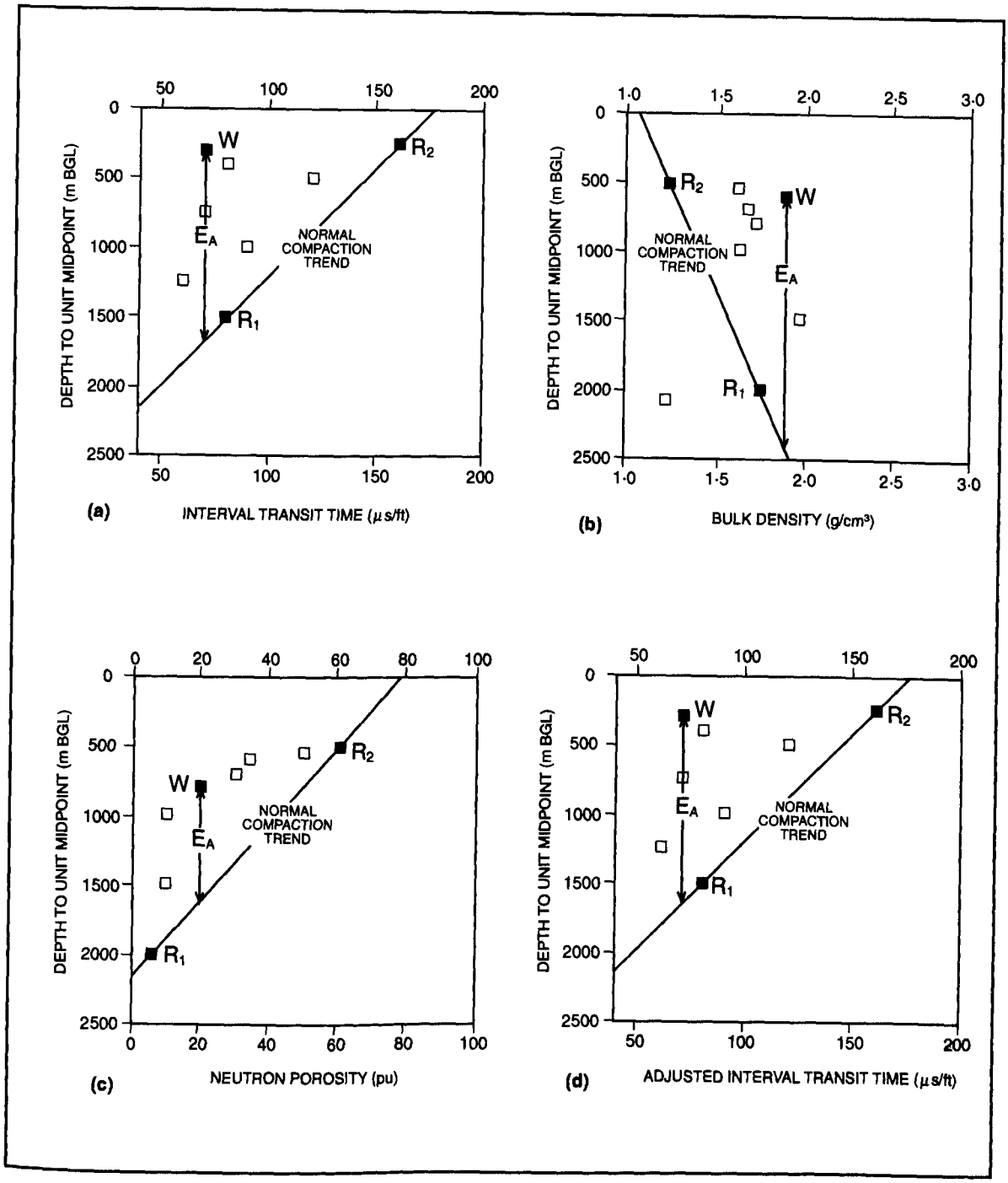

Figure 2.13. Determination of normal compaction trend in the (a), (b), (c) different porosity logs and the (d) adjusted sonic log, using the reference wells (R1, R2). For details see text, BGL: below ground level, E_A: apparent exhumation of the well under consideration (W).

exhumed from maximum burial-depth, all apparent exhumation values will be underestimated by the amount of exhumation undergone by the reference wells.

An additional constraint on the selection of the normal compaction relation/reference wells is that the surface intercept on the velocity/depth plots should have a value close to, or less than 189 μs/ft, 1.03 g/cm^3 or 100 porosity units, the approximate value for saltwater in each of the porosity logs. Similar constraint has been adopted by Magara (1976).

As many wells as possible, from as wide an area as possible, should be analysed to determine a true normal compaction relation. The greater the number of wells and the larger the study area, the more likely the reference wells are to be at maximum burial-depth. It is significant that in this study normal compaction relationships are based on the analysis of 206 wells throughout the entire Cooper and Eromanga Basins (Figure 2.14).

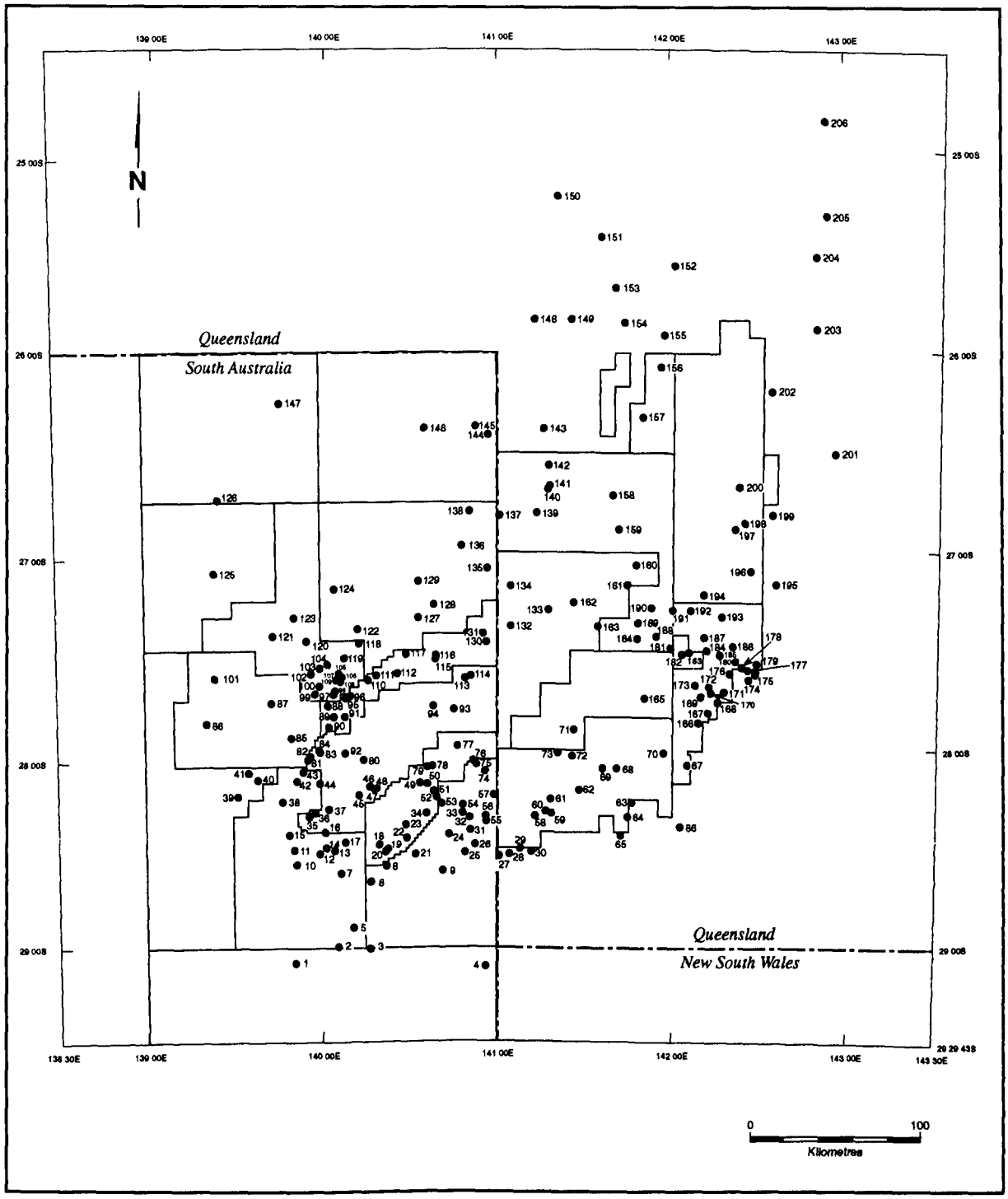

Figure 2.14. Location of wells used in compaction analysis. Exploration blocks are also shown.

Figure 2.14. Continued. List of wells used in compaction analysis as shown in Figure 2.14.

1. Weena-1
2. Tinga Tingana-1
3. Gurra-1
4. Paxton-1
5. Kumbarie-1
6. Kobari-1
7. Dunoon-1
8. Kiwarrick-1
9. Wuroopie-1
10. Padulla-1
11. Boxwood-1
12. Wancoocha-2
13. Garanjanie-2
14. Dirkala-2
15. Pando South-1
16. Thurakinna-5
17. Bungee-1
18. Alwyn-1
19. Limestone Creek-9
20. Biala-1
21. Battunga-1
22. Mckinlay-3
23. Buckinna-1
24. Keeto-2
25. Wirha-1
26. Azolla-1
27. Munkarie South-1
28. Paragilga-1
29. Gidgee-1
30. Munro-1
31. Toolachee-39
32. Toolachee-9
33. Toolachee-21
34. Childie-1
35. Daralingie-15
36. Daralingie-23
37. Cowan-3
38. Pintari-1
39. Lycium-1
40. Taloola-1
41. Sturt-6
42. Spencer-4
43. Muteroo-3
44. Arrakis-1
45. Moomba South-1
46. Moomba-57
47. Big Lake-26
48. Big Lake-35
49. Mudera-3
50. Marabooka-2
51. Strzelecki -27
52. Strzelecki-10
53. Baratta-1
54. Witchetty-1
55. Amyema-1
56. Marsilea-1
57. Kerna-5
58. Wills-1
59. Hydra-1
60. Mooliampah-1
61. Rheims-1
62. Belah-1
63. Wompi-1
64. Rho East-1
65. Naryilco-1
66. Atoll-1
67. Watson-1
68. Patroclus-1
69. Hume-1
70. Tennaperra South-1
71. Warnie East-1
72. Orientos-2
73. Lambda-1
74. Burke-2
75. Dullingari-3
76. Dullingari North-1
77. Three Queens-1
78. Della-10
79. Della-7
80. Moomba North-1
81. Kurunda-1
82. Mawson-1
83. Gidgealpa-42
84. Gidgealpa-20
85. Jack Lake-2
86. Lhotsky-1
87. Nulla-1
88. Cooba-1
89. Meranji-1
90. Snake Hole-1
91. Swan Lake-1
92. Moomba-27
93. Mcleod-1
94. Burley-2
95. Merrimelia-25
96. Merrimelia-7
97. Gooranie-2
98. Gooranie-1
99. Andree-1
100. Spectre-1
101. Kalladeina-1
102. Fly Lake-1
103. Fly Lake-4
104. Brolga-2
105. Tirrawarra North-1
106. Tirrawarra-26
107. Tirrawarra West-1
108. Tirrawarra-15
109. Tirrawarra-13
110. Deparanie-1
111. Minkie-1
112. Wantana-2
113. Kirby-1
114. Kirby-2
115. Pondrinie-5
116. Packsaddle-4
117. Bookabourdie-1
118. Lake Mcmillan-1
119. Moorari-4
120. Darter-1
121. Charo-1
122. Moolion-1
123. Yanta-1
124. Daer-1
125. Koonchera-1
126. Pandieburra-1
127. Wimma-1
128. Beanbush-1
129. Deramookoo-1
130. Innamincka-4
131. Turban-1
132. Innamincka-3
133. Pepita-2
134. Arrabury-1
135. Paning-1
136. Kenny-1
137. Yanbee-1
138. James-1
139. Doonmulla-1
140. Cook-1
141. Cook North-1
142. Wicho-1
143. Mackillop-1
144. Araburg-1
145. Potiron-1
146. Haddon Downs-1
147. Putamurdie-1
148. Curalle-1
149. Meeba-1
150. Copai-1
151. Morney-1
152. Ullenbury-1
153. Cuddapan-1
154. Denley-1
155. Tanbar North-1
156. Tanbar-1
157. Marengo-1
158. Tinchoo-1
159. Barrolka-1
160. Durham Downs-1
161. Keilor-1
162. Macadama-1
163. Challum-1
164. Yanda-2
165. Baryulah-1
166. Johba-1
167. Echuburra North-1
168. Bardoc-1
169. Wallawanny-1
170. Jarrar-1
171. Cooroo-1
172. Pallano-1
173. Kutyo-1
174. Jackson South-1
175. Richie-1
176. Karwin-1
177. Jackson-1
178. Graham-1
179. Bycoe-1
180. Tinpilla-1
181. Wackett-3
182. Naccowlah West-1
183. Naccowlah South-1
184. Naccowlah East-1
185. Bogala-1
186. Thurra-1
187. Carney-1
188. Munkah-2
189. Ballera-1
190. Karmona-2
191. Okotoko-1
192. Wippo-2
193. Yumba-1
194. Tartulla-1
195. Hooley-1
196. Kercummurra-1
197. Wareena-1
198. Navalla-1
199. Boldrewood-1
200. Toby-1
201. Coonavalla-1
202. Alkina-1
203. Russel-1
204. Ingella-1
205. Hammond-1
206. Steward-1

2.8.2 Normal Compaction Relations in Specific Units

The mean sonic interval transit time (Δt) for each unit was determined from the sonic log data and plotted against the depth of the midpoint of the unit (Figure 2.15). The above criteria define the normal compaction relationships and the reference wells for each of the units. The reference wells and the normal compaction relationships for each unit are summarised in Table 2.1.

The mean adjusted sonic interval transit time (Δt_{adj})for each unit was determined from the adjusted sonic log data and plotted against the depth of the midpoint of the unit (Figure 2.16). The above criteria again define the normal compaction relationships and the reference wells for each of the units. The reference wells and the normal compaction relationships for each unit are summarised in Table 2.2.

The mean bulk density (ρ_b) of the units examined was determined from the density log data and plotted against the depth of the midpoint of the unit. For all the units analysed, the criteria in Section 2.8.1 establish the normal compaction relation and the reference wells (Figure 2.17). However, the density log was run in less wells than the sonic log, and even when run, often did not cover the Winton, Mackunda, Allaru Mudstone-Oodnadatta and the Bulldog Shale-Wallumbilla Formations. Consequently, the reference wells for the density log are not the same as those for the sonic log (eg. the density log was not run in Tinga Tingana-1 well which was a reference well for the sonic log data in severed units). The reference wells and the normal compaction relationships for each unit are given in Table 2.3.

The mean neutron porosity (ϕ_N) of the units examined was determined from the neutron porosity log data and plotted against the depth of the midpoint of the unit. For all the units analysed, the criteria in Section 2.8.1 define the normal compaction relation and the reference wells (Figure 2.18). However, the number of wells in which the neutron log was run is extremely low for determining normal compaction relationships for the Winton, Mackunda, Allaru Mudstone-Oodnadatta and the Bulldog Shale-Wallumbilla Formations (Figure 2.18).

Indeed, in these units there are probably too few wells analysed to be confident of the normal compaction relation. Some of the reference wells in the underlying units are different from those of the sonic and bulk density log, for the same unit. The reference wells and the normal compaction relationships for each unit are given in Table 2.4.

As discussed in Section 2.7.1, the presence of coals in the Toolachee and Patchawarra Formations has a strong influence on the average compaction state of these units. Given the amount of coals in the formations is laterally variable, this would lead to anomalous exhumation values. Hence coal-free sections were analysed in these units. Figure 2.19 shows the porosity log/depth and velocity/depth plots for the entire Toolachee and Patchawarra Formations (including the coals). Figure 2.19 confirms that reasonable normal compaction relations cannot be determined for the entire Toolachee and Patchawarra Formations.

The location of the reference wells used to determine the normal compaction relationships is shown on Figure 2.20. The apparent exhumation values for the analysed units (along with the relevant depth and Δt, Δt_{adj}, ρ_b, and ϕ_N data) are listed in Appendix A.

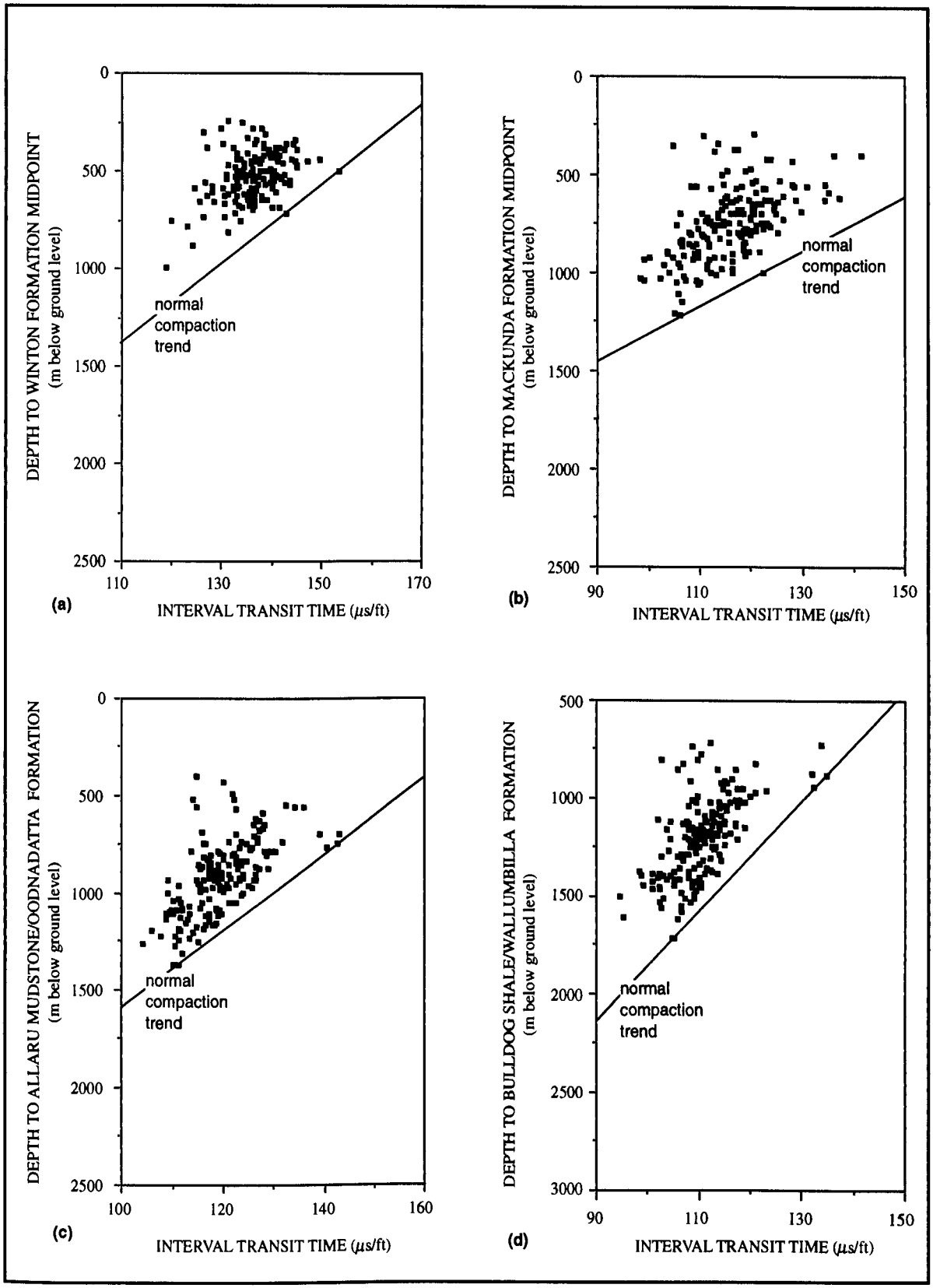

Figure 2.15a. Mean sonic Δt/depth to unit midpoint plots for units analysed in the Cooper-Eromanga Basins (a) the Winton Formation, (b) the Mackunda Formation, (c) the Allaru Mudstone/Oodnadatta Formation, and (d) the Bulldog Shale/Wallumbilla Formation. The normal compaction relationship for each unit (ie. that unaffected by exhumation, determined as outlined in the text) is also shown.

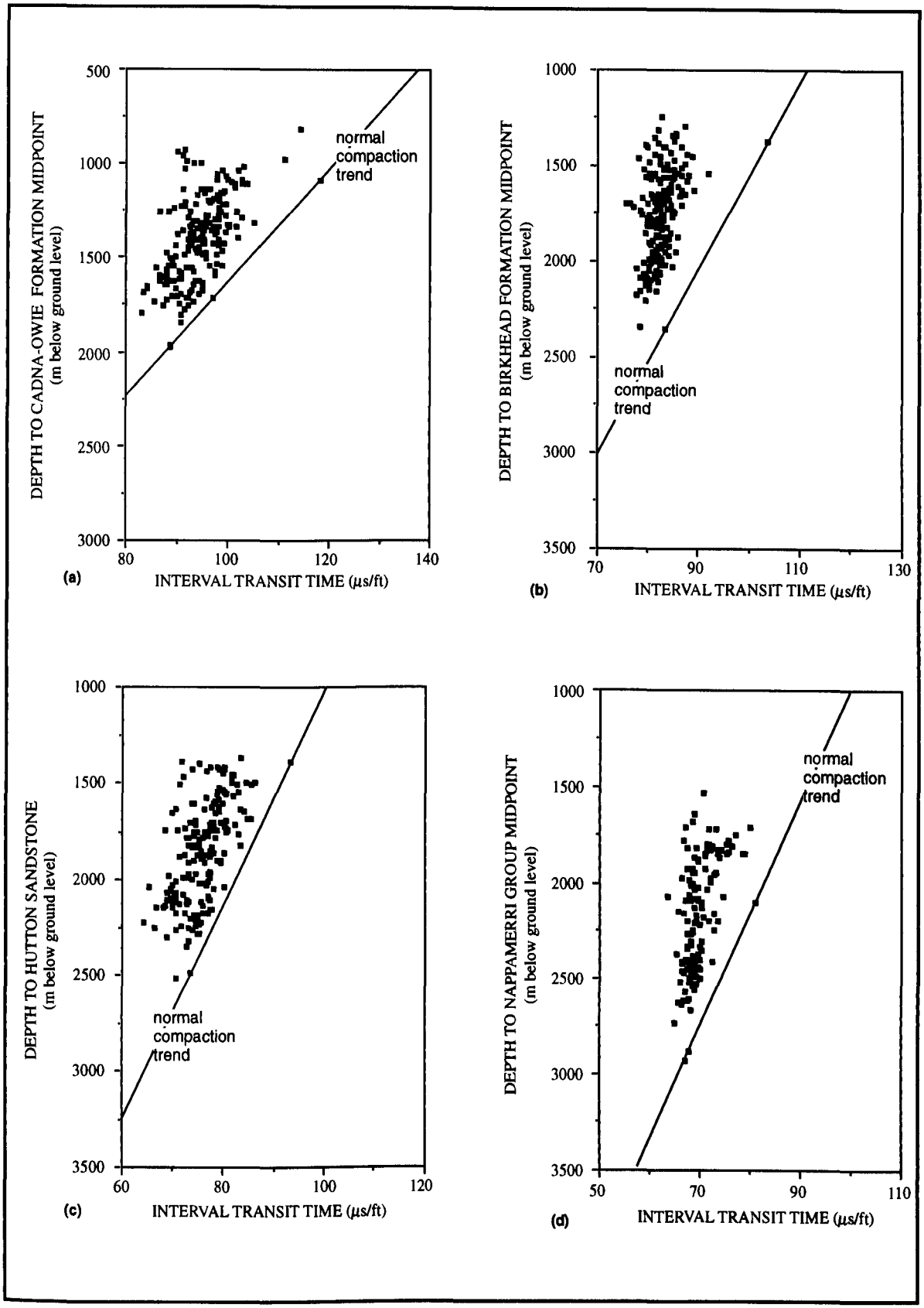

Figure 2.15b. Mean sonic Δt/depth to unit midpoint plots for units analysed in the Cooper-Eromanga Basins (a) the Cadna-owie Formation, (b) the Birkhead Formation, (c) the Hutton Sandstone, and (d) the Nappamerri Group. The normal compaction relationship for each unit (ie. that unaffected by exhumation, determined as outlined in the text) is also shown.

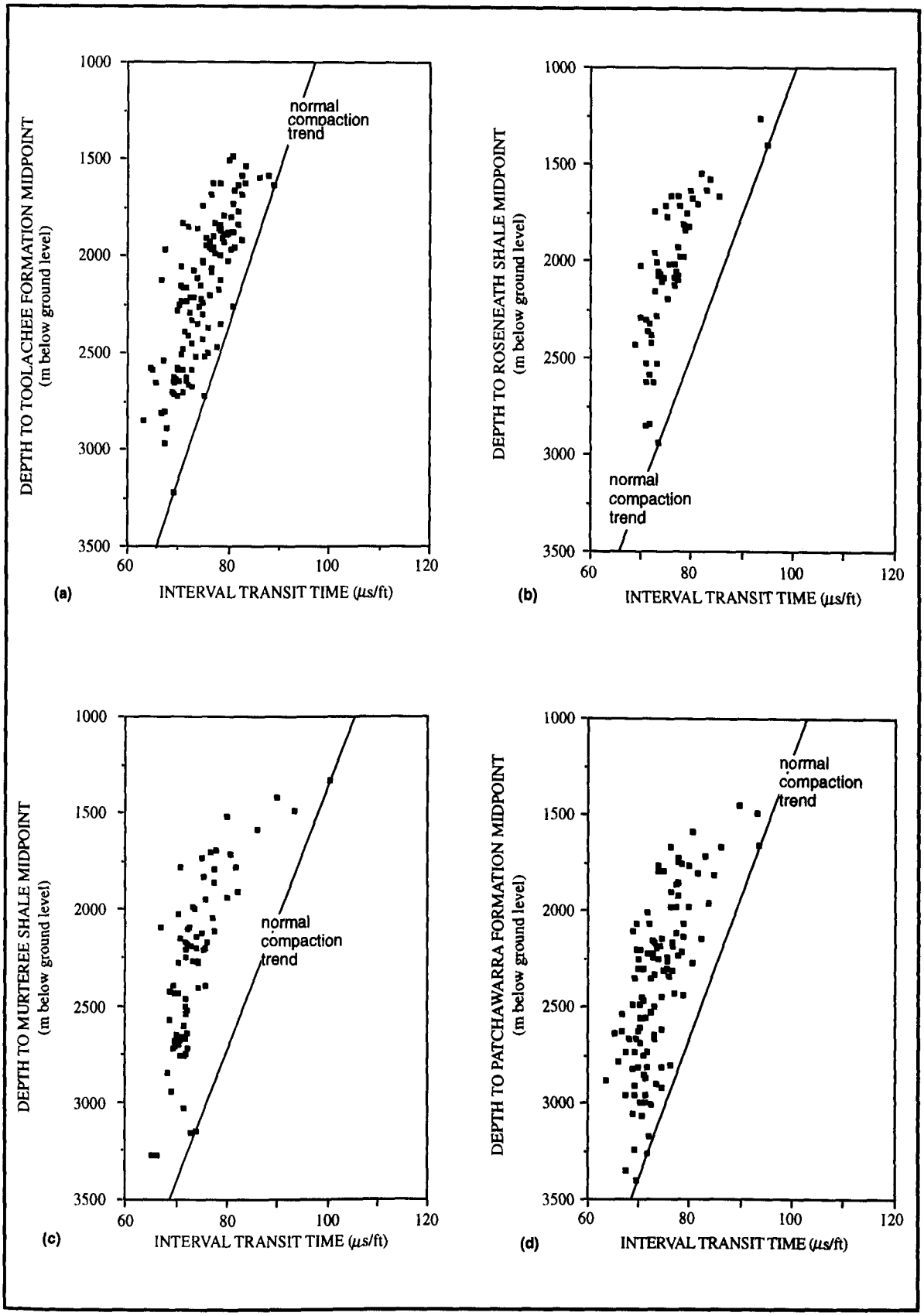

Figure 2.15c. Mean sonic Δt/depth to unit midpoint plots for units analysed in the Cooper-Eromanga Basins (a) the Toolachee Formation, (b) the Roseneath Shale, (c) the Murteree Shale, and (d) the Patchawarra Formation. The normal compaction relationship for each unit (ie. that unaffected by exhumation, determined as outlined in the text) is also shown.

Table 2.1. Sonic Log Data Defining Normal Compaction Relationships

Stratigraphic Unit	Normally Compacted Wells	Mean Δt (μs/ft)	Midpoint Depth (m bgl)*	Equation of Normal Compaction Relationship**
Eromanga Basin				
Winton Formation	Thurakinna-5 Tinga Tingana-1	142.713 153.622	712.759 495.629	Δt = 178.493 - 0.0502 dbgl
Mackunda Formation	Beanbush-1 Fly Lake-1	106.091 122.231	1220.208 1004.255	Δt = 197.248 - 0.0747 dbgl
Allaru Mudstone- Oodnadatta Formation	Tinga Tingana-1 Wimma-1	142.633 111.234	744.769 1370.657	Δt = 179.945 - 0.0501 dbgl
Bulldog Shale- Wallumbilla Formation	Beanbush-1 Weena-1	105.045 134.791	1717.333 884.693	Δt = 166.374 - 0.0357 dbgl
Cadna-owie Formation	Beanbush-1 Tinga Tingana-1	88.751 118.215	1971.093 1086.159	Δt = 154.275 - 0.0332 dbgl
Birkhead Formation	Tinga Tingana-1 Wimma-1	103.791 83.372	1374.944 2357.447	Δt = 132.252 - 0.0207 dbgl
Hutton Sandstone	Tinga Tingana-1 Wimma-1	93.463 73.606	1388.054 2492.777	Δt = 118.226 - 0.0179 dbgl
Cooper Basin				
Nappamerri Group	Steward-1 Wimma-1	81.133 67.918	2099.800 2889.167	Δt = 116.167 - 0.0167 dbgl
Toolachee Formation	Kirby-1 Wuroopie-1	75.262 89.015	2718.297 1634.312	Δt = 109.512 - 0.0126 dbgl
Roseneath Shale	Mcleod-1 Tinga Tingana-1	73.685 95.201	2935.685 1399.339	Δt = 114.791 - 0.0140 dbgl
Murteree Shale	Burley-2 Gurra-1	73.861 100.380	3153.549 1328.014	Δt = 119.643 - 0.0145 dbgl
Patchawarra Formation	Burley-2 Tinga Tingana-1	71.650 93.450	3260.035 1657.724	Δt = 115.995 - 0.0136 dbgl

*m bgl = meters below ground level.

**Δt = interval transit time (μs/ft); dbgl = depth below ground level (in metres).

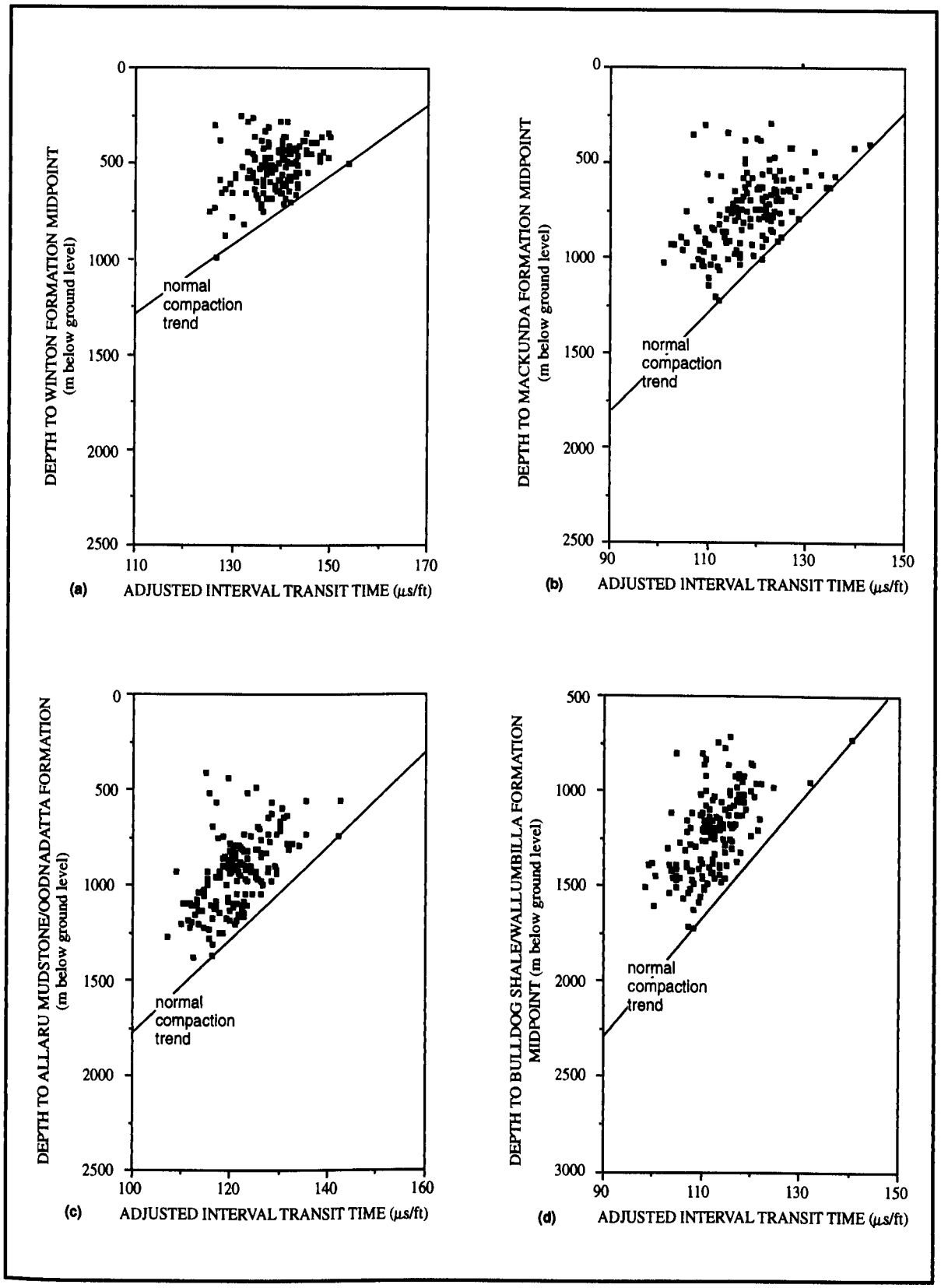

Figure 2.16a. Mean adjusted sonic Δt_{adj}/depth to unit midpoint plots for units analysed in the Cooper-Eromanga Basins (a) the Winton Formation, (b) the Mackunda Formation, (c) the Allaru Mudstone/Oodnadatta Formation, and (d) the Bulldog Shale/Wallumbilla Formation. The normal compaction relationship for each unit (ie. that unaffected by exhumation, determined as outlined in the text) is also shown.

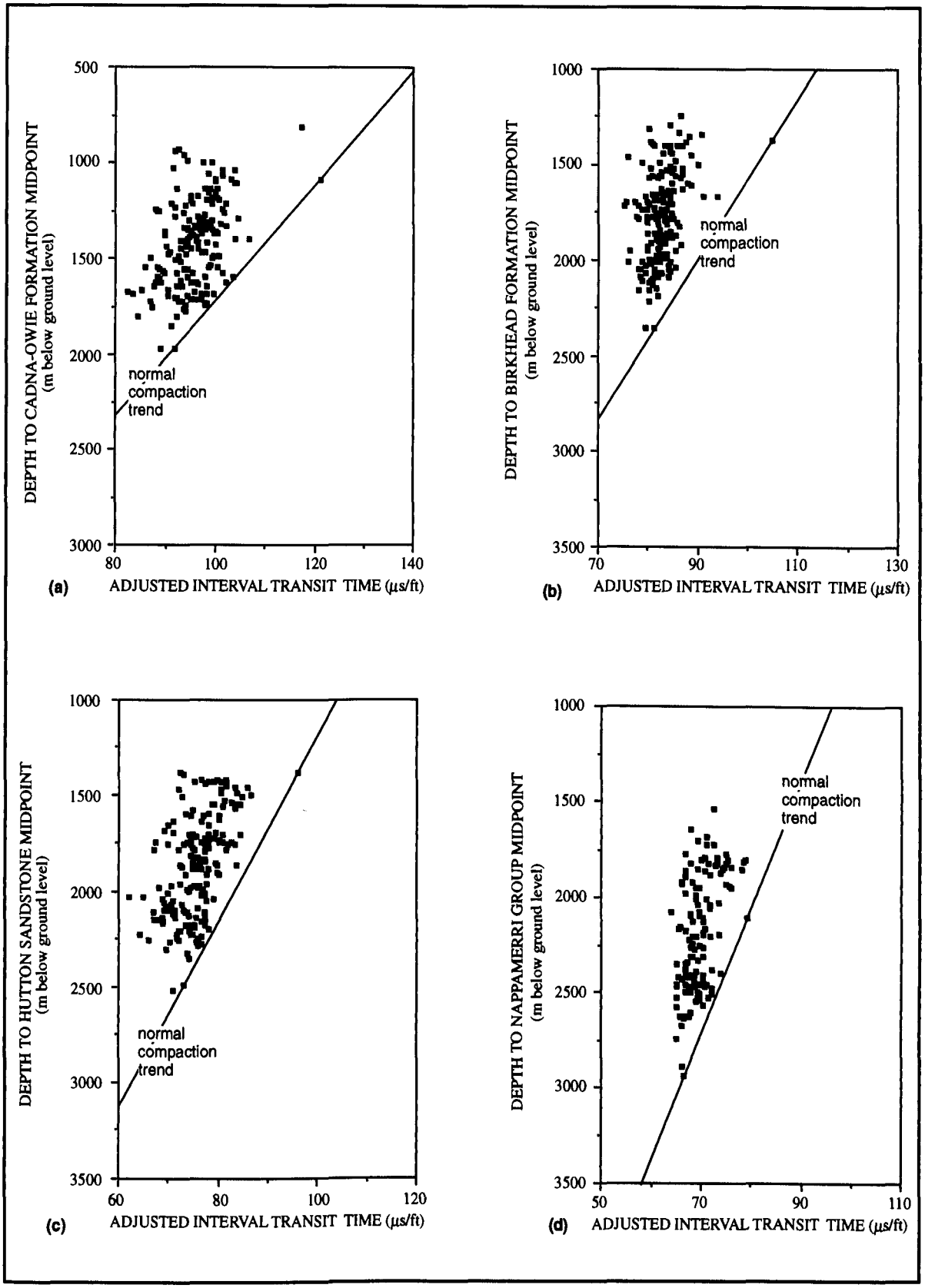

Figure 2.16b. Mean adjusted sonic Δt_{adj}/depth to unit midpoint plots for units analysed in the Cooper-Eromanga Basins (a) the Cadna-owie Formation, (b) the Birkhead Formation, (c) the Hutton Sandstone, and (d) the Nappamerri Group. The normal compaction relationship for each unit (ie. that unaffected by exhumation, determined as outlined in the text) is also shown.

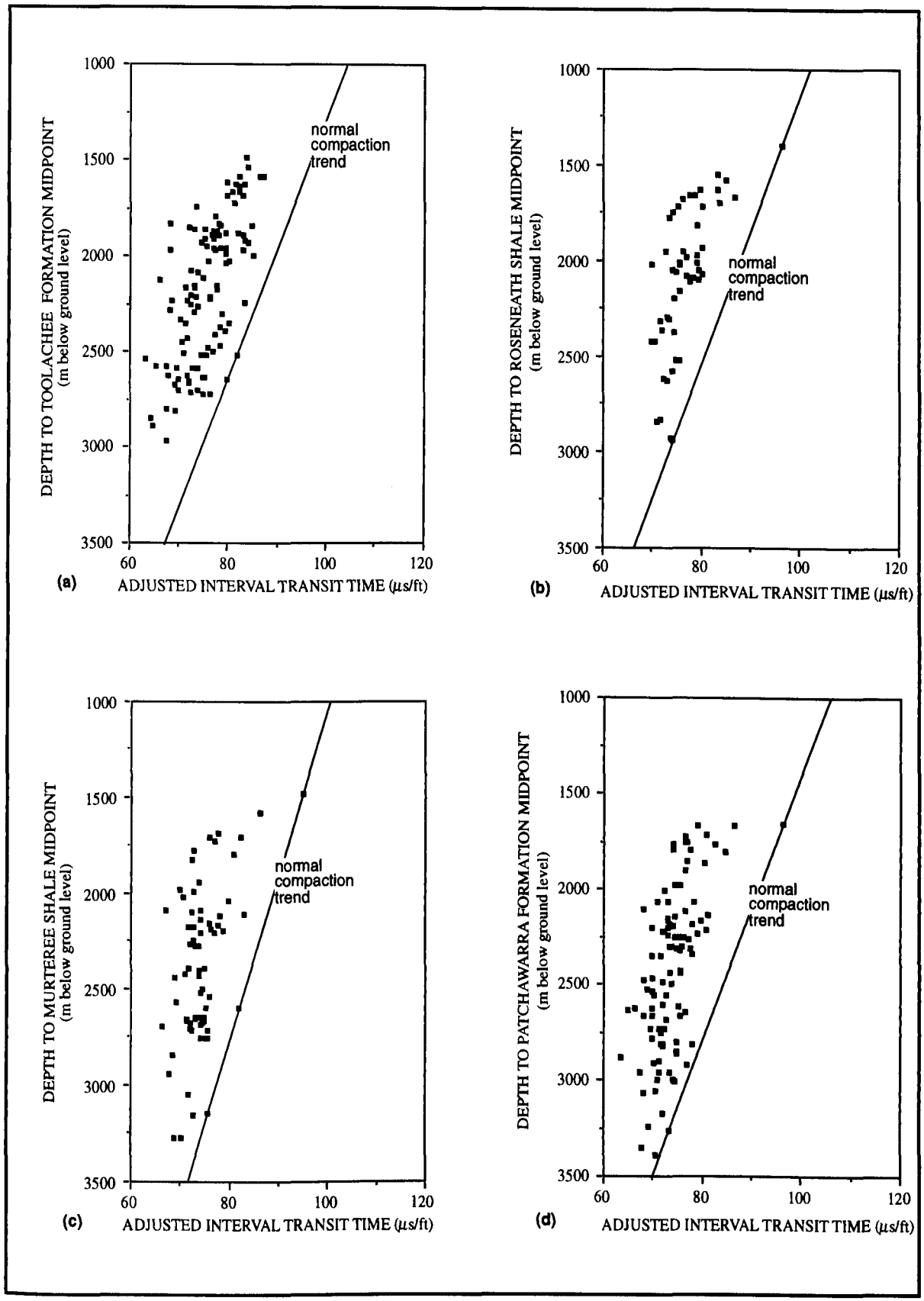

Figure 2.16c. Mean adjusted sonic Δt_{adj}/depth to unit midpoint plots for units analysed in the Cooper-Eromanga Basins (a) the Toolachee Formation, (b) the Roseneath Shale, (c) the Murteree Shale, and (d) the Patchawarra Formation. The normal compaction relationship for each unit (ie. that unaffected by exhumation, determined as outlined in the text) is also shown.

Table 2.2. Adjusted Sonic Log Data Defining Normal Compaction Relationships

Stratigraphic Unit	Normally Compacted Wells	Mean Δt_{adj} (μs/ft)	Midpoint Depth (m bgl)*	Equation of Normal Compaction Relationship**
Eromanga Basin				
Winton Formation	Beanbush-1 Tinga Tingana-1	126.697 153.621	990.463 495.629	Δt_{adj} = 180.578 - 0.0544 dbgl
Mackunda Formation	Beanbush-1 Fly Lake-1	112.200 121.009	1220.208 1004.255	Δt_{adj} = 161.862 - 0.0407 dbgl
Allaru Mudstone- Oodnadatta Formation	Tinga Tingana-1 Wimma-1	142.000 116.260	744.769 1370.657	Δt_{adj} = 172.594 - 0.0411 dbgl
Bulldog Shale- Wallumbilla Formation	Beanbush-1 Paxton-1	108.197 140.296	1717.333 726.324	Δt_{adj} = 163.666 - 0.0323 dbgl
Cadna-owie Formation	Beanbush-1 Tinga Tingana-1	91.864 121.095	1971.093 1086.159	Δt_{adj} = 156.910 - 0.0330 dbgl
Birkhead Formation	Tinga Tingana-1 Wimma-1	104.984 81.372	1374.944 2357.447	Δt_{adj} = 137.950 - 0.0240 dbgl
Hutton Sandstone	Tinga Tingana-1 Wimma-1	95.854 73.213	1388.054 2492.777	Δt_{adj} = 124.065 - 0.0204 dbgl
Cooper Basin				
Nappamerri Group	Steward-1 Beanbush-1	79.323 66.458	2099.800 2936.233	Δt_{adj} = 111.382 - 0.0153 dbgl
Toolachee Formation	Darter-1 Macadama-1	81.427 79.821	2519.390 2644.732	Δt_{adj} = 113.673 - 0.0128 dbgl
Roseneath Shale	Burley-2 Tinga Tingana-1	74.211 96.467	2941.930 1399.339	Δt_{adj} = 116.574 - 0.0144 dbgl
Murteree Shale	Burley-2 Tinga Tingana-1	76.255 95.361	3153.549 1480.874	Δt_{adj} = 112.205 - 0.0114 dbgl
Patchawarra Formation	Burley-2 Tinga Tingana-1	73.162 96.165	3260.035 1657.724	Δt_{adj} = 119.780 - 0.0143 dbgl

*m bgl = meters below ground level.

**Δt_{adj} = adjusted interval transit time (μs/ft); dbgl = depth below ground level (in metres).

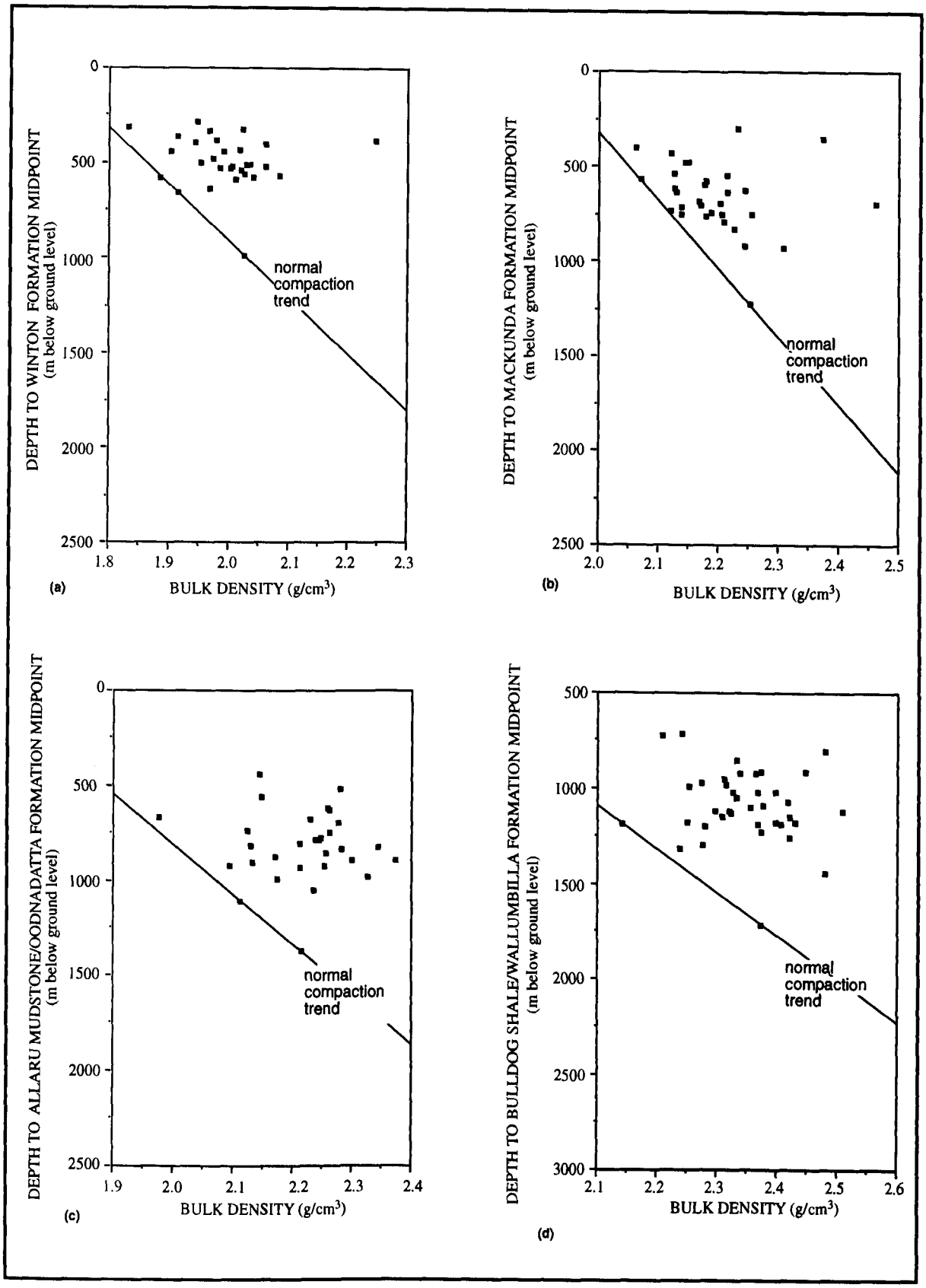

Figure 2.17a. Mean bulk density ρ_b/depth to unit midpoint plots for units analysed in the Cooper-Eromanga Basins (a) the Winton Formation, (b) the Mackunda Formation, (c) the Allaru Mudstone/Oodnadatta Formation, and (d) the Bulldog Shale/Wallumbilla Formation. The normal compaction relationship for each unit (ie. that unaffected by exhumation, determined as outlined in the text) is also shown.

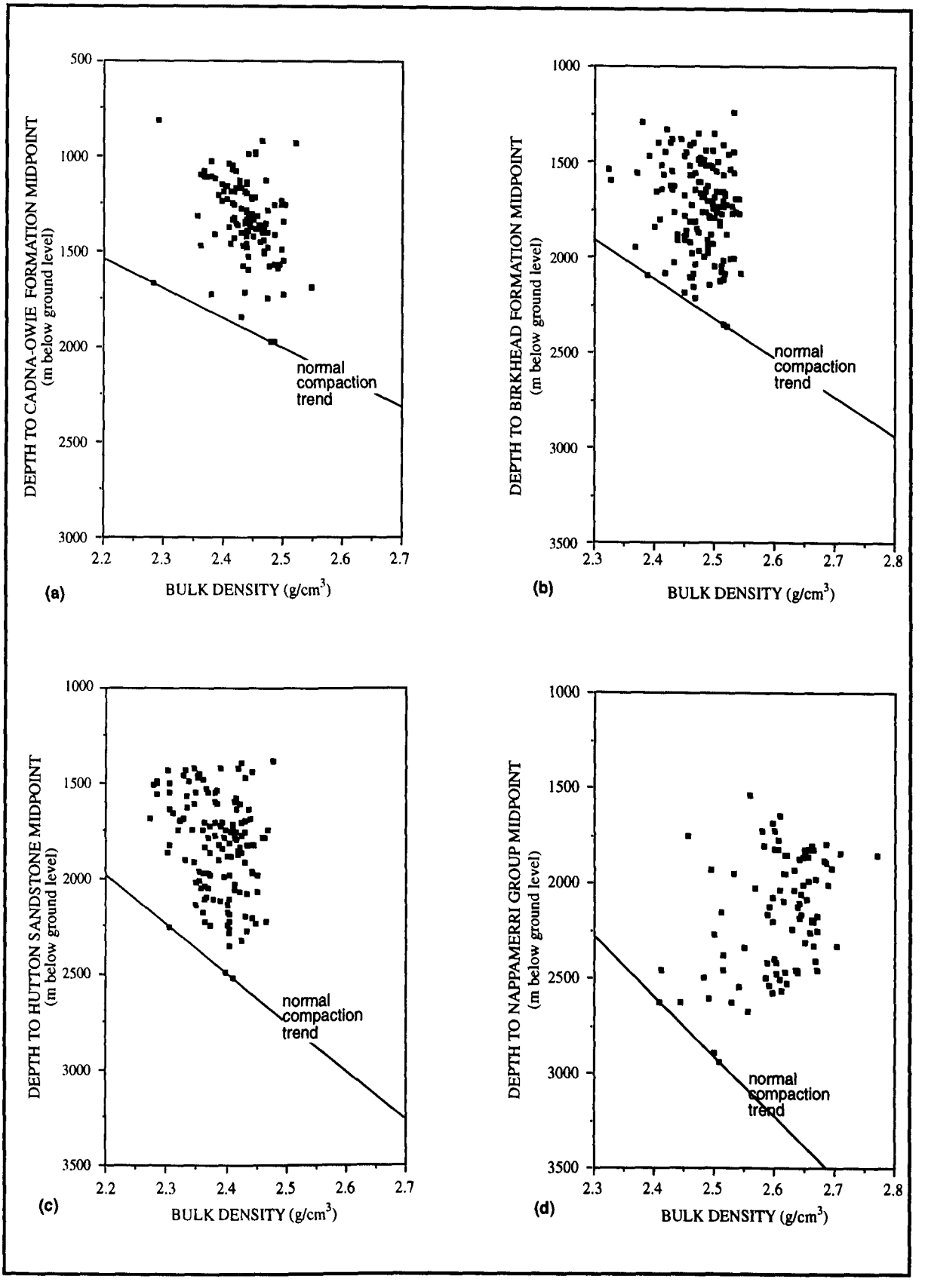

Figure 2.17b. Mean bulk density ρ_b/depth to unit midpoint plots for units analysed in the Cooper-Eromanga Basins (a) the Cadna-owie Formation, (b) the Birkhead Formation, (c) the Hutton Sandstone, and (d) the Nappamerri Group. The normal compaction relationship for each unit (ie. that unaffected by exhumation, determined as outlined in the text) is also shown.

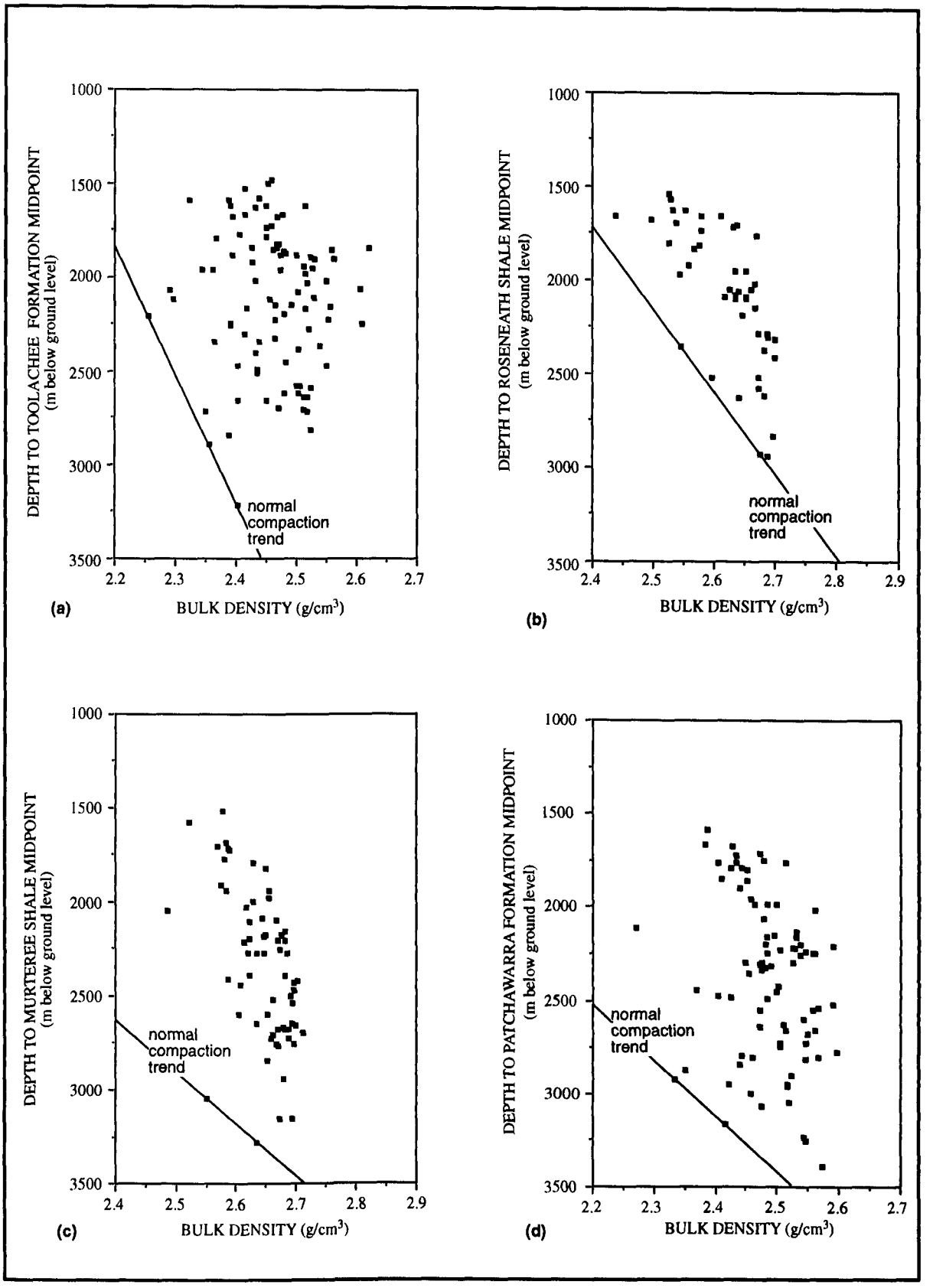

Figure 2.17c. Mean bulk density ρ_b/depth to unit midpoint plots for units analysed in the Cooper-Eromanga Basins (a) the Toolachee Formation, (b) the Roseneath Shale, (c) the Murteree Shale, and (d) the Patchawarra Formation. The normal compaction relationship for each unit (ie. that unaffected by exhumation, determined as outlined in the text) is also shown.

Table 2.3. Density Log Data Defining Normal Compaction Relationships

Stratigraphic Unit	Normally Compacted Wells	Mean ρ_b (g/cm³)	Midpoint Depth (m bgl)*	Equation of Normal Compaction Relationship**
Eromanga Basin				
Winton Formation	Beanbush-1	2.025	990.463	$\rho_b = 1.687 + 341.6 \times 10^{-6}$ dbgl
	Burley-2	1.884	578.025	
Mackunda Formation	Beanbush-1	2.253	1220.208	$\rho_b = 1.916 + 276.4 \times 10^{-6}$ dbgl
	Dunnon-1	2.072	565.276	
Allaru Mudstone-Oodnadatta Formation	Beanbush-1	2.216	1376.418	$\rho_b = 1.690 + 382.3 \times 10^{-6}$ dbgl
	Burley-2	2.113	1106.730	
Bulldog Shale-Wallumbilla Formation	Beanbush-1	2.372	1717.333	$\rho_b = 1.609 + 444.4 \times 10^{-6}$ dbgl
	Hume-1	2.140	1194.054	
Cadna-owie Formation	Beanbush-1	2.479	1971.093	$\rho_b = 1.193 + 652.3 \times 10^{-6}$ dbgl
	Paning-1	2.280	1666.738	
Birkhead Formation	Beanbush-1	2.512	2348.393	$\rho_b = 1.371 + 486.0 \times 10^{-6}$ dbgl
	Kenny-1	2.388	2092.455	
Hutton Sandstone	Beanbush-1	2.409	2522.923	$\rho_b = 1.428 + 388.6 \times 10^{-6}$ dbgl
	Russel-1	2.305	2256.136	
Cooper Basin				
Nappamerri Group	Beanbush-1	2.508	2936.233	$\rho_b = 1.580 + 316.3 \times 10^{-6}$ dbgl
	Russel-1	2.408	2619.461	
Toolachee Formation	Kirby-1	2.349	2718.297	$\rho_b = 1.564 + 288.9 \times 10^{-6}$ dbgl
	Russel-1	2.388	2851.411	
Roseneath Shale	Baryulah-1	2.548	2359.507	$\rho_b = 2.024 + 221.9 \times 10^{-6}$ dbgl
	Mcleod-1	2.676	2935.685	
Murteree Shale	Beanbush-1	2.634	3280.198	$\rho_b = 1.470 + 354.9 \times 10^{-6}$ dbgl
	Kirby-1	2.552	3049.429	
Patchawarra Formation	Kirby-1	2.416	3174.279	$\rho_b = 1.350 + 335.6 \times 10^{-6}$ dbgl
	Moolion-1	2.331	2923.000	

*m bgl = meters below ground level.

**ρ_b = bulk density (g/cm³); dbgl = depth below ground level (in metres).

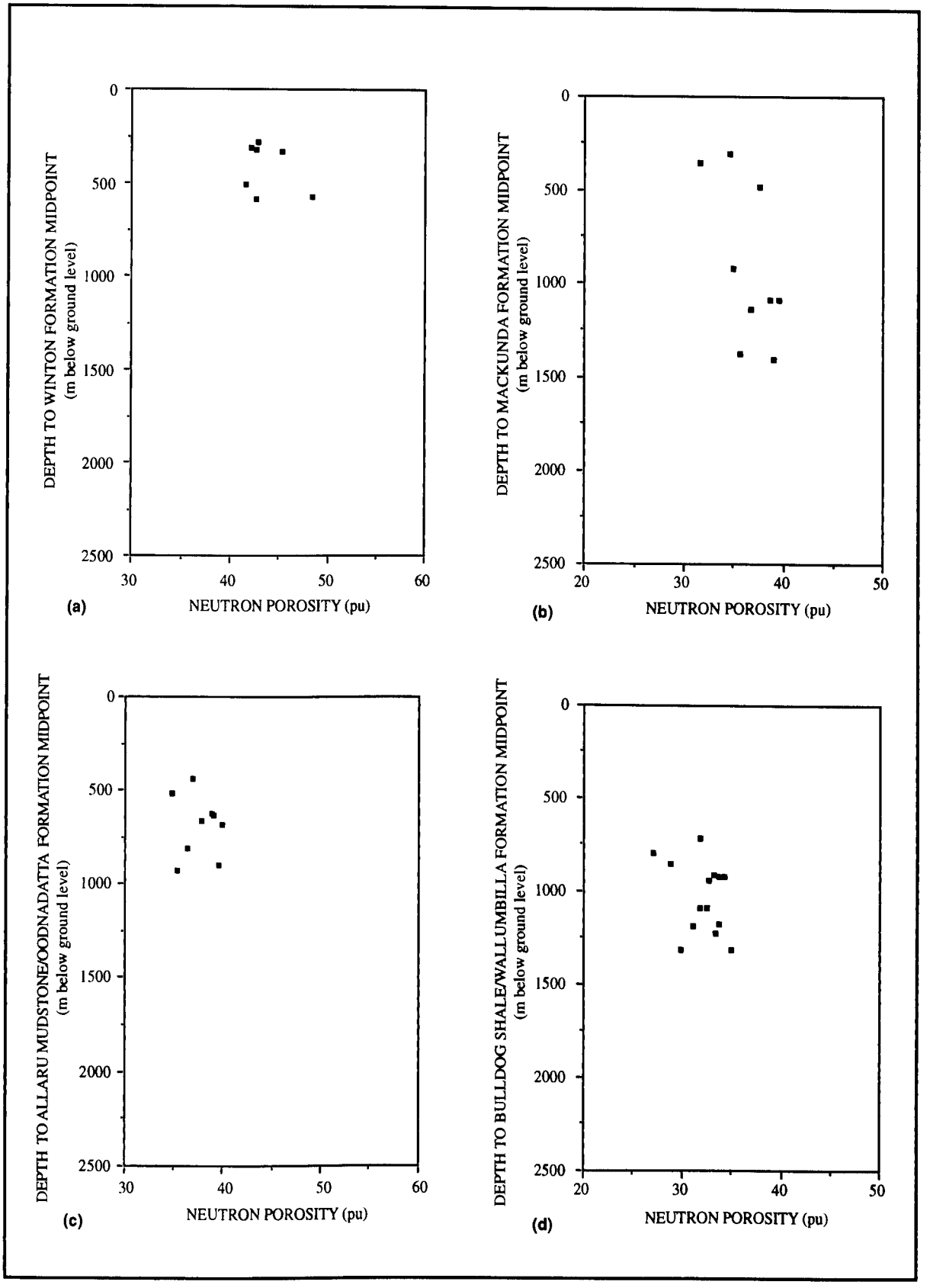

Figure 2.18a. Mean neutron porosity Φ_N/depth to unit midpoint plots for units analysed in the Cooper-Eromanga Basins (a) the Winton Formation, (b) the Mackunda Formation, (c) the Allaru Mudstone/ Oodnadatta Formation, and (d) the Bulldog Shale/Wallumbilla Formation. The normal compaction relationship for these units cannot be determined due to the low number of wells the neutron porosity log was run.

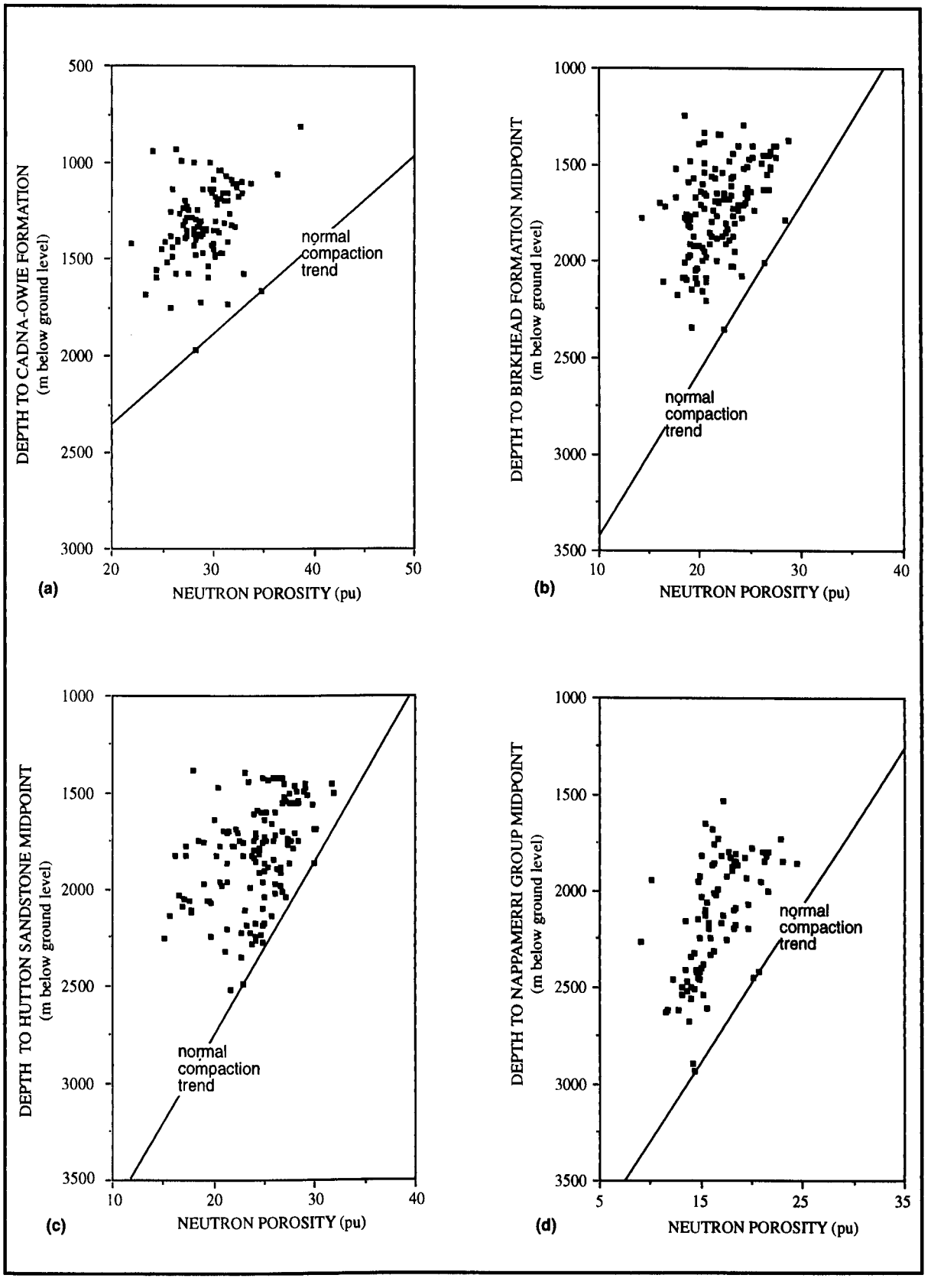

Figure 2.18b. Mean neutron porosity Φ_N/depth to unit midpoint plots for units analysed in the Cooper-Eromanga Basins (a) the Cadna-owie Formation, (b) the Birkhead Formation, (c) the Hutton Sandstone, and (d) the Nappamerri Group. The normal compaction relationship for each unit (ie. that unaffected by exhumation, determined as outlined in the text) is also shown.

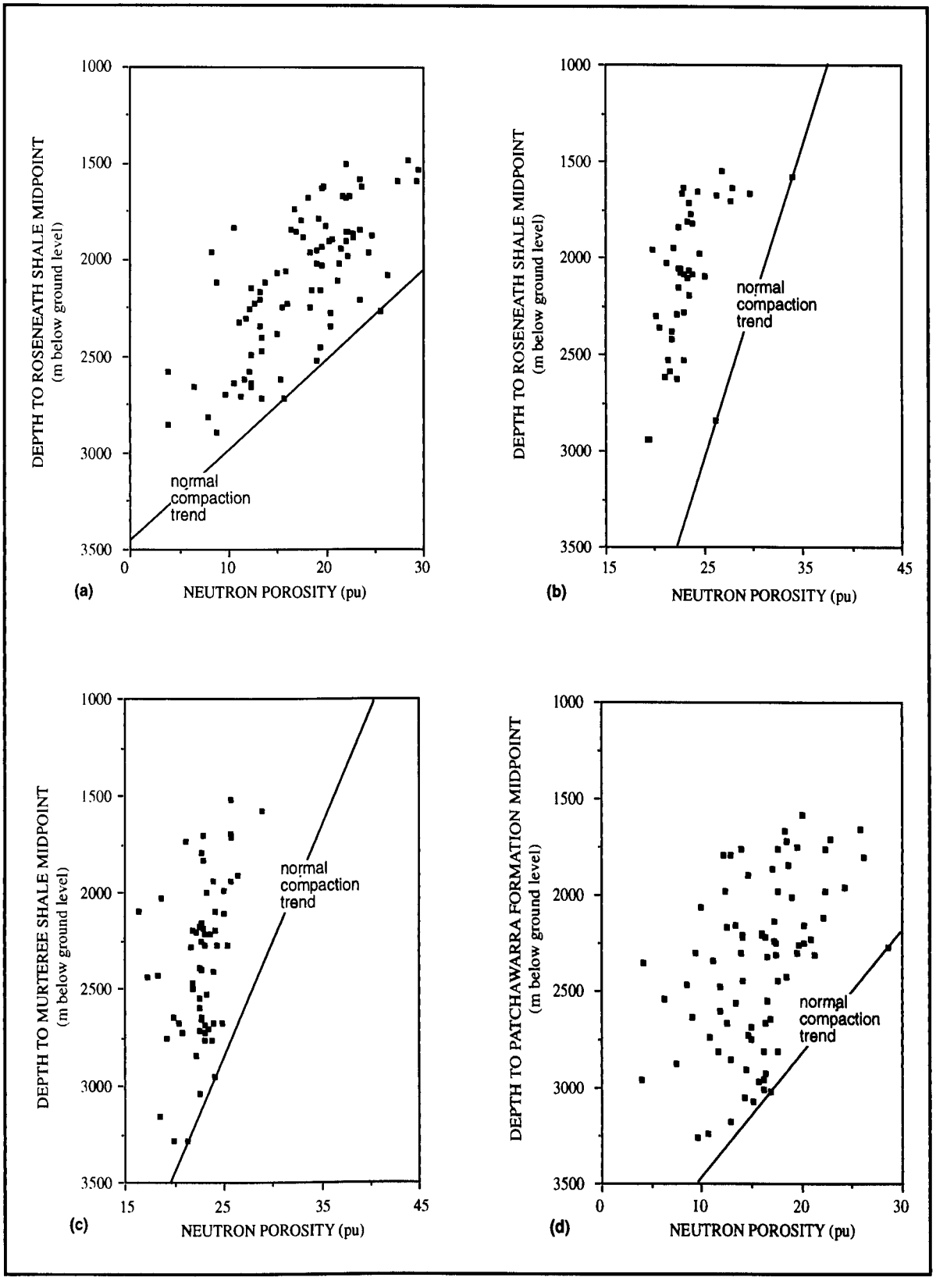

Figure 2.18c. Mean neutron porosity Φ_N/depth to unit midpoint plots for units analysed in the Cooper-Eromanga Basins (a) the Toolachee Formation, (b) the Roseneath Shale, (c) the Murteree Shale, and (d) the Patchawarra Formation. The normal compaction relationship for each unit (ie. that unaffected by exhumation, determined as outlined in the text) is also shown.

Table 2.4. Neutron Porosity Log Data Defining Normal Compaction Relationships

Stratigraphic Unit	Normally Compacted Wells	Mean ϕ_N (pu)	Midpoint Depth (m bgl)	Equation of Normal Compaction Relationship**
Eromanga Basin				
Winton Formation				
Mackunda Formation				
Allaru Mudstone-Oodnadatta Formation				
Bulldog Shale-Wallumbilla Formation				
Cadna-owie Formation	Paning-1 Wimma-1	34.671 28.333	1666.738 1969.437	ϕ_N = 69.494 - 0.0209 dbgl
Birkhead Formation	Kirby-1 Wimma-1	26.614 22.632	2010.929 2357.447	ϕ_N = 49.506 - 0.0114 dbgl
Hutton Sandstone	Wimma-1 Yumba-1	13.097 19.977	2492.777 1869.339	ϕ_N = 40.517 - 0.0110 dbgl
Cooper Basin				
Nappamerri Group	Beanbush-1 Kirby-1	14.290 20.717	2936.233 2425.929	ϕ_N = 50.992 - 0.0125 dbgl
Toolachee Formation	Kirby-1 Turban-1	15.696 25.446	2718.297 2263.906	ϕ_N = 73.888 - 0.0214 dbgl
Roseneath Shale	Jackson-1 Kirby-1	33.991 26.236	1577.949 2836.429	ϕ_N = 43.538 - 0.0061 dbgl
Murteree Shale	Beanbush-1 Lake Mcmillan-1	21.361 24.217	3280.198 2945.895	ϕ_N = 49.242 - 0.0085 dbgl
Patchawarra Formation	Paning-1 Turban-1	16.895 28.565	3021.078 2273.291	ϕ_N = 64.023 - 0.0156 dbgl

*m bgl = meters below ground level.

**ϕ_N = neutron porosity (pu); dbgl = depth below ground level (in metres).

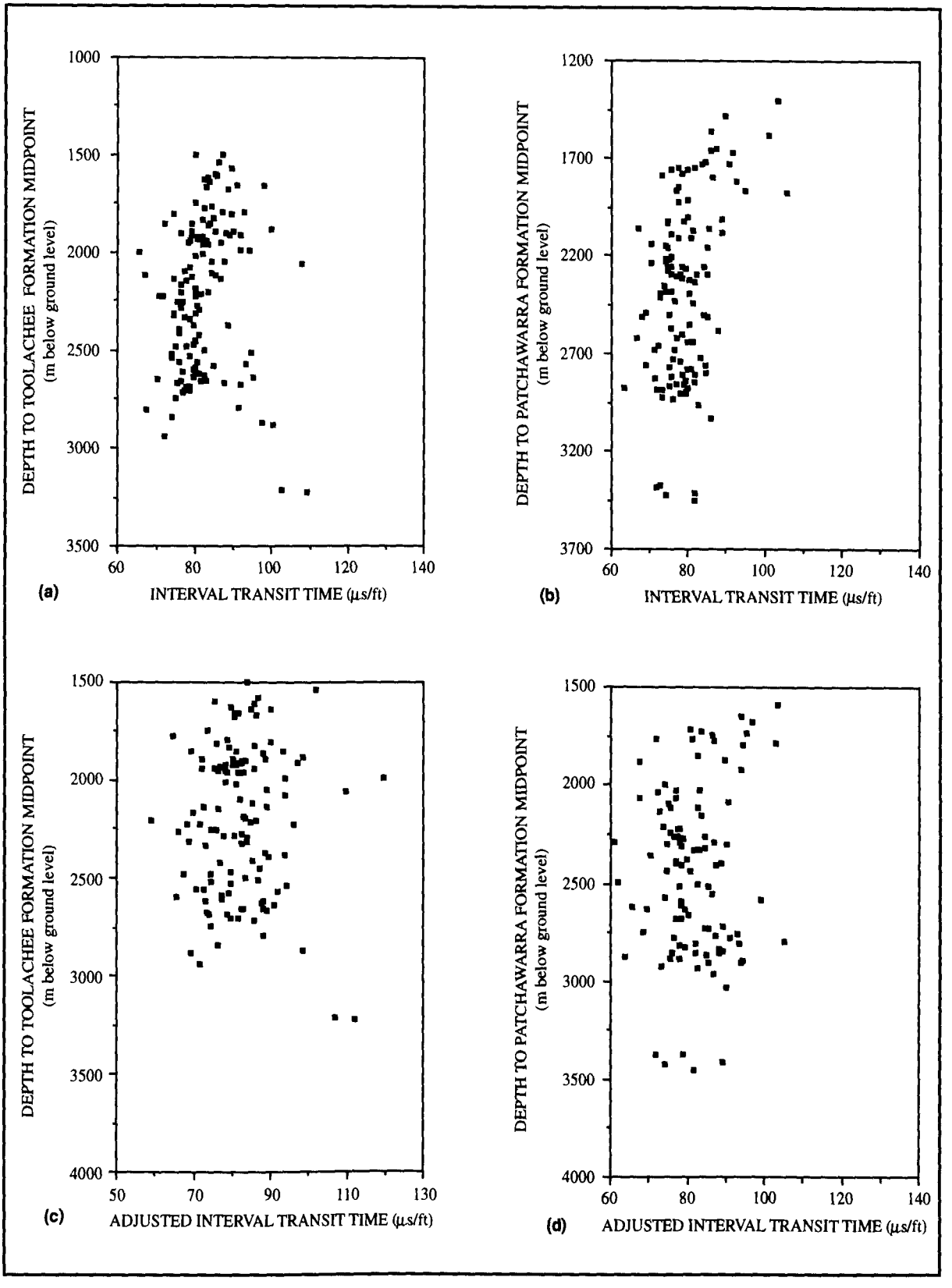

Figure 2.19a. Mean sonic Δt/depth to unit midpoint plots for (a) the Toolachee and (b) the Patchawarra Formations and mean adjusted sonic Δt_{adj}/depth to unit midpoint plots for (c) the Toolachee and (d) the Patchawarra Formations, including coals. The presence of coals in these formations makes impossible and/or difficult the determination of normal compaction relationships.

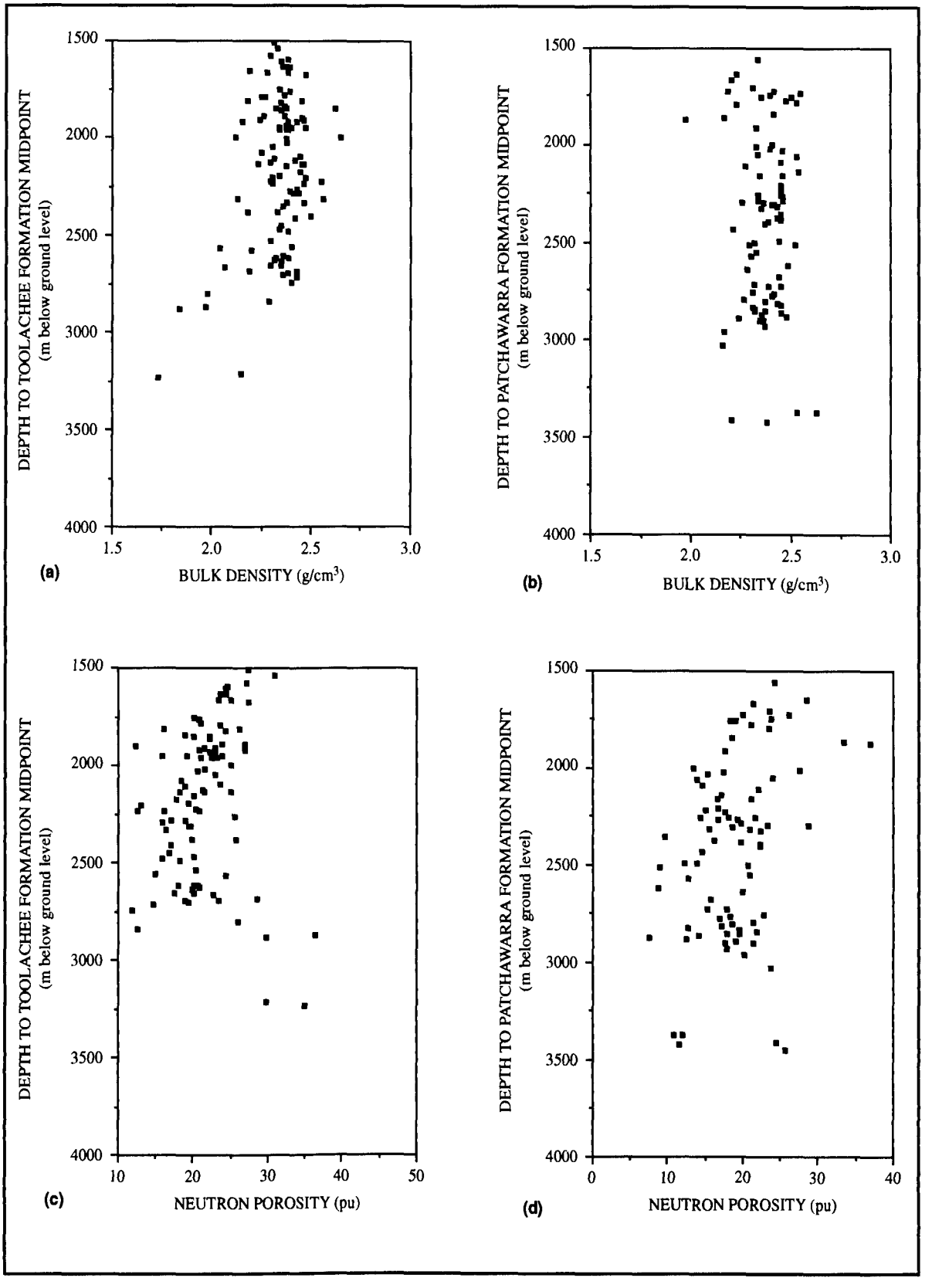

Figure 2.19b. Mean bulk ρ_b/depth to unit midpoint plots for (a) the Toolachee and (b) the Patchawarra Formations and mean neutron Φ_N/depth to unit midpoint plots for (c) the Toolachee and (d) the Patchawarra Formations, including coals. The presence of coals in these formations makes impossible and/or difficult the determination of normal compaction relationships.

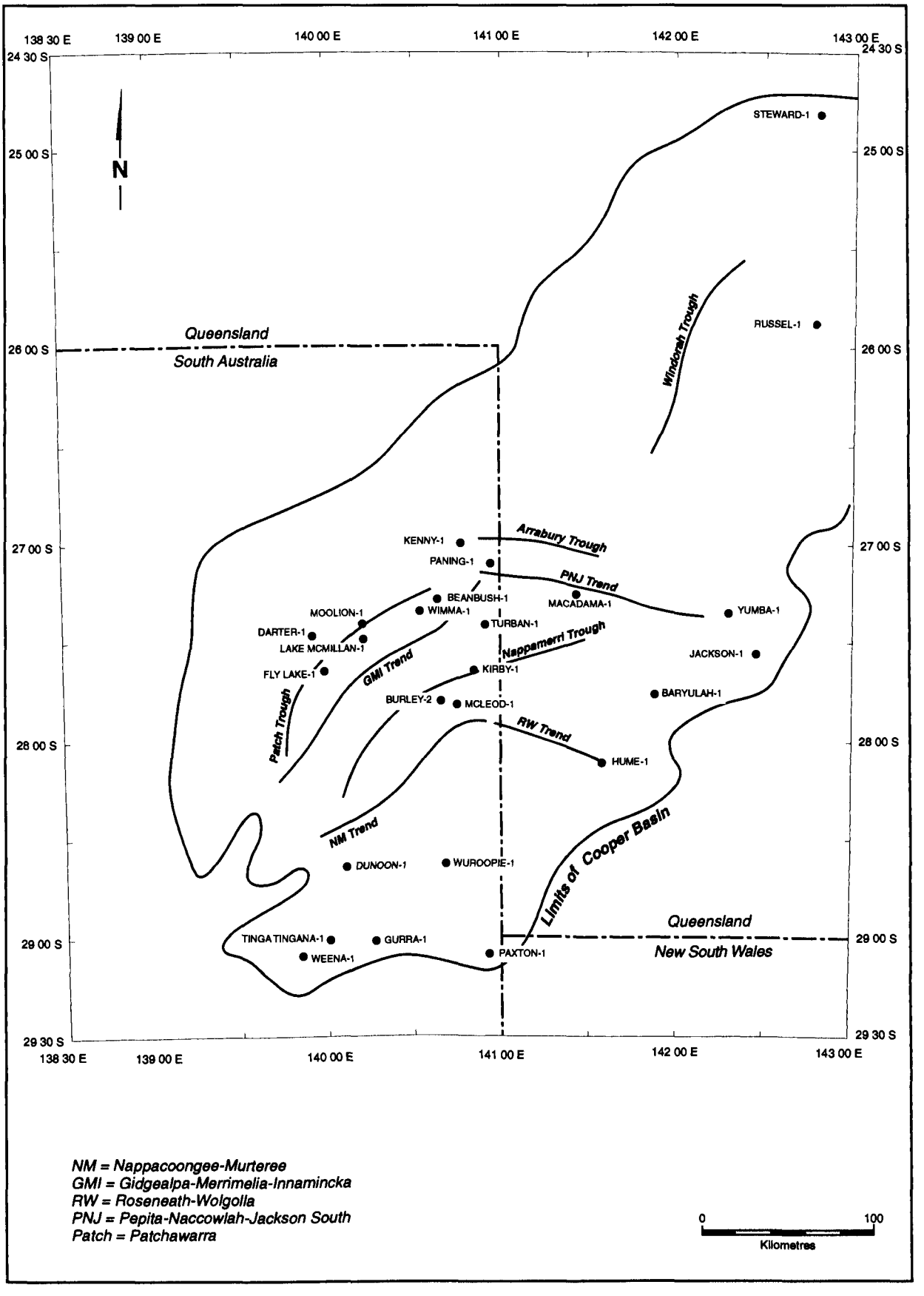

Figure 2.20. Location map of the reference wells. Major tectonic elements of the Cooper-Eromanga Basins are also shown.

3. RESULTS OF COMPACTION-BASED ANALYSIS OF EXHUMATION

3.1 Introduction

In this chapter apparent exhumation values determined using the compaction methodology, as described in Chapter 2, are discussed. Comparisons are made between the results from the different stratigraphic units and different logs. The mean of the apparent exhumation values from the Eromanga Basin and Cooper Basin units analysed are calculated, and the significance of the difference between these mean values is discussed. The distribution of Tertiary exhumation throughout the Eromanga Basin, as witnessed by the mean of the apparent exhumation values from the Eromanga Basin sequence, is discussed with respect to structural trends in the basin.

3.2 Comparison of Apparent Exhumation Results from Different Stratigraphic Units in the Eromanga Basin

Considering the sonic log data from the Eromanga Basin, there is an excellent correlation between apparent exhumation results from different stratigraphic units in the same well (Figure 3.1 and Table 3.1). Given this correlation, it seems probable that, at a formational and regional scale, overcompaction reflects previously greater burial-depth, rather than laterally varying sedimentological or diagenetic processes. Laterally variable sedimentological or diagenetic processes, such as calcite cementation in the Birkhead Formation and Hutton Sandstone (Schulz-Rojahn, 1993), or secondary porosity generation, would not be likely to generate the same degree of overcompaction in different stratigraphic units within the same well. Exhumation of the entire Eromanga Basin sequence is the only likely cause of the consistent degree of overcompaction of the seven units analysed. The Birkhead Formation does yield somewhat higher values than the other units in the Eromanga Basin. The higher

values from the Birkhead Formation are due to the relatively low velocity of the shallower reference well, Tinga Tingana-1, which may be anomalous (Figure 2.15b).

The correlation between exhumation values derived from different stratigraphic units in the same well in the Eromanga Basin is considerably better than has been observed in studies of exhumation from multiple stratigraphic units in various basins of the United Kingdom (Bulat and Stoker, 1987; Hillis *et al.*, 1994; Hillis, 1995; Menpes and Hillis, 1995). This may be due to the relative absence of carbonates and evaporites, and the dominance of clastics, especially shales, in the Eromanga Basin. The mean apparent exhumation value from such of the Eromanga Basin units as are present in each well has been determined. A high degree of confidence may be placed on these values as reflecting the height of the Eromanga Basin sequence above its maximum burial-depth. These values provide crucial input to modelling the maturation history of source rocks in the Cooper-Eromanga Basins, and to elucidating basin structure, thus migration pathways at the time of maximum burial-depth.

The apparent exhumation values from the adjusted sonic log show, similarly to the sonic log data, an excellent correlation between the different stratigraphic units in the same well (Figure 3.2 and Table 3.2), supporting the hypothesis that overcompaction reflects previously greater burial-depth, rather than laterally varying sedimentological or diagenetic processes. The Birkhead Formation again shows higher values than the other units in the Eromanga Basin. This is probably due again to the use of Tinga Tingana-1 as a reference well.

The apparent exhumation results from the density log in the Cadna-owie, Birkhead and Hutton units are also similar within the same well (Figure 3.3 and Table 3.3). These data further support the hypothesis that overcompaction reflects previously greater burial-depth, rather than laterally varying sedimentological or diagenetic processes. In the shallower units, where there are less data (ie. density log not often run), there is not such a clear correlation between exhumation values from different units in the same well. This is due to the paucity of density log data for these units, normal compaction relations are poorly constrained, and less reliable, in these units.

There are insufficient data from the neutron log to analyse units above the Cadna-owie, and there is some scatter between apparent exhumation results from the Cadna-owie, Birkhead and Hutton units (Figure 3.4 and Table 3.4). However, despite exhibiting more scatter than the results from the sonic and density logs, the neutron porosity-derived exhumation values from these units are broadly consistent with each other.

Regression analysis was used to determine least-squares, best-fit, linear relationships between the apparent exhumation values from the different units, and associated co-efficients of correlation. The t-statistic of each co-efficients of correlation was calcuclated and tested against the one-tailed Student's t-distribution in order to test the null hypothesis that the co-efficients of correlation come from a population whose mean value is zero (eg. Till, 1974). This hypothesis can be rejected at the 97.5% confidence level in the vast majority of all cases in all four logs (Tables 3.1 - 3.4). Hence the results of apparent exhumation as determined from the Eromanga Basin units in all logs are statistically similar.

3.3 Comparison of Apparent Exhumation Results from Different Stratigraphic Units in the Cooper Basin

Exhumation values from the five units analysed in the Cooper Basin are not as consistent, in the same well, as those in the Eromanga Basin (Figures 3.1-3.4 and Tables 3.1-3.4). The presence of coals, and the need to analyse relatively thin coal-free sections of the lower Toolachee and lower Patchawarra Formations, is probably largely responsible for poorer correlation between exhumation values involving these two units (Figures 2.9b and c). The poorest correlations between exhumation values involve the Toolachee Formation. Although coals are generally absent from the picked part of the lower Toolachee Formation, carbonaceous units are present. In retrospect, the Toolachee Formation is probably the least suitable of the units analysed for estimation of apparent exhumation. Exhumation values from units underlying the Toolachee Formation (Roseneath Shale, Murteree Shale and Patchawarra

Formation) are reasonably consistent in all four logs, though not as consistent as those from units in the Eromanga Basin sequence.

Regression analysis was used to determine least-squares, best-fit, linear relationships between the apparent exhumation values from the different units, and associated co-efficients of correlation. The t-statistic of each co-efficients of correlation was caluclated and tested against the one-tailed Student's t-distribution in order to test the null hypothesis that the co-efficients of correlation come from a population whose mean value is zero (eg. Till, 1974). This hypothesis can be rejected at the 97.5% confidence level in almost all cases in all four logs (Tables 3.1 - 3.4). Hence the results of apparent exhumation as determined from the Cooper Basin units in all logs are statistically similar.

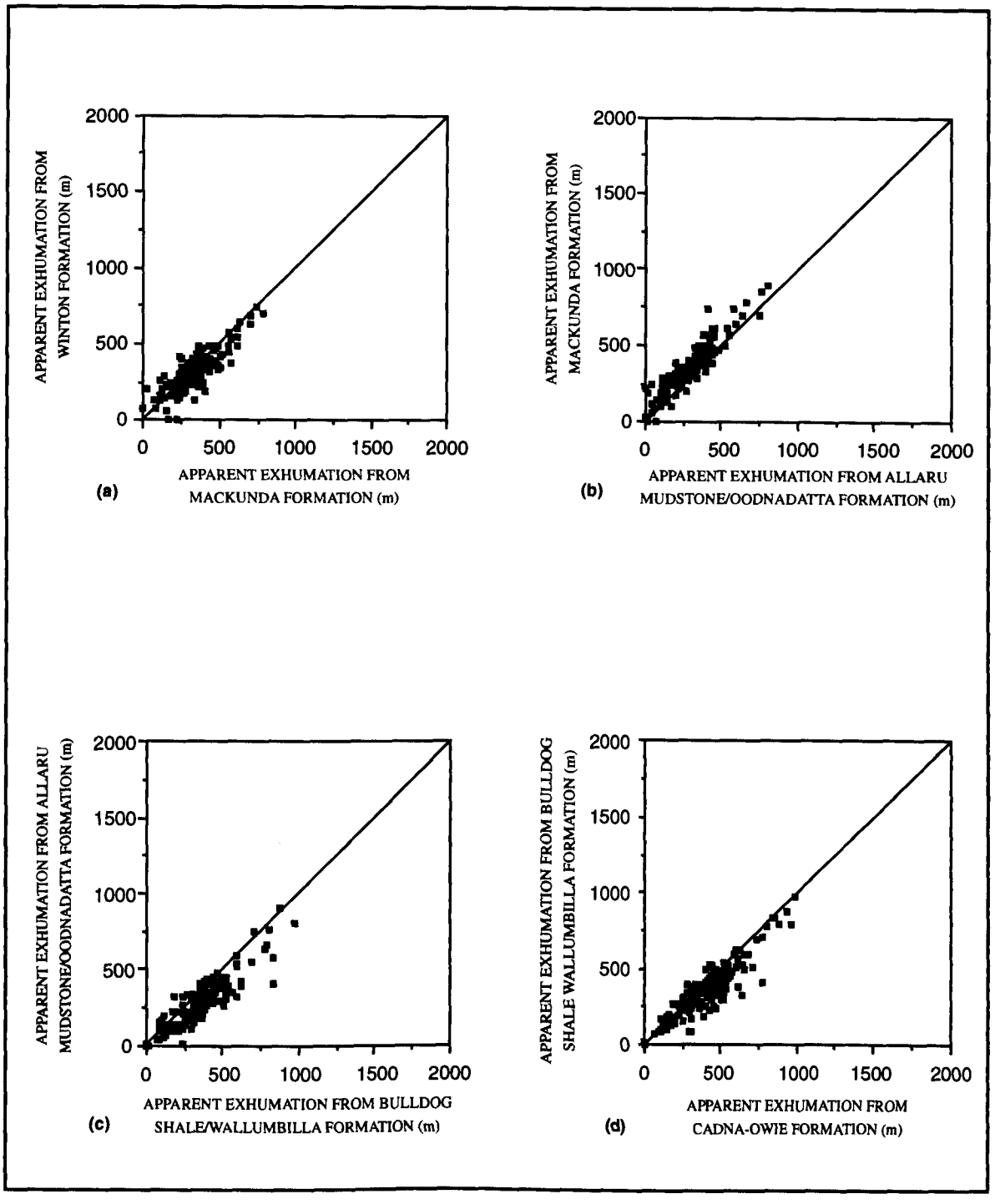

Figure 3.1. Crossplots of apparent exhumation (in metres) derived from sonic interval transit time in the stratigraphic units studied: (a) apparent exhumation from Winton Formation against those from the Mackunda Formation, (b) Mackunda Formation against AllaruMudstone/Oodnadatta Formation, (c) Allaru Mudstone/Oodnadatta Formation against Bulldog Shale/Wallumbilla Formation, (d) Bulldog Shale/Wallumbilla Formation against Cadna-owie Formation. The line illustrating the 1:1 relationship between apparent exhumation values from each pair of units analysed is shown.

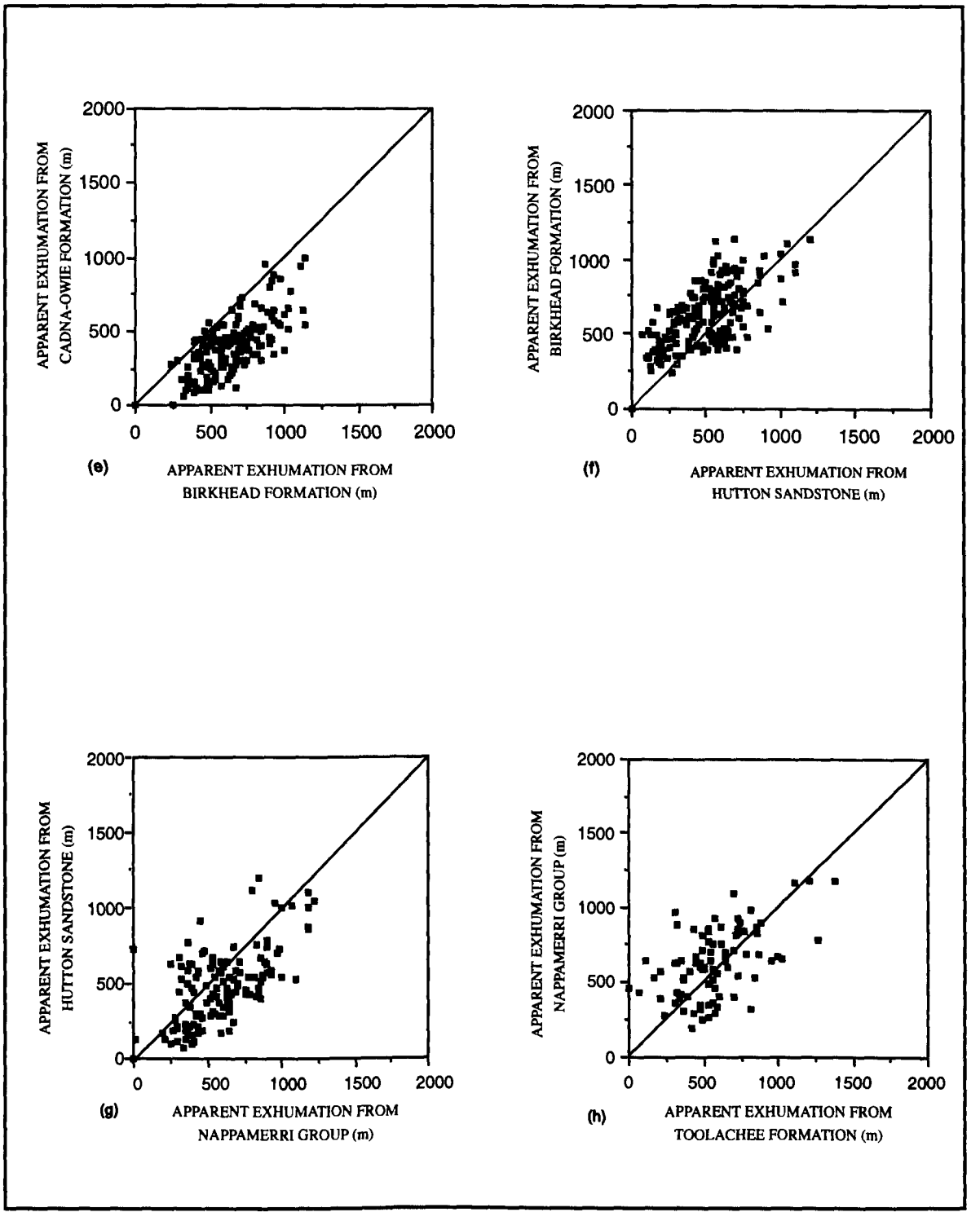

Figure 3.1. Continued. Crossplots of apparent exhumation (in meters) derived from sonic interval transit time in the stratigraphic units studied: (e) apparent exhumation from Cadna-owie Formation against those from the Birkhead Formation, (f) Birkhead Formation against Hutton Sandstone, (g) Hutton Sandstone against Nappamerri Group, and (h) Nappamerri Group against Toolachee Formation. The line illustrating the 1:1 relationship between apparent exhumation values from each pairs of units analysed is shown.

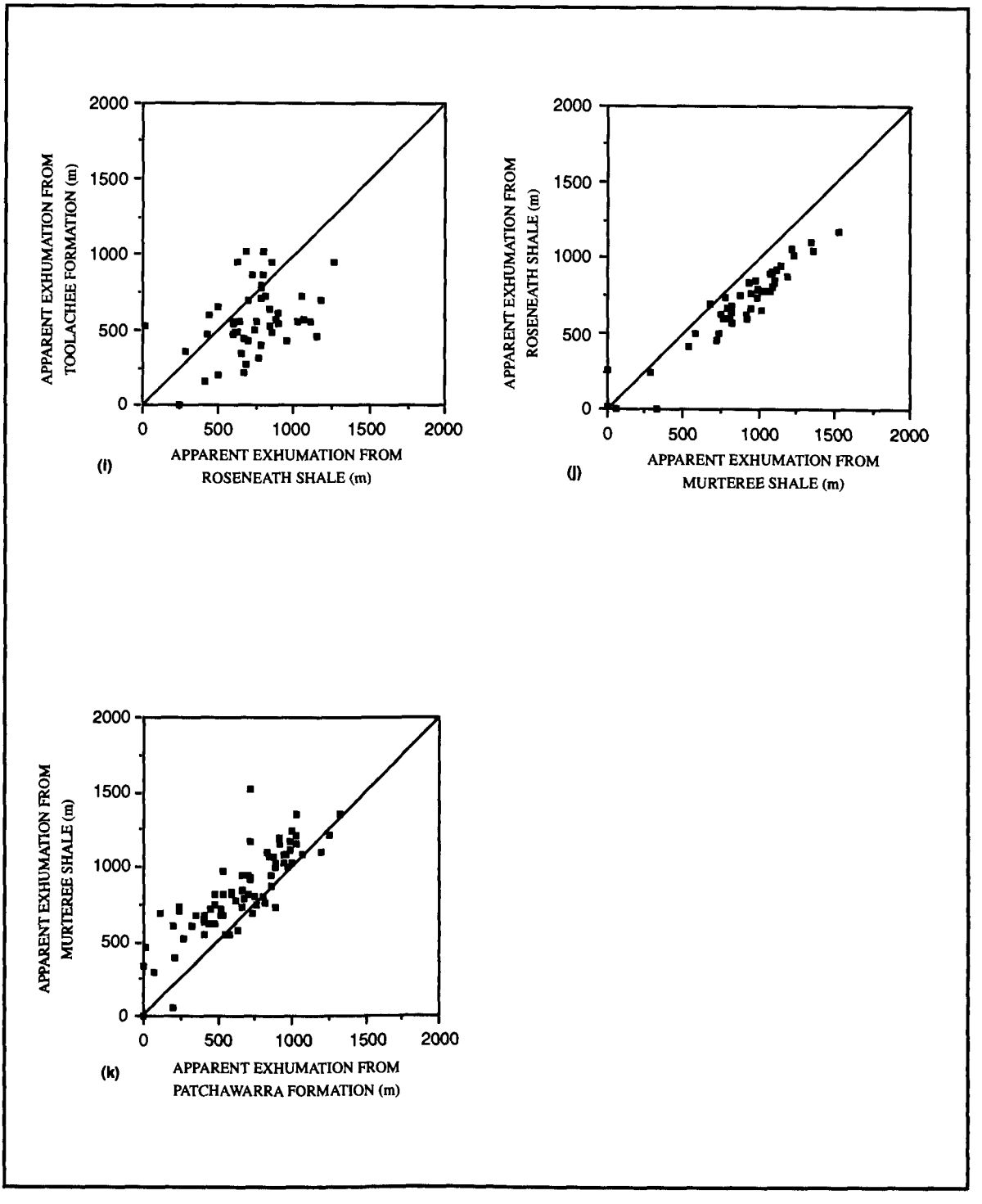

Figure 3.1. Continued. Crossplots of apparent exhumation (in meters) derived from sonic interval transit time in the stratigraphic units studied: (i) apparent exhumation from Toolachee Formation against those from Roseneath Shale, (j) Roseneath Shale against Murteree Shale, and (k) Murteree Shale against Patchawarra Formation. The line illustrating the 1:1 relationship between apparent exhumation values from each pairs of units analysed is shown.

Table 3.1. Correlation Between Apparent Exhumation Results Derived from Sonic Log from the Stratigraphic Units Analysed*

	Winton Formation (W)	Mackunda Formation (M)	Allaru Mudstone/ Oodnadatta Formation (A)	Bulldog Shale/ Wallumbilla Formation (BW)	Cadna-owie Formation (C)	Birkhead Formation (B)	Hutton Sandstone (H)	Nappamerri Group (N)	Toolachee Formation (T)	Roseneath Shale (R)	Murteree Shale (MS)
Mackunda Formation (M)	W = 61 + 0.769M M = 41 + 0.920W										
No of Wells Having Both Units	156										
Coefficient of Correlation**	0.841										
t-statistic***	19.3										
Allaru Mudstone/ Oodnadatta Formation (A)	W = 92 + 0.807A A = - 1 + 0.885W	M = 63 + 0.975A A = - 12 + 0.87M									
No of Wells Having Both Units	156	173									
Coefficient of Correlation**	0.844	0.921									
t-statistic***	19.5	30.9									
Bulldog Shale/Wallumbilla Formation (BW)	W = 80 + 0.682BW BW = 45 + 0.956W	M = 50 + 0.817BW BW = 19 + 0.985M	A = 4 + 0.790BW BW = 64 + 1.024A								
No of Wells Having Both Units	155	172	174								
Coefficient of Correlation**	0.807	0.896	0.899								
t-statistic***	16.9	26.3	26.9								
Cadna-owie Formation (C)	W = 95 + 0.565C C = 73 + 1.013W	M = 39 + 0.747C C = 45 + 1.053M	A = 5 + 0.696C C = 102 + 1.057A	BW = 20 + 0.835C C = 50 + 0.992BW							
No of Wells Having Both Units	156	172	174	176							
Coefficient of Correlation**	0.756	0.886	0.857	0.909							
t-statistic***	14.3	24.9	21.8	28.8							
Birkhead Formation (B)	W = 123 + 0.314B B = 398 + 0.715W	M = - 2 + 0.545B B = 319 + 0.906M	A = - 18 + 0.488B B = 372 + 0.891A	BW = - 9 + 0.588B B = 327 + 0.835BW	C = - 9 + 0.641B B = 311 + 0.803C						
No of Wells Having Both Units	149	159	161	162	178						
Coefficient of Correlation**	0.474	0.702	0.659	0.7	0.717						
t-statistic***	6.5	12.4	11	12.4	13.6						
Hutton Sandstone (H)	W = 113 + 0.411H H = 135 + 1.144N	M = 73 + 0.525H H = 116 + 1.156M	A = 31 + 0.503H H = 163 + 1.208A	BW = 38 + 0.632H H = 86 + 1.178BW	C = 80 + 0.623H H = 117 + 0.980C	B = 323 + 0.590H H = 47 + 0.726B					
No of Wells Having Both Units	153	165	167	168	183	187					
Coefficient of Correlation**	0.685	0.778	0.779	0.863	0.781	0.655					
t-statistic***	11.6	15.8	16	22	16.8	11.8					
Nappamerri Group (N)	W = 159 + 0.262N N = 342 + 0.824W	M = 40 + 0.464N N = 268 + 1.065M	A = 1 + 0.457N N = 305 + 1.100	BW = 64 + 0.468N N = 297 +0.899BW	C = 45 + 0.532N N = 271 + 0.909C	B = 229 + 0.578N N = - 3 + 1.042B	H = 134 + 0.589N N = 273 + 0.661H				
No of Wells Having Both Units	98	107	109	111	122	134	134				
Coefficient of Correlation**	0.464	0.702	0.709	0.648	0.695	0.776	0.623				
t-statistic***	5.1	10.1	10.4	8.9	10.6	14.1	9.2				
Toolachee Formation (T)	W = 223 + 0.153T T = 384 + 0.675W	M = 169 + 0.291T T = 308 + 0.864M	A = 161 + 0.212T T = 377 + 0.791A	BW = 185 + 0.269T T = 319 + 0.819BW	C = 189 + 0.318T T = 323 + 0.7C	B = 461 + 0.288T T = 279 + 0.476B	H = 248 + 0.383T T = 286 + 0.625H	N = 364 + 0.467T T = 208 + 0.571N			
No of Wells Having Both Units	84	91	91	91	102	107	108	88			
Coefficient of Correlation**	0.32	0.5	0.408	0.469	0.472	0.37	0.488	0.516			
t-statistic***	3.1	5.4	4.2	5	5.4	4.1	5.8	5.6			
Roseneath Shale (R)	W = 215 + 0.129R R = 551 + 0.563W	M = 260 + 0.126R R = 521 + 0.561M	A = 158 + 0.174R R = 445 + 0.963A	BW = 201 + 0.213R R = 349 + 1.020BW	C = 234 + 0.234R R = 375 + 0.805C	B = 404 + 0.413R R = 240 + 0.665B	H = 332 + 0.241R R = 343 + 0.715H	N = 357 + 0.453R R = 144 + 1.225N	T = 294 + 0.356R R = 534 + 0.362T		
No of Wells Having Both Units	45	47	47	46	54	54	54	37	49		
Coefficient of Correlation**	0.268	0.266	0.408	0.466	0.434	0.524	0.414	0.744	0.359		
t-statistic***	N	N	3	3.5	3.5	4.4	3.3	6.6	2.6		
Murteree Shale (MS)	W = 107 +0.150MS MS = 533 +1.416W	M = 107 + 0.176MS MS = 518 + 1.313M	A = 27 + 0.207MS MS = 543 + 1.538A	BW = 55 + 0.247MS MS = 465 + 1.452BW	C = 97 + 0.247MS MS = 530 + 1.002C	B = 163 + 0.478MS MS = 287 + 0.962B	H = 43 + 0.425MS MS = 505 + 0.835H	N = 54 + 0.618MS MS = 296 + 0.928N	T = 287 + 0.262MS MS = 651 + 0.438T	R = 12 + 0.769MS MS = 76 + 1.167R	
No of Wells Having Both Units	56	61	61	60	70	73	74	63	61	44	
Coefficient of Correlation**	0.46	0.48	0.563	0.598	0.497	0.684	0.595	0.756	0.339	0.947	
t-statistic***	3.8	4.2	5.2	5.7	4.7	7.9	6.3	9	2.8	19.1	
Patchawarra Formation (P)	W = 116 + 0.229P P = 348 + 1.397W	M = 78 + 0.300P P = 283 + 1.519M	A = 43 + 0.276P P = 367 + 1.503A	BW = 75 + 0.308P P = 244 + 1.616P	C = 96 + 0.337P P = 275 + 1.323C	B = 277 + 0.451P P = 81 + 1.052B	H = 105 + 0.461P P = 229 + 1.117H	N = 226 + 0.515P P = 108 + 0.996N	T = 359 + 0.249P P = 478 + 0.498T	R = 237 + 0.567P P = 209 + 0.852R	MS = 329 + 0.777P P = 107 + 0.908MS
No of Wells Having Both Units	80	87	87	87	98	104	105	88	85	51	74
Coefficient of Correlation**	0.565	0.674	0.644	0.705	0.667	0.689	0.717	0.716	0.352	0.694	0.839
t-statistic***	6	8.4	7.8	9.2	8.8	9.6	10.4	9.5	3.4	6.7	13.1

*Linear, best-fit, least-squares regression between apparent exhumation values derived from the 12 units analysed. Because there is no dependent variable, apparent exhumation from the shallower unit was regressed on that from the deeper unit (first or top equation) and vice versa (second or bottom equation).

**Coefficient of correlation between apparent exhumation values is derived from the two units in the examined wells.

***t-statistic for the coefficient of correlation. In most cases, comparison of the t-statistic with the one-tailed Student's t-distribution allows rejection of the null hypothesis (that the coefficients of correlation come from a population the mean of which is zero) at the 97.5% confidence level. N indicates that the coefficient of correlation is not significant at the stated confidence level.

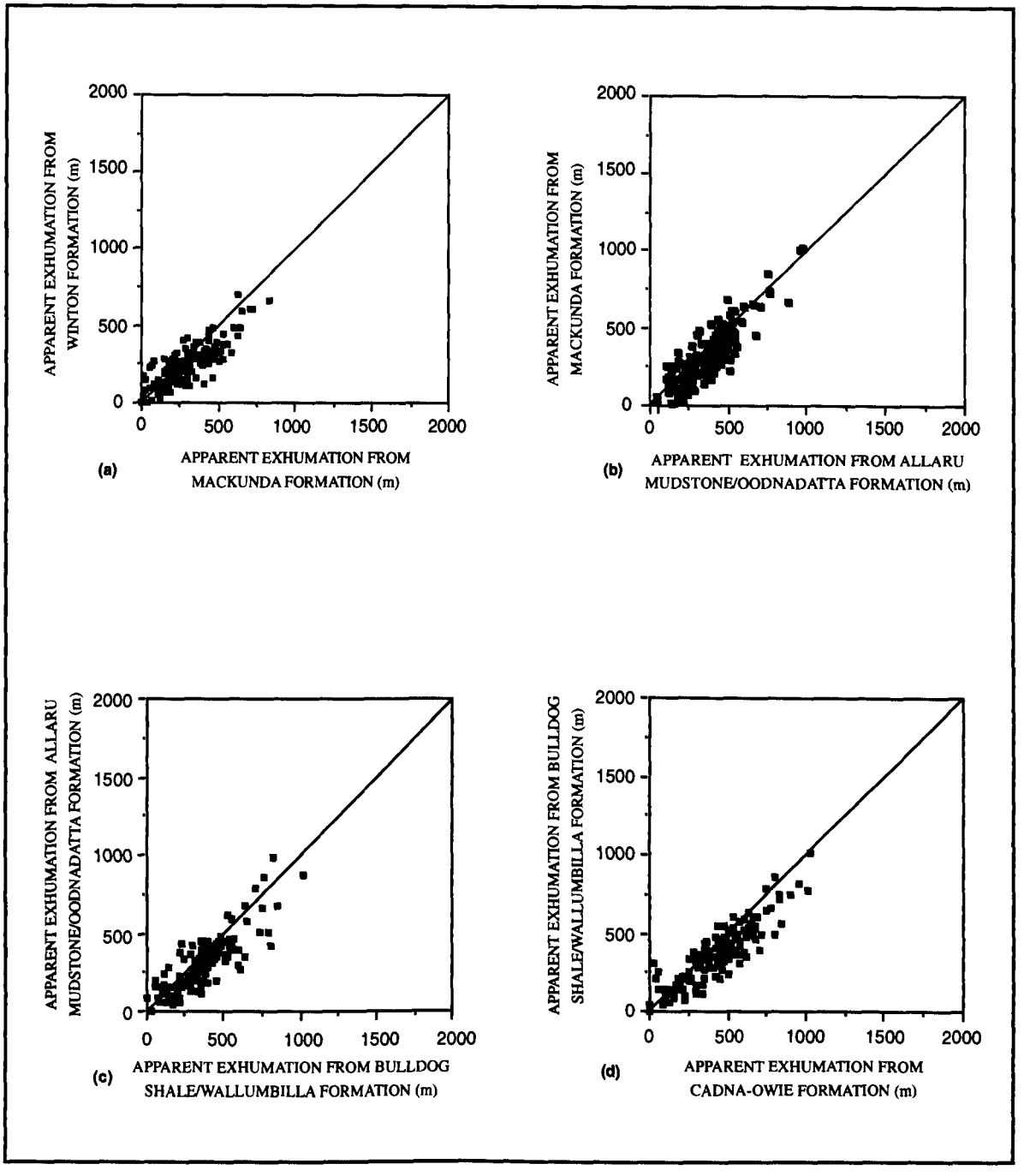

Figure 3.2. Crossplots of apparent exhumation (in metres) derived from adjusted sonic interval transit time in the stratigraphic units studied: (a) apparent exhumation from Winton Formation against those from the Mackunda Formation, (b) Mackunda Formation against AllaruMudstone/Oodnadatta Formation, (c) Allaru Mudstone/Oodnadatta Formation against Bulldog Shale/Wallumbilla Formation, and (d) Bulldog Shale/Wallumbilla Formation against Cadna-owie Formation. The line illustrating the 1:1 relationship between apparent exhumation values from each pair of units analysed is shown.

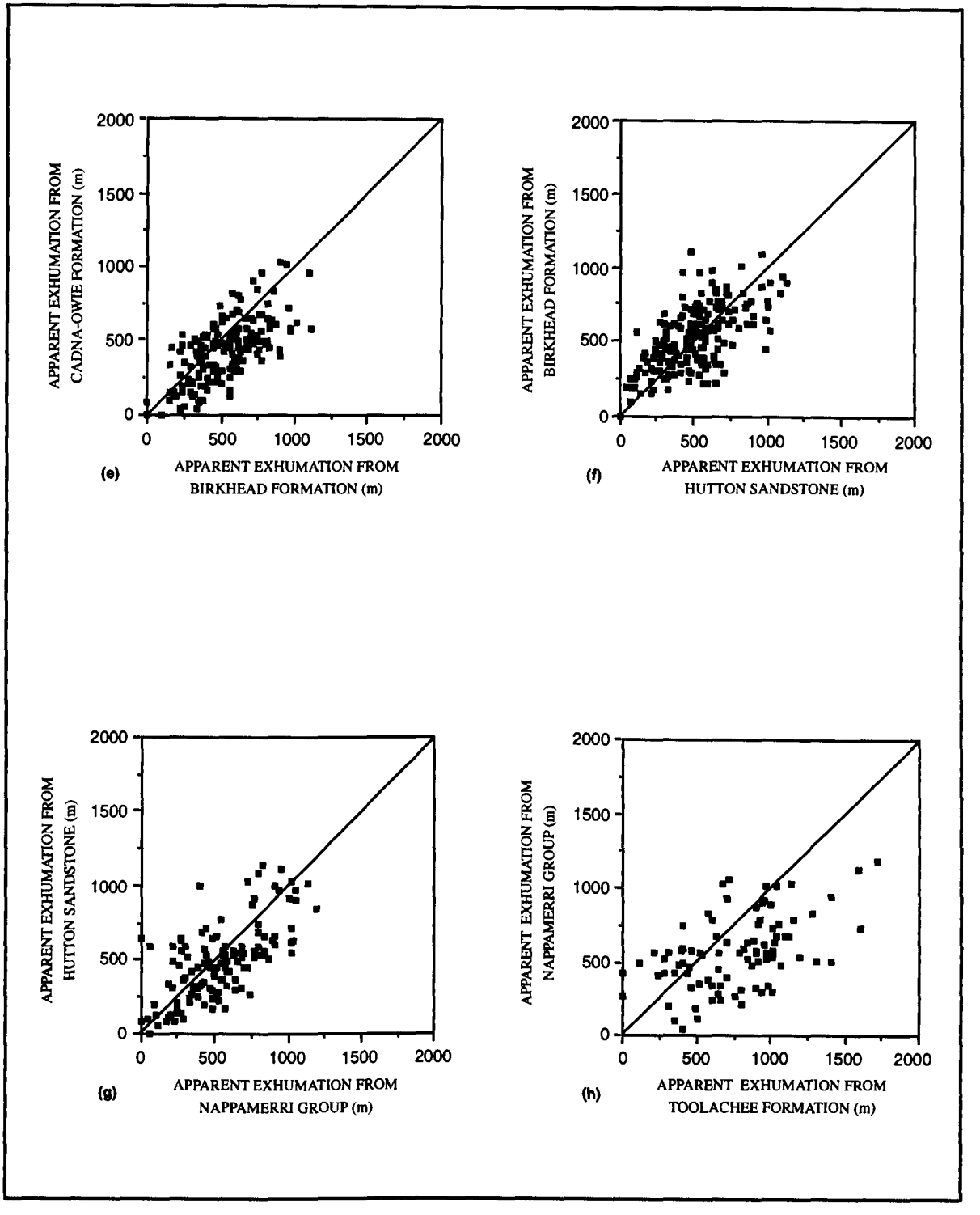

Figure 3.2. Continued. Crossplots of apparent exhumation (in metres) derived from adjusted sonic interval transit time in the stratigraphic units studied: (e) apparent exhumation from Cadna-owie Formation against those from the Birkhead Formation, (f) Birkhead Formation against Hutton Sandstone, (g) Hutton Sandstone against Nappamerri Group, and (h) Nappamerri Group against Toolachee Formation. The line illustrating the 1:1 relationship between apparent exhumation values from each pair of units analysed is shown.

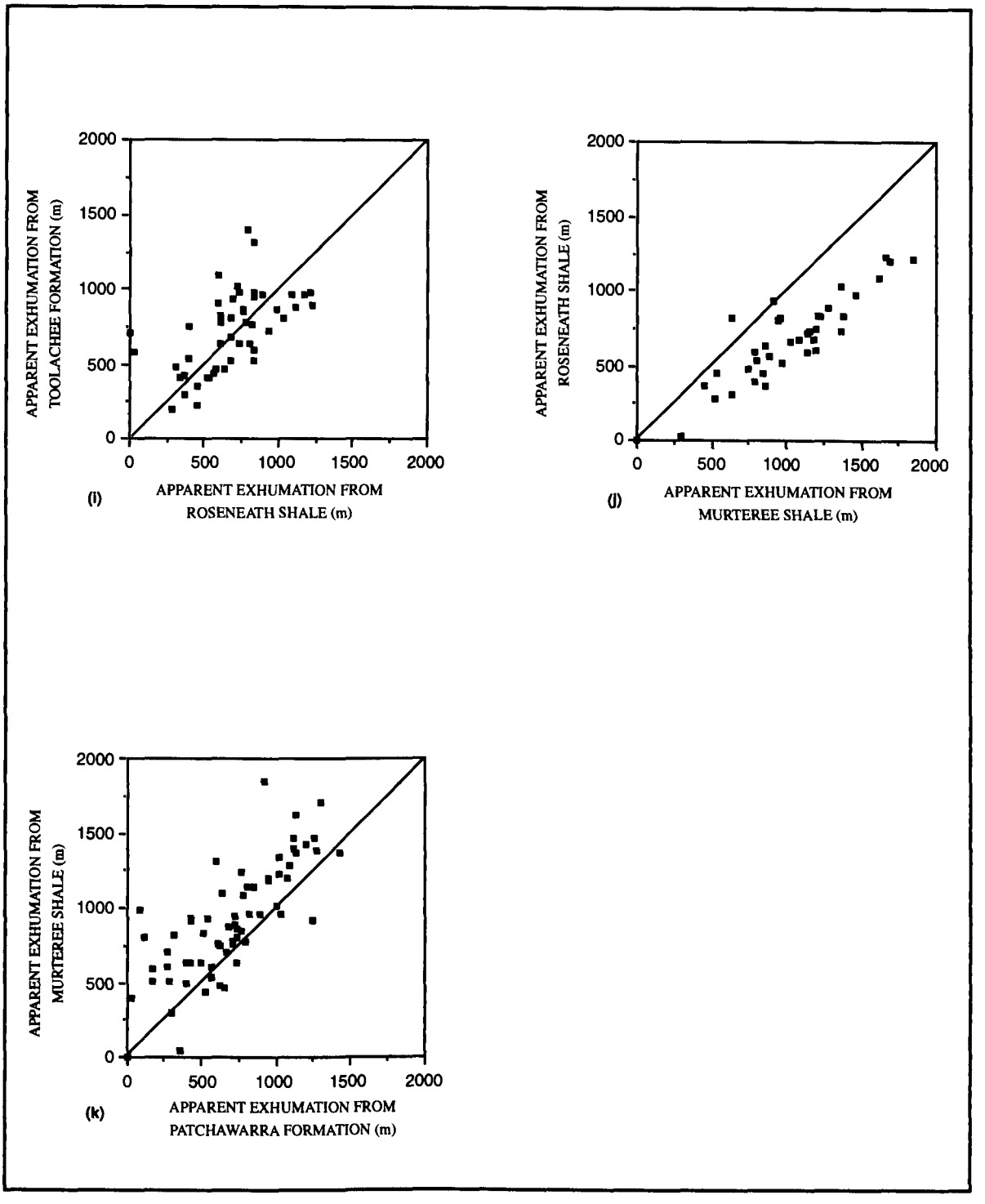

Figure 3.2. Continued. Crossplots of apparent exhumation (in metres) derived from adjusted sonic interval transit time in the stratigraphic units studied: (i) apparent exhumation from Toolachee Formation against those from Roseneath Shale, (j) Roseneath Shale against Murteree Shale, and (k) Murteree Shale against Patchawarra Formation. The line illustrating the 1:1 relationship between apparent exhumation values from each pair of units analysed is shown.

Table 3.2. Correlation Between Apparent Exhumation Results Derived from Adjusted Sonic Log from the Stratigraphic Units Analysed*

	Winton Formation (W)	Mackunda Formation (M)	Allaru Mudstone/ Oodnadatta Formation (A)	Bulldog Shale/ Wallumbilla Formation (BW)	Cadna-owie Formation (C)	Birkhead Formation (B)	Hutton Sandstone (H)	Nappamerri Group (N)	Toolachee Formation (T)	Roseneath Shale (R)	Murteree Shale (MS)
Mackunda Formation (M)	W = 48 + 0.657M M = 55 + 1.012W										
No of Wells Having Both Units	142										
Coefficient of Correlation**	0.814										
t-statistic***	16.6										
Allaru Mudstone/ Oodnadatta Formation (A)	W = 32 + 0.717A A = 71 + 0.934W	M = 13 + 0.980A A = 69 + 0.761M									
No of Wells Having Both Units	143	153									
Coefficient of Correlation**	0.818	0.863									
t-statistic***	16.9	21									
Bulldog Shale/Wallumbilla Formation (BW)	W = 30 + 0.601BW BW = 129 + 0.949W	M = 12 + 0.813BW BW = 123 + 0.794M	A = 23 + 0.773BW BW = 89 + 0.911A								
No of Wells Having Both Units	143	155	159								
Coefficient of Correlation**	0.754	0.803	0.839								
t-statistic***	13.6	16.7	19.3								
Cadna-owie Formation (C)	W = 30 + 0.505C C = 167 + 1.072W	M = 34 + 0.634C C = 193 + 0.799C	A = 26 + 0.645C C = 135 + 0.984A	BW = 36 + 0.762C C = 68 + 1.006BW							
No of Wells Having Both Units	143	155	161	162							
Coefficient of Correlation**	0.735	0.712	0.796	0.875							
t-statistic***	12.9	12.5	16.6	22.9							
Birkhead Formation (B)	W = 97 + 0.287B B = 343 + 0.749W	M = 161 + 0.292B B = 405 + 0.417M	A = 90 + 0.415B B = 313 + 0.710A	BW = 121 + 0.476B B = 265 + 0.720BW	C = 95 + 0.641B B = 216 + 0.718C						
No of Wells Having Both Units	141	151	157	158	170						
Coefficient of Correlation**	0.463	0.349	0.543	0.585	0.678						
t-statistic***	6.2	4.5	8.1	9	12						
Hutton Sandstone (H)	W = 50 + 0.398H H = 226 + 1.110W	M = 73 + 0.525H H = 227 + 0.902M	A = 48 + 0.512H H = 187 + 1.053A	BW = 60 + 0.617H H = 99 + 1.097BW	C = 110 + 0.635H H = 136 + 0.857C	B = 224 + 0.590H H = 134 + 0.708B					
No of Wells Having Both Units	141	151	157	158	170	179					
Coefficient of Correlation**	0.664	0.692	0.734	0.822	0.737	0.645					
t-statistic***	10.5	11.7	13.5	18	14.1	11.2					
Nappamerri Group (N)	W = 79 + 0.305N N = 304 + 1.006W	M = 113 + 0.394N N = 302 + 0.768M	A = 67 + 0.440N N = 274 + 0.910A	BW = 133 + 0.419N N = 268 + 0.793BW	C = 107 + 0.543N N = 227 + 0.794C	B = 168 + 0.544N N = 84 + 0.984B	H = 142 + 0.632 N = 200 + 0.700H				
No of Wells Having Both Units	94	102	109	109	120	130	130				
Coefficient of Correlation**	0.554	0.55	0.633	0.577	0.656	0.731	0.665				
t-statistic***	6.4	6.6	8.5	7.3	9.4	12.1	10.1				
Toolachee Formation (T)	W = 120 + 0.156T T = 563 + 0.967W	M = 120 + 0.255T T = 502 + 0.950M	A = 141 + 0.209T T = 508 + 0.976A	BW = 183 + 0.220T T = 436 + 1.039BW	C = 171 + 0.306T T = 433 + 0.877C	B = 333 + 0.232T T = 464 + 0.624B	H = 253 + 0.284T T = 454 + 0.695H	N = 292 + 0.360T T = 355 + 0.723N			
No of Wells Having Both Units	84	90	93	95	103	108	108	90			
Coefficient of Correlation**	0.388	0.491	0.451	0.478	0.517	0.38	0.443	0.509			
t-statistic***	3.8	5.3	4.8	5.2	6.1	4.2	5.1	5.5			
Roseneath Shale (R)	W = 159 + 0.124R R = 533 + 0.688W	M = 288 + 0.044R R = 646 + 0.188M	A = 181 + 0.177R R = 394 + 1.009A	BW = 284 + 0.141R R = 351 + 0.932BW	C = 287 + 0.236R R = 313 + 0.812C	B = 295 + 0.409R R = 239 + 0.763B	H = 363 + 0.211R R = 318 + 0.706H	N = 309 + 0.416R R = 181 + 0.759N	T = 348 + 0.547R R = 257 + 0.590T		
No of Wells Having Both Units	41	44	45	45	49	51	51	34	48		
Coefficient of Correlation**	0.293	0.089	0.423	0.361	0.438	0.558	0.386	0.562	0.567		
t-statistic***	N	0.6	3.1	2.5	3.3	4.7	2.9	3.8	4.7		
Murteree Shale (MS)	W = 53 + 0.122MS MS = 629 + 2.099W	M = 126 + 0.105MS MS = 709 + 1.196M	A = 80 + 0.140MS MS = 656 + 1.492A	BW = 137 + 0.151MS MS = 576 + 1.401BW	C = 122 + 0.217MS MS = 579 + 1.118C	B = 148 + 0.324MS MS = 394 + 1.195B	H = 115 + 0.297MS MS = 525 + 1.039H	N = 55 + 0.459MS MS = 414 + 1.043N	T = 333 + 0.348MS MS = 473 + 0.749T	R = 6 + 0.660MS MS = 166 + 1.249R	
No of Wells Having Both Units	52	55	57	57	64	70	70	60	58	39	
Coefficient of Correlation**	0.504	0.353	0.456	0.46	0.491	0.622	0.555	0.692	0.509	0.907	
t-statistic***	4.1	2.7	3.8	3.8	4.4	6.6	5.5	7.3	4.4	13.1	
Patchawarra Formation (P)	W = 65 + 0.189P P = 513 + 1.392W	M = 115 + 0.201P P = 542 + 0.999M	A = 74 + 0.241P P = 465 + 1.276A	BW = 115 + 0.255P P = 335 + 1.476BW	C = 83 + 0.367P P = 350 + 1.186C	B = 165 + 0.403P P = 257 + 1.094B	H = 101 + 0.416P P = 318 + 1.087H	N = 140 + 0.504P P = 261 + 0.934N	T = 388 + 0.401P P = 420 + 0.548T	R = 113 + 0.619P P = 236 + 0.965R	MS = 296 + 0.884P P = 54 + 0.705MS
No of Wells Having Both Units	77	83	85	87	95	102	102	85	85	46	68
Coefficient of Correlation**	0.511	0.448	0.554	0.613	0.659	0.663	0.672	0.686	0.469	0.772	0.789
t-statistic***	5.1	4.5	6.1	7.2	8.4	8.9	9.1	8.6	4.8	8.1	10.4

*Linear, best-fit, least-squares regression between apparent exhumation values derived from the 12 units analysed. Because there is no dependent variable, apparent exhumation from the shallower unit was regressed on that from the deeper unit (first or top equation) and vice versa (second or bottom equation).
**Coefficient of correlation between apparent exhumation values is derived from the two units in the examined wells.
***t-statistic for the coefficient of correlation. In most cases, comparison of the t-statistic with the one-tailed Student's t-distribution allows rejection of the null hypothesis (that the coefficients of correlation come from a population the mean of which is zero) at the 97.5% confidence level. N indicates that the coefficient of correlation is not significant at the stated confidence level.

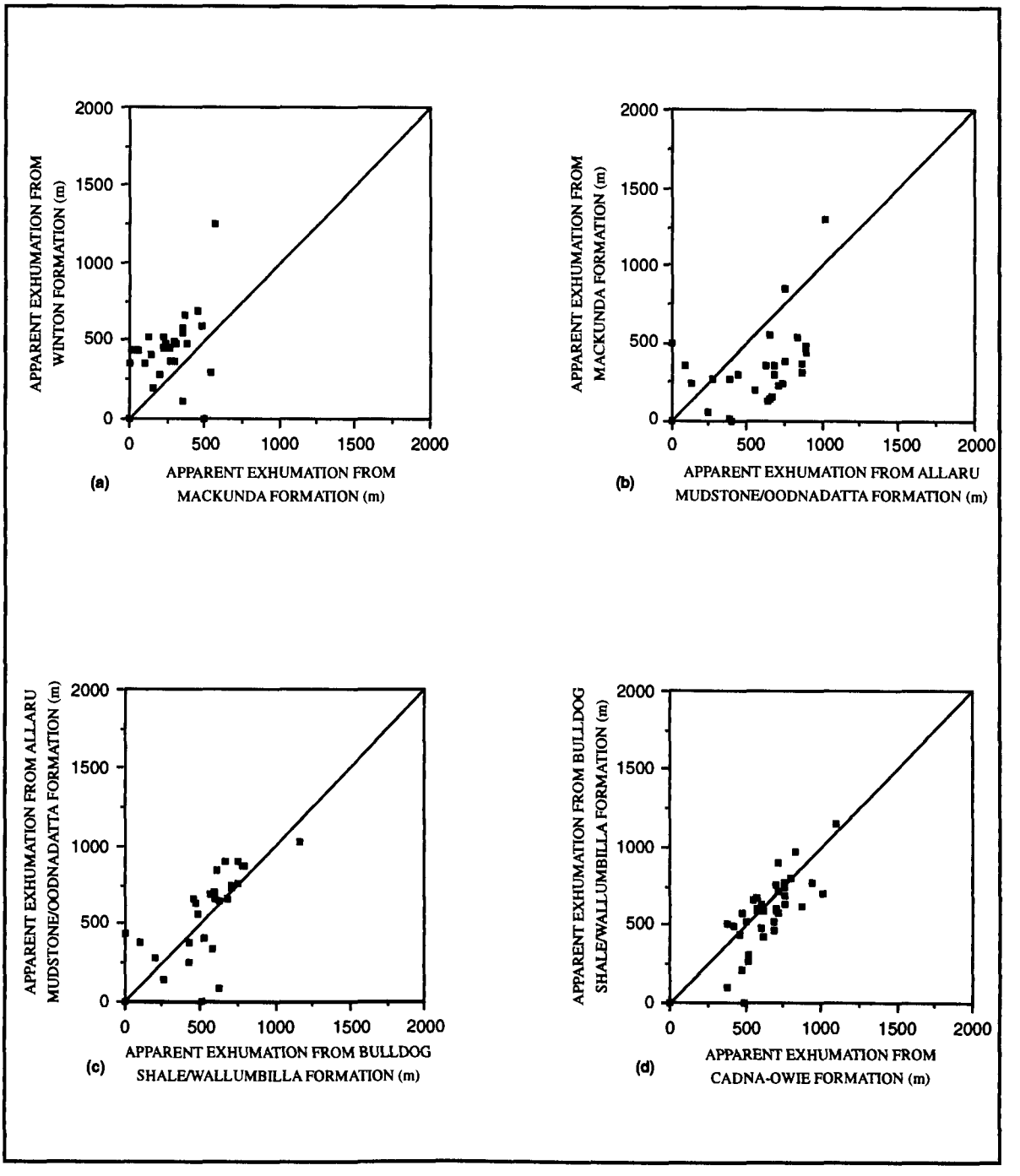

Figure 3.3. Crossplots of apparent exhumation (in metres) derived from bulk density in the stratigraphic units studied: (a) apparent exhumation from Winton Formation against those from the Mackunda Formation, (b) Mackunda Formation against AllaruMudstone/Oodnadatta Formation, (c) Allaru Mudstone/Oodnadatta Formation against Bulldog Shale/Wallumbilla Formation, and (d) Bulldog Shale/Wallumbilla Formation against Cadna-owie Formation. The line illustrating the 1:1 relationship between apparent exhumation values from each pair of units analysed is shown.

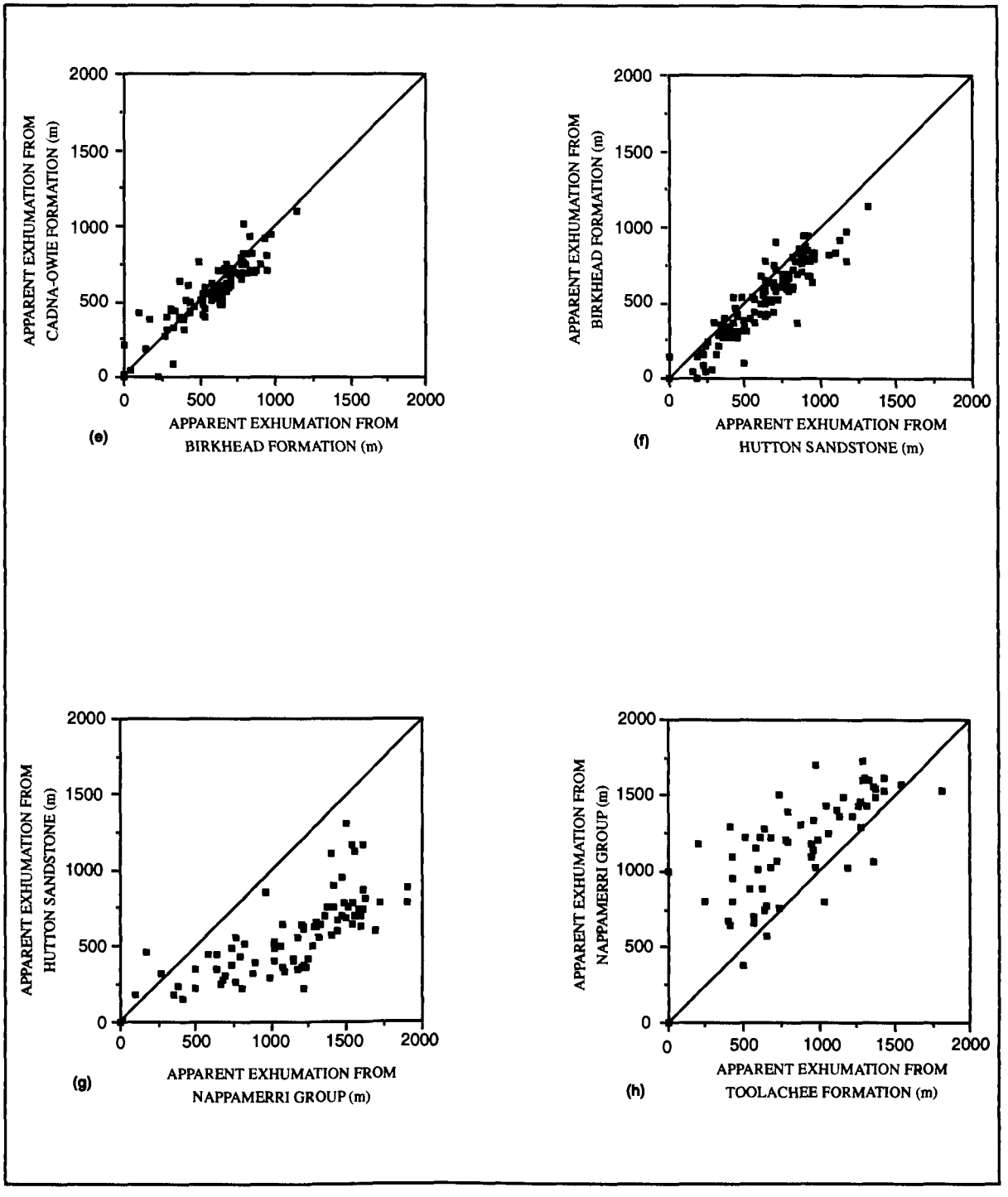

Figure 3.3. Continued. Crossplots of apparent exhumation (in metres) derived from bulk density in the stratigraphic units studied: (e) apparent exhumation from Cadna-owie Formation against those from the Birkhead Formation, (f) Birkhead Formation against Hutton Sandstone, (g) Hutton Sandstone against Nappamerri Group, and (h) Nappamerri Group against Toolachee Formation. The line illustrating the 1:1 relationship between apparent exhumation values from each pair of units analysed is shown.

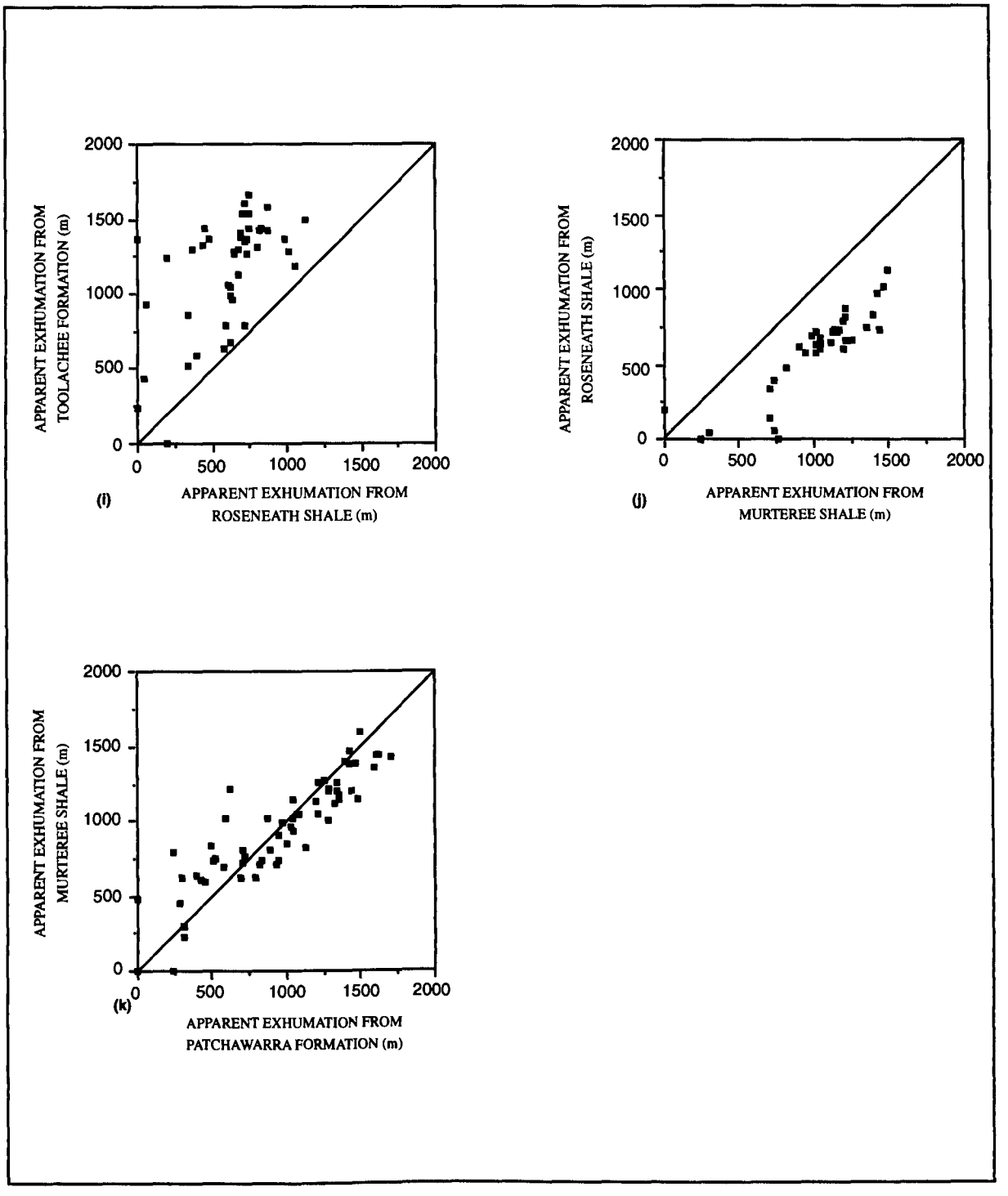

Figure 3.3. Continued. Crossplots of apparent exhumation (in metres) derived from bulk density in the stratigraphic units studied: (i) apparent exhumation from Toolachee Formation against those from the Roseneath Shale, (j) Roseneath Shale against Murteree Shale, and (k) Murteree Shale against Patchawarra Formation. The line illustrating the 1:1 relationship between apparent exhumation values from each pair of units analysed is shown.

Table 3.3. Correlation Between Apparent Exhumation Results from Bulk Density Log from the Stratigraphic Units Analysed*

	Winton Formation (W)	Mackunda Formation (M)	Allaru Mudstone/ Oodnadatta Formation (A)	Bulldog Shale/ Walhumbilla Formation (BW)	Cadna-owie Formation (C)	Birkhead Formation (B)	Hutton Sandstone (H)	Nappamerri Group (N)	Toolachee Formation (T)	Roseneath Shale (R)	Murteree Shale (MS)
Mackunda Formation (M)	W = 285 + 0.551M M = 159 + 0.255W										
No of Wells Having Both Units	27										
Coefficient of Correlation**	0.374										
t-statistic***	N										
Allaru Mudstone/ Oodnadatta Formation (A)	W = 142 + 0.529A A = 278 + 0.652W	M = 83 + 0.434A A = 405 + 0.501M									
No of Wells Having Both Units	26	29									
Coefficient of Correlation**	0.584	0.466									
t-statistic***	3.5	2.7									
Bulldog Shale/Walhumbilla Formation (BW)	W = 320 + 0.218BW BW = 427 + 0.190W	M = 11 + 0.594BW BW = 356 + 0.531M	A = 123 + 0.807BW BW = 197 + 0.613A								
No of Wells Having Both Units	26	29	29								
Coefficient of Correlation**	0.202	0.562	0.703								
t-statistic***	N	3.5	5.1								
Cadna-owie Formation (C)	W = 91 + 0.565C C = 471 + 0.311W	M = - 133 + 0.768C C = 522 + 0.319M	A = - 18 + 0.908C C = 374 + 0.471A	BW = - 45 + 0.951C C = 269 + 0.653BW							
No of Wells Having Both Units	27	31	31	37							
Coefficient of Correlation**	0.42	0.495	0.654	0.788							
t-statistic***	2.3	3.1	4.7	7.6							
Birkhead Formation (B)	W = 98 + 0.519B B = 453 + 0.383W	M = 11 + 0.547B B = 548 + 0.269M	A = 75 + 0.761B B = 375 + 0.482A	BW = 69 + 0.765B B = 316 + 0.586BW	C = 103 + 0.791B B = 21 + 0.999C						
No of Wells Having Both Units	27	29	29	36	107						
Coefficient of Correlation**	0.446	0.383	0.606	0.67	0.889						
t-statistic***	2.5	2.2	4	5.3	19.9						
Hutton Sandstone (H)	W = - 17 + 0.620H H = 172 + 0.516W	M = - 110 + 0.642H H = 590 + 0.399M	A = 75 + 0.655H H = 433 + 0.546A	BW = 70 + 0.652H H = 371 + 0.678BW	C = 28 + 0.772H H = 83 + 1.085C	B = - 14 + 0.863H H = 114 + 0.977B					
No of Wells Having Both Units	26	28	28	35	105	134					
Coefficient of Correlation**	0.566	0.506	0.598	0.665	0.915	0.918					
t-statistic***	3.4	3	3.8	5.1	23	26.6					
Nappamerri Group (N)	W = - 65 + 9.296N N = 734 + 1.654W	M = 134 + 0.217N N = 1130 + 0.411M	A = - 42 + 0.398N N = 883 + 0.916A	BW = 181 + 0.272N N = 1082 + 0.478BW	C = 65 + 0.356N N = 447 + 1.527C	B = - 33 + 0.429N N = 409 + 1.578B	H = 42 + 0.459N N = 374 + 1.331H				
No of Wells Having Both Units	9	11	11	18	59	82	83				
Coefficient of Correlation**	0.7	0.298	0.604	0.361	0.737	0.823	0.781				
t-statistic***	2.6	N	2.3	N	8.2	13	11.3				
Toolachee Formation (T)	W = - 20 + 0.310T T = 951 + 0.775W	M = 219 + 0.119T T = 1144 + 0.384M	A = 79 + 0.388T T = 1048 + 0.409A	BW = 446 + 0.074T T = 1161 + 0.135BW	C = 222 + 0.295T T = 425 + 1.298C	B = 115 + 0.396T T = 286 + 1.416B	H = 142 + 0.462T T = 178 + 1.374H	N = 602 + 0.647T T = - 76 + 0.818N			
No of Wells Having Both Units	15	15	14	20	60	79	79	64			
Coefficient of Correlation**	0.49	0.213	0.398	0.1	0.619	0.749	0.797	0.727			
t-statistic***	N	N	N	N	6	9.9	11.6	8.3			
Roseneath Shale (R)	W = 161 + 0.278R R = 428 + 0.502W	M = 464 - 0.144R R = 1449 - 2.293M	A = 388 + 0.333R R = 381 + 0.337A	BW = 688 - 0.189RR R =790 - 0.369BW	C = 542 + 0.122R R = 289 + 0.600C	B = 311 + 0.443R R = 199 + 0.727B	H = 411 + 0.412R R = 196 + 0.636H	N = 923 + 0.711R R = - 387 + 0.710N	T = 661 + 0.813R R = 126 + 0.412T		
No of Wells Having Both Units	11	9	9	9	29	37	39	24	44		
Coefficient of Correlation**	0.374	0.574	0.335	0.264	0.27	0.568	0.512	0.71	0.579		
t-statistic***	N	N	N	N	N	4.1	3.6	4.7	4.6		
Murteree Shale (MS)	W = - 105 + 0.382MS MS = 455 + 2.02W	M = 219 + 0.025MS MS = 1040 + 0.271M	A = - 44 + 0.415MS MS = 594 + 1.252A	BW = 167 + 0.214MS MS = 761 + 0.886BW	C = 9.916 + 0.440MS MS = 311 + 1.599C	B = - 91 + 0.543MS MS = 398 + 1.323B	H = - 23 + 0.562MS MS = 260 + 1.366H	N = 280 + 0.955MS MS = 65 + 0.724N	T = 1 + 0.985MS MS = 368 + 0.635T	R = - 150 + 0.732MS MS = 391 + 1.051R	
No of Wells Having Both Units	11	10	10	11	33	51	52	47	53	35	
Coefficient of Correlation**	0.878	0.082	0.72	0.436	0.839	0.847	0.876	0.831	0.791	0.878	
t-statistic***	5.5	N	2.9	N	8.6	11.2	12.8	10	9.2	10.5	
Patchawarra Formation (P)	W = - 37 + 0.297P P = 714 + 1.394W	M = 264 + 0.010P P = 1148.664 + 0.091M	A = 33 + 0.351P P = 827 + 0.726A	BW = 99 + 0.317P P = 644 + 1.023BW	C = 63 - 0.396P P = 343 + 1.559C	B = 5 + 0.452P P = 305 + 1.537B	H = 87 + 0.457P P = 212 + 1.463H	N = 429 + 0.765P P = 11 + 0.785N	T = 280 + 0.691P P = 251 + 0.778T	R = 105 + 0.406P P = 632 + 0.877R	MS = 207 + 0.705P P = - 99 + 1.113MS
No of Wells Having Both Units	13	12	12	14	51	71	72	61	69	41	62
Coefficient of Correlation**	0.633	0.031	0.505	0.57	0.786	0.834	0.818	0.775	0.733	0.597	0.886
t-statistic***	2.7	N	N	2.4	8.9	12.6	11.9	9.4	8.8	4.6	14.8

*Linear, best-fit, least-squares regression between apparent exhumation values derived from the 12 units analysed. Because there is no dependent variable, apparent exhumation from the shallower unit was regressed on that from the deeper unit (first or top equation) and vice versa (second or bottom equation).

**Coefficient of correlation between apparent exhumation values is derived from the two units in the examined wells.

***t-statistic for the coefficient of correlation. In most cases, comparison of the t-statistic with the one-tailed Student's t-distribution allows rejection of the null hypothesis (that the coefficients of correlation come from a population the mean of which is zero) at the 97.5% confidence level. N indicates that the coefficient of correlation is not significant at the stated confidence level.

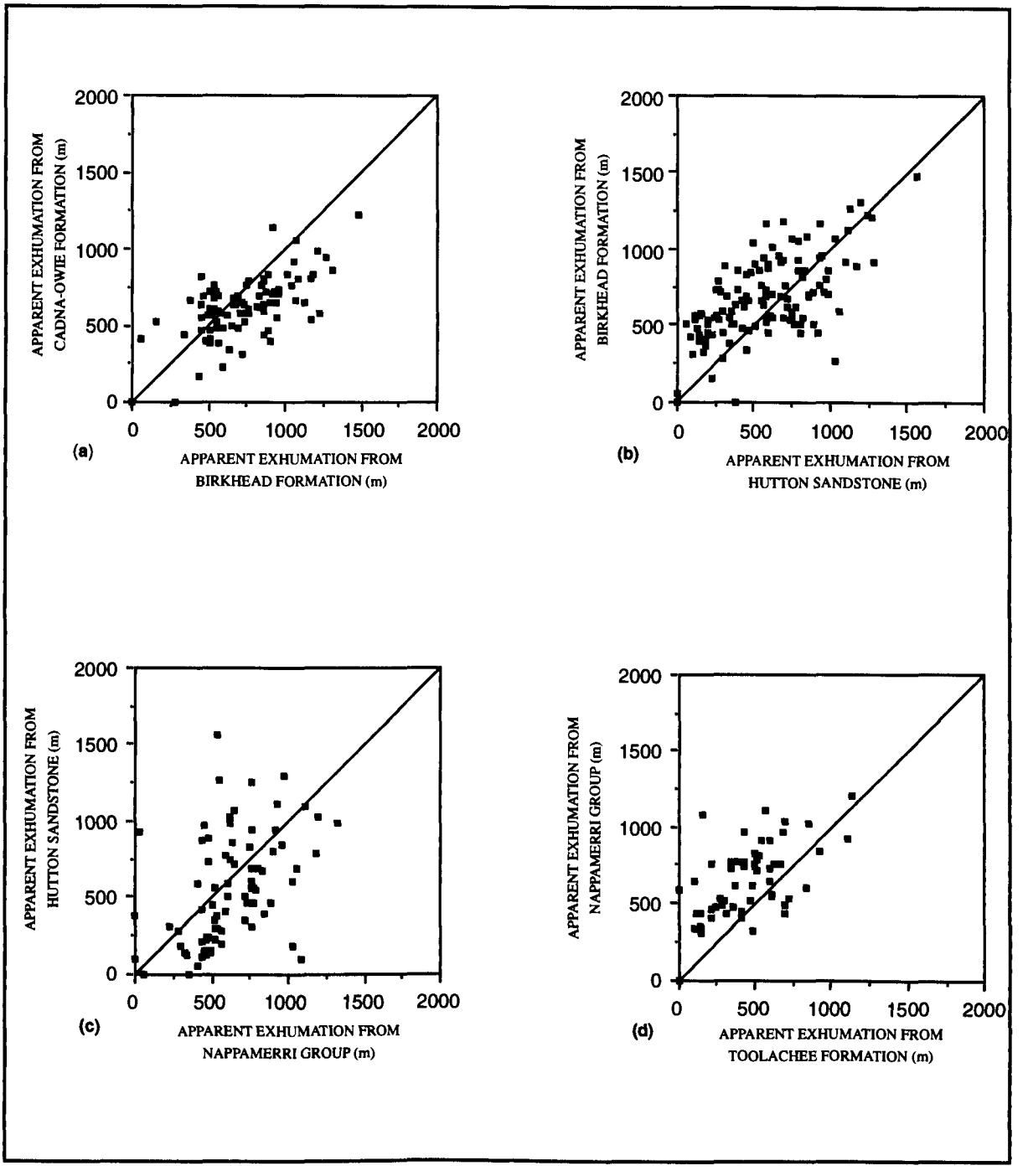

Figure 3.4. Crossplots of apparent exhumation (in metres) derived from neutron porosity in the stratigraphic units studied: (a) apparent exhumation from Cadna-owie against those from the Birkhead Formation, (b) Birkhead Formation against Hutton Sandstone, (c) Hutton Sandstone against Nappamerri Group, (d) Nappamerri Group against Toolachee Formation. The line illustrating the 1:1 relationship between apparent exhumation values from each pair of units analysed is shown.

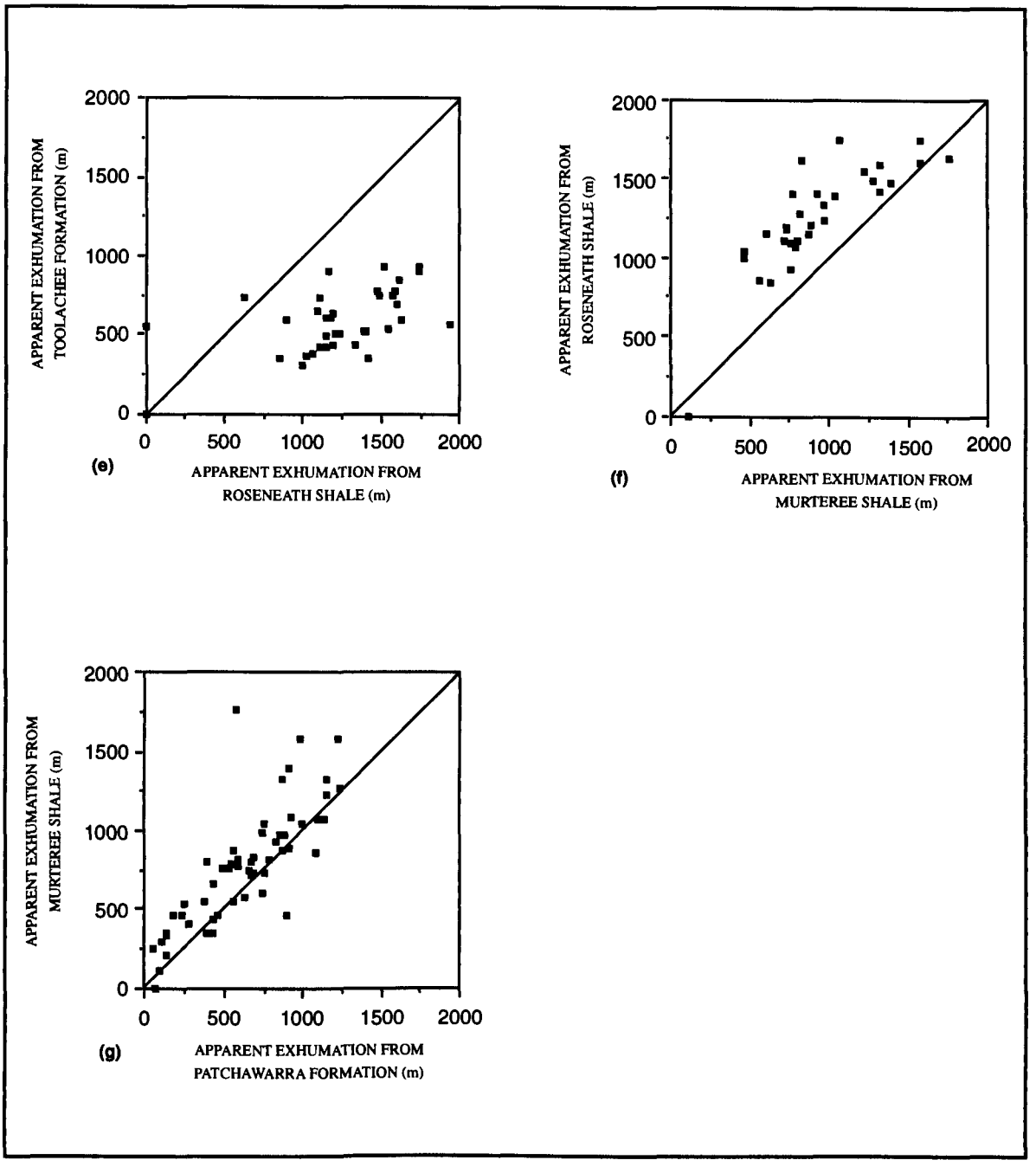

Figure 3.4. Continued. Crossplots of apparent exhumation (in metres) derived from neutron porosity in the stratigraphic units studied: (e) apparent exhumation from Toolachee Formation against those from the Roseneath Shale, (f) Roseneath Shale against Murteree Shale, and (g) Murteree Shale against Patchawarra Formation. The line illustrating the 1:1 relationship between apparent exhumation values from each pair of units analysed is shown.

Table 3.4. Correlation Between Apparent Exhumation Results Derived from Neutron Porosity Log from the Stratigraphic Units Analysed*

	Cadna-owie Formation (C)	Birkhead Formation (B)	Hutton Sandstone (H)	Nappamerri Group(N)	Toolachee Formation (T)	Roseneath Shale (R)	Murteree Shale (MS)
Birkhead Formation (B)	C = 288 + 0.459B B = 193 + 0.866C						
No of Wells Having Both Units	92						
Coefficient of Correlation**	0.63						
t-statistic***	7.7						
Hutton Sandstone (H)	C = 353 + 0.428H H = 31 + 0.967C	B = 372 + 0.539H H = 44 + 0.781B					
No of Wells Having Both Units	94	121					
Coefficient of Correlation**	0.642	0.648					
t-statistic***	8	9.3					
Nappamerri Group (N)	C = 197 + 0.562N N = 270 + 0.713C	B = 326 + 0.522N N = 302 + 0.495B	H = 193 + 0.575N N = 440 + 0.329H				
No of Wells Having Both Units	49	77	77				
Coefficient of Correlation**	0.633	0.507	0.434				
t-statistic***	5.6	5.1	4.2				
Toolachee Formation (T)	C = 456 + 0.279T T = 267 + 0.552C	B = 397 + 0.536T T = 166 + 0.521B	H = 336 + 0.421T T = 351 + 0.311H	N = 404 + 0.534T T = 72 + 0.592N			
No of Wells Having Both Units	49	69	71	57			
Coefficient of Correlation**	0.392	0.528	0.361	0.562			
t-statistic***	2.9	5.1	3.2	5			
Roseneath Shale (R)	C = 626 + 0.019R R = 1165 + 0.219C	B = 587 + 0.069R R = 1151 + 0.152B	H = 454 + 0.102R R = 1064 + 0.302H	N = 103 + 0.631R R = 333 + 1.327N	T = 254 + 0.267R R = 591 + 1.100T		
No of Wells Having Both Units	26	34	36	21	36		
Coefficient of Correlation**	0.063	0.1	0.176	0.914	0.542		
t-statistic***	N	N	N	9.8	3.8		
Murteree Shale (MS)	C = 180 + 0.366MS MS = 201 + 1.497C	B = 357 + 0.276MS MS = 308 + 0.811B	H = 131 + 0.416MS MS = 459 + 0.704H	N = 213 + 0.520MS MS = 60 + 1.305N	T = 131 + 0.429MS MS = 161 + 1.348T	R = 538 + 0.770MS MS = 173 + 0.880R	
No of Wells Having Both Units	26	48	50	45	45	30	
Coefficient of Correlation**	0.74	0.472	0.541	0.824	0.76	0.822	
t-statistic***	5.4	3.6	4.5	9.5	7.7	7.6	
Patchawarra Formation (P)	C = 322 + 0.284P P = 133 + 1.359C	B = 370 + 0.359P P = 101 + 1.013B	H = 230 + 0.366P P = 394 + 0.710H	N = 362 + 0.374P P = 50 + 1.128N	T = 172 + 0.422P P = 208 + 1.120T	R = 996 + 0.231P P = 588 + 0.205R	MS = 192 + 0.926P P = 92 + 0.693MS
No of Wells Having Both Units	43	66	68	56	61	36	56
Coefficient of Correlation**	0.621	0.602	0.509	0.649	0.687	0.216	0.801
t-statistic***	5.1	6	4.8	6.3	7.3	N	9.8

* Linear, best-fit, least-squares regression between apparent exhumation values derived from the 12 units analysed. Because there is no dependent variable, apparent exhumation from the shallower unit was regressed on that from the deeper unit (first or top equation) and vice versa (second or bottom equation).

** Coefficient of correlation between apparent exhumation values is derived from the two units in the examined wells.

***t-statistic for the coefficient of correlation. In most cases, comparison of the t-statistic with the one-tailed Student's t-distribution allows rejection of the null hypothesis (that the coefficients of correlation come from a population the mean of which is zero) at the 97.5% confidence level. N indicates that the coefficient of correlation is not significant at the stated confidence level.

3.4 Comparison of Apparent Exhumation Results from Different Stratigraphic Units Between the Cooper and Eromanga Basins

All four logs, but most noticeably the density log results, suggest consistently higher apparent exhumation results from the Nappamerri Group than from the Hutton Sandstone (Figure 3.1g, 3.2g, 3.3g and 3.4c). The Hutton Sandstone is the lowermost unit analysed in the Eromanga Basin, and the Nappamerri Group is the uppermost unit analysed in the Cooper Basin. If apparent exhumation is greater for the Cooper Basin, than for the Eromanga Basin, the Cooper Basin must, at least in some places, have attained its maximum burial-depth prior to the deposition of Eromanga Basin.

In order to further investigate this possible implication, the mean apparent exhumation value determined from the seven Eromanga Basin units was compared with the mean value from the five Cooper Basin units (Figure 3.5). In all four cases, mean apparent exhumation from Cooper Basin units is consistently greater than that from the Eromanga Basin units. Again this tendency is most developed in the density log data, and least developed in the neutron log data. Inspection of the raw log data plotted against depth (Figures 2.15 - 2.18) does indeed suggest that the units analysed in the Cooper Basin exhibit a greater spread (on the depth axis) than those in the Eromanga Basin, which implies that this phenomenon is not simply an artefact of the positioning of the normal compaction relation.

It is difficult to ascribe errors limits to the apparent exhumation values that have been determined. For individual units, and for the mean results based thereupon, systematic errors in the results are dependent on the extent to which the assumptions in the method are violated, principally, the extent to which units do not follow the normal compaction relation with burial in all wells, and the extent to which compaction is reversed by subsequent exhumation. Measurement errors are likely to be insignificant in comparison with the potential systematic errors. The spread of the exhumation values around the one-to-one relation for units within the Eromanga Basin gives an indication of the errors in exhumation values from these units, and, although no detailed statistical analysis has been undertaken, a value of ± 200 m seems

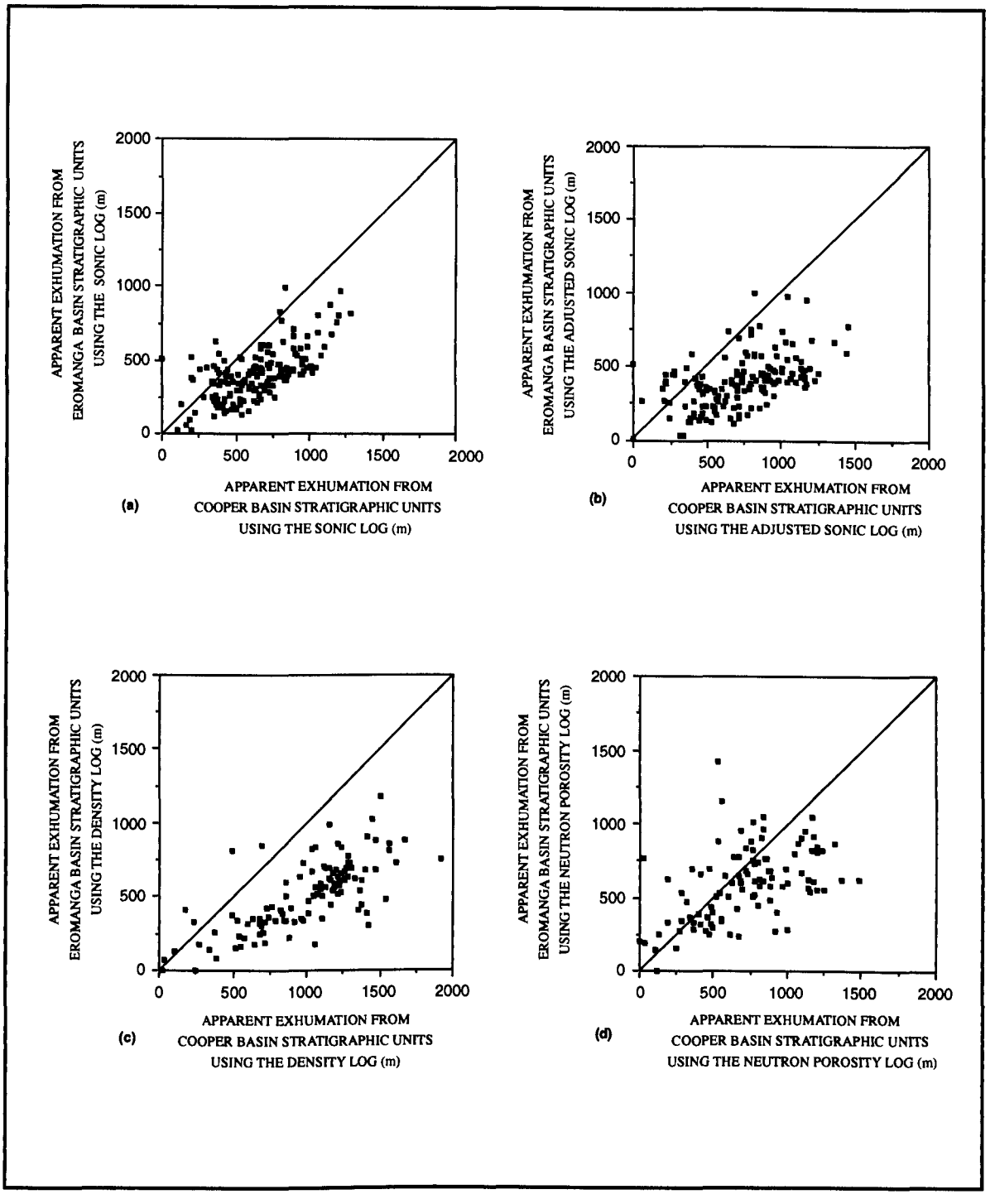

Figure 3.5. Crossplots of mean apparent exhumation (in metres) from Eromanga Basin units against mean apparent exhumation (in metres) from Cooper Basin units derived from the (a) sonic, (b) adjusted sonic, (c) density, and (d) neutron porosity logs. The line illustrating the 1:1 relationship between apparent exhumation values from each pair of units analysed is shown.

reasonable from inspection of Figures 3.1-3.4. An indication of the errors in the mean exhumation values derived from the units analysed in the Cooper and Eromanga Basins can be obtained by considering Figure 3.5. In the absence of major lateral tectonic movement (as may be reasonably assumed in the relatively tectonically quiescent Cooper-Eromanga Basins), any exhumation to which the Cooper Basin was subjected must also have affected the Eromanga Basin. Hence in the absence of errors, exhumation from units in Eromanga Basin could not exceed that from units in the Cooper Basin. In the case of the data from the neutron log, the tendency for Cooper Basin units to yield greater apparent exhumation values than those of the Eromanga Basin is thus within the demonstrable error limits of the data. In the case of the density, and to a lesser extent the sonic and the adjusted sonic logs, the tendency for Cooper Basin units to yield greater apparent exhumation values than those of the Eromanga Basin is beyond the demonstrable error limits of the data. It is thus inferred that some areas of the Cooper Basin did reach maximum burial-depth prior to the deposition of the Eromanga Basin sequence, the location and structural significance of these areas is discussed later in this chapter.

3.5 Comparison of Apparent Exhumation Results from the Different Logs

As discussed in Chapter 2, there is a reasonable theoretical basis for using all the porosity logs in studies of maximum burial-depth/exhumation, and not just the sonic log/sonic velocities, to which previous studies have generally been restricted. One of the purposes of this study was to analyse the suitability of the density and neutron logs for maximum burial-depth/exhumation analysis. The use of the sonic log is widely accepted in such work. Hence if the other porosity logs yield comparable results to the sonic log data, their use is justified. In order to test the viability of the density and neutron logs, the mean apparent exhumation values for the Eromanga Basin sequence and from the Cooper Basin sequence derived from each of the porosity logs were crossplotted against each other (Figure 3.6). The correlation between the exhumation values from the sonic and the adjusted sonic is excellent. It is significant that the reference wells used for determining the normal compaction relationships for the above two

logs are almost always the same (Tables 2.1 and 2.2), and that both data are based on the same physical property (sonic velocity), albeit measured at different frequencies. There is generally a good correlation between exhumation values from the different logs, with correlation coefficients of 0.597 - 0.955, and the use of the porosity logs is considered to be justified. The relationships and the correlations between mean apparent exhumation results from the different logs are summarised in Table 3.5.

Much of the scatter between the different logs can probably be attributed to the fact that neutron and density log coverage is not as extensive as the sonic and the adjusted sonic log coverage. Hence the reference wells for the normal compaction relations for a number of units were necessarily different in the different logs. This is probably responsible for the offset from the one-to-one relation of the crossplot of:

- sonic (and adjusted sonic) and neutron log from Eromanga Basin units;
- sonic (and adjusted sonic) and density log from Cooper Basin units; and
- density and neutron log from Cooper Basin units.

Random scatter in the crossplots is presumably linked to the different ways in which the different logs see porosity, thus compaction. For example, the sonic log, unlike the other two porosity logs, does not tend to see secondary, fracture or vugular porosity. For this reason alone, the sonic log is considered likely to be the most reliable indicator of maximum burial-depth/exhumation. However, differences in the ways the three porosity logs see porosity are considered likely to generate less differences between exhumation values than differences in the reference wells, and thus placement of the normal compaction relation.

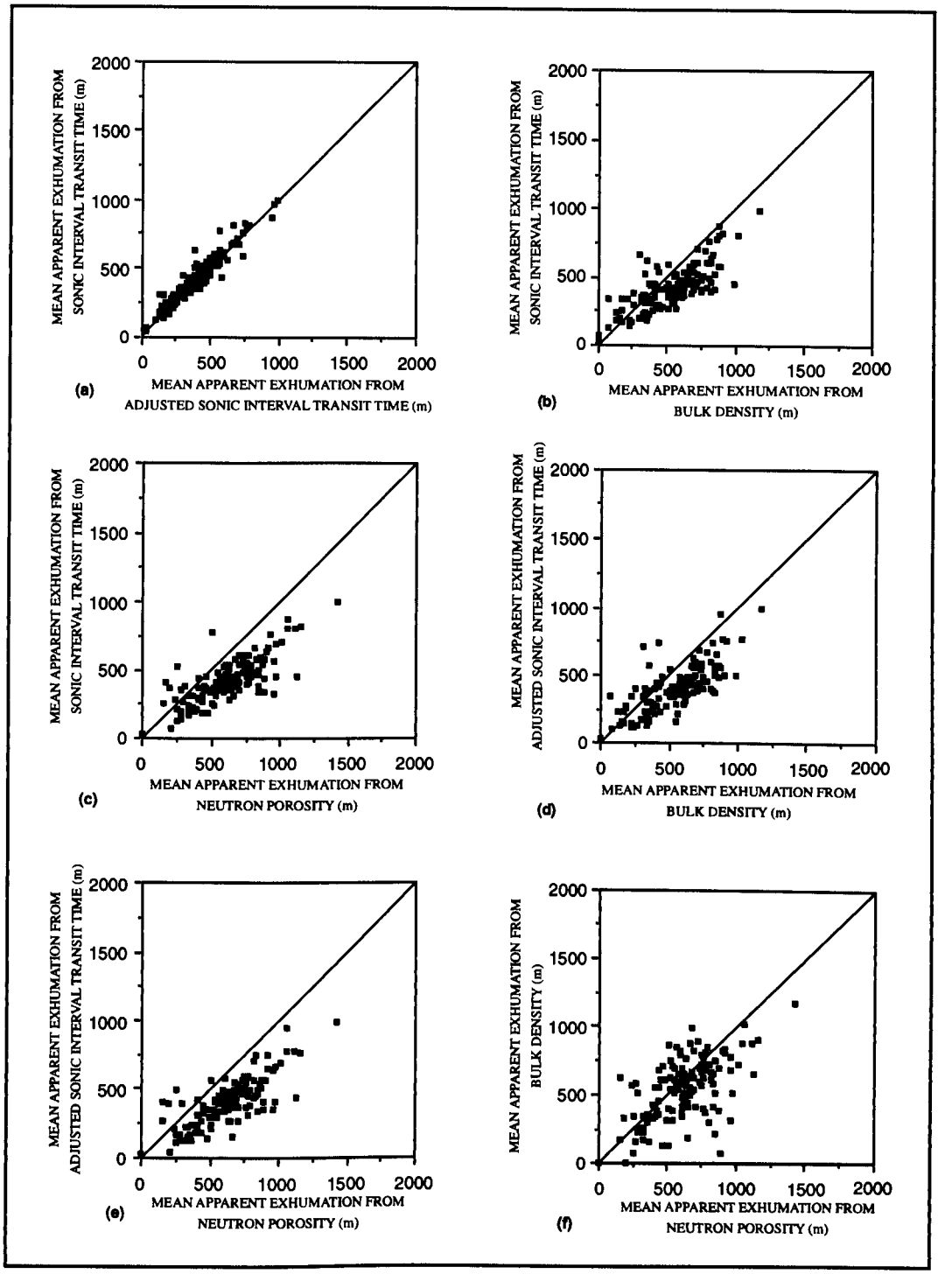

Figure 3.6a. Comparison of exhumation results from the different logs. Crossplots of mean apparent exhumation (in metres) derived from Eromanga Basin units (a) apparent exhumation from sonic interval transit time against those from the adjusted interval transit time, (b) apparent exhumation from sonic interval transit time against bulk density, (c) apparent exhumation from sonic interval transit time against neutron porosity, (d) apparent exhumation from adjusted sonic interval transit time against bulk density, (e) apparent exhumation from adjusted sonic interval transit time against neutron porosity, and (f) apparent exhumation from bulk density against neutron porosity. The line illustrating the 1:1 relationship between apparent exhumation values from each pair of units analysed is shown.

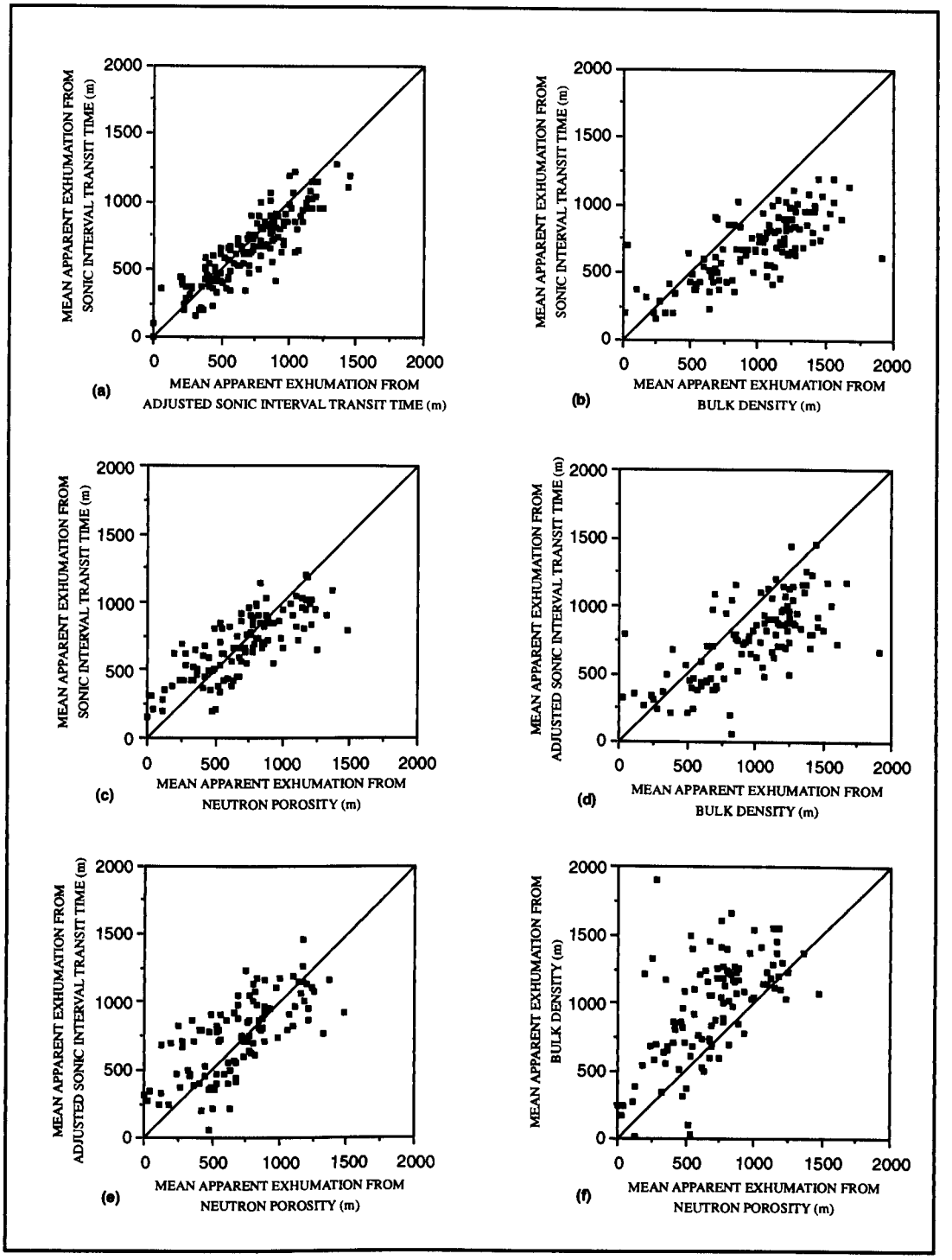

Figure 3.6b. Comparison of exhumation results from the different logs. Crossplots of mean apparent exhumation (in metres) derived from Cooper Basin units (a) apparent exhumation from sonic interval transit time against those from the adjusted interval transit time, (b) apparent exhumation from sonic interval transit time against bulk density, (c) apparent exhumation from sonic interval transit time against neutron porosity, (d) apparent exhumation from adjusted sonic interval transit time against bulk density, (e) apparent exhumation from adjusted sonic interval transit time against neutron porosity, and (f) apparent exhumation from bulk density against neutron porosity. The line illustrating the 1:1 relationship between apparent exhumation values from each pair of units analysed is shown.

Table 3.5a. Correlation Between Mean Apparent Exhumation Results in Eromanga Basin for the Different Logs Analysed*

	Adjusted Sonic Log (Δt_{adj})	Bulk Density Log (ρ_b)	Neutron Porosity (Φ_N)
Sonic Log (Δt)	$\Delta t = 51 + 0.932\Delta t_{adj}$	$\Delta t = 125 + 0.551\rho_b$	$\Delta t = 98 + 0.529\Phi_N$
	$\Delta t_{adj} = -15 + 0.978\Delta t$	$\rho_b = 91 + 1.061\Delta t$	$\Phi_N = 135 + 1.136\Delta t$
Coefficient of Correlation**	0.955	0.764	0.775
Adjusted Sonic Log (Δt_{adj})		$\Delta t_{adj} = 96 + 0.568\rho_b$	$\Delta t_{adj} = 54 + 0.564\Phi_N$
		$\rho_b = 138 + 0.994\Delta t_{adj}$	$\Phi_N = 190 + 1.070\Delta t_{adj}$
Coefficient of Correlation**		0.751	0.777
Bulk Density Log (ρ_b)			$\rho_b = 189 + 0.572\Phi_N$
			$\Phi_N = 279 + 0.623\rho_b$
Coefficient of Correlation**			0.597

Table 3.5b. Correlation Between Mean Apparent Exhumation Results in Cooper Basin for the Different Logs Analysed*

	Adjusted Sonic Log (Δt_{adj})	Bulk Density Log (ρ_b)	Neutron Porosity (Φ_N)
Sonic Log (Δt)	$\Delta t = 122 + 0.751\Delta t_{adj}$	$\Delta t = 229 + 0.467\rho_b$	$\Delta t = 289 + 0.560\Phi_N$
	$\Delta t_{adj} = 38 + 1.027\Delta t$	$\rho_b = 176 + 1.169\Delta t$	$\Phi_N = -11 + 1.047\Delta t$
Coefficient of Correlation**	0.878	0.739	0.766
Adjusted Sonic Log (Δt_{adj})		$\Delta t_{adj} = 246 + 0.517\rho_b$	$\Delta t_{adj} = 315 + 0.616\Phi_N$
		$\rho_b = 304 + 0.886\Delta t_{adj}$	$\Phi_N = 110 + 0.787\Delta t_{adj}$
Coefficient of Correlation**		0.677	0.696
Bulk Density Log (ρ_b)			$\rho_b = 469 + 0.721\Phi_N$
			$\Phi_N = 213 + 0.501\rho_b$
Coefficient of Correlation**			0.601

*Linear, best-fit, least-squares regression between apparent exhumation values derived from the logs used in compaction analysis. Because there is no dependent variable, apparent exhumation from one log was regressed on that from the rest (first or top equation) and vice versa (second or bottom equation).
**Coefficient of correlation between apparent exhumation values is derived from the two logs in the examined wells.

3.6 Apparent Exhumation in the Eromanga Basin

Maps of apparent exhumation derived from individual units in the Eromanga Basin sequence all show a very similar pattern (Figure 3.7). The map of apparent exhumation based on the mean of the Eromanga Basin units analysed shows the same pattern. It is this 'mean map' which is discussed below. The 'mean map' is considered to give the best description of the amount of Late Cretaceous - Tertiary exhumation of the area (Figure 3.8) because any sedimentological and/or diagenetic effects that might cause variation from the normal Δt/depth trend in individual units, and consequently violate the assumption that all units follow the normal compaction trend with burial depth, will tend to be reduced. Such variations are considered to be of second order with respect to burial-depth because of the statistically significant similarity between apparent exhumation values from the seven units.

The Patchawarra and Tenappera Troughs are at/or near maximum burial-depth, as they are the south-western and southern margins of the area. The boundary between the Patchawarra Trough and the anticlinal Gidgealpa-Merrimelia-Innamincka (GMI) Trend is apparent on the map of Late Cretaceous - Tertiary exhumation. This suggests that the GMI Trend has seen Late Cretaceous - Tertiary structural development. This evidence for Late Cretaceous - Tertiary exhumation of the GMI Trend is supported by structural interpretation of seismic data across the Merrimelia Field in which early Tertiary folding accompanied by faulting and erosion are apparent (Moore and Pitt, 1984). The evidence presented here suggests that the Eromanga Basin sequence (and thus also the Cooper Basin sequence) has been exhumed approximately 300 m from maximum burial-depth along the GMI Trend since Cenomanian times.

The Nappamerri Trough is separated from the Patchawarra Trough by the GMI Trend. Unlike the Patchawarra Trough, significant Late Cretaceous - Tertiary exhumation has occurred in the Nappamerri Trough. Late Cretaceous - Tertiary exhumation from maximum burial-depth increases from approximately 300 m in the south and west of the Nappamerri Trough to 600 m in its north-eastern/Queensland part. Vincent *et al.* (1985) argued, on essentially geochemical grounds, that the oil in the Hutton sandstone in the Jackson-Naccowlah area of Queensland

was sourced from the Jurassic of the Nappamerri Trough. The recognition of significant Late Cretaceous - Tertiary exhumation in the Nappamerri Trough has important implications for such models.

Broadly speaking, exhumation increases eastwards from the Patchawarra Trough, through the GMI Trend and Nappamerri Trough into Queensland, with values of approximately 600 m in the Jackson-Naccowlah area. These results are consistent with structural/stratigraphic interpretations which suggest that exhumation increases eastwards towards the Dividing Range (Shaw, 1991). Indeed, Shaw (1991) suggested that the uplifted eastern margin of the Eromanga Basin was the source of the Tertiary sediments deposited within the downwarps in the basin. Late Cretaceous - Tertiary exhumation reaches approximately 1 km, north of the Jackson-Naccowlah area. The other area of maximum Late Cretaceous - Tertiary exhumation, which also reaches approximately 1 km, lies near the extreme north-eastern boundary of South Australia, in the vicinity of the Curalle-1 well. This is beyond the limit of the Permian sequence of the Cooper Basin but still within the Eromanga Basin. The Betoota, Curalle and Morney anticlinal domes in this area show significant erosional thinning of the Winton Formation, but negligible thinning of the underlying Eromanga sequence (Moore and Pitt, 1984), which is consistent with the significant exhumation to which the area is believed to have been subjected. Shaw (1991) describes the Curalle Dome as a conspicuous anticlinal feature breached by reactivated basement faulting.

Exhumation witnessed by the units analysed in the Eromanga Basin (Figure 3.8) is, to some extent, the complement of Tertiary thickness (Figure 3.9). The Tertiary is absent or very thin over the maxima in exhumation to the north of the Jackson-Naccowlah area and in the vicinity of the Curalle-1 well. The region of lower exhumation between these two maxima (Windorah Trough) corresponds to a minor depocentre which holds in excess of 100 m of Tertiary sediments. The Patchawarra Trough is part of the major Tertiary depocentre of the area (with up to 300 m of Tertiary sediments), and this is consistent with the interpretation that it is currently at maximum burial-depth. This Tertiary depocentre does, however, extend south of the Patchawarra Trough, extending over the GMI Trend and into the southern part of the

Nappamerri Trough. The trend of the Tertiary depocentre follows the Patchawarra Trough, and may have been inherited from it. However, the structural grain of the GMI Trend and Nappamerri Trough appears to have exerted little influence on the Tertiary depocentre.

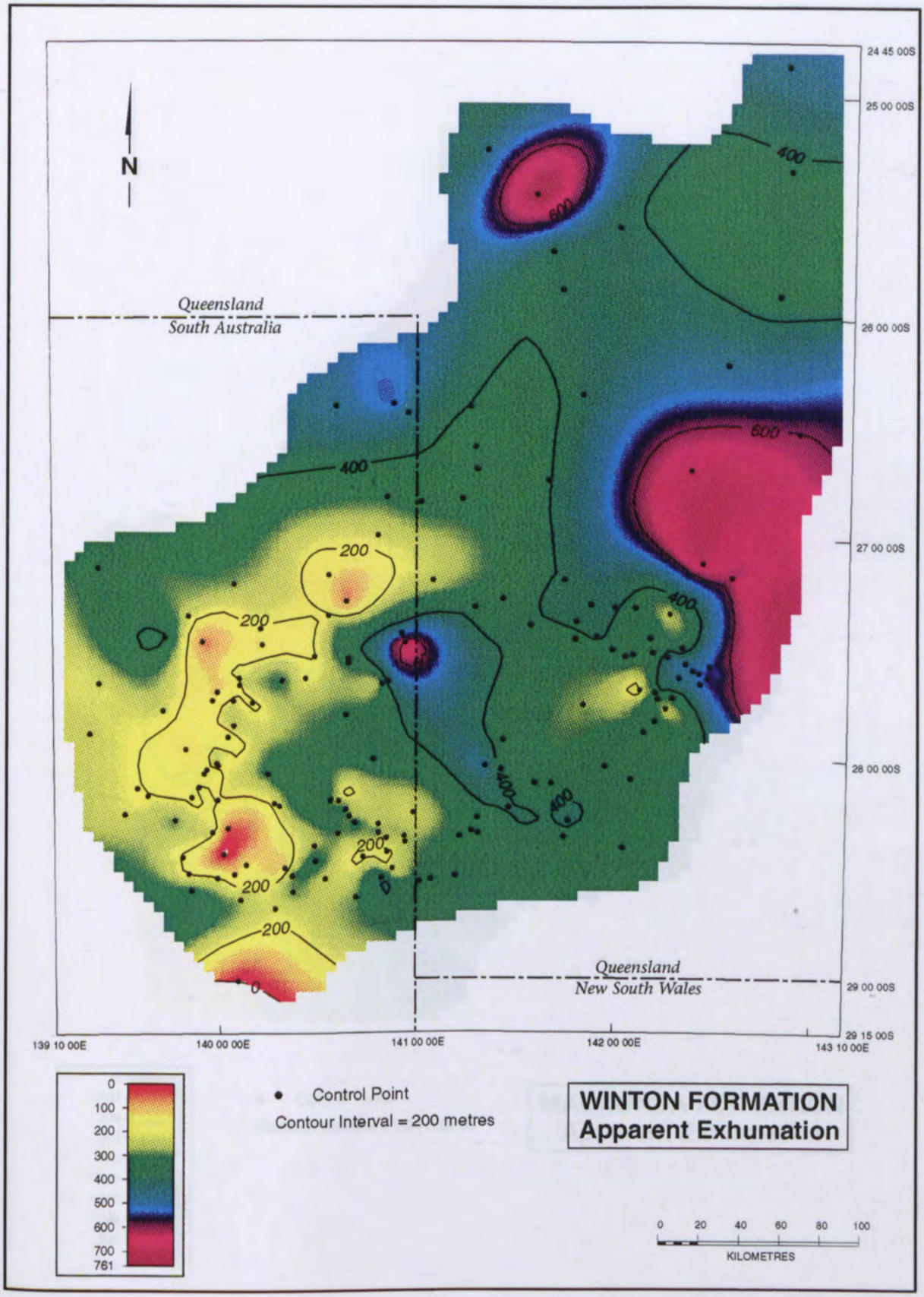

Figure 3.7. Apparent exhumation based on sonic log velocity in the Winton Formation. Well control points are also shown.

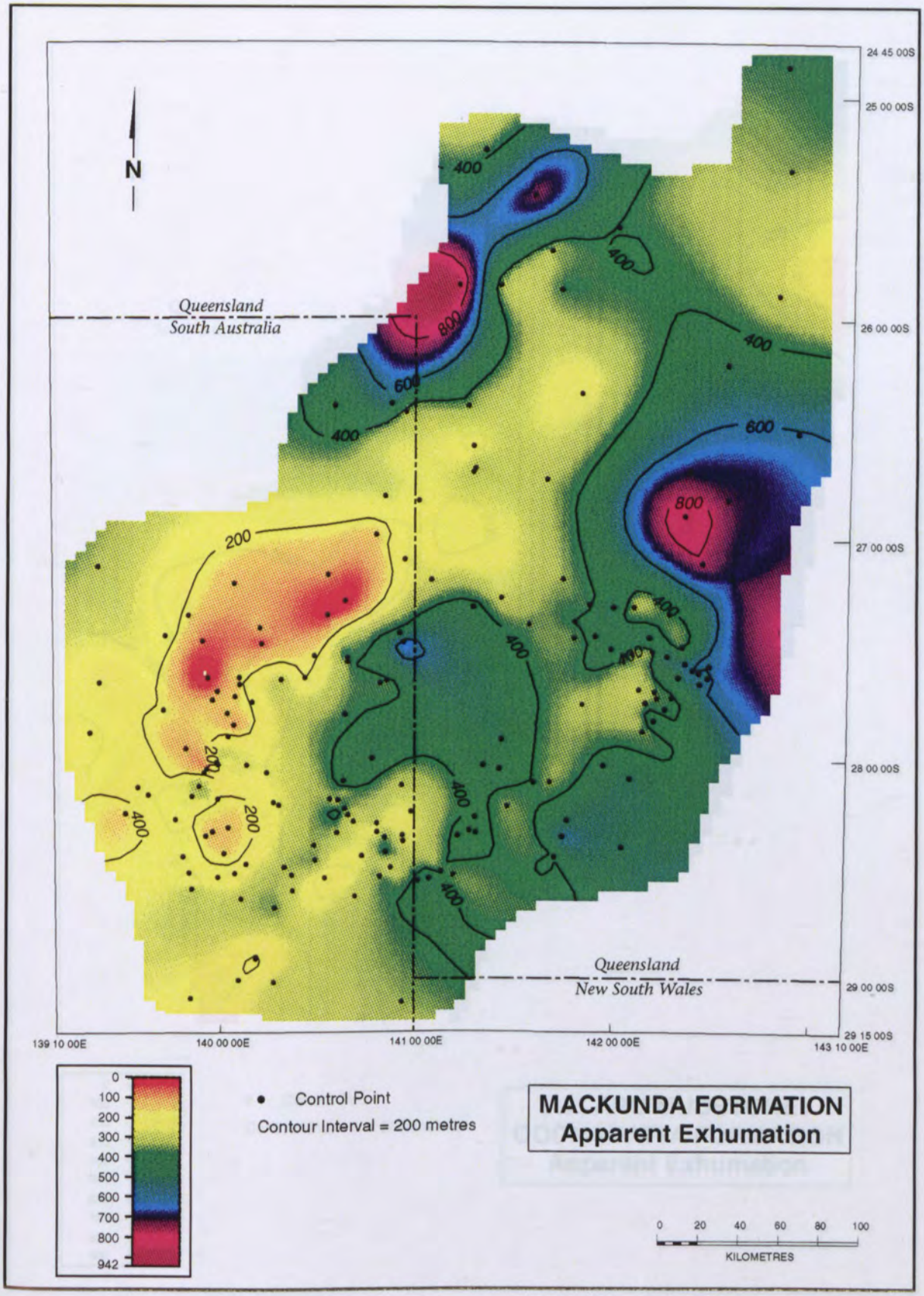

Figure 3.7. Continued. Apparent exhumation based on sonic log velocity in the Mackunda Formation. Well control points are also shown.

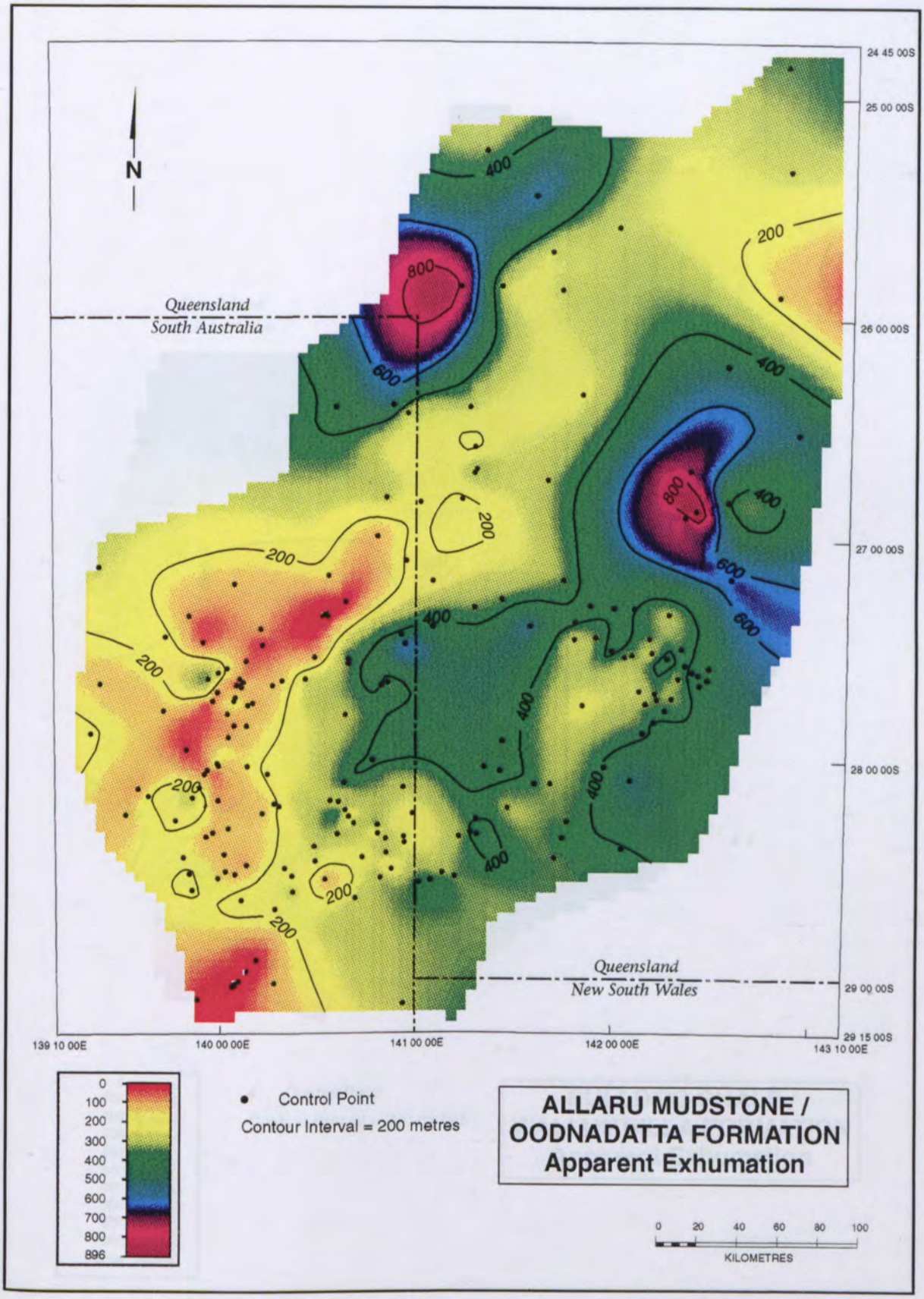

Figure 3.7. Continued. Apparent exhumation based on sonic log velocity in the Allaru Mudstone/Oodnadatta Formation. Well control points are also shown.

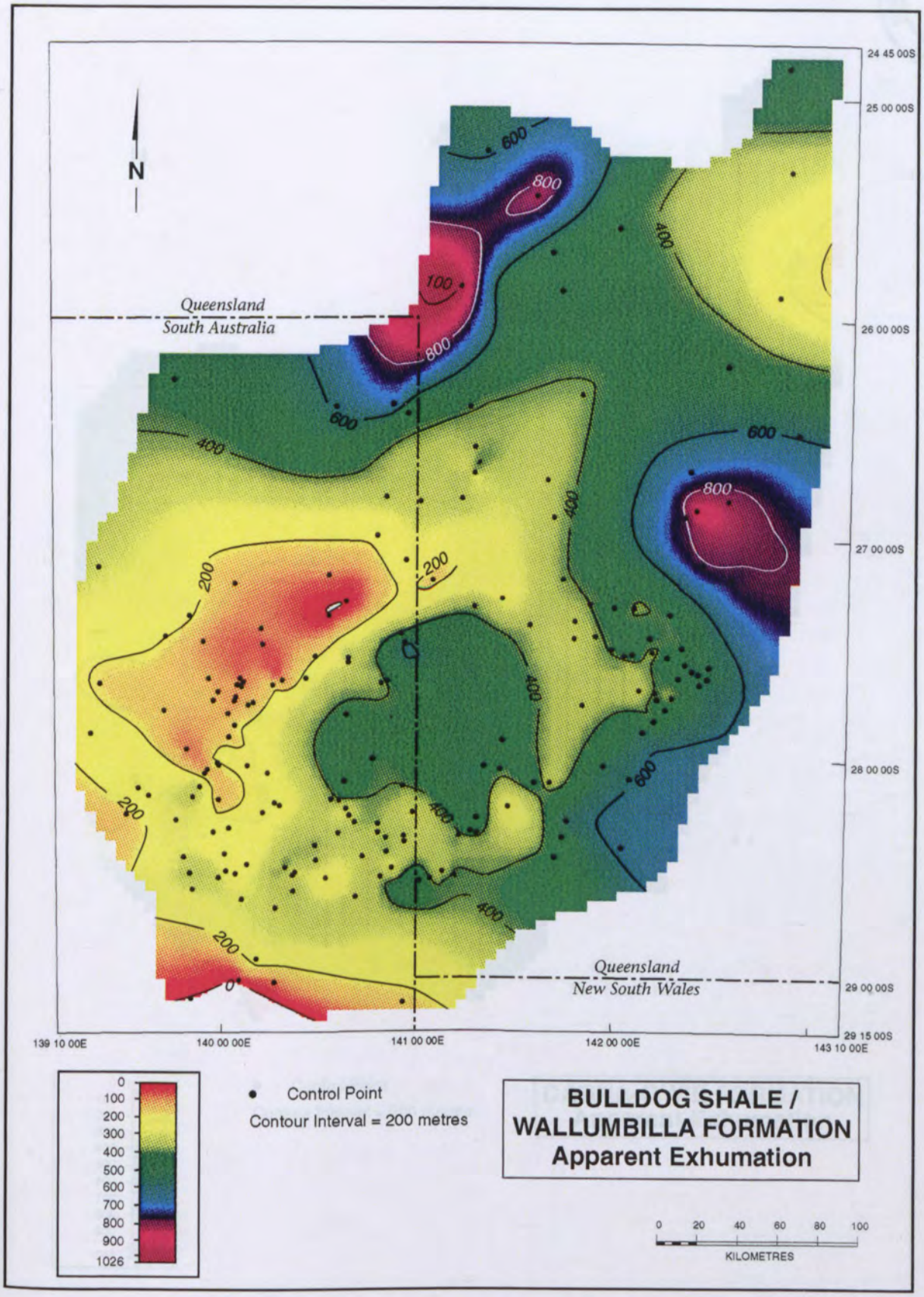

Figure 3.7. Continued. Apparent exhumation based on sonic log velocity in the Bulldog Shale/Wallumbilla Formation. Well control points are also shown.

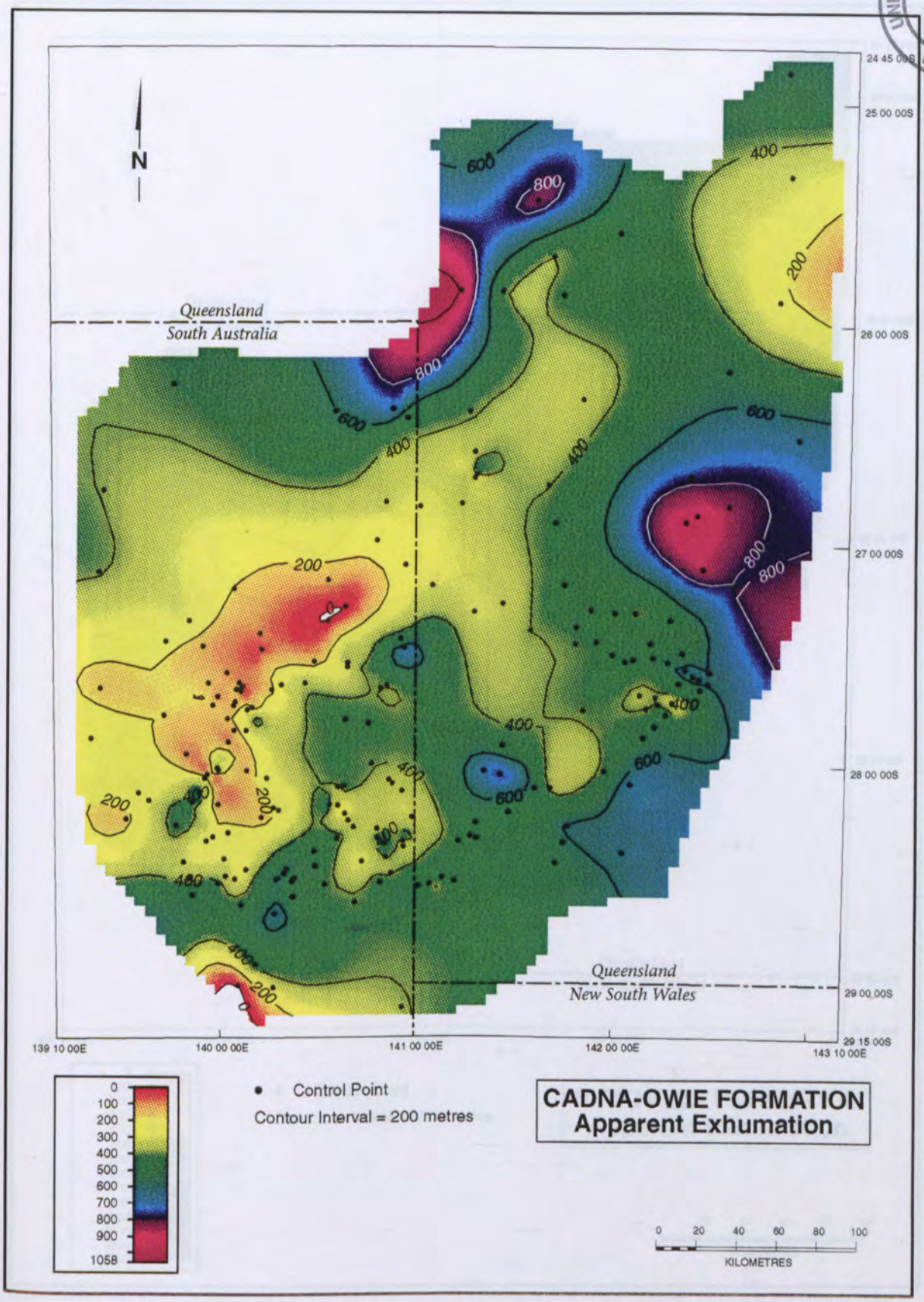

Figure 3.7. Continued. Apparent exhumation based on sonic log velocity in the Cadna-owie Formation. Well control points are also shown.

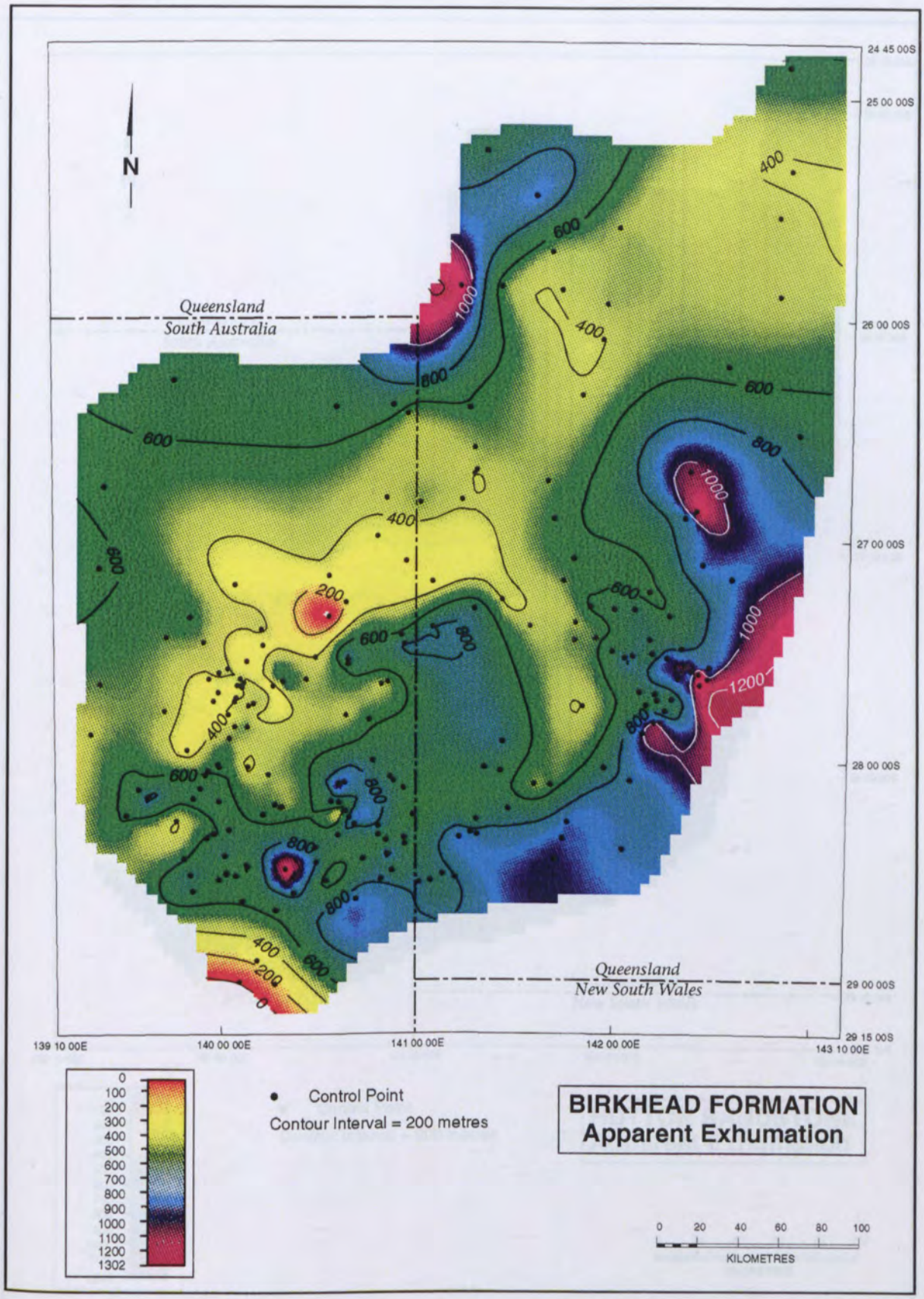

Figure 3.7. Continued. Apparent exhumation based on sonic log velocity in the Birkhead Formation. Well control points are also shown.

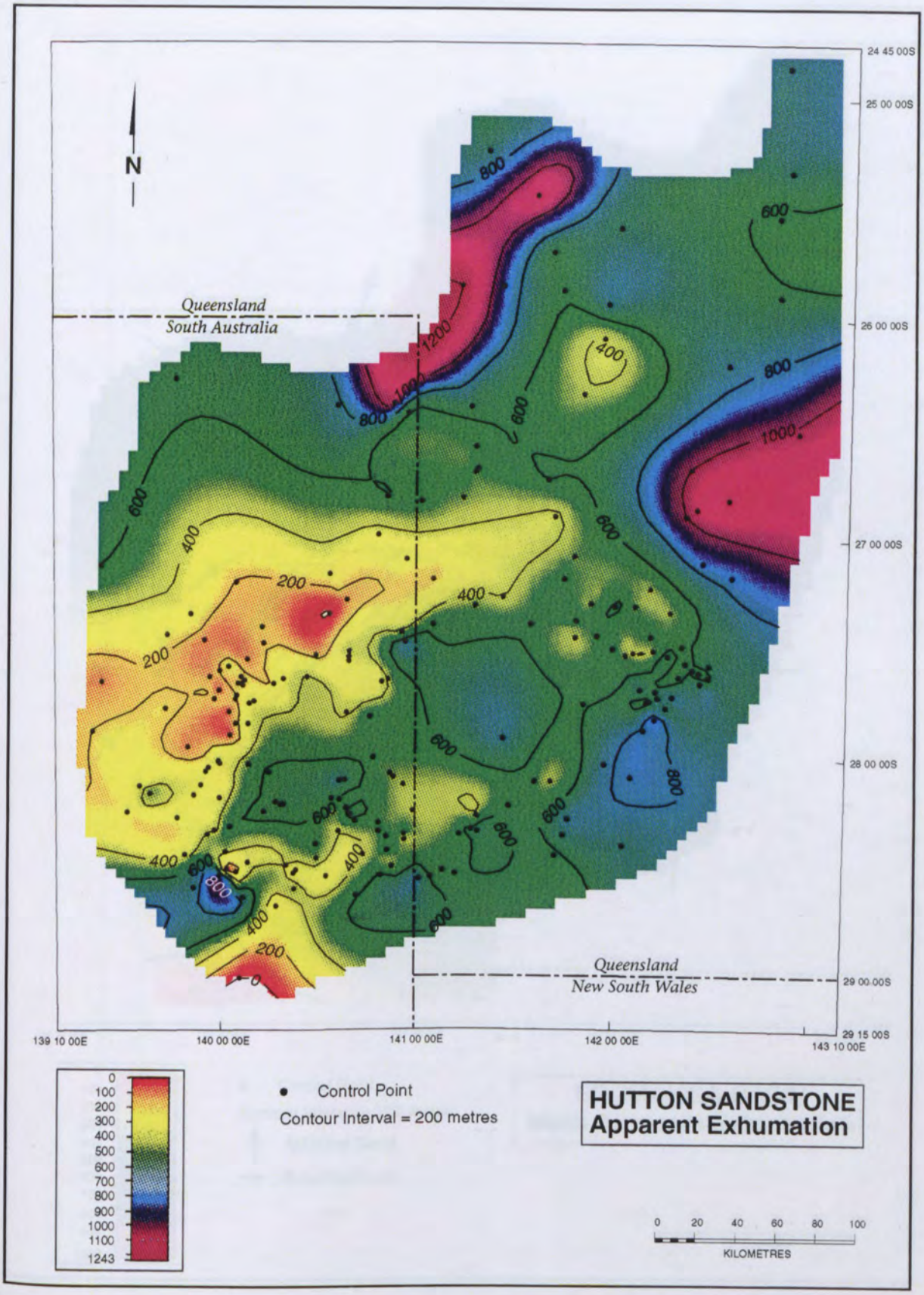

Figure 3.7. Continued. Apparent exhumation based on sonic log velocity in the Hutton Sandstone. Well control points are also shown.

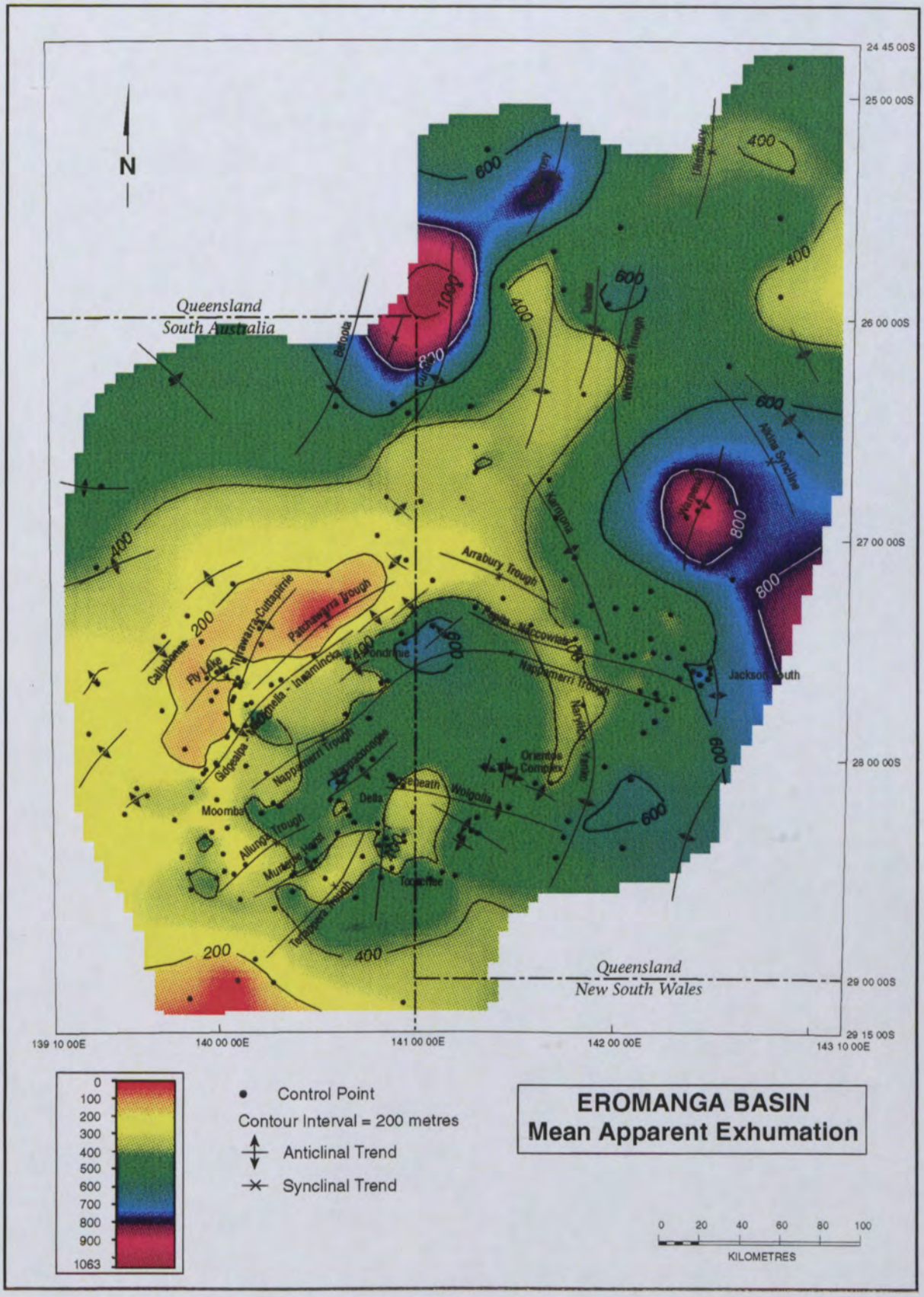

Figure 3.8. Mean apparent exhumation based on sonic log velocity in Eromanga Basin stratigraphic units. Well control points and tectonic elements are also shown.

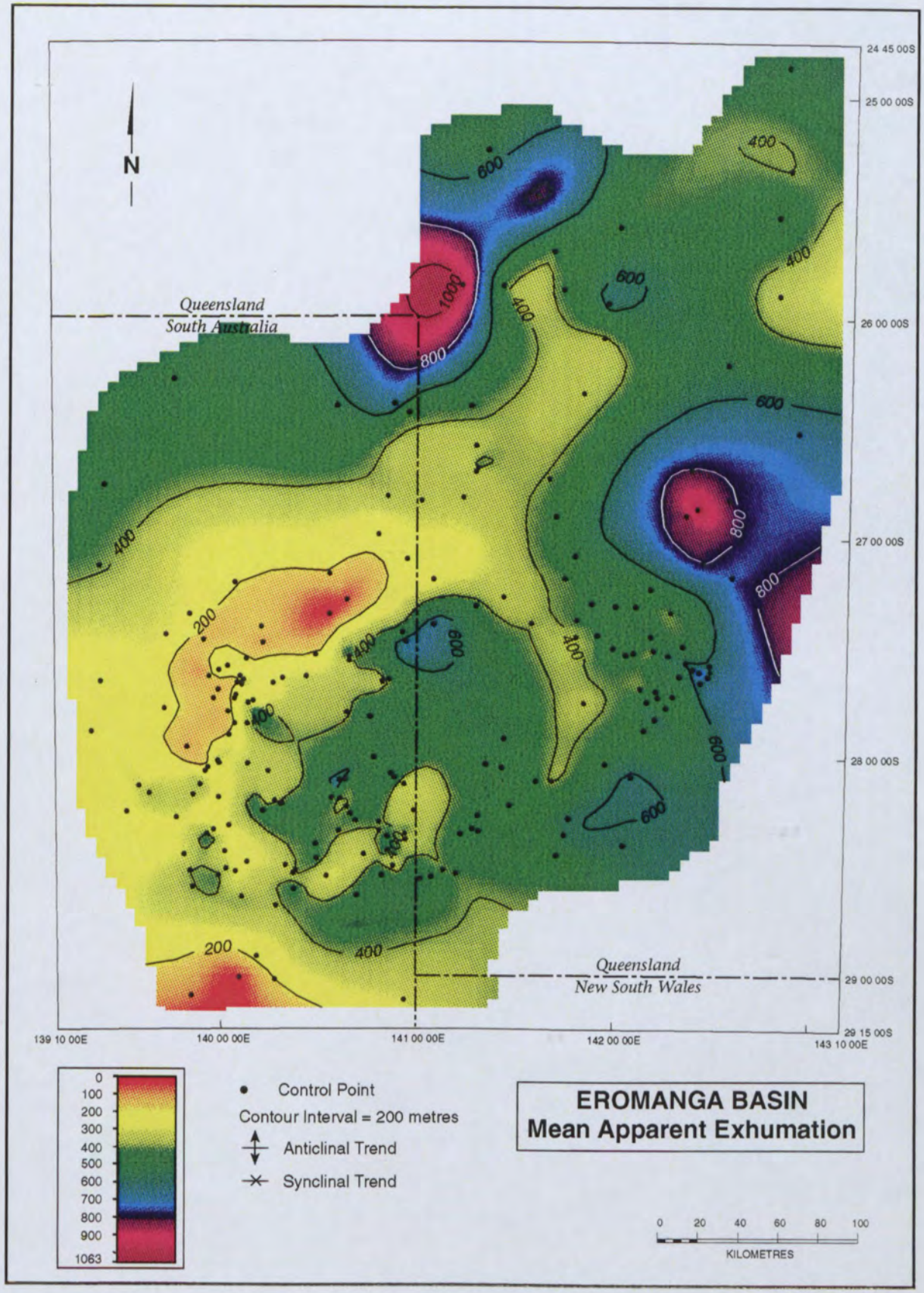

Figure 3.8. Mean apparent exhumation based on sonic log velocity in Eromanga Basin stratigraphic units. Well control points and tectonic elements are also shown.

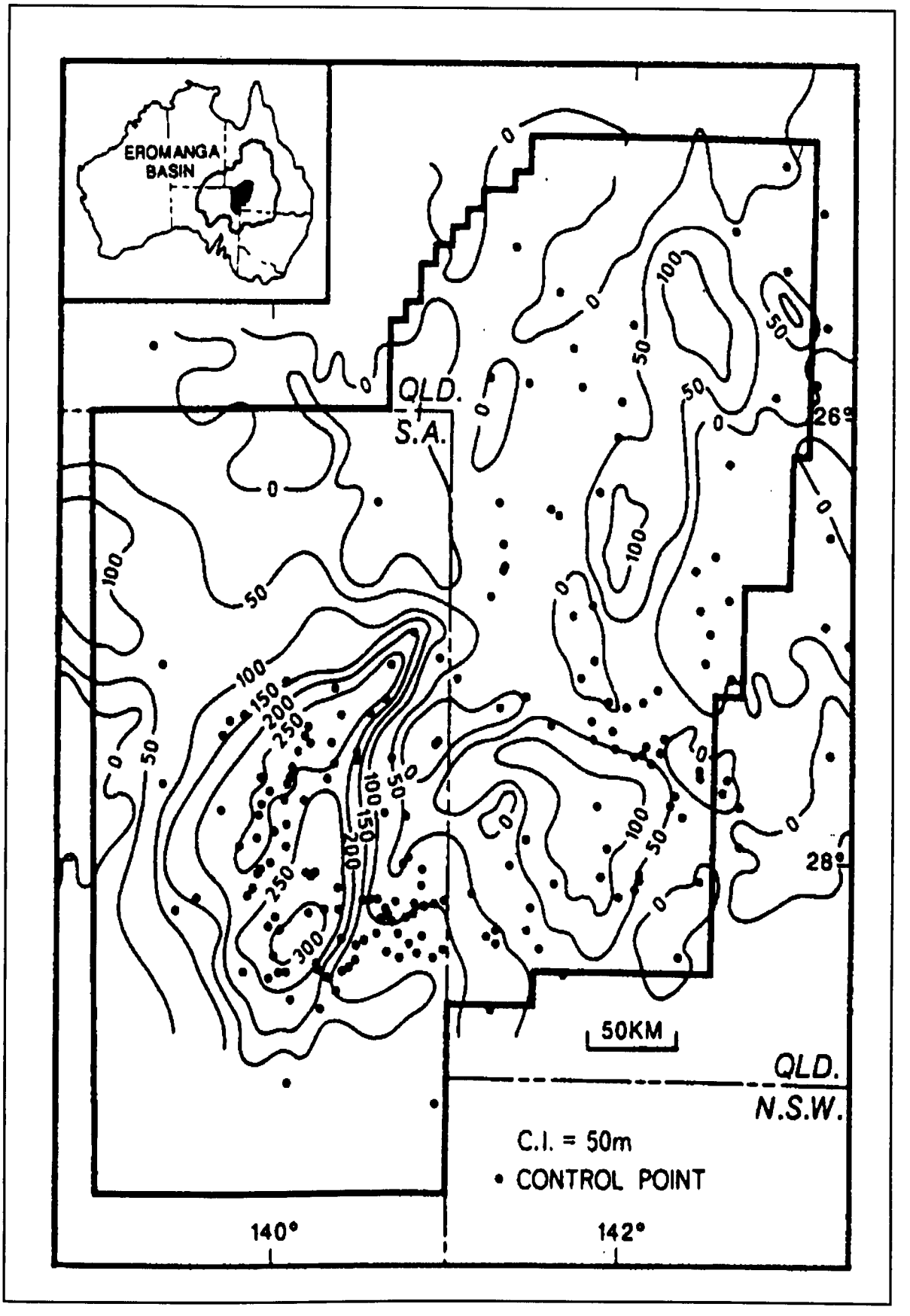

Figure 3.9. Tertiary isopach map for Queensland and South Australia. Based on data from Morton (1987) and the Geological Survey of Queensland (unpublished). The inset shows the study area and the Eromanga Basin (after Rodgers *et al.*, 1991).

3.7 Apparent Exhumation in the Cooper Basin

The maps of apparent exhumation from the five Cooper Basin units analysed are shown in Figure 3.10. The map of the mean of the apparent exhumation values from such units are present in each well is shown in Figure 3.11. The Cooper Basin, underlying the Eromanga Basin was, of course, subject to the same Late Cretaceous - Tertiary exhumation that is witnessed by the overcompaction of the units analysed in the Eromanga Basin sequence. However, as discussed above, the Cooper Basin appears, at least locally, to have been subject to a more major period of exhumation in Late Triassic - Early Jurassic times, prior to the deposition of the Eromanga Basin. This is apparent in higher apparent exhumation values mapped for the Cooper Basin than the Eromanga Basin (compare Figures 3.8 and 3.11). In order to further analyse the greater exhumation values yielded by Cooper Basin units, the difference between the mean exhumation value yielded by the sonic log data from the Cooper Basin units and those from the Eromanga Basin units has been plotted on Figure 3.12. Given a $\pm$ 200 m error on exhumation values from individual units, much of the excess of Cooper Basin apparent exhumation over that of the Eromanga Basin is within error limits. However, there are significant areas where the difference is in excess of 400 m, and, perhaps even more importantly, the map of the difference between Cooper and Eromanga Basin exhumation (Figure 3.12) has a demonstrable link with the structural history of the basins. The major Troughs within the Cooper-Eromanga Basins: Patchawarra, Nappamerri, Arrabury and Windorah, which were depocentres during the development of the Cooper Basin (Zwigulis, 1983; Stuart *et al.*, 1988; Heath, 1989), correspond with areas where maximum burial-depth was attained subsequent to the deposition of the Eromanga Basin. A number of the areas where Cooper Basin exhumation is significantly greater than that of the Eromanga Basin are Permo-Triassic structural highs such as the Callabonna anticline, Pondrinie, Naccowlah and a significant area centred on the Toolachee Field.

A major region of hydrocarbon accumulations from Fly Lake through Gidgealpa, Moomba and Della lie between the Nappamerri Trough, where maximum burial-depth was attained after deposition of the Eromanga Basin, and a NNW-SSE trending axis where the Cooper Basin

attained maximum burial-depth prior to the deposition of the Eromanga Basin. The Toolachee and surrounding fields are located in another region where the Cooper Basin attained maximum burial-depth prior to the deposition of the Eromanga Basin. Given that Permian-sourced oils are highly unlikely to be preserved where the sources attained maximum burial-depth prior to the deposition of the Eromanga Basin, it is suggested that the Nappamerri Trough, or other more local areas where maximum burial-depth was attained after deposition of the Eromanga Basin, are the primary source of Permian hydrocarbons. This implies some degree of lateral migration of these hydrocarbons to reservoirs located on structural highs where maximum burial-depth was attained prior to the deposition of the Eromanga Basin.

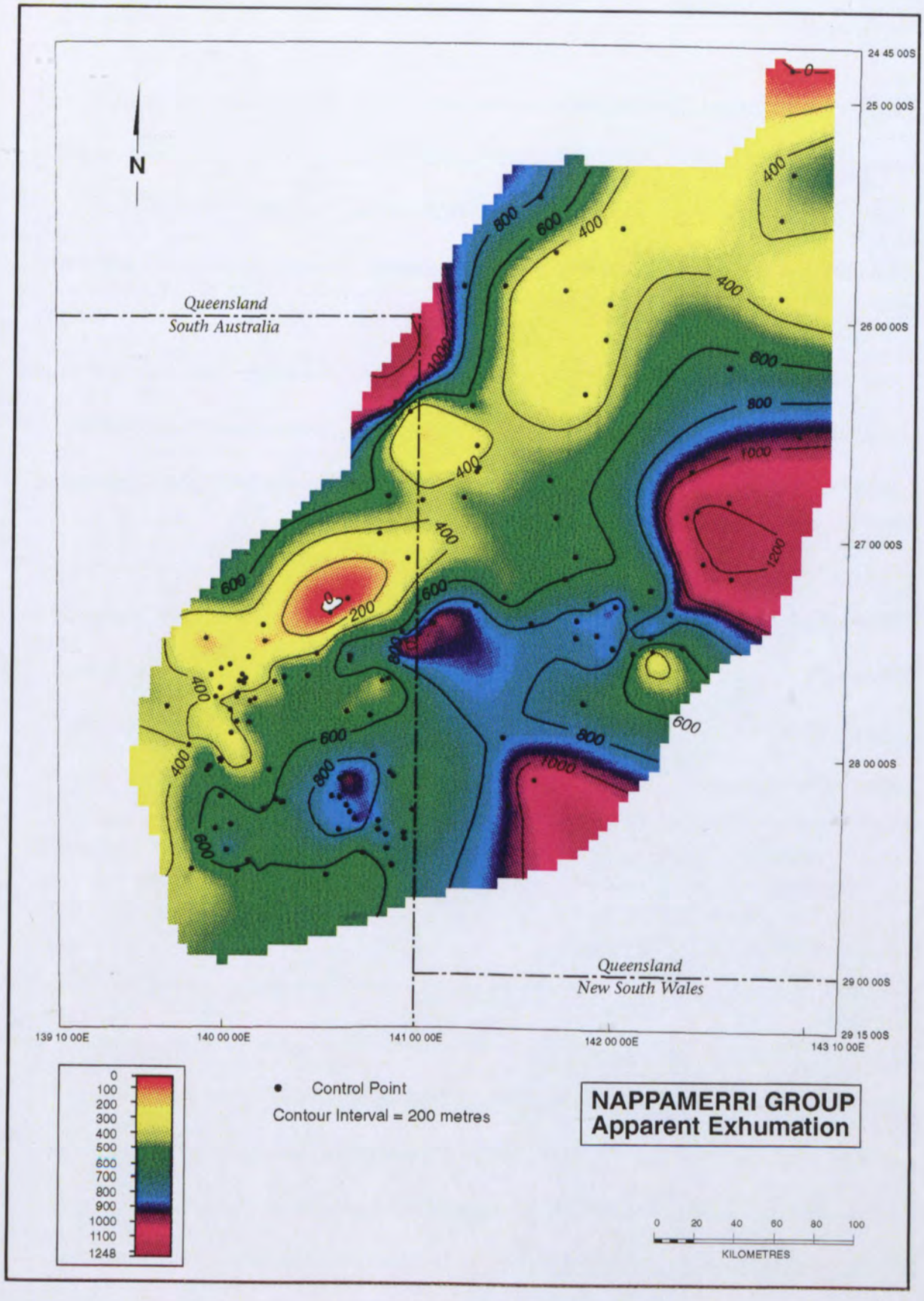

Figure 3.10. Apparent exhumation based on sonic log velocity in the Nappamerri Group. Well control points are also shown.

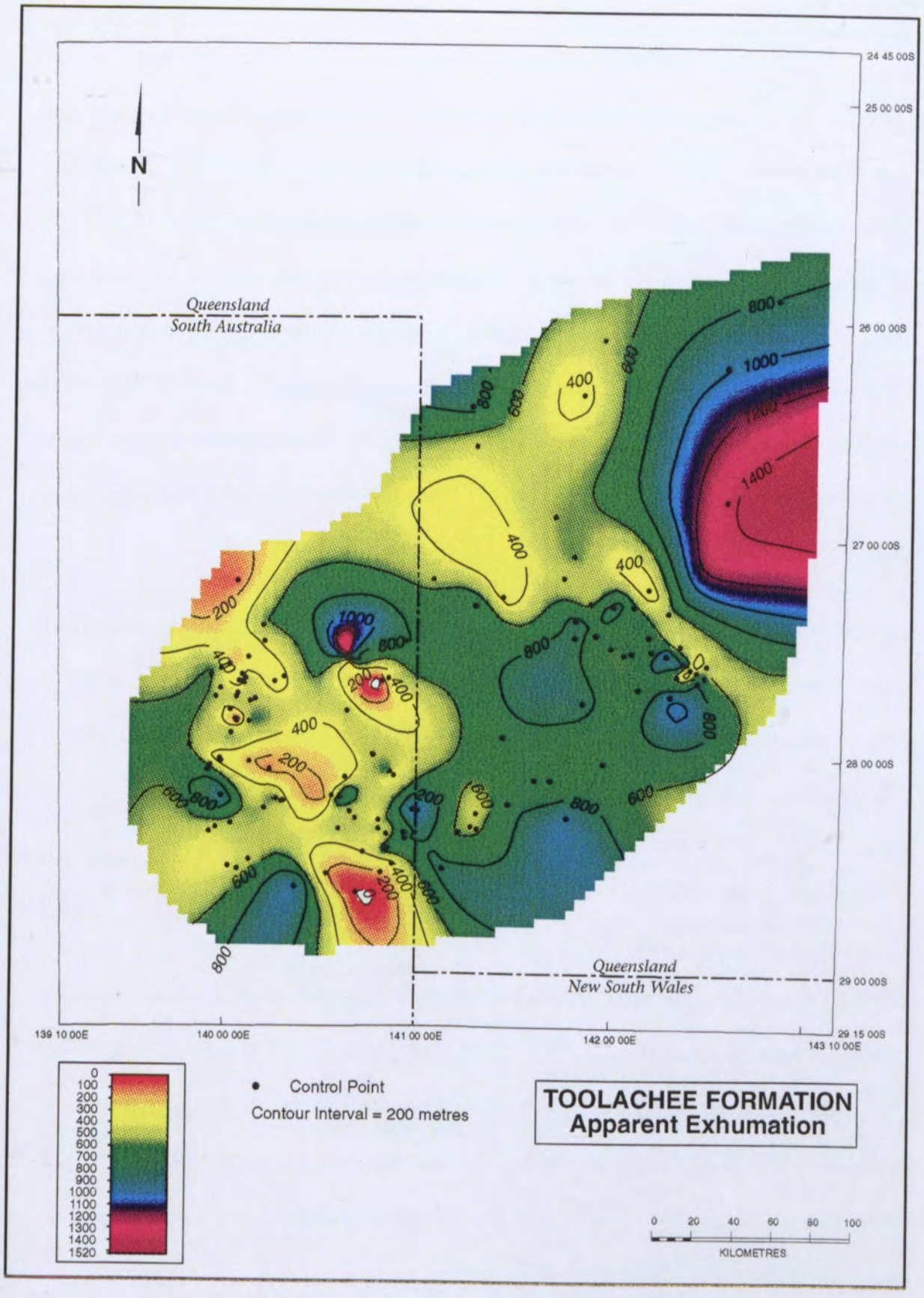

Figure 3.10. Continued. Apparent exhumation based on sonic log velocity in the Toolachee Formation. Well control points are also shown.

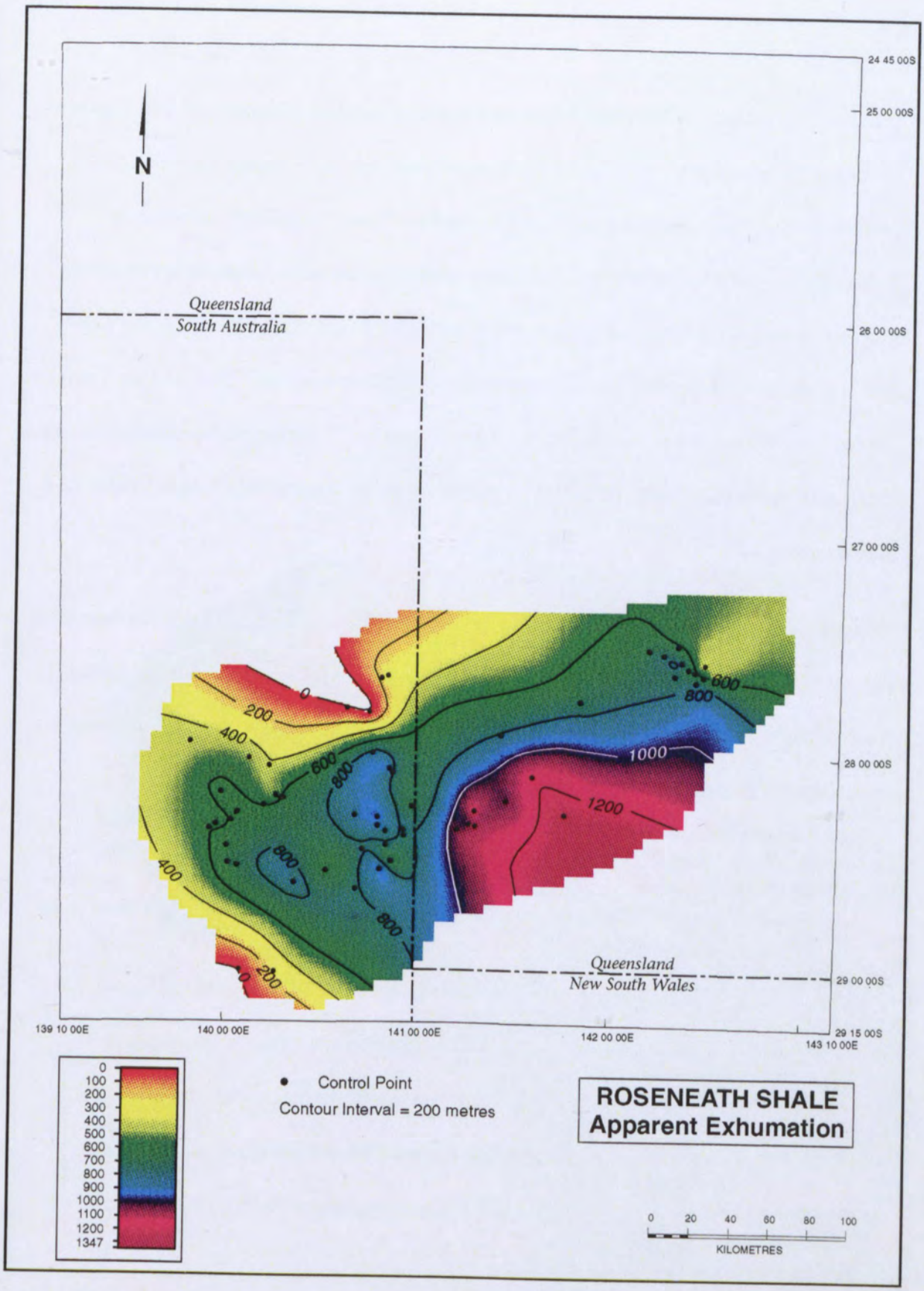

Figure 3.10. Continued. Apparent exhumation based on sonic log velocity in the Roseneath Shale. Well control points are also shown.

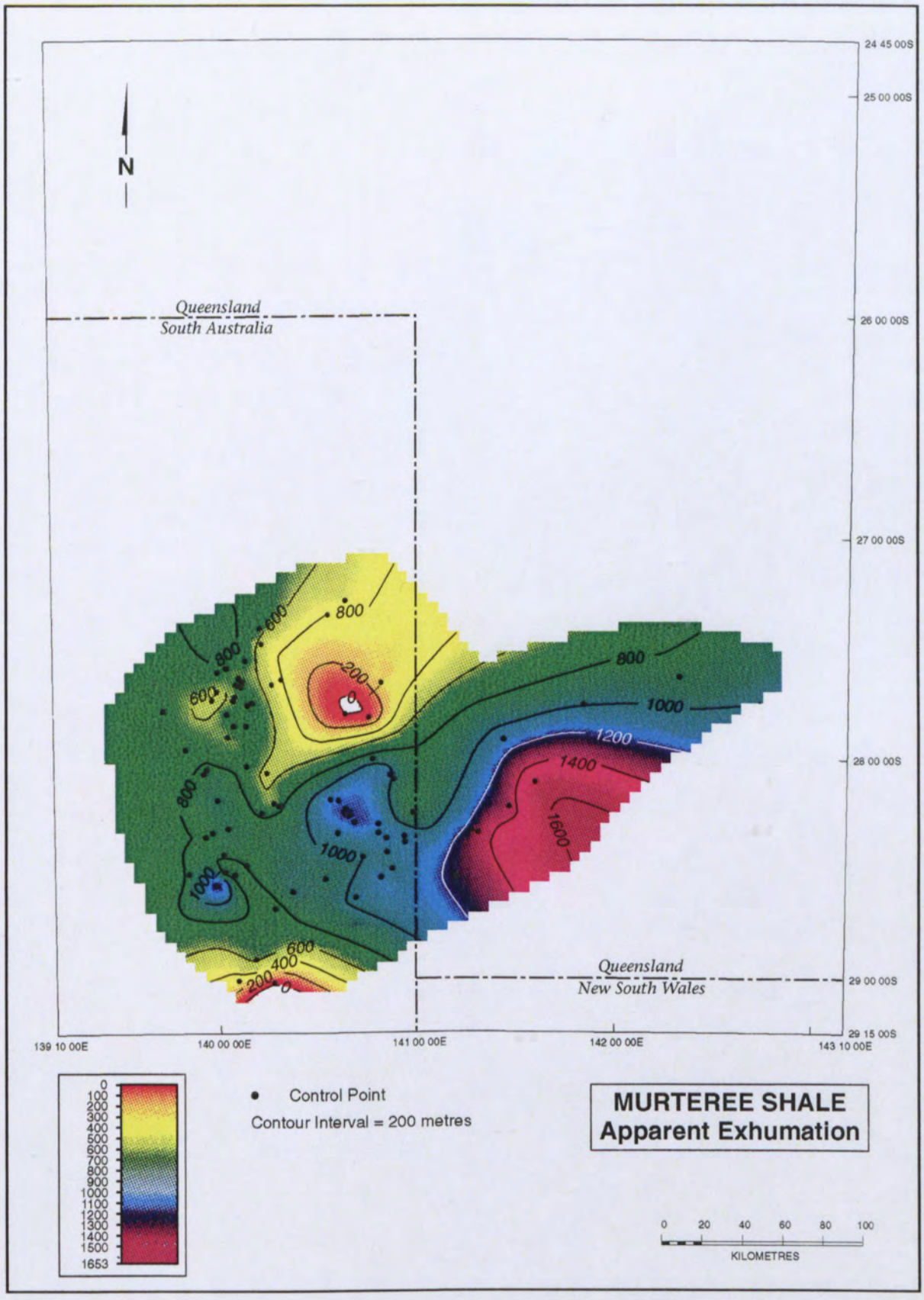

Figure 3.10. Continued. Apparent exhumation based on sonic log velocity in the Murteree Shale. Well control points are also shown.

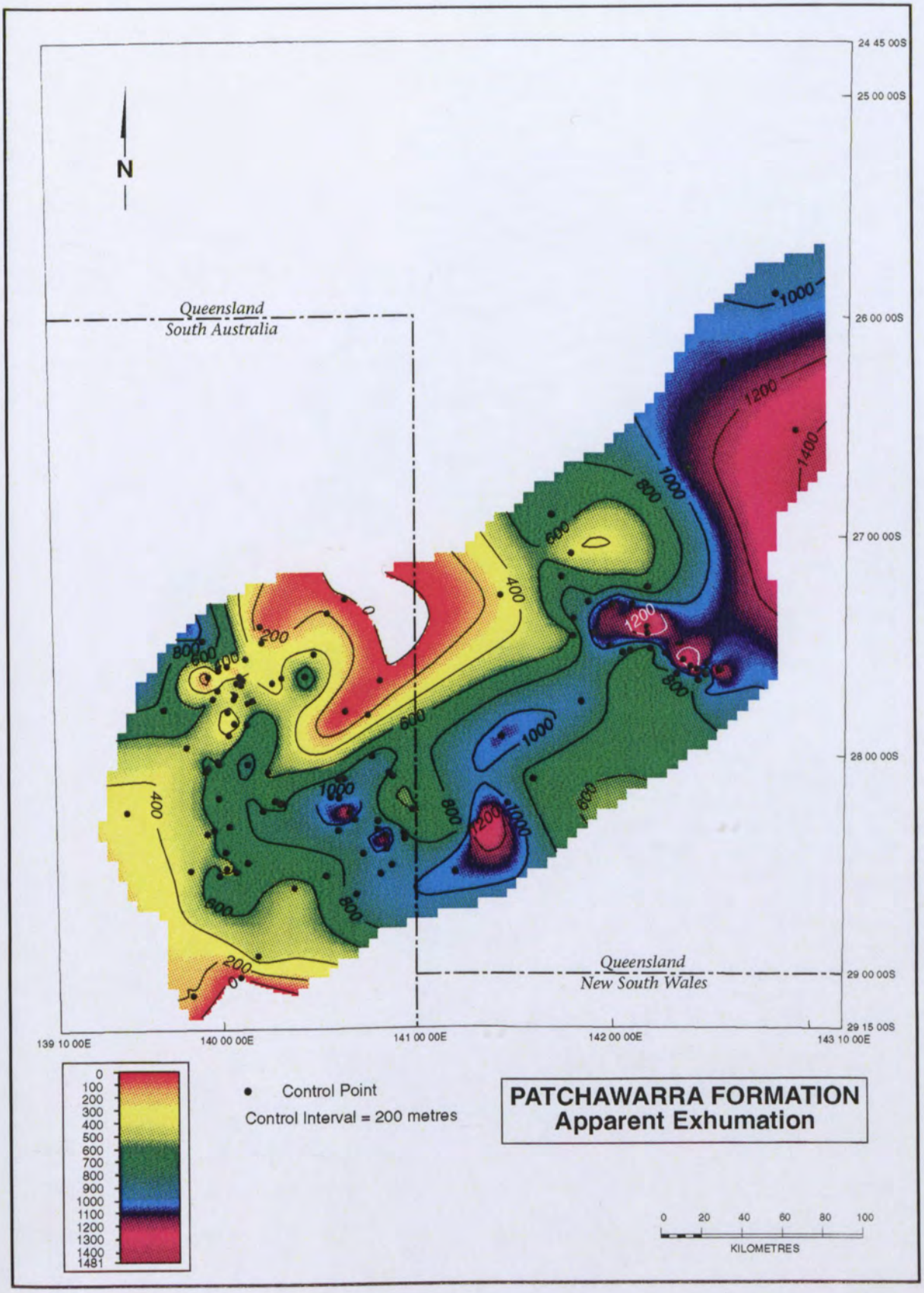

Figure 3.10. Continued. Apparent exhumation based on sonic log velocity in the Patchawarra Formation. Well control points are also shown.

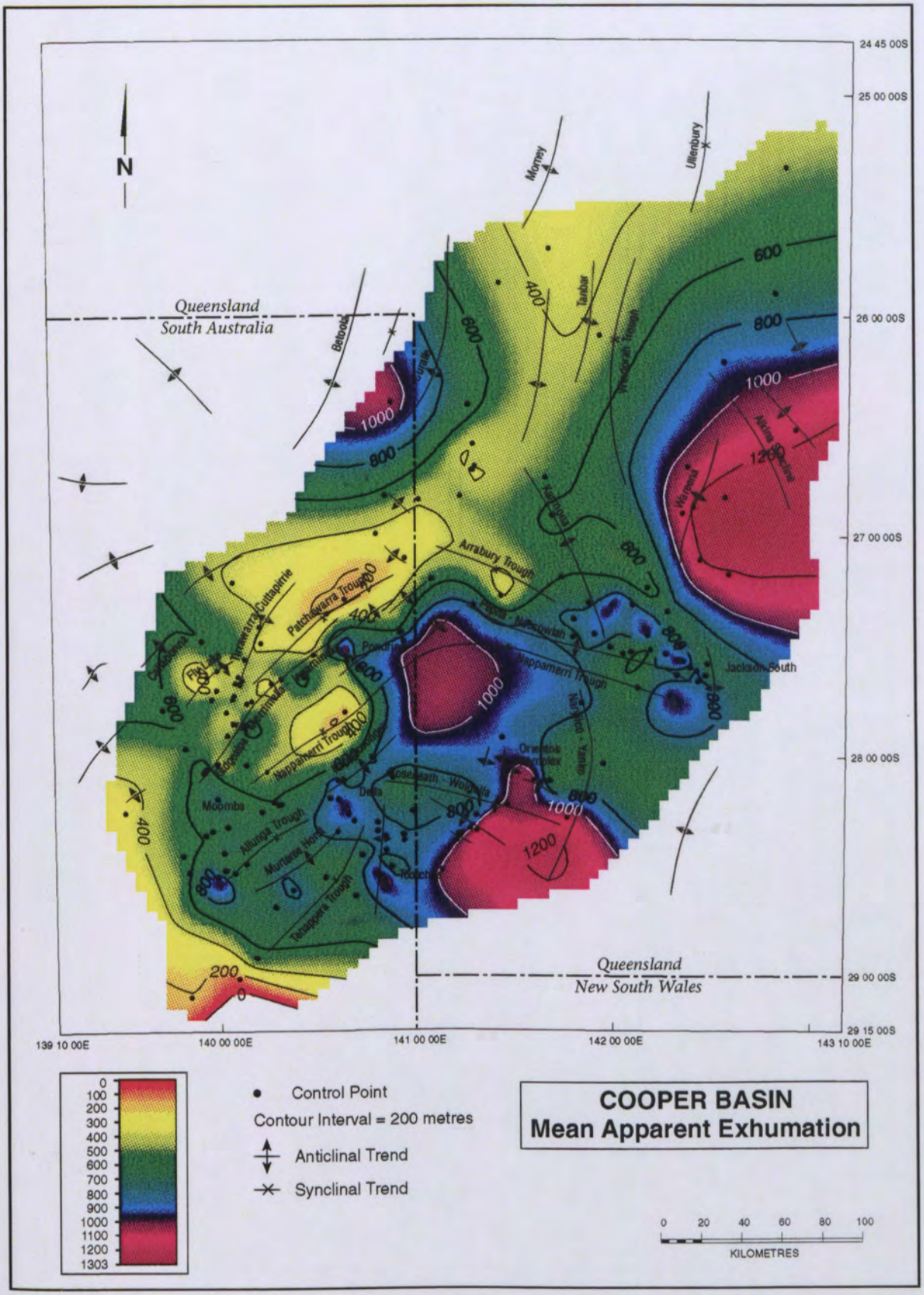

Figure 3.11. Mean apparent exhumation based on sonic log velocity in Cooper Basin stratigraphic units. Well control points and tectonic elements are also shown.

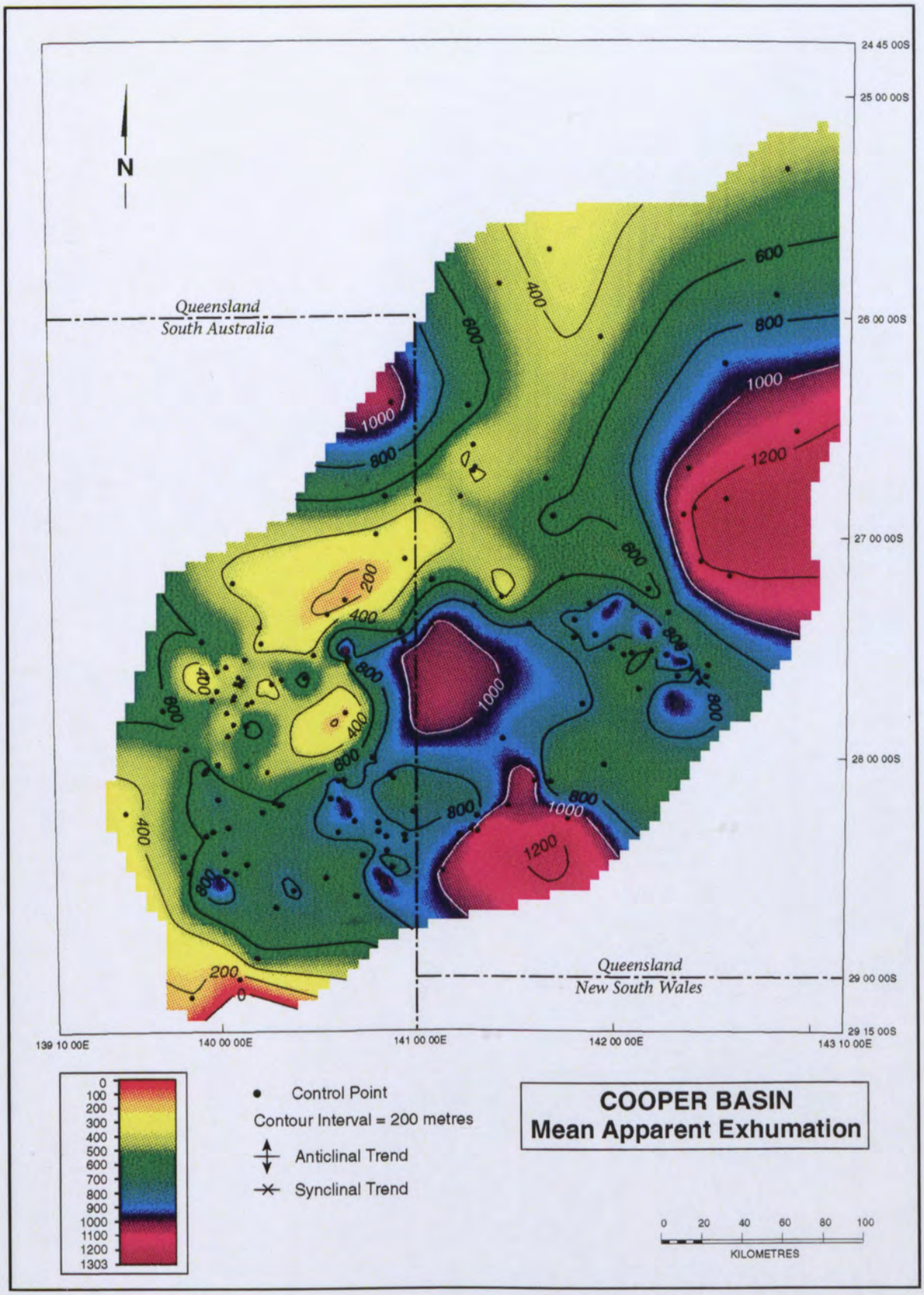

Figure 3.11. Mean apparent exhumation based on sonic log velocity in Cooper Basin stratigraphic units. Well control points and tectonic elements are also shown.

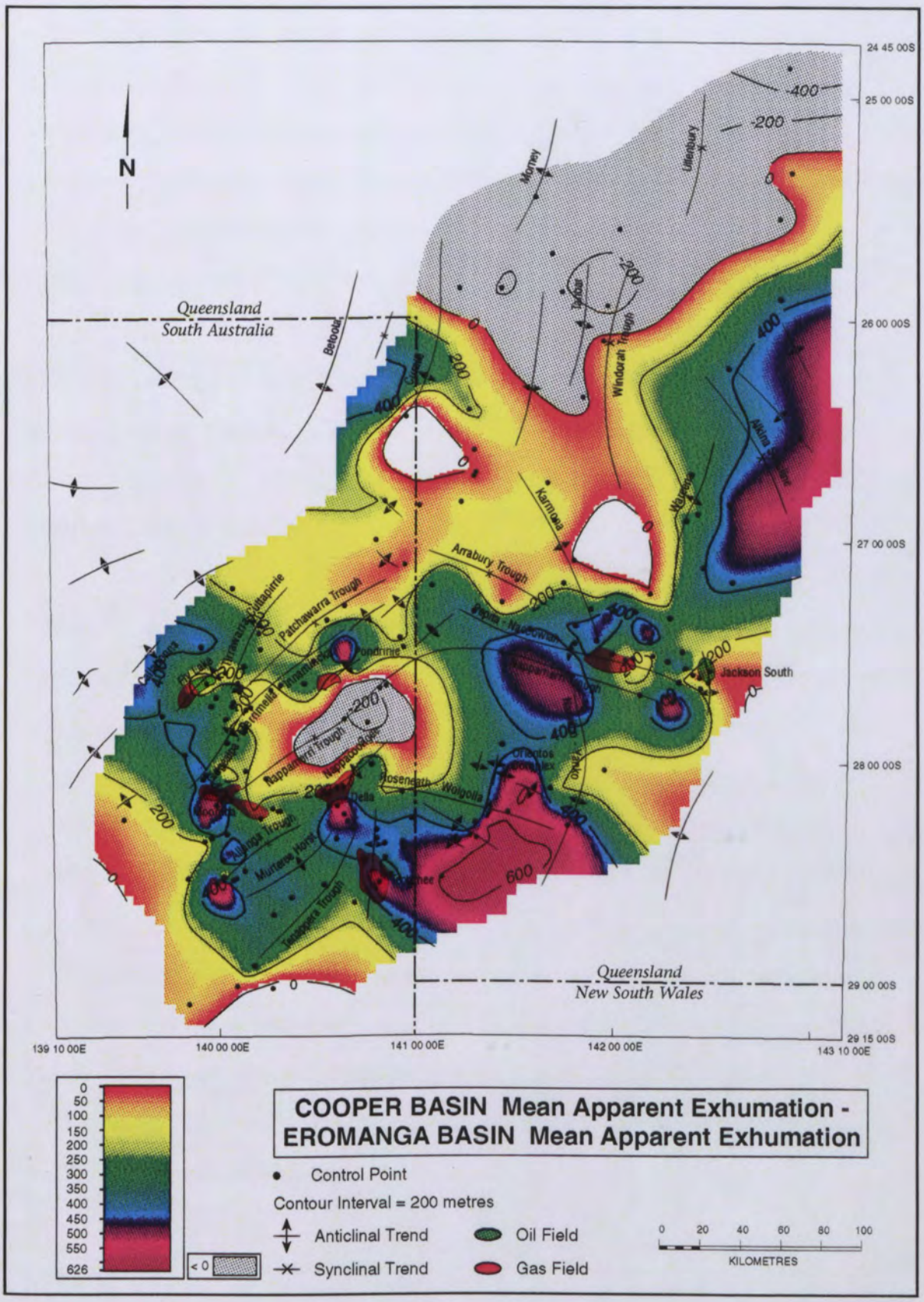

Figure 3.12. Map of difference between mean apparent exhumation in Cooper Basin and Eromanga Basin ($E_{A_{Cooper}} - E_{A_{Eromanga}}$). Well control points and tectonic elements are also shown.

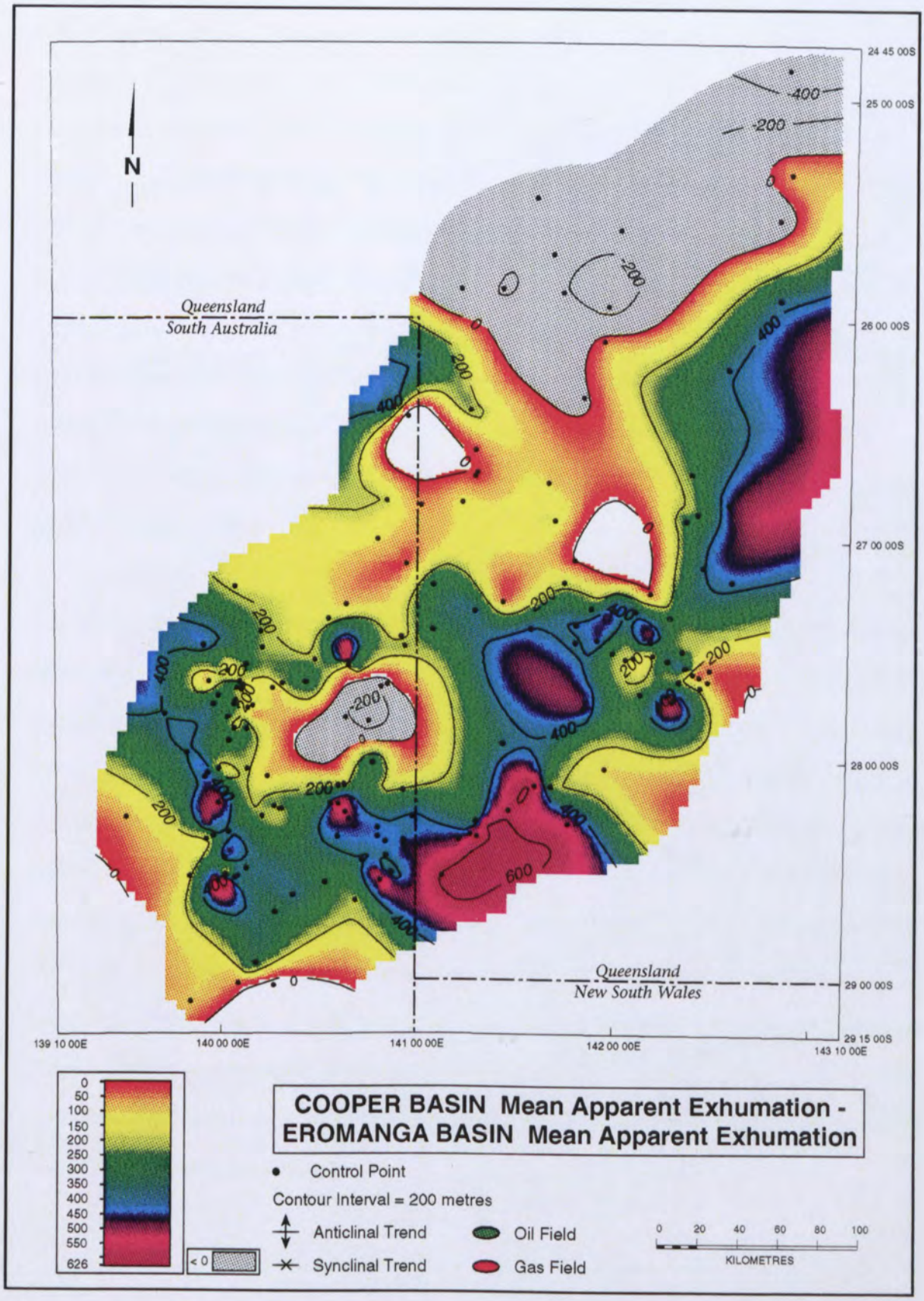

Figure 3.12. Map of difference between mean apparent exhumation in Cooper Basin and Eromanga Basin ($E_{ACooper}$ - $E_{AEromanga}$). Well control points and tectonic elements are also shown.

3.8 Comparison of Results with Other Studies

On the basis of structural/stratigraphic reconstruction, Shaw (1991) suggested that the entire eastern margin of the Eromanga Basin (somewhat east of the margin of this study) had been uplifted, and estimated that this uplift locally exceeded 1200 m. Again on structural/stratigraphic grounds, Moore and Pitt (1984) suggested that Late Cretaceous - Tertiary erosion was most severe in southwestern Queensland where up to 800 m of Winton Formation has been removed. Both of these estimates are broadly consistent with the estimates presented here of approximately 600 m of Late Cretaceous - Tertiary exhumation from maximum burial-depth in the Jackson-Naccowlah area, increasing to approximately 1 km to the north of Jackson-Naccowlah.

Rodgers *et al.* (1991) estimated the amount of Tertiary section loss in the Eromanga Basin based on interval velocities from well velocity surveys in the Wallumbilla Formation and overlying Allaru Mudstone. Rodgers *et al.* (1991) followed the compaction methodology essentially as outlined here. Their map of Tertiary section loss was based on the average of results from the Wallumbilla Formation and the Allaru Mudstone. Unfortunately, they did not compare the individual results from the Wallumbilla Formation and the Allaru Mudstone. Rodgers *et al.*'s (1991) map of mean Wallumbilla Formation/Allaru Mudstone exhumation is similar to the map of apparent exhumation presented here based on the mean of the seven Eromanga Basin units analysed (Figure 3.13). Rodgers *et al.* (1991) show that Patchawarra Trough is at or near maximum burial-depth, with exhumation increasing eastwards over the GMI Trend and reaching around 600 m in the Jackson-Naccowlah area, and in excess of 800 m north of Jackson-Naccowlah.

There are two major differences between the results of Rodgers *et al.* (1991) and those presented here. Rodgers *et al.* (1991) show approximately 500 m (as opposed to approximately 1 km) of section loss in the vicinity of the Curalle-1 well. However, the value of approximately 500 m indicated on their map of section loss is hard to reconcile with their velocity/depth plot for the Allaru Mudstone, which indicates that the Curalle-1 well is

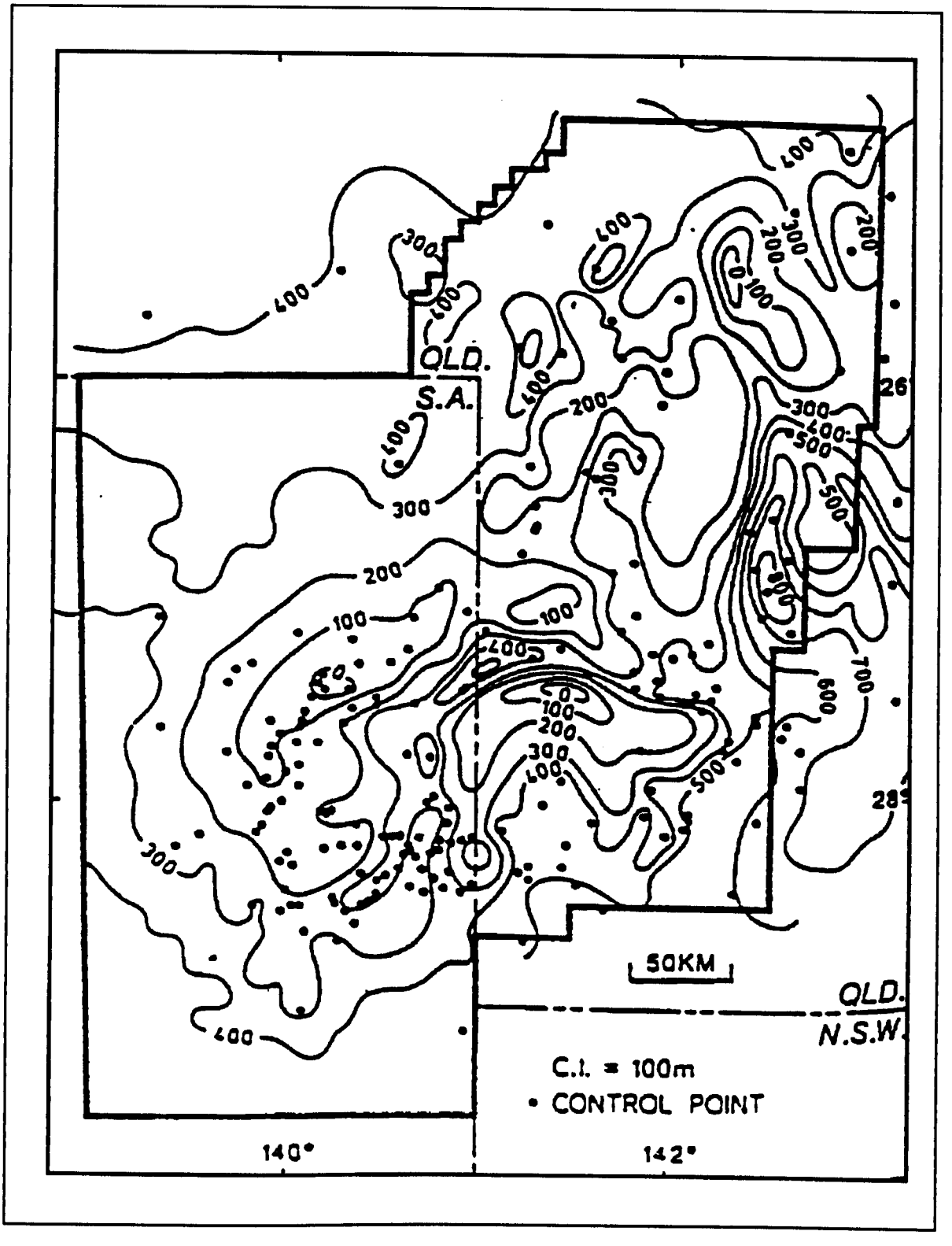

Figure 3.13. Tertiary section loss for Queensland and South Australia (after Rodgers *et al.*, 1991).

approximately 1.1 km above maximum burial-depth. The six Eromanga Basin units analysed in this study at the Curalle-1 well (the Winton Formation is absent, presumably due to erosion) consistently indicate apparent exhumation ranging from 800 - 1200 m. Combined with the strong structural evidence of Tertiary deformation in the area (Moore and Pitt, 1984; Shaw, 1991), a high degree of confidence is placed in the value of approximately 1 km of exhumation from maximum burial-depth in the vicinity of the Curalle-1 well which has been determined in this study. Rodgers *et al.* (1991) indicate a low in apparent exhumation in the north-western (Queensland) part of the Nappamerri Trough. However, there are very few data points constraining this low, and it may be an artefact of their contouring method. Despite the fact that the contours suggest there was no exhumation in the centre of this low, there are no wells that indicate less than 200 m of section loss. In this study, two wells constrain the high of 600 m of exhumation in the north-western part of the Nappamerri Trough, on the Queensland/South Australia border (Figure 3.8), which is immediately east of the low indicated by Rodgers *et al.* (1991). A number of other wells confirm values of approximately 400 m surrounding this high. Again, given the additional stratigraphic units and wells analysed, a higher degree of confidence is placed in the results presented herein.

3.9 Total Exhumation of the Eromanga Basin

The quantity determined from the log data is referred to as apparent exhumation because it is exhumation not reversed by subsequent burial. If renewed burial follows exhumation, the magnitude of apparent exhumation is reduced by the amount of that subsequent burial (Section 2.6.2). In order to determine the magnitude of exhumation that occurred at the time the rocks were being elevated, it is thus necessary to know the timing of the exhumation, and the magnitude of post-exhumational burial.

Figure 3.14 shows total exhumation, at the time of denudation for the Late Cretaceous - Tertiary exhumation of the Eromanga Basin, calculated assuming that maximum burial-depth was attained prior to the deposition of the Eocene Eyre Formation (further discussion of the

timing of exhumation is presented in Chapter 6). Since the Tertiary units are relatively thin, ie. post-exhumational burial is equal and/or close to 0 m for the majority of the examined wells, the map of total exhumation is very similar to the map of mean apparent exhumation (compare Figures 3.8 and 3.14). Post-exhumational burial and total exhumational values are listed in Table 3.6.

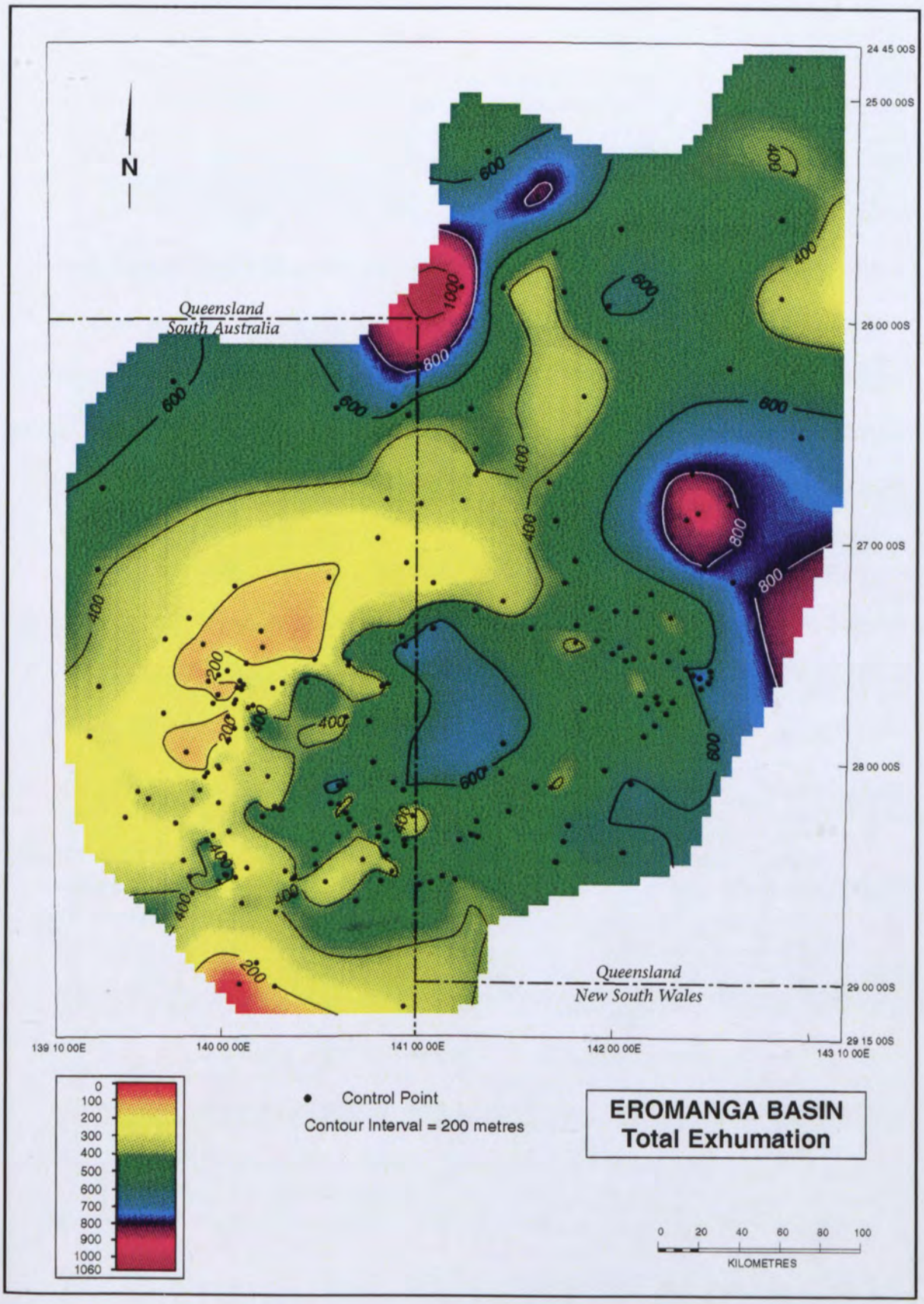

Figure 3.14. Total exhumation based on sonic log velocity in Eromanga Basin stratigraphic units ($E_T = E_A + B_E$). Well control points are also shown.

Table 3.6. Post-Exhumational Burial and Total Exhumation Results for Eromanga Basin Units

Well	Post-Exhumational Burial (B_E)	Total Exhumation (E_T)	Well	Post-Exhumational Burial (B_E)	Total Exhumation (E_T)	Well	Post-Exhumational Burial (B_E)	Total Exhumation (E_T)	Well	Post-Exhumational Burial (B_E)	Total Exhumation (E_T)
Alkina-1	0.0	529.1	Dirkala-2	315.8	673.2	Macadama-1	0.0	335.9	Snake Hole-1	0.0	186.9
Alwyn-1	0.0	353.1	Doonmulla-1	0.0	356.5	Mackillop-1	0.0	446.2	Spectre-1	0.0	146.2
Amyema-1	108.0	474.3	Dullingari-3	0.0	513.6	Marabooka-2	0.0	401.2	Spencer-4	0.0	356.4
Andree-1	97.5	264.4	Dullingari North-1			Marengo-1	0.0	353.8	Steward-1	0.0	513.7
Araburg-1	0.0	460.9	Dunoon-1	0.0	393.9	Marsilea-1	0.0	408.2	Strzelecki-10	124.4	558.5
Arrabury-1	0.0	243.3	Durham Downs-1	0.0	528.1	Mawson-1	0.0	214.9	Strzelecki -27	0.0	382.9
Arrakis-1	0.0	253.1	Echuburra North-1	0.0	584.5	Mckinlay-3	0.0	444.9	Sturt-6	0.0	313.7
Atoll-1	0.0	577.4	Fly Lake-1	0.0	142.9	Mcleod-1	0.0	517.3	Swan Lake-1	0.0	351.1
Azolla-1	0.0	357.0	Fly Lake-4	0.0	304.8	Meeba-1	0.0	438.1	Taloola-1	0.0	364.7
Ballera-1	50.6	488.1	Garanjanie-2	30.5	296.5	Meranji-1	0.0	209.8	Tanbar-1	57.6	446.4
Baratta-1	0.0	429.6	Gidgealpa-20	0.0	345.5	Merrimelia-7	0.0	227.6	Tanbar North-1	0.0	625.2
Bardoc-1	0.0	468.6	Gidgealpa-42	0.0	266.1	Merrimelia-25	0.0	349.5	Tartulla-1	4.6	510.4
Barrolka-1	0.0	456.0	Gidgee-1	0.0	414.8	Minkie-1	0.0	295.0	Tennaperra South-1	0.0	518.8
Baryulah-1	99.7	466.0	Gooranie-1	0.0	204.6	Mooliampah-1	18.1	531.7	Three Queens-1	0.0	476.7
Battunga-1	0.0	302.2	Gooranie-2	0.0	245.4	Moolion-1	0.0	179.2	Thurakinna-5	0.0	287.6
Beanbush-1	238.0	*	Graham-1	0.0	603.4	Moomba-27	0.0	335.1	Thurra-1	0.0	473.8
Belah-1	0.0	434.3	Gurra-1	0.0	200.2	Moomba-57	0.0	324.3	Tinchoo-1	0.0	407.8
Biala-1	0.0	337.1	Haddon Downs-1	0.0	577.5	Moomba North-1	0.0	345.5	Tinga Tingana-1	0.0	33.2
Big Lake-26	0.0	583.2	Hammond-1	0.0	398.4	Moomba South-1	0.0	449.5	Tinpilla-1	0.0	596.4
Big Lake-35	0.0	334.0	Hooley-1	0.0	757.3	Moorari-4	0.0	199.7	Tirrawarra-13	0.0	306.0
Bogala-1	0.0	578.3	Hume-1	72.4	522.1	Morney-1	0.0	823.7	Tirrawarra-15	0.0	279.2
Boldrewood-1	0.0	818.6	Hydra-1	0.0	533.9	Mudera-3	103.6	556.3	Tirrawarra-26	0.0	349.0
Bookabourdie-1	0.0	201.1	Ingella-1	0.0	501.3	Munkah-2	0.0	435.1	Tirrawarra North-1	0.0	185.3
Boxwood-1	0.0	401.4	Innamincka-3	0.0	666.5	Munkarie South-1	56.0	590.6	Tirrawarra West-1	0.0	168.7
Brolga-2	0.0	260.2	Innamincka-4	0.0	666.2	Munro-1	0.0	426.9	Toby-1	0.0	805.6
Buckinna-1	0.0	434.4	Jack Lake-2	0.0	137.1	Muteroo-3	0.0	385.4	Toolachee-9	0.0	445.3
Bungee-1	0.0	277.9	Jackson-1	0.0	774.5	Naccowlah East-1	0.0	414.5	Toolachee-21	93.1	490.1
Burke-2	239.7	572.5	Jackson South-1	0.0	632.7	Naccowlah South-1	75.6	533.8	Toolachee-39	0.0	436.7
Burley-2	0.0	385.3	James-1	0.0	371.2	Naccowlah West-1	0.0	482.7	Turban-1	0.0	457.0
Bycoe-1	0.0	609.0	Jarrar-1	0.0	458.1	Naryilco-1	31.7	494.0	Ullenbury-1	29.9	482.9
Carney-1	0.0	485.5	Johba-1	0.0	497.2	Navalla-1	0.0	971.8	Wackett-3	105.2	588.1
Challum-1	61.0	449.8	Kalladeina-1	133.1	357.4	Nulla-1	0.0	229.8	Wallawanny-1	0.0	523.3
Charo-1	0.0	294.1	Karmona-2	32.3	478.9	Okotoko-1	0.0	516.9	Wancoocha-2	0.0	408.4
Childie-1	51.8	462.7	Karwin-1	0.0	542.2	Orientos-2	0.0	486.9	Wantana-2	161.5	467.8
Cooba-1	0.0	162.9	Keeto-2	0.0	332.8	Packsaddle-4	0.0	457.4	Wareena-1	0.0	871.2
Cook-1	0.0	349.6	Keilor-1	0.0	425.3	Padulla-1	0.0	396.5	Warnie East-1	140.2	681.7
Cook North-1	0.0	414.9	Kenny-1	0.0	241.3	Pallano-1	0.0	453.1	Watson-1	0.0	613.0
Coonavalla-1	0.0	678.0	Kercummurra-1	0.0	802.0	Pandieburra-1	95.7	576.1	Weena-1	230.7	*
Cooroo-1	0.0	453.0	Kerna-5	0.0	337.7	Pando South-1	0.0	310.8	Wicho-1	58.6	419.0
Copai-1	0.0	531.1	Kirby-1	0.0	373.0	Paning-1	0.0	253.3	Wills-1	107.4	588.1
Cowan-3	36.6	331.0	Kirby-2	0.0	415.0	Paragilga-1	0.0	468.0	Wimma-1	237.0	*
Cuddapan-1	0.0	439.2	Kiwarrick-1	0.0	441.2	Patroclus-1	0.0	393.9	Wippo-2	0.0	441.1
Curalle-1	0.0	996.4	Kohari-1	0.0	385.9	Paxton-1	0.0	310.5	Wirha-1	0.0	469.1
Daer-1	0.0	205.3	Koonchera-1	0.0	410.6	Pepita-2	0.0	430.9	Witchetty-1	0.0	418.5
Daralingie-15	0.0	428.4	Kumbarie-1	0.0	228.2	Pintari-1	0.0	298.4	Wompi-1	0.0	588.4
Daralingie-23	0.0	276.7	Kurunda-1	0.0	246.1	Pondrinie-5	0.0	352.8	Wuroopie-1	0.0	443.8
Darter-1	0.0	155.0	Kutyo-1	0.0	405.3	Potiron-1	0.0	686.6	Yanbee-1	0.0	355.3
Della-7	0.0	708.7	Lake Mcmillan-1	0.0	125.1	Putamurdie-1	68.4	610.5	Yanda-2	0.0	382.0
Della-10	0.0	557.8	Lambda-1	104.3	653.9	Rheims-1	0.0	474.5	Yanta-1	0.0	275.5
Denley-1	0.0	437.8	Lhotsky-1	29.9	297.1	Rho East-1	0.0	575.1	Yumba-1	0.0	412.3
Deparanie-1	0.0	227.9	Limestone Creek-9	0.0	409.5	Richie-1	0.0	604.8			
Deramookoo-1	0.0	189.1	Lycium-1	0.0	250.4	Russel-1	0.0	337.4			

*Apparent exhumation (E_A) is less than post-exhumational burial (B_E). The well is currently at maximum burial-depth.

3.10 Maximum Burial-Depth in the Cooper-Eromanga Basins

Apparent exhumation is equal to the height of the rocks above their maximum burial-depth. Hence the maximum burial-depth of any unit is the sum of its present burial-depth and the apparent exhumation at that location (Section 2.6.2). The maximum burial-depth of the base of Hutton Sandstone and Patchawarra Formation, prior to Tertiary exhumation, have been calculated (Appendix B) and contoured (Figures 3.15 and 3.16). For comparison, the present burial-depths of the base of Hutton Sandstone and Patchawarra Formation have also been contoured (Figures 3.15 and 3.16). These maps are based only on burial-depths at the well localities, and the maximum burial-depth maps were determined using the mean apparent exhumation data from the Eromanga Basin units analysed.

For the well locations analysed, base Hutton Sandstone maximum burial-depths are up to:

- 2.6 km in the Tanbar Anticline in the NNE of the study area (Tanbar North-1 well);
- 2.6 km in the Karmona Anticline (Durham Downs-1 well);
- 2.6 km in the Arrabury Trough, close to the borders of South Australia and Queensland (Yanbee-1 and Doonmulla-1 wells); and
- 2.6 km in the Nappamerri and Patchawarra Troughs (wells Burley-2 and Beanbush-1 respectively).

For the well locations analysed, base Patchawarra Formation maximum burial-depths are up to:

- 3.4 km in the southwestern end of the Nappamerri Trough, (Big Lake-26 well)
- 3.5 - 3.6 km in the Patchawarra Trough, (Beanbush-1 and Wimma-1 wells); and
- 3.9 - 4.1 km in the Nappamerri Trough, (Burley-2, Kirby-1 and Mcleod-1 wells).

The major maxima in maximum burial-depth in both maps are concentrated in the north-east (Windorah Trough and Alkina Syncline) and south-west (Nappamerri and Patchawarra Troughs). However, the major maxima in present burial-depth are concentrated in the south-west. This supports the suggestion of Shaw (1991), that, on a regional scale, the uplifted

eastern margin of the Eromanga Basin provide was the source of Cenozoic sediments deposited within the Tertiary depocentres of the Nappamerri and Patchawarra Troughs.

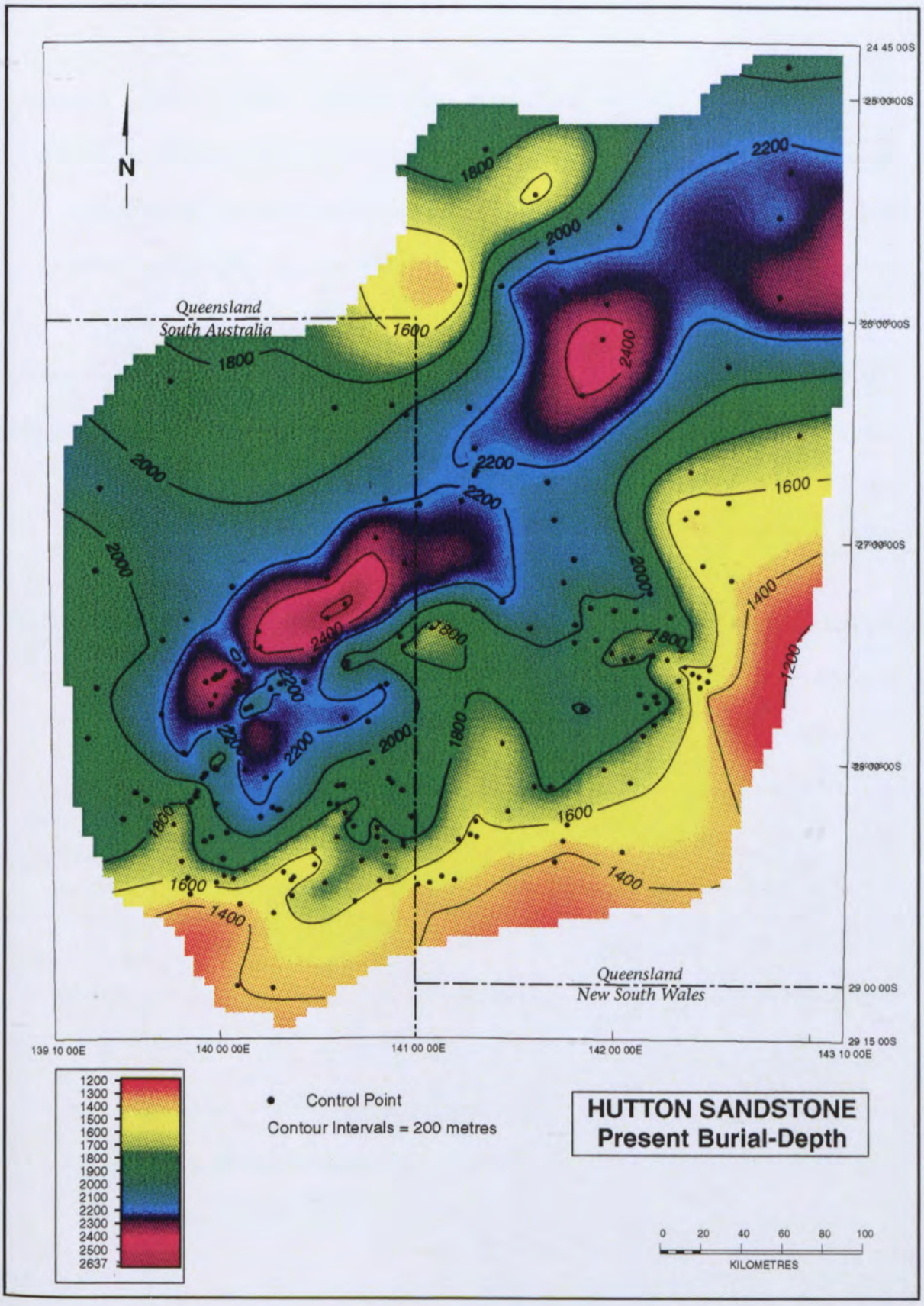

Figure 3.15a. Map of present burial-depth of the base of the Hutton Sandstone. Well control points are also shown.

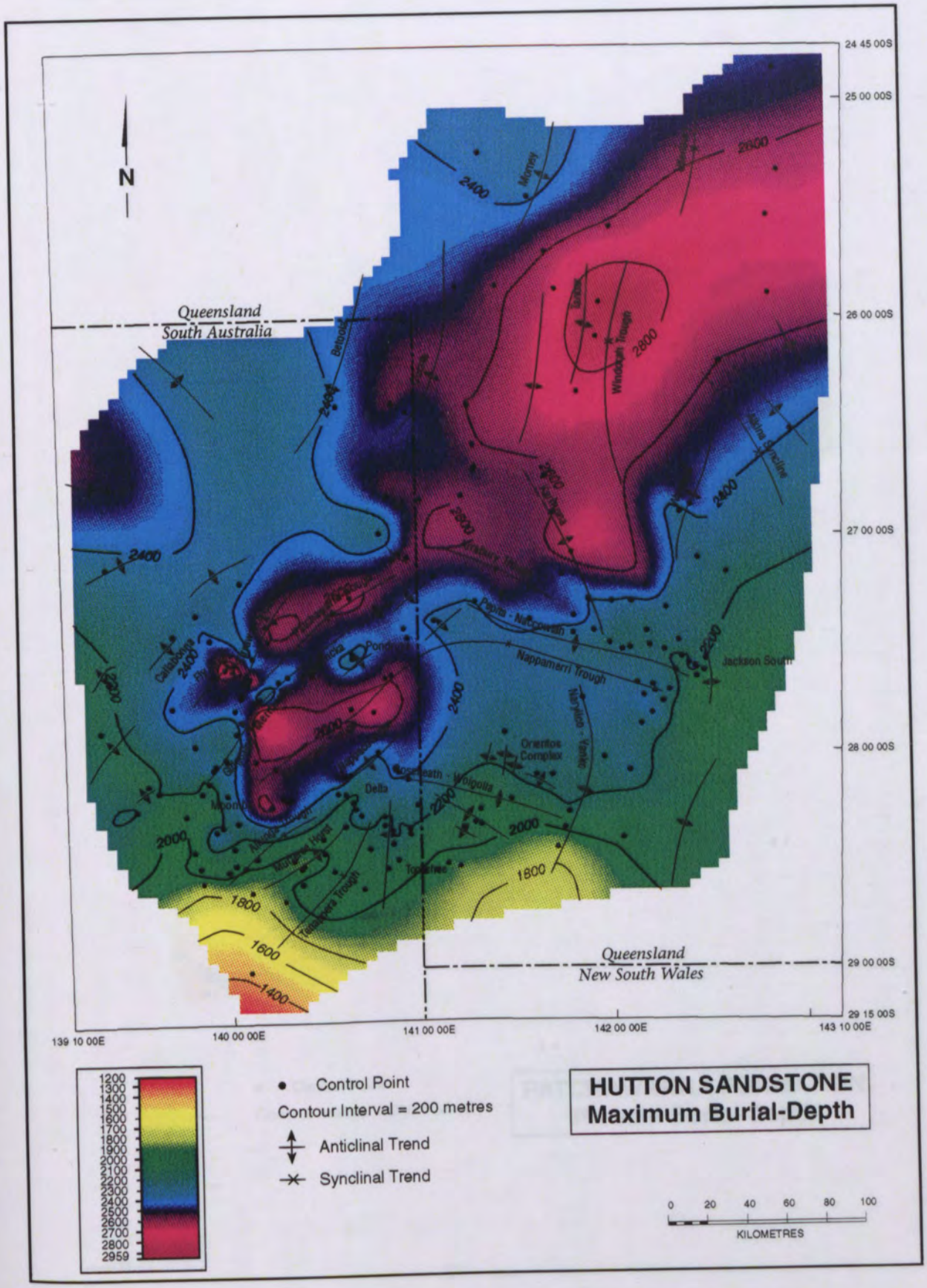

Figure 3.15b. Map of maximum burial-depth of the base of the Hutton Sandstone in Late Cretaceous - Tertiary times, based on the addition of the mean apparent exhumation (E_A) values from the Eromanga Basin stratigraphic units to present burial-depths ($B_T = E_A + B_P$). Well control points and tectonic elements are also shown.

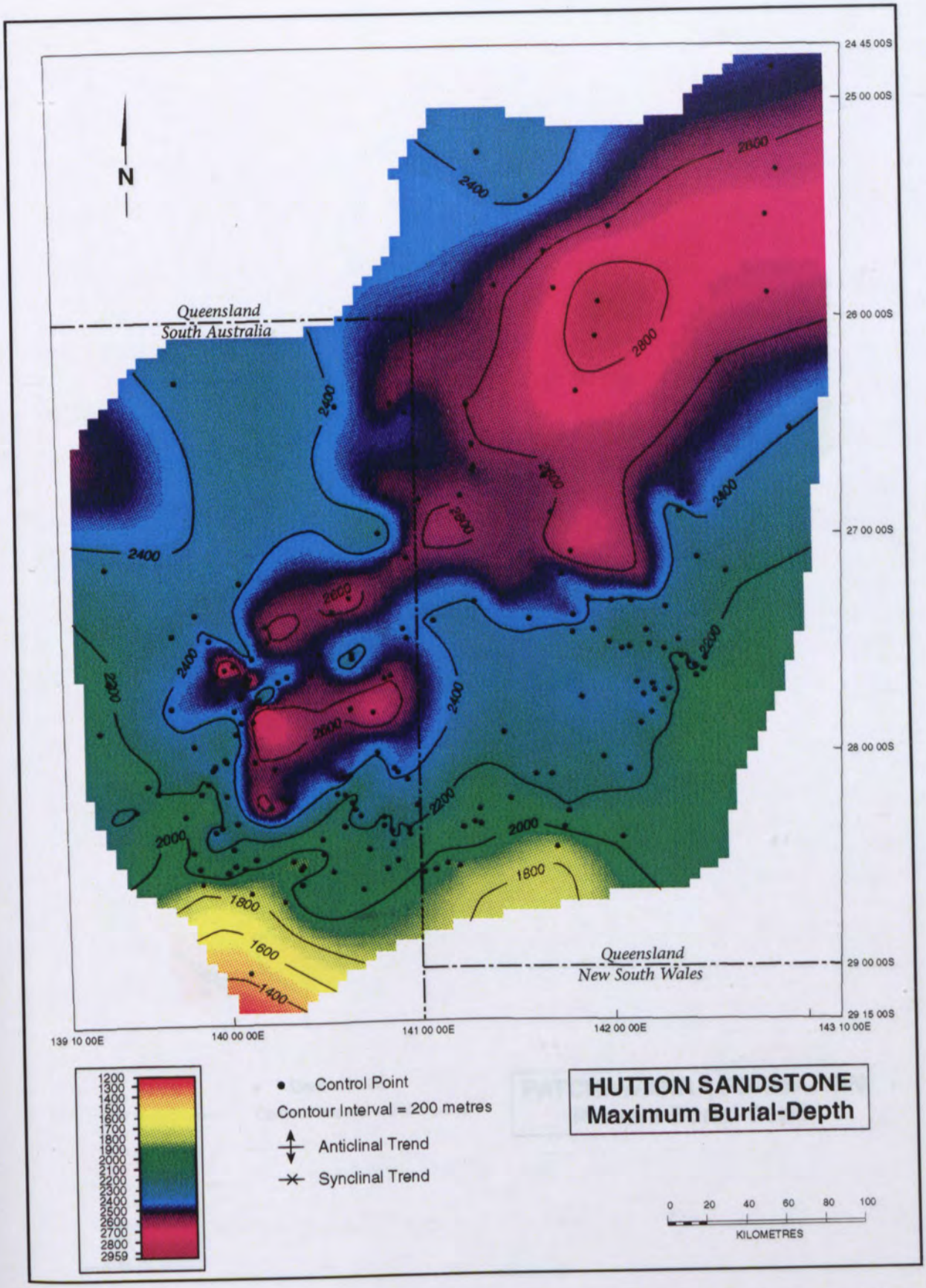

Figure 3.15b. Map of maximum burial-depth of the base of the Hutton Sandstone in Late Cretaceous - Tertiary times, based on the addition of the mean apparent exhumation (E_A) values from the Eromanga Basin stratigraphic units to present burial-depths ($B_T = E_A + B_P$). Well control points and tectonic elements are also shown.

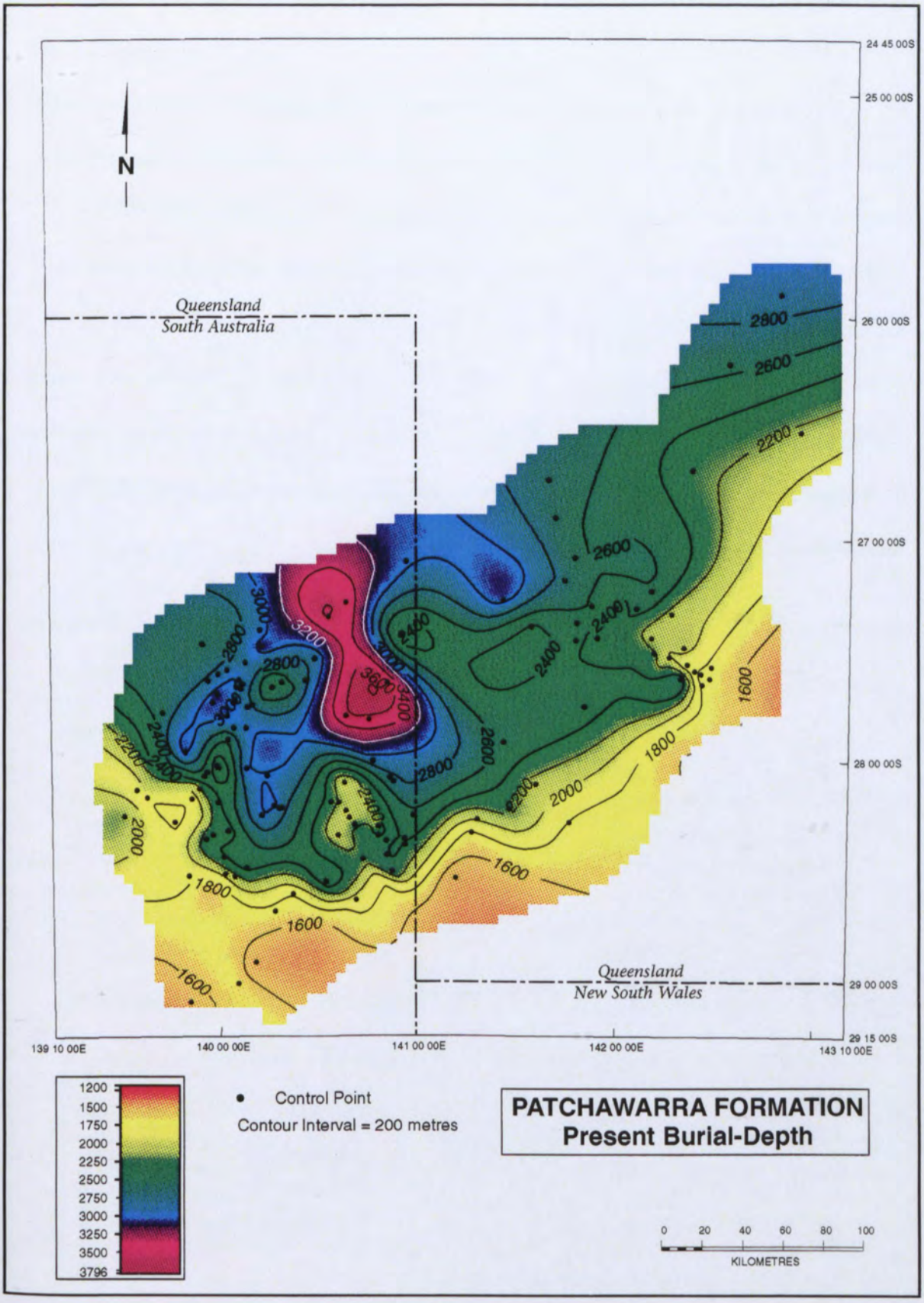

Figure 3.16a. Map of present burial-depth of the base of the Patchawarra Formation. Well control points are also shown.

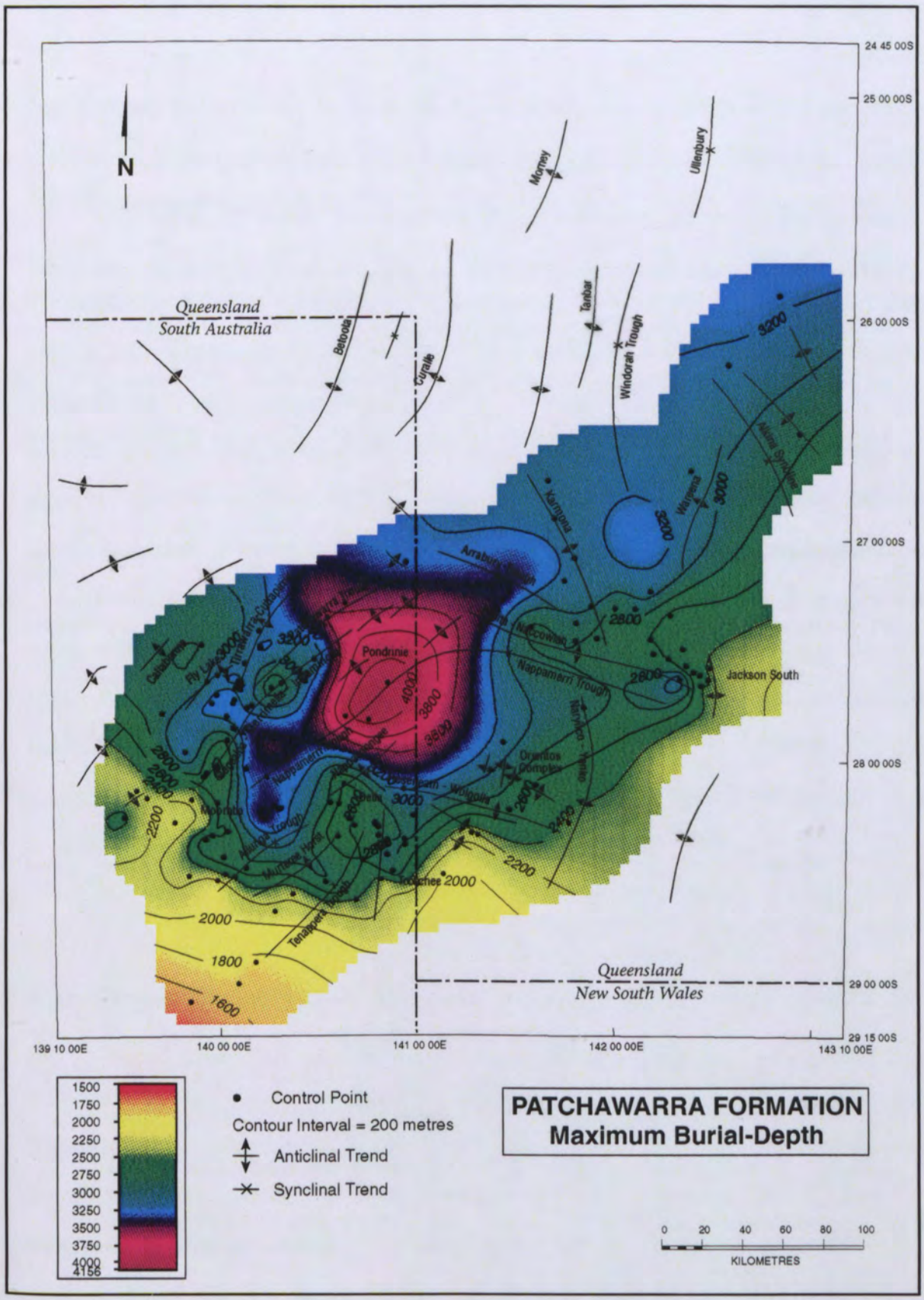

Figure 3.16b. Map of maximum burial-depth of the base of the Patchawarra Formation in Late Cretaceous - Tertiary times, based on the addition of the mean apparent exhumation (E_A) values from the Eromanga Basin stratigraphic units to present burial-depths ($B_T = E_A + B_P$). Well control points and tectonic elements are also shown.

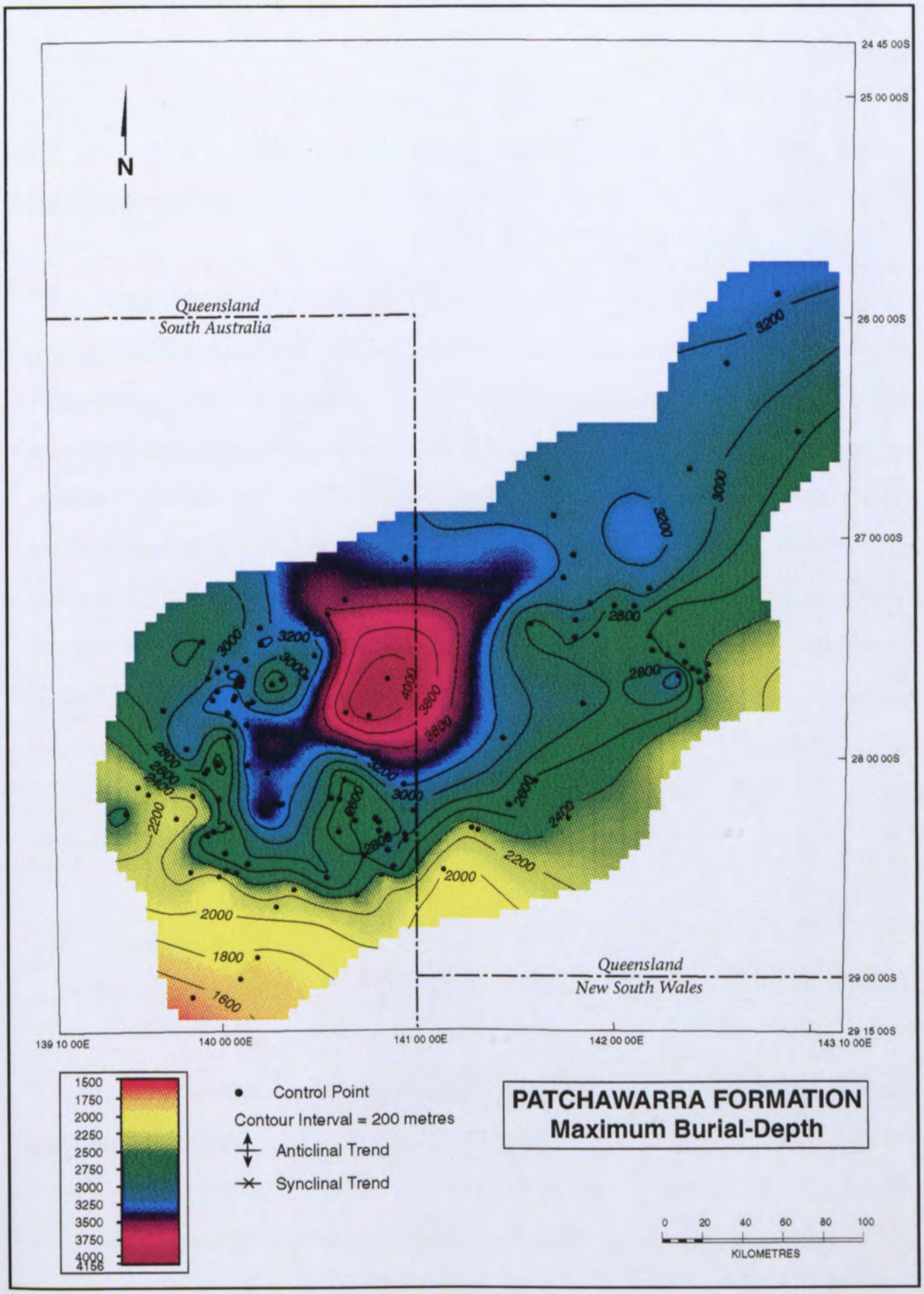

Figure 3.16b. Map of maximum burial-depth of the base of the Patchawarra Formation in Late Cretaceous - Tertiary times, based on the addition of the mean apparent exhumation (E_A) values from the Eromanga Basin stratigraphic units to present burial-depths ($B_T = E_A + B_P$). Well control points and tectonic elements are also shown.

4. QUANTIFYING EXHUMATION USING VITRINITE REFLECTANCE

4.1 Introduction

This chapter deals with the estimation of exhumation in the Cooper-Eromanga Basins using the vitrinite reflectance method. The purpose of this analysis is to investigate whether exhumation values derived from vitrinite reflectance modelling are consistent with those derived in the previous chapters using the compaction methodology. No new analytical determinations of vitrinite reflectance were made in this study, and all reflectance measurements were taken from previous reports. However, this analysis provides a consistent approach to the modelling of vitrinite reflectance data throughout the Cooper-Eromanga Basins, and to its interpretation in terms of exhumation. After a brief review of the vitrinite reflectance methodology, and its application to quantifying exhumation, the methodology and results of the analysis undertaken herein are presented. Finally, previous vitrinite reflectance work in the Cooper-Eromanga Basins is summarised, and the results of previous work, and that presented herein are discussed.

4.2 Vitrinite Reflectance

Vitrinite reflectance is the percentage of light reflected by the maceral vitrinite in terrestrial organic matter. Vitrinite reflectance is the most widely used, and most precise measurement of organic diagenesis (Bustin, 1989). The monotonic increase in the intensity of vitrinite reflectance through the entire range of thermal maturation permits semiquantitative reconstructions of the burial and temperature histories of stratigraphic sequences (eg. Kalkreuth and McMechan, 1984). Methods of quantitative palaeotemperature assessment, such as vitrinite reflectance and apatite fission track analysis (AFTA), may be used to estimate the amount of exhumation (uplift of rocks with the surface) associated with unconformities in the sequence, provided that palaeogeothermal gradients are known.

Vitrinite reflectance has an advantage over many palaeogeothermometers currently in use (eg. clay mineralogy, zeolites, fluid inclusions, apatite and zircon fission-track annealing, stable isotopes) because it can be used in temperatures ranging from 25°C to at least 400°C (Price and Barker, 1985). Since the application of other commonly available maturity parameters has created no fewer, and possibly more, problems than vitrinite reflectance (Khorasani and Michelsen, 1994), vitrinite reflectance is considered by many investigators to be the single most powerful maturation measure in petroleum geochemistry (Tissot and Welte, 1978; Hunt, 1979; Russell and Baillie, 1989).

4.2.1 Modelling Vitrinite Reflectance

The most commonly used kinetic model in vitrinite reflectance (%Ro) involves the correlation of a calculated time-temperature index (TTI) to vitrinite reflectance, based on the assumption that organic reaction rates increase by approximately a factor of two with each 10°C rise in temperature (eg. Lopatin, 1971; Waples, 1980; Issler, 1984; Horváth *et al.*, 1988). However, the TTI method, which assumes that the rate of petroleum generation doubles for every 10°C increase in temperature, has been shown to give unreliable results (Burnham and Sweeney, 1989; Waples *et al.*, 1992a; Waples, 1994). In fact, reaction rates double for a 3 to 5°C temperature increase, given typical subsurface temperatures (Tissot *et al.*, 1987). As a consequence, the TTI method overestimates the influence of geologic time, which may lead to significant errors. Furthermore, the TTI method relies upon the hypothesis of universal kinetic behaviour of all kerogens which, as discussed below, is not the case.

A less widely applied method of modelling vitrinite reflectance involves the derivation of thermal history from the empirical observation that $\log(\%R_o)$ values increase linearly with burial depth (Dow, 1977; Middleton, 1982). Erosional unconformities have been assumed to create breaks in vitrinite reflectance profiles that show higher maturities below an unconformity than above it. In a manner exactly analogous to that used in the compaction methodology in the previous Chapters, the magnitude of such vitrinite reflectance breaks has been used to

estimate the thickness of eroded section (eg. Dow, 1977; Figure 4.1). However, this methodology has been criticised and modified by Katz *et al.* (1988), Armagnac *et al.* (1985; 1989), and Waples *et al.* (1992b), who showed that breaks in profiles of vitrinite reflectance, like those in compaction profiles (Section 2.6.2), anneal during re-burial and thus must be used cautiously in working out amounts of erosion (eg. Waples, 1994; Figure 4.1). The graphical approach to estimating removal suggested by Dow (1977) can lead to serious errors where annealing has occurred (Waples, 1994).

Recently, more theoretically rigorous methods of modelling vitrinite reflectance have been developed. The maturation of vitrinite is tested as a series of parallel first-order Arrhenius-type reactions, each characterised by a different activation energy (Tissot and Espitalié, 1975; Quigley *et al.*, 1987; Espitalié *et al.*, 1988; Burnham, 1989; Burnham and Sweeney, 1989; BEICIP, 1990; Castelli *et al.*, 1990; Sweeney and Burnham, 1990). These models describe the process of maturation in terms of the Arrhenius equation:

$$k = A \exp(-E/RT)$$

where k is the rate constant (s^{-1}), E is the activation energy (kcal/mole), A is the pre-exponential factor (s^{-1}), R is the gas constant (0.001987 kcal/mole/K), and T is the Kelvin temperature (K).

These Arrhenius-based simulations of vitrinite reflectance have superseded earlier multiple-reaction algorithms such as those of Larter (1988) and Wood (1988). Examples of kinetic data for standard kerogen types I, II, and III are shown in Figure 4.2. Each kerogen is thought to contain several bond types differing in activation energy by one or two kcal/mole. In most models, the pre-exponential factor is considered to be the same for all bonds in the kerogen, generally in the order of 10^{13}-10^{16}/s. If pre-exponential factors are the same for all bondtypes, changes in activation energy as small as a few kcal/mole can lead to major differences in the temperature and timing of hydrocarbon generation.

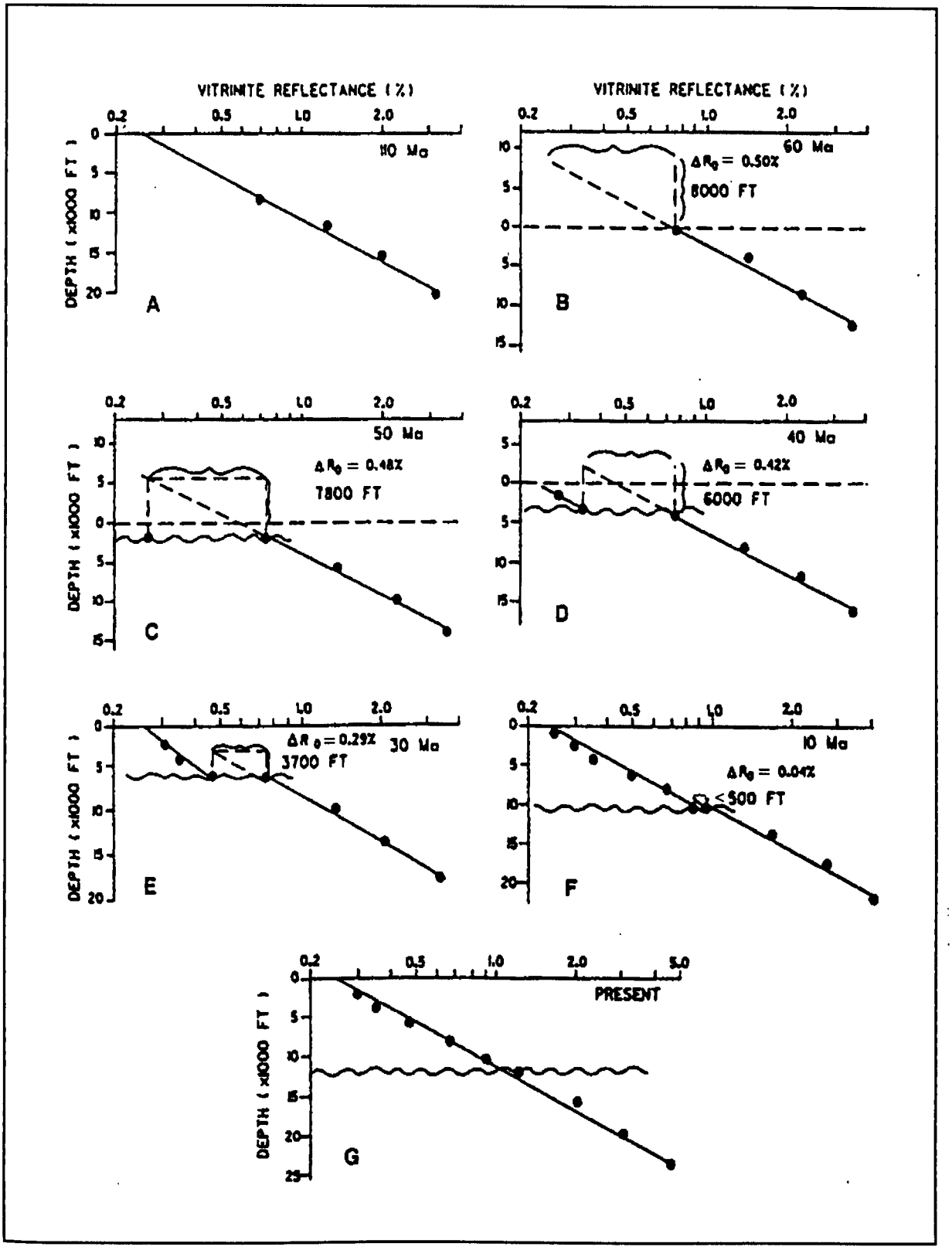

Figure 4.1. Development and gradual annealing of a break in a vitrinite profile during burial, erosion, and reburial. Erosion between the times represented in (A) and (B) leads to a surface Ro (0.75%) that is 0.5% higher than normal. (C) After 2000 ft of reburial, the gap has shrunk to 0.48%; (E) after 6000 ft, 0.29%; (F) after 10,000 ft, 0.04%; and (G) after 12,000 ft, the slope is unbroken (after Katz *et al.*, 1988).

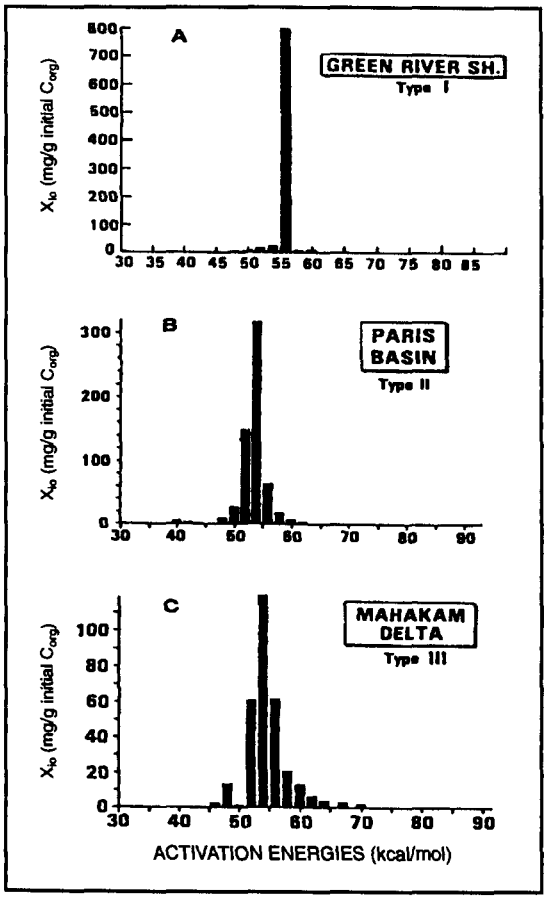

Figure 4.2. Histograms of activation energies for various bond strengths in the IFP kinetic model for (A) typeI, (B) type II, and (C) type III kerogens. The y-axis in each histogram represents the mass of hydrocarbon formed per gram of organic carbon and thus is directly comperable among all there kerogen types (after Tissot *et al.*, 1987).

Such kinetic methods are becoming the recognised approach for calculating organic maturity and petroleum generation. Differences in the predictions of two of the most widely used kinetic models for hydrocarbon generation, the IFP (Institut Français du Pétrole) and LLNL (Lawrence Livermore National Laboratory) models, are minimal compared to other uncertainties in the modelling process (Waples *et al.*, 1992b). These models are considered the best currently available to represent the Arrhenius-type approach (Ungerer *et al.*, 1990; Morrow and Issler, 1993). In this study the IFP kinetic model as incorporated in the MATOIL program (BEICIP, 1990) was used.

4.2.2 Limitations of Vitrinite Reflectance Analysis

Although vitrinite reflectance is a powerful tool, there are a number of problems associated with modelling vitrinite reflectance data. Ungerer (1993) stated that vitrinite reflectance cannot be modelled with great accuracy because of the chemical variability of vitrinites. Some other problems are summarised below.

- Suppression is the phenomenon of measured vitrinite reflectance values being lower than expected values at a given regional rank. Vitrinite reflectance is greatly suppressed in vitrinite macerals associated with hydrogen-rich kerogen. Vitrinite reflectance can be significantly suppressed solely by variations in the percentages of the different vitrinite macerals themselves (Hutton and Cook, 1980; Fang and Jianyu, 1992; Beardsmore and O'Sullivan, 1995).
- By contrast, enhancement is the phenomenon that the measured vitrinite reflectance values are higher than expected values for a given regional rank (Wenger and Baker, 1987; Fang and Jianyu, 1992).
- There is a subjectivity problem in choosing the correct vitrinite submaceral to use. There are many different submacerals, and each follows a different maturation path. In other words, for a given set of burial conditions, different vitrinite reflectance values will result for each different maceral type (Valceva, 1979; Smith and Cook, 1980).
- Technical errors can also arise in reflectance analysis in relation to instrument reliability, reflectance standards, sample polish quality and sample moisture content (Suggate and Lowery, 1982).
- Subjectivity on the part of the microscope operator is also a problem, partly caused by the presence of oxidised or recycled vitrinite in the sample (Price and Barker, 1985).

The author relied on measured vitrinite reflectance data as listed in file reports. No new analytical determinations of vitrinite reflectance were undertaken in this study. As a

consequence, the above problems cannot be addressed. Many of these problems are commonly ignored in vitrinite reflectance studies. However, the results of modelling should be interpreted with some caution, bearing in mind the above limitations.

4.3 Methodology of Vitrinite Reflectance Modelling in the Cooper-Eromanga Basins

Vitrinite reflectance-depth data from 21 wells were taken from well completion reports[1]. The selected wells provide regional coverage (Figure 4.3), and the vitrinite reflectance-depth profile of each well is representative of the area in which it is located.

Present geothermal gradients in the Cooper-Eromanga Basins range between 30 and 60°C/km (Figure 4.4). They are considerably higher than the 25°C/km commonly assumed appropriate for Palaeozoic terrains (Middleton, 1979; Pitt, 1982; 1986; Kantsler *et al.*, 1983, 1986). Pitt (1986) undertook a comprehensive study of the available borehole data, and found that geothermal gradients generally exceed 40°C/km in the Nappamerri Trough, having values between 50 and 60°C/km in the vicinity of Moomba and Strzelecki Fields. The Patchawarra

---

[1] Vitrinite Reflectance data were assimilated from the following reports:

Baily, T. (1988). Battunga-1. Well completion report prepared for Santos Ltd.
Beech, A.J. (1988). Bungee-1. Well completion report compiled for Santos Ltd.
Boothby, P. (1986). Warnie East-1. Well completion report compiled for Delhi Petroleum Pty Ltd.
Boothby, P. (1987). Okotoko-1. Well completion report compiled for Delhi Petroleum Pty Ltd.
Boothby, P. and Pietsch, A. (1987). Mackillop-1. Well completion report compiled for Delhi Petroleum Pty Ltd.
Burnett, P.J. (1981). Beanbush-1. Well completion report compiled for Delhi Petroleum Pty Ltd.
Campbell, I.R. and Harrison, J. (1963). Putamurdie-1. Well completion report compiled for Delhi Petroleum Pty Ltd.
Elliott, P. (1984). Innamincka-4. Well completion report compiled for Delhi Petroleum Pty Ltd.
Elliott, P. (1985). Burley-2. Well completion report compiled for Delhi Petroleum Pty Ltd.
Gauld, T. (1981). Curalle-1. Well completion report compiled for Delhi Petroleum Pty Ltd.
Gauld, T.D. (1981). Wareena-1. Well completion report compiled for Delhi Petroleum Pty Ltd.
Hall, R. (1982). Alkina-1. Well completion report compiled for Delhi Petroleum Pty Ltd.
Hollis, N. (1986). Nulla-1. Well completion report compiled for Delhi Petroleum Pty Ltd.
Martin, C. (1986). Macadama-1. Well completion report compiled for Delhi Petroleum Pty Ltd.
Mielnik, V. (1984). Tirrawarra North-1. Well completion report compiled for Delhi Petroleum Pty Ltd.
Mielnik, V. (1985). Russel-1. Well completion report compiled for Delhi Petroleum Pty Ltd.
Mielnik, V. (1985). Ullenbury-1. Well completion report compiled for Delhi Petroleum Pty Ltd.
Moore, M.J. (1985). Baryulah-1. Well completion report compiled for Delhi Petroleum Pty Ltd.
Nugent, O.W. (1990). Lycium-1. Well completion report compiled for Santos Ltd.
Robinson, S. (1982). Jackson-1. Well completion report compiled for Delhi Petroleum Pty Ltd.
Robinson, S. (1988). Copai-1. Well completion report compiled for Delhi Petroleum Pty Ltd.

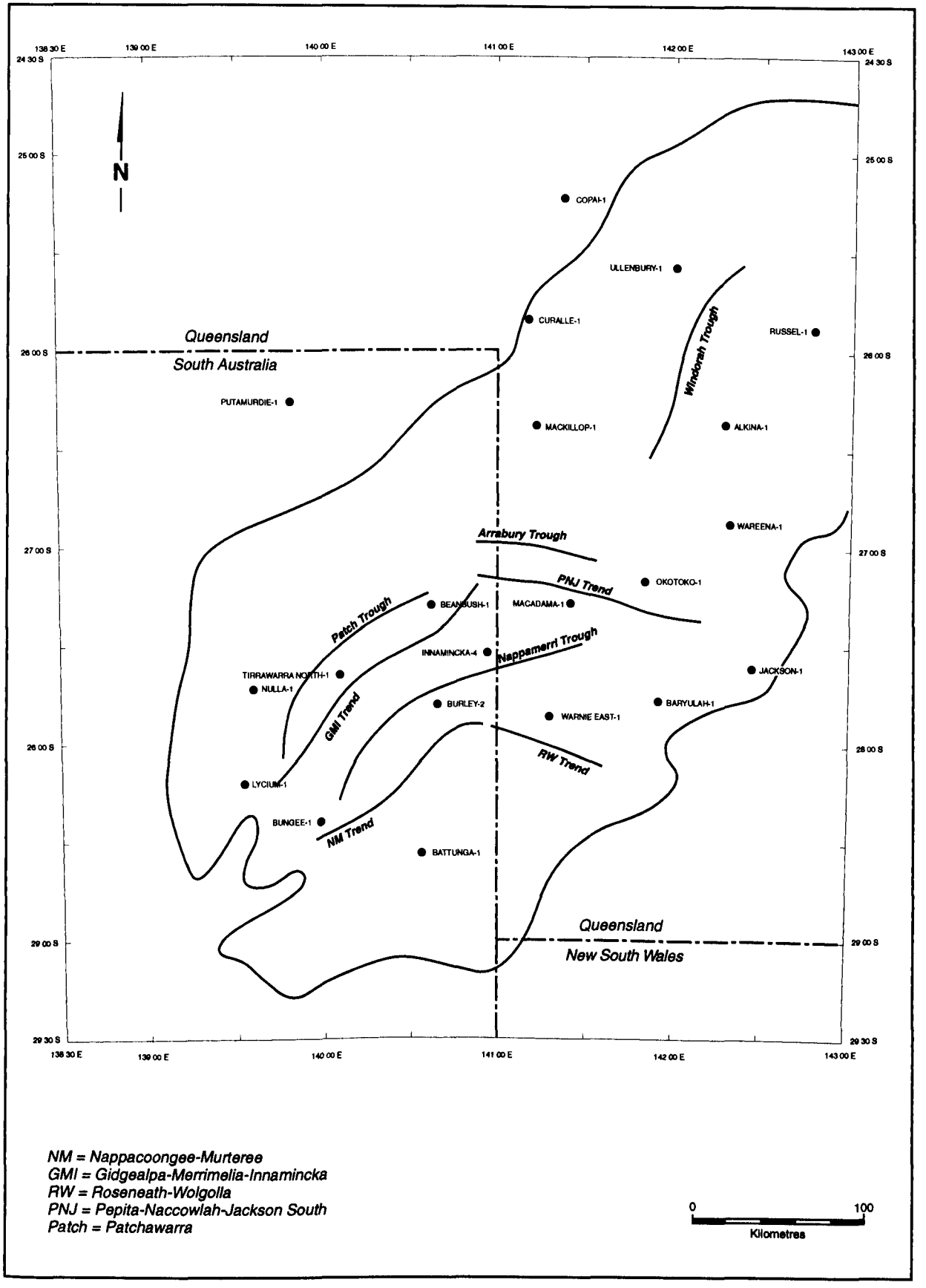

Figure 4.3. Location of wells used for modelling. Major tectonic elements are also shown.

Trough has lower gradients, typically of 30 to 40°C/km. For further details of the distribution of present geothermal gradients in the Cooper-Eromanga Basins, see Pitt (1986).

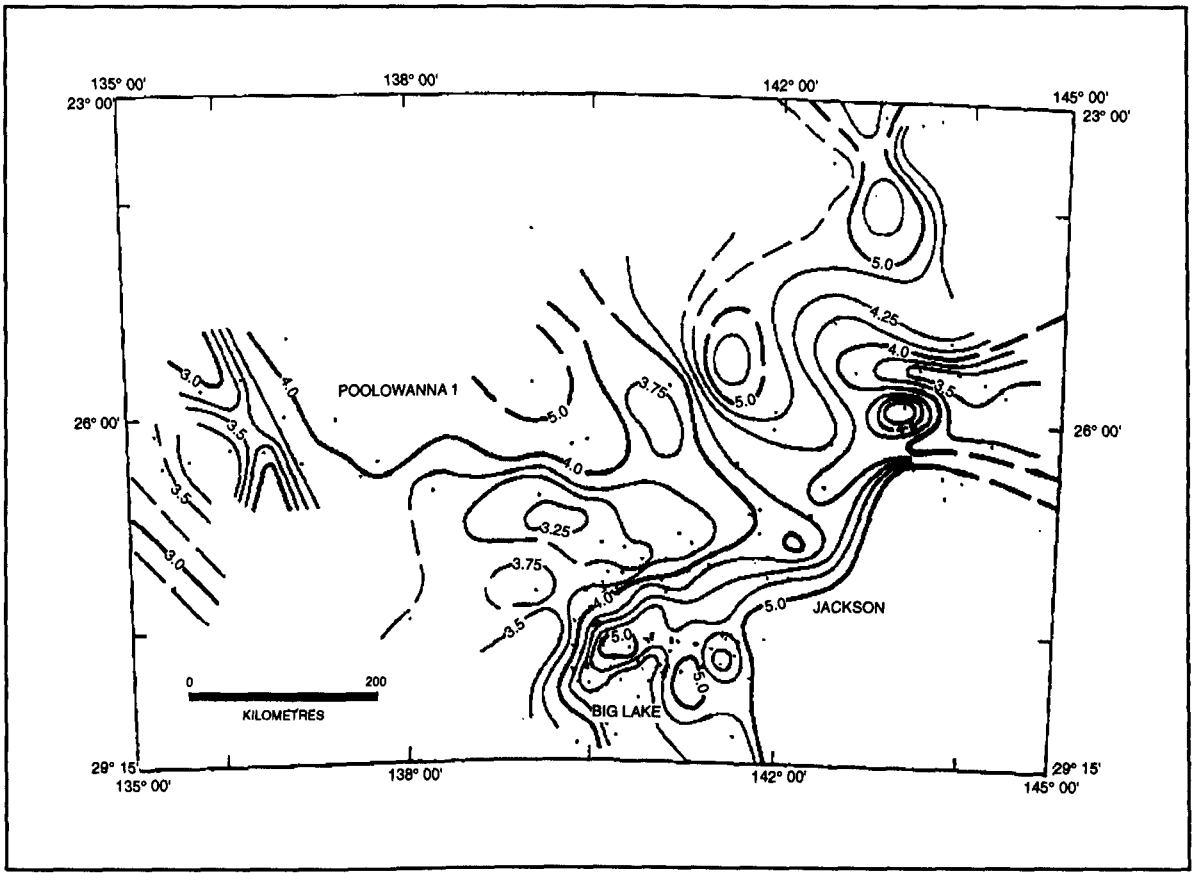

Figure 4.4. Distribution of basement-to-surface geothermal gradients in Eromanga-Cooper Basin region. C.I. = 0.25°C/100m (after Pitt, 1986).

In this study, present geothermal gradients were calculated using bottom hole temperatures (corrected for time since circulation of drilling muds), and temperatures determined from drill stem tests. Cao *et al.*(1988) and Russell and Baillie (1989) suggest that such values provide the most reliable formation temperatures. It is argued that the baseline temperature to which the most meaningful overall thermal gradient is drawn is not the temperature at ground surface, which is subject to diurnal and seasonal variations, but the rock temperature some metres or tens of metres below the ground. This temperature is probably 18-20°C in the region under discussion (Pitt, 1986). A surface temperature of 20°C was used in this study.

The kinetic modelling of the MATOIL program (BEICIP, 1990) used in this study includes both primary cracking (ie. transformation of kerogen to petroleum) and secondary cracking (ie.

progressive degradation of petroleum to gas and to a carbon residue). In modelling, MATOIL's default thermal conductivities, and compaction/decompaction parameters for given lithologies were used.

The two most important variables that govern the modelling of vitrinite reflectance are:

- burial/exhumation history, and ;
- palaeogeothermal gradients.

Waples (1994) recommended that preliminary estimates of exhumation should be incorporated in vitrinite reflectance modelling. Where such estimates are available, they allow palaeogeothermal gradients to be evaluated more accurately from vitrinite reflectance data. However, the aim of this study was to compare exhumation estimates from vitrinite reflectance modelling with those determined using the compaction methodology (Chapters 2 and 3). Hence, three different assumed palaeogeothermal histories were used, and the exhumation during the Late Triassic - Early Jurassic unconformity, and that during the Late Cretaceous - Tertiary unconformity, were varied in order that the modelled vitrinite reflectance gave the best fit to observed vitrinite reflectance.

Following the principle of Occam's razor (ie. the simplest hypothesis that fits the data is the best hypothesis), vitrinite reflectance was first modelled assuming that palaeogeothermal gradients were constant and equal to the present geothermal gradients, ie. *Geothermal History A* (Figure 4.5). As shown by the results (Section 4.4), reflectances predicted by *Geothermal History A* are higher than those observed for the Eromanga Basin. This indicates that the present high geothermal gradients are a relatively recent phenomenon with which vitrinite reflectance has not fully equilibrated. This observation is consistent with the results of AFTA (Gleadow *et al.*, 1988).

Since *Geothermal History A* proved unsatisfactory, a second geothermal history was used. In *Geothermal History B*, the palaeogeothermal gradients increase over the last 90 Ma from lower values to the present gradients (Figure 4.5). The assumed increases in geothermal gradients the last 90 Ma were as follows:

Present Geothermal Gradient	Increase in Geothermal Gradient from 90 Ma to Present Day
≤35°C/km	5°C/km
36-44°C/km	10°C/km
≥45°C/km	15°C/km.

As shown by the results in Section 4.4, *Geothermal History B* implies extremely high, and probably unreasonable, exhumation values associated with the Late Triassic - Early Jurassic unconformity for the majority of the examined wells.

As a consequence, vitrinite reflectance modelling was undertaken using a third and preferred geothermal history. In *Geothermal History C*, geothermal gradients during the deposition of the Eromanga Basin were the same as in *Geothermal History B* (ie. increasing over the last 90 Ma), but the gradients during the deposition of the Cooper Basin were taken to be 5°C/km higher than the present geothermal gradients (Figure 4.5). The effect of increasing the geothermal gradients during the deposition of the Cooper Basin is to reduce the amount of exhumation required at the time of Late Triassic - Early Jurassic unconformity (ie. between the deposition of the Cooper and Eromanga Basins).

The precise geothermal histories used for each well in each of the three scenarios (*A*, *B* and *C*) are summarised in Table 4.1.

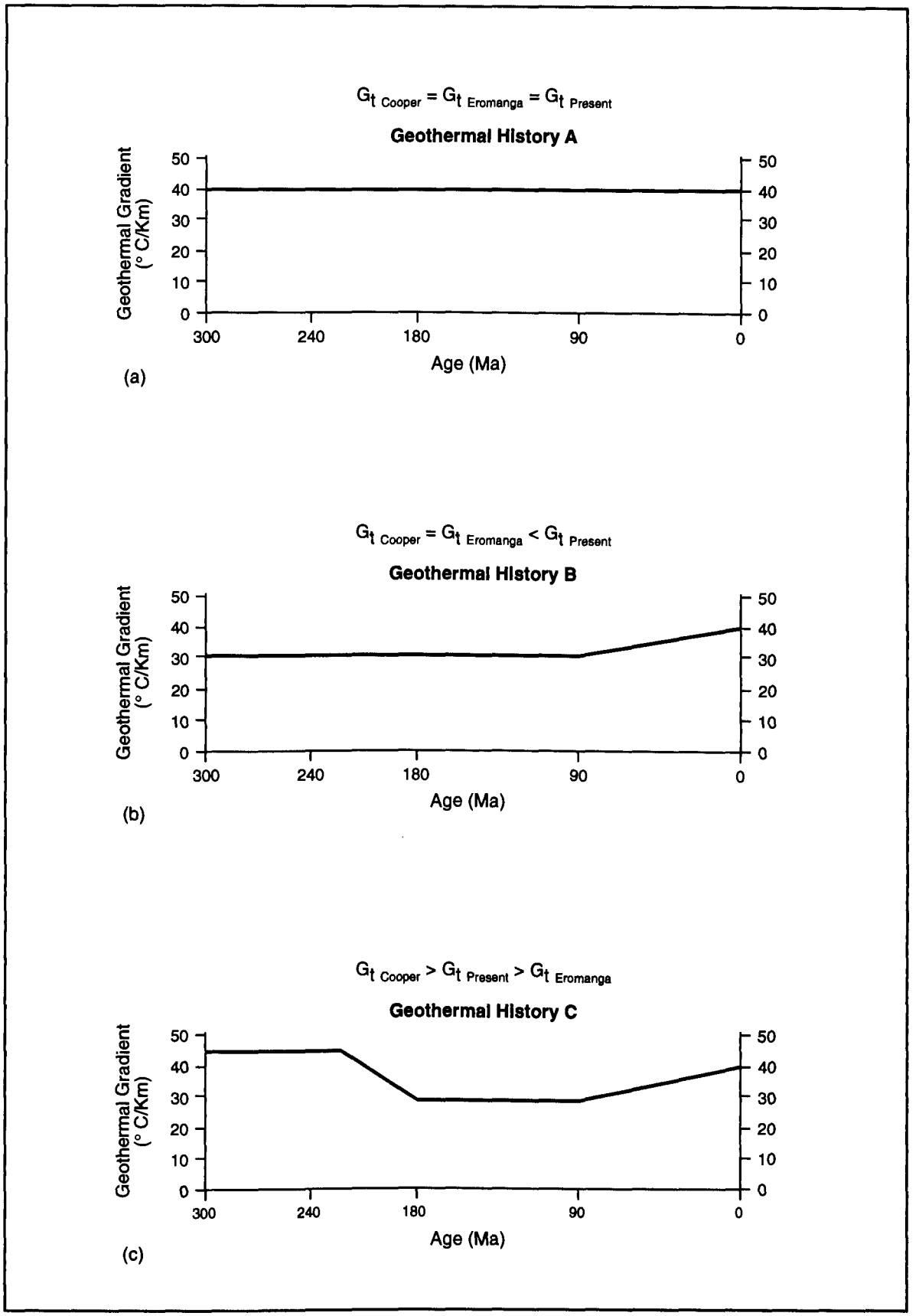

Figure 4.5. Summary of geothermal gradient histories in the three types of maturity modelling. Gradients value at any point in time reflects average gradient of existing basinal section. Details for each well are given in Table 4.1. G_t = Geothermal gradient.

Table 4.1. Table of Present and Palaeogeothermal Gradients That Best Fit Vitrinite Reflectance Data Assuming *Geothermal History A , B* and *C* .

Well	*Geothermal History A* Age (Ma)	*Geothermal History A* Geothermal Gradient (°C/km)	*Geothermal History B* Age (Ma)	*Geothermal History B* Geothermal Gradient (°C/km)	*Geothermal History C* Age (Ma)	*Geothermal History C* Geothermal Gradient (°C/km)
Alkina-1	0	45	0	45	0	45
	91	45	91	30	91	30
	198	45	198	30	198	30
	286	45	286	30	286	50
Baryulah-1	0	45	0	45	0	45
	91	45	91	30	91	30
	208	45	208	30	208	30
	286	45	286	30	286	50
Battunga-1	0	40	0	40	0	40
	10	40	10	30	10	30
	91	40	91	30	91	30
	183	40	183	30	183	30
	286	40	286	30	286	45
Beanbush-1	0	37	0	37	0	37
	91	37	91	27	91	27
	225	37	225	27	225	27
	286	37	286	27	286	42
Bungee-1	0	44	0	44	0	44
	88	44	88	34	88	34
	193	44	193	34	193	34
	286	44	286	34	286	49
Burley-2	0	55	0	55	0	55
	91	55	91	40	91	40
	193	55	193	40	193	40
	286	55	286	40	286	60
Copai-1	0	45	0	45	0	45
	91	45	91	30	91	30
	193	45	193	30	193	30
Curalle-1	0	48	0	48	0	48
	91	48	91	33	91	33
	198	48	198	33	198	33
	250	48	250	33	250	53
Innamincka-4	0	47	0	47	0	47
	91	47	91	32	91	32
	193	47	193	32	193	32
	258	47	258	32	258	52
Jackson-1	0	44	0	44	0	44
	10	44	10	34	10	34
	91	44	91	34	91	34
	193	44	193	34	193	34
	286	44	286	34	286	49
Lycium-1	0	38	0	38	0	38
	10	38	10	28	10	28
	91	38	91	28	91	28
	193	38	193	28	193	28
	268	38	268	28	268	43
Macadama-1	0	44	0	44	0	44
	91	44	91	34	91	34
	183	44	183	34	183	34
	286	44	286	34	286	49

Table 4.1. Continued.

Well	*Geothermal History A* Age (Ma)	Geothermal Gradient (°C/km)	*Geothermal History B* Age (Ma)	Geothermal Gradient (°C/km)	*Geothermal History C* Age (Ma)	Geothermal Gradient (°C/km)
Mackillop-1	0	45	0	45	0	45
	91	45	91	30	91	30
	193	45	193	30	193	30
	258	45	258	30	258	50
Nulla-1	0	37	0	37	0	37
	90	37	90	27	97	27
	193	37	193	27	193	27
	286	37	286	27	286	42
Okotoko-1	0	41	0	41	0	41
	91	41	91	31	91	31
	193	41	193	31	193	31
	286	41	286	31	286	46
Putamurdie-1	0	40	0	40	0	40
	90	40	90	30	90	30
	193	40	193	30	193	30
Russel-1	0	42	0	42	0	42
	10	42	10	32	10	32
	91	42	91	32	91	32
	193	42	193	32	193	32
	258	42	258	32	258	47
Tirrawarra North-1	0	35	0	35	0	35
	91	35	91	30	91	30
	193	35	193	30	193	30
	286	35	286	30	286	40
Ullenbury-1	0	42	0	42	0	42
	91	42	91	32	91	32
	204	42	204	32	204	32
	245	42	245	32	245	47
Wareena-1	0	43	0	43	0	43
	91	43	91	33	91	33
	198	43	198	33	198	33
	253	43	253	33	253	48
Warnie East-1	0	52	0	52	0	52
	10	52	10	37	10	37
	91	52	91	37	91	37
	193	52	193	37	193	37
	286	52	286	37	286	57

4.4 Results of Vitrinite Reflectance Modelling in the Cooper-Eromanga Basins

Assuming *Geothermal History A*, modelled vitrinite reflectance, especially for the Eromanga Basin sequence, is generally too high, ie. vitrinite reflectances have not yet reached equilibrium with the current high temperatures (Figure 4.6). As stated previously, this indicates that the present high geothermal gradients have not been in existence throughout the deposition of the Eromanga Basin sequence.

At Beanbush-1, Bungee-1, Mackillop-1 and Russel-1, assuming *Geothermal History A*, the modelled vitrinite reflectance of the Eromanga sequence is the most in excess of the observed data (Figure 4.6). In these wells, the modelled vitrinite reflectance of the Cooper Basin sequence does, however, provide a reasonable match for the observed data. Hence at these wells no exhumation is inferred either in Late Cretaceous - Tertiary or Late Triassic - Early Jurassic times. Given that *Geothermal History A* predicts vitrinite reflectance that is too high for the Eromanga Basin sequence, but approximately correct for the Cooper Basin sequence in these wells, it is immediately clear that there is a major reflectance break between the Cooper and Eromanga Basins (Figure 4.6). This major break, apparent in most wells, is consistent with the suggestions in the previous Chapter, based on the compaction methodology, that the Cooper Basin has been more deeply buried than the Eromanga Basin. However, it could also indicate higher geothermal gradients during the deposition of the Cooper Basin, or some combination of the two factors. The major difficulty faced in the vitrinite reflectance modelling is that with two key variables (burial/exhumation history and geothermal gradient) and one known (vitrinite reflectance), the resultant models are inherently non-unique.

Assuming *Geothermal History A*, the best fit to the observed vitrinite reflectance data, implies no Late Cretaceous - Tertiary exhumation at: Alkina-1, Battunga-1, Burley-2, Innamincka-4, Lycium-1, Macadama-1, Nulla-1, Tirrawarra North-1 and Warnie East-1. However (unlike Beanbush-1, Bungee-1, Mackillop-1 and Russel-1 which exhibit no Late Cretaceous - Tertiary or Late Triassic - Early Jurassic exhumation) assuming *Geothermal History A*, these wells are best modelled by incorporating Late Triassic - Early Jurassic exhumation. In some wells

(Alkina-1, Battunga-1, Lycium-1 and Ullenbury-1) the amount of Late Triassic - Early Jurassic exhumation was less than subsequent burial. Hence in these wells the Cooper Basin sequence reached maximum burial-depth in Late Cretaceous - Tertiary times. In other wells (Baryulah-1, Curalle-1, Jackson-1, Okotoko-1, and Wareena-1), assuming *Geothermal History A*, the Cooper Basin sequence reached maximum burial-depth prior to deposition of Eromanga Basin sequence.

Figure 4.9 shows apparent exhumation inferred from vitrinite reflectance measurements in the Cooper Basin crossplotted against apparent exhumation inferred from vitrinite reflectance measurements in the Eromanga Basin, assuming *Geothermal History A*.

Given that *Geothermal History A* predicts vitrinite reflectance in excess of that observed for the Eromanga Basin, the data were next modelled using *Geothermal History B* which assumes that present high geothermal gradients result from a steady increase in geothermal gradient since 90 Ma (Turonian) as discussed in Section 4.3.

Assuming *Geothermal History B*, unlike *Geothermal History A*, there are no wells where vitrinite reflectance is best modelled with no exhumation at either Late Cretaceous - Tertiary or Late Triassic - Early Jurassic unconformity (Figure 4.7). Assuming *Geothermal History B*, the best fit to the observed vitrinite reflectance data implies no Late Cretaceous - Tertiary exhumation at: Beanbush-1, Bungee-1, Innamincka-4, and Tirrawarra North-1. In the rest of the wells, except Copai-1 and Putamurdie-1 (Alkina-1, Baryulah-1, Battunga-1, Burley-2, Curalle-1, Jackson-1, Lycium-1, Macadama-1, Mackillop-1, Nulla-1, Okotoko-1, Russel-1, Ullenbury-1, Wareena-1 and Warnie East-1), assuming *Geothermal History B*, Late Cretaceous - Tertiary exhumation is inferred, but the Cooper Basin sequence reached maximum burial-depth prior to deposition of Eromanga Basin sequence.

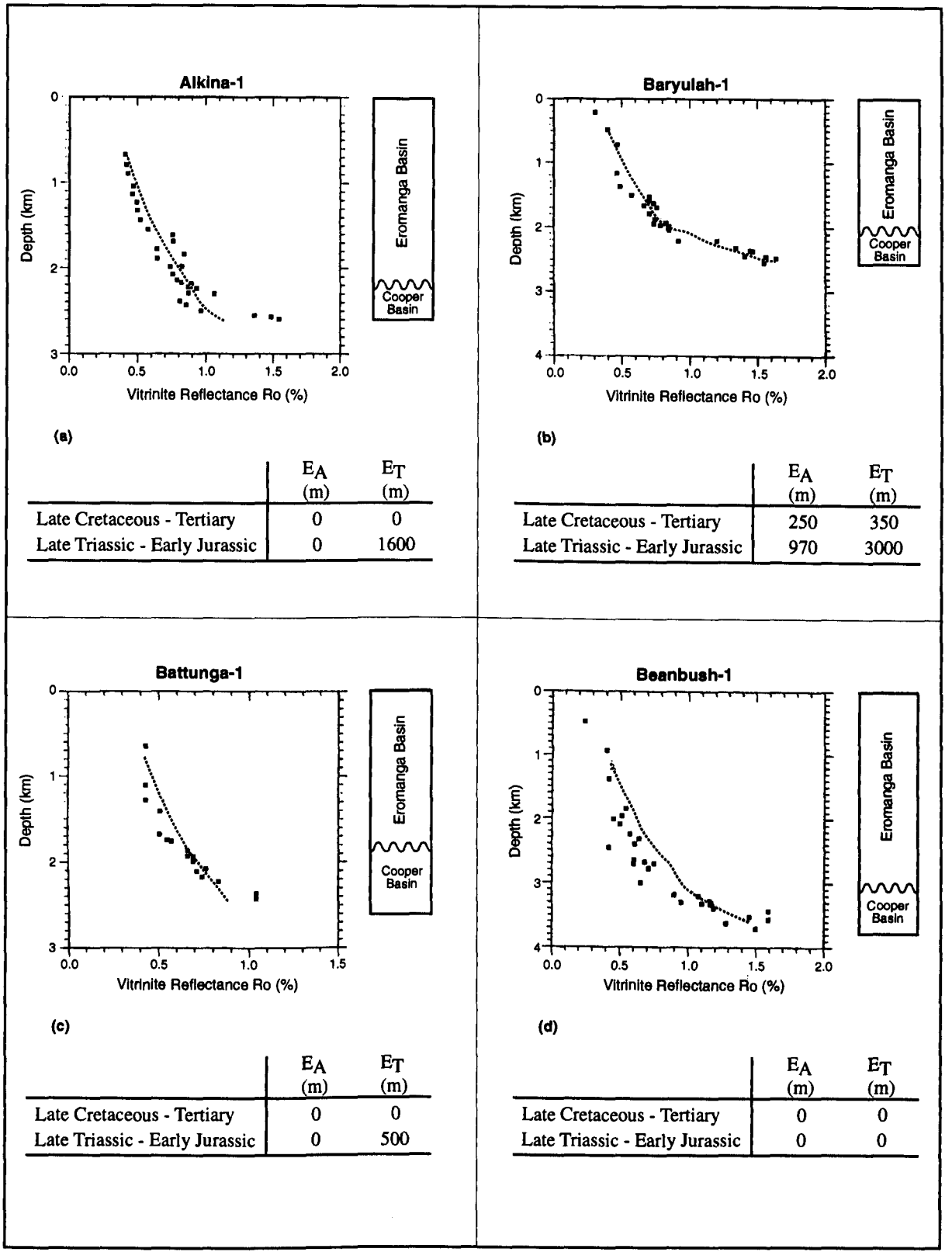

	E_A (m)	E_T (m)
Late Cretaceous - Tertiary	0	0
Late Triassic - Early Jurassic	0	1600

	E_A (m)	E_T (m)
Late Cretaceous - Tertiary	250	350
Late Triassic - Early Jurassic	970	3000

	E_A (m)	E_T (m)
Late Cretaceous - Tertiary	0	0
Late Triassic - Early Jurassic	0	500

	E_A (m)	E_T (m)
Late Cretaceous - Tertiary	0	0
Late Triassic - Early Jurassic	0	0

Figure 4.6. Plots of observed (black dots) and modelled (broken line) vitrinite reflectance Ro (%) vs depth (in km), assuming *Geothermal History A*. Modelling assumes that burial/exhumational events took place in Late Triassic - Early Jurassic times, after the deposition of the Cooper Basin, and in Late Cretaceous - Tertiary times, after the deposition of the Eromanga Basin. Apparent exhumation (E_A) and total exhumation (E_T) values (in metres) used in the modelling are also shown.

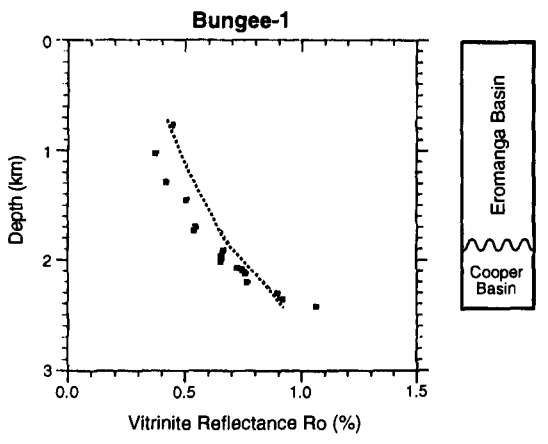

(e)

	E_A (m)	E_T (m)
Late Cretaceous - Tertiary	0	0
Late Triassic - Early Jurassic	0	0

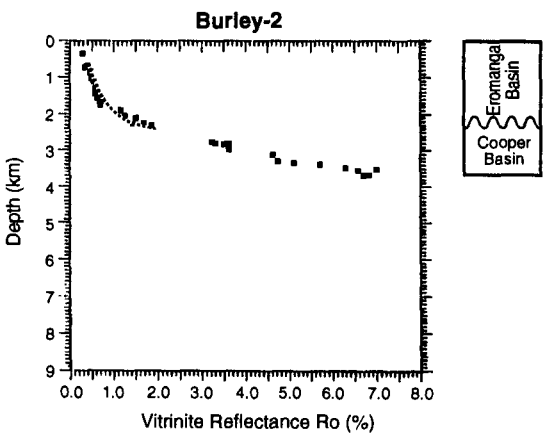

(f)

	E_A (m)	E_T (m)
Late Cretaceous - Tertiary	0	0
Late Triassic - Early Jurassic	3200	5500

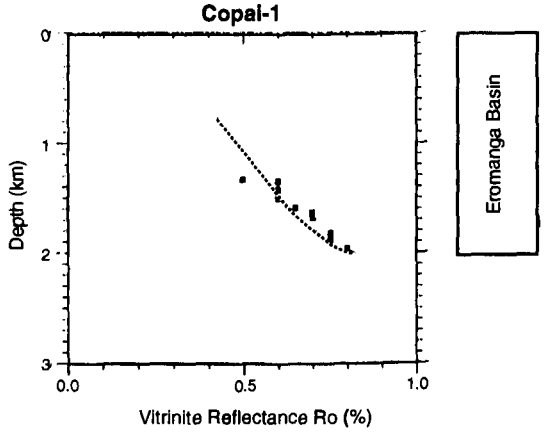

(g)

	E_A (m)	E_T (m)
Late Cretaceous - Tertiary	100	100
Late Triassic - Early Jurassic	IM*	IM*

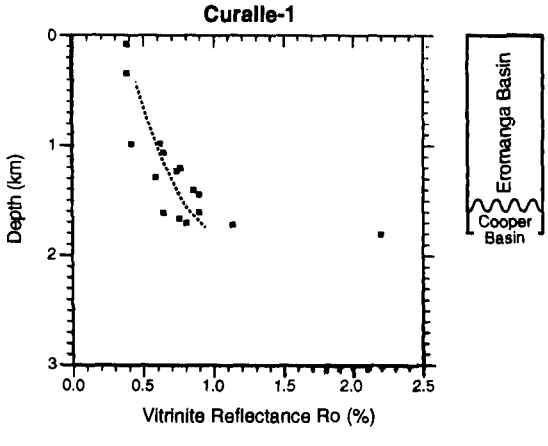

(h)

	E_A (m)	E_T (m)
Late Cretaceous - Tertiary	550	550
Late Triassic - Early Jurassic	900	2600

Figure 4.6. Continued.

*IM = Interval Missing.

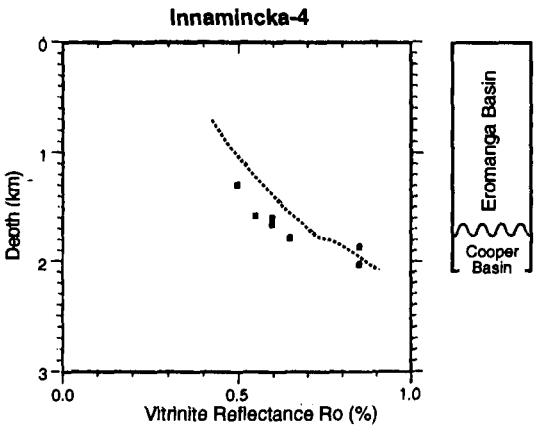

(i)

	E_A (m)	E_T (m)
Late Cretaceous - Tertiary	0	0
Late Triassic - Early Jurassic	410	2200

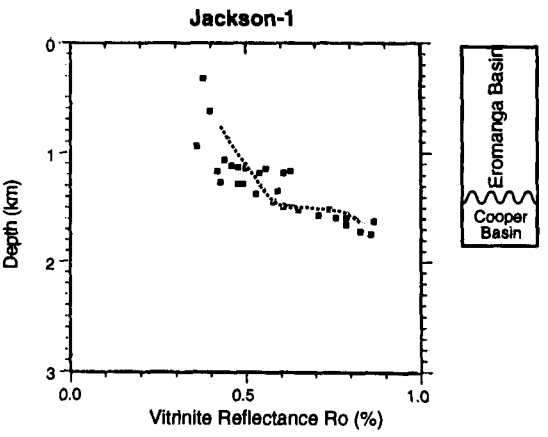

(j)

	E_A (m)	E_T (m)
Late Cretaceous - Tertiary	100	100
Late Triassic - Early Jurassic	1010	2500

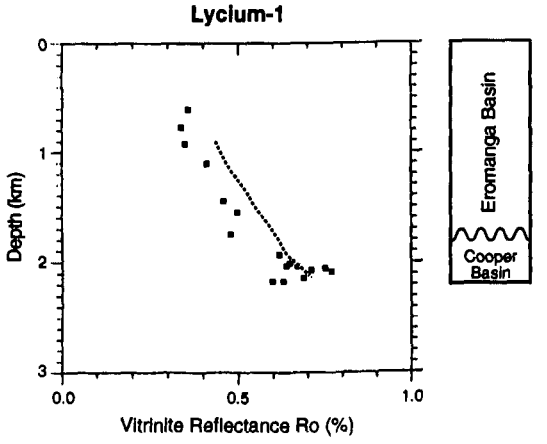

(k)

	E_A (m)	E_T (m)
Late Cretaceous - Tertiary	0	0
Late Triassic - Early Jurassic	0	1900

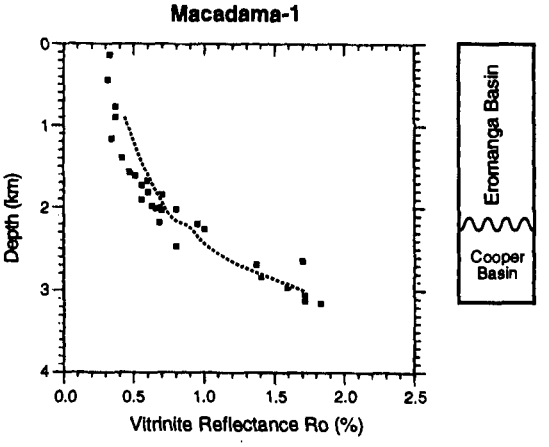

(l)

	E_A (m)	E_T (m)
Late Cretaceous - Tertiary	0	0
Late Triassic - Early Jurassic	600	2800

Figure 4.6. Continued.

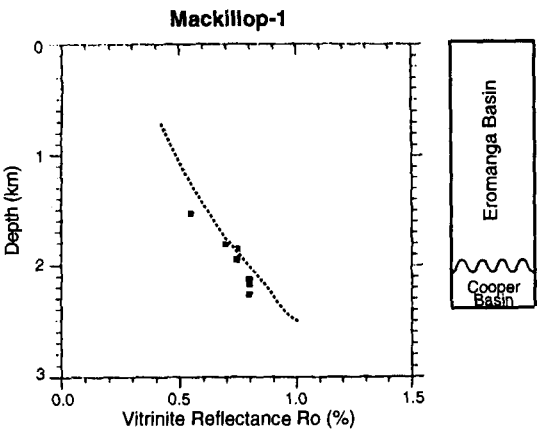

(m)

	E_A (m)	E_T (m)
Late Cretaceous - Tertiary	0	0
Late Triassic - Early Jurassic	0	0

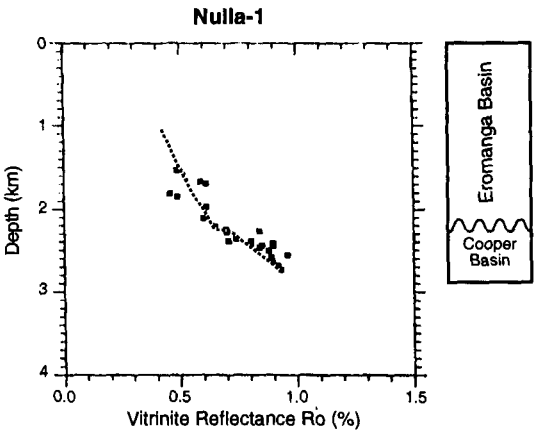

(n)

	E_A (m)	E_T (m)
Late Cretaceous - Tertiary	0	0
Late Triassic - Early Jurassic	660	2900

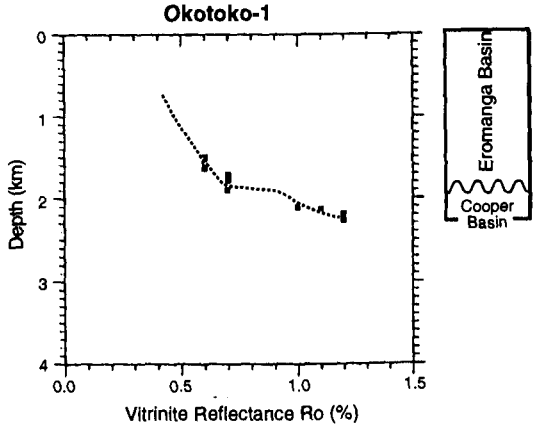

(o)

	E_A (m)	E_T (m)
Late Cretaceous - Tertiary	200	200
Late Triassic - Early Jurassic	1220	3100

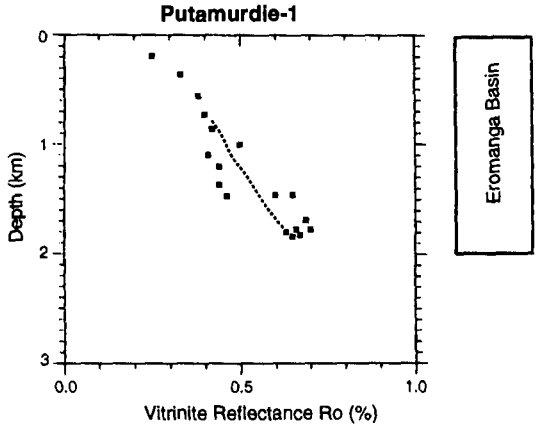

(p)

	E_A (m)	E_T (m)
Late Cretaceous - Tertiary	130	200
Late Triassic - Early Jurassic	*IM	*IM

Figure 4.6. Continued.

*IM = Interval Missing.

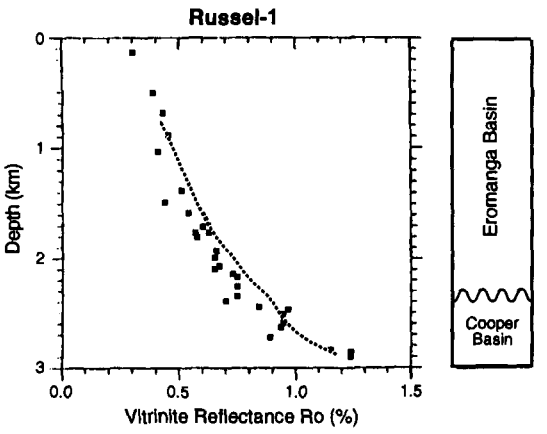

(q)	E_A (m)	E_T (m)
Late Cretaceous - Tertiary	0	0
Late Triassic - Early Jurassic	0	0

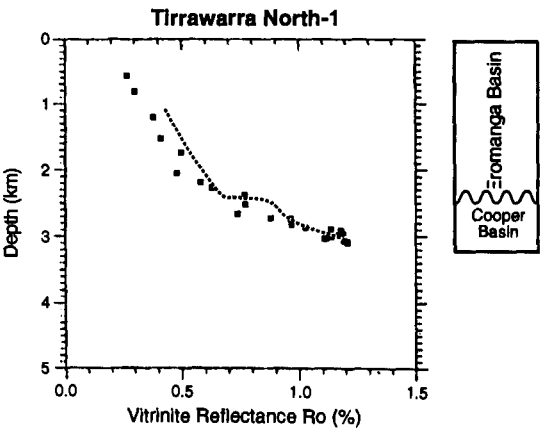

(r)	E_A (m)	E_T (m)
Late Cretaceous - Tertiary	0	0
Late Triassic - Early Jurassic	1100	3500

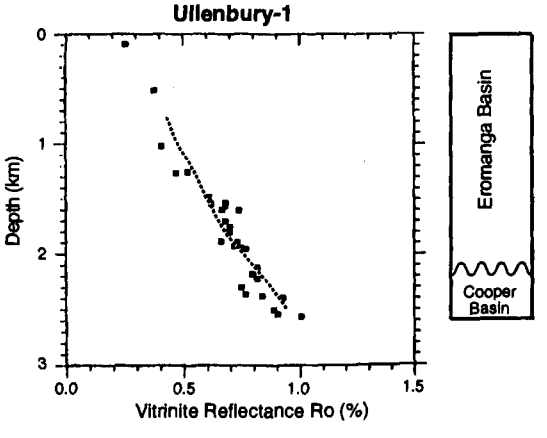

(s)	E_A (m)	E_T (m)
Late Cretaceous - Tertiary	170	200
Late Triassic - Early Jurassic	0	2200

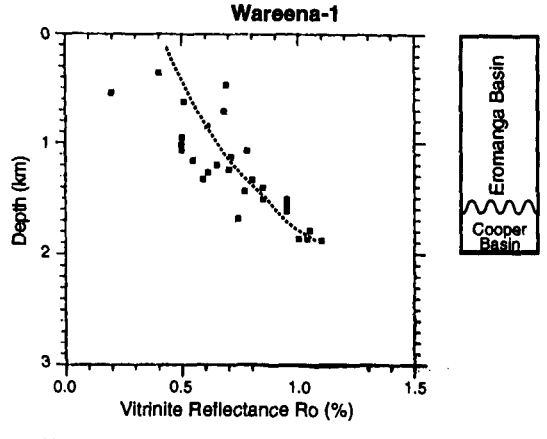

(t)	E_A (m)	E_T (m)
Late Cretaceous - Tertiary	600	600
Late Triassic - Early Jurassic	880	2400

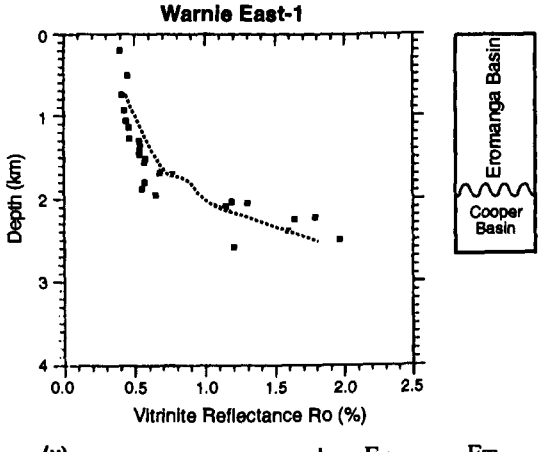

(u)	E_A (m)	E_T (m)
Late Cretaceous - Tertiary	0	0
Late Triassic - Early Jurassic	580	2300

Figure 4.6. Continued.

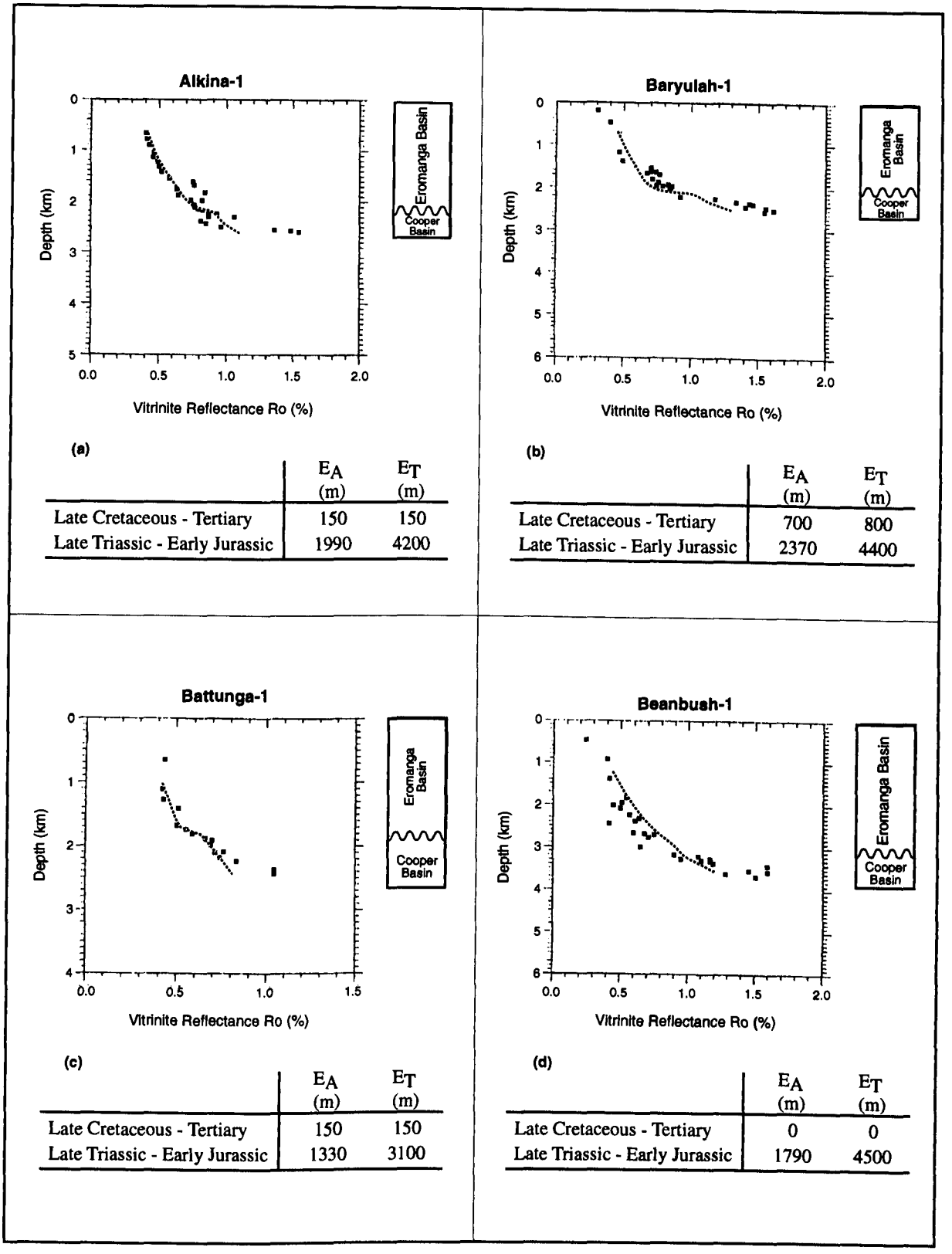

	E_A (m)	E_T (m)
Late Cretaceous - Tertiary	150	150
Late Triassic - Early Jurassic	1990	4200

	E_A (m)	E_T (m)
Late Cretaceous - Tertiary	700	800
Late Triassic - Early Jurassic	2370	4400

	E_A (m)	E_T (m)
Late Cretaceous - Tertiary	150	150
Late Triassic - Early Jurassic	1330	3100

	E_A (m)	E_T (m)
Late Cretaceous - Tertiary	0	0
Late Triassic - Early Jurassic	1790	4500

Figure 4.7. Plots of observed (black dots) and modelled (broken line) vitrinite reflectance Ro (%) vs depth (in km), assuming *Geothermal History B*. Modelling assumes that burial/exhumational events took place in Late Triassic - Early Jurassic times, after the deposition of the Cooper Basin, and in Late Cretaceous - Tertiary times, after the deposition of the Eromanga Basin. Apparent exhumation (E_A) and total exhumation (E_T) values (in metres) used in the modelling are also shown.

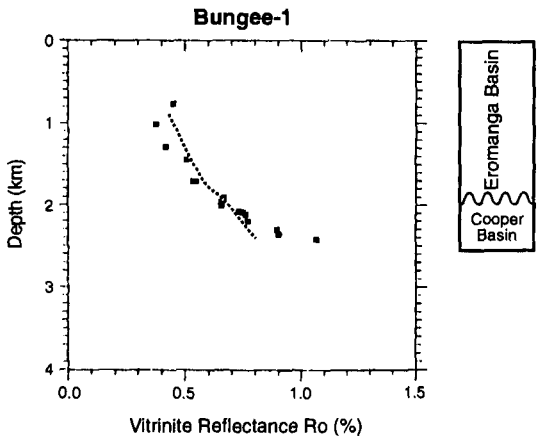

(e)

	E_A (m)	E_T (m)
Late Cretaceous - Tertiary	0	0
Late Triassic - Early Jurassic	900	2700

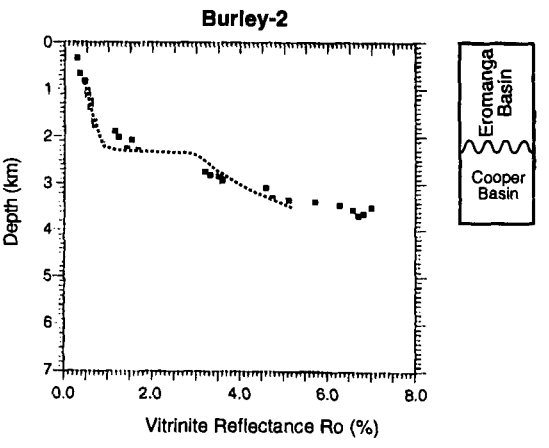

(f)

	E_A (m)	E_T (m)
Late Cretaceous - Tertiary	200	200
Late Triassic - Early Jurassic	4830	7500

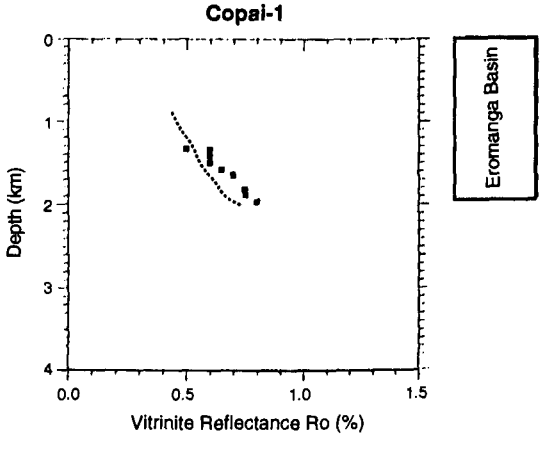

(g)

	E_A (m)	E_T (m)
Late Cretaceous - Tertiary	600	600
Late Triassic - Early Jurassic	*IM	*IM

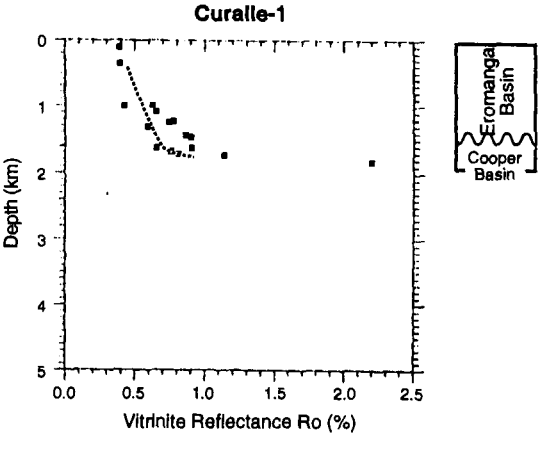

(h)

	E_A (m)	E_T (m)
Late Cretaceous - Tertiary	1000	1000
Late Triassic - Early Jurassic	2190	3900

Figure 4.7. Continued.

*IM = Interval Missing.

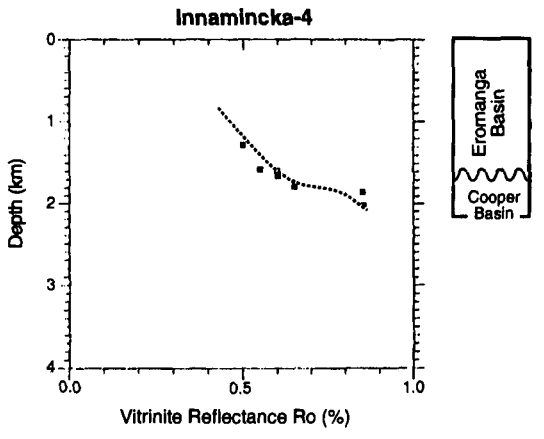

(i)

	E_A (m)	E_T (m)
Late Cretaceous - Tertiary	0	0
Late Triassic - Early Jurassic	810	2600

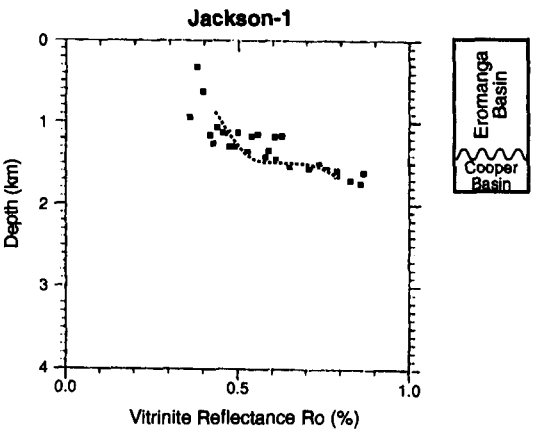

(j)

	E_A (m)	E_T (m)
Late Cretaceous - Tertiary	350	350
Late Triassic - Early Jurassic	1610	3100

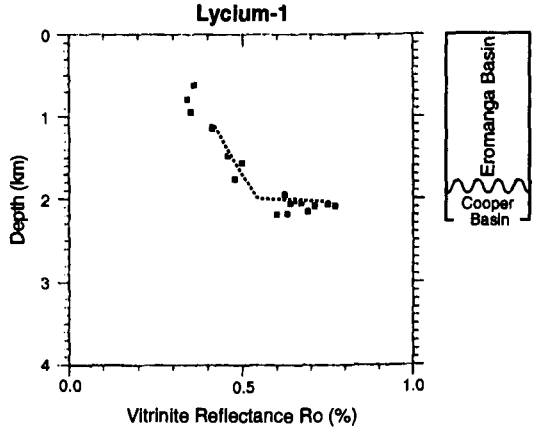

(k)

	E_A (m)	E_T (m)
Late Cretaceous - Tertiary	150	150
Late Triassic - Early Jurassic	1510	3500

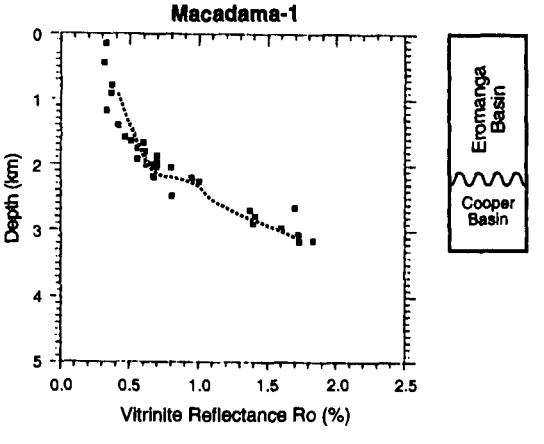

(l)

	E_A (m)	E_T (m)
Late Cretaceous - Tertiary	300	300
Late Triassic - Early Jurassic	1500	3700

Figure 4.7. Continued.

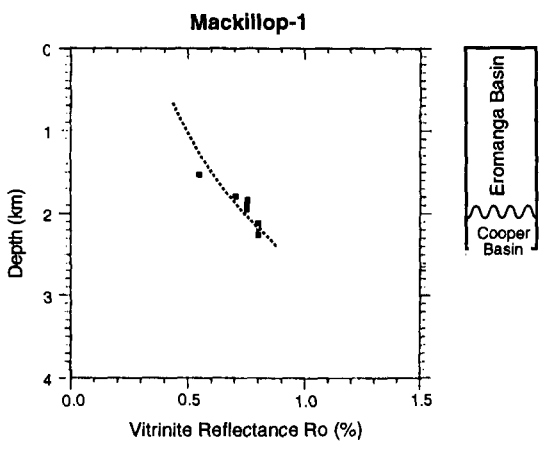

(m)

	E_A (m)	E_T (m)
Late Cretaceous - Tertiary	450	450
Late Triassic - Early Jurassic	720	3000

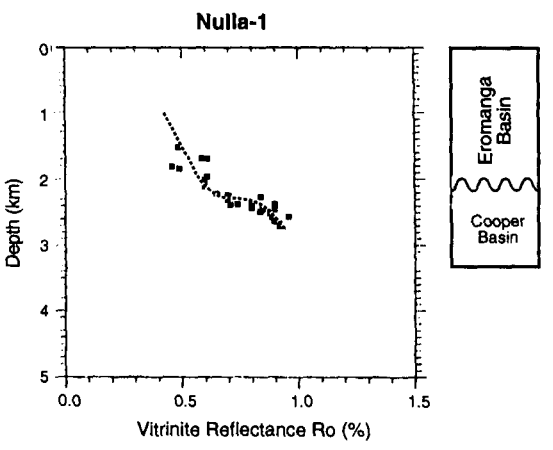

(n)

	E_A (m)	E_T (m)
Late Cretaceous - Tertiary	400	400
Late Triassic - Early Jurassic	2060	4300

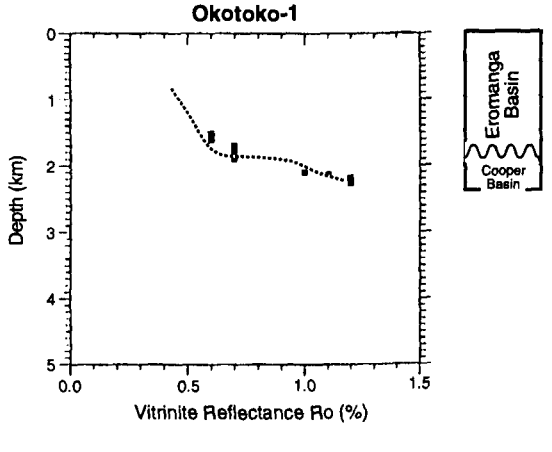

(o)

	E_A (m)	E_T (m)
Late Cretaceous - Tertiary	400	400
Late Triassic - Early Jurassic	2320	4200

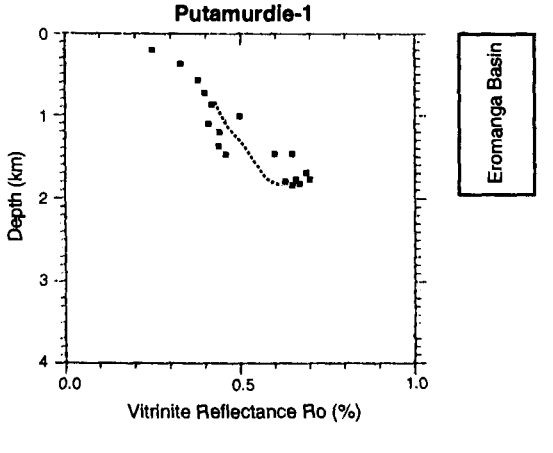

(p)

	E_A (m)	E_T (m)
Late Cretaceous - Tertiary	530	600
Late Triassic - Early Jurassic	*IM	*IM

Figure 4.7. Continued.

*IM = Interval Missing.

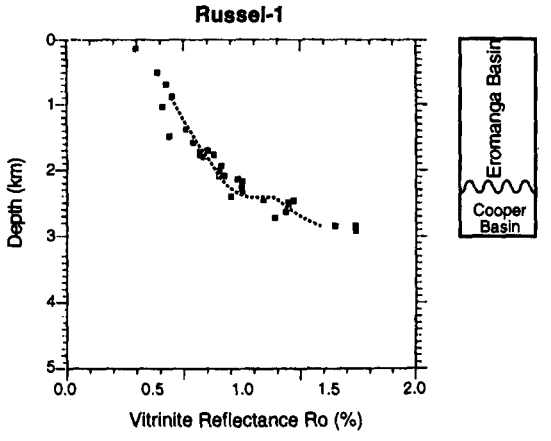

(q)

	E_A (m)	E_T (m)
Late Cretaceous - Tertiary	400	400
Late Triassic - Early Jurassic	1480	3900

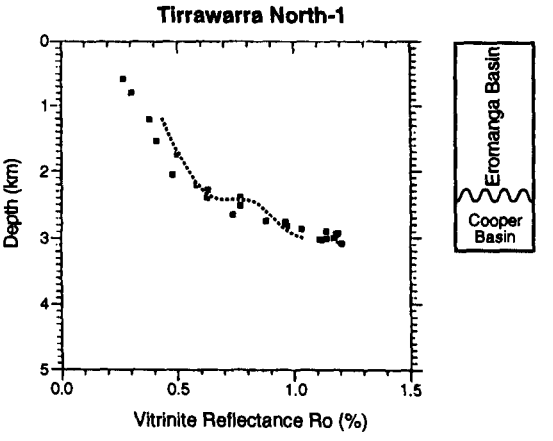

(r)

	E_A (m)	E_T (m)
Late Cretaceous - Tertiary	0	0
Late Triassic - Early Jurassic	1600	4000

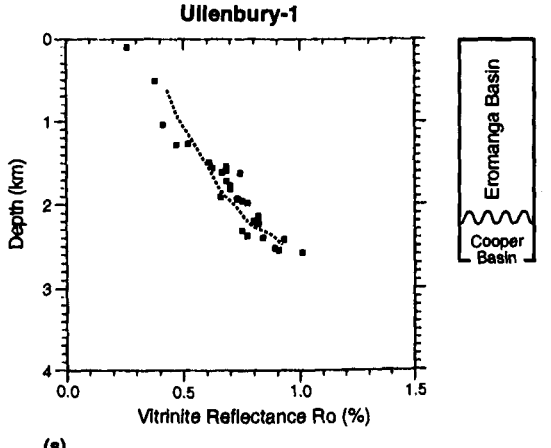

(s)

	E_A (m)	E_T (m)
Late Cretaceous - Tertiary	570	600
Late Triassic - Early Jurassic	1440	3800

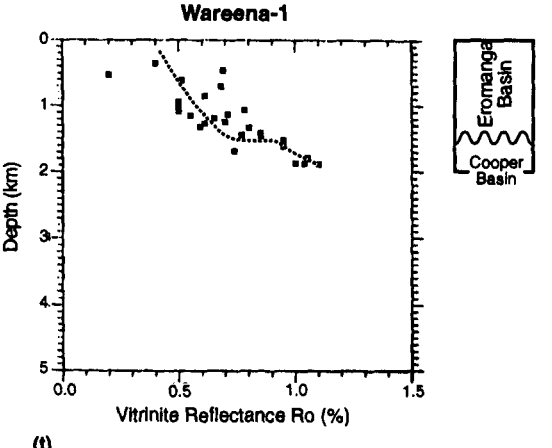

(t)

	E_A (m)	E_T (m)
Late Cretaceous - Tertiary	1100	1100
Late Triassic - Early Jurassic	2380	3900

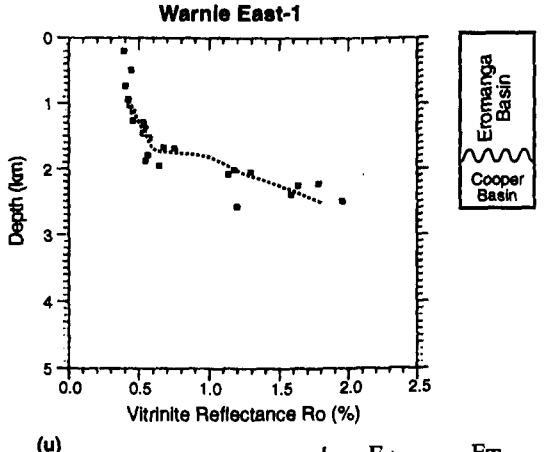

(u)

	E_A (m)	E_T (m)
Late Cretaceous - Tertiary	60	200
Late Triassic - Early Jurassic	1880	3600

Figure 4.7. Continued.

The mean Late Cretaceous - Tertiary apparent exhumation value assuming *Geothermal History B* is approximately 360 m. This is 260 m higher than the mean Late Cretaceous - Tertiary apparent exhumation value assuming *Geothermal History A*. The mean Late Triassic - Early Jurassic apparent exhumation value assuming *Geothermal History B* is approximately 1830 m. This is 1220 m higher than the mean Late Triassic - Early Jurassic apparent exhumation value assuming *Geothermal History A*.

Figure 4.9 shows apparent exhumation inferred from Cooper Basin vitrinite reflectance crossplotted against apparent exhumation inferred from Eromanga Basin vitrinite reflectance, assuming *Geothermal History B*.

The vitrinite reflectance trend in the Burley-2 well merits special mention. This well exhibits the most pronounced change of vitrinite reflectance trend with depth between Cooper and Eromanga Basins of all the wells studied. In order to match this change in trend, assuming *Geothermal History B*, in excess of 7500 m of Late Triassic - Early Jurassic exhumation must be inferred (7500 m was used in the modelling and so additional exhumation would be required to match the Cooper Basin vitrinite reflectance trend). This amount of exhumation is considered geologically unreasonable, and the break in vitrinite reflectance trend in this well presumably reflects both Late Triassic - Early Jurassic exhumation, and higher geothermal gradients during the deposition of the Cooper Basin.

Geothermal histories *B* and *C* were altered slightly to model vitrinite reflectance in the Battunga-1, Jackson-1, Lycium-1, Russel-1 and Warnie East-1 wells. In these wells the increase in geothermal gradients was assumed to occur over the last 10 Ma and not the last 90 Ma (Table 4.1). This allowed a better fit to vitrinite reflectance data from the Eromanga sequence, but does not otherwise affect the conclusions.

In an attempt to match the vitrinite reflectance trends of the Cooper Basin without invoking such extreme Late Triassic - Early Jurassic exhumation as required by *Geothermal History B*, modelling was undertaken using *Geothermal History C*. In *Geothermal History C*, higher

geothermal gradients were assumed during the deposition of the Cooper Basin (see Section 4.3 and Table 4.1 for details).

Assuming *Geothermal History C*, there are no wells where vitrinite reflectance is best modelled with no exhumation associated with both the Late Cretaceous - Tertiary and Late Triassic - Early Jurassic unconformities (Figure 4.8). Assuming *Geothermal History C*, the best fit to the observed vitrinite reflectance data, implies no Late Cretaceous - Tertiary exhumation at: Beanbush-1, Bungee-1, Innamincka-4, and Tirrawarra North-1. In the rest of the wells, assuming *Geothermal History C*, Late Cretaceous - Tertiary exhumation is inferred, but the Cooper Basin sequence reached maximum burial-depth prior to deposition of Eromanga Basin sequence.

Figure 4.9 shows apparent exhumation inferred from Cooper Basin vitrinite reflectance crossplotted against apparent exhumation inferred from Eromanga Basin vitrinite reflectance, assuming *Geothermal History C*.

The Late Cretaceous - Tertiary exhumation values inferred by vitrinite reflectance modelling using *Geothermal History B* and *Geothermal History C* are very similar. This is to be expected since they assume the same geothermal history during the deposition of the Eromanga Basin sequence. The mean Late Triassic - Early Jurassic apparent exhumation value assuming *Geothermal History C* is 600 m. This is 1230 m less than the mean Late Triassic - Early Jurassic apparent exhumation value assuming *Geothermal History B*. This reduction, of course, reflects the higher geothermal gradients assumed by *Geothermal History C* during the deposition of the Cooper Basin sequence. The interpretation and significance of the results are discussed in Section 4.6. However, the exhumation values inferred from *Geothermal History C* are considered the most reliable. The Late Cretaceous - Tertiary exhumation values assuming *Geothermal History C* are plotted on Figure 4.10 and these values are used for comparisons between the methods of estimating exhumation (Chapter 6).

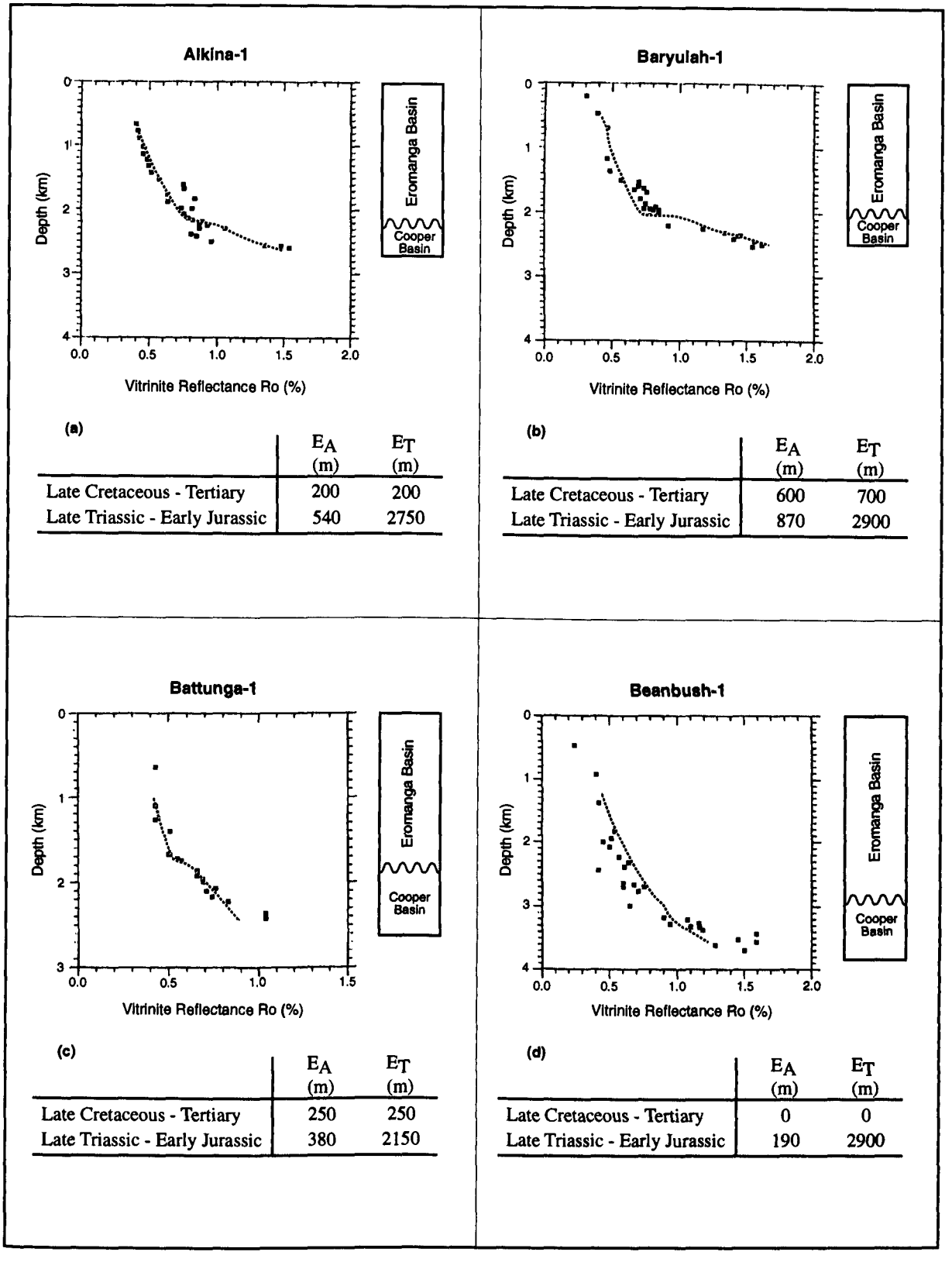

(a)

	E_A (m)	E_T (m)
Late Cretaceous - Tertiary	200	200
Late Triassic - Early Jurassic	540	2750

(b)

	E_A (m)	E_T (m)
Late Cretaceous - Tertiary	600	700
Late Triassic - Early Jurassic	870	2900

(c)

	E_A (m)	E_T (m)
Late Cretaceous - Tertiary	250	250
Late Triassic - Early Jurassic	380	2150

(d)

	E_A (m)	E_T (m)
Late Cretaceous - Tertiary	0	0
Late Triassic - Early Jurassic	190	2900

Figure 4.8. Plots of observed (black dots) and modelled (broken line) vitrinite reflectance Ro (%) vs depth (in km), assuming *Geothermal History C*. Modelling assumes that burial/exhumational events took place in Late Triassic - Early Jurassic times, after the deposition of the Cooper Basin, and in Late Cretaceous - Tertiary times, after the deposition of the Eromanga Basin. Apparent exhumation (E_A) and total exhumation (E_T) values (in metres) used in the modelling are also shown.

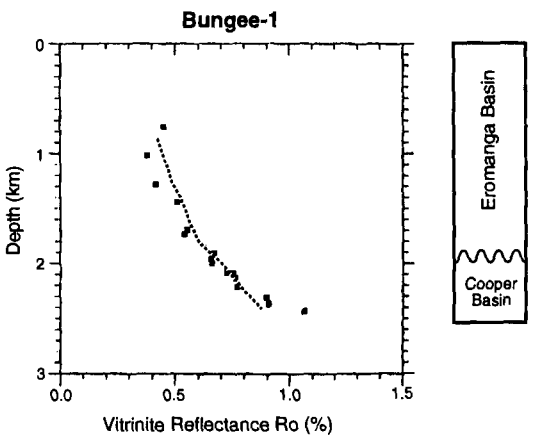

(e)

	E_A (m)	E_T (m)
Late Cretaceous - Tertiary	0	0
Late Triassic - Early Jurassic	250	2050

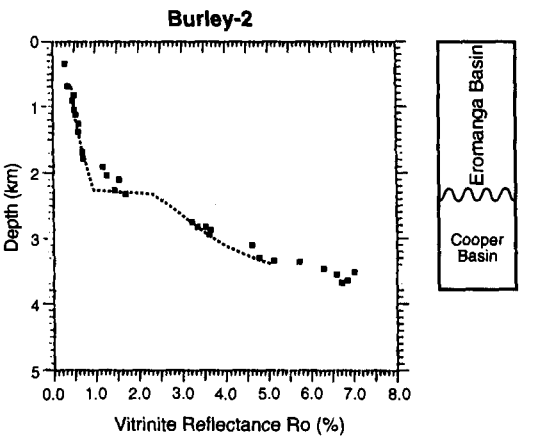

(f)

	E_A (m)	E_T (m)
Late Cretaceous - Tertiary	200	200
Late Triassic - Early Jurassic	1730	4000

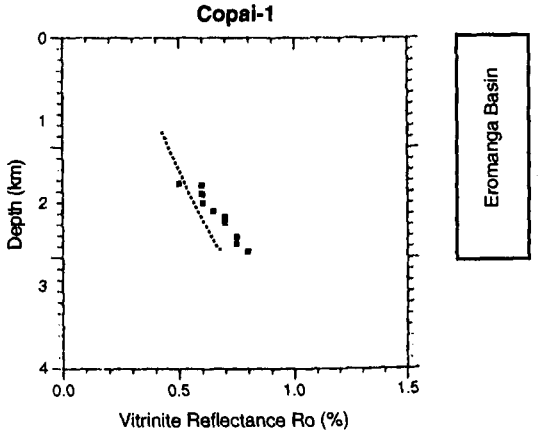

(g)

	E_A (m)	E_T (m)
Late Cretaceous - Tertiary	300	300
Late Triassic - Early Jurassic	*IM	*IM

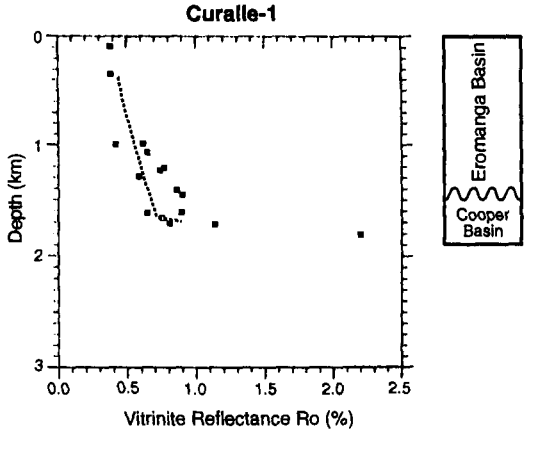

(h)

	E_A (m)	E_T (m)
Late Cretaceous - Tertiary	800	800
Late Triassic - Early Jurassic	1190	2900

Figure 4.8. Continued.

*IM = Interval Missing.

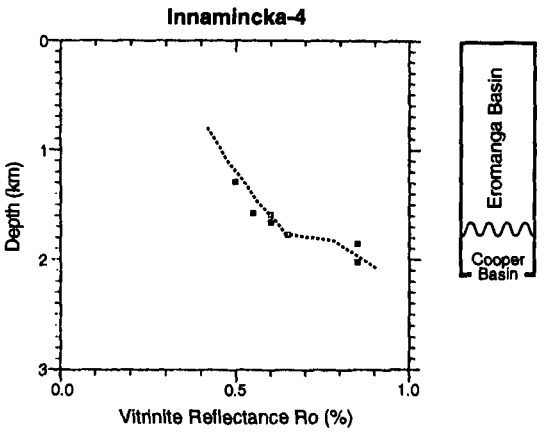

(i)

	E_A (m)	E_T (m)
Late Cretaceous - Tertiary	0	0
Late Triassic - Early Jurassic	310	2100

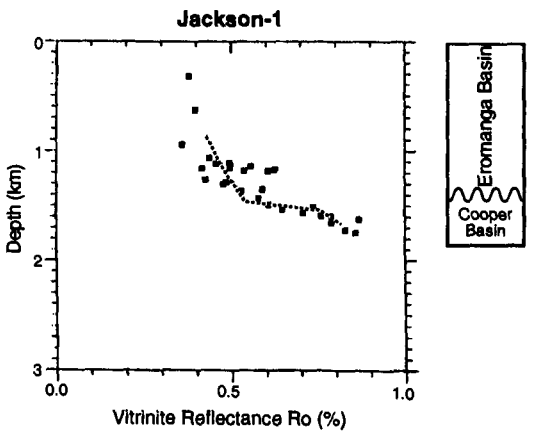

(j)

	E_A (m)	E_T (m)
Late Cretaceous - Tertiary	400	400
Late Triassic - Early Jurassic	710	2200

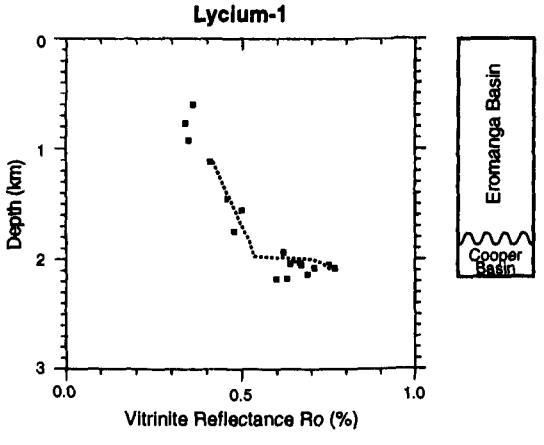

(k)

	E_A (m)	E_T (m)
Late Cretaceous - Tertiary	150	150
Late Triassic - Early Jurassic	310	2300

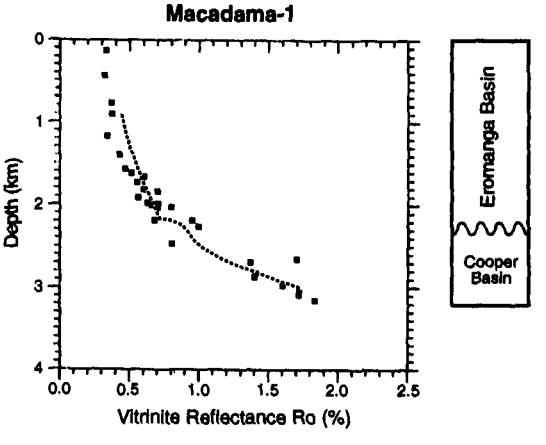

(l)

	E_A (m)	E_T (m)
Late Cretaceous - Tertiary	300	300
Late Triassic - Early Jurassic	500	2700

Figure 4.8. Continued.

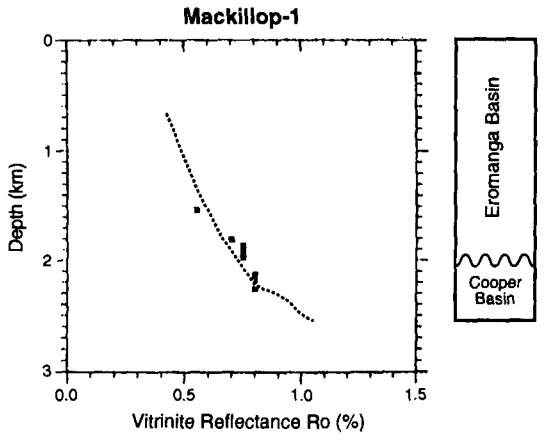

(m)	E_A (m)	E_T (m)
Late Cretaceous - Tertiary	350	350
Late Triassic - Early Jurassic	470	2750

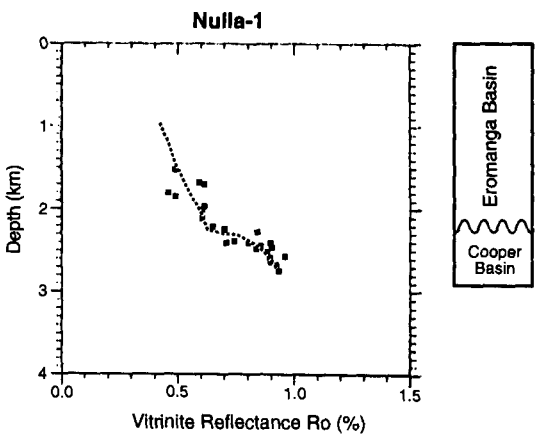

(n)	E_A (m)	E_T (m)
Late Cretaceous - Tertiary	300	300
Late Triassic - Early Jurassic	610	2850

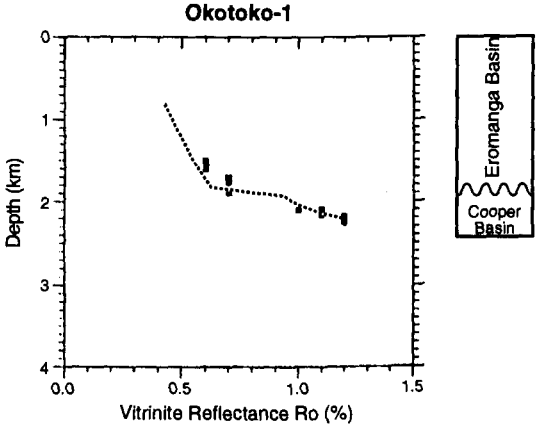

(o)	E_A (m)	E_T (m)
Late Cretaceous - Tertiary	350	350
Late Triassic - Early Jurassic	620	2500

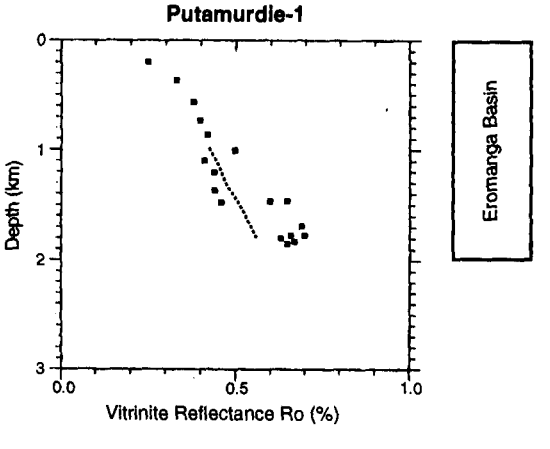

(p)	E_A (m)	E_T (m)
Late Cretaceous - Tertiary	230	300
Late Triassic - Early Jurassic	*IM	*IM

Figure 4.8. Continued.

*IM = Interval Missing.

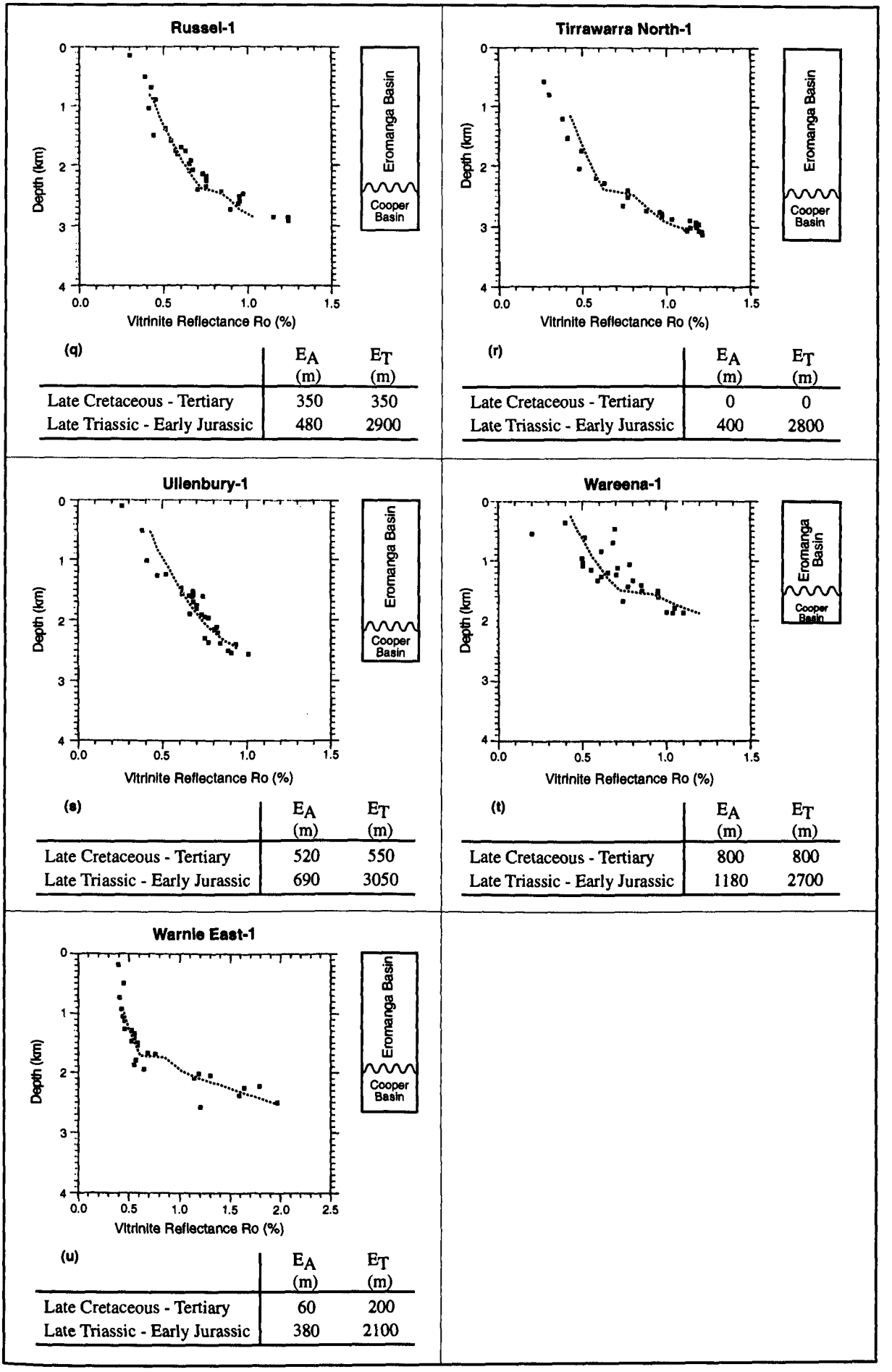

(q)

	E_A (m)	E_T (m)
Late Cretaceous - Tertiary	350	350
Late Triassic - Early Jurassic	480	2900

(r)

	E_A (m)	E_T (m)
Late Cretaceous - Tertiary	0	0
Late Triassic - Early Jurassic	400	2800

(s)

	E_A (m)	E_T (m)
Late Cretaceous - Tertiary	520	550
Late Triassic - Early Jurassic	690	3050

(t)

	E_A (m)	E_T (m)
Late Cretaceous - Tertiary	800	800
Late Triassic - Early Jurassic	1180	2700

(u)

	E_A (m)	E_T (m)
Late Cretaceous - Tertiary	60	200
Late Triassic - Early Jurassic	380	2100

Figure 4.8. Continued.

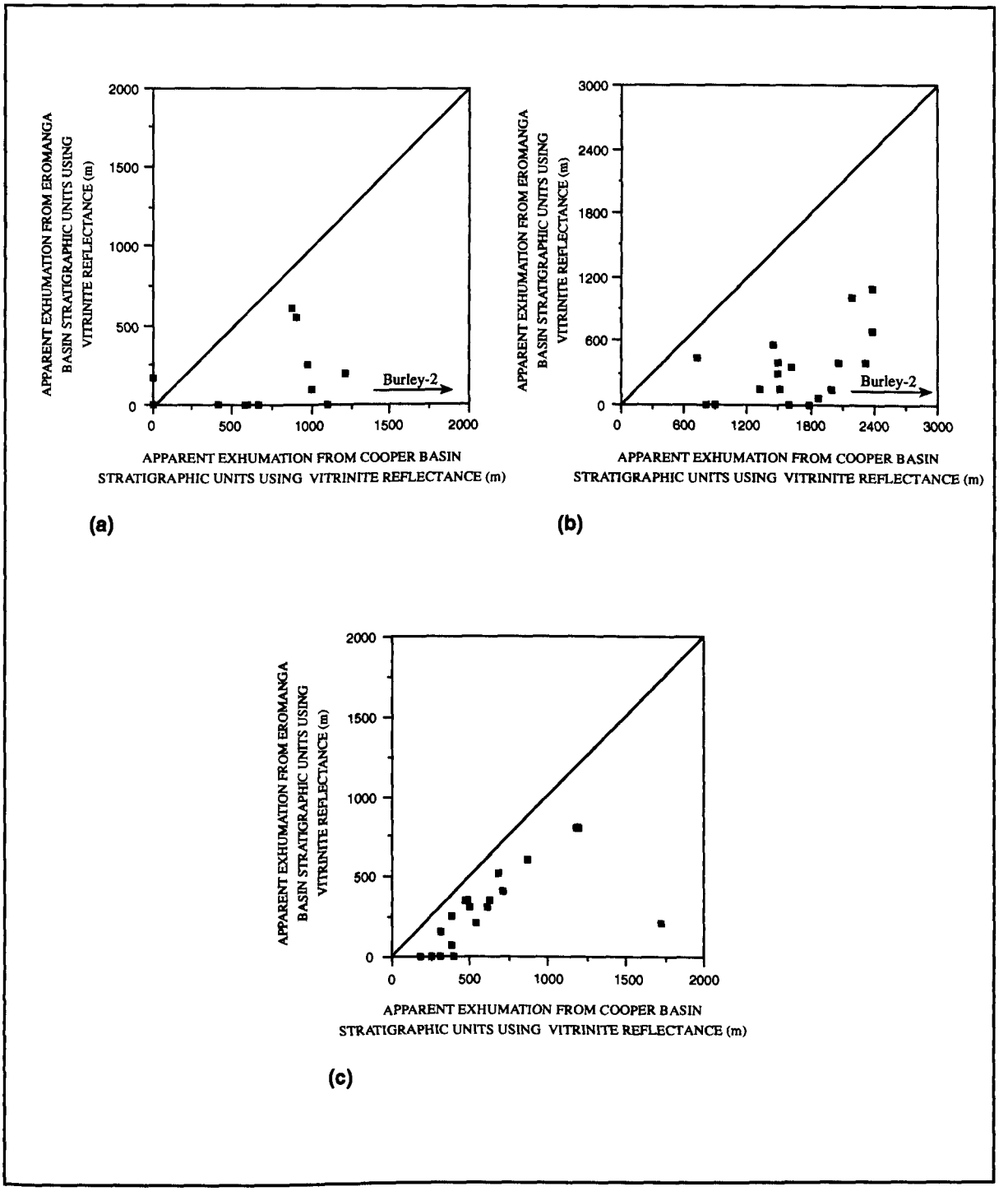

Figure 4.9. Crossplots of apparent exhumation (in metres) from Eromanga Basin units against apparent exhumation (in metres) from Cooper Basin units derived from (a) *Geothermal History A*, (b) *Geothermal History B*, and (c) *Geothermal History C*. The line illustrating the 1:1 relationship between apparent exhumation values from each pair of units analysed is shown.

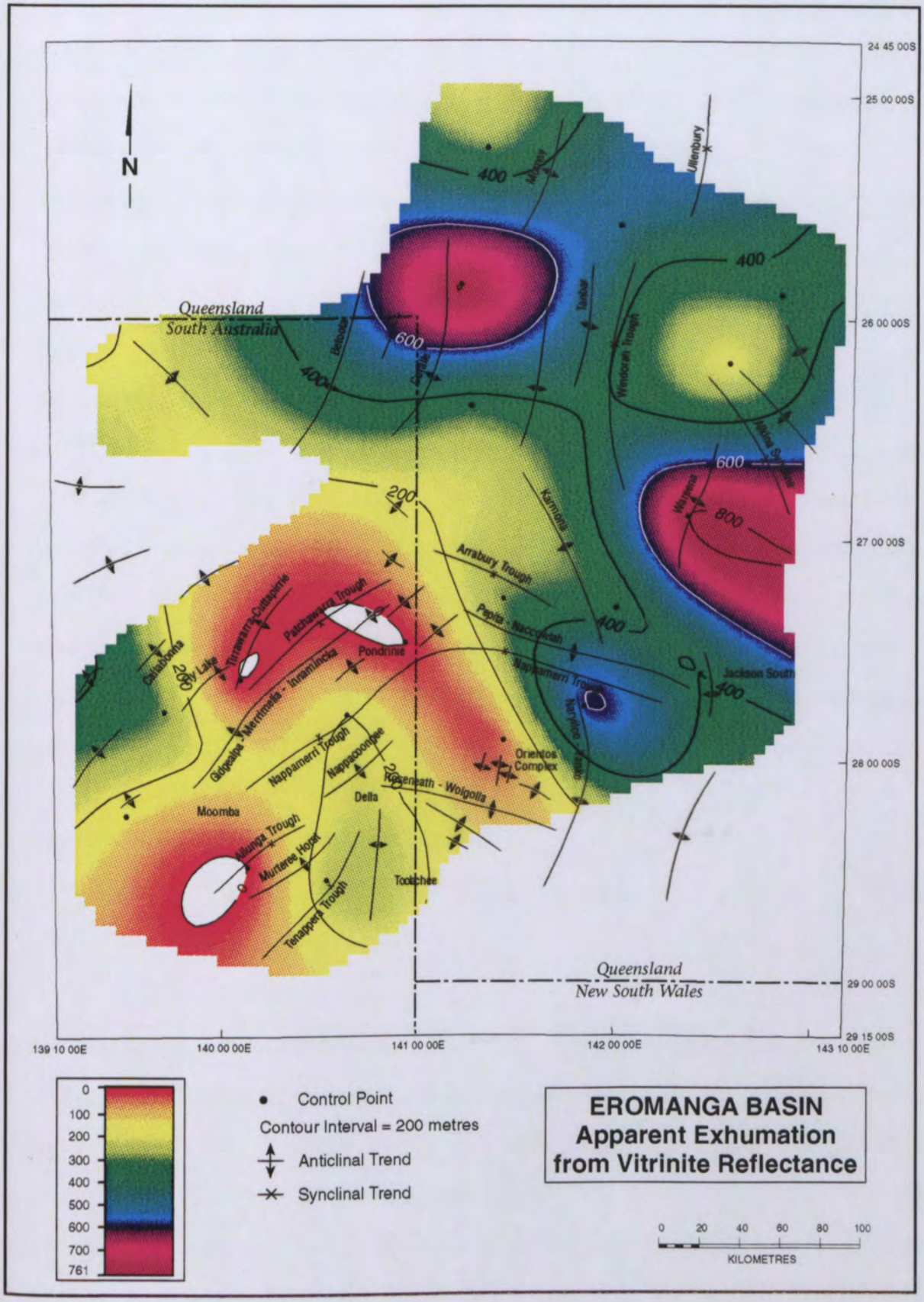

Figure 4.10. Apparent exhumation based on vitrinite reflectance in Eromanga Basin stratigraphic units. Well control points and tectonic elements are also shown.

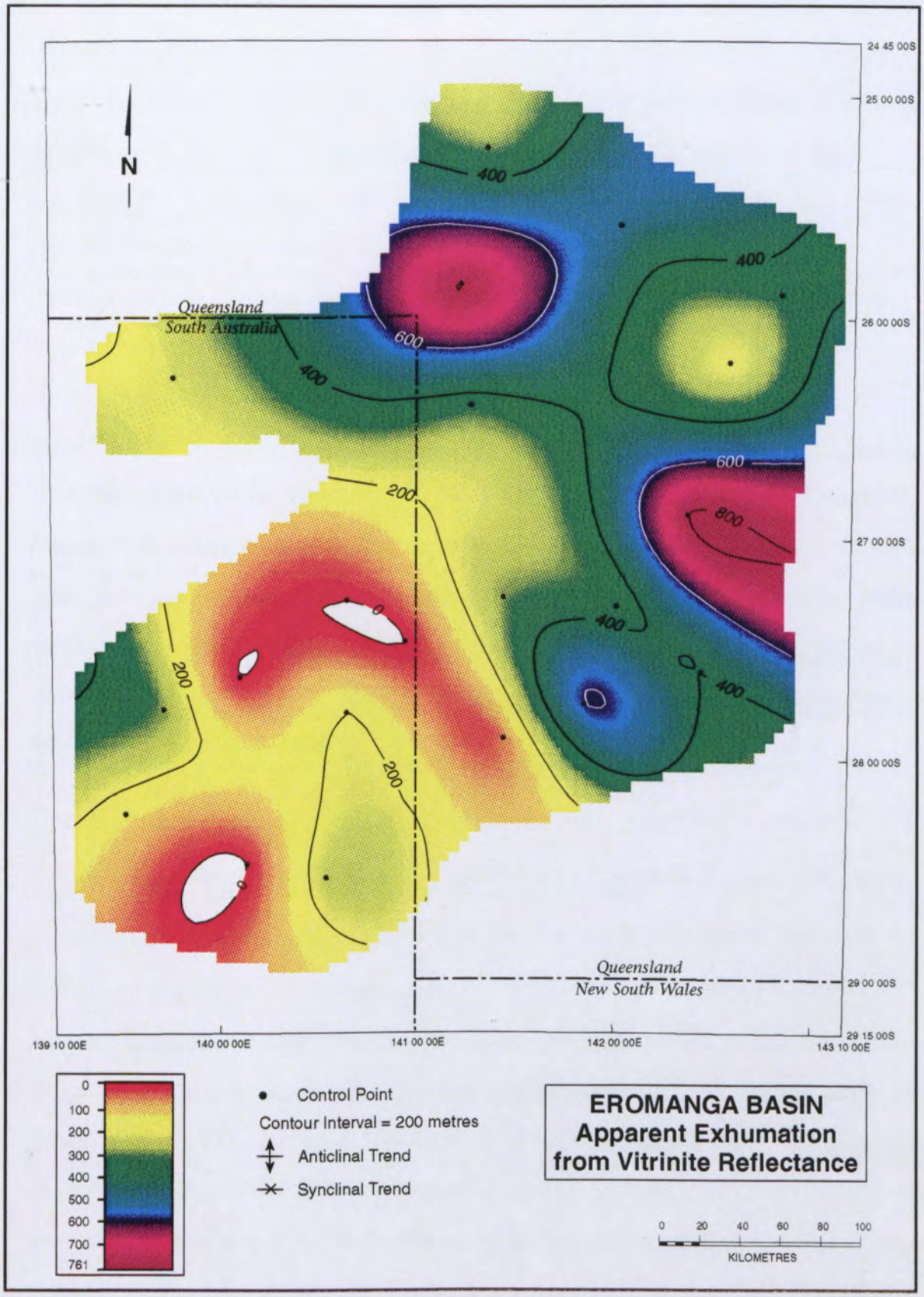

Figure 4.10. Apparent exhumation based on vitrinite reflectance in Eromanga Basin stratigraphic units. Well control points and tectonic elements are also shown.

The results of *Geothermal History C* suggest that Late Cretaceous - Tertiary exhumation from maximum burial-depth increases from approximately 200 m in the south and west of the Nappamerri Trough to 800 m in the north-eastern/Queensland part of the Nappamerri Trough (Figure 4.10). This supports the evidence of Shaw (1991) that exhumation increases eastwards and is in broad agreement with the results of the compaction analysis (Section 3.6). The tendency for exhumation values, from compaction analysis, to increase from the Patchawarra to Nappamerri Trough, is not borne out by the vitrinite reflectance modelling. This may simply be because less wells were analysed in the vitrinite reflectance modelling than in the compaction analysis. Late Cretaceous - Tertiary exhumation inferred from vitrinite reflectance assuming *Geothermal History C* reaches maximum values of approximately 800 m in the Wareena Anticline (north of the Jackson-Naccowlah area) and of approximately 700 m in the Naryilco Anticline (south of the Jackson-Naccowlah area). The other area of maximum Late Cretaceous - Tertiary exhumation, inferred from vitrinite reflectance modelling, which reaches approximately 800 m, is near the north-eastern boundary of South Australia, in the vicinity of the Curalle-1 well. These results are consistent with those based on compaction analysis, and with the fact that the Tertiary is absent or very thin over these areas.

4.5 Previous Vitrinite Reflectance Analyses in the Cooper-Eromanga Basins

Most previous studies of vitrinite reflectance in the Cooper-Eromanga Basins have been concerned with predicting the maturity of source rocks with respect to hydrocarbon generation (Shibaoka *et al.*, 1973; Powell and McKirdy, 1976; Shibaoka and Bennett, 1977; Kantsler *et al.*, 1978a, 1978b, 1983, 1986; Middleton, 1979, 1983; McKirdy, 1982; Pitt, 1986; Russell and Bone, 1989; Stuart *et al.*, 1993). The main purpose of these studies was to predict the most gas-prone kitchen areas of the Cooper-Eromanga Basins. In this study, the vitrinite reflectance method is used for estimating exhumation across the entire region. Nonetheless, the previous studies are relevant to the present investigation. This Section and Table 4.2 summarise the palaeogeothermal gradients used, and exhumation results revealed by these previous studies.

Table 4.2. Total Exhumation Values from Vitrinite Reflectance in Previous Studies and in This Study (*Geothermal History C*). Geothermal Histories are Also Shown.

	Vitrinite Reflectance Results from Kantsler *et al*. (1986)					Vitrinite Reflectance Results from Pitt (1986)					Vitrinite Reflectance Results from Russell and Bone (1989)					Vitrinite Reflectance Results from Stuart *et al.* (1993)					Vitrinite Reflectance Results from *Geothermal History C*				
		Total Exhumation		Geothermal History			Total Exhumation		Geothermal History			Total Exhumation		Geothermal History*			Total Exhumation		Geothermal History			Total Exhumation		Geothermal History	
Tectonic Province	Well	Late Triassic-Early Jurassic (m)	Late Cretaceous-Tertiary (m)	Age (Ma)	Geothermal Gradient (°C/km)	Well	Late Triassic-Early Jurassic (m)	Late Cretaceous-Tertiary (m)	Age (Ma)	Geothermal Gradient (°C/km)	Well	Late Triassic-Early Jurassic (m)	Late Cretaceous-Tertiary (m)	Age (Ma)	Range of Maximum Geothermal Gradient (°C/km)	Well	Late Triassic-Early Jurassic (m)	Late Cretaceous-Tertiary (m)	Age (Ma)	Geothermal Gradient (°C/km)	Well	Late Triassic-Early Jurassic (m)	Late Cretaceous-Tertiary (m)	Age (Ma)	Geothermal Gradient (°C/km)
Caralle Anticline						Caralle-1	0	550	0	45											Caralle-1	2900	800	0	48
									2	42														91	33
									198	42														198	33
									245	42														245	53
GMI Trend											Innaminicka-2	0	553	0	52-81						Innaminicka-4	2100	0	0	47
														91	52-81									91	32
														193	52-81									193	32
														258	52-81									286	52
Karmona Trend											Tallaka-1	1607	0	0	75-116						Okototo-1	2500	350	0	41
														91	75-116									91	31
														193	75-116									193	31
														286	75-116									286	46
Nappamerri Trough	Kirby-1	0	500	0	66	Moomba-3	55	200	0	56	Burley-1	0	34	0	71-121	Burley-2	1530	0	0	55	Burley-2	>4000	200	0	55
				91	66				91	40				91	71-121				10	<55				91	40
				193	66				193	55				193	71-121				91	<55				193	40
				286	66				286	55				286	71-121				193	160				286	70
											Moomba-6	1447	0	0	96-148				286	160					
														91	96-148										
														193	96-148										
														286	96-148										
Patchawarra Trough	Cuttapirrie-1	500	0	0	40	Beanbush-1	50	0	0	35	Beanbush-1	1227	630	0	29-46						Beanbush-1	2900	0	0	37
				91	40				10	25				91	29-46									91	27
				225	40				91	25				225	29-46									225	27
				286	40				225	25				286	29-46									286	42
									286	25															
											Tirrawarra-1	1253	0	0	87-113						Tirrawarra North-1	2800	0	0	35
														91	87-113									91	30
														193	87-113									193	30
														286	87-113									286	40
Warcena Anticline						Tarnalla-1	(Low values)	200	0	40											Warcena-1	2700	1050	0	43
									5	30														91	33
									198	30														198	33
									253	30														253	48

* Palaeogeothermal history is not specified.

Kantsler *et al.* (1983) noted the discontinuity in vitrinite reflectance gradient between the Cooper and Eromanga Basins. He suggested that it implies not only a Permian - Late Triassic heating event, but also the loss of up to 500 m of sedimentary section in the Late Triassic. Using the Lopatin (1971) TTI method, Kantsler *et al.* (1983) concluded that constant palaeogeothermal gradients as high as 50-70°C/km are required throughout the deposition of the Cooper-Eromanga Basins to model observed vitrinite reflectance in the Big Lake area of the Nappamerri Trough. However, palaeogeothermal gradients less than 40°C/km are required to model vitrinite reflectance in the north-western Patchawarra Trough Kantsler *et al.* (1983). On the basis of more recent thermal maturation calculations, Kantsler *et al.* (1986) suggested that observed vitrinite reflectance values are consistent with either a decrease in palaeogeothermal gradient from a Late Carboniferous - Early Permian heating event associated with a maximum geothermal gradient of 100°C/km, or a Late Cretaceous - Tertiary heating event with geothermal gradients up to about 70°C/km. However, the Late Cretaceous - Tertiary heating event cannot alone account for the discontinuity in vitrinite reflectance values associated with the unconformity between the Cooper-Eromanga Basins. Kantsler *et al.'s* (1983; 1986) use of higher geothermal gradients than those used here subdue the magnitude of modelled exhumation with respect to these determined here.

Middleton (1983) suggested that the difference in vitrinite reflectance gradient between the Cooper and Eromanga Basins can be explained by the loss of 200 m or more of Triassic sediments due to uplift and erosion which occurred in association with a Late Triassic - Jurassic heating event. However, Middleton's (1979; 1983) method in estimating present geothermal gradients was criticised by Cao *et al.* (1988) and Russell and Baillie (1989). Cao *et al.* (1988) compared their formation temperature estimation (FTE) method with that of Middleton (1979) and showed that the latter method yielded static bottom hole temperature values that were 13 to 18°C higher than those calculated by the FTE method. For depths of 2 to 3 km the Middleton method could overestimate geothermal gradient by some 5 to 10°C/km (Cao *et al.*, 1988).

Pitt (1986), again using the Lopatin (1971) TTI method, reported the results of vitrinite reflectance modelling of selected wells. He used constant geothermal gradients throughout the

deposition of the Cooper and Eromanga Basins. Pitt (1986) calculated that palaeogeothermal gradients of 25°C/km for Beanbush-1, in the Patchawarra Trough, and 45 to 55°C/km for Moomba-3, in the Nappamerri Trough, are required to model observed vitrinite reflectance/depth trends. Although Pitt's (1986) geothermal gradients are lower than those inferred for the Permian - Early Triassic by Kantsler *et al.* (1983; 1986), they do also indicate that the Nappamerri Trough has been subjected to a higher geothermal gradient than the Patchawarra Trough. Pitt (1986) assumed exhumation values of 50 m and 55 m during Late Triassic - Early Jurassic times for the Patchawarra and Nappamerri Trough, respectively; and 0 m, 200 m and 550 m during Late Cretaceous - Tertiary times for the Patchawarra Trough, Nappamerri Trough and Curalle Anticline, respectively.

Russell and Bone (1989), using Dow's (1977) method, calculated exhumation values of 1200 to 2040 m, 1400 to 1670 m, and 1100 to 1600 m during the Late Triassic - Early Jurassic times for the Patchawarra Trough, Nappamerri Trough and Murteree-Nappacoongee Trend, respectively; and 630 to 800 m and 500 to 1250 m during the Late Cretaceous - Tertiary times for the Patchawarra Trough, and GMI Trend, respectively. They concluded that minor post-Cretaceous uplift and an Upper Triassic/Jurassic uplift of more than 500 m, account for the high vitrinite reflectance data in the Nappamerri Trough.

More recently Stuart *et al.* (1993), using the LLNL (Lawrence Livermore National Laboratory) kinetic model, determined that even at present high heat flows, the Permian section in Nappamerri Trough would have been buried to depths of approximately 5 km, with approximately 3 km of Triassic section eroded prior to basal Jurassic deposition. As they suggested, vitrinite reflectance is probably better modelled by a combination of exhumation, of the order of 1500 m, and an extremely elevated palaeogeothermal gradient, of the order of 160°C/km.

4.6 Discussion

The change of gradient in the vitrinite reflectance/depth profiles between the Cooper and Eromanga Basins is characteristic of the majority of the wells studied. This change occurs at the unconformity between the Cooper and the Eromanga Basins. Observed vitrinite reflectances were difficult to model consistently. The data points from the Eromanga Basin were lower than expected at shallow levels and those from the Cooper Basin higher than expected at deeper levels.

Authors of previous maturation studies (Section 4.5) agree that it is difficult to model the available reflectance data, partly due to their complexity, and also due to the limitations of the modelling packages used. Kantsler *et al.* (1983), Middleton (1983) and Pitt (1986) used the Lopatin (1971) TTI model, the disadvantages of which were discussed in Section 4.2.1. Indeed, Kantsler (1978b) stated that the Lopatin (1971) TTI model had failed to provide satisfactory results for many Australian sedimentary basins, including the Cooper Basin.

A key feature of the observed vitrinite reflectance data from the Cooper-Eromanga Basins is that, as demonstrated by the modelling based on *Geothermal History A*, measured vitrinite reflectances are lower than would be expected from present temperatures, particularly in the Eromanga Basin. This demonstrates that the present high geothermal gradients in the area, typically 40-50°C/km, are a relatively recent phenomenon.

The cause of this increase in geothermal gradient is unclear. The results of the compaction analysis indicate significant exhumation over the area. Hence, it is tempting to suggest that advective transfer of heat to the surface associated with exhumation may have been responsible for the increase in geothermal gradient. However, if this was so, vitrinite reflectances should be consistent with present temperatures. Alternatively, as suggested by Stuart *et al.* (1993), there may have been significant heat transport through groundwater movement in aquifers. The Eromanga Basin is, of course, part of the Great Artesian Basin, and thus subject to groundwater movement through its aquifers. Furthermore, there is significant contemporary hot spring activity in the Flinders Ranges (eg. Paralana Hot Springs) to the south of the

Cooper-Eromanga Basins (Foster *et al.*, 1994), where the presumed basement of the area outcrops. The role played by the basement granites in producing the high geothermal gradients is discussed later in this section.

Given that geothermal gradients must have increased in Late Cretaceous - Tertiary times, it is difficult to obtain reliable estimates of Late Cretaceous - Tertiary exhumation. Essentially, one can reduce the palaeogeothermal gradient during the deposition of the Eromanga Basin from that of the present day such that observed reflectances in the Eromanga Basin are modelled without invoking exhumation, or one can reduce the palaeogeothermal gradient further, and invoke exhumation. It is fully recognised that the reduction of palaeogeothermal gradient during the deposition of the Eromanga Basin used in *Geothermal Histories B and C* is somewhat arbitrary. This problem has been faced by all who have modelled vitrinite reflectance in the Cooper-Eromanga Basins (Section 4.5).

The most striking feature of the observed vitrinite reflectance data from the Cooper-Eromanga Basins is the increase in vitrinite reflectance/depth gradient from the Eromanga Basin sequence to the Cooper Basin sequence. This increase in gradient reflects exhumation during Late Triassic - Early Jurassic times, and/or higher palaeogeothermal gradients during the deposition of the Cooper Basin sequence, prior to Late Triassic - Early Jurassic exhumation. Again, the balance of exhumation and/or palaeogeothermal gradient used to model the observed vitrinite reflectance trends is inherently a non-unique one. Indeed, it is clear from the previous section that there almost as many different estimates of exhumation and palaeogeothermal gradients as there are vitrinite reflectance modelling studies in the area.

High geothermal gradients during the deposition of the Cooper Basin sequence are likely to be the consequence of Carboniferous tectonic activity and associated igneous intrusion. Powell (1984) indicated that older Palaeozoic sequences of the Adavale and Drummond Basins (underlying the eastern Cooper-Eromanga Basins) were deformed as part of the continent-wide Kanimblan Orogeny during the middle Carboniferous. After these events, the region was effectively part of cratonic Australia, with subsequent tectonic events taking place further east (Finlayson *et al.*, 1988).

Granites have been widely postulated to play a role in both high present and high palaeogeothermal gradients in the area (eg. Pitt, 1986; Gallagher, 1988). Kantsler *et al.* (1983) suggested that the high geothermal gradients could have existed for 300 Myr with even higher gradients in the Permo-Triassic, on the basis that the early high gradients were associated with granite intrusion. Much of the Nappamerri Trough is underlain by granites (Gatehouse, 1986). The granites encountered in wells in the area are dated radiometrically at about 305-360 Ma (Gatehouse, 1986), which implies that the elevated geothermal gradients may have existed for up to 50 Myr before the onset of sediment deposition in the Late Carboniferous-Early Permian. The distribution of granites must be considered, laterally, more extensive underneath the basement lithologies than the represented by intersection wells (Gallagher, 1988).

Present-day high geothermal gradients in the Nappamerri Trough are considered to reflect the fact that the area is underlain by 'hot' granitic basement (Russell and Bone, 1989). In contrast, lower geothermal gradients in the Patchawarra Trough may reflect the fact that this area is underlain by older, mid Palaeozoic (meta-) sediments of the Warburton Basin (Kantsler *et al.*, 1983; 1986; Gallagher, 1988). The GMI trend appears to represent a 'thermal hinge' between the Patchawarra and Nappamerri Troughs.

The period of lower geothermal gradients during the deposition of Eromanga Basin sediments may have been anomalous if the basement granites of the area are responsible for the long term high geothermal gradients. Lower geothermal gradients at this time may have been associated with thermal blanketing due to rapid Jurassic - Early Cretaceous sedimentation. Alternatively, the high heat flow associated with granites may have decayed during Jurassic - Early Cretaceous times and the recent increase may have a different origin.

It is significant that in areas such as Strzelecki and Jackson, where there is no evidence of granites, that there is a present thermal high (Pitt, 1986), suggesting that the more recent increase in geothermal gradients is not everywhere associated with the granites and that it may be related to groundwater movement (Stuart *et al.*, 1993). Clearly granite intrusion prior to the

onset of Cooper Basin sedimentation cannot alone account for high geothermal gradients during the deposition of the Cooper Basin and the recent increase in geothermal gradients.

In this Chapter, following the principle of Occam's razor, progressively more complex geothermal histories were used to model observed vitrinite reflectances. Given that the purpose of the modelling was to investigate whether exhumation values derived from vitrinite reflectance modelling were consistent with those based on compaction analysis, it is ironic that the modelling has fairly convincingly demonstrated a Late Cretaceous - Tertiary increase in geothermal gradient and higher geothermal gradients during the deposition of the Cooper Basin. However, because the magnitudes of the Late Cretaceous - Tertiary increase in geothermal gradient and of the higher gradients during the deposition of the Cooper Basin cannot be independently ascertained, the magnitude of Late Cretaceous - Tertiary and Late Triassic - Early Jurassic exhumation cannot be determined with confidence from the vitrinite reflectance data.

This study has the advantage over previous studies that it uses the most recent kinetic models of increase of vitrinite reflectance with time and temperature incorporated in the MATOIL software (BEICIP, 1990), as opposed to Dow's (1977) simplistic vitrinite reflectance trend offset method used by Russell and Bone (1989), or the Lopatin (1971) TTI method used by Kantsler *et al.* (1983) and Pitt (1986). Nonetheless, the most recent kinetic models still require inputs of burial/exhumation history and palaeogeothermal gradient.

Section 4.2.2 highlighted a number of sources of potential error in the determination of vitrinite reflectance (including suppression, enhancement and selection of maceral) that need to be borne in mind, particularly because no new analytical determinations of vitrinite reflectance were made in this study, and because the vitrinite reflectance data used come from a number of different reports. Such analytical errors do, of course, need to be borne in mind when using the vitrinite reflectance data to assess thermal maturity and hydrocarbon generation. However, these errors are not likely to be of great significance in the estimates of exhumation produced herein, given the uncertainties associated with palaeogeothermal gradients discussed above.

It is clear from this study that the Cooper-Eromanga Basin with its complex thermal history is not an ideal area in which to investigate whether exhumation values yielded by modelling vitrinite reflectance are consistent with those from the compaction methodology. The main use of vitrinite reflectance modelling is, of course, in analysing thermal maturity and the history of hydrocarbon generation. It is suggested, given the inevitable compromises between exhumation and geothermal gradient, that estimates of exhumation from compaction should be used to constrain vitrinite reflectance modelling. This does not allow comparisons of exhumation estimates between the two methods, as initially desired from this work, but does ensure that an independent constraint on exhumation history is incorporated into modelling the history of hydrocarbon generation from observed vitrinite reflectances, as recommended by Waples (1994).

5. EVIDENCE OF EXHUMATION FROM APATITE FISSION TRACK ANALYSIS AND FLUID INCLUSION HOMOGENIZATION TEMPERATURES

5.1 Introduction

This chapter reviews evidence of exhumation and palaeo-thermal history in the Cooper-Eromanga Basins based on previous apatite fission track analysis (AFTA) and fluid inclusion homogenization temperatures. This chapter is solely a review of previously results of these techniques, and their implications for this study, and unlike the chapters on compaction and vitrinite reflectance, neither new analytical nor new modelling work has been undertaken. AFTA results are available for 12 wells in Cooper-Eromanga Basins, and fluid inclusion homogenization temperatures for four wells. Previous works using these techniques have tended to focus their research in the palaeo-thermal history, rather than exhumation magnitudes, indeed thermal annealing witnessed by AFTA and associated with the recent/present high geothermal gradients precludes estimation of exhumation at the Cooper-Eromanga Basins unconformity. After a brief review of AFTA and fluid inclusion homogenization temperatures results, the implications for this study are then discussed.

5.2 Apatite Fission Track Analysis

5.2.1 Introduction

Apatite fission track analysis (AFTA) is used to elucidate the thermal histories of sedimentary basins particularly in the context of hydrocarbon resource evaluation. The technique depends on the observation that fission tracks in minerals, which form due to spontaneous nuclear fission of ^{238}U, anneal as a function of temperature and time. Hence the number of tracks gives an idea of geological age, and the degree to which they have annealed, an idea of thermal

history. Under geological conditions the temperature interval over which fission track annealing occurs in the mineral apatite (60° to 125°C) is broadly coincident that required for the generation of liquid hydrocarbons. The pattern of apatite fission track ages, together with detailed analyses of the distributions of track lengths, yields information on thermal history, unobtainable by other methods, for the evaluation of low-temperature thermal histories in sedimentary basins. For more details of the AFTA methodology, the reader is inferred to Gleadow *et al.* (1983); Green *et al.* (1989); Naeser *et al.* (1990); and Arne (1992).

5.2.2 Apatite Fission Track Analysis in the Cooper-Eromanga Basins

The first application of AFTA to the Cooper-Eromanga Basins was by Gleadow *et al.* (1988), and covered the South Australian sector of the study area. The samples used for that analysis were taken from the Dullingari-1, Merrimellia-1, 3 and 8, Namur-2, Putamurdie-1, Tinga Tingana-1, and Toolachee-1 wells (Figure 5.1). The second application was by Geotrack (1988), and covered the Queensland sector of the study area. The samples in that analysis were taken from the Jackson-1, Morney-1, Pepita-1, and Watson-1 wells (Figure 5.1). Details of the technique in terms of apatite fission track parameters (eg. fission track age, length measurements and pooled or maximum probability ages), and the interpreted thermal histories are outlined by Hurford and Green (1983) and Gleadow *et al.* (1983). Only the most important conclusions relevant to burial/exhumational events are summarised here.

AFTA in South Australia: The samples from the Dullingari-1 well cover a present temperature range of 41 to 142°C. The shallowest samples (Winton Formation, Allaru Mudstone and Cadna-owie Formation) from Dullingari-1 give fission track ages that are similar to their stratigraphic ages. Samples from the Namur Sandstone and underlying units have fission track ages much less than their stratigraphic ages. This shows that the samples from the Namur Sandstone and underlying units have been subjected to considerable annealing, implying temperatures of around 70°C or above (Figure 5.2). Gleadow *et al.* (1988) concluded that samples overlying the Murta Member are currently at their maximum temperatures, and that these maximum temperatures have been attained for less than

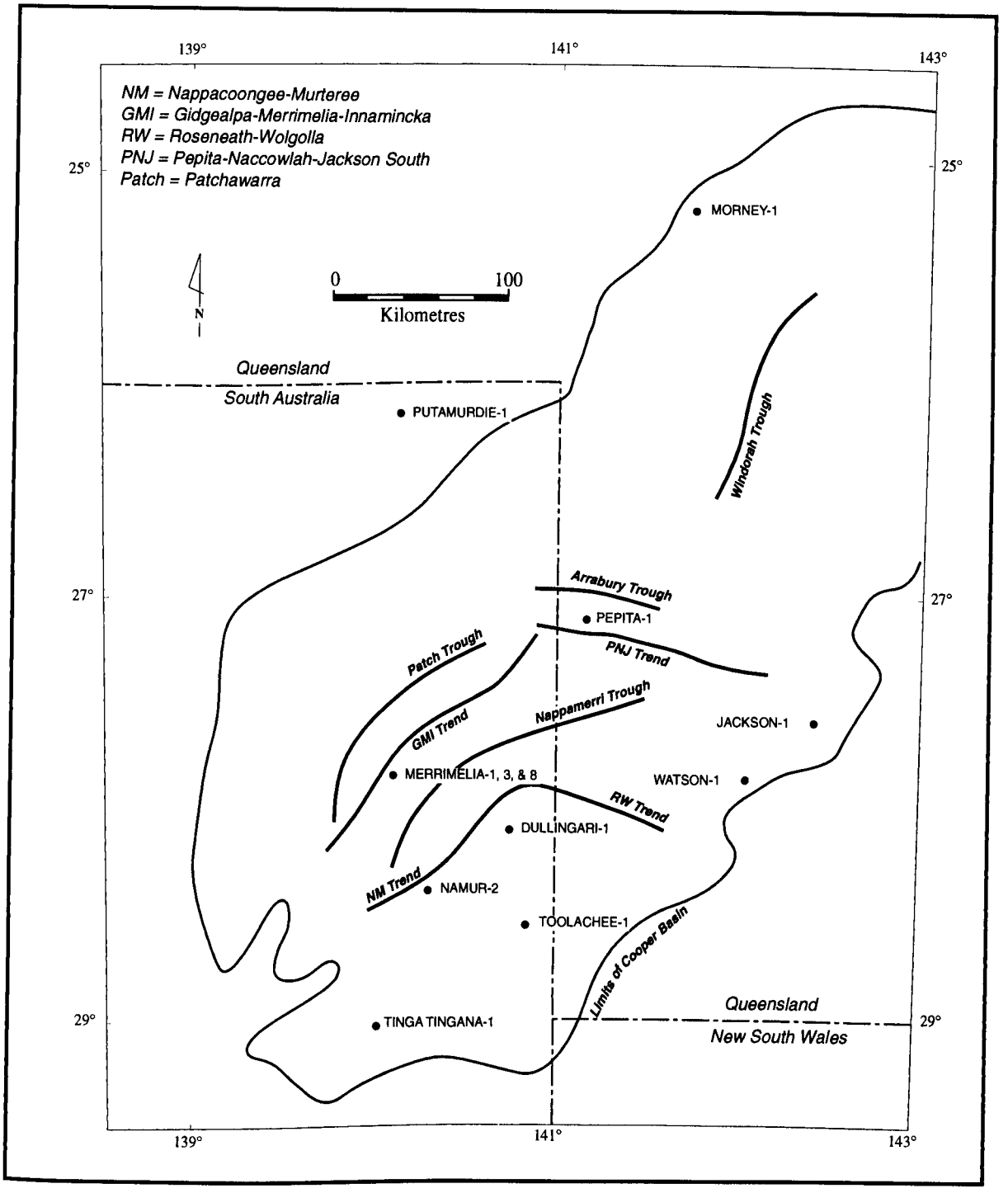

Figure 5.1. Location map of the wells used in AFTA. Major tectonic elements of the Cooper-Eromanga Basins are also shown.

about 10 Ma. On the other hand, as indicated by the sharp change in apparent fission track age between the Murta Member and the Namur Sandstone, samples below the Namur Sandstone have probably been subjected to temperatures sufficient to totally anneal all previously formed tracks, during a period of peak temperatures prior to the recent temperature increase. The nature of this event is not known, and Gleadow *et al.* (1988) suggested it is most likely due to thermal perturbations associated with the passage of hot fluids in the Namur/Murta and

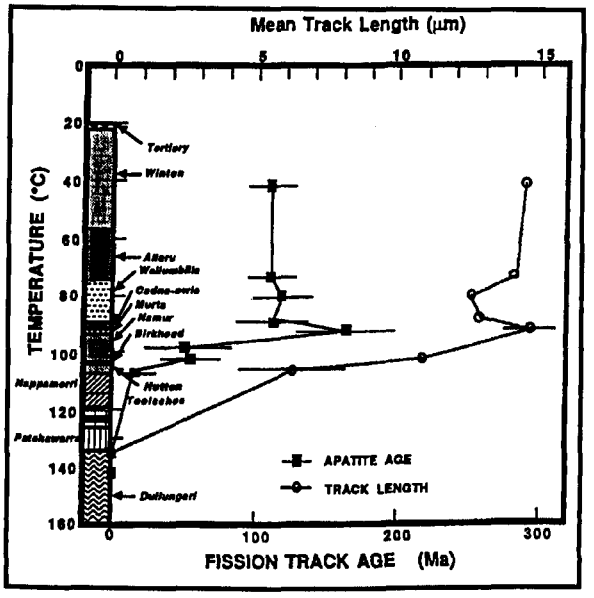

Figure 5.2a. The variation of apparent fission track age and mean track length with downhole temperature for apatites from Dullingari-1 (after Gleadow *et al.*, 1988).

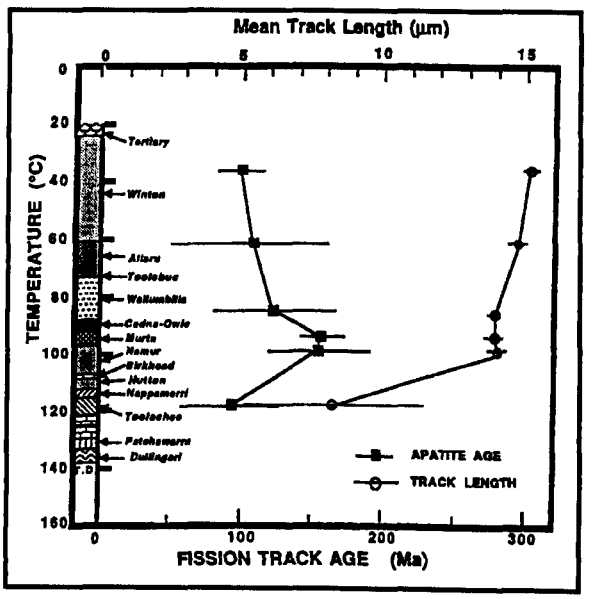

Figure 5.2b. The variation of apparent fission track age and mean track length with downhole temperature for apatites from Toolachee-1 (after Gleadow *et al.*, 1988).

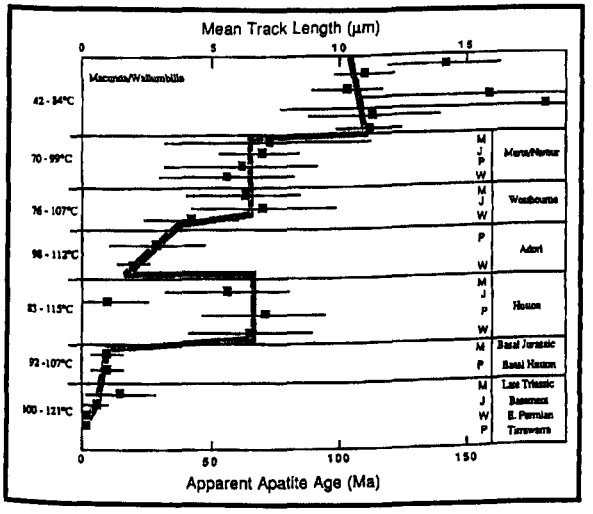

Figure 5.2c. The variation of apparent fission track age with stratigraphy for Morney-1, Pepita-1, Jackson-1 and Watson-1, Eromanga Basin. A very similar pattern is present in all four wells regardless of the large range in present temperatures covered by individual formations (after Geotrack, 1988).

Hutton/Birkhead aquifer systems. The break in fission track age at this level could also be explained by 1-2 km of exhumation between the Namur Sandstone and Murta Member. However, the compaction data presented herein show no evidence of major exhumation at this time, and support the opinion of Gleadow *et al.* (1988) that exhumation at this time is not a likely explanation of the break in fission track ages.

Samples from the Toolachee-1 well cover a present temperature range from 36 to 118°C. Again, the AFTA data indicate that the present high temperatures can only have been attained for about the last 10 Ma. The only data available for the other wells analysed come from one or two core samples per well, and suggest that most of their tracks have been annealed at sometime in the past, at temperatures in excess of approximately 100°C. The data for all the wells indicate that the present high temperatures were relatively recently attained, during the last 10 Ma.

Gleadow *et al.* (1988) did not report amounts of Late Cretaceous - Tertiary exhumation because of the annealing effects of the recent heating event in the majority of the samples in all of the stratigraphic units analysed.

AFTA in Queensland: The results of AFTA undertaken in wells in the Queensland sector of the Cooper-Eromanga Basins consistently showed that formations below the Wallumbilla Formation have experienced palaeotemperatures in the range of approximately 90 to 110°C, or greater. The present temperatures of these formations range between 70 to 110°C. Temperatures attained in these units were sufficient to reduce the apatite fission track ages to around 20 to 70 Ma, much less than the appropriate stratigraphic ages, (Figure 5.2). As concluded Geotrack (1988), such a pattern might be due to uplift and erosion of the entire section during the Tertiary, implying a significant loss of Winton Formation and/or overlying units. Geotrack (1988) suggested the AFTA results were consisted with the following magnitudes of exhumation:

- 457 m in Jackson-1;
- 975 m in Morney-1;
- 460 m in Pepita-1, and;
- 549 m in Watson-1.

However, data from samples in the Wallumbilla and younger formations cannot be readily explained by post-Winton Formation exhumation alone, because there is a marked break in fission track ages between those and the underlying units (Figure 5.2). Geotrack (1988) suggested there may have been differential heating of the pre-Wallumbilla section by circulation of hot fluids during Tertiary times. Temperatures involved were in the range of approximately 90-110°C and cooling probably took place in Oligocene or Miocene times, but may have been at any time between approximately 70 Ma and 5 Ma. Geotrack (1988) concluded that a combination of post-Winton uplift and erosion and hot fluid circulation could be invoked to explain the data, but they suggested that hot fluid circulation is the more likely explanation. Despite this interpretation, Geotrack (1988) admit that it is difficult to model the data from Morney-1 well without assuming significant exhumation.

5.2.3 Fission Track Analysis in the Eastern Eromanga Basin (Eromanga-Brisbane Geoscience Transect) and Western Margin of the Eromanga Basin

In addition to the AFTA undertaken in the Cooper-Eromanga Basins, and described above, AFTA has been undertaken on a series of samples from the Cooper-Eromanga to Brisbane areas not included in this thesis (Figure 5.3; Gallagher *et al.*, 1994).

On the basis of AFTA, Gallagher *et al.* (1994) suggested that the Eromanga Basin had undergone 1 km late Cretaceous-middle Tertiary exhumation, and that the basins to the east (Clarence-Moreton, eastern Surat) had undergone even more erosion (approximately 2.5 km). Erosion was probably initiated earlier in the eastern basins (Gallagher *et al.*, 1994).
The data from some of the Eromanga Basin wells are interpreted in terms of a recent (<10 Ma)

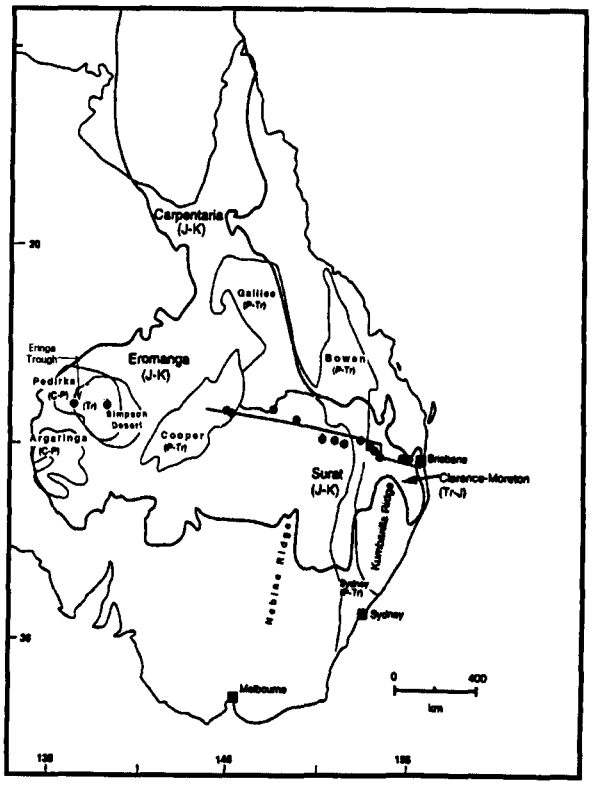

Figure 5.3. The boundary of the Mesozoic (J-K) basins in eastern Australia (bold line). The finer boundaries represent generally concealed Permo-Triassic basins. Locations of wells used in AFTA (black dots) are also shown (modified after Gallagher *et al.*, 1994).

increase in temperature of 20-30°C. Gallagher *et al.* (1994) concluded that the cause of a regional temperature increase, as indicated by the fission track data, is problematic. However, they did argue, unlike Gleadow *et al.* (1988) and Geotrack (1988) that since hydrological flow perturbs the thermal regime only locally, it cannot be considered as a complete possible explanation for the examined area.

More recently, an AFTA and vitrinite reflectance study in the Eringa Trough (Figure 5.3) showed that elevated palaeotemperatures may have occurred over a large part of the western Eromanga Basin margin (Tingate *et al.*, 1996). The authors of this study concluded that likely causes for these elevated palaeotemperatures are burial prior to uplift and erosion of Cretaceous section and heating related to hot water moving through Mesozoic aquifers. Again the authors state that there are difficulties in distinguishing the relative importance of these two heating mechanisms. Tingate *et al.* (1996) concluded that significant erosion of Cretaceous section in the late Cretaceous-early Tertiary and later in the mid Tertiary is likely. Evidence of significant relatively young cooling is not confined to the Eringa Trough. AFTA outcrop and well data from the Arunta and Musgrave Blocks, Amadeus and Officer Basins also indicate cooling of approximately 40°C during the last 100 Ma (Tingate *et al.*, 1996).

5.3 Exhumation Estimates Using Fluid Inclusion Homogenization Temperatures

Fluid inclusion homogenization temperatures (FIHT) have been used to elucidate the palaeo-thermal history of sedimentary basins in the context of hydrocarbon resource evaluation. The use of FIHT studies in geological problems was reviewed by Hollister and Crawford (1981) and Roedder (1984). The most important conclusions from FIHT studies in the Cooper-Eromanga Basins by Eadington *et al.* (1989) and Russell and Bone (1989), are briefly reviewed here.

Fluid inclusion homogenization temperatures together with stable isotope and chemical kinetic models of diagenetic cements have been used to investigate the thermal and liquid hydrocarbon history of Hutton Sandstone samples from wells in south-west Queensland by Eadington *et al.* (1989). The mean FIHT range from 82 to 108°C, and present temperatures from 82 to 135°C. On a temperature-pressure (-depth) graph, the intercepts of sample depth on isochore lie above the average regional geothermal gradient of 45°C/km, deduced from the bottomhole temperatures (Figure 5.4). The amount of exhumation thus indicated from the FIHT are:

- 380 m in Bogala-1;
- 190 m in Challum-1;
- 280 m in Jackson-1, and;
- 280 m in Tintaburra-1.

The FIHT results show that either the quartz overgrowths were formed at greater depths than present, or that the geothermal gradient was higher (approximately 57°C/km) than at present. Eadington *et al.* (1989) concluded that such gradients (ie. 57°C/km) would have had a marked effect on the maturity of carbonaceous matter, such as is not observed (Kantsler *et al.*, 1986), and hence that very high gradients can be discounted. Eadington *et al.* (1989) suggested that the most straightforward interpretation of the FIHT is a constant geothermal gradient of about

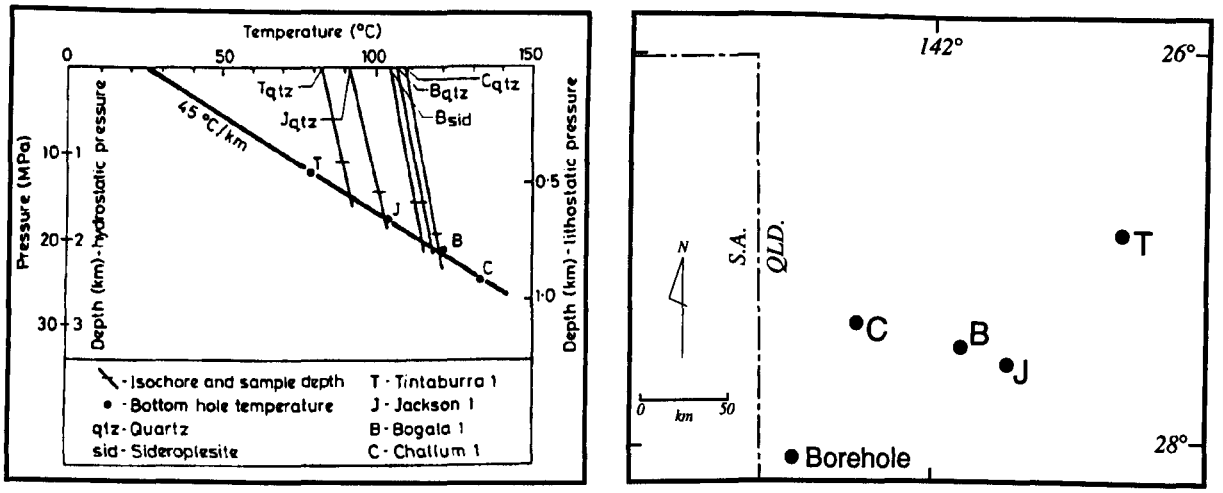

Figure 5.4a. Temperature-pressure depth relationships from aqueous inclusion data. Fluid inclusion homogenisation temperatures define minimum temperature and isochores along which the inclusions were trapped. The intercept of pressure on the isochore defines the temperature of entrapment. If pore fluid pressures were hydrostatic then the pressure axis can be transformed to a depth scale and the geothermal gradient used to deduce the trapping temperature locations of the wells sampled and also shown. Location map of wells used is also shown (after Eadington *et al.*, 1989).

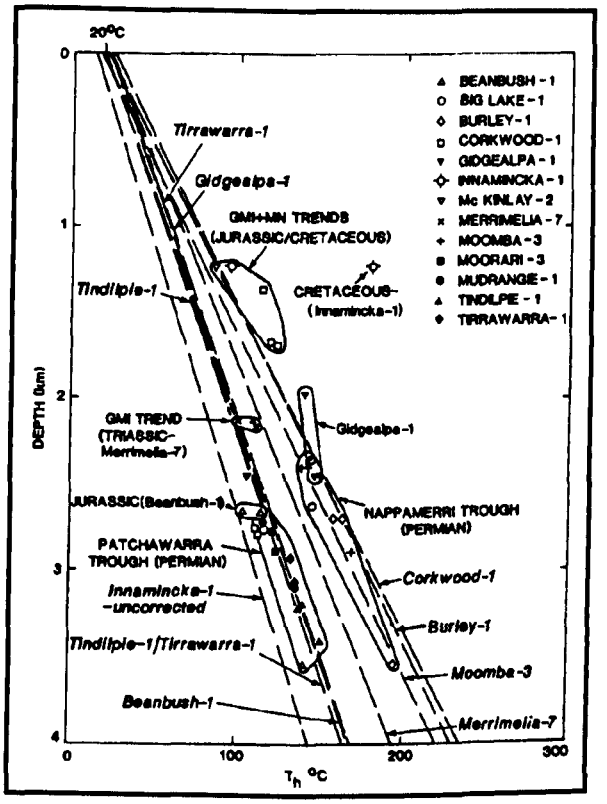

Figure 5.4b. Depth/temperature plot comparison of fluid inclusion homogenisation temperature [T_h] values and present-day geothermal trends in the Cooper and Eromanga Basins. Data points distinguished by well, age and structural domain (after Russell and Bone, 1989).

45°C in the Mid to Late Cretaceous with quartz overgrowths having been formed at depths 190 m to 380 m grater than at present.

Russell and Bone (1989), recorded fluid inclusion homogenization temperature values similar to the present-day formation temperatures in the Patchawarra and Nappamerri Troughs. However, the fluid inclusion homogenization temperature values recorded from the GMI and MN Trends are higher than the present-day formation temperatures (Figure 5.4) indicating greater burial-depths than the present burial-depths and/or higher palaeogeothermal gradients. Russell and Bone (1989) did not suggest likely exhumation magnitudes.

5.4 Discussion

In summary, the reduction in AFT ages, below the Murta Member in South Australia area and below the Wallumbilla Formation in Queensland area, compared to the stratigraphic ages for the majority of the samples, suggests that fission track annealing was an important process in the Cooper-Eromanga Basins. Thermal annealing is primarily controlled by the maximum temperatures (between 60°C and 125°C) experienced by the samples (Green *et al.*, 1986). This implies that formations below the Murta Member and Wallumbilla Formation, have at some time during their depositional history been at a higher temperature than that of the present. The thermal annealing events in the Cooper-Eromanga Basins are discussed below with particular reference to the burial/exhumation history of the basin.

No estimates of exhumation during Late Triassic - Early Jurassic times have been made from AFT data. In fission track dating it is assumed that there has been no loss of tracks since the time of formation of the fission track-uranium system. The geological interpretation of fission track ages depends initially on understanding the extent to which this assumption is valid for any particular sample. Where loss of tracks has occurred, the fission track clock will date not the original formation of the crystal, but some later stage in its thermal history (Gleadow *et al.*, 1983). Hence, the AFT technique is applied most usefully in sedimentary sections which have

been much hotter in the past than they are at the present (Bray *et al.*, 1992). Temperatures in the Cooper-Eromanga Basins have increased during the last 10 Ma as shown, by both vitrinite reflectance (*Geothermal History A*, Sections 4.4 and 4.6) and AFT studies. The highly annealed nature of Permian-Triassic samples means that they cannot give temperature information regarding Late Triassic - Early Jurassic burial, prior to exhumation.

The thermal annealing events recognised in the Cooper Basin samples may have a similar origin to the high palaeogeothermal gradients during the deposition of the Cooper Basin discussed with regard to vitrinite reflectance results in Section 4.6 (eg. the consequence of Carboniferous tectonic activity and associated granite intrusion). Given that the wells examined are not located in the Nappamerri Trough, which is largely underlain by granites, the AFTA results, similarly to those from vitrinite reflectance, might indicate that the distribution of basement granites extends beyond the Nappamerri Trough as suggested by Gallagher (1988).

A consistent result from AFT studies is that the markedly high present geothermal gradients are a relatively recent phenomenon, and probably developed over the last 10 Ma in the South Australia area and around 20 to 70 Ma in the Queensland area (Section 5.2.2). Gleadow *et al.* (1988) favoured the passage of hot fluids in the Namur Sandstone/Murta Member and in Birkhead Formation/Hutton Sandstone aquifer systems, as the origin of the increase in geothermal gradients, whereas Geotrack (1988) favoured a combination of circulation of hot fluids and burial/exhumational events as the explanation for the annealing events and the recent heating event. Tingate *et al.* (1996), studying the western margin of the basin, similarly favoured a combination of hot fluids and burial/exhumational events (Section 5.2.3).

The preserved approximately 100 m of irregularly distributed Tertiary sediments are too thin to account for the heating event over the last 10 Ma. From the fission track results alone, we cannot discriminate heating due to burial/exhumation, and that due to ingress of hot fluids. Toupin (1993) argued that the current artesian system of the Eromanga Basin was initiated in the Plio-Pleistocene (<2 Ma) with the uplift of the northeastern margin, creating a topographically-driven confined groundwater system. While the artesian system may

contribute to heating in discharge areas, and in aquifers, it could not have systematically have elevated thermal gradients through non-aquifer units over a large area in central Eromanga Basin. It seems likely that heating associated with burial (and subsequent exhumation) played an important role in the fission track annealing events witnessed in the Eromanga Basin samples.

Granites alone cannot account for the relatively recent increase in geothermal gradients to those of the present-day. Firstly, although the granites which are of Carboniferous age (Gatehouse, 1986) could be responsible for high geothermal gradients since Carboniferous times, they cannot be responsible for a relatively recent heating event. Secondly, in areas such as Jackson, and the other samples from Queensland, where there is no evidence of granites, there is a present thermal high as evidenced by AFT and vitrinite reflectance studies (Section 4.6).

The AFT and fluid inclusion homogenization temperatures methods show evidence of exhumation primarily in the Queensland sector of the Cooper-Eromanga Basins. Although capable of estimating the magnitude of exhumation in the Queensland area, AFTA is largely unable to constrain detailed exhumational events in the present hot area of the South Australia, and only indications of the palaeotemperatures can be deduced (Figure 5.5). It should be mentioned that the objectives of the AFT studies were to define the palaeo-thermal history of the region, and not specifically to elucidate the amounts of exhumation during the major unconformities in the basins. As discussed above, the relative importance of hot fluids, burial/exhumation and/or other heating processes is unclear. Nonetheless, where reported, exhumation results from AFTA and fluid inclusion homogenization temperatures are in a broad agreement with those from compaction analysis and vitrinite reflectance.

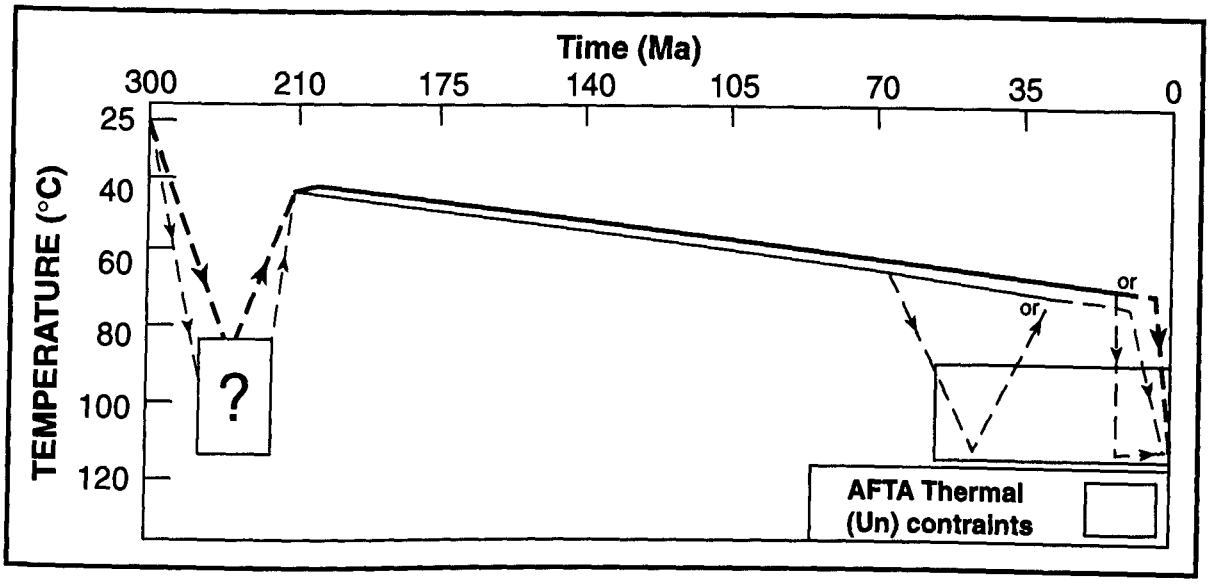

Figure 5.5. Schematic illustration of possible thermal history interpretations for the wells analysed in South Australia (thick line) and Queensland (thin line), using AFTA. Dashed lines represent times without good time/temperature control by AFTA. The AFTA data shows that samples experienced temperatures of 100°C or greater at around 20 to 70 Ma (or 10 to 70 Ma) in Queensland and around 10 to 1Ma in South Australia.

6. COMPARISON OF EXHUMATION RESULTS FROM THE DIFFERENT METHODS AND INFERRED BURIAL/EXHUMATION HISTORIES FOR THE COOPER-EROMANGA BASINS

6.1 Introduction

The previous chapters have shown that significant exhumation occurred after the deposition of the Cooper Basin (except in AFTA, Chapter 5), during Late Triassic - Early Jurassic times, and also after the deposition of the Eromanga Basin, during Late Cretaceous - Tertiary times. This chapter compares estimates of exhumation based on analysis of compaction, vitrinite reflectance, AFTA and fluid inclusion homogenization temperatures. The timing and duration of exhumational events during the major unconformities is also discussed and the results are synthesised to determine the burial/exhumation history of representative wells.

6.2 Comparison of Exhumation Estimates

The methodologies used in estimating exhumation from sedimentary rock compaction, vitrinite reflectance, AFTA and fluid inclusion homogenization temperatures have been discussed in the preceding chapters. This section compares the results from the different techniques and considers the extent to which they are compatible.

As discussed in Section 3.5, exhumation estimates based on the sonic log are considered more reliable than those based on the other logs. Hence sonic log-based estimates of exhumation are used for the comparisons in this chapter. As discussed in Section 4.3, overmaturity witnessed by vitrinite reflectance can be ascribed to exhumation from previously greater burial-depth and/or higher palaeogeothermal gradients. Hence exhumation values obtained from vitrinite reflectance are strongly influenced by the palaeogeothermal history that is selected.

Geothermal History C was considered the most reasonable (Section 4.4), and estimates of exhumation based on *Geothermal History C* are used for the comparisons in this chapter.

The exhumation values derived from the sonic log for the Eromanga Basin sequence are comparable with, or greater than those derived from vitrinite reflectance (Table 6.1 and Figure 6.1a). The differences between exhumation values for the two techniques are less than 350 m except at Innamincka-4, Jackson-1, and Warnie East-1, where the differences are 650, 370, and 480 m respectively. In the case of the Cooper Basin sequence, the majority of the wells show exhumation values derived from the sonic log that are broadly comparable with those derived from vitrinite reflectance (Table 6.1 and Figure 6.1b). Again, the differences between exhumation values from the two techniques are less than 350 m except at Bungee-1, Innamincka-4, and Warnie East-1, where the differences are 400, 580, and 520 m respectively. The greatest difference is at Burley-2, where the vitrinite reflectance method suggests some 1500 m more exhumation than the compaction analysis.

The broad patterns of exhumation revealed by the compaction and vitrinite reflectance methods are comparable (Figures 3.8 and 4.10). Both methods suggest lower Late Cretaceous - Tertiary exhumation values in the Patchawarra Trough and the Nappamerri Trough and an increase in exhumation in the Jackson-Naccowlah area (to approximately 600 m) and the Curalle anticline (to approximately 1000 m) (Figures 3.8 and 4.10). However, discrimination between the Patchawarra Trough and the anticlinal GMI Trend witnessed by compaction-based exhumation values (Section 3.6; Figure 3.8) is not apparent from the vitrinite reflectance data (Section 4.4; Figure 4.10). There are insufficient vitrinite reflectance data to reveal such a trend, even if it is witnessed by reflectances in those areas.

The reported exhumation values from the AFTA and fluid inclusion homogenization temperature methods are also in broad agreement with those derived from compaction analysis (Table 6.1 and Figures 6.1c and d). The greatest difference is at the Jackson-1 well, where compaction analysis gives values 300 and 500 m greater than those from the AFTA and fluid inclusion homogenization temperatures, respectively.

Table 6.1. Apparent Exhumation Estimates*

Well	Apparent Exhumation (in metres) Based on **Sonic Interval Transit Time** Eromanga Basin	Cooper Basin	Apparent Exhumation (in metres) Based on **Vitrinite Reflectance** Eromanga Basin	Cooper Basin	Apparent Exhumation (in metres) Based on **AFTA** Eromanga Basin	Apparent Exhumation (in metres) Based on **Fluid Inclusion Homogenization Temperatures** Eromanga Basin
Alkina-1	529	914	200	540		
Baryulah-1	366	852	600	870		
Battunga-1	302	619	250	380		
Beanbush-1	67	159	0	190		
Bogala-1	578	944				380
Bungee-1	278	660	0	250		
Burley-2	385	204 **	200	1730		
Copai-1	531	I M ***	300	I M ***		
Challum-1	389	839				190
Curalle-1	996	839 **	800	1190		
Innamincka-4	666	896	0	310		
Jackson-1	775	814	400	710	457	280
Lycium-1	250	342	150	310		
Macadama-1	336	387	300	500		
Mackillop-1	446	682	350	470		
Morney-1	824	798 **			975	
Nulla-1	230	625	300	610		
Okotoko-1	517	975	350	620		
Pepita-2	431	806			460	
Putamurdie-1	542	I M ***	230	I M ***		
Russel-1	337	705	350	480		
Tirrawarra North-1	185	376	0	400		
Ullenbury-1	453	310 **	520	690		
Wareena-1	871	1142	800	1180		
Warnie East-1	542	906	60	380		
Watson-1	613	I M ***		I M ***	549	

*Wells without apparent exhumation values means that no data have been collected (ie. in Vitrinite Reflectance) or reported (ie. in AFTA and Fluid Inclusion Homogenization Temperatures).

* *Values where exhumation derived from Cooper Basin units is less than exhumation derived from Eromanga Basin units, ie. no distinct phase of pre-Eromanga Basin exhumation can be distinguished.

***I M = Interval Missing

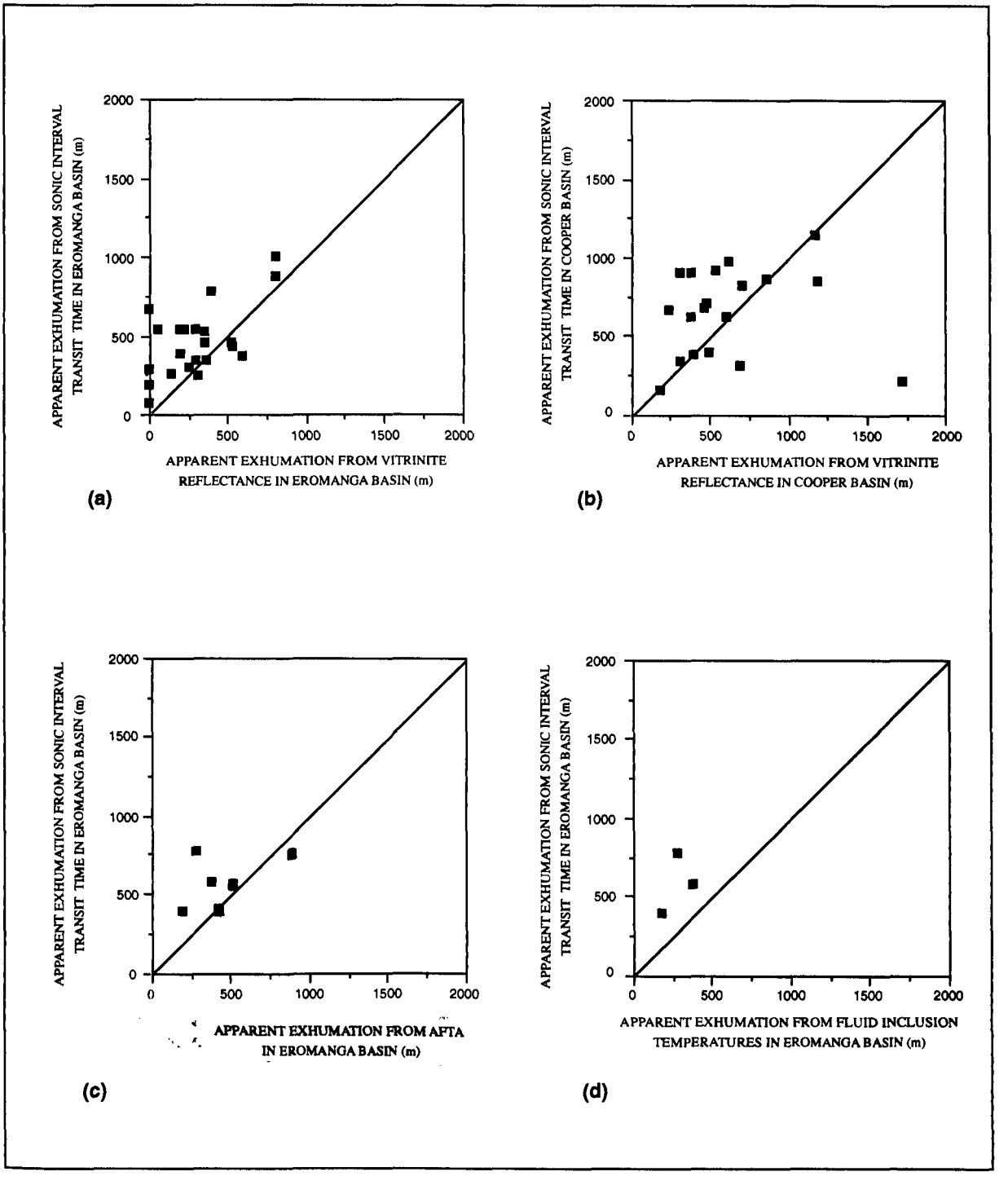

Figure 6.1. Comparison of apparent exhumation (in metres) from the different methods: (a) compaction based (sonic log) values from Eromanga Basin sequence vs those from vitrinite reflectance, (b) compaction based (sonic log) values from Cooper Basin sequence vs those from vitrinite reflectance, (c) compaction based (sonic log) values from Eromanga Basin sequence vs those from AFTA, (d) compaction based (sonic log) values from Eromanga Basin sequence vs those from fluid inclusion homogenization temperatures. The line illustrating the 1:1 relationship between apparent exhumation values from each pair of units analysed is shown.

There are clearly much more data available from compaction and vitrinite reflectance-based methods than from AFTA and fluid inclusion homogenization temperatures. The compaction and vitrinite reflectance methods have the advantage over other methods in that they are based on data that are commonly available from exploration wells and do not necessarily require extra laboratory costs (Skagen, 1992). Furthermore, recent investigations of exhumation in the Barents Sea, using different techniques showed that the shale compaction and the vitrinite reflectance give the most accurate results (Nyland *et al.*, 1992; Skagen, 1992; Jensen and Schmidt, 1993).

Unlike the workers in the Barents Sea, the author does not feel able to say with confidence which method(s) are more accurate, such would seem to require knowledge of 'true' exhumation values. *However, given that, albeit with some exceptions, the compaction-based values of exhumation derived from the sonic log are consistent with those based on the other techniques, and that the compaction-based data provides the most extensive set of results, these data are considered the best available for characterising exhumational events in the Cooper-Eromanga Basins.*

The compaction-based values of exhumation derived from the sonic log are used in the burial/exhumation histories presented in Section 6.4. However, in order to determine burial/exhumation histories for the Cooper-Eromanga Basins it is also necessary to constrain, as far as possible, the timing of the major periods of exhumation. The timing of these events is discussed in the following section.

6.3 Timing of Major Periods of Exhumation in the Cooper-Eromanga Basins

6.3.1 The Daralingie and Nappamerri Unconformities

A hiatus witnessed by the absence of palynological zones between the Early and Late Permian

is apparent in the rock record as the Daralingie unconformity (eg. Heath, 1989; also Figure 1.4). At the end of Early Permian/beginning of Late Permian times, a compressional phase resulted in rejuvenation of older basement structures and produced, for example the large, northeast-orientated, GMI Trend (Apak *et al.*, 1993). Although the tectonic activity along pre-Permian fault trends (Stuart, 1976; Stanmore and Johnstone, 1988) caused uplift and erosion of previously deposited sediments, sediment accumulation was continuous in deeper parts of the basin (Stuart, 1976; Battersby, 1976). There is no offset in the amounts of exhumation determined from the Lower Permian units (Patchawarra Formation, Murteree Shale and Roseneath Shale) and those determined from Upper Permian and Triassic units (Toolachee Formation and Nappamerri Group). Hence it appears that the pre-Daralingie, Lower Permian units did not reach maximum burial-depth during the hiatus associated with the Daralingie unconformity, and thus compaction analysis cannot detect the amount of exhumation during this hiatus.

Deposition of the Cooper Basin sequence was terminated by major uplift in Late Triassic - Early Jurassic times which resulted in a northeasterly tilting of the Cooper Basin (Kuang, 1985), rejuvenation of pre-existing structures and a basin-wide unconformity (Thorton, 1979; Kuang, 1985; Channon and Wood, 1989). Kuang (1985) considered this event was due to wrench-induced northeast-southwest compressional stress. Wiltshire (1982a) and Gallagher *et al.* (1994) related the unconformity to the Mid - Late Triassic Hunter/Bowen orogeny in the New England Fold Belt. It would seem reasonable to correlate the unconformities, with more intense deformation observed in the Sydney and Bowen Basins to the east (Veevers, 1984). Detailed mapping of seismic lines in the Bowen and Surat Basins has shown major unconformities developed near thrust and reverse faults in response to compressional reactivation of these faults (Elliot, 1993).

In the Cooper-Eromanga Basins, the timing of erosion associated with the Triassic-Jurassic unconformity is locally constrained where the Late Triassic Cuddapan Formation is observed (Figure 1.4). However, the Cuddapan Formation is limited to the Windorah Trough and the Patchawarra Trough, having a maximum thickness of 50 m (Powis, 1989). Powis (1989)

argued that erosion prior to deposition of the Lower Jurassic Poolowanna Formation resulted in these isolated remnant 'puddles' of Late Triassic strata. However, Wiltshire (1982b) noticed that the thickest development of the unit is in areas where Lower Jurassic sediments are also thick, ie. this Late Triassic sedimentation was apparently a precursor of Eromanga Basin sedimentation. Wiltshire (1982b) argued that the unit in terms of lithology, log character and area of distribution has much greater affinity to the overlying Eromanga Basin sequence than to the Cooper Basin, and thus it presumably post-dates erosion.

Powis (1989) argued that the boundary between the Lower and Middle Triassic Arrabury and Tinchoo Formations, which is a mappable seismic marker in northern ATP 259P (Queensland sector of the study area), is associated with a tectonic event. Powis (1989) suggested that this was a major event (of Early/Middle Triassic age) that initiated the termination of the Cooper Basin phase of deposition.

In order to check whether the Arrabury/Tinchoo boundary represented the main uplift event between the Cooper and Eromanga Basins, the compaction method was applied separately to the Arrabury and Tinchoo Formations in 37 wells selected to provide regional coverage (Figure 6.2a). Apparent exhumation values from both units are very consistent and do not support Powis's (1989) suggestion that the Arrabury/Tinchoo boundary represents the Cooper-Eromanga transition (Figures 6.2b and c).

Hence, accepting Wiltshire's (1982b) interpretation that the Cuddapan Formation is part of the Eromanga Basin sequence, where the Cooper Basin is believed to have reached maximum burial-depth prior to the deposition of the Eromanga Basin (as discussed in Section 3.4), this is inferred to have occurred in Late Triassic times.

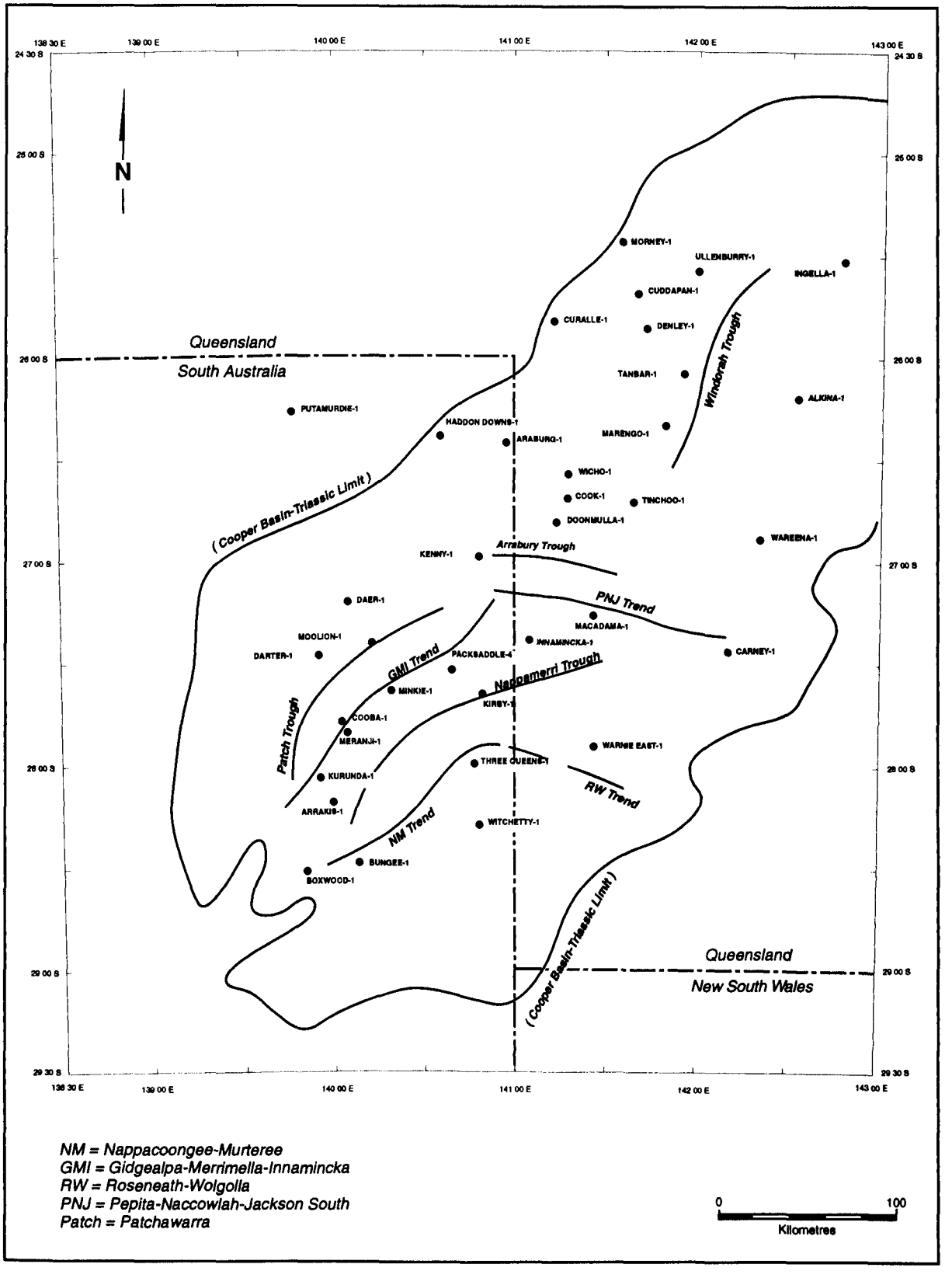

Figure 6.2a. Location map of the wells used in compaction analysis of the Tinchoo and Arrabury Formations. Major tectonic elements are also shown.

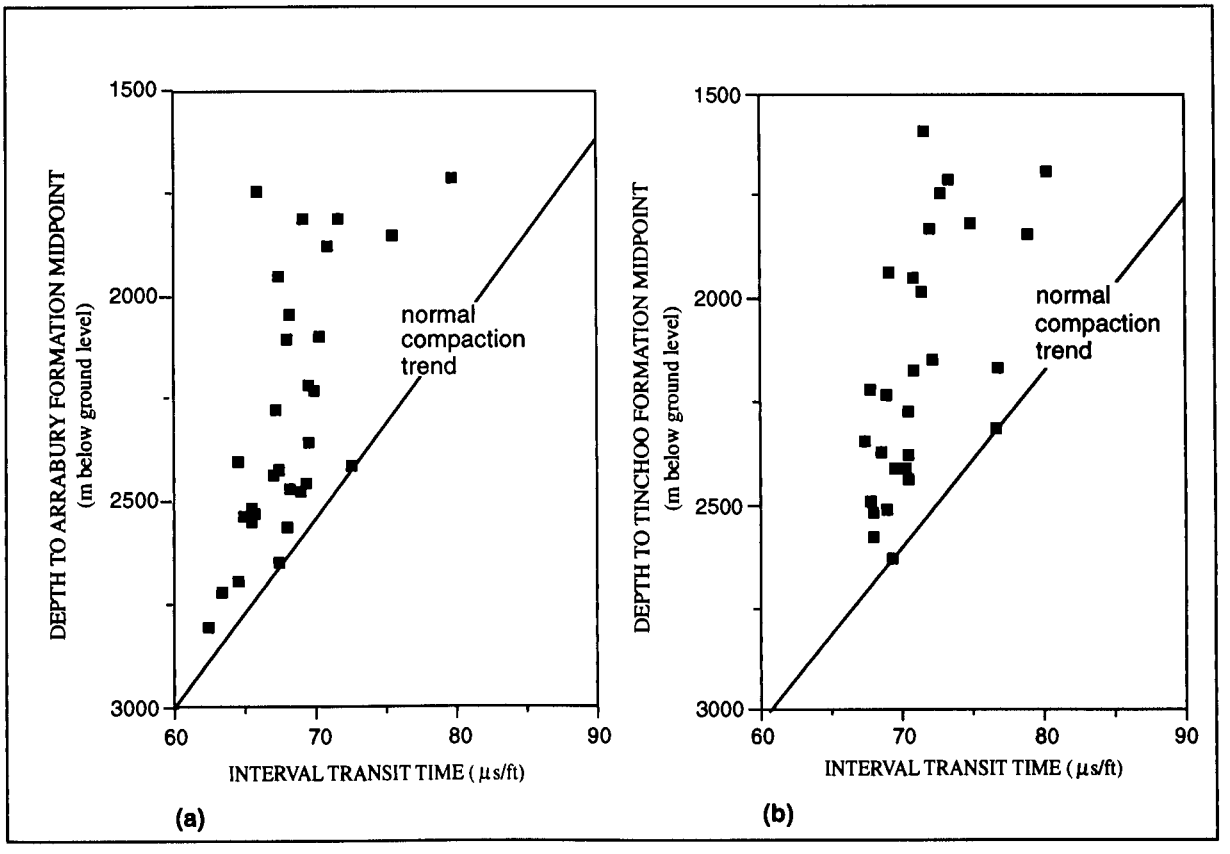

Figure 6.2b. Mean Δt/depth to unit midpoint for (a) Arrabury Formation and (b) Tinchoo Formation. The normal compaction relationship for each unit is also shown.

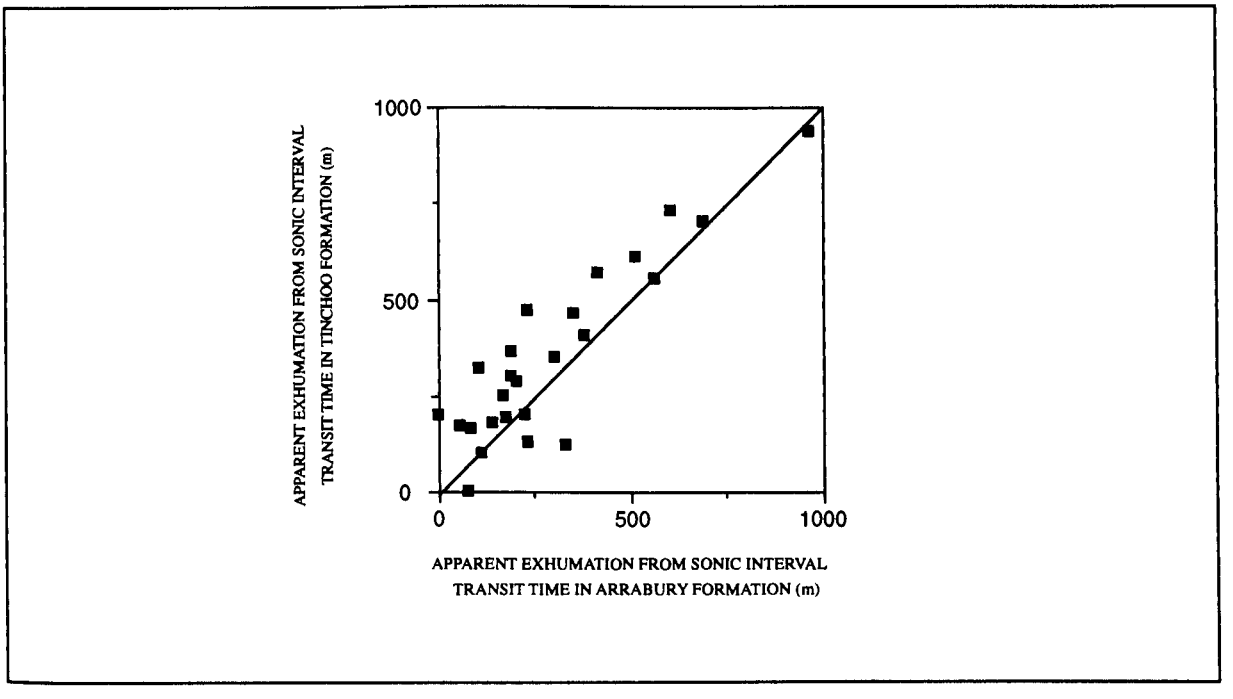

Figure 6.2c. Crossplot of apparent exhumation (in metres) derived from Δt in Tinchoo Formation against those from Arrabury Formation. The line illustrating the 1:1 relationship between apparent exhumation values from each pair of units analysed is shown.

6.3.2 Late Cretaceous - Tertiary Unconformities

Deposition of the Winton Formation ceased in Late Cenomanian or Early Turonian times (Moore and Pitt, 1984). The Winton Formation is unconformably overlain by the Late Palaeocene - Late Eocene Eyre Formation. The Eyre Formation is itself unconformably overlain by the Early-Middle Miocene Etadunna Formation (Figure 6.3).

Unfortunately, no log data are available for the units overlying the Winton Formation, thus it is not possible to date the exhumation beyond post-Cenomanian using the compaction methodology. Since the Tertiary units are relatively thin, the timing of Late Cretaceous - Tertiary structuration, which may be contemporaneous with exhumation, cannot be determined from seismic reflection data using standard techniques (ie. interpretation of Tertiary units affected/unaffected by structuration). Information on the age of Tertiary structuration and exhumation is restricted to analysis of the outcropping Tertiary.

Even in the subsurface, the Winton Formation is deeply weathered in its upper part (Wopfner *et al.*, 1974; Senior *et al.*, 1978; Williams and Moriarty, 1986), indicating that it was subject to a long period of exposure, and potentially exhumation, prior to Tertiary deposition. Furthermore, an angular unconformity of a few degrees separates the Winton and Eyre Formations on the crests of major anticlines (Sprigg, 1958; Wopfner *et al.*, 1974). Hence there was a period of exposure and structuration prior to deposition of the Eyre Formation.

Deep chemical weathering during late Eocene-Oligocene times, between the deposition of the Eyre and Etadunna Formations, caused silicification the Eyre and Winton Formations. This period may also have been one of significant exhumation. Structuring continued subsequent to the deposition of the Eyre Formation, producing the major surface anticlines and the uplifted silcrete-covered tablelands seen today (Moore and Pitt, 1984).

Regionally, Late Miocene-Recent exhumation, subsequent to the deposition of the Etadunna Formation, is witnessed by the uplift of the Sturgon Volcanics in central Queensland

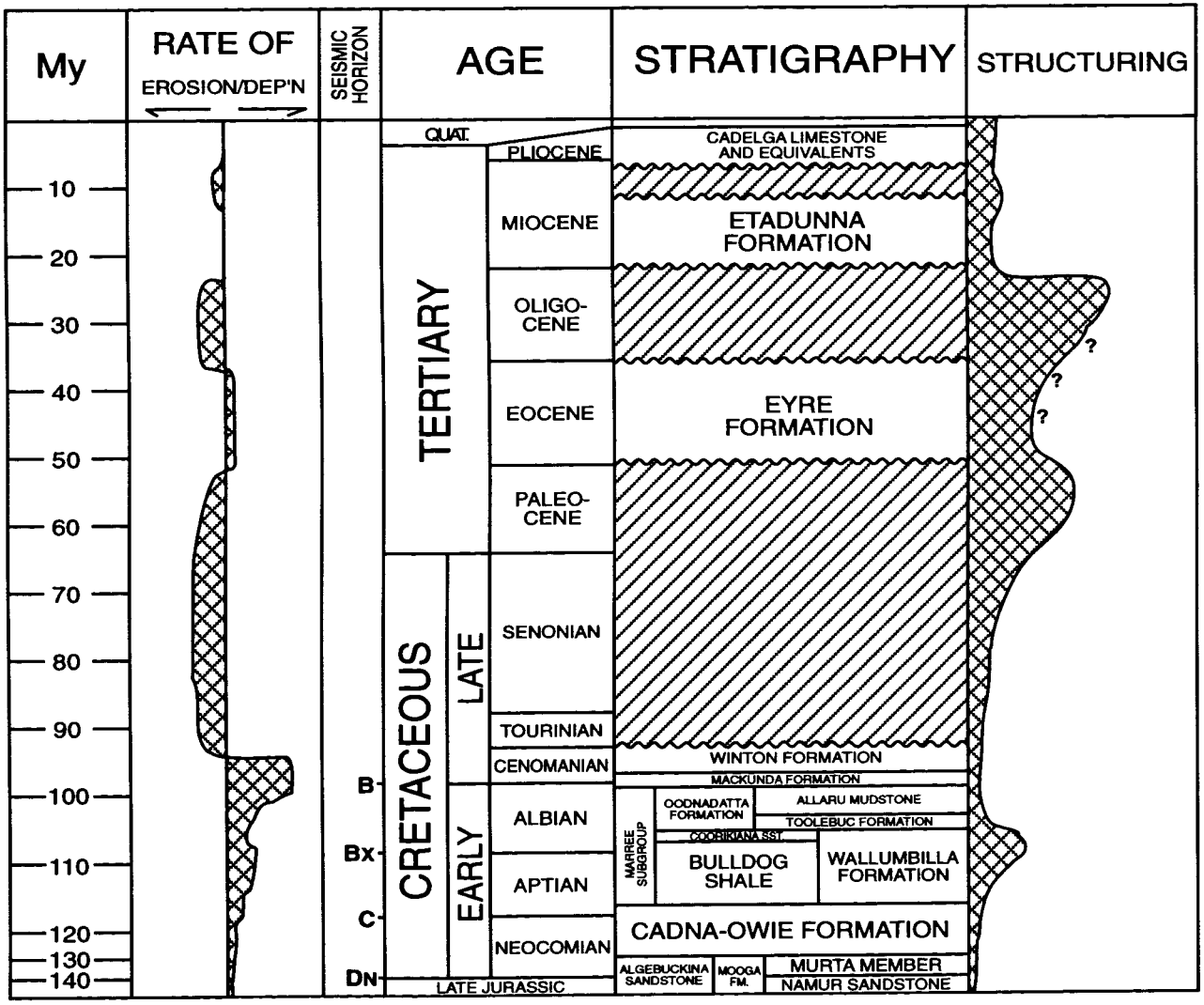

Figure 6.3. Summary of stratigraphy, structuring in Eromanga-Tertiary sediments (modified after Santos, 1991).

(Coventry *et al.*, 1985), and by uplift of the Flinders Ranges (Callen and Tedford, 1986). However, Moore and Pitt (1984) suggested that there is no clear evidence of post-Etadunna folding of Eromanga Basin sediments.

In summary, although the chronology of Late Cretaceous - Tertiary basin development is not well constrained, uplift and structuration appears to have been multi-phase or episodic throughout Late Cretaceous and Tertiary times (Moore and Pitt, 1984; Shaw, 1991). Given that such Tertiary sequences as are preserved are relatively thin and separated by marked unconformities/weathered surfaces, it is suggested that exhumation rather than sedimentation dominated the Tertiary, and that in exhumed areas, maximum burial-depth was attained in Late Cretaceous times.

6.4 Burial/Exhumation History of the Cooper-Eromanga Basins

6.4.1 Sediment Decompaction

In order to re-create burial/exhumation history through time, the preserved rock record must be decompacted. Sedimentary rock decompaction aims to restore the original depositional thickness of now-buried and compacted stratigraphic units and thus re-create burial history (eg. Sclater and Christie, 1980; Falvey and Deighton, 1982). To restore the original thickness of a stratigraphic unit, its normal porosity/depth relationship and maximum burial-depth must be determined. Restored thicknesses are calculated from the porosity (hence, associated volume) increase indicated by the porosity/depth relationship as the rock unit is raised from its maximum burial-depth to the surface.

To illustrate the technique of sediment decompaction, the decompacted depth to the base Permian in the Beanbush-1 well is calculated by removing and decompacting the overlying sediment sequence unit-by-unit (Figure 6.4). The top unit (1), from which there are no well returns, is removed first and the underlying units are decompacted, increasing in thickness.

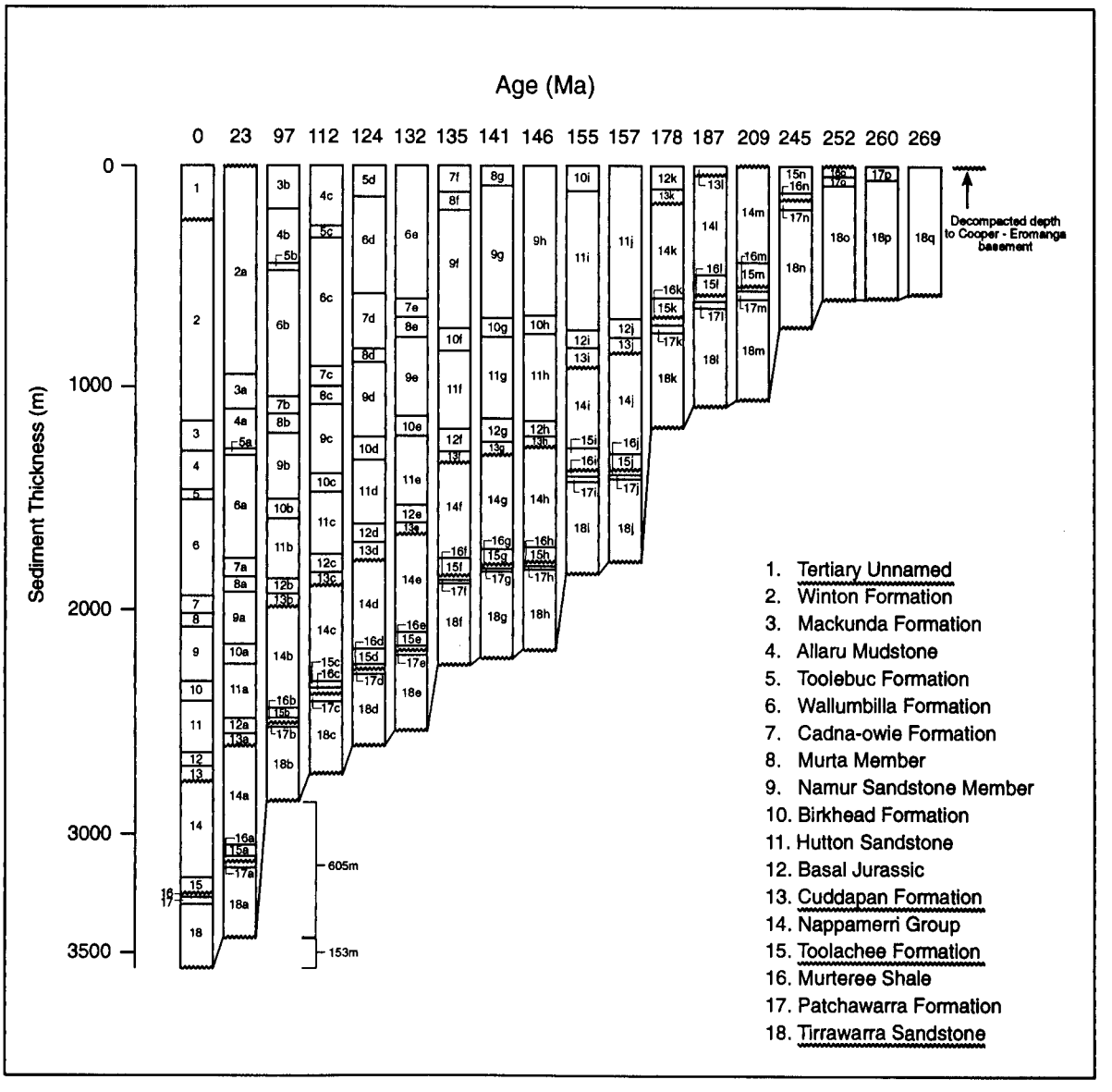

Figure 6.4. Progressive decompaction of the Cooper-Eromanga sequence in well Beanbush-1.

The thickness increase of underlying units counteracts the removal of the top 240 m of sediments, hence the decrease in decompacted depth to "basement" from the present to the end of the Miocene, with removal of the topmost 240 m, is only 150 m. The Cenomanian Winton Formation is removed next: its thickness has increased from 910 m (2) to 950 m (2a) due to the removal of the top unit, however, the decompaction of the underlying sediments as the 950 m of Winton Formation is removed means that the decrease in decompacted depth to basement is only 600 m. This continues until approximately the middle of the sequence where the decompaction of the unit being removed becomes greater than the decompaction of the underlying units due to its removal, and decompacted depths to "basement" change by more than the present-day thickness of the unit being backstripped. Decompacting a sediment

sequence hence predicts more rapid early and slower later subsidence than present well thicknesses. An important assumption is that levels beneath compaction basement are fully compacted prior to the onset of sedimentation and do not compact further during subsequent deposition.

Several algorithms for decompaction have been proposed based on the rate of reduction of porosity with depth and conservation of the solid volume of sediments (Athy, 1930; Perrier and Quiblier, 1974; Sclater and Christie, 1980; Baldwin and Butler, 1985; Stam *et al.*, 1987). Among these algorithms, Perrier and Quiblier's (1974) and Sclater and Christie's (1980) are the most representative (Liu and Roaldset, 1994). In this study, Sclater and Christie's (1980) algorithm, as incorporated in the BasinMod™ software (Platte River Associates, 1995), was used. It has been used in this study with porosity-depth parameters derived from the Cooper-Eromanga Basins as discussed in the next section.

6.4.2 Porosity-Depth Relations and Sediment Decompaction in the Cooper-Eromanga Basins

In order to decompact sedimentary rocks in exhumed wells, their undisturbed porosity-depth trend and the amount of exhumation must be known. Like the normal velocity-depth trend used to estimate exhumation, the normal porosity-depth trend is defined by the wells which are the least compacted (highest porosity) for their burial-depth. In order to determine porosity-depth trends, the sonic log values (determined in Chapter 2) were converted to porosity values using Hansen's (1996) equation for shales (equation 6.1) and Raiga-Clemenceau *et al.*'s (1988) equation for sandstones (equation 6.2):

$$\phi = (1/1.57)([\Delta t - 59]/[189 - 59]) \qquad (6.1)$$

$$\phi = 1 - \left(\frac{\Delta t_{ma}}{\Delta t}\right)^{1/x} \qquad (6.2)$$

where Δt_{ma} (μsec/ft) = 55.5 and x = 1.6 (Raiga-Clemenceau *et al.*, 1988).

Most of the stratigraphic units are combinations of the above lithologies, the above equations were modified according to the approximate fraction of the lithology in each unit. The relationships applied are summarised in Table 6.2 and Figure 6.5.

Sclater and Christie's (1980) method is based on the Rubey and Hubbert's (1959) equation relating porosity (ϕ) to depth (z):

$$\phi_z = \phi_0 e^{-cz} \qquad (6.3)$$

where ϕ_z and ϕ_0 are porosity at depth z and surface porosity respectively and c is the exponential factor to allow for the varying compressibilities of different lithologies. Rubey and Hubbert's (1959) equation has been fitted to the least compacted porosity-depth points for each unit (Figure 6.6). Surface porosities have been taken from the literature. Schlumberger (1974) suggested 63% for shales, while Pryor (1973) showed that sandstone surface porosity is facies-dependent and a simple average of these facies which is 46%, was taken to represent the varied sandstone facies of the Cooper-Eromanga Basins. Sediment grain densities were taken from Sclumberger (1987) and these are 2.72 gcm^{-3} and 2.65 gcm^{-3} for shales and sandstones respectively. The surface porosity and density values were assigned according to the fraction of each lithology in each unit. Table 6.3 summarises the porosity-depth values used in sediment decompaction.

The ages of the tops and bases of units were taken from those on operators' composite logs and calibrated according to the geological time scale of Harland *et al.* (1989). The hiatus associated with the Daralingie unconformity was treated as a phase of non-deposition because there is no evidence from compaction of exhumation at this time (Section 6.3.1). Mean total exhumation values from the Cooper Basin and Eromanga Basin units, were added to the observed stratigraphy in Late Triassic - Early Jurassic and Late Cretaceous - Tertiary times, respectively. The following section discusses the burial/exhumation history of six representative wells in the Cooper-Eromanga Basins (Figure 6.7).

Table 6.2. Relationships Between Porosity and Interval Transit Time for the Units to be Backstripped in the Cooper-Eromanga Basins

Lithology	Stratigraphic Unit	Interval Transit Time-Porosity Equation
Sandstone		
	Hutton Sandstone	$\phi = 1 - (55.5/\Delta t)^{1/1.6}$
Shale		
	Bulldog Shale/ Wallumbilla Formation / Roseneath Shale / Murteree Shale	$\phi = (1/1.57)([\Delta t - 59]/[189 - 59])$
Sandy Shale		
• 80% Shale - 20% Sandstone	Allaru Mudstone/ Oodnadatta Formation	$\phi = 0.8(1/1.57)([\Delta t - 59]/[189 - 59]) + 0.2(1 - (55.5/\Delta t)^{1/1.6})$
• 70% Shale - 30% Sandstone	Winton Formation / Cadna-owie Formation / Birkhead Formation / Nappamerri Group	$\phi = 0.7(1/1.57)([\Delta t - 59]/[189 - 59]) + 0.3(1 - (55.5/\Delta t)^{1/1.6})$
• 65% Shale - 35% Sandstone	Patchawarra Formation	$\phi = 0.65(1/1.57)([\Delta t - 59]/[189 - 59]) + 0.35(1 - (55.5/\Delta t)^{1/1.6})$
• 60% Shale - 40% Sandstone	Mackunda Formation / Toolachee Formation	$\phi = 0.6(1/1.57)([\Delta t - 59]/[189 - 59]) + 0.4(1 - (55.5/\Delta t)^{1/1.6})$

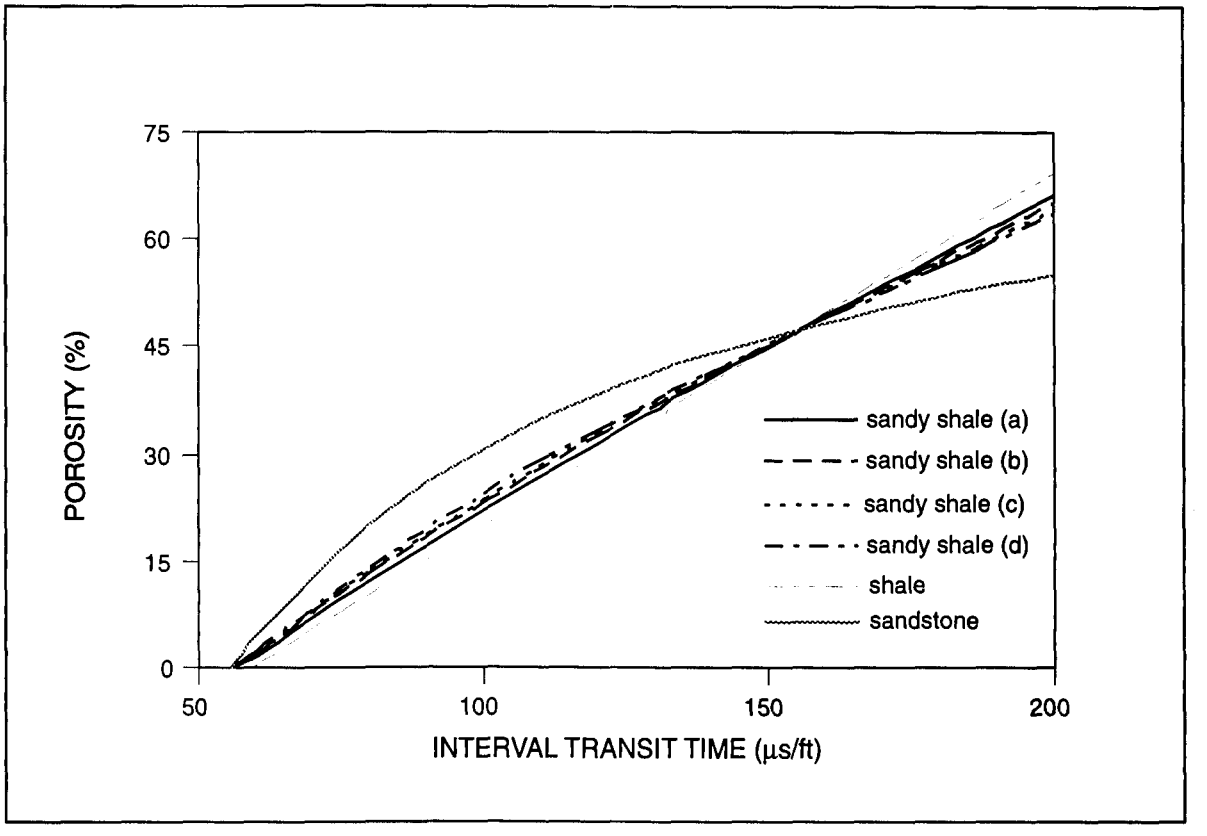

Figure 6.5. Interval transit time (Δt) / porosity relationships. Sandstone interval transit time/porosity relationship is after Raiga-Clemenceau *et al.* (1988) and was used to convert sonic log based Δt to porosity in the Hutton Sandstone. Shale interval transit time (Δt) / porosity relationship is after Hansen (1966) and was used to convert sonic log based Δt to porosity in the Bulldog Shale/Wallumbilla Formation, Roseneath and Murteree Shales. Sandy shale interval transit time (Δt) / porosity relationships are combinations of a: (a) 80% shale and 20% sandstone relations suitable for the Allaru Mudstone/Oodnadatta Formation, (b) 70% shale and 30% sandstone relations suitable for the Winton Formation, Cadna-owie Formation, Birkhead Formation, and Nappamerri Group, (c) 65% shale and 35% sandstone relations suitable for the Patchawarra Formation and (d) 60% shale and 40% sandstone relations suitable for the Mackunda and Toolachee Formations.

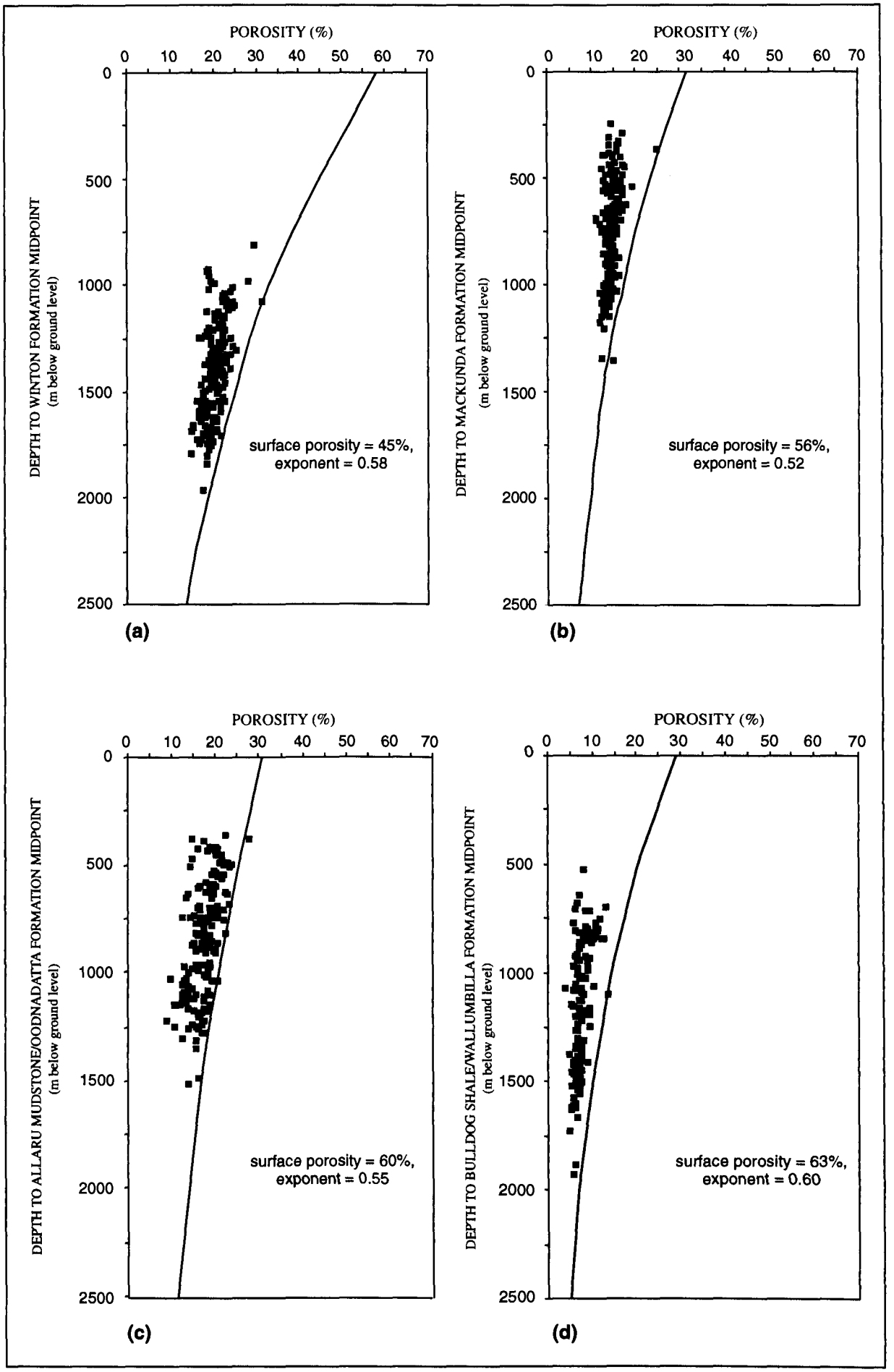

Figure 6.6. Porosity/mid-point depth plots for units backstripped in the Cooper-Eromanga Basins (a) the Winton Formation, (b) the Mackunda Formation, (c) the Allaru Mudstone/Oodnadatta Formation, and (d) the Bulldog Shale/Wallumbilla Formation.

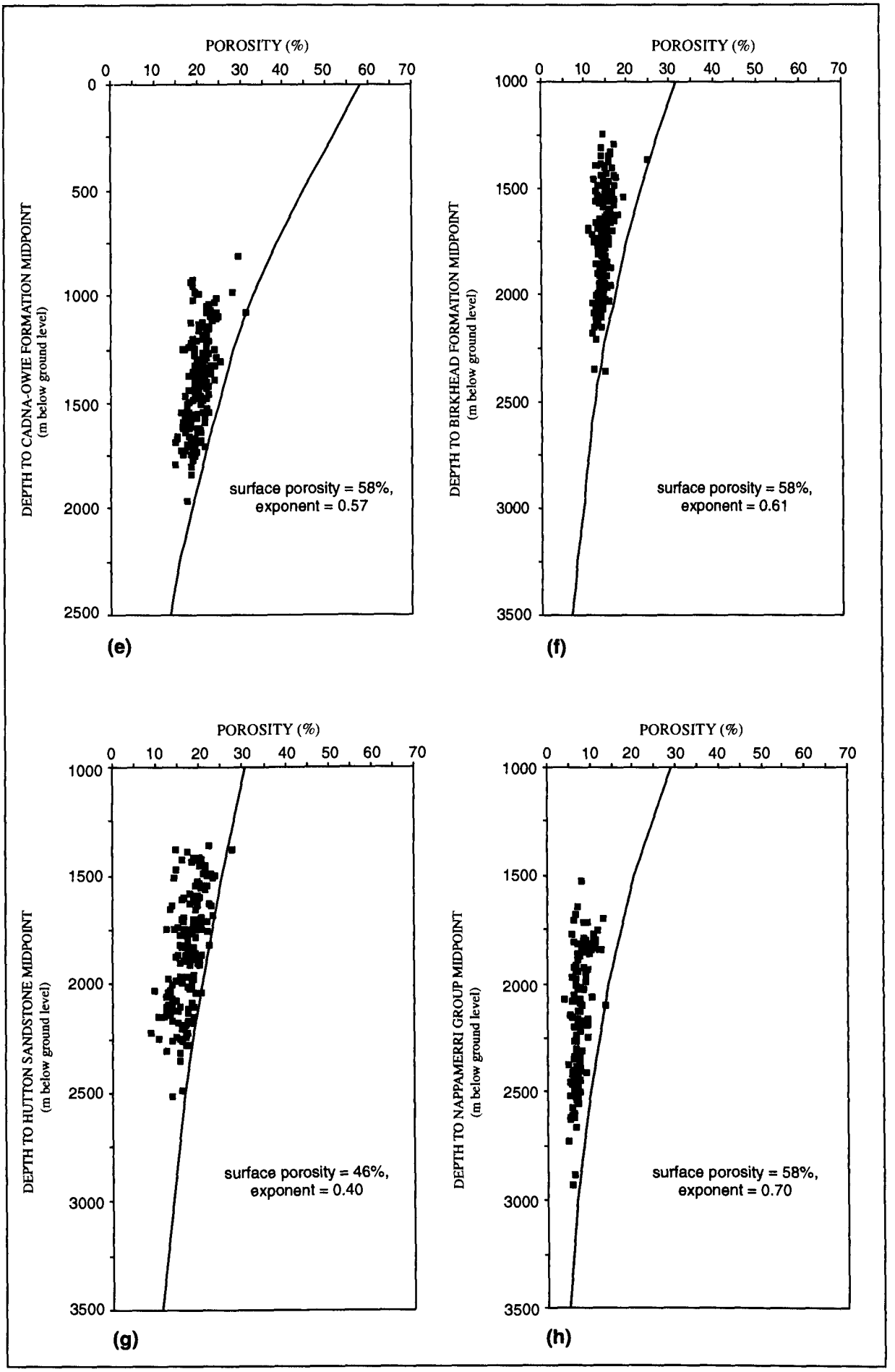

Figure 6.6. Continued. Porosity/mid-point depth plots for units backstripped in the Cooper-Eromanga Basins (e) the Cadna-owie Formation, (f) the Birkhead Formation, (g) the Hutton Sandstone, and (h) the Nappamerri Group.

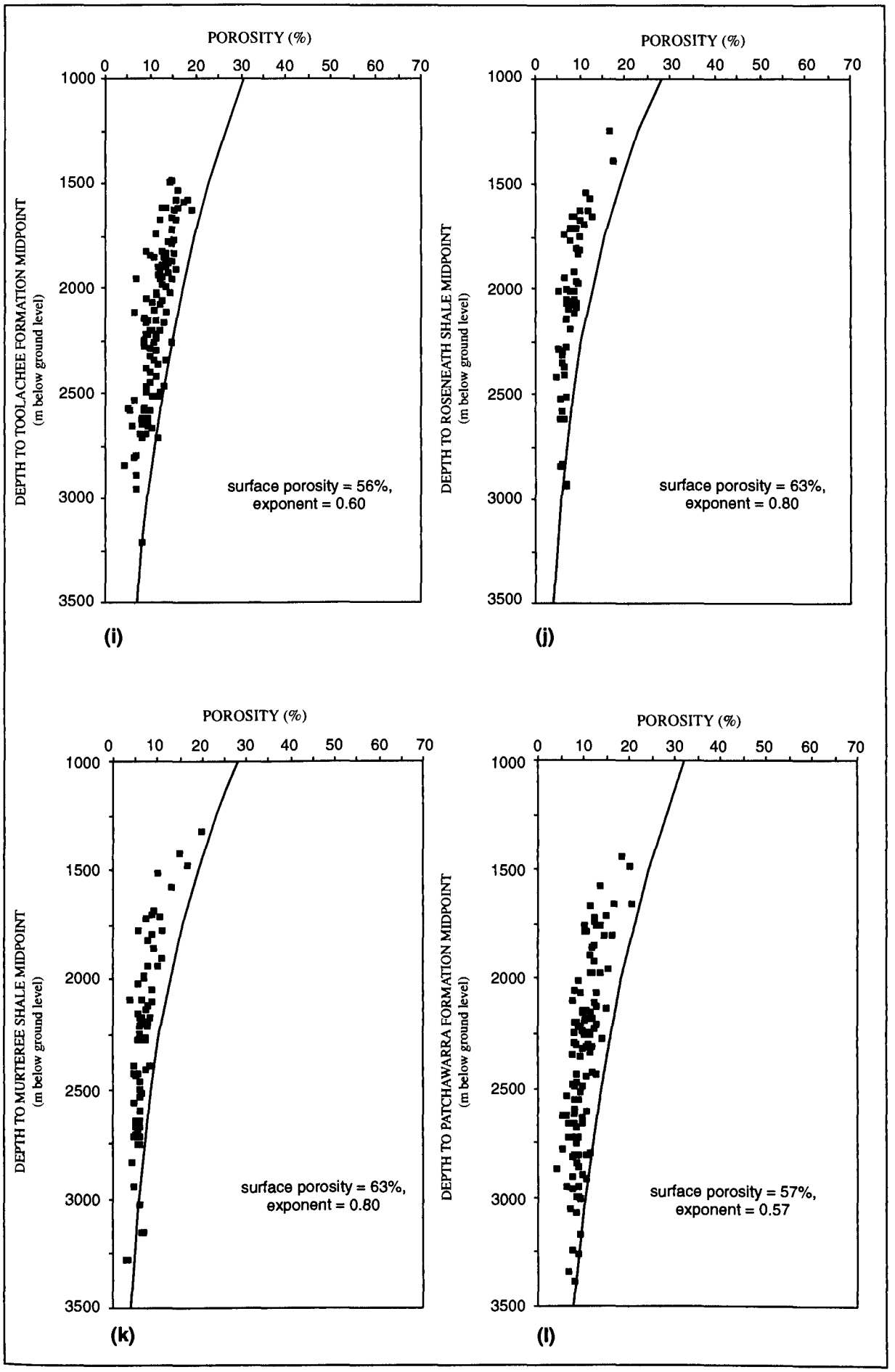

Figure 6.6. Continued. Porosity/mid-point depth plots for units backstripped in the Cooper-Eromanga Basins (i) the Toolachee Formation, (j) the Roseneath Shale, (k) the Murteree Shale, and (l) the Patchawarra Formation.

Table 6.3. Porosity-Depth Parameters and Sediment Grain (Matrix) Densities Used in Sediment Decompaction

Unit	ϕ_0 (%)	c (km^{-1})	ρ_{ma} (gcm^{-3})
Eromanga Basin			
Winton Formation	58	0.45	2.69
Mackunda Formation	56	0.52	2.69
Allaru Mudstone/	60	0.55	2.70
Oodnadatta Formation			
Bulldog Shale/	63	0.60	2.72
Wallumbilla Formation			
Cadna-owie Formation	58	0.57	2.69
Birkhead Formation	58	0.61	2.69
Hutton Sandstone	46	0.40	2.65
Cooper Basin			
Nappamerri Group	58	0.70	2.69
Toolachee Formation	56	0.60	2.69
Roseneath Shale and	63	0.80	2.72
Murteree Shale			
Patchawarra Formation	57	0.57	2.69

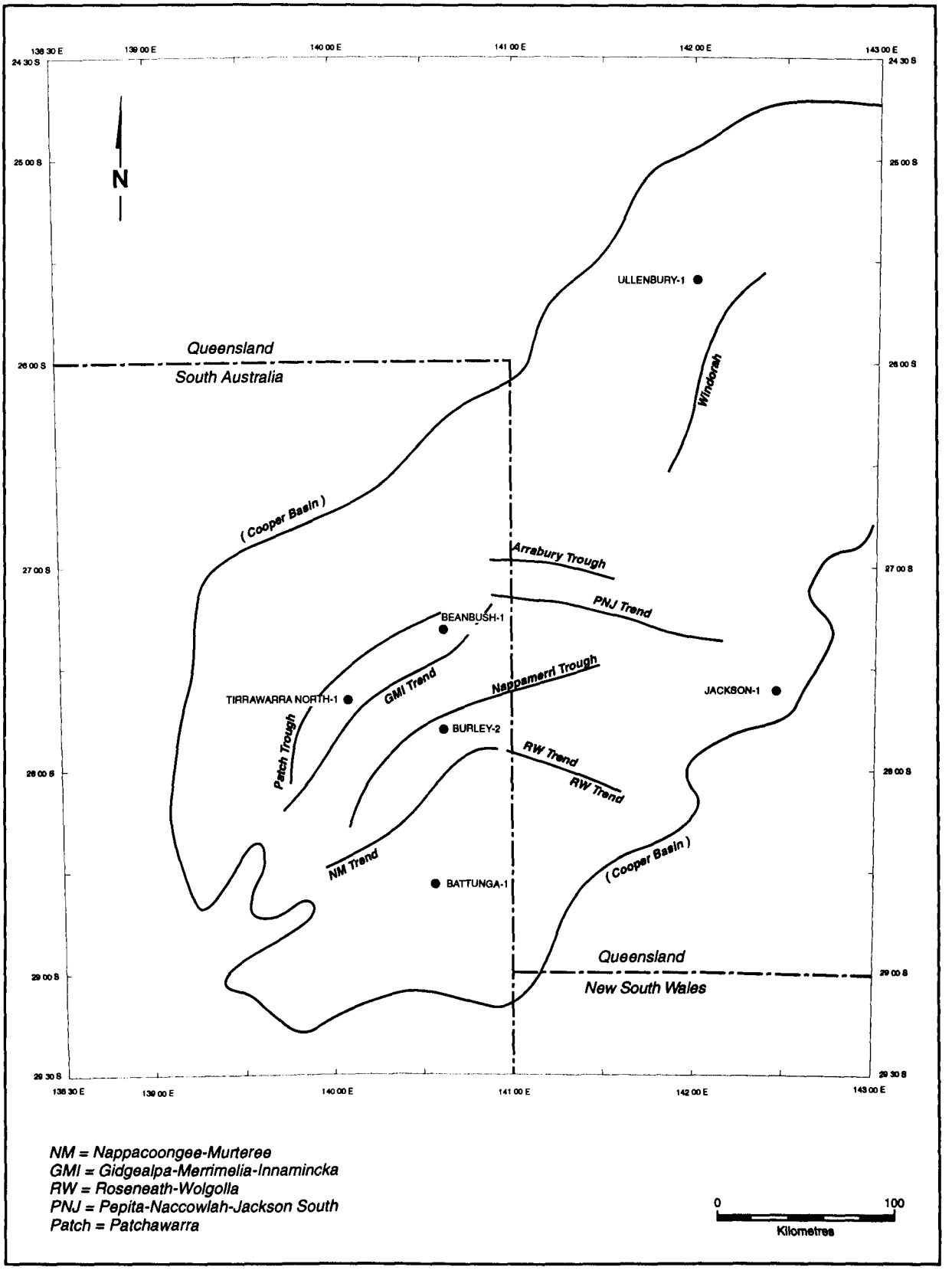

Figure 6.7. Location of representative wells used in burial/exhumation histories. Major tectonic elements of the Cooper-Eromanga Basins are also shown.

6.4.3 Discussion of Burial/Exhumation Histories

Considering the relative significance of the major periods of exhumation in the Cooper/Eromanga Basins, which is the main focus of this thesis, three broad types of burial/exhumation histories can be distinguished (Figure 6.8):

- maximum burial-depth of the Cooper Basin sequence attained prior to the deposition of the Eromanga Basin sequence, ie. Late Triassic - Early Jurassic exhumation was of greater magnitude than subsequent burial during development of the Eromanga Basin;
- maximum burial-depth of the Cooper and Eromanga Basin sequences attained in Late Cretaceous times, prior to Tertiary exhumation, and;
- currently at maximum burial-depth.

There are relatively few wells where the stratigraphic units analysed lie on or close to the normal velocity/depth compaction trends (Figure 2.15). Hence it is inferred that few wells are currently at maximum burial-depth. In the vast majority of wells (187 of those analysed), the mean exhumation yielded from compaction analysis of the Cooper Basin units is greater than the mean value yielded from the Eromanga Basin units. As discussed in Section 3.4, in these wells it is inferred that the Cooper Basin sequence attained maximum burial-depth prior to the deposition of the Eromanga Basin sequence. However, it should be mentioned that in many cases, the difference is less than the sum of the probable error bounds on the two estimates of exhumation. In 16 wells the mean exhumation yielded from compaction analysis of the Cooper Basin units is less than the mean value yielded from the Eromanga Basin units. In these wells there is no evidence, from compaction analysis, of exhumation in Late Triassic - Early Jurassic times. However, in the absence of major lateral tectonic movement, the Cooper Basin units must have been subjected to the same magnitude of Late Cretaceous - Tertiary exhumation as the Eromanga Basin units. Thus the wells in which exhumation indicated by the compaction of the Cooper Basin units is less than the mean value indicated by the Eromanga Basin units give an indication of the error associated with the method (Section 3.4).

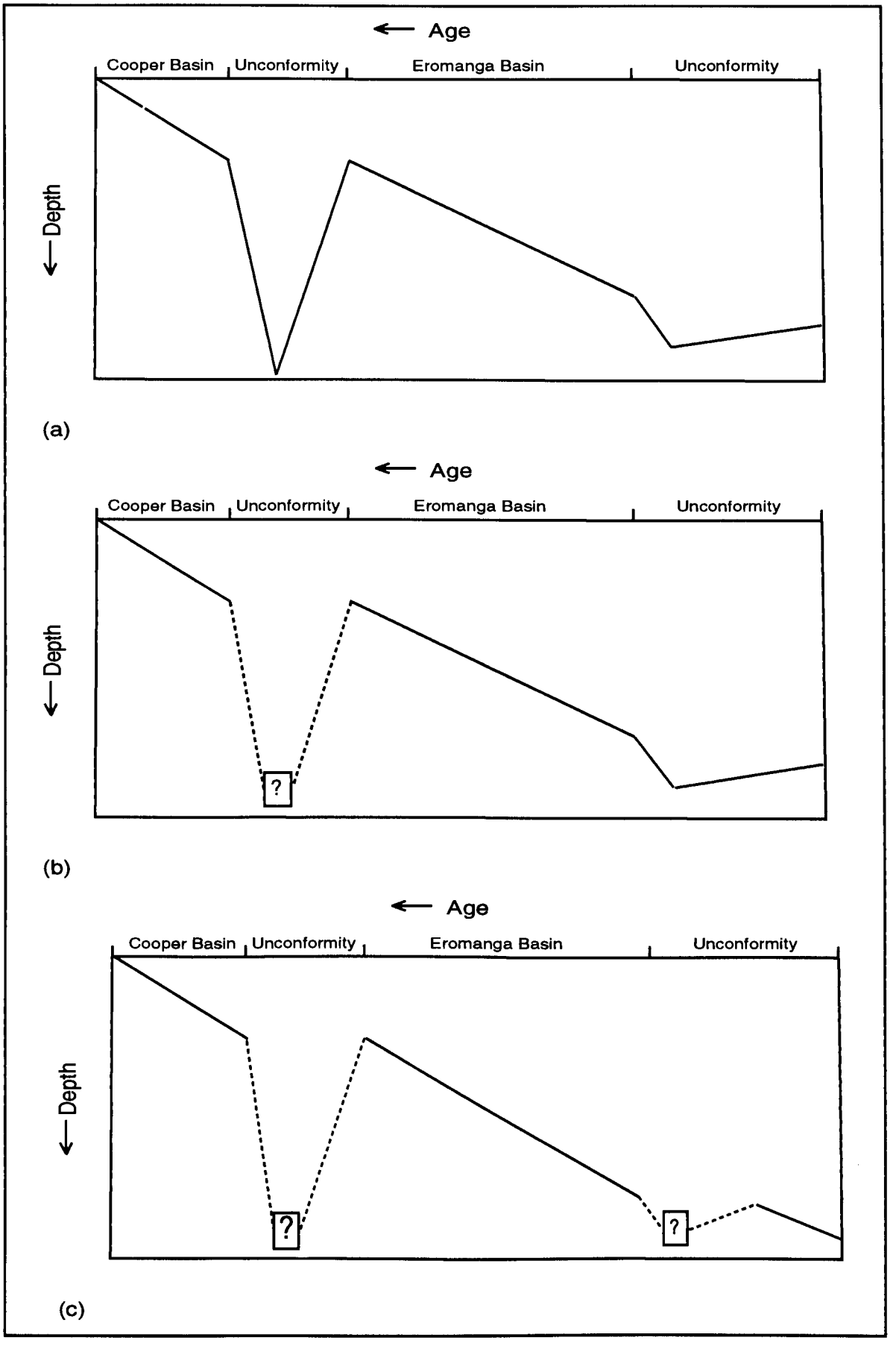

Figure 6.8. Types of burial/exhumation histories for the Cooper-Eromanga Basins. In type (a) burial/exhumation events at both the Cooper and Eromanga unconformities are visible, in type (b) the burial/exhumation event in the Cooper Basin unconformity is not apparent, and in type (c) the well is at maximum burial-depth and no previous burial/exhumation events are apparent.

Figure 6.9 illustrates the burial/exhumation history for several wells where the Cooper Basin sequence attained maximum burial-depth prior to the deposition of the Eromanga Basin sequence. Since Late Triassic - Early Jurassic exhumation was of greater magnitude than subsequent burial during development of the Eromanga Basin, the pre-exhumation (Cooper Basin) units would not have compacted during deposition of the Eromanga Basin sequence. Hence the Cooper Basin sequence acts as compaction basement during decompaction of the Eromanga Basin units, ie. all horizons in the Cooper Basin would have followed a burial/exhumation path parallel to that illustrated for the base Permian. In practice, Cooper Basin units were decompacted as a separate sequence, with the addition of 2700 m of sediments inferred to have been removed during Late Triassic - Early Jurassic exhumation. These wells also exhibit significant Late Cretaceous - Tertiary exhumation. The incorporation of the Late Cretaceous - Tertiary exhumation into the burial histories of these wells significantly increases maximum burial-depth of the Eromanga Basin sequence from that observed at the present day. Consequently the Eromanga Basin decompacts considerably more when allowance is made for Late Cretaceous - Tertiary exhumation.

Figure 6.10 illustrates the burial/exhumation history for wells where maximum burial-depth was attained in Late Cretaceous times. All that can be said with confidence about any Late Triassic - Early Jurassic exhumation in such wells is that it was of lesser magnitude than subsequent burial during the deposition of the Eromanga Basin. Given that many wells in the Cooper-Eromanga Basin show major exhumation at this time, and that there is a regional angular unconformity between the Cooper and Eromanga Basins, it seems unlikely that these wells were not subject to any exhumation at this time. Figure 6.10 shows a dotted line which indicates the maximum possible burial and subsequent exhumation during Late Triassic - Early Jurassic times in these wells. The true amount of burial and exhumation at this time may have been anywhere between none and that indicated by the dotted line. Given, the magnitude of exhumation in other wells and the regional angular unconformity, the author believes that it is closer to the latter than the former. In these wells the effect on decompaction of incorporating Late Cretaceous - Tertiary exhumation is more readily apparent than it is in the wells illustrated

in Figure 6.9, because the Cooper Basin sequence is not acting as compaction basement during decompaction of the Eromanga Basin units.

Figure 6.11 illustrates the burial/exhumation history for a well believed to currently be at maximum burial-depth. There are only three such wells in this study. There is no evidence, from compaction trends, of exhumation either in Late Triassic - Jurassic or Late Cretaceous - Tertiary times in these wells. Indeed these are the wells that were used as reference wells in the compaction plots, ie. wells defining the normal compaction relation. It is, of course, possible that these wells are above maximum burial-depth and that the amount of exhumation inferred in all wells is reduced from the true amount by the amount of exhumation to which these reference wells were subjected. However, comparing normal compaction trends in this study with those published world-wide (eg. Figure 2.2), suggests that if such is the case, the amount of exhumation is not significant. Exhumation is seen in wells in close proximity to the reference wells, both during Late Triassic - Early Jurassic and during Late Cretaceous - Tertiary times. Hence it is considered likely that the reference wells were exhumed at these times, but by a smaller amount than subsequent burial. The dotted lines in Figure 6.11 indicate the minimum (zero) and maximum amount of exhumation to which these wells may have been subjected.

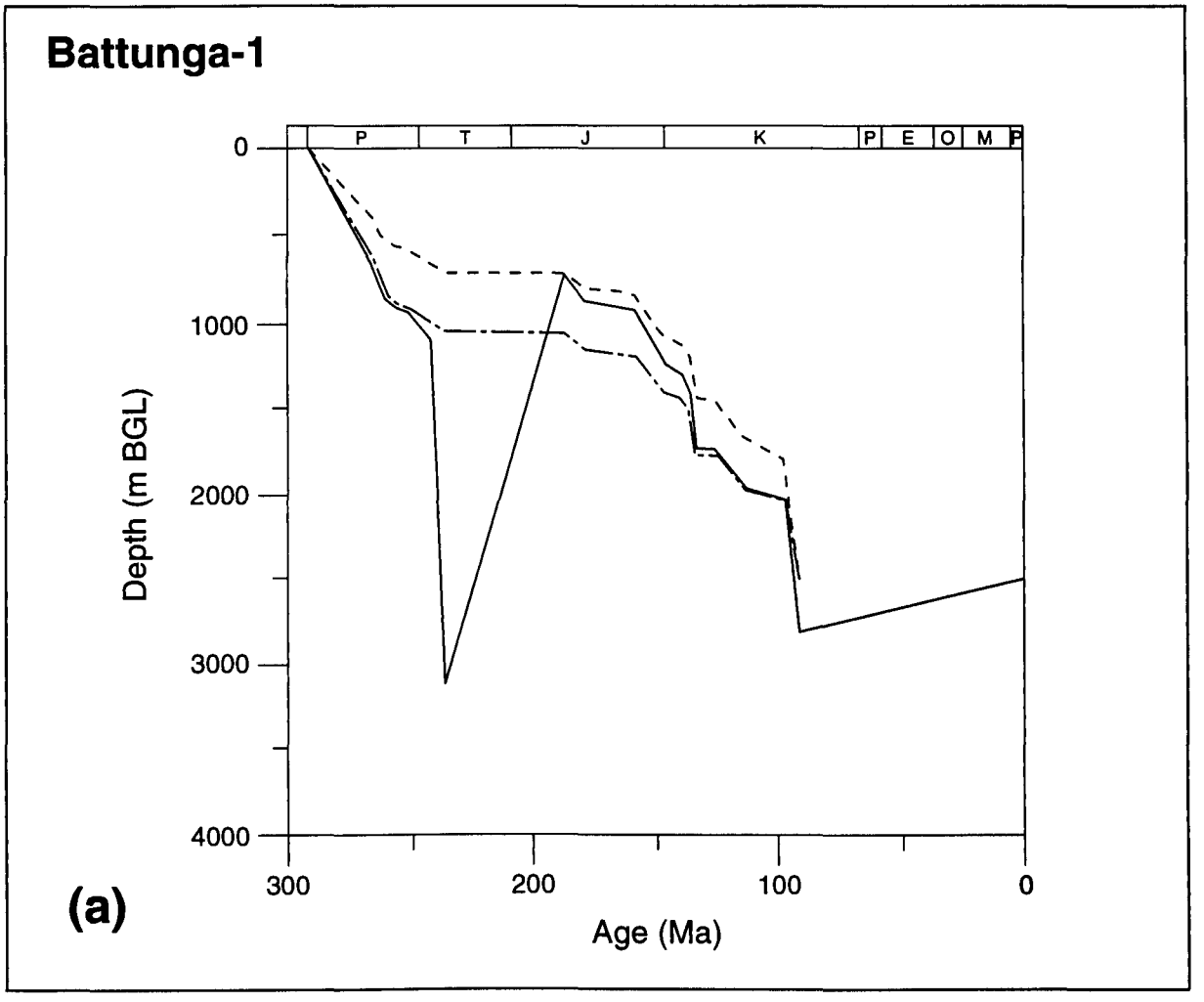

Figure 6.9. Burial/exhumation history for the base Permian in wells (a) Battunga-1, (b) Jackson-1 and (c) Tirrawarra North-1. The dashed line indicates the preserved stratigraphy. The long dash-dotted line indicates preserved stratigraphy corrected for compaction. The black line indicates the decompacted burial/exhumation history of the base Permian allowing for Late Triassic - Early Jurassic and Late Cretaceous - Tertiary exhumation. Note that because the Cooper Basin sequence reached maximum burial-depth in these wells prior to the deposition of the Eromanga sequence, the Cooper Basin sequence acts as compaction basement during Eromanga Basin burial (ie. all Cooper Basin units follow parallel burial histories during Eromanga Basin burial).

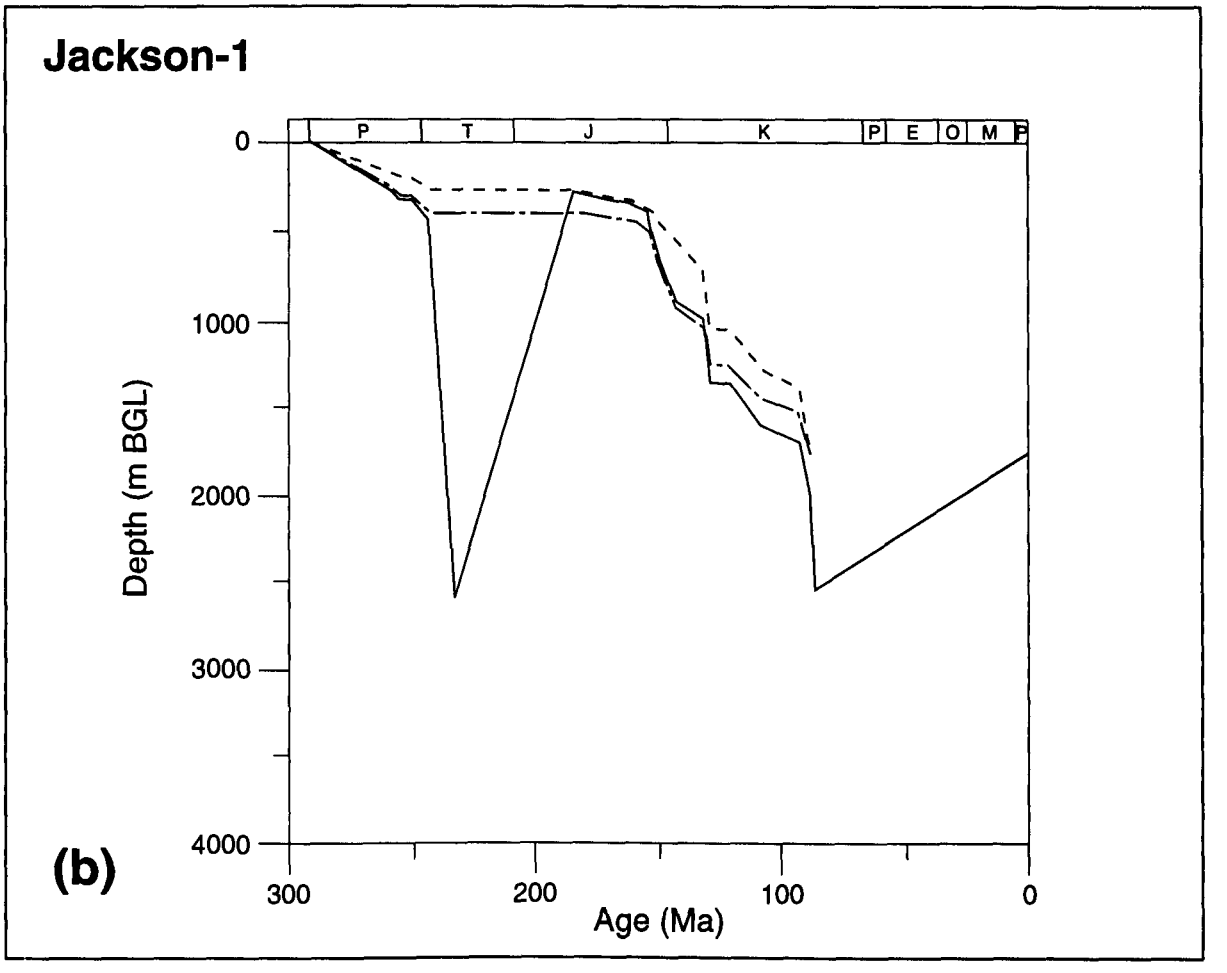

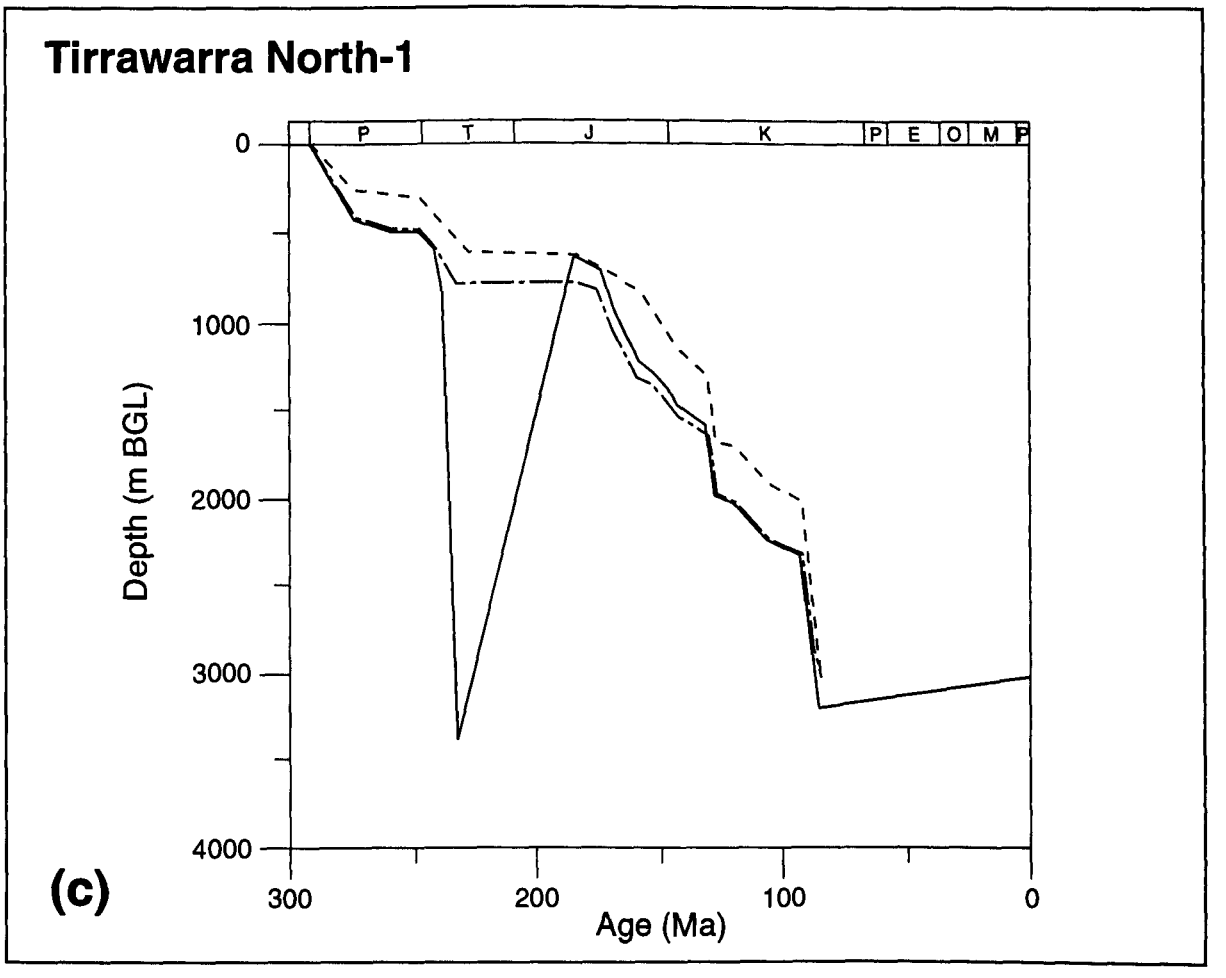

Figure 6.9. Continued.

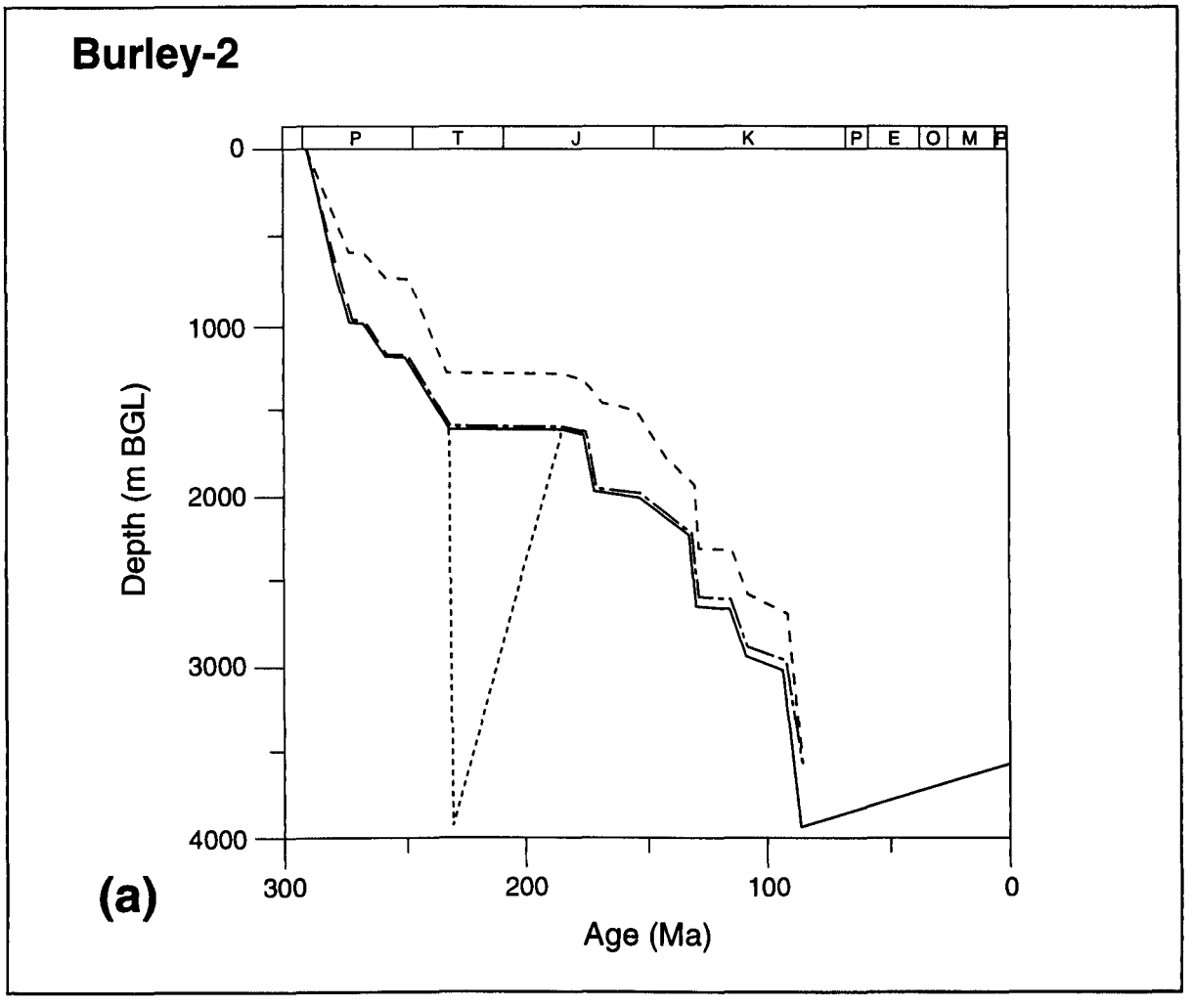

Figure 6.10. Burial/exhumation history (a) for the base Permian in the Burley-2 well and (b) for the base Triassic in the Ullenbury-1 well. The dash line indicates the preserved stratigraphy. The long dash-dotted line indicates preserved stratigraphy corrected for compaction. The black line indicates the decompacted burial/exhumation history of the base Permian in well Burley-2 and of the base Triassic in well Ullenbury-1 allowing for Late Cretaceous - Tertiary exhumation. There is no evidence from the compaction method of Cooper Basin having reached maximum burial-depth before the deposition of the Eromanga Basin in both wells. The dotted line indicates the maximum amount of Late Triassic - Early Jurassic burial/exhumation that could have occured without being witnessed by the compaction method.

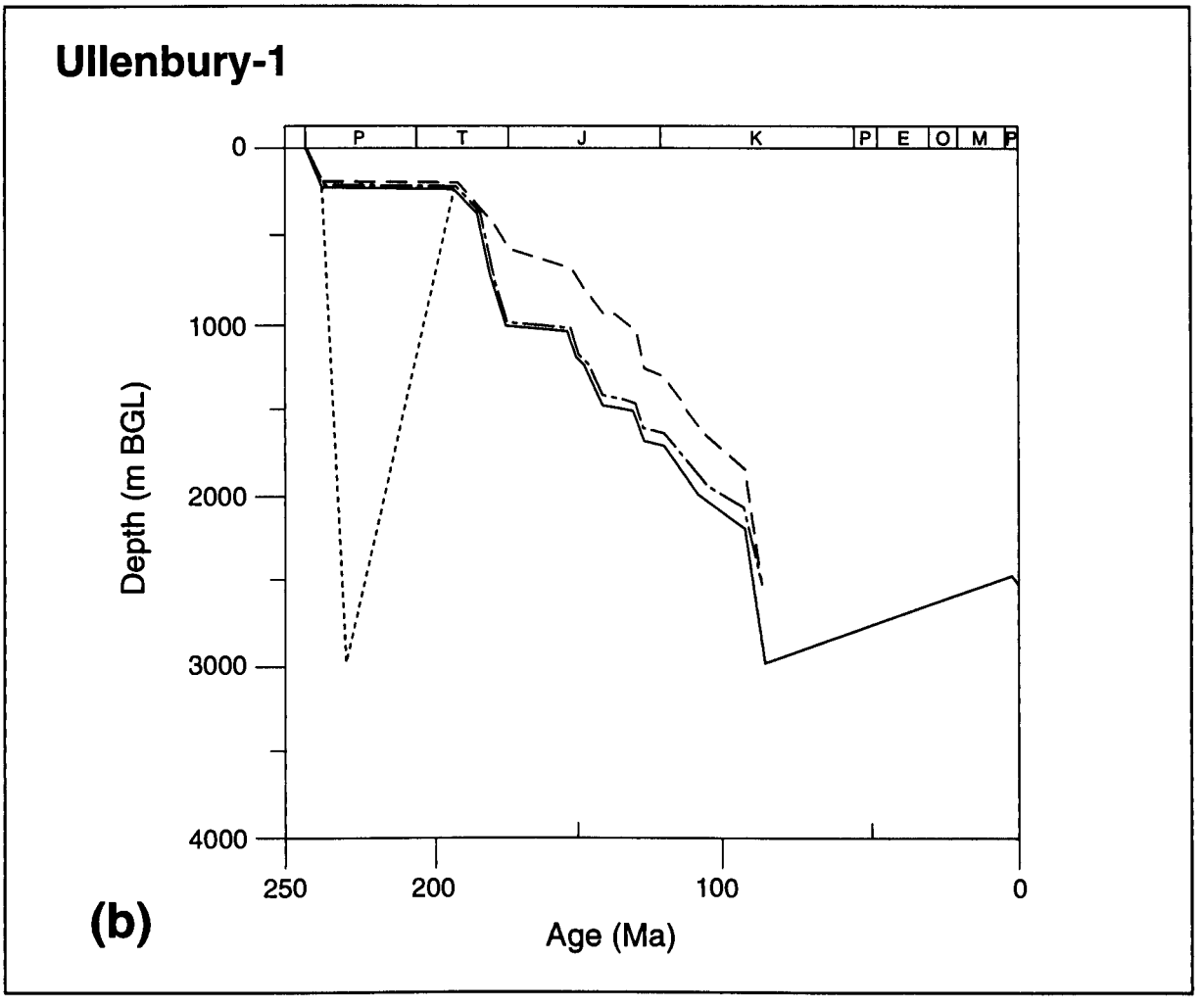

Figure 6.10. Continued.

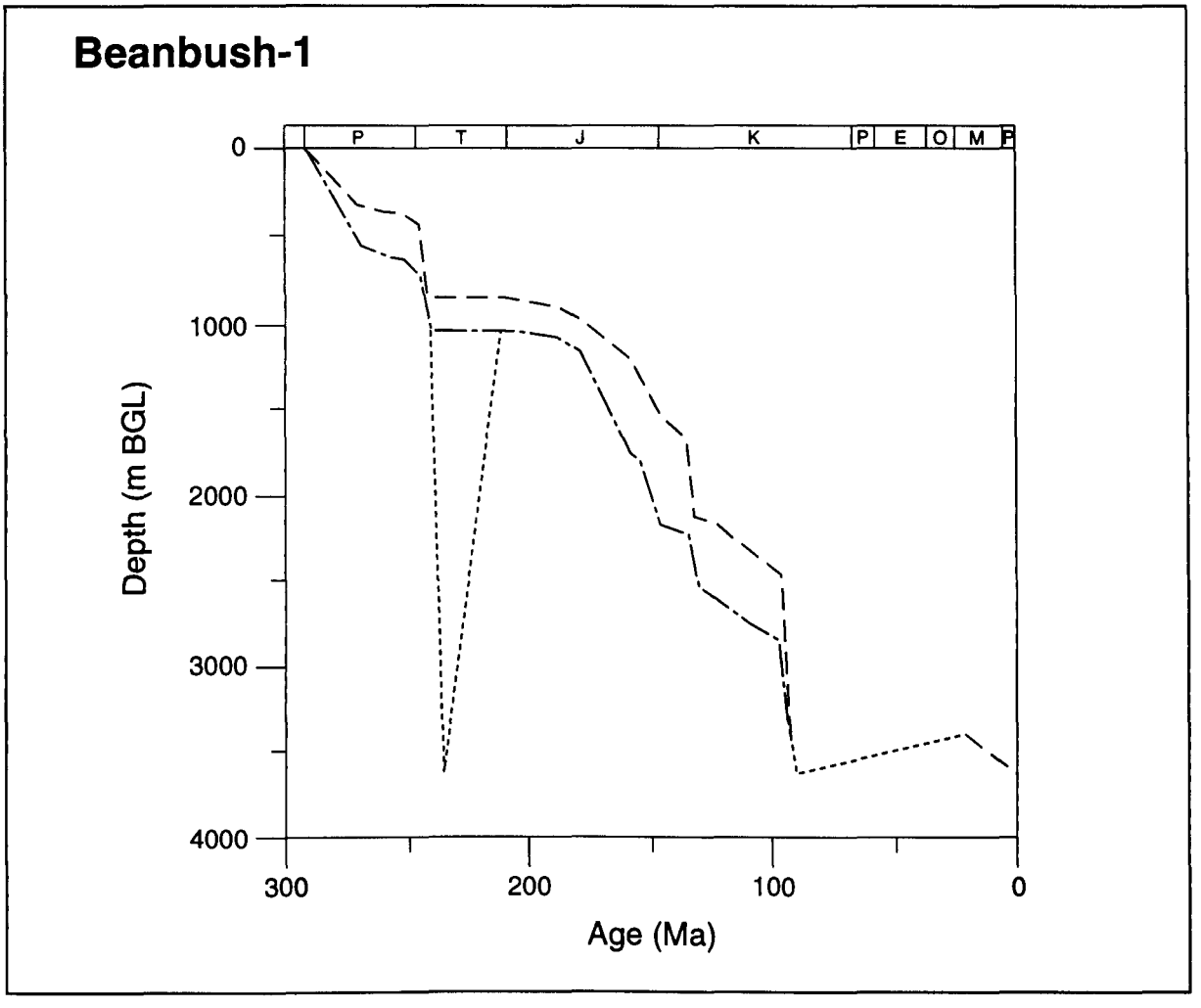

Figure 6.11. Burial/exhumation history for the base Permian in the Beanbush-1 well. The dash line indicates the preserved stratigraphy. The long dash-dotted line indicates preserved stratigraphy corrected for compaction. There is no evidence from the compaction method of Cooper-Eromanga Basins having reached maximum burial-depth before the deposition of the Tertiary sequence in Beanbush-1. The dotted line indicates the maximum amount of Late Triassic - Early Jurassic and Late Cretaceous - Tertiary burial/exhumation that could have occured without being witnessed by the compaction method.

7. STRUCTURAL FRAMEWORK AND TECTONIC MECHANISMS OF UPLIFT AND EROSION

7.1 Introduction

The amount of uplift and erosion in the Cooper-Eromanga Basins has been determined in previous chapters. This chapter investigates the structural expression of and controls on uplift using seismic sections, and considers possible tectonic driving forces for uplift. Seismic reflection profiles show that many of the major structural elements of the Cooper-Eromanga Basins have been reactivated in association with uplift.

7.2 Structural Evolution of the Cooper-Eromanga Basins

Seismic reflection profiles have been interpreted in order to determine the nature of deformation during Late Triassic - Early Jurassic and Late Cretaceous - Tertiary times (ie. during the major periods of uplift), as well as the broader structural history of the basins. The results of the seismic interpretation in the South Australian sector of the Cooper-Eromanga Basins and associated literature review, are summarised below. Insufficient good quality data were available in the Queensland sector of the Cooper-Eromanga Basins to include that area in this structural analysis herein. The locations of the seismic sections discussed in this chapter are shown in Figure 7.1.

The inception of the Cooper Basin structures and associated faults is closely associated with the rejuvenation of the pre-existing basement structures (Wopfner, 1960; Sprigg, 1961; Stuart, 1976; Moore and Pitt, 1984; Gravestock *et al.*, 1995). In the studied area, reactivation of major northeast-southwest direction thrust faults of the underlying Warburton Basin have controlled the structural configuration of the Cooper Basin. The presence of these faults are clearly defined by the strong Cambrian reflectors (Figure 7.2).

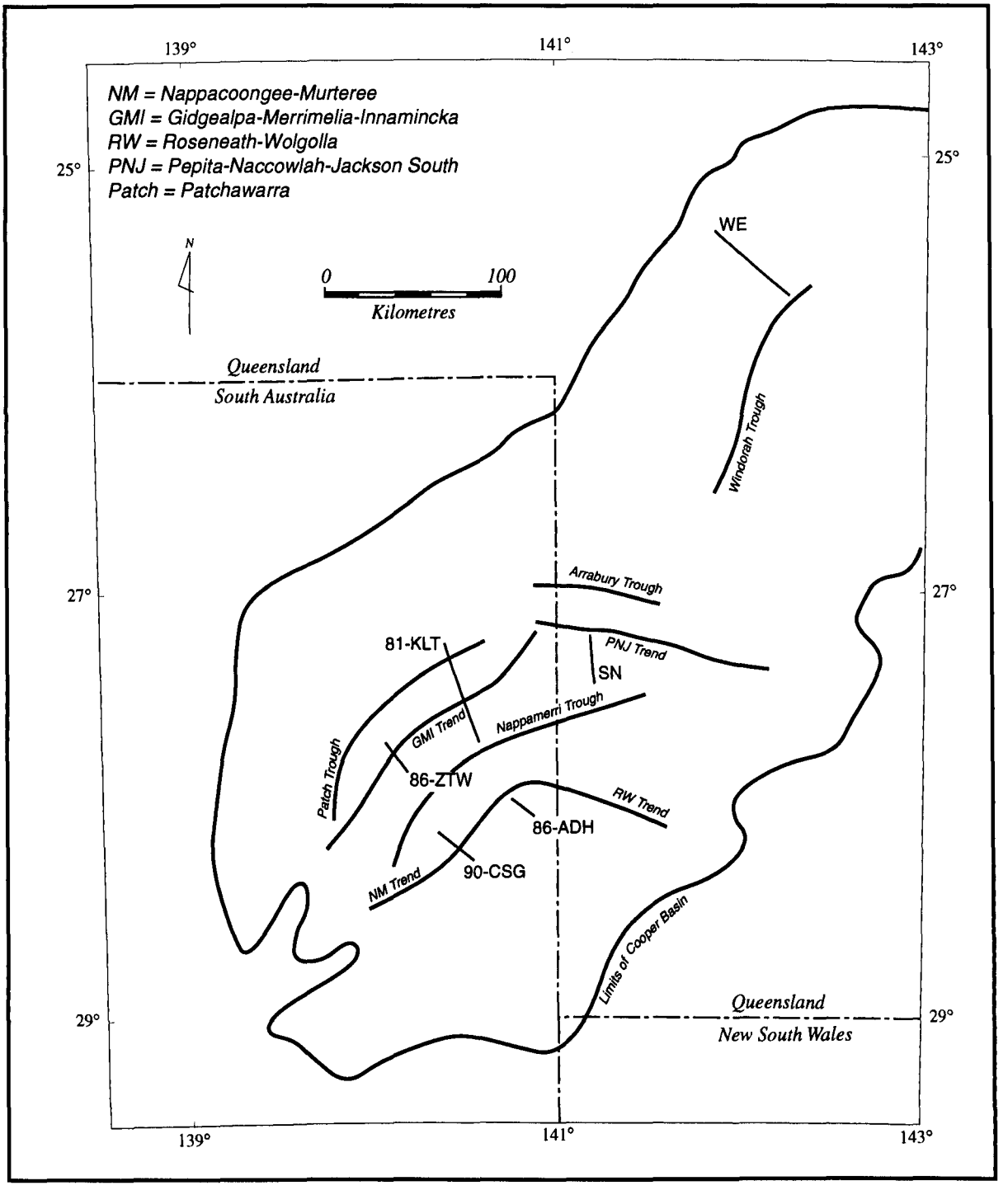

Figure 7.1. Location map of the seismic lines. Major tectonic elements of the Cooper-Eromanga Basins are also shown.

During deposition of the Tirrawarra Sandstone in Late Carboniferous - Early Permian times, the reactivated thrust faults gave rise to major fault escarpments. Between these thrust faults mainly tensional regimes existed, with tilted horsts, grabens and half grabens (Kuang, 1985). At that time, the origination of the northeast trending GMI anticlinal Trend, the most prominent of the basin's thrust fault systems, was reactivated and separated the Patchawarra Trough to

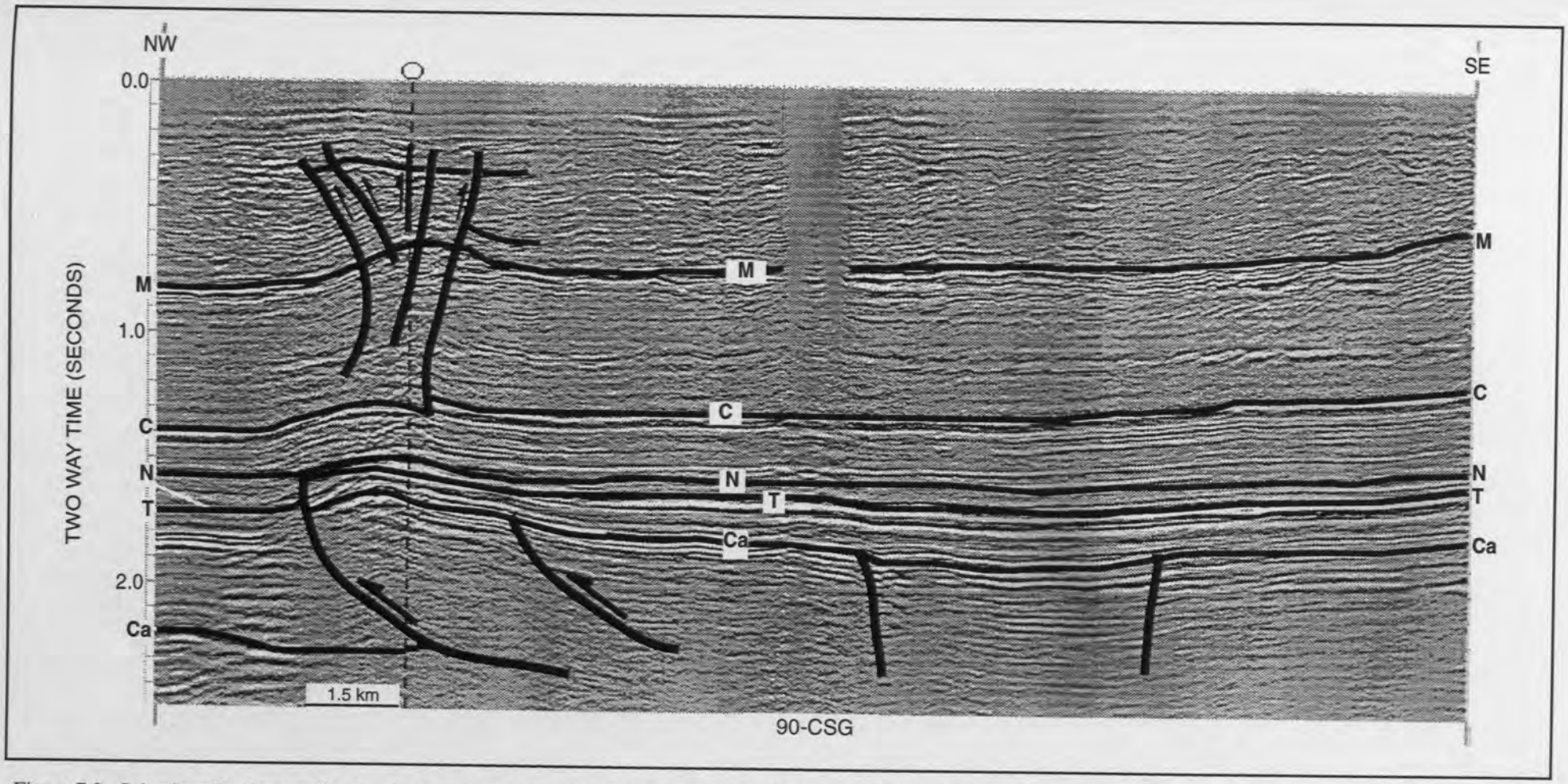

Figure 7.2. Seismic reflection profile showing inverted structure in Cooper-Eromanga Basins units. Thinning and onlapping of the Cooper Basin units on the crest of the inverted sequence is apparent, indicating Late Triassic - Early Jurassic reactivation of Cambrian faults. Strike-slip features cut through the Eromanga Basin units (above the Cadna-owie Formation). Later reactivation is constrained as Late Cretaceous - Tertiary because Nappamerri Group and Cadna-owie Formation reflectors are almost parallel. Ca = Top Cambrian, T = Top Toolachee Formation, N = Top Nappamerri Group, C = Top Cadna-owie Formation and M = Top Mackunda Formation.

Nappamerri Trough to the south. The reactivated GMI thrust faults have a strike-slip component and small wrench related structures are generated (Kuang, 1985) (Figure 7.3). In Queensland, the Jackson-Naccowlah trend originated as a right lateral wrench and effectively acted as a basin hingeline during the deposition of the Cooper Basin (Kuang, 1985).

Facilitated by the reactivated faults, the Cooper Basin developed quite rapidly in Early Permian times. The basin continued to develop by down-warping in a quiescent tectonic phase during the deposition of the Murteree, Epsilon, Roseneath and Daralingie units. After the Daralingie Formation was deposited, an overall compressional stress developed within the Copper Basin and resulted in accentuation of pre-existing faults and crestal unconformities (Kuang, 1985). Following deposition of the Toolachee Formation and the Triassic Nappamerri Group, the whole basin underwent in a severe uplift as discussed in previous chapters. The Cooper Basin's sedimentary strata thin markedly over the structural highs and in some places are absent due to exhumation. Thickening of the Nappamerri Formation on the downthrown side of reverse faults witnesses reactivation of these faults in Middle to Late Triassic times (Figure 7.4). A Late Triassic compressional stress over most of the basin, in response to plate margin behaviour, is postulated to be the cause of the basin wide Nappamerri unconformity. Kuang (1985) related this event to a wrench-induced northeast-southwest compressional stress and Middleton and Hunt (1989) related it to an east-west compressional stress field. Although it is difficult to determine the exact orientation of stresses in Early Triassic - Early Jurassic times, associated deformation was severe (Figures 7.2 - 7.4). The depositional pattern changed and in late Early Jurassic times the Nappamerri and Patchawarra Troughs became the most important depocentres.

Eromanga Basin deposition occurred during a tectonically quiescent period as witnessed by the uniformity of the associated isopachs (Figure 2.8). After deposition of the Jurassic-Cretaceous Eromanga Basin, the region underwent another basin-modifying tectonic episode of a compressional nature. Finlayson *et al.* (1988) suggested a northeast-southwest crustal shortening, whereas Kuang (1985) favoured on east-west direction. The exact timing of the Late Cretaceous - Tertiary unconformity is unclear and has been discussed in Section 6.3.2.

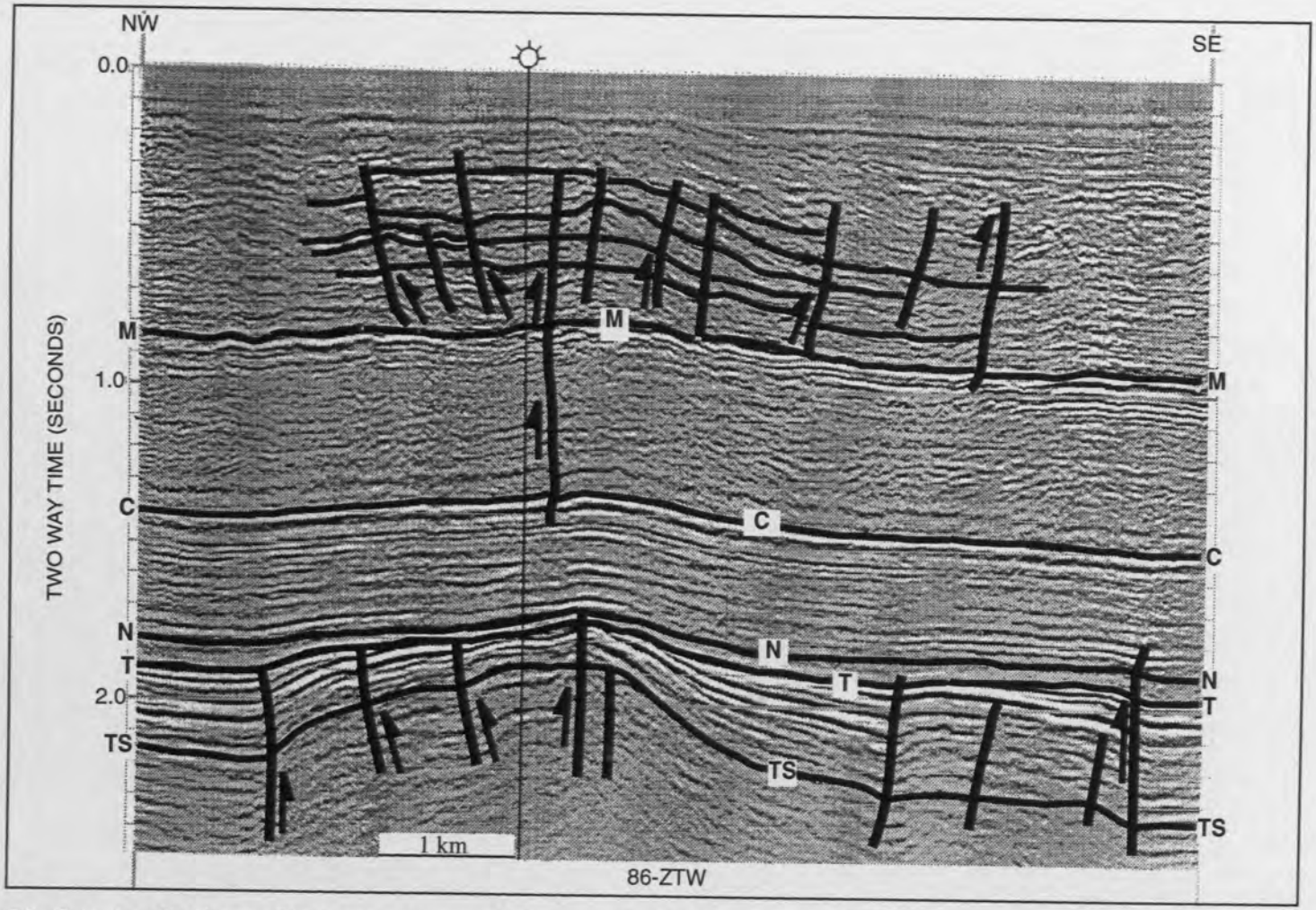

Figure 7.3. Seismic reflection profile showing the wrench character (positive flower) of the GMI Trend in Cooper Basin, which is overprinted by the same structural style in the Eromanga Basin. TS = Top Tirrawarra Sandstone, T = Top Toolachee Formation, N = Top Nappamerri Group, C = Top Cadna-owie Formation and M = Top Mackunda Formation.

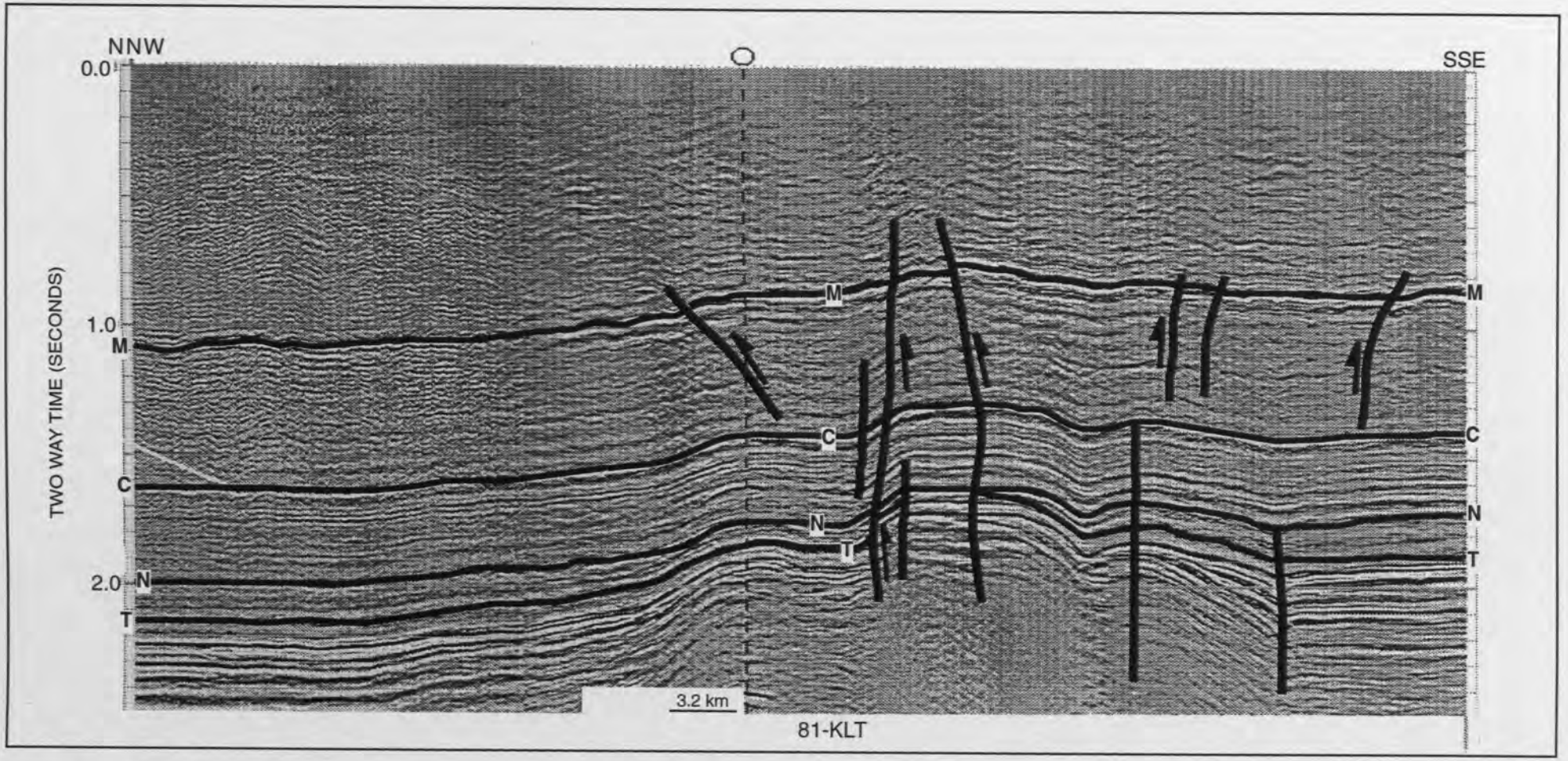

Figure 7.4. Seismic reflection profile showing reactivation of basement structure that continues until Late Cretaceous time. Near vertical faulting and the helicoidal structures are indicative of strike-slip movement. Note truncation of the Nappamerri Group on the crest of the anticline, indicating the exhumational event post-dates its deposition. T = Top Toolachee Formation, N = Top Nappamerri Group, C = Top Cadna-owie Formation and M = Top Mackunda Formation.

Unfortunately the application of seismic interpretation for the exact chronology of the Tertiary structuring is limited due to minimal sediment accumulation since the Late Cretaceous and strong coherent noise events on reflection records in the near surface. On a regional scale, this compressional phase has resulted in the uplift of the entire eastern margin of the Eromanga Basin, its exhumation and subsequent retreat to the west leaving exposed, in surface outcrop, sediments of the underlying easternmost Galilee and Drummond Basins (Shaw, 1991). The exhumation witnessed by the compaction analysis confirm the regional extent of this event (Section 3.10). This new structural phase resulted in rejuvenation of many older structures and associated faults (Figure 7.4) and in several Late Cretaceous - Tertiary unconformities (Section 6.3.2). Seismic profiles indicate extensive reverse and normal faulting, anticlines with variable asymmetry, and monoclines (Figure 7.5). In a broad sense, it is evident from the seismic profiles (Figure 7.2 - 7.5) that the dominant fault style, in the Eromanga Basin, is compressive with strike-slip components. Similar conclusions have been drawn from previous structural studies in this area (eg. Kuang, 1985; Apak, 1993; Finlayson, 1988; Shaw, 1991). Similar structural style in the Queensland Cooper-Eromanga area to South Australia Cooper-Eromanga is illustrated from the seismic profiles of Wecker (1989) the extensive area between Windorah Trough and over the Jackson-Naccowlah trend (Figure 7.6).

In conclusion, the seismic reflection profiles indicate the compressive nature of the structural style associated with the major uplift events in the Cooper-Eromanga Basins. Inversion geometries and reactivated features attest to a period of compression during Late Triassic - Early Jurassic times. In the Eromanga Basin, compressional structural styles associated with Late Cretaceous - Tertiary are apparent. However normal/extensional geometries also occur and these may reflect earlier basin-forming structures and/or complex variation in structural style associated with the Late Cretaceous - Tertiary event. Tertiary deformation has reactivated older structures increasing the amount of structural relief in the Cooper Basin units. Many of the areas of clear local Late Cretaceous - Tertiary structuration (such as the Morney and Curalle Domes) coincide with highs in Late Cretaceous - Tertiary exhumation (Figure 3.14). Exhumation in these areas is clearly controlled by the structuration apparent on reflection seismic data. However, Late Cretaceous - Tertiary exhumation is much more widespread than the relatively localized areas of Tertiary structuration. Regional exhumation must have a more

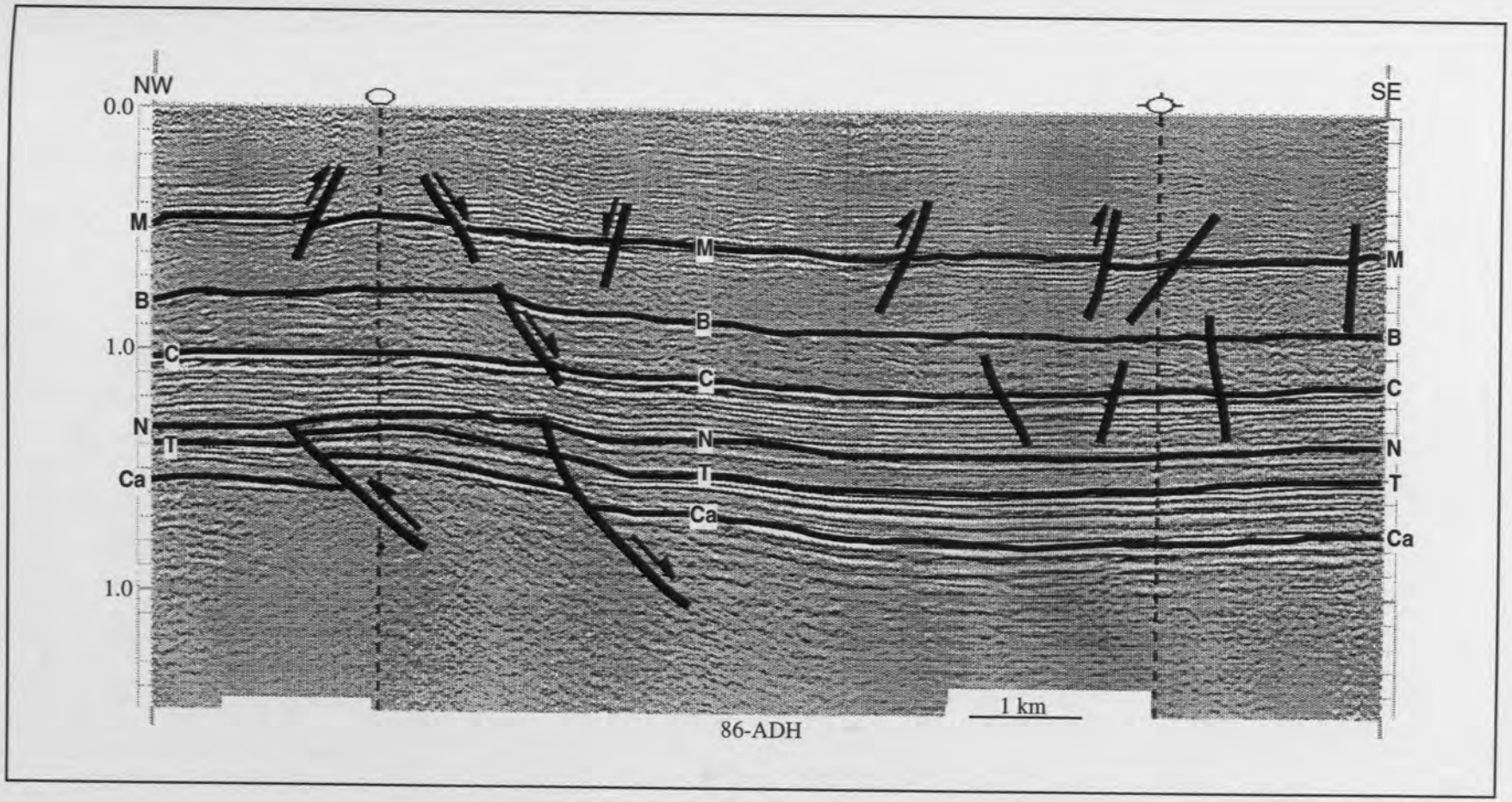

Figure 7.5. Seismic reflection profile showing structures associated with uplift in Cooper Basin and reverse and normal faulting in the Eromanga Basin. The onlapping and thinning of the Nappamerri Group due to Late Triassic - Early Jurassic exhumation is shown. The similarity of tectonic styles and reactivation link between Late Triassic - Early Jurassic and Late Cretaceous - Tertiary exhumation events is noted. Ca = Top Cambrian, T = Top Toolachee Formation, N = Top Nappamerri Group, C = Top Cadna-owie Formation, B = Top Bulldog Shale and M = Top Mackunda Formation.

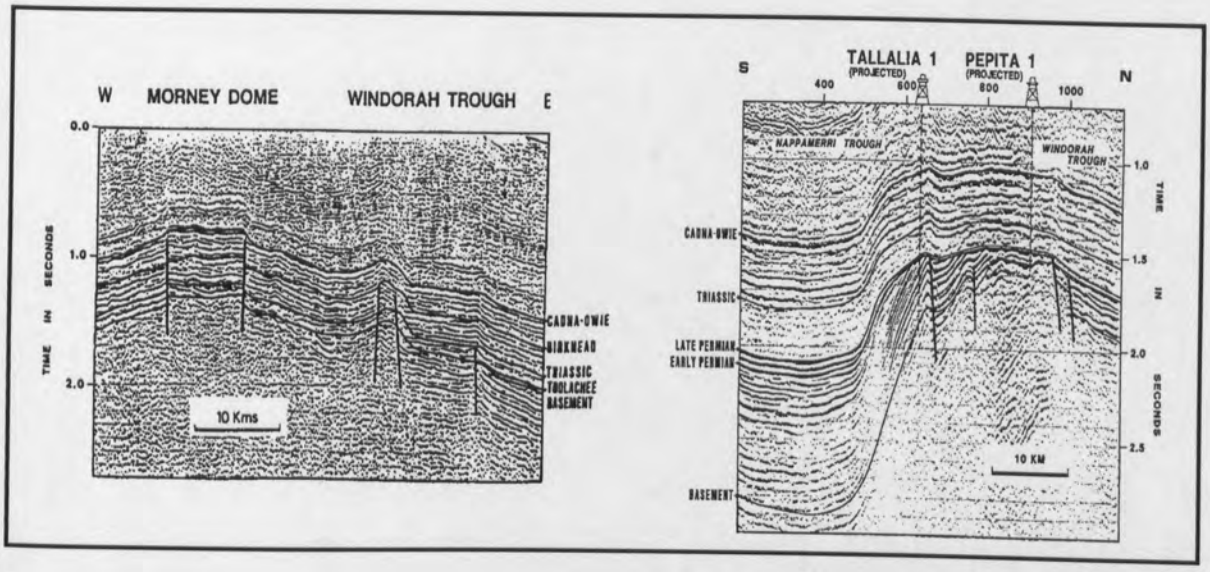

Figure 7.6. Seismic lines over the Morney and Pepita Anticlines, illustrating the similarity of structural style throughout the Eromanga Basin. Line locations are shown in Figure 7.1 (after Wecker, 1989).

deep-rooted origin. Perhaps the key structural observation in the context of regional exhumation is the gentle tilting of the Cooper-Eromanga Basins in Late Cretaceous - Tertiary times. This regional tilting which cannot be seen on the relatively local seismic records presented was mentioned above and by Shaw (1991).

7.3 Cause of Regional Tertiary Uplift

7.3.1 Introduction

In the following sections the distinction between tectonically-driven uplift and exhumation as revealed by the compaction and other methods are discussed and the potential mechanisms which might account for the regional uplift are also addressed.

7.3.2 Tectonic Uplift Versus Exhumation

As mentioned in Section 2.6.3 only surface uplift (as opposed to exhumation) requires work against gravity, and hence it is necessary to prove regional surface uplift to invoke a tectonic

driving force. Because the scale of tectonic processes controlling uplift is at least that of crustal thickness, only uplifts that occur over a region of at least 10^3-10^4 km^2 are of potential tectonic significance (England and Molnar, 1990). Clearly the approximately 130,000 km^2 (13×10^4 km^2) over exhumation occurred in the Cooper-Eromanga Basins, and indeed over a wide area in eastern Australia (1×10^6 km^2) (Gallagher, *et al.* 1994), is potentially significant sensu tectonic processes.

Exhumation exhibits a maxima in areas that show Late Cretaceous - Tertiary structuration (Section 3.6 and Figure 3.14). However there is no evidence of structural reactivation away from basin controling structures, for example in the vicinity of Nappamerri Trough (South Australia and Queensland sector) and Windorah Trough, where exhumation is approximately 0.6 km. Regional exhumation of the type seen in the Cooper-Eromanga Basins induces isostatic crustal rebound to counterbalance the weight of the rocks removed. One must correct for the amplification of any initial uplift caused by this isostatic rebound to calculate the tectonic component (ie. that caused by changes in the density distribution within the lithosphere) of the observed uplift. The tectonic component (U_T) of regional exhumation (E_T) is given by

$$U_T = E_T(1-\rho_s/\rho_m)$$

where ρ_m and ρ_s are mantle (approximately 3.3 gcm^{-3}) and sedimentary rock (approximately 2.3 gcm^{-3}) densities. Given these densities, erosion of an initial surface (tectonic) uplift of 0.18 km would generate the observed, Late Cretaceous - Tertiary, regional exhumation of 0.6 km. The amount of tectonic uplift also needs to be corrected for any change in sedimentary base level, here taken as sea level, which might induce erosion. Assuming no change in elevation (with respect to sea level before and after exhumation), a sea level fall of 0.18 km is required to alone account for the observed regional exhumation (without an additional tectonic component). According to Hallam (1984) and the first-order curve of Haq *et al.* (1987), the major eustatic sea level falls in Late Cretaceous - Tertiary times do not significantly exceed 0.1 km, and although these figures may be in error, Late Cretaceous - Tertiary eustatic sea level falls are unlikely to be as great as 0.18 km. Given that maximum

Late Cretaceous - Tertiary sea level changes of the order of 0.1 km, the tectonic component of regional Late Cretaceous - Tertiary exhumation is 0.18 ± 0.1 km.

7.3.3 Mechanisms of Uplift

The key observations for which any model of Late Cretaceous - Tertiary tectonic evolution of the Cooper-Eromanga Basins and for the eastern Permo-Cretaceous basins (eg. Bowen-Surat and Esk Trough-Moreton Basins) (Figure 7.7), must account are:

- tectonic uplift of structured areas that occurred in association with (upper) crustal compression/thickening;
- regional tectonic uplift (0.18 ± 0.1 km) without associated upper lithospheric compression/thickening; and
- burial prior to uplift, during which the rocks became overcompacted (Section 6.4.3).

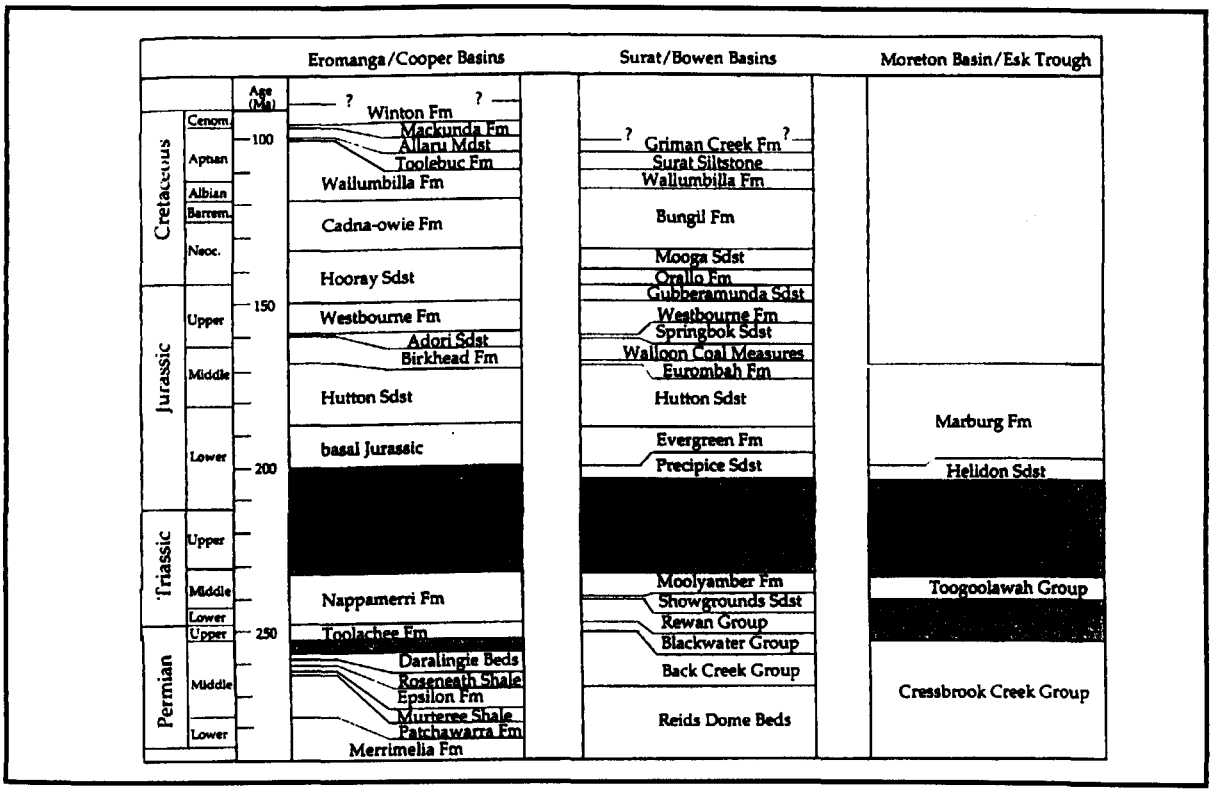

Figure 7.7. Stratigraphic nomenclature of the eastern Australian platform basins. The time scale is after Harland *et al.* (1982) (after Gallagher, 1990).

In areas where there is evidence of crustal compression and hence crustal thickening, tectonic uplift is readily explained, indeed required, by the isostatic response to crustal thickening (Chadwick, 1985; Murrell, 1986). However, the origin of the tectonic force driving the regional component of 0.18 ± 0.1 km uplift, where there is no evidence of crustal compression and thickening, is more enigmatic. The following paragraphs review possible mechanisms that may account for the regional uplift.

Two-layer model of lithospheric compression: A decoupled or two-layer model of lithospheric compression, as proposed by Hillis (1992), may account for the regional uplift of areas where there is no crustal thickening (Figure 7.8). In the model, compression and thickening in the lower lithosphere (possibly equivalent to the mantle part of the lithosphere) is decoupled and laterally displaced from that in the upper crust. Such a two-layer model is directly analogous to the decoupled, two-layer models of lithospheric extension (eg. Hellinger and Sclater, 1983; Kuznir *et al.*, 1987; White and McKenzie, 1989). As proposed by Hillis (1992) pure shear shortening and thickening of the mantle lithosphere is decoupled and may be displaced from crustal thickening which is concentrated along pre-existing zones of crustal weakness (detachments). In areas where Late Cretaceous-Tertiary uplift and erosion occurred without attendant crustal shortening and thickening, such as the Nappamerri, Tenappera and Patchawarra Troughs, it is proposed that the mantle part of lithosphere was compressed and thickened without thickening of the overlying crust (Figure 7.8). Submersion of cold, dense mantle lithosphere into the surrounding asthenosphere would have caused an initial, isostatically-driven subsidence. Subsequent warming of the lithosphere would have caused uplift. Hence thickening of the mantle lithosphere without thickening of the overlying crust can account for the initial subsidence then uplift of uninverted, platform areas inferred from the compaction method (Figure 7.8). The stresses responsible for two-layer lithopsheric compression are considered to have resulted from the onset of drift along the southern margin at 90-100 Ma (Cande and Mutter, 1982; Veevers, 1986). Another possible source of stressses can be related to the opening of the Coral Sea (Crook and Belbin, 1978) which led to the development of the Great Escarpment and the uplift of the Eastern Highlands (Ollier, 1982; Figure 7.9) and has been dated as beginning in the Early Tertiary 50-60 My ago (Jones and Veevers, 1982).

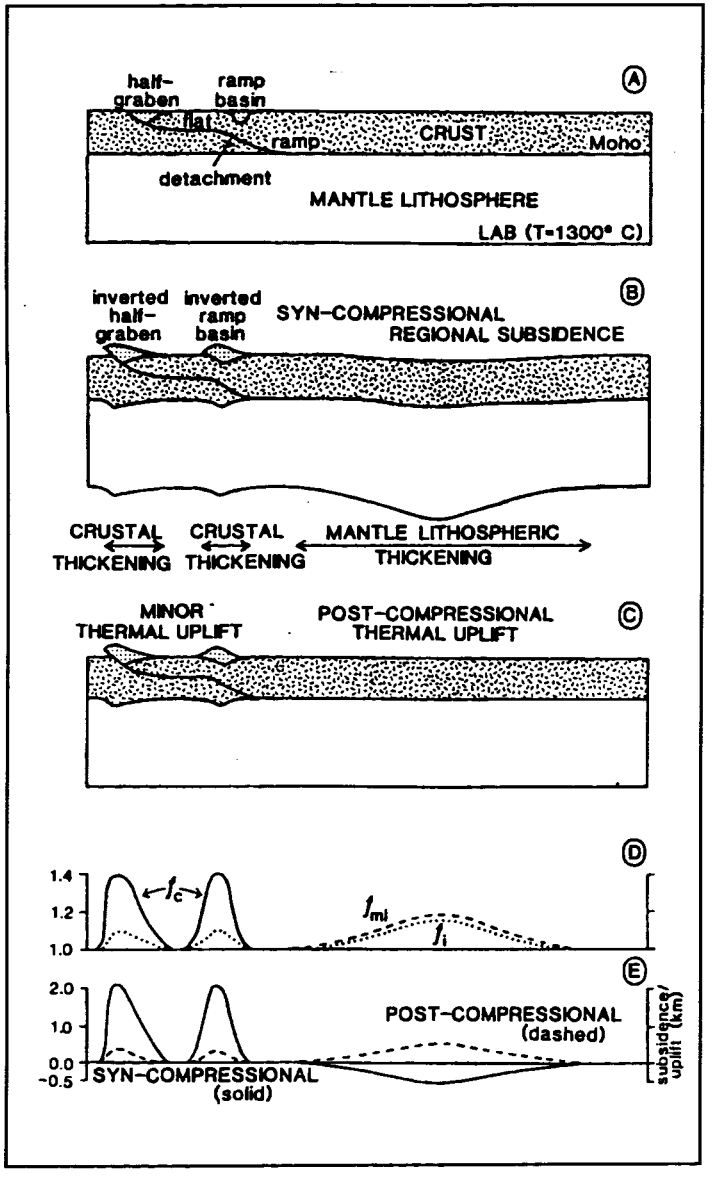

Figure 7.8. Decoupled, two-layer lithospheric compression and thickening. (A) Cooper-Eromanga Troughs such as the Nappamerri, Patchawarra and Tenappera formed above ramps in a major during extension. (B) Compression reactivates the major fault, inverting the Cooper-Eromanga depocentres. Mantle lithospheric thickening is decoupled and laterally displaced from that in the crust and causes initial subsidence: the subsidence phase prior to uplift. (C) The lithosphere thermally re-equilibrates to its pre-compressional level, uplifting the region of mantle lithospheric thickening: the regional uplift phase. (D) Balanced distribution of lithospheric thickening similar to that illustrated schematically in (A)-(C). The crustal thickening factor (f_c-solid line) is the ratio of thickness of the deformed crust to its initial thickness (Sandiford and Powell, 1990). Similarly, f_{ml} is mantle lithospheric thickening (dashed) and f_l is the whole lithospheric thickening (dotted). (E) Surface elevation changes associated with the distribution of lithospheric thickening shown in (D), assuming local isostasy and no surface loading (Sandiford and Powell, 1990). Syn-compressional elevation changes are shown by the solid lines, and post-compressional, thermal uplift is shown by the dashed line (after Hillis, 1992).

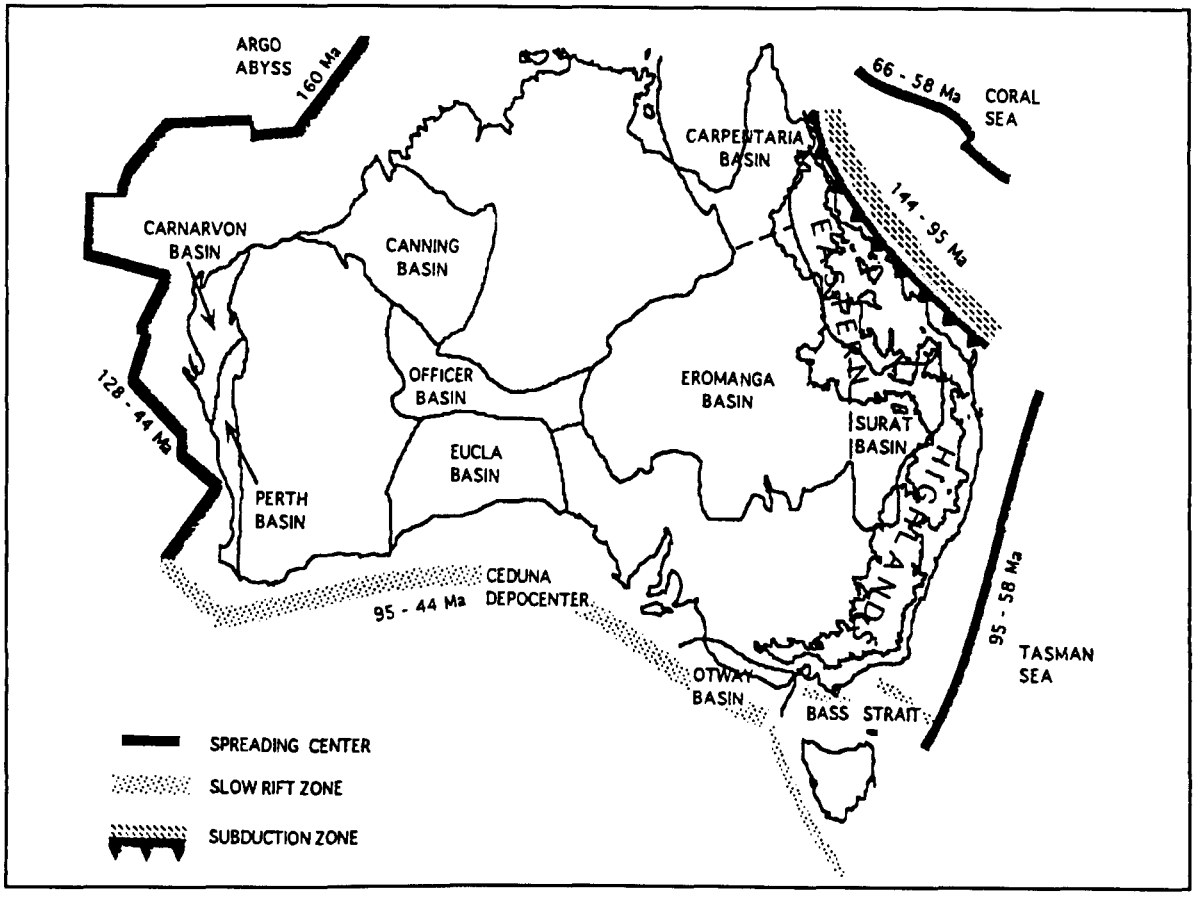

Figure 7.9. Map of Australia showing the locations of major Mesozoic depocentres, the positions of rift zones and convergent margins active since the Mesozoic, and age interval over which they were active (after Russell and Gurnis, 1994).

Continental tilting: Mitrovica *et al.* (1989) proposed a model which predicts epeirogenic motion of cratonic regions as a direct result of viscous flow induced by a cold subducting lithospheric slab, and discussed the application of this model to the western interior of North America. The basis of this model is that the cold slab induces flow which tilts the overlying platform down towards the subduction zone (Figure 7.10). Subsidence may occur over distances of more than 1000 km from the trench, the horizontal scale depending primarily on the dip of the subducting slab. The temperature contrast between the slab and the mantle, and the isostatic response of the overlying lithosphere are important in determining the vertical deflection of the overlying plate. Furthermore, these models predict uplift when subduction ceases and differential subsidence and uplift can occur contemporaneously as the dip of the subducting slab varies. This mechanism may be a plausible explanation for the widespread subsidence and uplift of eastern Australia during the Mesozoic and Cenozoic (Gallagher, *et al.* 1994). The cessation of plate convergence on the eastern margin and the subsequent opening

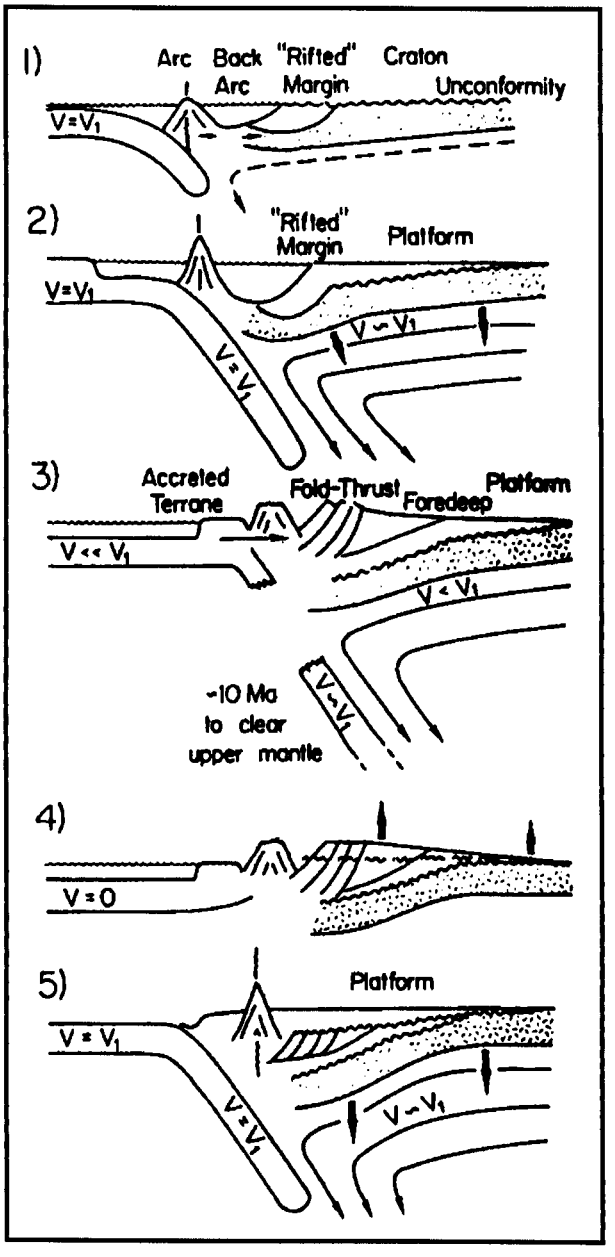

Figure 7.10. Schematic diagram illustrating the proposed mechanism for large horizontal scale platform subsidence and uplift caused by subduction. (1) Subduction is initiated. The coupled sublithospheric flow produces platform subsidence and sedimentation in the interior of the craton. (2) The tilt of the basement continues for as long as the convergence remains active. (3) Convergence is slowed, or stopped entirely, due to the accretion of terrane, and, as the subducted limb breaks off and continues to descend, the sublithospheric flow is reduced. (4) With the removal of the driving force the platform begins to rebound, creating an unconformity and an exhumational phase. (5) It may be possible, depending on the physical situation, that subduction could be initiated a second time, and as with the first cycle, the consequent submergence would be evident in the sedimentary record (after Mitrovica *et al.*, 1989).

of the Tasman Sea would have been accompanied by a major change in both the stress and thermal regimes of the region, and may have led to regional uplift of the eastern margin as the deeper convection pattern adjusted. This model can be invoked as a possible explanation of the uplift in the Eromanga Basin which is some 1000 km from the former subduction zone at the eastern margin (Gallagher, *et al.* 1994; Russell and Gurnis, 1994). However, the model predicts a stratigraphic sequence that thins away from the subduction zone. This is in contrast to the Eromanga Basin where the thickest sediments were deposited in the central and western areas and the strata generally dip towards this region from all directions.

Downwelling plumes: Middleton (1989) developed a model which relates the early Palaeozoic evolution of the Canning Basin, Western Australia, to mantle convection by examining the effect of downwelling plumes on surface elevation. Middleton (1989) showed that a descending mantle plume can produce a basin by rapid subsidence, due to the topographic low associated with the plume, followed by slow subsidence from cooling of the lithosphere. Subsidence is followed by a period of uplift and erosion. Uplift occurs when the convective regime reverts from a descending plume to either horizontal or an upward plume, because the downward pull of the plume vanishes and thermal recovery (heating) of the lithosphere occurs. Stresses induced by the mechanism are compressive, but are less than the yield strength of crustal rocks. Therefore, major normal faults are not common. This model provides an explanation for circular intracratonic basins with little evidence of normal faulting or widespread thermal activity. However, without appealing to a series of downwelling plumes, it seems unlikely that the model alone is an appropriate mechanism for the extensive subsidence and exhumation in central-eastern Australia. Furthermore, uplift due to thermal stabilization after the removal of the plume would have thermally relaxed by recent times and hence no overcompaction would currently be observed.

Magmatic underplating: Brodie and White (1995) have proposed that magmatic underplating could have generated regional Tertiary uplift offshore northwest of Britain. Magmatic underplating at the base of the crust by igneous material produced by adiabatic decompression of mantle material will generate uplift that unlike dynamic thermal uplift, does not subsequently collapse (White and McKenzie, 1989; Brodie and White, 1995). Wellman (1987) believed that the coincidence of volcanism and uplift supports an underplating mechanism in the area of eastern highlands, in mid-Cretaceous and Cainozoic times, due to the opening of the Tasman Sea. Shaw (1990) agreed that heat flow and volcanism increased during the opening of the Tasman Sea and uplift associated with this event resulted in erosion of 1-2 km of sediments from the eastern flank of the Clarence-Moreton Basin. However, the uplift associated with this event could have extended only at 100 km landward (Shaw, 1990) and hence the regional uplift evidenced in eastern Australia and further west in the study area must have a different cause. In addition, the compressive style of the structural deformation mentioned in Section

7.2, and the absence of significant volcanism in the study area, suggest that magmatic underplating is not a major mechanism of uplift.

Intraplate stresses: There is evidence of intraplate deformation throughout the Australian continent during the Cainozoic associated with the contact of northern Australian crust with the Indonesian Archipelago (Etheridge *et al.*, 1991). However the timing of these events and the transmission of stresses post-dates Eocence and hence precedes the likely main phases of Late Cretaceous - Tertiary in age uplift (Section 6.3.2). The opening of the Tasman Sea and the Coral Seas, as mentioned previously, can lead to stresses transmission in the interior of the continent. However, stresses are only likely to generate up to 100 m of uplift (Cloetingh *et al.*, 1985) and furthermore the Mesozoic depocentre of the Eromanga Basin would be expected to subside in response to compression, and its flanks would be expected to be uplifted (Cloetingh *et al.*, 1985). Such a pattern does not account for the observed regional uplift of the area.

The above discussion of uplift mechanisms has been largely qualitative and there is clearly a need for quantitative analysis which is beyond the scope of this thesis. Quantitative tectonic modelling of Late Cretaceous - Tertiary regional uplift requires a detailed knowledge of the magnitude and timing of tectonic uplift throughout the whole (including the eastern part) Eromanga Basin. While a number of mechanisms may have contributed to regional Late Cretaceous - Tertiary exhumation, the two-layer lithospheric compression model is considered by the author as the most complete explanation of uplift of the areas subject to compression and crustal thickening and of regional uplift and the preceding subsidence of areas not subject to any apparent Late Cretaceous - Tertiary structuration.

8. IMPLICATIONS OF EXHUMATION IN THE COOPER-EROMANGA BASINS FOR HYDROCARBON EXPLORATION

8.1 Introduction

The quantification of exhumation has critical implications for exploration that are largely related to the burial/exhumation history of the source and reservoir rocks. The burial/exhumation history of the Cooper-Eromanga Basins has already been discussed (Chapter 6), and in this chapter the specific implications of burial/exhumation for source rock maturity, depth-conversion and reservoir porosity are discussed.

8.2 Influence of Exhumation on Source Rock Maturity

Source rock maturity is a function of temperature and time (eg. Sweeney and Burnham, 1990; Suzuki *et al.*, 1993). The source rock thermal history required to model observed maturity is generally determined from burial history and palaeogeothermal gradients or palaeo-heatflow/thermal conductivity (eg. Falvey and Deighton, 1982; Bray *et al.*, 1992). To asses the influence of Late Triassic - Early Jurassic and Late Cretaceous - Tertiary exhumation on source rock maturity, vitrinite reflectance levels have been modelled in two wells where Late Triassic - Early Jurassic exhumation was of greater magnitude than subsequent burial during development of the Eromanga Basin, namely Jackson-1 and Tirrawarra North-1 (Section 6.4.3). Vitrinite reflectance has also been modelled in Burley-2, where Late Triassic - Early Jurassic exhumation was of lesser magnitude than subsequent burial during development of the Eromanga Basin. The palaeogeothermal gradients used in modelling were those of *Geothermal History C* (Section 4.3 and Table 4.1). For each of the wells, source rock maturity has been modelled (in terms of vitrinite reflectance) for the following three scenarios:

- without considering exhumation;
- considering exhumation only in Late Cretaceous - Tertiary times and
- considering exhumation in Late Triassic - Early Jurassic and Late Cretaceous - Tertiary times (Figure 8.1 - 8.3).

Modelling was undertaken using the Platte River Associates (1995) BasinMod™ software in which vitrinite reflectance is calculated using the kinetics of Sweeney and Burnham (1990).

The major potential source rocks for liquid hydrocarbon generation are the Patchawarra and Toolachee Formations in the Cooper Basin (Jenkins, 1989), and the basal Jurassic (Hawkins *et al.*, 1989), Birkhead Formation (Jenkins, 1989) and Murta Member (Michaelsen and McKirdy, 1989) in the Eromanga Basin.

In the Jackson-1 well, without allowance for burial/exhumation, the Patchawarra Formation reaches a vitrinite reflectance level of 0.5%R_o, equivalent to early maturity for oil generation during Late Cretaceous times and the rest of the source rocks during Tertiary times. Without allowance for exhumation no source rocks reach mid maturity (0.7 - 1.0%R_o) (Figure 8.1a). However, with the incorporation of Late Cretaceous - Tertiary exhumation, all source rocks reach a vitrinite reflectance of 0.5%R_o, during Late Cretaceous times and the Patchawarra Formation reaches a vitrinite reflectance of 0.7%R_o, equivalent to mid maturity for oil generation during Tertiary times (Figure 8.1b). When maturation modelling incorporates Late Triassic - Early Jurassic exhumation the Patchawarra and Toolachee Formations pass through early oil generation during Mid Triassic times and the Patchawarra Formation reaches mid mature during Late Triassic times (Figure 8.1c). Considering Late Triassic - Early Jurassic exhumation, the Toolachee Formation reaches mid mature oil generation at around the Late Cretaceous/Tertiary boundary. Robinson (1982) quoted observed reflectances in the Jackson-1 well, which include 0.56% at 1.1 km in the Murta Member, 0.58% at 1.4 km in the Birkhead Formation, 0.74% at 1.5 km in the Toolachee Formation and 0.87% at 1.6 km in the Patchawarra Formation. Hence, the only maturation modelling that is consistent with the observed reflectances in the Jackson-1 well is that which

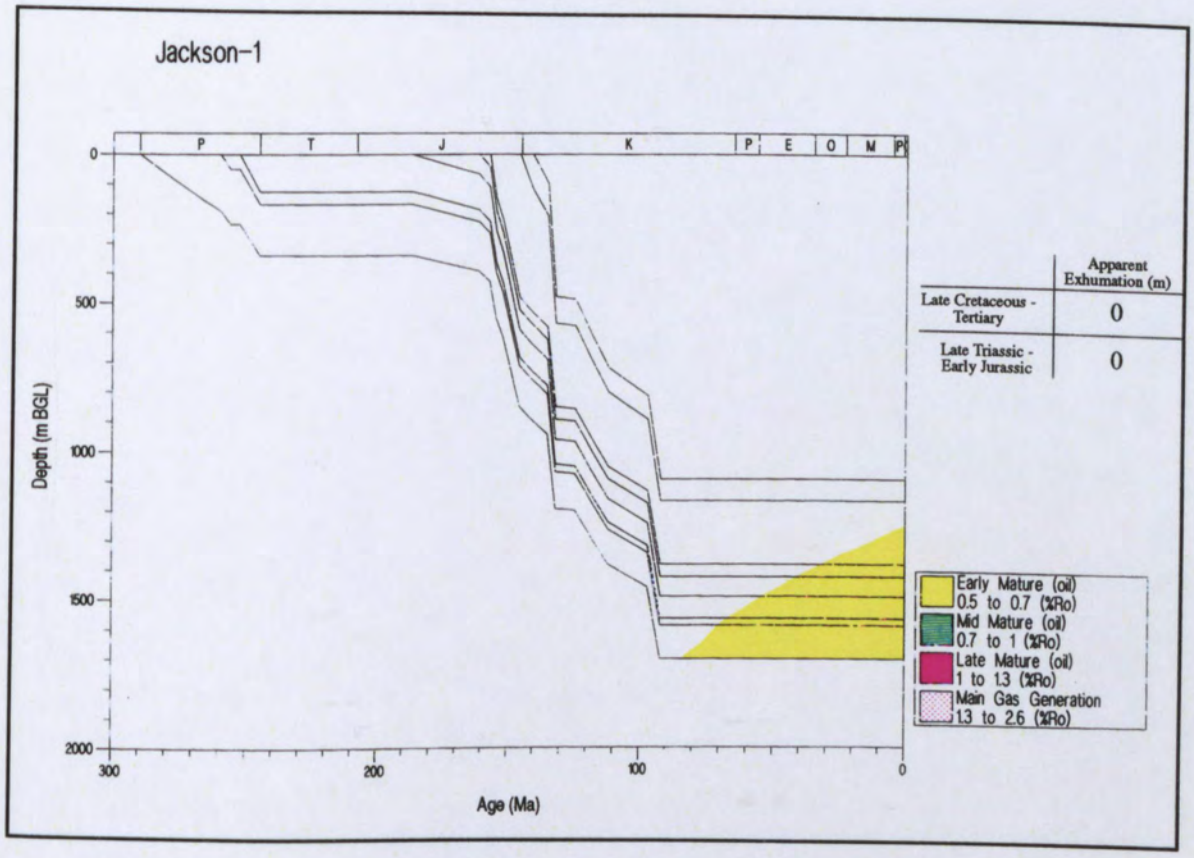

(a)

Figure 8.1. Burial/exhumation and maturity histories for the Jackson-1 well (a) without allowance for exhumation, (b) with allowance for Late Cretaceous - Tertiary exhumation and (c) with allowance for Late Cretaceous - Tertiary and Late Triassic - Early Jurassic exhumation. All burial/exhumation histories were decompacted using the methodology of Sclater and Christie (1980) with the decompaction parameters defined in Section 6.4.2. Ages were taken from the operators' composite logs and geochronologically calibrated after the time scale of Harland *et al.* (1989). The apparent exhumation values (in metres) used in each case are shown. Incorporation of Late Cretaceous - Tertiary and Late Cretaceous - Early Jurassic exhumation increases significantly the level of thermal maturity of a given stratigraphic level.

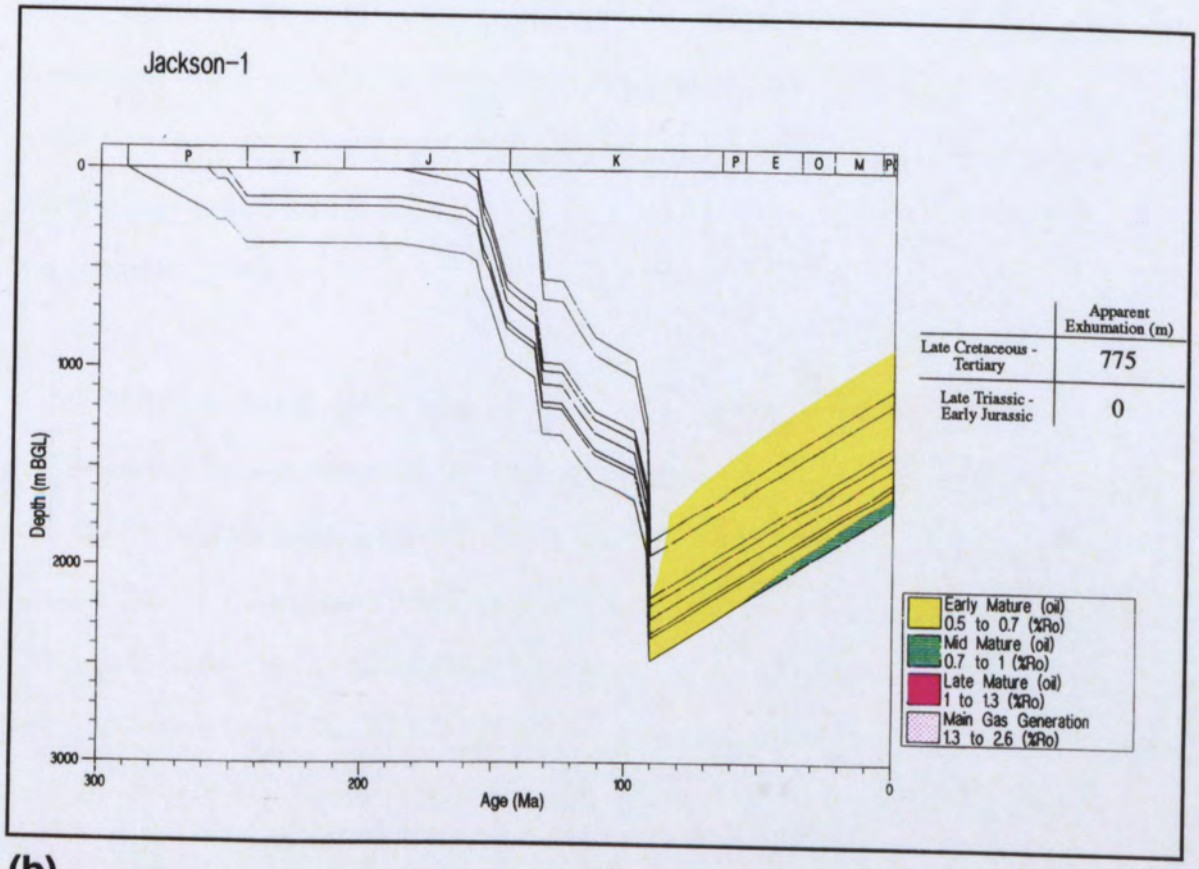

(b)

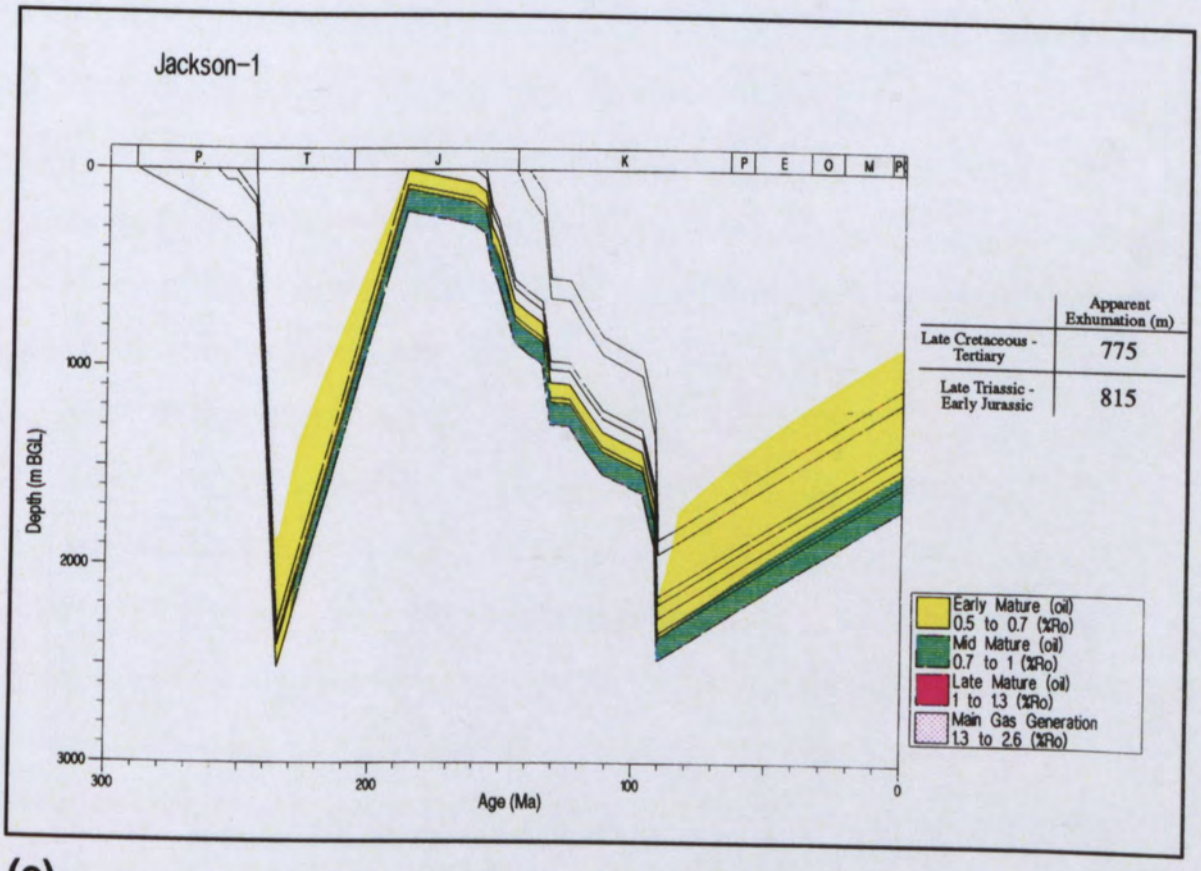

(c)

Figure 8.1. Continued.

incorporates Late Triassic - Early Jurassic and Late Cretaceous - Tertiary exhumation. More broadly, incorporating Late Triassic - Early Jurassic and Late Cretaceous - Tertiary exhumation in maturation modelling is consistent with the sourcing of the oil fields of the Jackson-Naccowlah area, in southwestern Queensland, from the above source rocks (Vincent *et al.*, 1985).

In the Tirrawarra North-1 well, without allowance for burial/exhumation, the Patchawarra and Toolachee Formations reach a vitrinite reflectance level of 0.5%R_o, equivalent to early maturity for oil generation during Early Cretaceous times. Without allowance for exhumation, the Patchawarra and Toolachee Formations reach mid maturity (0.7 - 1%R_o) during Late Cretaceous and Early Tertiary times, respectively. The basal Jurassic and Birkhead Formation reach early oil generation during Late Cretaceous time and the Murta Member during Early Tertiary times. Near the end of Tertiary times, the basal Jurassic reaches the stage of mid maturity (Figure 8.2a). This maturity history, without considering exhumation, is consistent with the sourcing of the oil fields of the Tirrawarra area, the largest oil field in Australia (Yew and Mills, 1989), from the above source rocks. The incorporation of Late Cretaceous - Tertiary exhumation, which is less than 200 m, does not cause any significant difference to the maturity history (Figure 8.2b). However, maturation modelling that incorporates Late Triassic - Early Jurassic exhumation results in Cooper Basin source rocks reaching early and mid maturity during Mid - Late Triassic times (Figure 8.2c). Mielnik (1984) quoted observed reflectances in the Tirrawarra North-1 well, of 0.5% at 1.8 km in the Murta Member, 0.56% at 2.1 km in the Birkhead Formation, 0.77% at 2.4 km in the basal Jurassic, and 0.88% at 2.7 km in the Toolachee Formation. These values are broadly consistent with all three maturity histories presented in Figure 8.2. However, Mielnik (1984) quoted observed reflectances of more than 1% at depths greater than 2.8 km in the Patchawarra Formation which is not consistent with the maturation modelling presented here since late mature oil generation is not predicted even with the incorporation of Late Triassic - Early Jurassic exhumation. This suggests that the palaeogeothermal gradients and/or the exhumation values used in modelling should be higher (Section 4.4).

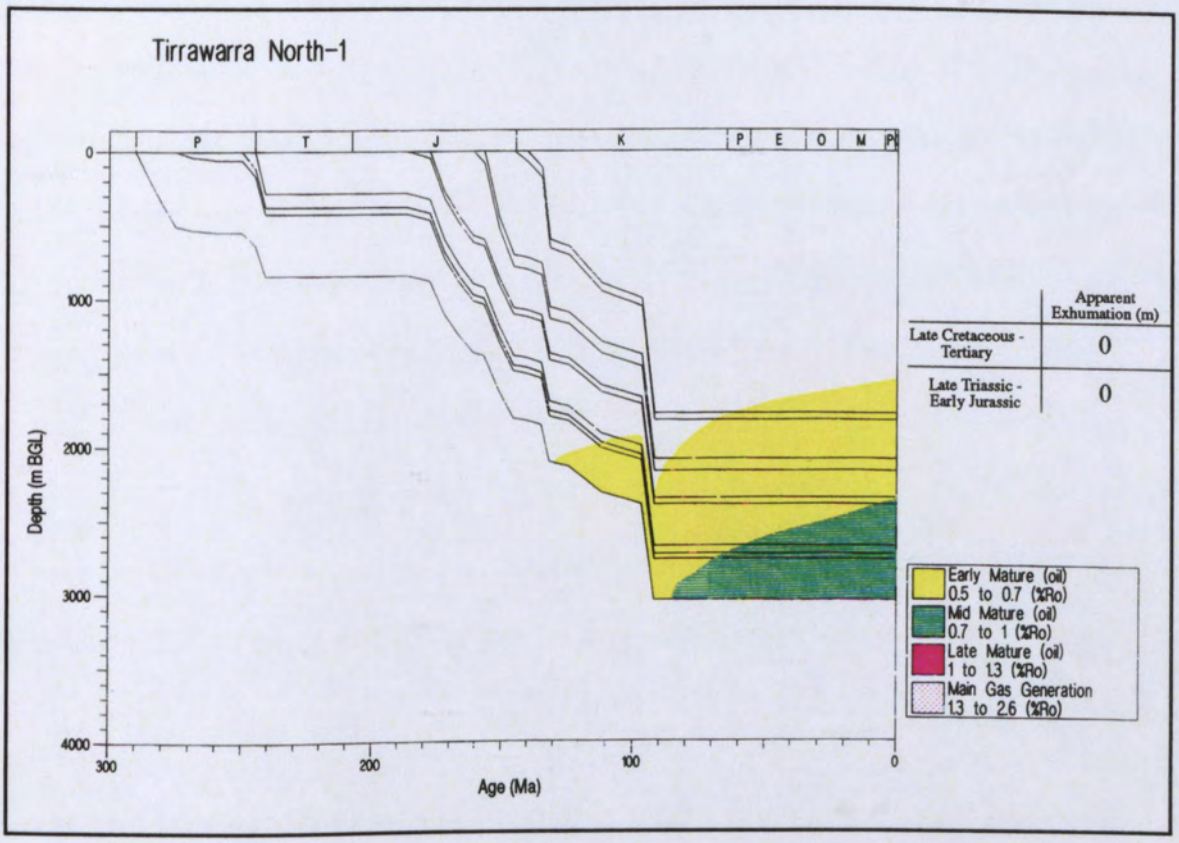

(a)

Figure 8.2. Burial/exhumation and maturity histories for the Tirrawarra North-1 well (a) without allowance for exhumation, (b) with allowance for Late Cretaceous - Tertiary exhumation and (c) with allowance for Late Cretaceous - Tertiary and Late Triassic - Early Jurassic exhumation. All burial/exhumation histories were decompacted using the methodology of Sclater and Christie (1980) with the decompaction parameters defined in Section 6.4.2. Ages were taken from the operators' composite logs and geochronologically calibrated after the time scale of Harland *et al.* (1989). The apparent exhumation values (in metres) used in each case are shown.

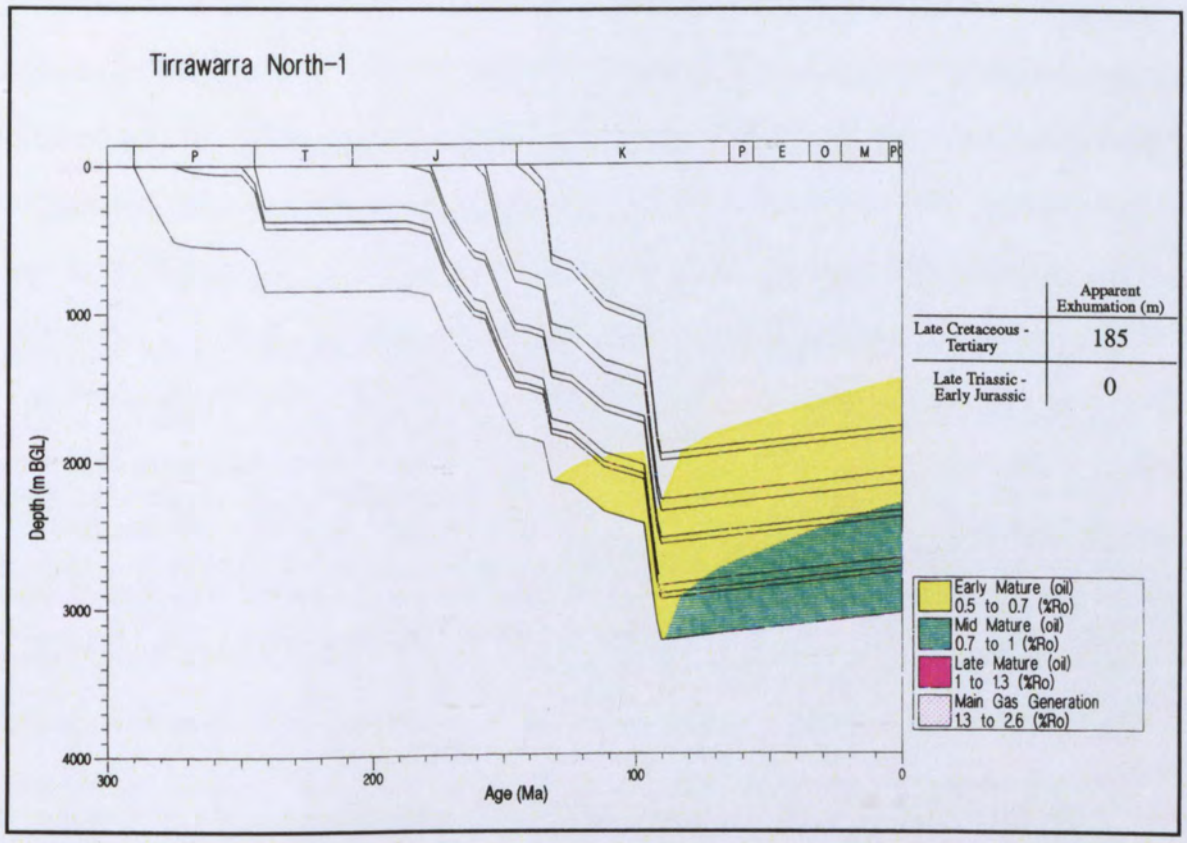

(b)

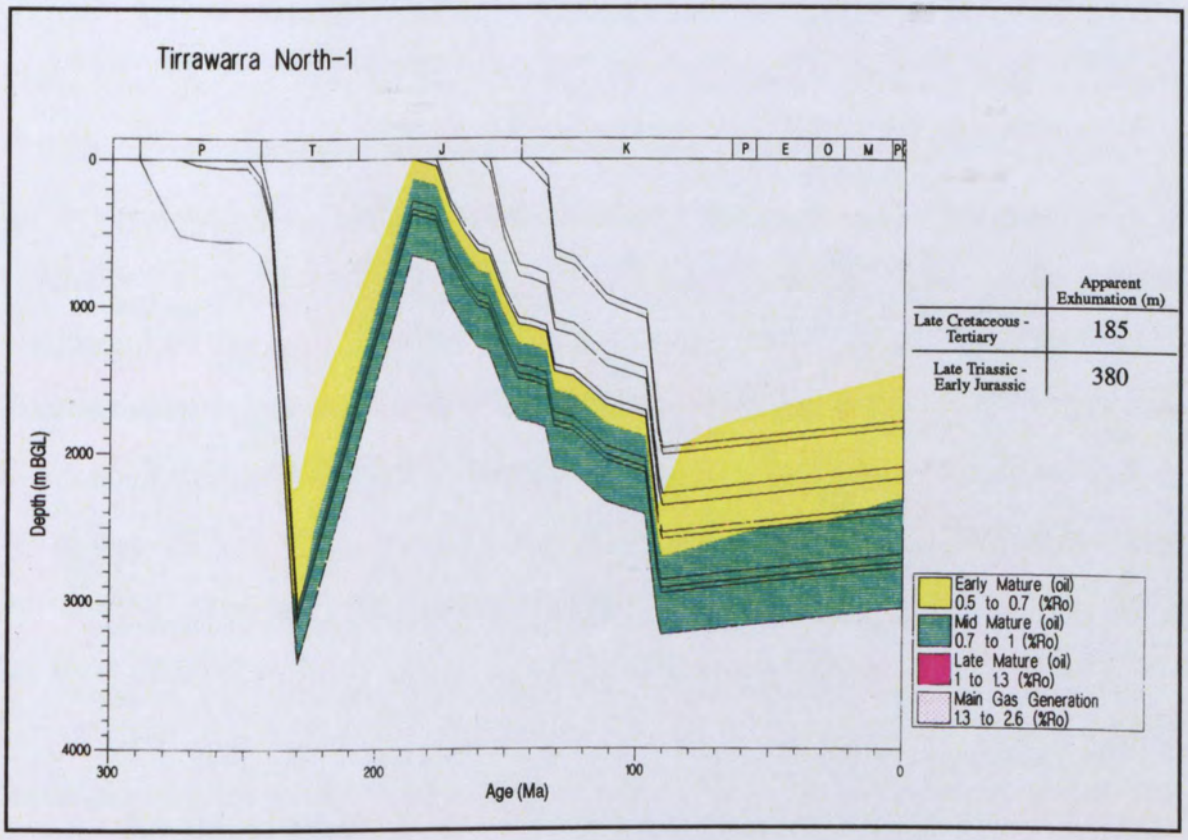

(c)

Figure 8.2. Continued.

In the Burley-2 well, without allowance for burial/exhumation, the Patchawarra Formation reaches a vitrinite reflectance level of 0.5%R_o, equivalent to early maturity for oil generation during Early Permian times; a vitrinite reflectance of 0.7%R_o, equivalent to mid maturity for oil generation during Early Cretaceous times; a vitrinite reflectance of 1%R_o, equivalent to late maturity for oil generation at around the Early/Late Cretaceous boundary; and a vitrinite reflectance of 1.3%R_o, equivalent to mature for gas generation during Late Cretaceous times. The Toolachee Formation reaches the threshold of early, mid, and late maturity for oil and main gas generation around Early Cretaceous, Early/Late Cretaceous, Late Cretaceous/Early Tertiary and Tertiary times, respectively. The basal Jurassic reaches the threshold of early, mid and late maturity for oil generation around Early/Late Cretaceous, Late Cretaceous and Late Tertiary times, respectively. The Birkhead Formation reaches the threshold of early and mid maturity for oil generation, around Early/Late Cretaceous and Late Cretaceous times, respectively. Finally, the Murta Member reaches the threshold of early and mid maturity for oil generation around Early/Late Cretaceous and Tertiary times, respectively (Figure 8.3a). Minor changes in maturation are manifested with the incorporation of Late Cretaceous - Tertiary exhumation. The Murta Member reaches a vitrinite reflectance level of 0.5%R_o, equivalent to early maturity for oil generation during Late Cretaceous times and the Birkhead reaches a vitrinite reflectance level of 1%R_o, equivalent to late maturity for oil generation during Tertiary times (Figure 8.3b). However, with the incorporation of possible maximum Late Triassic - Early Jurassic exhumation (Section 6.4.3), the Patchawarra and Toolachee Formations pass through the stage of gas generation in Mid Triassic whereas the Eromanga Basin's source rocks have a similar maturation history as in previously modellings. Elliott (1985) quoted observed reflectances in the Burley-2 well, which include 0.69% at 1.8 km in the Murta Member, 1.5% at 2.1 km in the Birkhead Formation, 1.67% at 2.2 km in the basal Jurassic, 3.2% at 2.7 km in the Toolachee Formation and 5.7% at 3.3 km in the Patchawarra Formation. The values for the Toolachee and Patchawarra Formations are broadly consistent with all three maturity histories presented in Figure 8.3. However, the observed reflectances for the basal Jurassic and Birkhead Formation indicate that these units reached the phase of gas generation whereas the modelling presented in Figure 8.3 predicts that these formations reach the stage of late mature oil. Possible causes are

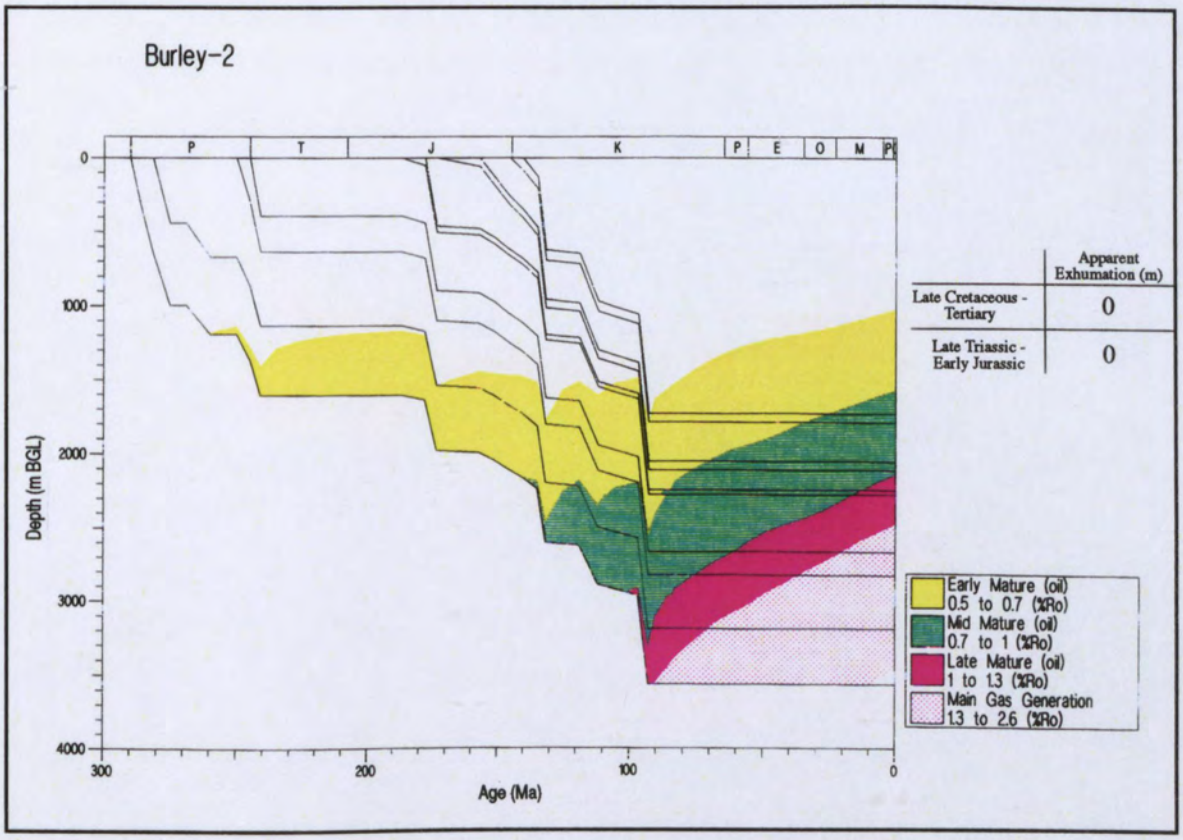

(a)

Figure 8.3. Burial/exhumation and maturity histories for the Burley-2 well (a) without allowance for exhumation, (b) with allowance for Late Cretaceous - Tertiary exhumation and (c) with allowance for Late Cretaceous - Tertiary and maximum possible Late Triassic - Early Jurassic exhumation. All burial/exhumation histories were decompacted using the methodology of Sclater and Christie (1980) with the decompaction parameters defined in Section 6.4.2. Ages were taken from the operators' composite logs and geochronologically calibrated after the time scale of Harland *et al.* (1989). The apparent exhumation values (in metres) used in each case are shown.

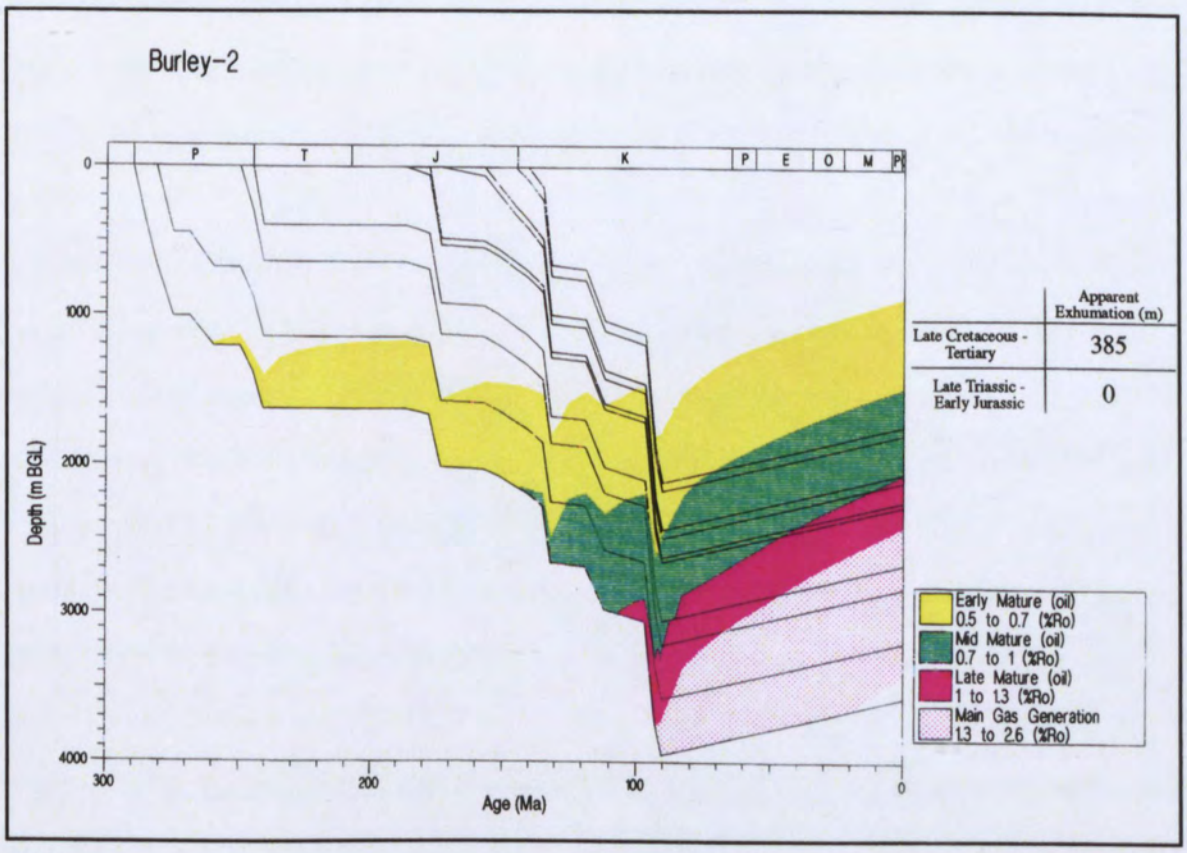

(b)

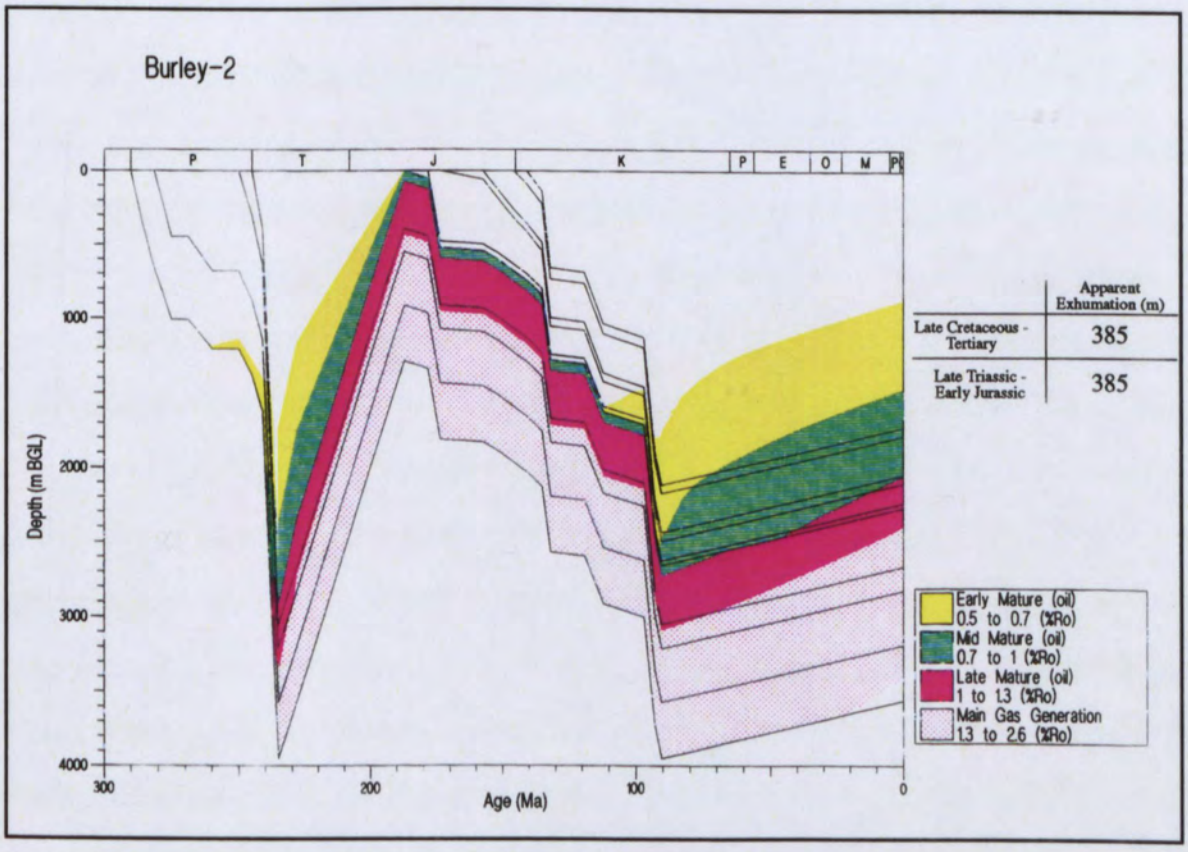

(c)

Figure 8.3. Continued.

palaeogeothermal gradients and/or the exhumation values used in this modelling (Section 4.4). As shown previously, all types of maturation modelling are consistent with the sourcing of the gas and oil fields of the Nappamerri Trough (Kantsler *et al.*, 1986).

In summary, the combination of any given palaeogeothermal gradients with a burial history plot for a potential hydrocarbon source that allows for exhumation indicates earlier and higher levels of organic maturity than the same palaeogeothermal gradients combined with a burial history plot that does not allow for exhumation. This is more discernible when Late Triassic - Early Jurassic exhumation is incorporated in maturation modelling. Thus, estimates of exhumation, such as those presented, should be incorporated in maturation modelling of wells not at their maximum burial-depth.

Discussion: A question that continues to be debated amongst explorationists in the Cooper-Eromanga Basins is whether the hydrocarbons located in Eromanga reservoirs were sourced primarily from rocks in the Eromanga Basin or those in the Cooper Basin. In the Cooper Basin, the location of oil and gas fields is closely linked to the distribution of maturity in the source rocks. For example, most of the gas fields are located in or near the hot Nappamerri Trough, whereas the cooler Patchawarra Trough is the area of the oil fields (Kantsler *et al.*, 1983; Hunt *et al.*, 1989). In the Eromanga Basin, the distribution of oil and gas is not so closely related to surrounding maturation levels (Hunt *et al.*, 1989). Most of the oil pools in the Eromanga Basin are located over and adjacent to the margins of the Cooper Basin (Heath *et al.*, 1989). Stratigraphically the Eromanga fields are characterised by vertically stacked pools, with the largest accumulation of oil usually located just below the deepest, most competent seal (Heath *et al.*, 1989). Heath *et al.* (1989) used the above and other factors to argue that much of the oil and gas in the Eromanga Basin was sourced from the underlying Cooper Basin. A drilling program carried out at the edge of southwestern Cooper Basin, where the confining Nappamerri 'bed' is absent, largely confirmed this hypothesis, yielding commercial discoveries of oil in Eromanga reservoirs that are hydraulically connected to the underlying Cooper source rocks (Heath *et al.*, 1989). A chemical biomarker study by Jenkins (1989) supports the field-based conclusions for a dominantly Permian source for

Eromanga hydrocarbons. If the oil and gas reservoired in the Eromanga Basin are sourced largely from underlying Cooper rocks, as the above arguments suggest, then the timing of the oil and gas generation and expulsion relative to the creation of trapping structures in the Eromanga Basin is very critical. For example if oil was generated and expelled from source rocks before structures were formed, such as during the burial/exhumation of the Cooper Basin, then no significant accumulations would be expected to be found. This hypothesis has been used to explain the absence of hydrocarbon discoveries in many Eromanga structures that would have expected to yield oil or gas (Kantsler *et al.*, 1983).

It is worth noting that in both Jackson-1 and Tirrawarra North-1 (Figures 8.1 and 8.2) the excess of Late Triassic - Early Jurassic exhumation over subsequent burial is relatively small, and greater maturities are attained by Cooper Basin source rocks in Tertiary times than were attained in Late Triassic - Early Jurassic times. Hence hydrocarbons generated by Cooper Basin source rocks could have charged reservoirs in these areas in Tertiary times. Where the excess of Late Triassic - Early Jurassic exhumation over subsequent burial is relatively small:

- Cooper Basin sourced oils could have directly charged Eromanga Basin reservoirs
- Cooper Basin reservoirs may have been charged with Cooper Basin sourced oils in Late Tertiary times, and such oils need not have been preserved in reservoirs since Late Triassic - Early Jurassic times.

However, where the excess of Late Triassic - Early Jurassic exhumation over subsequent burial is large (in excess of at least 400 m) it is considered unlikely that Cooper Basin sources could have filled Eromanga Basin reservoirs.

Indeed recent geochemical work (Michaelsen and McKirdy, 1989) has suggested that Eromanga Basin sourced oils form a significant component of Eromanga Basin reservoired oils. There are not yet sufficient geochemical data to compare geochemically-based determinations of source rock with the exhumation values determined herein. However, in the future it may be possible to investigate whether areas where Cooper Basin sources are

currently at maximum maturity based on exhumation values coincide with areas where Cooper Basin sourced oils dominate, and whether areas where Cooper Basin sources have not re-attained maturity levels attained in Late Triassic - Early Jurassic are dominated by Eromanga Basin sourced oils.

8.3 Influence of Exhumation on Velocity/Depth Conversion

A single velocity/depth function cannot be used for depth conversion of seismic two-way times in an area which has undergone severe exhumation. Maps of raw interval velocities are also often unreliable for predicting velocities at undrilled locations because of relatively rapid spatial changes in exhumation which cause rapid velocity variations. The accuracy of depth-conversion may be improved by using the velocity anomaly method of Jaspen (1993). Velocity anomaly is essentially the same as apparent exhumation. If instead of mapping raw interval velocity, the velocity anomaly is mapped, velocity variations due to variations in present burial-depth are removed and those due to variations in exhumation are more easily resolved. Hence a velocity anomaly map is more likely to be successfully predictive than a raw interval velocity map.

Hillis *et al.* (1995) in a study of depth-conversion in Petroleum Exploration Licences (PELs) 5 and 6 of the Cooper-Eromanga Basins showed that the velocity anomaly method is significantly more accurate than the interval velocity method. Hillis *et al.* (1995) calculated the velocity anomaly, based on seismic isochron and checkshot/sonic log-derived data, for three layers: surface to top of the Mackunda Formation, top of the Mackunda to top of the Cadna-owie Formation and top of the Cadna-owie Formation to top of the Toolachee Formation. The velocity anomaly maps for top of the Mackunda to top of the Cadna-owie Formation and top of the Cadna-owie Formation to top of the Toolachee Formation are broadly similar, showing a general west-east increase across the area (Figure 8.4). In the first layer (surface to top of the Mackunda Formation) velocity anomalies are generally smaller than those for the rest of the layers. This suggests that exhumation from maximum

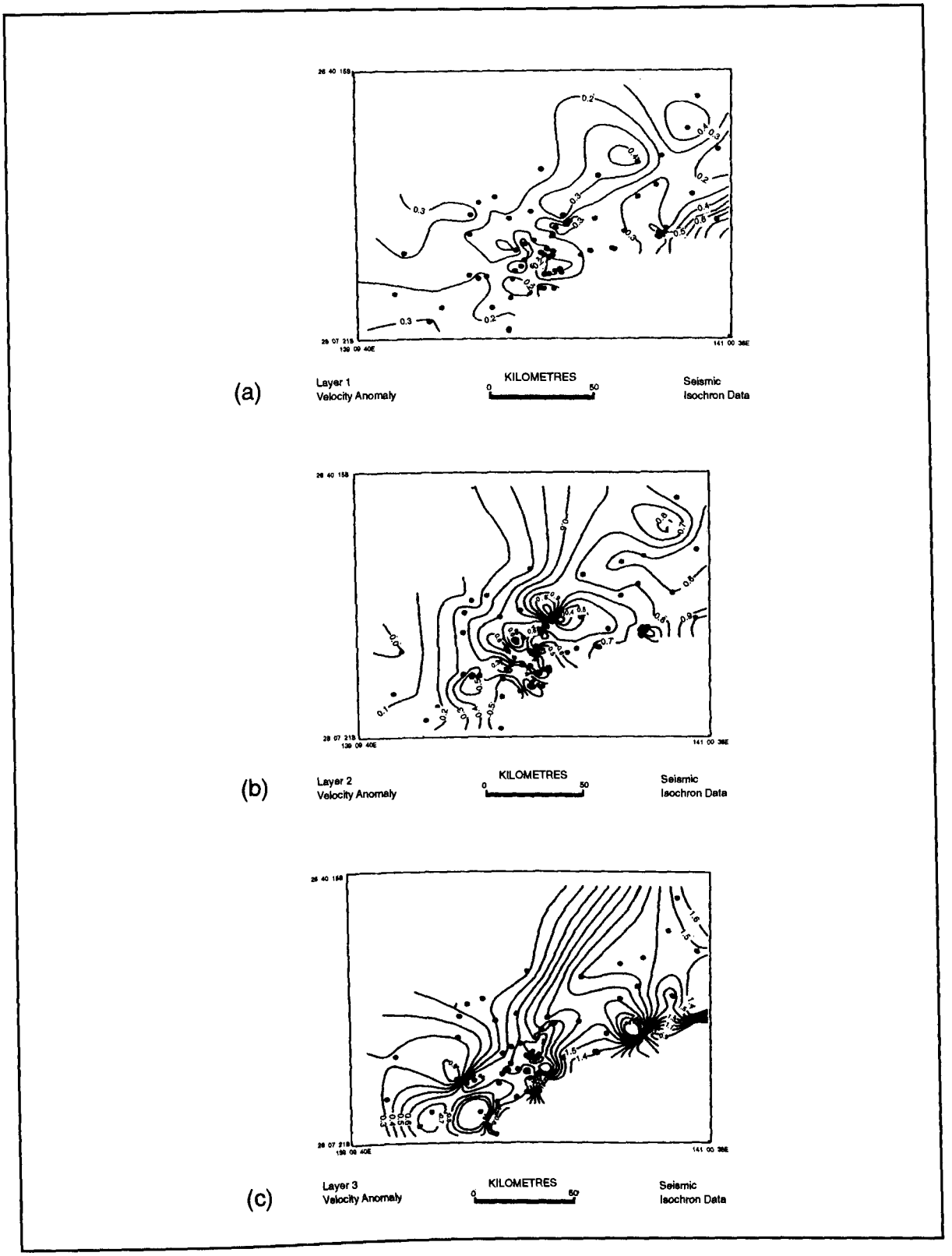

Figure 8.4. Velocity anomaly maps for (a) surface to top of the Mackunda Formation; (b) top of the Mackunda Formation to top of the Cadna-owie Formation; and (c) top of the Cadna-owie Formation to top of the Toolachee Formation. The mapped area is PELs 5 and 6 in South Australia sector of the Cooper-Eromanga Basins. The regional eastward increase of velocity anomaly in Mackunda to Cadna-owie Formation and Cadna-owie to Toolachee Formation is believed to represent increasing exhumation from previous maximum burial-depth and the relatively low velocity anomalies in surface to Mackunda Formation are believed to illustrate that exhumation from maximum burial-depth pre-dated the deposition of at least part of surface to Mackunda Formation sequence (after Hillis *et al.*, 1995).

burial-depth pre-dated the deposition of at least part of this layer. Indeed, as discussed in Section 6.3.2 and as suggested by Rodgers *et al.* (1991), the major period of Tertiary exhumation occurred during the Late Cretaceous to Palaeocene and resulted in the regional angular unconformity between the Winton Formation and the overlying Eocene Eyre Formation. The Tertiary sequence, which is up to 300 m thick in the depth-conversion study area of Hillis *et al.* (1995), is a significant part of their first layer. The Tertiary sequence is less affected by exhumation than the underlying units and would thus exhibit relatively little velocity anomaly, reducing the velocity anomaly of their first layer as an whole.

Hillis *et al.*'s (1995) study covered only a portion of the South Australia sector of the Cooper-Eromanga Basins. Although beyond the scope of this thesis, the data presented herein could form the basis of determining more regional velocity anomaly maps for the entire Cooper-Eromanga Basins.

8.4 Influence of Exhumation on Reservoir Porosity

To a first order, reservoir porosity is controlled by maximum burial-depth. This is demonstrated by the fact that apparent exhumation values from the Hutton Sandstone, the principal reservoir unit in the Eromanga Basin, are consistent with those from shaly units in the Eromanga Basin sequence (Section 3.2). In assessing hydrocarbon volumes and thus the economic viability of prospects in the Cooper-Eromanga Basins it is necessary to estimate reservoir porosity. Hence predicted reservoir porosity is an important factor in ranking prospects in the Cooper-Eromanga Basins.

Porosities from the Hutton Sandstone, the most important reservoir rock in the Eromanga Basin (Passmore, 1989), and the Toolachee Formation, an important reservoir unit in the Cooper Basin (Stanmore, 1989), show a very poor relationship with present burial-depth because of the effects of exhumation (Figures 8.5 and 8.6). However, porosities show a much improved relationships with maximum burial-depths as defined in this study

(Figures 8.5 and 8.6). Hence it is recommended that maximum burial-depth should be incorporated into procedures for estimating porosities in calculating the potential hydrocarbon volumes in undrilled prospects.

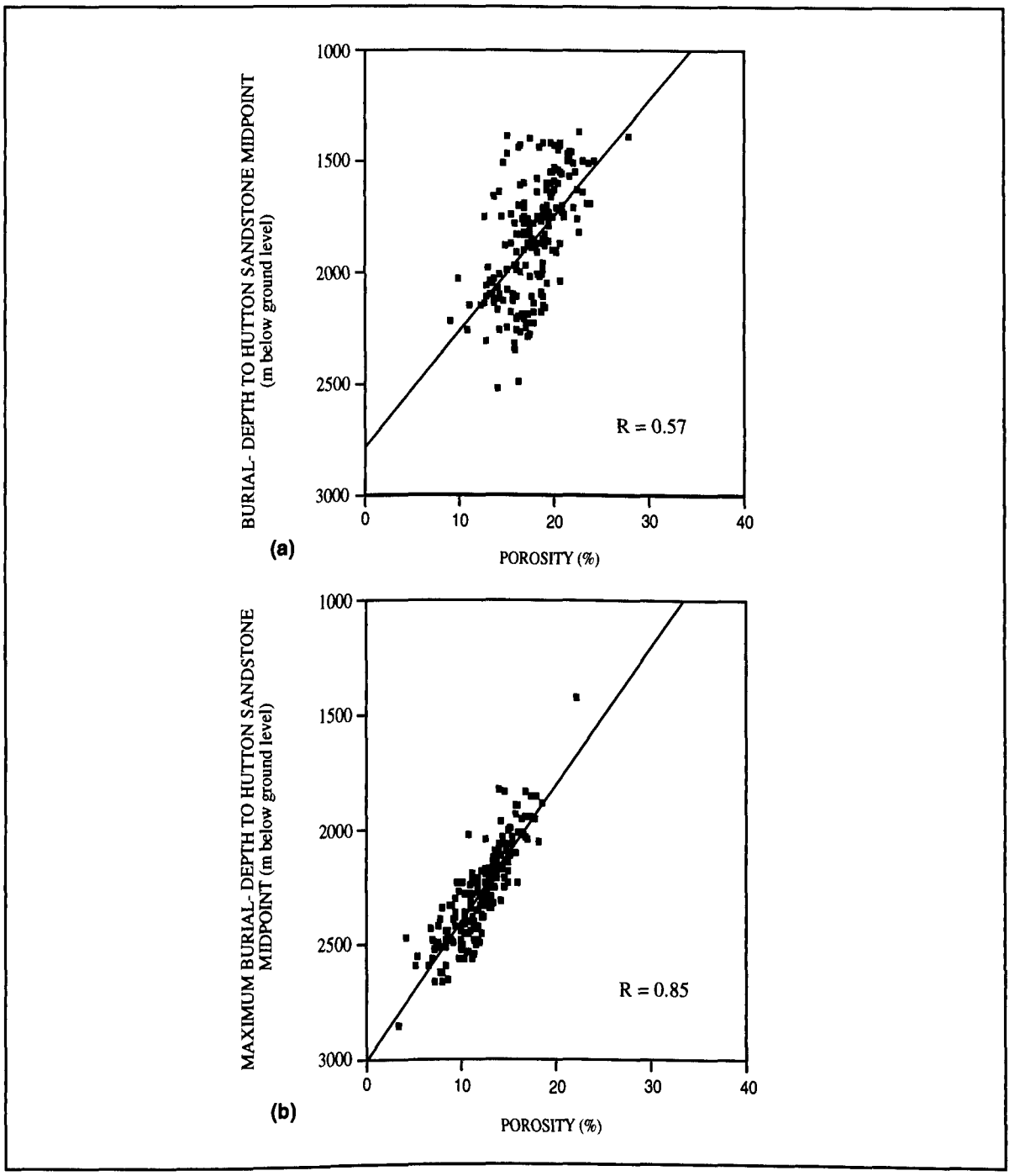

Figure 8.5. Porosity of Hutton Sandstone vs (a) midpoint present burial-depth and (b) midpoint maximum burial-depth. R = correlation coefficient. The porosities used here are the mean porosities of the entire Hutton Sandstone unit, determined from sonic log.

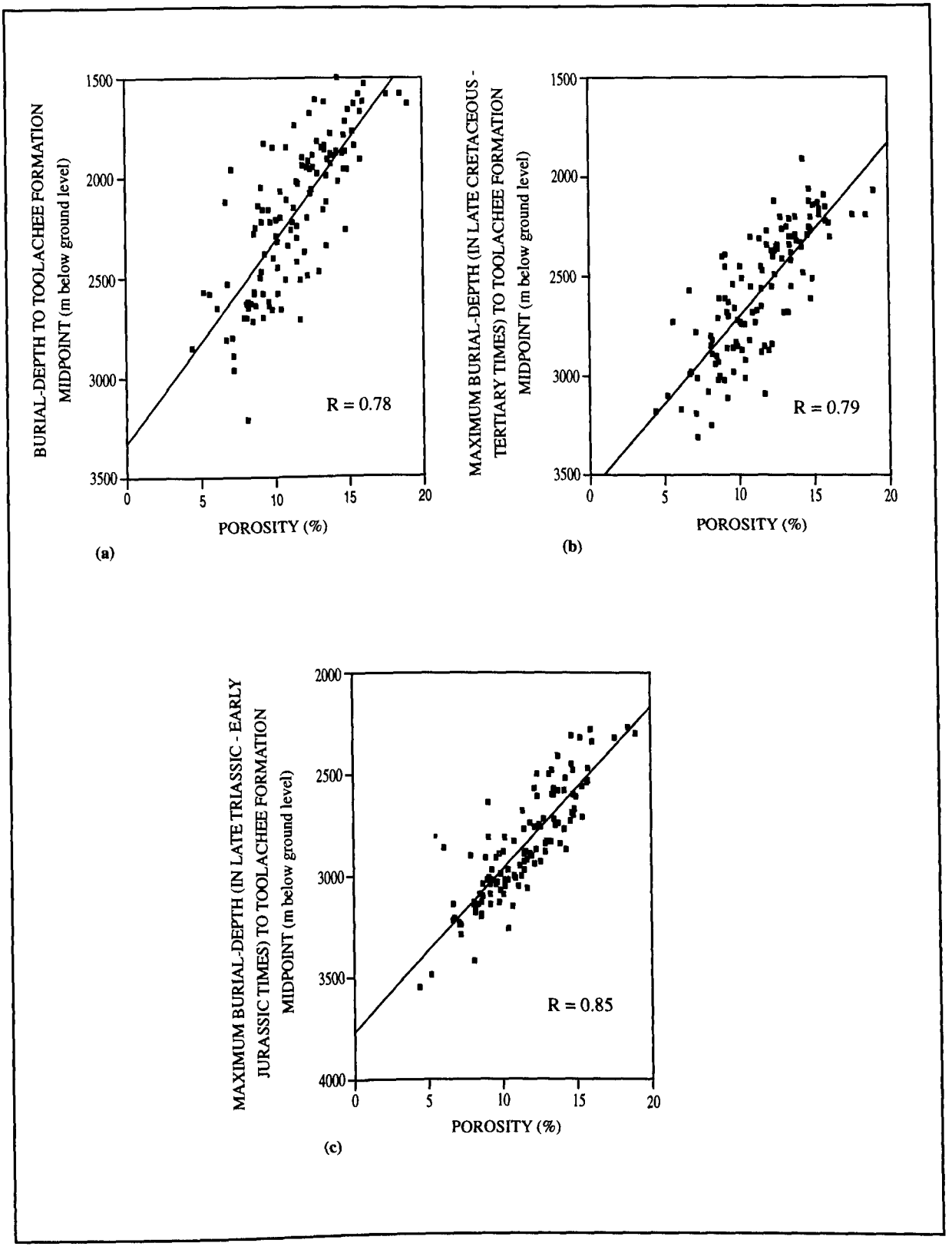

Figure 8.6. Porosity of Toolachee Formation vs (a) midpoint present burial-depth, (b) midpoint maximum burial-depth, derived from Eromanga Basin units (ie. $B_T = E_{A(Eromanga)} + B_P$), and (c) midpoint maximum burial-depth, derived from Cooper Basin units (ie. $B_T = E_{A(Cooper)} + B_P$). R = correlation coefficient. The porosities used here are the mean porosities of the entire Toolachee Formationt, determined from sonic log. Porosities show better correlation with maximum burial-depth derived from Cooper Basin units.

9. SUMMARY AND CONCLUSIONS

The aim of this thesis was to determine the amount of exhumation in the Cooper-Eromanga Basins. The compaction method was applied in order to achieve this aim. In the compaction-based method of determining exhumation the main assumption is that, at the formational and regional scale, burial-depth exerts the primary control on compaction. Since porosity describes compaction state, the porosity logs are all appropriate indicators of compaction, and hence are appropriate for quantifying exhumation from compaction. The porosity logs (sonic, density and neutron), and the velocity survey (check-shot) data, from more than 200 wells, have been used. This thesis thus expands the traditional use of the sonic log as the main 'tool' in compaction-based analysis. Another aspect of the compaction technique relatively rarely applied but used herein, was the use of units of a range of stratigraphic age. Furthermore, most, but not all, of the units analysed were of shaly lithology. The seven units selected for analysis from the Eromanga Basin were the: Winton Formation, Allaru Mudstone/Oodnadatta Formation, Bulldog Shale/Walumbilla Formation, Cadna-owie Formation, Birkhead Formation and Hutton Sandstone. The five units selected for analysis from the Cooper Basin were the: Nappamerri Group, Toolachee Formation, Roseneath Shale, Murteree Shale and Patchawarra Formation. The use of multiple lithologies in the compaction-based analysis of maximum burial-depth has several advantages over the analysis of a single unit and these were discussed in Sections 2.5.2 and 2.5.3.

Considering the sonic log data from the *Eromanga Basin*, there is an excellent correlation between apparent exhumation results from different stratigraphic units in the same well. This correlation confirms that, at a formational and regional scale, overcompaction reflects previously greater burial-depth, rather than laterally varying sedimentological or diagenetic processes. The apparent exhumation values from the adjusted sonic log show, similarly to the sonic log, excellent correlations between different units. The apparent exhumation results from the density log in the Cadna-owie, Birkhead and Hutton units are also similar within the same well. Although exhibiting more scatter than the results from the sonic and the adjusted sonic log, the density and neutron porosity-derived exhumation values from these units are broadly consistent with each other.

Exhumation values from the five units analysed in the *Cooper Basin* are not as consistent as those in the Eromanga Basin. The presence of coals, and the need to analyse relatively thin coal-free sections of the lower Toolachee and lower Patchawarra Formations, is probably largely responsible for poorer correlation between exhumation values involving these two units.

One of the purposes of this study was to analyse the suitability of the density and neutron logs for maximum burial-depth/exhumation analysis. There is generally a good correlation between exhumation values from the different logs, and the use of all the porosity logs is considered to be justified. Much of the scatter, in exhumation values, between the different logs can probably be attributed to the fact that neutron and density log coverage is not as extensive as the sonic and the adjusted sonic log coverage. Random scatter in the crossplots is presumably linked to the different ways in which the different logs see porosity, thus compaction. For example, the sonic log, unlike the other two porosity logs, does not tend to see secondary, fracture or vugular porosity. For this reason alone, the *sonic log is considered likely to be the most reliable indicator of maximum burial-depth/exhumation.*

Maps of apparent exhumation derived from individual units in the Eromanga Basin sequence all show a very similar pattern. The map of apparent exhumation based on the mean of the Eromanga Basin units analysed is considered to give the most reliable description of the amount of Late Cretaceous - Tertiary exhumation because any sedimentological and/or diagenetic effects that might cause variation from the normal Δt/depth trend in individual units, and consequently violate the assumption that all units follow the normal compaction trend with burial depth, will tend to be reduced.

Broadly speaking, exhumation increases eastwards from the Patchawarra Trough, through the GMI Trend and Nappamerri Trough into Queensland, with values of approximately 600 m in the Jackson-Naccowlah area. Late Cretaceous - Tertiary exhumation reaches approximately 1 km, north of the Jackson-Naccowlah area. The other area of maximum Late Cretaceous - Tertiary exhumation, which also reaches approximately 1 km, lies near the extreme north-eastern boundary of South Australia, in the vicinity of the Curalle-1 well.

The Tertiary is absent or very thin over the maxima in exhumation to the north of the Jackson-Naccowlah area and in the vicinity of the Curalle-1 well. The region of lower exhumation between these two maxima (Windorah Trough) corresponds to a minor depocentre which contains in excess of 100 m of Tertiary sediments. The Patchawarra Trough is part of the major Tertiary depocentre of the area (with up to 300 m of Tertiary sediments), and this is consistent with the interpretation that it is currently at maximum burial-depth. This Tertiary depocentre does, however, extend south of the Patchawarra Trough, extending over the GMI Trend and into the southern part of the Nappamerri Trough. The trend of the Tertiary depocentre follows the Patchawarra Trough, and may have been inherited from it. However, the structural grain of the GMI Trend and Nappamerri Trough appears to have exerted little influence on the Tertiary depocentre.

One of the key results of this thesis is that in many cases the Cooper Basin units exhibit more overcompaction than the Eromanga Basin units in the same well. Given a ± 200 m error on exhumation values from individual units, much of the excess of apparent exhumation of the Cooper Basin over that of the Eromanga Basin is within error limits. However, there are significant areas where the difference is in excess of 400 m, and, perhaps even more importantly, the map of the difference between Cooper and Eromanga Basin exhumation has a demonstrable link with the structural history of the basins. The major Troughs within the Cooper-Eromanga Basins, eg. Patchawarra, Nappamerri, Arrabury and Windorah, which were depocentres during the development of the Cooper Basin correspond with areas where maximum burial-depth was attained subsequent to the deposition of the Eromanga Basin. A number of the areas where Cooper Basin exhumation is significantly greater than that of the Eromanga Basin are Permo-Triassic structural highs such as the Callabonna anticline, Pondrinie, Naccowlah and a significant area centred on the Toolachee Field.

In order to further investigate the exhumation in the Cooper-Eromanga Basins the *vitrinite reflectance* method was also utilised. However, in order to use vitrinite reflectance to quantify exhumation the geothermal history must be known. Following the principle of Occam's razor, vitrinite reflectance was first modelled assuming that palaeogeothermal gradients were constant and equal to the present geothermal gradients, ie. *Geothermal History A* . Given that

Geothermal History A predicts vitrinite reflectance in excess of that observed for the Eromanga Basin, the data were next modelled using *Geothermal History B* which assumes that present high geothermal gradients result from a steady increase in geothermal gradient since 90 Ma. In an attempt to match the vitrinite reflectance trends of the Cooper Basin without invoking such extreme Late Triassic - Early Jurassic exhumation as required by *Geothermal History B*, modelling was undertaken using *Geothermal History C*. In *Geothermal History C*, which was considered as the most reliable, higher geothermal gradients were assumed during the deposition of the Cooper Basin. The results of *Geothermal History C* are consistent with those based on compaction analysis. However, the tendency for exhumation values, from compaction analysis, to increase from the Patchawarra to Nappamerri Trough, is not borne out by the vitrinite reflectance modelling. This may simply be because less wells were analysed in the vitrinite reflectance modelling than by the compaction analysis. Indeed it is a major advantage of the compaction method that it does not require laboratory-based analytical work and many wells can be analysed in a short time and at low cost.

A key feature of the vitrinite reflectance data, especially in the Eromanga Basin, is that, assuming palaeogeothermal gradients equal to the present day predicts reflectances in excess of these that are observed. This demonstrates that the present high geothermal gradients in the area, typically 40-50°C/km, are a relatively recent phenomenon. The cause of this increase in geothermal gradient is unclear. Given that geothermal gradients must have increased in Late Cretaceous - Tertiary times, it is difficult to obtain reliable estimates of Late Cretaceous - Tertiary exhumation.

The most striking feature of the vitrinite reflectance data from the Cooper-Eromanga Basins is the observed increase in vitrinite reflectance/depth gradient from the Eromanga Basin sequence to the Cooper Basin sequence. This increase in gradient is consistent with compaction based indication that at least parts of the Cooper Basin reached maximum burial-depth before deposition of the Eromanga Basin. It reflects exhumation during Late Triassic - Early Jurassic times, and/or higher palaeogeothermal gradients during the deposition of the Cooper Basin sequence, prior to Late Triassic - Early Jurassic exhumation. Unfortunately, the balance of

exhumation and/or palaeogeothermal gradient used to model the observed vitrinite reflectance trends is inherently a non-unique one.

Given that the purpose of the vitrinite reflectance modelling was to investigate whether exhumation values derived from vitrinite reflectance modelling were consistent with those based on compaction analysis, it is perhaps ironic that the modelling has fairly convincingly demonstrated a Late Cretaceous - Tertiary increase in geothermal gradient and higher geothermal gradients during the deposition of the Cooper Basin. However, because the magnitudes of the Late Cretaceous - Tertiary increase in geothermal gradient and of the higher gradients during the deposition of the Cooper Basin cannot be independently ascertained, the magnitude of Late Cretaceous - Tertiary and Late Triassic - Early Jurassic exhumation cannot be determined with confidence from the vitrinite reflectance data. It is clear from this study that the Cooper-Eromanga Basins, with their complex thermal history are not an ideal area in which to investigate whether exhumation values yielded by modelling vitrinite reflectance are consistent with those from the compaction methodology.

Apatite fission track analysis and fluid inclusion homogenisation temperatures in the Cooper-Eromanga Basins have been analysed by several authors. Although capable of estimating the magnitude of exhumation in the Queensland area, AFTA is largely unable to constrain exhumational events in the present hot area of South Australia, and only indications of the palaeotemperatures can be deduced. AFTA studies help to define the palaeo-thermal history of the region, but do not specifically elucidate the amounts of exhumation during the major unconformities in the basins. Nonetheless, where reported, exhumation results from AFTA and fluid inclusion homogenization temperatures are in a broad agreement with those from compaction analysis and vitrinite reflectance.

The compaction-based values of exhumation derived from sonic log data are consistent with those based on the other techniques. Given that the sonic log-based compaction analysis provides the most extensive set of results, these data are considered the best available for characterising exhumational events in the Cooper-Eromanga Basins.

Unfortunately, no log data are available for the units overlying the Winton Formation, thus it is not possible to date exhumation beyond Late Cretaceous - Tertiary using the compaction methodology. Since the Tertiary units are relatively thin, the timing of Late Cretaceous - Tertiary structuration, which may be contemporaneous with exhumation, cannot be determined from seismic reflection data using standard techniques (ie. interpretation of Tertiary units affected/unaffected by structuration). Given that such Tertiary sequences as are preserved are relatively thin and separated by marked unconformities/weathered surfaces, it is suggested that exhumation rather than sedimentation dominated the Tertiary, and that in exhumed areas, maximum burial-depth was attained in Late Cretaceous times.

In the vast majority of wells (187 wells) the mean exhumation yielded from compaction analysis of the Cooper Basin units is greater than the mean value yielded from the Eromanga Basin units. In these wells it is inferred that the Cooper Basin sequence attained maximum burial-depth prior to the deposition of the Eromanga Basin sequence. However, it should be mentioned that in many cases the difference is less than the sum of the probable error bounds on the two estimates of exhumation. In 16 wells the mean exhumation yielded from compaction analysis of the Cooper Basin units is less than the mean value yielded from the Eromanga Basin units. In these wells there is no evidence, from compaction analysis, of exhumation in Late Triassic - Early Jurassic times. However, in the absence of major lateral tectonic movement, the Cooper Basin units must have been subjected to the same magnitude of Late Cretaceous - Tertiary exhumation as the Eromanga Basin units. Indeed these wells are used to estimate the likely error bounds on the compaction methodology.

The Permian hiatus associated with the Daralingie unconformity was treated as a phase of non-deposition because there is no evidence from compaction, and other methods, of exhumation at this time. However, all methods of quantifying exhumation based on rock properties are intrinsically insensitive to exhumation associated with now deeply buried unconformities, because rock properties are unlikely to hold a memory of such events.

Examination of seismic reflection profiles indicate, the compressive nature of the structural style associated with the major uplift events in the Cooper-Eromanga Basins. Inversion

geometries and reactivated features attest to a period of compression during Late Triassic - Early Jurassic times. In the Eromanga Basin, compressional structural styles associated with Late Cretaceous - Tertiary uplift are apparent. Tertiary deformation has reactivated older structures, increasing the amount of structural relief in the Cooper Basin units. Although a number of mechanisms may have contributed to regional Late Cretaceous - Tertiary exhumation, the two-layer lithospheric compression model is considered as the most complete explanation of both the uplift of areas subject to compression and crustal thickening, and of the regional uplift (and preceding subsidence) of areas not subject to any apparent Late Cretaceous - Tertiary compression.

The combination of any given palaeogeothermal gradients with a burial history plot for a potential hydrocarbon source that allows for exhumation indicates earlier and higher levels of organic maturity than the same palaeogeothermal gradients combined with a burial history plot that does not allow for exhumation. Hence, estimates of exhumation, such as those presented in this thesis, should be incorporated in maturation modelling of wells not at their maximum burial-depth. Since a single velocity/depth function cannot be used for depth conversion of seismic two-way times due to severe exhumation the data presented herein could form the basis of determining more regional velocity anomaly maps for the entire Cooper-Eromanga Basins. Porosities from the Hutton Sandstone, the most important reservoir rock in the Eromanga Basin, and the Toolachee Formation, an important reservoir unit in the Cooper Basin, show a much improved relationships with maximum burial-depths than with present burial-depths. Therefore maximum burial-depth should be incorporated into procedures for estimating porosities in calculating the potential hydrocarbon volumes in undrilled prospects.

In conclusion, this thesis has shown that a considerable amount of exhumation happened after the deposition of the Cooper Basin, in Late Triassic - Early Jurassic times and after the deposition of the Eromanga Basin, in Late Cretaceous - Tertiary times. However, previous work has generally paid little attention to exhumation in these basins and its consequences. In particular the significance of Late Triassic - Early Jurassic times, has not been widely recognised. It is not surprising that maturation studies which have not incorporated the effects of exhumation have failed to produce satisfactory models. To the best of the author's

knowledge this is the most detailed exhumation study in the Cooper-Eromanga Basins. The results of this thesis will contribute to research into basin formation and uplift and to petroleum exploration projects. In addition, it has been shown that the use of multiple lithologies and the use of all the porosity logs gives reasonable results and the same approach is recommended in exhumation studies in other parts of the world.

Recommendations for Further Research:

Although this thesis has helped elucidate exhumation in the Cooper-Eromanga Basins, little is known about exhumation in the other geologically and economically important basins of Australia's eastern area. Similar age unconformities to those in Cooper-Eromanga Basins, are observed in the other basins of eastern Australia. Due to the availability of petrophysical data and the low cost of the technique, it is suggested that compaction analysis could be used to quantify the amount of Late Triassic - Early Jurassic exhumation between the Galilee and Eromanga Basins, between the Bowen and Surat Basins, and between the Esk Trough and Moreton Basins. The compaction methodology could also be applied to determine Late Cretaceous - Tertiary exhumation in the Surat and Moreton Basins. Given the broad lithological similarity of these basins to the Cooper-Eromanga Basins, normal compaction relations would be expected to be similar to those determined herein. Accurate knowledge of exhumation in the eastern part of the Australian continent will be a useful to petroleum exploration in these areas to applying a regional tectonic model for the formation and evolution of the eastern part of the continent and its sedimentary basins.

APPENDIX A: MIDPOINT DEPTHS, MEAN LOG DATA AND APPARENT EXHUMATION RESULTS

Table 1. Midpoint Depth and Mean Interval Transit time Data and Apparent Exhumation Results

Eromanga Basin Stratigraphic Units

	Winton Formation			Mackunda Formation			Allaru Mudstone-Oodnadatta Formation			Bulldog Shale-Wallumbilla Formation			Cadna-owie Formation			Birkhead Formation			Hutton Sandstone			Mean[1]
Well	Midpoint Depth (m bgl*)	Mean Δt** (µs/ft)	E_A*** (m)	Midpoint Depth (m bgl*)	Mean Δt** (µs/ft)	E_A*** (m)	Midpoint Depth (m bgl*)	Mean Δt** (µs/ft)	E_A*** (m)	Midpoint Depth (m bgl*)	Mean Δt** (µs/ft)	E_A*** (m)	Midpoint Depth (m bgl*)	Mean Δt** (µs/ft)	E_A*** (m)	Midpoint Depth (m bgl*)	Mean Δt** (µs/ft)	E_A*** (m)	Midpoint Depth (m bgl*)	Mean Δt** (µs/ft)	E_A*** (m)	E_A*** (m)
Alkina-1	440.2	133.0	466.7	755.2	105.4	474.8	931.9	109.1	481.5	1271.9	104.3	467.3	1473.9	87.9	523.7	1841.4	82.8	541.8	1977.4	69.4	747.9	529.1
Alwyn-1	443.4	149.5	134.1	613.4	126.2	337.5	785.9	128.2	247.5	1021.7	116.0	388.3	1154.4	95.4	616.0				1496.0	84.4	395.2	353.1
Amyema-1	617.1	134.3	263.4	776.8	118.9	271.5	963.8	119.1	249.1	1212.1	111.3	330.3	1374.1	97.3	339.2	1700.7	83.2	663.2	1747.5	79.0	447.9	366.4
Andree-1	696.6	136.2	145.2	1040.6	109.4	135.1	1182.9	116.0	92.1	1512.6	107.4	139.8	1747.0	90.5	170.8	2115.3	82.1	303.3	2246.4	74.8	181.7	166.9
Araburg-1	554.5	126.5	481.4	802.6	110.4	359.9	995.1	115.4	292.7	1299.5	102.7	482.4	1442.0	89.9	496.0	1750.7	85.2	517.7	1909.8	73.4	596.1	460.9
Arrabury-1	515.8	140.6	238.1	864.5	111.9	278.0	1029.1	117.3	219.7	1359.5	111.5	176.0	1615.9	90.4	306.8	1959.0	85.8	283.8	2098.7	77.1	201.0	243.3
Arrakis-1	468.1	145.1	197.1	848.2	118.9	200.0	1104.3	119.3	106.6	1387.8	111.3	154.7	1544.7	98.9	122.0	1860.2	79.7	672.7	1964.6	77.4	318.5	253.1
Atoll-1	357.0	144.1	327.4	437.0	127.9	491.6	554.0	132.4	394.9	858.3	113.7	616.3	1041.7	98.9	625.6	1378.6	85.4	880.6	1421.7	80.2	705.5	577.4
Azolla-1	616.5	136.0	229.0	751.9	120.9	270.3	928.5	123.1	204.8	1191.9	113.8	279.9	1337.6	97.3	377.7	1667.3	83.4	689.5	1705.7	79.7	447.6	357.0
Ballera-1	453.9	134.6	421.3	791.0	108.0	403.2	964.0	111.1	408.9	1282.8	108.1	349.5	1514.4	88.9	450.8	1881.3	83.4	475.1	1969.4	73.1	553.5	437.5
Baratta-1	593.0	132.2	329.9	828.0	114.1	285.1	983.0	116.6	280.5	1252.1	108.5	369.1	1427.6	95.3	345.6	1759.2	78.9	814.9	1813.6	75.4	582.2	429.6
Bardoc-1	439.4	143.8	251.4	674.8	118.2	382.9	825.1	120.0	370.6	1155.8	108.8	455.5	1346.8	94.7	445.1	1706.6	82.1	713.4	1758.5	74.9	661.5	468.6
Barrolka-1													1499.9	89.7	443.2	1864.9	82.1	554.8	2020.5	75.4	370.0	456.0
Baryulah-1	489.5	139.8	280.4	857.8	109.4	318.2	1048.4	115.9	230.1	1356.0	106.1	332.2	1572.8	88.0	422.1	1951.1	83.6	393.1	1990.7	72.1	588.2	366.3
Batunga-1	498.5	140.4	259.8	764.9	123.9	216.6	930.3	126.4	138.3	1175.6	116.3	227.8	1334.4	95.5	433.0	1662.5	86.3	554.9	1710.4	82.5	284.9	302.2
Beanbush-1	990.5	124.9	76.2	1220.2	106.1	0.0 (R*)	1376.4	110.2	15.8	1717.3	105.0	0.0 (R*)	1971.1	88.8	0.0 (R*)	2348.4	78.5	244.4	2522.9	70.7	132.3	66.7
Belah-1	431.0	136.4	407.2	666.0	120.8	357.9	858.2	120.9	318.9	1248.6	113.3	237.5	1289.8	95.9	467.2	1625.5	84.2	692.7	1661.0	78.5	558.6	434.3
Biala-1	524.6	137.4	294.0	635.8	125.3	328.0	781.3	129.1	233.7	1017.9	118.4	326.4	1158.1	98.5	520.0				1513.2	85.5	320.4	337.1
Big Lake-26																1952.1	81.1	516.6	2032.7	70.2	649.7	583.2
Big Lake-35	655.1	132.6	259.3	957.3	105.9	266.1	1131.3	111.7	230.2	1443.2	105.3	267.0	1646.5	93.3	189.4	1969.6	81.5	477.6	2053.7	69.8	648.5	334.0
Bogala-1	359.9	138.1	444.1	550.5	114.6	555.5	694.0	122.4	454.4	978.1	115.7	441.9	1195.0	96.1	554.0	1538.8	80.5	955.9	1605.4	78.0	642.2	578.3
Boldrewood-1				291.5	120.5	735.2	869.1	115.7	411.8	824.8	107.0	838.7	1030.2	91.6	855.4	1401.9	83.0	971.2	1508.9	71.5	1099.3	818.6
Bookabourdie-1	682.9	134.2	198.6	1020.9	106.9	189.1	1178.5	114.8	120.3	1481.4	106.6	192.9	1720.1	91.9	155.7	2102.2	80.6	389.7	2231.1	75.4	161.2	201.1
Boxwood-1	519.1	142.7	194.8	685.6	129.8	217.3	864.1	126.2	207.3	1137.5	112.7	365.1	1277.5	99.5	371.5	1557.6	84.3	755.1	1635.6	76.5	698.7	401.4
Brolga-2													1758.5	92.0	113.8	2130.2	79.6	408.1	2257.7	73.2	258.7	260.2
Buckinna-1	507.4	140.0	260.0	682.4	120.3	347.4	834.5	124.4	273.8	1051.0	115.2	381.2	1194.5	98.0	498.2	1520.6	85.4	738.5	1557.5	80.7	541.7	434.4
Bungee-1	545.8	143.7	147.8	802.1	120.1	231.3	1002.8	124.0	113.2	1259.8	112.9	238.5	1403.4	98.1	286.0	1705.5	84.7	588.6	1755.0	80.8	340.3	277.9
Burke-2				791.0	115.7	301.2	993.7	115.4	294.4	1293.5	105.9	400.3	1482.0	93.9	335.4							332.8
Burley-2	578.0	133.5	318.1	926.7	100.0	374.7	1106.7	109.4	300.6	1447.1	99.3	432.2	1687.8	83.4	443.0	2082.2	79.8	445.6	2177.0	72.4	382.6	385.3
Bycoe-1	327.1	135.0	539.5	482.1	115.3	615.1	622.1	126.2	449.8	921.8	115.5	503.5	1135.9	96.5	602.7	1491.7	82.4	910.5	1553.7	79.0	641.6	609.0
Carney-1	444.9	136.6	390.5	642.4	114.4	466.6	798.4	122.3	351.6	1072.9	112.5	435.9	1273.4	95.8	486.0	1635.4	83.4	722.2	1704.4	78.0	545.7	485.5
Challum-1	581.4	133.2	321.5	822.1	111.4	327.4	959.5	115.6	324.4	1282.4	107.7	360.2	1489.4	91.5	400.4	1853.3	84.7	442.6	1967.0	73.3	545.2	388.8
Charo-1	473.3	134.4	404.3	815.2	118.2	242.4	970.4	120.4	218.5	1233.7	115.1	201.2	1426.8	99.4	224.7	1766.5	84.9	515.5	1913.7	79.5	252.4	294.1
Childie-1	443.9	141.0	303.5	699.8	120.6	326.5	889.6	119.3	319.4	1176.7	111.6	356.7	1335.9	95.8	422.6	1659.3	82.6	736.7	1695.8	80.5	410.9	410.9
Cooba-1				985.1	114.3	125.6	1132.3	117.1	122.1	1449.3	110.2	123.8	1675.8	92.8	172.4	2025.0	83.4	331.4	2160.1	77.8	102.1	162.9
Cook-1	517.5	135.2	345.5	916.2	106.8	293.9	1111.2	108.9	306.7	1417.3	105.2	294.8	1591.2	90.8	317.0	1920.4	84.4	385.6	2076.1	72.0	504.1	349.6
Cook North-1	628.0	126.9	400.1	918.7	104.9	317.7	1093.6	109.7	308.3	1404.4	102.1	396.0	1596.7	86.5	441.8	1934.7	82.8	452.0	2067.2	70.7	588.7	414.9
Coonavalla-1	362.8	130.0	602.5	564.1	109.5	611.0	743.6	116.0	531.4	1014.3	108.8	596.6	1209.8	91.6	674.6	1555.0	85.4	707.3	1659.7	70.2	1023.1	678.0
Cooroo-1	430.0	140.1	335.2	699.7	116.2	385.9	890.6	119.2	321.3	1183.1	110.4	384.0	1366.0	97.8	332.7	1726.7	82.5	672.1	1781.4	73.1	739.7	453.0
Copai-1	438.9	133.7	453.7	693.9	118.1	365.7	903.4	118.1	329.5	1156.9	103.9	592.8	1285.4	92.0	586.7	1602.3	84.7	690.3	1752.5	74.4	698.9	531.1
Cowan-3	678.9	141.3	61.3	893.9	119.7	144.0	1079.3	118.7	143.2	1356.1	109.0	250.2	1511.4	95.8	249.5	1817.8	80.9	659.9	1897.1	74.4	553.0	294.5
Cuddapan-1	571.7	128.1	431.1	851.2	107.8	346.6	1086.7	111.9	270.3	1390.2	98.8	503.0	1546.2	89.6	400.5	1879.2	83.2	485.3	2010.2	70.8	637.7	439.2
Curalle-1				350.4	104.8	886.5	518.9	113.9	799.3	802.9	102.8	978.3	939.9	90.2	986.6	1246.9	82.9	1131.8	1387.8	72.0	1195.7	996.4
Daer-1	665.8	130.4	292.4	914.8	118.7	136.7	1092.8	118.5	133.7	1371.3	112.4	139.2	1546.3	96.3	196.8	1876.8	86.2	345.5	2046.3	78.2	192.9	205.3

Table 1. Continued.

	Winton Formation			Mackunda Formation			Allaru Mudstone-Oodnadatta Formation			Bulldog Shale-Wallumbilla Formation			Cadna-owie Formation			Birkhead Formation			Hutton Sandstone			Mean[1]
Well	Midpoint Depth (m bgl*)	Mean Δt** (μs/ft)	E_A*** (m)	Midpoint Depth (m bgl*)	Mean Δt** (μs/ft)	E_A*** (m)	Midpoint Depth (m bgl*)	Mean Δt** (μs/ft)	E_A*** (m)	Midpoint Depth (m bgl*)	Mean Δt** (μs/ft)	E_A*** (m)	Midpoint Depth (m bgl*)	Mean Δt** (μs/ft)	E_A*** (m)	Midpoint Depth (m bgl*)	Mean Δt** (μs/ft)	E_A*** (m)	Midpoint Depth (m bgl*)	Mean Δt** (μs/ft)	E_A*** (m)	E_A*** (m)
Daralingie-15													1483.3	97.8	217.4	1788.6	81.9	640.5	1857.8	77.3	427.3	428.4
Daralingie-23	727.9	130.4	229.7	941.4	116.3	141.8	1090.6	119.2	122.3	1320.7	111.0	231.0	1496.3	95.8	264.2	1791.5	83.1	580.9	1863.2	78.3	366.8	276.7
Darter-1	683.9	140.0	82.2	1001.4	116.3	82.5	1172.4	118.3	58.0	1452.9	110.5	112.5	1643.9	95.0	139.4	2000.9	80.8	480.6	2153.6	77.4	129.9	155.0
Della-7													1353.6	96.8	376.3	1695.6	76.4	999.6	1781.1	72.9	750.4	708.7
Della-10				674.6	114.4	434.4	860.4	117.6	383.8	1157.3	108.1	474.6	1338.4	94.7	454.1	1670.6	79.0	896.1	1755.8	74.2	703.5	557.8
Denley-1	498.5	132.9	410.1	931.9	99.0	382.7	1200.9	105.8	277.9	1502.7	94.5	508.7	1660.9	84.3	445.4	2005.6	82.2	407.7	2149.5	68.4	632.2	437.8
Deparanie-1										1402.0	110.2	172.1	1623.4	94.4	178.1	1970.9	84.1	351.4	2086.0	77.1	209.9	227.9
Deramookoo-1	558.1	142.7	155.1	979.3	116.3	103.9	1195.1	111.6	167.7	1503.1	108.9	105.3	1716.6	92.4	146.1	2058.1	82.4	348.1	2203.1	73.5	297.4	189.1
Dirkala-2													1343.9	97.6	362.6	1627.6	86.7	570.1	1689.0	85.5	139.7	357.5
Doonmulla-1							1153.9	112.7	186.6	1456.9	102.4	335.8	1642.0	88.0	351.9	1987.3	82.4	417.0	2128.7	71.4	489.2	356.5
Dullingari-3													1445.5	94.4	356.3	1800.6	80.2	707.2	1870.4	76.2	477.2	513.6
Dullingari North-1																						
Dunoon-1	391.5	144.9	278.6	565.3	130.8	324.7	732.8	131.6	230.9	973.9	120.9	299.5	1109.0	102.7	443.4				1423.4	78.7	786.0	393.9
Durham Downs-1																1866.2	81.7	574.0	1999.5	73.8	482.2	528.1
Echuburra North-1	462.0	135.8	389.0	658.2	115.0	443.4	845.2	117.1	407.8	1155.1	109.9	426.5	1342.2	92.5	515.1	1699.1	75.8	1021.3	1747.5	71.0	888.5	584.5
Fly Lake-1				1004.3	122.2	0.0 (R*)	1156.7	118.7	64.8	1471.8	109.4	123.8	1714.0	92.2	154.0	2068.0	81.6	374.2	2228.8	75.8	140.7	142.9
Fly Lake-4																2087.1	80.2	423.0	2239.4	74.8	186.6	304.8
Garanjanie-2	567.8	143.4	130.3	780.1	122.5	220.6	960.3	125.1	133.7	1193.8	115.1	241.7	1340.5	100.3	284.7	1629.6	84.5	675.9	1686.9	84.9	175.1	266.0
Gidgealpa-20	541.3	138.4	257.5	850.5	111.8	293.9	973.7	121.0	202.1	1247.1	112.6	257.6	1465.8	92.3	399.0	1801.7	82.4	603.8	1869.2	77.5	404.9	345.5
Gidgealpa-42	671.8	135.5	185.3	849.2	115.8	241.3	1012.5	123.6	111.5	1283.8	113.9	186.3	1464.6	98.9	203.1	1808.7	81.6	635.5	1903.8	78.8	300.0	266.1
Gidgee-1				547.8	128.0	378.6	770.0	125.7	312.5	1010.3	117.8	351.2	1125.2	101.2	470.7				1477.5	81.8	561.0	414.8
Gooranie-1	615.4	136.5	220.9	981.3	111.5	166.5	1140.1	112.8	198.8	1456.2	110.5	107.6	1681.0	95.0	103.0	2046.7	80.5	448.4	2177.8	75.9	187.2	204.6
Gooranie-2													1682.5	92.7	170.1	2069.7	82.5	329.8	2188.9	74.8	236.3	245.4
Graham-1	338.4	136.8	492.7	500.8	114.3	608.9	645.8	125.9	431.8	929.3	114.4	526.6	1139.5	95.3	635.2	1481.3	82.4	920.8	1542.0	79.8	607.3	603.4
Gurra-1				552.4	134.6	286.9	701.5	138.9	116.8	875.7	132.1	85.4	983.9	111.2	311.7							200.2
Haddon Downs-1	410.8	133.1	493.2	631.3	117.1	441.5	825.3	117.3	424.9	1118.1	104.4	616.3	1258.6	92.5	599.9	1542.8	86.1	682.9	1701.8	73.7	783.9	577.5
Hammond-1	525.1	132.6	388.5	902.8	103.6	350.7	1138.7	108.8	280.3	1463.2	102.4	327.8	1629.9	88.8	339.0	2005.6	82.6	389.0	2150.2	66.9	713.3	398.4
Hooley-1	257.2	133.9	630.7	376.9	116.8	700.6	520.3	122.2	632.5	803.4	109.8	781.6	997.1	94.6	798.5	1346.8	85.7	900.1	1424.6	77.4	856.8	757.3
Hume-1	506.7	135.9	341.8	748.4	111.7	396.9	928.9	114.6	373.8	1194.1	107.3	460.1	1377.1	90.0	556.6	1706.1	86.8	488.8	1748.3	77.5	529.3	449.6
Hydra-1	422.0	141.6	312.4	569.5	122.2	434.6	734.5	121.1	440.1				1170.2	97.7	532.2	1497.8	84.0	828.9	1527.8	79.2	655.2	533.9
Ingella-1																1979.0	82.3	430.0	2122.0	70.0	572.5	501.3
Innamincka-3																1525.2	84.3	788.8	1643.3	79.1	544.2	666.5
Innamincka-4	382.6	126.9	644.9	557.8	108.1	635.1	692.1	115.8	586.9	996.4	109.7	592.0	1228.8	90.9	676.7	1595.5	82.6	799.4	1712.4	74.5	728.3	666.2
Jack Lake-2	649.1	138.0	157.9	1048.1	110.2	117.3	1254.6	115.1	38.4	1533.2	108.4	90.4	1696.1	94.4	106.1	2065.0	82.6	330.5	2178.3	77.1	118.8	137.1
Jackson-1													1055.8	98.0	637.8	1402.2	79.9	1122.5	1459.1	82.1	563.3	774.5
Jackson South-1	283.7	138.0	523.6	422.3	123.0	571.1	594.0	127.9	444.9	858.2	117.1	522.5	1035.5	101.9	540.0	1396.9	79.7	1139.1	1454.6	79.9	687.4	632.7
James-1	615.7	131.2	325.8	906.0	109.0	275.4	1107.2	110.0	287.1	1413.7	103.7	340.4	1578.7	90.4	341.4	1912.6	83.6	433.1	2067.0	70.6	594.9	371.2
Jarrar-1	544.5	134.8	326.5	737.3	114.5	369.9	883.9	118.9	334.1	1118.7	111.4	419.9	1405.7	93.3	430.2	1774.5	82.1	645.2	1826.3	73.3	681.0	458.1
Johba-1	485.8	136.1	359.6	692.8	118.7	358.9	808.8	120.0	387.2	1134.0	106.9	532.8	1329.5	92.8	519.5				1737.3	72.3	825.4	497.2
Kalladeina-1	537.4	140.0	228.5	731.2	126.2	220.3	877.5	129.0	139.1	1146.0	118.8	185.7	1314.1	105.0	167.6	1652.8	87.4	511.5	1820.7	83.6	117.4	224.3
Karmona-2	539.7	130.9	409.0	682.1	117.5	385.3	851.8	115.2	439.3	1195.4	109.7	393.0	1434.1	92.6	421.8	1791.0	82.3	617.0	1887.9	76.2	460.4	446.6
Karwin-1	356.8	136.4	482.0	534.7	120.9	487.8	735.1	126.6	329.0	1029.6	114.0	437.1	1209.3	96.3	534.9	1563.3	79.7	970.9	1626.2	79.2	553.8	542.2
Keeto-2	647.1	136.6	187.5	788.6	120.1	244.3	955.5	120.6	228.0	1201.5	111.1	346.5	1363.0	99.7	278.2	1689.2	83.2	676.8	1732.8	80.6	369.4	332.8
Keilor-1	465.0	134.4	413.3	784.7	112.9	344.4	953.9	115.0	342.0	1285.3	106.7	386.6	1508.6	88.8	459.9	1878.2	82.8	508.8	1986.1	73.3	521.9	425.3
Kenny-1	592.7	136.7	239.0	1042.7	107.3	161.5	1250.7	111.3	118.6	1559.7	102.7	223.2	1753.1	87.4	259.0	2092.5	81.7	344.6	2248.5	71.8	343.4	241.3
Kercummurra-1	246.3	131.3	694.5	342.0	113.7	776.9	488.6	121.9	669.0	774.9	110.3	794.0	986.0	92.0	886.3	1351.0	85.1	925.5	1442.6	76.9	867.7	802.0
Kerna-5	640.9	135.2	220.9	807.4	117.8	256.7	983.9	119.4	224.1	1279.1	109.5	312.5	1481.3	94.7	312.1	1825.5	81.8	608.3	1870.0	77.1	429.7	337.7
Kirby-1	537.9	136.7	295.3	839.9	106.1	380.0	1000.9	108.9	415.4	1390.4	103.1	380.7	1629.4	86.6	405.2	2010.9	80.9	464.7	2113.9	75.6	269.5	373.0
Kirby-2	512.2	130.8	438.6	839.7	106.6	373.3	1039.9	110.2	352.2	1382.9	102.4	407.9	1610.4	87.4	402.7	1997.3	80.5	499.5	2103.9	72.9	430.4	415.0
Kiwarrick-1	499.2	138.5	297.7	673.3	124.5	300.1	831.9	124.6	272.1	1059.4	115.3	371.5	1195.3	96.8	533.9	1518.5	83.1	851.0	1567.4	81.9	462.0	441.2
Kobari-1	451.4	144.5	225.1	632.6	122.9	363.3	809.5	128.5	217.2	1043.8	117.5	325.7	1172.1	94.1	638.8	1451.6	88.8	646.1	1499.6	86.3	285.2	385.9

Table 1. Continued.

	Winton Formation			Mackunda Formation			Allaru Mudstone-Oodnadatta Formation			Bulldog Shale-Wallumbilla Formation			Cadna-owie Formation			Birdhead Formation			Hutton Sandstone			Mean[1]
Well	Midpoint Depth (m bgl*)	Mean Δt** (μs/ft)	E_A*** (m)	Midpoint Depth (m bgl*)	Mean Δt** (μs/ft)	E_A*** (m)	Midpoint Depth (m bgl*)	Mean Δt** (μs/ft)	E_A*** (m)	Midpoint Depth (m bgl*)	Mean Δt** (μs/ft)	E_A*** (m)	Midpoint Depth (m bgl*)	Mean Δt** (μs/ft)	E_A*** (m)	Midpoint Depth (m bgl*)	Mean Δt** (μs/ft)	E_A*** (m)	Midpoint Depth (m bgl*)	Mean Δt** (μs/ft)	E_A*** (m)	E_A*** (m)
Koonchera-1	518.5	136.2	323.4	696.3	120.3	333.5	849.8	123.7	272.2	1122.8	115.1	313.6	1300.3	97.5	408.7	1609.3	85.9	624.5	1795.3	75.4	598.5	410.6
Kumbarie-1				615.9	137.1	189.5	768.9	140.4	20.0	963.8	123.2	245.1	1088.0	102.9	458.3							228.2
Kurunda-1	678.1	136.5	158.5	927.1	114.5	180.9	1123.8	118.9	95.0	1426.0	109.7	160.2	1575.6	93.3	258.6	1913.3	80.7	570.3	2024.6	76.6	299.0	246.1
Kutyo-1	621.9	137.9	187.5	790.8	117.3	279.2	938.0	119.0	278.5	1257.4	109.3	341.8	1453.6	93.7	368.1	1814.4	80.1	701.0	1869.0	72.6	681.3	405.3
Lake Mcmillan-1	754.3	133.8	135.0	1149.2	106.5	65.6	1312.5	112.0	42.9	1624.6	105.9	69.9	1848.0	90.8	60.5	2212.7	79.6	324.5	2353.5	72.9	177.1	125.1
Lambda-1	405.4	135.1	459.2	634.5	115.9	454.8	820.1	116.2	452.0	1070.3	109.7	515.8	1240.7	89.3	712.8	1558.8	85.4	703.3				549.7
Lhotsky-1	585.4	136.7	246.7	750.4	122.0	256.7	902.9	124.0	212.4	1143.2	117.2	234.2	1288.4	102.6	267.4	1627.2	89.2	451.2	1760.2	83.1	202.2	267.2
Limestone Creek-9										1021.2	119.0	305.3	1157.7	98.7	513.6							409.5
Lycium-1	628.9	135.3	232.0	796.9	125.2	167.9	936.4	126.0	139.4	1204.4	117.5	165.4	1401.1	101.9	174.4	1757.8	82.9	622.1	1865.7	80.4	251.9	250.4
Macadama-1	508.8	136.2	333.2	889.3	109.7	283.2	1029.8	111.2	341.1	1373.3	107.9	265.0	1622.4	89.3	333.3	1992.2	82.8	394.6	2112.3	73.2	400.7	335.9
Mackillop-1	605.0	128.2	397.6	893.1	103.7	358.8	1093.1	110.8	285.7	1421.3	100.9	413.1	1568.5	88.1	421.0	1891.6	81.1	577.1	2045.2	69.6	670.0	446.2
Marabooka-2	525.5	140.4	232.4	712.7	120.0	320.9	899.6	121.2	272.9	1196.2	109.3	401.0	1368.8	99.6	276.1	1712.0	81.7	726.6	1781.8	76.0	578.4	401.2
Marengo-1	747.3	119.9	420.3	1033.4	102.4	236.6	1270.8	104.2	240.4	1607.3	95.2	385.0	1799.5	83.2	337.3	2161.2	78.8	416.9	2306.3	69.1	440.0	353.8
Marsilea-1	624.6	133.1	280.2	783.1	118.6	269.2	973.7	117.9	263.4	1241.4	109.2	358.4	1397.3	93.2	439.3	1739.4	81.4	714.5	1773.4	77.0	532.7	408.2
Mawson-1	663.6	136.6	171.5	888.9	121.6	124.3	1110.4	119.5	95.3	1434.1	110.6	126.7	1578.9	97.5	128.7	1893.8	81.1	573.1	2012.4	77.1	285.1	214.9
Mckinlay-3	462.9	137.5	353.6	628.9	123.7	356.3	782.2	128.0	253.7	1011.7	117.2	364.7	1153.0	99.1	507.1	1469.9	85.3	792.9	1506.0	82.6	485.8	444.9
Mcleod-1													1670.0	84.0	443.2	2046.4	78.1	566.5	2142.6	70.2	542.1	517.3
Meeba-1				864.9	106.5	349.8	1098.7	109.5	305.6	1380.0	98.3	526.0	1543.7	88.5	435.7	1872.8	82.4	531.6	2034.1	65.4	917.8	438.1
Meranji-1	587.7	135.9	260.3	1013.1	113.3	110.8	1167.1	116.4	101.0	1426.2	108.6	191.2	1634.6	95.0	148.8	1982.4	81.1	483.5	2105.6	77.5	172.6	209.8
Merrimelia-7	583.4	139.9	184.7	918.3	113.0	209.7	1047.1	121.9	111.1	1317.2	114.2	144.5	1532.7	97.8	167.1	1874.8	83.4	481.6	1981.8	77.5	294.1	227.6
Merrimelia-25													1559.8	91.9	316.7	1881.2	84.3	433.3	1987.3	77.3	298.5	349.5
Minkie-1	727.8	126.2	314.6	960.8	103.0	301.1	1121.5	116.3	147.8	1387.0	113.6	90.0	1555.0	93.0	287.4	1905.8	80.3	598.9	2014.6	76.4	325.2	295.0
Mooliampah-1	361.0	143.0	346.7	585.1	121.1	435.0	763.4	123.2	369.0	1019.4	114.1	443.4	1186.7	98.3	496.5	1513.2	83.3	845.5	1548.2	78.7	658.8	513.6
Moolion-1	713.9	132.5	202.3	1105.5	105.8	118.4	1279.8	110.6	103.6	1579.9	106.6	94.9	1804.1	90.9	103.7	2183.1	78.0	433.0	2323.2	73.1	198.4	179.2
Moomba-27													1720.6	92.1	148.9	2067.3	81.6	374.2	2171.4	70.7	482.2	335.1
Moomba-57	647.0	135.4	212.3	1004.5	103.9	244.4	1199.3	111.1	173.5	1507.8	102.9	268.8	1694.6	90.6	219.6	2011.0	79.5	533.6	2096.2	69.6	617.9	324.3
Moomba North-1	781.9	123.3	318.1	1044.2	99.3	267.2	1222.6	107.7	219.4	1514.0	103.0	260.9	1703.9	89.1	257.8	2029.7	80.4	470.7	2139.1	68.7	624.7	345.5
Moomba South-1													1686.4	92.5	170.8	2013.4	79.4	534.9	2109.3	68.9	643.0	449.5
Moorari-4																2158.4	81.8	273.6	2285.7	75.1	125.9	199.7
Morney-1	300.4	126.3	739.3	385.4	113.0	742.0	566.4	122.4	582.0	859.0	105.7	839.9	995.4	93.1	844.0	1332.7	85.8	909.6	1472.9	72.0	1109.2	823.7
Mudera-3	574.5	132.4	343.2	744.3	115.8	346.1	921.6	119.2	290.4	1224.7	109.1	379.2	1412.0	93.2	424.7	1763.1	80.4	735.6	1829.3	73.9	649.5	452.7
Munkah-2	447.7	135.7	404.6	696.5	113.5	424.7	865.9	119.1	347.4	1170.7	111.0	378.7	1390.3	93.1	451.5	1766.6	84.9	518.2	1854.4	75.7	520.6	435.1
Munkarie South-1	336.5	144.7	336.7	533.5	125.7	424.3	682.4	127.0	373.8	920.7	115.0	518.9	1084.8	100.1	545.5	1404.9	86.8	786.8	1429.4	79.1	756.0	534.6
Munro-1	419.2	138.4	378.8	556.3	128.3	367.1	717.8	126.6	346.2	958.4	117.6	407.3	1109.8	101.5	479.1				1459.4	81.7	582.6	426.9
Muteroo-3	525.7	141.4	213.5	808.8	108.1	383.9	990.9	120.1	202.9	1244.7	110.1	331.3	1365.0	93.0	477.0	1677.3	82.9	703.9				385.4
Naccowlah East-1	497.0	137.6	318.0	694.5	117.1	378.5	836.2	123.6	288.0	1120.2	112.9	376.2	1343.0	95.2	434.7	1699.0	83.2	666.4	1783.4	78.4	440.1	414.5
Naccowlah South-1	409.6	139.9	359.5	649.6	121.4	366.1	808.7	121.9	348.8	1093.1	111.1	455.7	1303.7	94.0	510.7	1653.4	82.1	763.3	1722.6	80.2	403.2	458.2
Naccowlah West-1	389.0	139.3	392.7	633.9	119.6	405.1	813.6	122.6	331.5	1096.3	112.7	407.7	1304.3	93.4	528.2	1661.2	80.9	813.4	1731.9	78.3	500.3	482.7
Naryilco-1				402.2	136.3	413.6	555.7	134.3	355.7	828.6	120.9	444.9	1014.8	103.2	521.6				1370.8	83.4	576.1	462.3
Navalla-1							407.9	114.6	895.4	739.6	108.6	877.9	962.3	91.3	933.2	1314.0	82.1	1103.8	1428.8	73.9	1048.5	971.8
Nulla-1	561.4	138.6	233.2	958.8	111.5	188.8	1112.2	117.0	142.8	1361.6	112.1	157.0	1627.8	93.7	193.6	1998.7	81.1	469.3	2137.1	76.0	223.8	229.8
Okotoko-1	478.8	132.7	434.1	698.8	106.3	519.2	828.0	117.0	427.9	1149.6	108.6	468.1	1376.9	92.5	480.9	1732.9	82.6	659.4	1825.0	74.3	628.7	516.9
Orientos-2	433.8	137.9	374.9	623.8	118.0	437.4	788.1	118.9	429.8	1053.1	114.0	414.1	1254.3	86.7	778.4							486.9
Packsaddle-4	506.3	133.6	388.1	739.4	111.2	412.0	872.0	117.1	381.1	1173.3	112.1	347.5	1394.0	94.6	400.0	1736.1	78.7	846.9	1848.2	77.5	426.4	457.4
Padulla-1	384.9	142.6	329.3	627.4	128.6	291.8	788.0	130.2	205.0	993.2	120.0	304.3	1098.3	100.6	518.3				1433.2	79.5	730.4	396.5
Pallano-1	512.7	133.8	377.2	752.9	114.5	354.8	900.5	117.6	343.9	1222.1	108.4	400.9	1414.6	94.9	372.8	1773.9	80.7	710.6	1828.5	74.5	611.8	453.1
Pandieburra-1													1296.1	98.1	393.7	1580.1	87.7	567.1				480.4
Pando South-1	541.1	141.7	191.1	698.9	125.0	268.6	871.9	127.0	184.4	1128.5	115.1	307.6	1255.6	101.7	325.1	1554.8	88.0	579.8	1633.3	83.3	319.2	310.8
Paning-1				918.2	109.8	252.4	1082.6	115.3	207.1	1411.3	106.3	270.6	1666.7	89.8	272.7	2037.1	85.1	239.4	2186.9	74.1	277.7	253.3
Paragilga-1	412.9	140.7	340.2	538.5	120.4	489.8	705.1	126.0	371.2	956.6	118.6	380.2	1107.2	103.8	411.4	1441.3	87.7	708.5	1467.6	81.7	574.8	468.0
Patroclus-1				757.6	114.7	347.6	926.3	117.2	324.6	1314.3	106.9	352.2	1404.2	95.3	369.3	1738.5	85.1	533.6	1788.0	78.4	436.3	393.9
Paxton-1				400.4	141.4	346.9	559.5	136.0	317.8	726.3	133.8	186.3	815.8	114.2	391.1							310.5

Table 1. Continued.

	Winton Formation			Mackunda Formation			Allaru Mudstone-Oodnadatta Formation			Bulldog Shale-Wallumbilla Formation			Cadna-owie Formation			Birkhead Formation			Hutton Sandstone			Mean*
Well	Midpoint Depth (m bgl*)	Mean Δt ** (μs/ft)	E_A *** (m)	Midpoint Depth (m bgl*)	Mean Δt ** (μs/ft)	E_A *** (m)	Midpoint Depth (m bgl*)	Mean Δt ** (μs/ft)	E_A *** (m)	Midpoint Depth (m bgl*)	Mean Δt ** (μs/ft)	E_A *** (m)	Midpoint Depth (m bgl*)	Mean Δt ** (μs/ft)	E_A *** (m)	Midpoint Depth (m bgl*)	Mean Δt ** (μs/ft)	E_A *** (m)	Midpoint Depth (m bgl*)	Mean Δt ** (μs/ft)	E_A *** (m)	E_A *** (m)
Pepita-2	551.1	133.0	354.0	740.5	109.4	435.4	884.3	118.7	337.7	1188.2	110.3	383.0	1423.2	97.0	301.5	1773.6	80.4	729.1	1884.6	76.0	475.8	430.9
Pintari-1	499.8	138.8	290.2	759.5	123.6	227.0	919.6	123.1	214.9	1125.8	117.2	251.0	1239.5	98.2	448.0	1541.7	92.0	398.6	1643.0	84.2	258.7	298.4
Pondrinie-5	627.8	130.4	329.2	812.8	110.8	345.1	936.2	116.1	337.9	1206.2	112.7	297.2	1432.4	98.0	259.4	1790.4	81.7	645.9	1900.3	79.7	255.0	352.8
Potiron-1	378.4	132.3	540.6	573.2	112.1	567.2	781.7	113.5	542.9	1109.1	102.1	690.8	1256.6	88.2	729.7	1568.1	84.9	717.5	1748.4	68.7	1017.6	686.6
Putamurdie-1										1105.9	111.1	441.2	1218.4	99.5	431.0	1491.8	87.4	669.8	1626.6	77.9	626.5	542.1
Rheims-1	423.8	138.4	374.0	574.4	122.6	425.1	732.6	123.6	391.8	1019.8	112.2	498.0	1185.8	97.0	536.2	1517.8	86.8	676.3	1550.1	83.0	420.1	474.5
Rho East-1	381.9	140.7	371.1	482.6	118.7	569.0	644.2	128.0	393.1	906.6	116.6	488.0	1071.2	99.6	574.0	1407.4	83.7	933.3	1429.4	80.2	696.9	575.1
Richie-1	280.2	136.1	564.9	425.0	123.7	560.2	630.8	127.1	423.5	916.1	115.0	523.4	1087.1	97.8	611.0	1446.1	81.6	997.4	1496.1	81.6	553.3	604.8
Russel-1	588.1	130.3	372.1	1031.9	98.4	291.6	1225.3	110.6	158.1	1534.7	102.4	257.8	1707.8	90.0	224.5	2106.8	79.5	434.9	2256.1	66.7	622.5	337.4
Snake Hole-1	606.8	140.8	144.1	928.4	111.8	215.8	1145.4	117.1	108.4	1453.9	108.5	165.4	1597.5	97.7	106.3	1929.2	82.1	489.9	2040.6	80.3	78.6	186.9
Spectre-1	814.6	131.2	127.2	1064.4	109.8	106.3	1235.8	113.3	93.4	1552.7	106.6	121.7	1773.3	91.5	113.8	2146.7	80.5	348.8	2278.8	75.4	112.3	146.2
Spencer-4	446.3	147.0	181.2	778.8	119.2	266.0	920.7	119.8	278.8	1192.4	111.8	335.4	1331.7	95.5	437.9	1640.6	84.7	651.5	1743.2	80.9	344.2	356.4
Steward-1	464.4	131.2	476.7	698.5	116.3	385.6	897.7	117.3	351.3	1213.0	104.5	519.0	1358.1	91.2	540.9	1733.4	84.0	593.7	1877.0	71.6	728.6	513.7
Strzelecki-10	457.5	142.1	267.0	744.9	117.6	320.9	923.8	123.8	196.4	1180.6	113.1	312.2	1354.7	97.8	345.4	1719.5	77.3	928.6	1778.4	74.4	668.7	434.2
Strzelecki -27	531.4	134.7	341.6	720.2	113.4	401.9	897.4	118.1	337.1	1163.4	113.9	306.7	1333.0	101.7	248.8	1655.1	87.5	504.1	1707.9	78.0	539.8	382.9
Sturt-6	549.0	140.4	209.1	794.2	119.3	249.4	974.0	125.5	112.6	1206.2	112.8	295.3	1332.7	99.9	304.3	1648.1	83.9	684.7	1745.9	80.9	340.5	313.7
Swan Lake-1													1727.5	88.1	263.3	2089.6	78.6	496.4	2208.3	73.4	293.6	351.1
Taloola-1	563.9	140.0	203.7	782.5	120.8	240.6	950.6	122.5	195.5	1193.2	113.6	286.0	1326.2	100.3	296.5	1649.8	80.7	838.4	1746.1	78.2	492.5	364.7
Tanbar-1																2107.9	80.3	395.7	2262.2	70.9	381.9	388.8
Tanbar North-1																2074.2	79.4	475.0	2225.0	64.5	775.3	625.2
Tartulla-1																1877.6	81.8	554.0	1972.2	74.7	457.6	505.8
Tennaperra South-1	380.0	141.6	354.2	639.5	116.2	444.9	872.1	115.5	413.1	1115.9	107.7	527.1	1315.2	96.4	426.0	1656.3	83.0	719.6	1692.1	74.6	746.6	518.8
Three Queens-1	406.7	139.2	375.1	693.2	110.3	470.1	872.2	115.5	412.5	1209.3	108.1	422.3	1410.3	93.8	410.3	1777.4	80.8	706.2	1871.3	75.1	540.4	476.7
Thurakinna-5	712.8	142.7	0.0 (R*)	883.0	118.7	168.7	1050.2	120.9	127.4	1331.7	110.2	241.7	1487.7	94.8	300.3	1782.2	79.9	744.0	1834.6	77.7	431.0	287.6
Thurra-1	418.7	139.7	354.4	652.0	120.4	376.5	858.7	118.9	358.4	1142.2	110.6	420.4	1314.6	95.4	456.6	1685.3	81.3	772.3	1755.8	76.5	577.9	473.8
Tinchoo-1	655.5	125.7	395.5	864.0	108.8	320.2	1055.3	111.6	308.5	1377.1	105.2	337.2	1593.8	88.1	397.0	1944.7	81.7	494.8	2099.9	69.9	601.3	407.8
Tinga Tingana-1	495.6	153.6	0.0 (R*)	625.9	134.3	217.4	744.8	142.6	0.0 (R*)	942.1	132.2	15.4	1086.2	118.2	0.0 (R*)	1374.9	103.8	0.0 (R*)	1388.1	93.5	0.0 (R*)	33.2
Tinpilla-1	312.1	138.5	484.5	473.5	119.8	562.9	664.8	127.8	375.8	949.1	114.6	502.1	1136.3	94.8	653.5	1487.0	80.3	1019.3	1547.9	80.2	576.5	596.4
Tirrawarra-13																2047.7	81.7	392.6	2192.6	75.1	219.3	306.0
Tirrawarra-15																2024.8	82.6	370.6	2176.4	75.9	187.9	279.2
Tirrawarra-26																2048.3	80.2	459.6	2208.6	74.4	238.5	349.0
Tirrawarra North-1	678.2	133.2	224.4	1046.5	105.4	182.7	1207.0	114.1	106.3	1513.6	109.2	87.5	1739.8	93.3	95.7	2124.8	80.2	384.5	2267.1	73.8	215.6	185.3
Tirrawarra West-1	640.7	138.9	148.4	997.9	112.2	140.2	1165.6	117.9	72.2	1489.9	109.0	116.2	1716.3	92.3	147.6	2089.0	81.5	359.8	2227.9	74.8	196.3	168.7
Toby-1	281.1	130.0	684.9	371.1	117.5	696.0	563.6	114.6	740.9	916.5	108.4	706.3	1134.3	91.0	769.0	1519.3	79.2	1038.6	1638.6	70.9	1003.6	805.6
Toolachee-9				754.9	113.8	362.0	933.7	118.3	295.7	1189.4	110.5	374.2	1349.3	94.1	460.9	1680.3	84.4	628.7	1728.6	77.4	550.4	445.3
Toolachee-21	545.3	136.1	298.8	753.9	123.6	232.2	927.6	121.6	236.6	1192.8	111.1	355.0	1359.4	95.4	412.6	1689.4	81.9	740.4	1747.6	78.0	503.0	396.9
Toolachee-39	481.7	145.1	184.5	739.9	112.3	397.7	916.7	119.2	294.3	1207.9	110.0	370.8	1378.8	94.9	407.3	1697.4	79.9	828.0	1752.6	76.6	574.4	436.7
Turban-1	585.4	124.4	492.1	712.5	111.3	437.7	860.3	115.5	424.7	1156.6	111.0	394.3	1382.3	93.3	450.8	1761.3	83.0	611.9	1884.9	77.6	387.4	457.0
Ullenbury-1	465.8	134.5	411.3	777.4	109.6	395.8	1078.1	112.0	276.4	1389.6	101.1	437.8	1552.2	86.0	502.1	1911.7	82.9	466.2	2064.1	69.1	681.2	453.0
Wackett-3	435.4	137.6	379.6	623.1	115.1	476.8	793.3	119.2	419.0	1083.2	113.1	407.9	1282.1	96.0	471.5	1643.3	84.4	666.1	1714.6	77.6	558.8	482.8
Wallawanny-1													1409.3	94.3	394.2	1782.8	82.5	616.7	1830.7	75.5	559.1	523.3
Wancoocha-2	554.1	139.9	215.5	750.4	123.3	240.0	907.4	126.4	160.1	1122.0	115.1	315.2	1263.2	98.1	426.0	1550.2	86.8	640.2	1612.2	73.9	862.2	408.4
Wantana-2	648.9	135.5	207.9	859.0	118.4	197.1	1070.2	113.2	261.3	1401.5	107.9	236.5	1647.8	87.7	355.5	2006.2	80.8	472.7	2130.3	72.7	412.7	306.2
Wareena-1				306.8	110.7	852.0	437.7	120.1	755.5	715.2	112.3	798.3	927.8	91.7	956.0	1294.4	87.5	866.7	1397.5	75.3	998.6	871.2
Warnie East-1	522.7	133.9	365.6	610.2	115.2	488.1	800.9	117.7	441.8	1132.9	108.1	498.4	1320.4	94.7	471.7	1667.1	81.7	771.2	1702.6	74.3	753.8	541.5
Watson-1	427.0	139.7	345.2	561.3	118.2	496.5	750.6	116.4	517.7	1043.5	108.1	588.1	1227.3	91.5	660.3	1568.8	82.3	839.4	1603.9	74.4	843.9	613.0
Weena-1				586.1	135.2	244.8	698.5	143.1	37.6	884.7	134.8	0.0 (R*)										94.1
Wicho-1	654.5	128.5	340.9	972.5	106.1	247.2	1183.9	111.2	187.1	1458.8	101.0	371.6	1624.6	88.0	368.2	1966.6	81.5	481.7	2119.3	70.8	526.9	360.5
Wills-1	428.2	140.4	331.0	591.2	121.0	429.8	773.1	125.2	319.1	1046.7	115.0	392.4	1215.2	99.0	447.0	1570.5	80.9	906.0	1605.2	79.9	539.7	480.7
Wimma-1	879.9	124.1	202.9	1204.3	105.2	27.6	1370.7	111.2	0.0 (R*)	1714.3	105.0	4.8	1969.4	88.8	1.3	2357.4	83.4	0.0 (R*)	2492.8	73.6	0.0 (R*)	33.8
Wippo-2	527.1	134.2	355.1	644.6	124.4	330.6	842.7	117.7	399.1	1188.1	110.1	387.4	1424.2	93.1	416.9	1805.0	80.1	710.0	1886.8	75.7	488.4	441.1

Table 1. Continued.

Well	Winton Formation			Mackunda Formation			Allaru Mudstone-Oodnadatta Formation			Bulldog Shale-Wallumbilla Formation			Cadna-owie Formation			Birkhead Formation			Hutton Sandstone			Mean[‡]
	Midpoint Depth (m bgl*)	Mean Δt** (µs/ft)	E_A*** (m)	Midpoint Depth (m bgl*)	Mean Δt** (µs/ft)	E_A*** (m)	Midpoint Depth (m bgl*)	Mean Δt** (µs/ft)	E_A*** (m)	Midpoint Depth (m bgl*)	Mean Δt** (µs/ft)	E_A*** (m)	Midpoint Depth (m bgl*)	Mean Δt** (µs/ft)	E_A*** (m)	Midpoint Depth (m bgl*)	Mean Δt** (µs/ft)	E_A*** (m)	Midpoint Depth (m bgl*)	Mean Δt** (µs/ft)	E_A*** (m)	E_A*** (m)
Wirha-1	496.8	133.9	391.5	647.9	122.0	359.2	848.2	122.4	300.1	1091.4	114.5	362.0	1246.7	98.2	441.6	1559.3	83.1	809.3	1595.5	78.6	620.0	469.1
Witchetty-1	567.3	137.1	256.9	726.3	120.1	306.9	910.3	118.1	323.3	1175.3	110.9	377.9	1339.5	98.2	348.3	1673.8	81.1	792.4	1734.2	77.8	523.6	418.5
Wompi-1	380.4	138.4	418.0	574.2	117.0	500.4	746.0	124.7	355.7	1021.1	109.5	571.7	1215.1	93.5	612.8	1555.5	81.0	918.3	1582.4	76.6	741.5	588.4
Wuroopie-1	483.3	139.6	292.2	700.8	122.2	304.4	873.3	122.9	264.0	1128.4	114.0	338.8	1260.4	98.5	417.2	1544.5	81.6	899.0	1591.1	79.2	591.0	443.8
Yanbee-1	651.1	128.6	342.8	933.5	108.5	254.8	1104.8	113.3	224.0	1397.5	104.4	336.6	1618.3	90.8	290.8	1953.6	81.6	489.9	2100.5	70.8	548.1	355.3
Yanda-2	520.4	134.8	349.0	759.5	113.2	365.4	919.8	119.3	290.9	1229.3	111.1	318.5	1448.2	92.2	419.7	1827.0	83.8	508.1	1912.7	76.4	422.7	382.0
Yanta-1	605.6	135.6	249.7	898.9	116.5	182.2	1049.4	122.4	99.6	1303.2	112.2	215.1	1472.2	95.7	291.5	1810.1	82.8	573.5	1972.7	77.3	317.3	275.5
Yumba-1	567.1	137.3	253.3	751.9	112.4	383.7	897.6	119.5	307.5	1177.1	109.2	423.5	1406.0	92.1	464.0	1790.7	82.5	607.5	1869.3	76.8	446.8	412.3

Cooper Basin Stratigraphic Units

Well	Nappamerri Group			Toolachee Formation			Roseneath Shale			Murteree Shale			Patchawarra Formation			Mean[‡]
	Midpoint Depth (m bgl*)	Mean Δt** (µs/ft)	E_A*** (m)	Midpoint Depth (m bgl*)	Mean Δt** (µs/ft)	E_A*** (m)	Midpoint Depth (m bgl*)	Mean Δt** (µs/ft)	E_A*** (m)	Midpoint Depth (m bgl*)	Mean Δt** (µs/ft)	E_A*** (m)	Midpoint Depth (m bgl*)	Mean Δt** (µs/ft)	E_A*** (m)	E_A*** (m)
Alkina-1	2379.9	65.3	667.8	2579.0	64.5	991.0							2633.5	65.4	1083.6	914.1
Alwyn-1																
Amyema-1	1824.1	74.2	689.3	1909.2	75.6	786.4	2088.2	74.7	777.2	2211.1	71.9	1080.3	2254.1	73.9	840.9	834.8
Andree-1	2521.2	68.0	365.9	2636.9	69.1	564.1				2721.7	72.1	554.7	2753.9	71.0	552.0	509.2
Araburg-1	2196.0	73.5	358.0													358.0
Arrabury-1				2654.7	69.3	533.1										533.1
Arrakis-1	2101.7	70.4	638.3	2149.8	70.5	947.6	2194.7	75.3	626.8	2273.2	73.3	918.3	2315.0	74.8	716.8	769.5
Atoll-1																
Azolla-1	1775.3	75.8	643.8	1842.6	81.9	348.9	2053.6	76.9	652.5	2191.2	72.9	1025.6	2242.5	72.7	939.4	722.1
Ballera-1	2148.6	65.8	868.5	2280.9	70.0	856.0							2472.1	71.0	839.3	854.6
Baratta-1	1921.5	68.7	920.3	1988.0	77.3	566.7	2079.4	73.4	879.4	2155.3	71.0	1195.9	2197.4	73.6	920.3	896.5
Bardoc-1																
Barrolka-1	2347.1	67.5	565.8	2571.1	70.0	559.5							2622.6	69.9	767.6	631.0
Baryulah-1	2128.2	69.2	686.2	2250.5	70.2	868.5	2359.5	71.5	731.2	2439.5	69.7	998.6	2483.3	69.0	974.3	851.7
Battunga-1	1804.9	76.5	571.1	1918.8	82.7	210.3	1972.1	77.8	670.0	2120.0	75.1	945.7	2183.2	76.8	698.6	619.1
Beanbush-1	2936.2	67.1	3.2							3280.2	65.2	466.7	3395.1	69.7	8.3	159.4
Belah-1	1724.3	71.8	930.1	1827.9	77.3	728.4	1952.7	72.8	1044.8	2026.8	70.5	1355.2	2224.5	71.7	1030.6	1017.8
Biala-1																
Big Lake-26	2171.1	69.4	632.0	2304.8	74.9	438.6	2376.2	72.2	663.2	2499.9	71.7	801.1	2558.4	70.2	805.7	668.1
Big Lake-35	2201.6	67.5	713.3	2347.6	73.8	482.8	2419.5	72.1	628.4	2544.0	71.8	752.4	2605.6	70.3	753.3	666.0
Bogala-1				1740.9	74.8	1015.9	1813.1	78.3	791.8				1900.9	76.2	1024.6	944.1
Boldrewood-1	1774.5	66.8	1181.9	1965.0	67.4	1369.0										1275.5
Bookabourdie-1	2498.3	67.9	390.8										2815.8	71.7	440.7	415.8
Boxwood-1	1705.9	80.1	456.3							1776.7	81.9	822.3	1807.5	84.9	479.2	585.9
Broiga-2	2527.8	69.4	273.5	2668.5	72.9	235.0				2690.5	70.4	701.7	2903.5	73.4	231.0	360.3
Buckinna-1																
Bungee-1	1844.7	75.3	603.8	1930.1	79.0	493.4				2109.3	77.4	801.3	2161.1	76.5	740.6	659.8
Burke-2																
Burley-2	2470.3	66.9	482.7	2701.3	68.8	523.2	2941.9	73.4	15.2	3153.5	73.9	0.0 (R*)	3260.0	71.7	0.0 (R*)	204.2
Bycoe-1				1622.5	83.2	473.5	1663.2	85.5	430.2				1723.8	77.7	1089.2	664.3
Carney-1	1806.6	72.5	811.2	1923.9	76.3	712.3							2062.6	69.7	1341.3	955.0
Challum-1	2162.3	66.8	794.2													794.2
Charo-1																
Childie-1	1794.4	71.9	857.2	1886.0	79.1	533.5				1942.8	75.6	1089.0	1981.9	76.3	937.2	854.2
Cooba-1	2427.6	69.1	388.3	2580.7	72.7	337.9				2662.3	71.0	685.2	2999.2	70.5	346.6	439.5
Cook-1	2401.7	70.2	354.0													354.0

Table 1. Continued.

	Nappamerri Group			Toolachee Formation			Roseneath Shale			Murteree Shale			Patchawarra Formation			Mean[‡]
Well	Midpoint Depth (m bgl*)	Mean Δt ** (µs/ft)	E_A *** (m)	Midpoint Depth (m bgl*)	Mean Δt ** (µs/ft)	E_A *** (m)	Midpoint Depth (m bgl*)	Mean Δt ** (µs/ft)	E_A *** (m)	Midpoint Depth (m bgl*)	Mean Δt ** (µs/ft)	E_A *** (m)	Midpoint Depth (m bgl*)	Mean Δt ** (µs/ft)	E_A *** (m)	E_A *** (m)
Cook North-1	2415.5	68.6	434.3													434.3
Coonavalla-1	1920.9	68.1	957.7										2103.0	69.0	1351.1	1154.4
Cooroo-1				1856.6	73.7	981.7										981.7
Copai-1																
Cowan-3	1992.8	72.1	649.3	2061.9	76.6	547.9	2121.1	76.7	601.6	2205.4	74.2	927.9	2247.7	75.7	715.4	688.4
Cuddapan-1	2406.7	69.8	370.8													370.8
Curalle-1	1722.0	73.4	839.5													839.5
Daer-1	2268.3	67.6	640.7	2348.3	78.5	111.4										376.0
Daralingie-15	1941.9	73.4	622.6	1999.8	78.5	466.6	2074.0	77.4	594.8	2174.3	76.3	813.8	2215.9	78.6	534.7	606.5
Daralingie-23	1952.2	72.8	644.0				2097.8	77.5	565.0	2196.1	75.8	823.6	2233.9	77.6	591.2	655.9
Darter-1	2412.7	72.5	199.9										2628.2	66.9	981.2	590.5
Della-7	1877.8	69.8	896.4													896.4
Della-10	1863.1	68.8	970.7	1961.4	81.0	301.9							1981.4	77.3	863.8	712.1
Denley-1	2504.9	70.1	252.7													252.7
Deparanie-1	2312.0	70.5	425.2	2426.6	74.9	316.6							2437.6	78.7	307.2	349.7
Deramookoo-1																
Dirkala-2				1775.9	81.9	422.5	1819.2	79.5	698.6	1908.4	82.1	681.2	1959.5	83.7	412.1	553.6
Doonmulla-1	2466.9	66.9	482.4													482.4
Dullingari-3	2033.6	71.6	635.2	2169.6	78.1	321.9	2317.2	71.6	767.2	2431.5	70.6	943.6	2498.0	73.1	653.5	664.3
Dullingari North-1	2022.5	69.7	759.3	2155.9	74.6	618.2	2290.6	70.1	898.4	2396.0	69.3	1074.1	2444.1	70.8	877.1	845.4
Dunoon-1																
Durham Downs-1	2309.2	68.2	561.4	2501.8	70.6	584.2							2615.4	74.6	427.1	524.2
Echuburra North-1																
Fly Lake-1	2477.4	69.0	347.0										2801.8	76.4	108.4	227.7
Fly Lake-4	2506.2	69.9	263.1	2637.6	69.5	532.0				2648.6	70.3	750.7	2666.1	73.3	472.2	504.5
Garanjanie-2	1753.1	77.1	590.4	1796.8	80.7	496.4	1837.5	78.8	734.6	1937.8	80.1	785.6	1982.1	79.9	672.7	655.9
Gidgealpa-20																
Gidgealpa-42	2072.0	74.7	414.9	2121.2	78.5	345.7							2134.7	78.8	598.7	453.1
Gidgee-1				1502.1	80.0	843.4				1517.0	80.1	1207.9	1582.4	80.5	1025.4	1025.6
Gooranie-1	2425.9	68.1	455.2	2623.3	69.2	571.9				2670.8	71.7	628.2	2963.3	69.4	460.0	528.8
Gooranie-2	2462.5	68.4	397.2	2621.8	71.6	382.1				2673.7	72.1	604.3	2958.3	71.4	317.4	425.3
Graham-1				1590.0	86.2	268.7	1700.3	81.4	686.6				1790.9	74.8	1236.5	730.6
Gurra-1							1256.7	93.5	263.2	1328.0	100.4	0.0 (R+)				131.6
Haddon Downs-1																
Hammond-1	2527.1	66.0	475.6													475.6
Hooley-1	1533.4	70.8	1185.8													1185.8
Hume-1	1816.3	67.6	1089.0	1897.9	76.9	691.8	2023.1	70.0	1176.7	2091.5	67.1	1526.0	2114.7	77.4	722.5	1041.2
Hydra-1				1633.6	82.0	553.7	1661.3	76.1	1101.8	1728.9	74.9	1352.0	1762.0	74.0	1328.5	1084.0
Ingella-1	2457.9	68.0	426.0													426.0
Innamincka-3	1818.3	69.3	990.6													990.6
Innamincka-4	1926.3	67.7	975.9	2075.5	73.1	816.9										896.4
Jack Lake-2	2374.9	69.8	403.8	2473.8	70.8	595.8	2522.9	73.2	449.3	2600.2	71.5	719.2	2641.3	73.1	513.5	536.3
Jackson-1				1535.4	83.3	548.2	1577.9	83.8	637.1				1668.6	76.2	1257.7	814.3
Jackson South-1				1488.6	80.7	800.5	1546.4	82.1	785.8				1761.1	80.0	886.4	824.2
James-1	2339.5	67.6	565.8													565.8
Jarrar-1																
Johba-1																
Kalladeina-1																
Karmona-2	2079.5	68.8	755.4	2225.0	74.4	558.6							2490.0	70.3	870.3	728.1
Karwin-1				1727.1	80.9	548.8	1928.4	77.2	754.2	2046.7	77.3	872.8	2254.6	73.7	853.1	757.2
Keeto-2	1809.3	76.4	574.7	1874.4	80.8	405.1	2016.5	75.5	787.7	2141.3	74.1	996.7	2184.2	74.3	880.1	728.9
Keilor-1	2243.6	68.7	598.0	2451.1	72.7	472.6							2555.2	71.3	731.3	600.6

Table 1. Continued.

	Nappamerri Group			Toolachee Formation			Roseneath Shale			Murteree Shale			Patchawarra Formation			Mean[#]
Well	Midpoint Depth (m bgl*)	Mean Δt ** (µs/ft)	E_A*** (m)	Midpoint Depth (m bgl*)	Mean Δt ** (µs/ft)	E_A*** (m)	Midpoint Depth (m bgl*)	Mean Δt ** (µs/ft)	E_A*** (m)	Midpoint Depth (m bgl*)	Mean Δt ** (µs/ft)	E_A*** (m)	Midpoint Depth (m bgl*)	Mean Δt ** (µs/ft)	E_A*** (m)	E_A*** (m)
Keany-1	2628.4	66.0	377.5													377.5
Kercummurra-1	1645.6	69.0	1181.6	1832.3	71.1	1213.5										1197.5
Kerna-5	1972.7	72.3	654.6	2058.9	70.7	1016.3	2284.2	73.2	683.6	2467.3	71.8	828.7	2452.1	74.6	589.0	754.5
Kirby-1	2452.9	67.5	462.8	2718.3	75.3	0.0 (R+)	2836.4	71.7	240.6	3032.6	71.4	291.2	3174.3	72.0	61.3	211.2
Kirby-2	2411.7	67.1	529.0	2700.9	70.9	360.7	2845.0	70.9	287.1							392.2
Kiwarrick-1				1681.5	76.4	943.4	1632.5	80.0	855.0	1712.2	80.7	973.2	1661.4	86.1	537.3	827.2
Kobari-1										1580.1	86.2	727.0				727.0
Koonchera-1																
Kumbarie-1										1421.4	90.0	620.9	1448.2	89.8	478.4	549.6
Kurunda-1	2177.9	70.8	537.8	2210.5	72.5	728.1				2276.3	74.5	833.3	2311.2	76.6	586.1	671.3
Kutyo-1				1964.9	76.6	649.8										649.8
Lake Mcmillan-1	2673.6	68.3	192.3	2892.9	67.7	422.8				2945.9	69.2	527.9	3069.9	70.6	263.8	351.7
Lambda-1																
Lhotsky-1																
Limestone Creek-9																
Lycium-1													2140.3	82.2	342.1	342.1
Macadama-1	2412.1	67.2	522.1	2644.7	71.6	363.1							3001.2	71.4	275.0	386.7
Mackillop-1	2400.6	67.3	524.1	2533.9	66.9	840.5										682.3
Marabooka-2	1890.5	69.6	898.7	1943.4	75.6	746.6				1996.7	73.6	1172.8	2162.8	73.2	983.9	950.5
Marengo-1	2737.2	65.3	310.6	2962.9	67.6	359.3										335.0
Marsilea-1	1864.4	73.9	665.0	1955.1	76.8	641.7	2154.5	73.0	833.2	2278.3	70.6	1103.1	2326.8	73.1	826.3	813.9
Mawson-1	2195.5	69.5	597.2	2244.4	74.9	500.0				2271.1	74.4	844.9	2302.6	75.6	663.8	651.5
Mckinlay-3																
Mcleod-1	2422.1	66.6	546.6				2935.7	73.7	0.0 (R+)	3157.3	72.9	64.0	3243.7	69.2	199.6	202.6
Meeba-1	2384.1	68.8	451.8													451.8
Meranji-1	2333.1	69.9	436.1	2470.9	77.6	63.9				2522.7	72.3	736.7	2813.2	74.5	237.1	368.5
Merrimelia-7	2165.1	73.0	420.4													420.4
Merrimelia-25	2199.4	72.0	446.0													446.0
Minkie-1	2221.2	70.2	529.5													529.5
Mooliampah-1				1586.3	82.5	561.0	1658.3	77.3	1020.7	1705.5	76.9	1238.6	1757.2	78.5	999.4	954.9
Moolion-1	2621.9	67.5	289.4	2813.2	66.8	571.0				2842.9	68.4	689.1	2923.0	74.7	115.3	416.2
Moomba-27	2353.5	70.4	389.8	2517.9	75.2	205.7	2627.3	71.0	499.0	2722.5	69.4	739.6	2781.6	66.1	889.6	544.8
Moomba-57	2264.6	68.3	599.1	2384.6	71.2	656.1	2583.1	71.7	493.3	2755.5	71.2	583.8	2819.1	69.0	632.9	593.0
Moomba North-1	2328.1	68.3	535.4	2496.3	76.1	157.7	2619.2	72.4	411.4	2753.2	71.7	547.4	2811.4	69.9	578.0	446.0
Moomba South-1	2256.6	68.7	587.3	2408.8	72.1	556.6	2524.4	71.0	602.2	2677.6	69.7	764.4	2734.5	67.6	820.8	666.2
Moorari-4	2541.0	68.8	296.3							2710.3	69.9	718.0	2849.2	71.2	445.9	486.7
Morney-1	1818.4	72.5	797.7													797.7
Mudera-3	1947.1	68.9	881.1	2028.0	79.9	324.2				2099.0	72.4	1157.8	2152.7	72.7	1028.4	847.9
Munkah-2	2009.2	68.3	855.7	2115.4	73.8	721.1							2297.9	69.9	1089.9	888.9
Munkarie South-1																
Munro-1																
Muteroo-3																
Naccowlah East-1	1851.1	78.6	398.8	1955.5	76.1	693.3	2014.8	76.8	698.1				2065.5	78.7	679.0	617.3
Naccowlah South-1	1796.5	75.6	636.7	1844.0	78.3	636.4										636.5
Naccowlah West-1																
Naryilco-1																
Navalla-1	1707.5	67.3	1216.2													1216.2
Nulla-1	2311.5	70.3	438.2							2409.3	74.5	699.3	2664.6	69.7	736.3	624.6
Okotoko-1	1986.1	68.1	892.5	2166.3	71.0	888.2							2203.8	70.5	1144.2	975.0
Orientos-2																
Packsaddle-4	2032.6	69.1	786.1	2122.5	66.8	1264.1										1025.1
Padulla-1																

Table 1. Continued.

	Nappamerri Group			Toolachee Formation			Roseneath Shale			Murteree Shale			Patchawarra Formation			Mean[‡]
Well	Midpoint Depth (m bgl*)	Mean Δt ** (µs/ft)	E_A*** (m)	Midpoint Depth (m bgl*)	Mean Δt ** (µs/ft)	E_A*** (m)	Midpoint Depth (m bgl*)	Mean Δt ** (µs/ft)	E_A*** (m)	Midpoint Depth (m bgl*)	Mean Δt ** (µs/ft)	E_A*** (m)	Midpoint Depth (m bgl*)	Mean Δt ** (µs/ft)	E_A*** (m)	E_A*** (m)
Paliano-1																
Pandieburra-1																
Pando South-1																
Paning-1	2606.3	67.9	282.5													282.5
Paragilga-1																
Patroclus-1				1858.2	78.0	646.9										646.9
Paxton-1																
Pepita-2	2089.4	67.1	845.9	2229.6	71.7	766.5										806.2
Pintari-1																
Pondrinie-5	2095.8	69.9	676.8	2204.6	76.1	445.7										561.2
Potiron-1	2073.5	63.8	1061.1													1061.1
Putamurdie-1																
Rheims-1				1679.1	82.7	456.1	1712.7	74.8	1142.7							799.4
Rho East-1																
Richie-1							1633.4	82.9	644.8							
Russel-1	2619.5	67.0	323.8	2851.4	63.3	809.4							1802.9	81.5	732.7	688.8
Snake Hole-1	2250.5	73.0	336.6	2325.8	72.7	592.1							2878.1	63.5	980.8	704.7
Spectre-1	2561.4	69.2	253.2	2709.3	69.2	490.5				2394.1	75.9	620.2	2428.9	77.1	427.7	494.2
Spencer-4										2759.2	71.5	557.5	3055.8	68.9	410.1	427.8
Steward-1	2099.8	81.1	0.0 (R*)													0.0
Strzelecki-10	1848.8	71.1	849.8	1890.8	79.1	523.9										
Strzelecki -27										1984.2	73.3	1207.8	2012.1	71.6	1252.1	958.4
Sturt-6																
Swan Lake-1	2409.3	67.4	509.4	2581.7	69.9	560.2										
Taloola-1										2649.8	70.0	772.7	2956.8	67.5	611.1	613.4
Tanbar-1	2636.3	66.3	346.7	2802.6	67.6	523.3										
Tanbar North-1	2575.9	67.1	360.0													435.0
Tartulla-1	2304.8	68.9	625.0	2370.4	75.8	304.1										360.0
Tennaperra South-1				1786.5	79.1	631.6							2525.4	72.3	685.9	538.3
Three Queens-1	2089.9	68.4	772.4	2262.9	74.3	532.5	2427.1	69.0	840.8							631.6
Thurakinna-5	1929.2	71.3	760.2				2088.0	76.6	636.3	2569.7	68.7	940.4	2665.1	68.1	854.8	788.2
Thurra-1	1839.9	75.7	586.4	1877.9	79.8	483.0	1978.2	78.4	620.1	2211.6	75.5	826.4	2259.0	75.8	696.3	729.8
Tinchoo-1	2461.9	66.4	517.9										2068.0	72.2	1154.9	711.1
Tinga Tingana-1							1399.3	95.2	0.0 (R*)	1480.9	93.3	333.3	1657.7	93.5	0.0 (R*)	517.9
Tinpilla-1				1620.9	78.2	861.9	1677.5	80.1	800.8				1789.9	73.9	1302.0	111.1
Tirrawarra-13	2455.8	68.9	371.8										2682.5	70.5	664.9	988.3
Tirrawarra-15	2446.8	69.6	341.1	2585.3	71.0	468.0				2659.4	70.4	733.2	2865.8	71.5	404.5	590.0
Tirrawarra-26	2470.9	69.1	344.9							2646.0	72.1	630.7	2907.1	69.4	516.4	461.1
Tirrawarra North-1	2535.3	69.0	288.2	2720.8	69.8	425.3				2681.2	70.8	681.1	3007.8	72.5	189.6	514.1
Tirrawarra West-1	2496.0	68.4	361.9	2663.9	72.0	309.0				2760.7	70.8	601.5	2730.0	71.6	536.0	376.2
Toby-1	1973.7	66.6	995.6							2700.1	70.6	674.8	2253.3	70.0	1126.9	470.4
Toolachee-9	1823.9	72.1	817.0	1885.5	79.7	486.2	2062.7	74.0	849.8	2175.0	72.0	1105.7	2208.4	69.7	1193.5	1061.2
Toolachee-21	1848.2	73.6	704.1	1910.3	78.6	545.7	2054.5	73.4	902.5	2180.2	72.2	1085.6	2224.2	72.7	961.6	890.4
Toolachee-39	1829.7	73.8	711.1	2034.1	75.0	704.2	2104.0	74.3	785.4	2251.3	71.9	1037.6	2302.1	71.1	1001.3	839.9
Turban-1	2127.2	70.3	622.3													847.9
Ullenbury-1	2452.5	70.0	310.1													622.3
Wacketi-3	1801.2	71.6	870.4	1865.4	78.3	609.7										310.1
Wallawanny-1																740.1
Wancoocha-2																
Wantana-2	2413.9	66.5	561.8							1689.8	78.0	1177.3	1714.6	83.0	711.9	944.6
Wareena-1	1681.2	68.5	1172.2	1851.8	72.1	1112.1							2732.7	69.1	711.5	636.6
Warnie East-1	1857.8	71.3	830.8	2026.4	74.8	725.5	2304.3	71.1	813.2	2426.7	68.6	1089.7	2541.2	66.9	1071.3	1142.1 906.1

Table 1. Continued.

	Nappamerri Group			Toolachee Formation			Roseneath Shale			Murteree Shale			Patchawarra Formation			Mean[‡]
Well	Midpoint Depth (m bgl*)	Mean Δt ** (µs/ft)	E_A *** (m)	Midpoint Depth (m bgl*)	Mean Δt ** (µs/ft)	E_A *** (m)	Midpoint Depth (m bgl*)	Mean Δt ** (µs/ft)	E_A *** (m)	Midpoint Depth (m bgl*)	Mean Δt ** (µs/ft)	E_A *** (m)	Midpoint Depth (m bgl*)	Mean Δt ** (µs/ft)	E_A *** (m)	E_A *** (m)
Watson-1																
Weena-1													1486.1	93.2	190.7	190.7
Wicho-1	2491.6	69.2	320.0	2646.2	70.1	478.5										399.3
Wills-1				1667.9	81.3	575.9	1771.0	75.2	1059.5	1826.8	75.4	1218.7				951.4
Wimma-1	2889.2	67.9	0.0 (R*)							3279.4	66.3	395.5	3348.9	67.6	209.9	201.8
Wippo-2	2079.3	69.8	696.7	2290.8	72.5	647.0							2348.3	69.4	1078.8	807.5
Wirha-1							1715.8	77.8	926.5	1794.1	77.4	1117.1	1861.2	77.3	987.2	1010.3
Witchetty-1	1816.8	71.6	850.0	1880.1	80.4	430.9	2008.3	73.3	956.0	2095.5	72.5	1151.7	2148.1	74.4	910.1	859.7
Wompi-1				1619.4	77.1	950.8	1742.4	72.8	1255.5							1103.1
Wuroopie-1				1634.3	89.0	0.0 (R*)	1754.2	79.3	781.1	1862.9	77.7	1027.7	1923.2	77.7	890.1	674.7
Yanbee-1	2420.9	68.7	419.3													419.3
Yanda-2	2059.0	68.0	824.4	2161.4	71.6	847.1							2342.1	75.9	603.5	758.3
Yanta-1																
Yumba-1	2003.3	68.7	840.8	2081.8	76.6	533.1										687.0

*m bgl = meters below ground level.

**Δt = interval transit time.

***E_A = apparent exhumation.

‡Mean = mean of the apparent exhumation values from such of the Eromanga Basin Formations as are present in any given well.

‡‡Mean = mean of the apparent exhumation values from such of the Cooper Basin Formations as are present in any given well.

R* = reference well, ie. well used to define normal compaction relationship.

Table 2. Midpoint Depth and Mean Adjusted Interval Transit time Data and Apparent Exhumation Results

	Eromanga Basin Stratigraphic Units																					
	Winton Formation			Mackunda Formation			Allaru Mudstone-Oodnadatta Formation			Bulldog Shale-Wallumbilla Formation			Cadna-owie Formation			Birkhead Formation			Hutton Sandstone			Mean[1]
Well	Midpoint Depth (m bgl*)	Mean Δt_{adj}** (µs/ft)	E_A*** (m)	Midpoint Depth (m bgl*)	Mean Δt_{adj}** (µs/ft)	E_A*** (m)	Midpoint Depth (m bgl*)	Mean Δt_{adj}** (µs/ft)	E_A*** (m)	Midpoint Depth (m bgl*)	Mean Δt_{adj}** (µs/ft)	E_A*** (m)	Midpoint Depth (m bgl*)	Mean Δt_{adj}** (µs/ft)	E_A*** (m)	Midpoint Depth (m bgl*)	Mean Δt_{adj}** (µs/ft)	E_A*** (m)	Midpoint Depth (m bgl*)	Mean Δt_{adj}** (µs/ft)	E_A*** (m)	E_A*** (m)
Alkina-1	440.2	133.0	435.2	755.2	105.6	626.1	931.9	109.1	613.8	1271.9	105.4	531.5	1473.9	90.5	538.9	1841.4	82.3	476.3	1977.4	68.0	769.8	570.2
Alwyn-1	443.4	146.1	191.2	613.4	130.7	153.8	785.9	131.7	209.7	1021.7	120.6	311.4	1154.4	99.9	573.8	1461.8	76.1	1113.5	1496.0	83.8	480.2	433.4
Amyema-1	617.1	138.5	156.1	776.8	122.4	192.9	963.8	123.2	239.2	1212.1	111.9	391.4	1374.1	100.2	344.1	1700.7	83.2	580.6	1747.5	76.6	582.2	355.2
Andree-1	696.6	141.7	18.3	1040.6	116.6	73.0	1182.9	121.4	62.2	1512.6	110.3	138.4	1747.0	94.0	160.2	2115.3	80.2	291.9	2246.4	75.8	119.7	123.4
Araburg-1	554.5	130.6	364.2	802.6	115.3	341.5	995.1	115.4	396.9	1299.5	103.2	572.7	1442.0	90.1	581.2	1750.7	84.8	463.7	1909.8	73.5	566.7	469.6
Arrabury-1																						
Arrakis-1	468.1	149.4	104.2	848.2	122.9	109.1	1104.3	123.6	88.5	1387.8	113.5	166.1	1544.7	100.3	169.5	1860.2	79.8	564.1	1964.6	77.6	314.3	216.6
Atoll-1	357.0	150.0	205.4	437.0	131.7	305.9	554.0	135.4	351.8	858.3	115.4	636.7	1041.7	101.5	639.0	1378.6	87.5	722.2	1421.7	81.7	658.9	502.9
Azolla-1	616.5	140.8	115.6	751.9	121.8	232.3	928.5	125.2	224.2	1191.9	116.3	276.6	1337.6	97.6	461.0	1667.3	91.1	287.0	1705.7	80.8	417.8	287.8
Ballera-1	453.9	140.0	292.3	791.0	113.7	393.3	964.0	115.3	430.4	1282.8	114.8	231.3	1514.4	93.0	422.2	1881.3	84.7	339.7	1969.4	70.5	654.7	394.9
Baratta-1	593.0	134.8	248.1	828.0	118.5	238.5	983.0	123.6	209.3	1252.1	112.7	326.5	1427.6	100.0	296.4	1759.2	81.7	585.9	1813.6	74.3	626.0	361.5
Bardoc-1	439.4	148.3	154.0	674.8	121.9	307.7	825.1	123.3	373.2	1155.8	111.1	472.7	1346.8	94.5	545.2	1706.6	80.1	705.3	1758.5	73.1	739.1	471.0
Barrolka-1													1499.9	87.0	617.3	1864.9	81.2	498.4	2020.5	76.6	305.2	473.6
Baryulah-1	489.5	142.7	206.8	857.8	113.6	327.7	1048.4	124.6	119.2	1356.0	109.6	317.6	1572.8	89.8	461.5	1951.1	85.4	240.2	1990.7	73.8	475.8	307.0
Battunga-1	498.5	142.6	199.7	764.9	124.7	149.9	930.3	127.6	165.1	1175.6	116.9	272.8	1334.4	97.8	457.0	1662.5	93.9	173.0	1710.4	84.5	233.6	235.9
Beanbush-1	990.5	126.7	0.0 (R*)	1220.2	112.2	0.0 (R*)		112.5	85.9	1717.3	108.2	0.0 (R*)	1971.1	91.9	0.0 (R*)	2348.4	79.4	89.3	2522.9	71.0	79.8	36.4
Belah-1	431.0	139.6	323.1	666.0	122.7	297.1	858.2	123.5	335.8	1248.6	115.6	239.7	1289.8	97.6	509.2	1625.5	82.6	678.8	1661.0	78.0	598.5	426.0
Biala-1	524.6	137.8	261.6	635.8	128.4	188.4	781.3	132.6	193.1	1017.9	118.7	376.3	1158.1	98.6	607.6				1513.2	84.7	418.9	341.0
Big Lake-26																1952.1	76.2	618.6	2032.7	64.9	864.7	741.6
Big Lake-35	655.1	136.0	163.6	957.3	108.4	355.4	1131.3	113.6	304.2	1443.2	105.0	373.3	1646.5	93.3	280.8	1969.6	82.3	351.2	2053.7	70.8	555.4	340.5
Bogala-1	359.9	140.9	370.0	550.5	117.9	530.9	694.0	125.6	450.3	978.1	117.1	465.1	1195.0	95.1	677.8	1538.8	82.5	771.0	1605.4	77.0	700.7	566.5
Boldrewood-1				291.5	122.7	671.6	869.1	119.7	417.4	824.8	110.8	811.0	1030.2	91.5	952.6	1401.9	85.7	774.9	1508.9	72.7	1010.9	662.6
Bookabourdie-1	682.9	138.0	99.8	1020.9	108.6	287.2	1178.5	116.2	193.1	1481.4	108.4	231.2	1720.1	93.3	208.3	2102.2	80.8	279.1	2231.1	71.8	332.8	233.1
Boxwood-1																						
Brolga-2													1758.5	93.8	155.0	2130.2	81.0	243.3	2257.7	71.9	300.5	232.9
Buckinna-1	507.4	143.1	181.3	682.4	124.3	240.1	834.5	127.2	270.8	1051.0	118.6	344.0	1194.5	100.9	504.1	1520.6	84.3	715.7	1557.5	80.7	571.7	403.9
Bungee-1	545.8	145.2	103.7	802.1	122.8	157.1	1002.8	126.8	112.4	1259.8	116.2	209.2	1403.4	103.8	205.7	1705.5	84.7	511.8	1755.0	81.9	312.4	230.3
Burke-2				791.0	118.7	271.0	993.7	119.0	309.2	1293.5	108.8	406.5	1482.0	93.9	428.8							353.9
Burley-2	578.0	134.1	276.8	926.7	102.2	537.6	1106.7	112.1	364.9	1447.1	100.5	506.4	1687.8	83.5	535.1	2082.2	82.1	243.5	2177.0	73.3	309.7	396.3
Bycoe-1	327.1	136.6	481.6	482.1	117.7	603.0	622.1	128.3	454.8	921.8	118.5	478.4	1135.9	99.0	620.4	1491.7	82.2	831.9	1553.7	79.1	652.5	588.9
Carney-1	444.9	141.7	270.5	642.4	115.3	501.3	798.4	122.0	432.8	1072.9	116.3	393.7	1273.4	97.8	518.9	1635.4	85.2	564.7	1704.4	77.9	560.9	463.3
Challum-1	581.4	136.2	235.3	822.1	112.2	398.2	959.5	117.2	387.5	1282.4	107.8	448.7	1489.4	92.7	457.2	1853.3	84.3	382.6	1967.0	72.4	566.7	410.9
Charo-1	473.3	140.1	271.5	815.2	125.0	92.0	970.4	125.6	172.4	1233.7	120.1	116.3	1426.8	100.2	293.0	1766.5	84.7	450.6	1913.7	80.0	246.0	234.5
Childie-1	443.9	141.2	279.3	699.8	125.0	205.5	889.6	122.5	329.4	1176.7	115.6	311.8	1335.9	98.3	441.1	1659.3	81.5	691.3	1695.8	79.3	501.4	394.3
Cooba-1				985.1	119.2	64.3	1132.3	120.1	145.5	1449.3	110.2	205.4	1675.8	95.8	174.7	2025.0	79.5	412.2	2160.1	76.5	172.2	195.7
Cook-1	517.5	140.8	214.3	916.2	113.7	268.1	1111.2	117.0	240.7	1417.3	107.7	314.2	1591.2	103.6	25.1	1920.4	86.5	224.0	2076.1	69.6	593.1	268.5
Cook North-1	628.0	128.4	331.7	918.7	105.6	463.8	1093.6	110.3	421.8	1404.4	104.7	421.8	1596.7	88.4	478.2	1934.7	79.8	487.6	2067.2	72.6	453.8	436.9
Coonavalla-1	362.8	134.3	488.0	564.1	112.7	643.4	743.6	118.5	571.7	1014.3	109.6	658.6	1209.8	91.4	776.1	1555.0	85.4	635.6	1659.7	69.9	993.7	681.0
Cooroo-1	430.0	140.8	301.8	699.7	116.5	415.5	890.6	120.0	390.0	1183.1	110.9	450.9	1366.0	97.2	442.9	1726.7	81.2	636.7	1781.4	72.2	762.2	485.7
Copai-1	438.9	139.3	320.0	693.9	124.0	236.0	903.4	123.1	300.3	1156.9	106.8	603.3	1285.4	91.8	688.6	1602.3	84.7	617.0	1752.5	74.6	674.0	491.3
Cowan-3																						
Cuddapan-1	571.7	133.0	302.2	851.2	111.3	390.6	1086.7	116.9	267.5	1390.2	99.1	607.4	1546.2	88.5	526.7	1879.2	83.2	402.5	2010.2	69.9	644.3	448.7
Curalle-1				350.4	106.9	999.8	518.9	115.6	867.7	802.9	104.7	1021.1	939.9	91.8	1031.7	1246.9	86.6	893.5	1387.8	72.5	1138.6	992.1
Daer-1	665.8	134.6	179.7	914.8	124.1	13.5	1092.8	121.5	151.2	1371.3	117.3	64.8	1546.3	98.6	222.1	1876.8	85.6	303.6	2046.3	77.7	226.1	165.9
Daralingie-15													1483.3	100.6	224.1	1788.6	84.0	460.8	1857.8	79.5	326.2	337.0
Daralingie-23	727.9	135.8	94.9	941.4	121.1	61.8	1090.6	122.9	119.8	1320.7	114.7	196.7	1496.3	99.3	250.9	1791.5	83.4	481.9	1863.2	79.9	303.5	215.6
Darter-1	683.9	140.7	49.6	1001.4	116.7	109.7	1172.4	119.2	127.0	1452.9	112.5	131.5	1643.9	98.1	139.0	2000.9	82.2	321.6	2153.6	77.4	133.7	144.6
Della-7							860.4	120.4	408.5				1353.6	97.9	433.4	1695.6	75.6	901.6	1781.1	66.9	1019.1	690.6

Table 2. Continued.

	Winton Formation			Mackunda Formation			Allaru Mudstone-Oodnadatta Formation			Bulldog Shale-Wallumbilla Formation			Cadna-owie Formation			Birkhead Formation			Hutton Sandstone			Mean[1]
	Midpoint	Mean		Midpoint	Mean		Midpoint	Mean		Midpoint	Mean		Midpoint	Mean		Midpoint	Mean		Midpoint	Mean		
	Depth	Δt_{sa}[**]	E_A[***]	Depth	Δt_{sa}[**]	E_A[***]	Depth	Δt_{sa}[**]	E_A[***]	Depth	Δt_{sa}[**]	E_A[***]	Depth	Δt_{sa}[**]	E_A[***]	Depth	Δt_{sa}[**]	E_A[***]	Depth	Δt_{sa}[**]	E_A[***]	E_A[***]
Well	(m bgl[*])	(µs/ft)	(m)	(m bgl[*])	(µs/ft)	(m)	(m bgl[*])	(µs/ft)	(m)	(m bgl[*])	(µs/ft)	(m)	(m bgl[*])	(µs/ft)	(m)	(m bgl[*])	(µs/ft)	(m)	(m bgl[*])	(µs/ft)	(m)	(m)
Della-10				674.6	117.3	419.9				1157.3	110.4	491.6	1338.4	94.3	559.6	1670.6	79.4	769.9	1755.8	70.0	894.0	627.0
Denley-1	498.5	136.3	315.1	931.9	103.2	509.5	1200.9	110.1	319.5	1502.7	98.5	514.6	1660.9	85.2	511.0	2005.6	82.2	319.0	2149.5	68.3	583.4	438.9
Deparanie-1							1100.5	120.8	160.3	1402.0	113.7	145.7	1623.4	96.3	213.7	1970.9	83.4	304.0	2086.0	75.8	278.8	220.5
Deramookoo-1	558.1	142.7	138.4	979.3	116.5	134.8	1195.1	112.1	276.8	1503.1	110.5	142.0	1716.6	95.9	133.4	2058.1	84.3	175.5	2203.1	72.4	330.4	190.2
Dirkala-2																						
Doonmulla-1							1153.9	112.8	301.5	1456.9	105.7	338.4	1642.0	92.1	321.7	1987.3	83.3	289.8	2128.7	77.2	171.7	284.6
Dullingari-3							947.6	122.1	282.2	1256.7	111.0	375.0	1445.5	96.6	382.9	1800.6	80.0	615.9	1870.4	74.7	549.4	441.1
Dullingari North-1																1780.9	78.3	706.2	1855.6	76.1	494.3	600.2
Dunoon-1	391.5	146.2	241.2	565.3	135.9	74.9	732.8	135.6	168.4	973.9	124.5	239.3	1109.0	103.8	499.6	1407.1	84.6	817.9	1423.4	79.9	743.7	397.8
Durham Downs-1							924.6	124.3	251.4	1241.6	111.9	362.8	1468.3	90.8	535.5	1866.2	83.7	393.8	1999.5	74.1	450.3	398.7
Echuburra North-1	462.0	136.3	351.7	658.2	117.8	425.1	845.2	120.4	425.3	1155.1	112.1	442.2	1342.2	93.8	571.3	1699.1	77.4	825.7	1747.5	73.7	721.0	537.5
Fly Lake-1				1004.3	121.0	0.0 (R*)	1156.7	121.6	84.0	1471.8	113.9	69.1	1714.0	97.0	100.4	2068.0	79.6	361.3	2228.8	74.8	187.8	133.8
Fly Lake-4													1733.5	98.1	48.5	2087.1	81.9	248.4	2239.4	76.6	88.6	128.5
Garanjanie-2																						
Gidgealpa-20	541.3	142.8	152.4	850.5	116.7	260.1	973.7	126.2	154.4	1247.1	114.2	285.8	1465.8	98.0	319.2	1801.7	85.8	371.4	1869.2	75.2	525.5	295.5
Gidgealpa-42																						
Gidgee-1																						
Gooranie-1	615.4	140.1	128.1	981.3	115.4	159.5	1140.1	117.9	190.2	1456.2	114.8	55.9	1681.0	97.3	126.9	2046.7	81.3	312.7	2177.8	75.1	221.5	170.7
Gooranie-2										1462.3	108.1	257.9	1682.5	99.8	47.7	2069.7	82.8	226.6	2188.9	75.1	211.9	186.0
Graham-1	338.4	145.0	316.2	500.8	117.5	590.0	645.8	127.7	447.2	929.3	117.5	502.3	1139.5	97.9	648.9	1481.3	85.4	708.4	1542.0	82.8	485.5	528.4
Gurra-1																						
Haddon Downs-1	410.8	137.0	389.7	631.3	121.2	368.7	825.3	122.6	391.8	1118.1	108.1	601.3	1258.6	93.8	654.2	1542.8	85.0	664.8	1701.8	70.8	908.3	568.4
Hammond-1	525.1	138.1	255.2	902.8	109.3	388.7	1138.7	114.3	278.4	1463.2	104.9	354.6	1629.9	89.0	427.4	2005.6	84.6	217.5	2150.2	67.0	645.8	366.8
Hooley-1	257.2	134.0	599.1	376.9	117.5	713.5	520.3	123.5	674.9	803.4	110.0	858.2	997.1	97.7	797.8	1346.8	90.8	620.0	1424.6	76.5	907.6	738.7
Hume-1	506.7	135.8	316.4	748.4	114.6	413.4	928.9	115.4	462.0	1194.1	107.8	535.6	1377.1	89.9	654.0	1706.1	84.3	531.0	1748.3	77.2	548.5	494.4
Hydra-1	422.0	142.7	274.3	569.5	123.4	375.8	734.5	122.7	478.8	995.9	115.7	489.8	1170.2	96.4	663.8	1497.8	90.0	501.1	1527.8	81.0	584.9	481.2
Ingella-1																1979.0	83.7	283.0	2122.0	70.9	483.4	383.2
Innamincka-3																1525.2	83.9	728.6	1643.3	76.4	692.3	710.4
Innamincka-4	382.6	127.3	597.1	557.8	109.6	725.4	692.1	116.4	675.6	996.4	110.7	644.9	1228.8	92.0	739.3	1595.5	88.0	486.6	1712.4	74.7	708.9	654.0
Jack Lake-2	649.1	139.8	100.7	1048.1	112.0	175.8	1254.6	118.5	61.0	1533.2	107.2	215.9	1696.1	94.4	199.3	2065.0	82.6	240.4	2178.3	77.5	106.9	157.1
Jackson-1				422.3	139.8	120.1				851.8	120.0	500.0	1055.8	98.4	716.3	1402.2	81.2	960.8	1459.1	83.2	546.5	568.8
Jackson South-1	283.7	139.8	465.7	422.3	127.1	432.1	594.0	130.7	426.8	858.2	120.2	487.1	1035.5	104.0	568.1	1396.9	81.0	974.6	1454.6	81.6	630.0	569.2
James-1	615.7	136.0	204.3	906.0	114.4	261.1	1107.2	115.9	271.3	1413.7	108.1	307.7	1578.7	92.4	376.2	1912.6	83.5	354.6	2067.0	70.6	553.5	332.7
Jarrar-1	544.5	137.0	257.2	737.3	115.6	398.7	883.9	119.8	401.4	1118.7	109.8	548.1	1405.7	96.2	434.0	1774.5	80.0	641.5	1826.3	75.1	575.4	465.2
Johba-1	485.8	141.0	241.8	692.8	124.5	227.0	808.8	125.5	336.5	1134.0	113.0	436.0	1329.5	98.9	427.8	1687.1	82.2	636.1	1737.3	74.5	691.2	428.1
Kalladeina-1																						
Karmona-2	539.7	134.0	316.4	682.1	121.0	321.7	851.8	118.8	456.6	1195.4	113.4	362.2	1434.1	94.1	469.5	1791.0	83.7	471.4	1887.9	78.1	368.7	395.2
Karwin-1	356.8	140.2	385.8	534.7	124.7	378.9	735.1	129.5	312.7	1029.6	117.6	398.2	1209.3	99.3	536.5	1563.3	82.5	748.9	1626.2	80.2	525.3	469.5
Keeto-2	647.1	141.5	70.7	788.6	122.0	191.1	955.5	125.1	199.1	1201.5	110.2	452.7	1363.0	99.9	366.0	1689.2	83.2	592.3	1732.8	80.2	417.2	327.0
Keilor-1	465.0	140.3	276.1	784.7	116.1	339.0	953.9	117.9	377.3	1285.3	108.7	417.8	1508.6	92.0	457.6	1878.2	84.2	363.4	1986.1	74.3	452.1	383.3
Kenny-1	592.7	137.4	201.4	1042.7	110.4	222.2	1250.7	118.0	78.9	1559.7	106.4	214.1	1753.1	87.4	352.6	2092.5	81.6	256.0	2248.5	71.5	326.1	235.9
Kercummurra-1	246.3	131.4	658.1	342.0	113.9	837.7	488.6	125.2	663.6	774.9	114.5	747.3	986.0	94.5	906.0	1351.0	88.2	723.7	1442.6	77.4	845.6	768.8
Kerna-5																						
Kirby-1	537.9	133.5	328.4	839.9	110.9	411.3	1000.9	115.4	391.1	1390.4	103.4	473.8	1629.4	89.2	422.6	2010.9	80.8	371.3	2113.9	73.5	365.8	394.9
Kirby-2	512.2	131.8	384.3	839.7	107.8	487.7	1039.9	113.5	398.4	1382.9	106.8	377.8	1610.4	88.7	455.0	1997.3	80.5	397.3	2103.9	72.9	403.4	415.3
Kiwarrick-1	499.2	141.9	211.5	673.3	127.7	166.4	831.9	126.5	288.8	1059.4	117.7	363.1	1195.3	98.3	581.0	1518.5	85.3	677.1	1567.4	83.4	428.1	388.0
Kobari-1	451.4	147.6	154.5	632.6	126.5	236.3	809.5	131.8	184.3	1043.8	117.1	397.4	1172.1	95.1	699.7	1451.6	88.8	597.2	1499.6	86.5	344.8	373.4
Koonchera-1	518.5	138.4	257.1	696.3	123.9	236.5	849.8	126.3	277.6	1122.8	117.3	313.2	1300.3	99.2	447.5	1609.3	88.6	446.0	1795.3	77.5	490.8	352.6
Kumbarie-1																						
Kurunda-1	678.1	136.7	128.4	927.1	118.9	128.6	1123.8	122.6	93.9	1426.0	112.3	166.1	1575.6	95.3	291.1	1913.3	80.6	476.8	2024.6	77.4	265.0	221.4
Kutyo-1	621.9	143.1	66.7	790.8	122.2	184.9	938.0	121.6	303.2	1257.4	110.0	404.6	1453.6	95.2	416.0	1814.4	82.0	518.8	1869.0	72.4	665.7	365.7

Table 2. Continued.

	Winton Formation			Mackunda Formation			Allaru Mudstone-Oodnadatta Formation			Bulldog Shale-Wallumbilla Formation			Cadna-owie Formation			Birkhead Formation			Hutton Sandstone			Mean[1]
	Midpoint	Mean		Midpoint	Mean		Midpoint	Mean		Midpoint	Mean		Midpoint	Mean		Midpoint	Mean		Midpoint	Mean		
	Depth	Δt_{sdj}[**]	E_A[***]	Depth	Δt_{sdj}[**]	E_A[***]	Depth	Δt_{sdj}[**]	E_A[***]	Depth	Δt_{sdj}[**]	E_A[***]	Depth	Δt_{sdj}[**]	E_A[***]	Depth	Δt_{sdj}[**]	E_A[***]	Depth	Δt_{sdj}[**]	E_A[***]	E_A[***]
Well	(m bgl[*])	(µs/ft)	(m)	(m bgl[*])	(µs/ft)	(m)	(m bgl[*])	(µs/ft)	(m)	(m bgl[*])	(µs/ft)	(m)	(m bgl[*])	(µs/ft)	(m)	(m bgl[*])	(µs/ft)	(m)	(m bgl[*])	(µs/ft)	(m)	(m)
Lake Mcmillan-1	754.3	136.2	60.9	1149.2	110.1	121.3	1312.5	116.3	58.1	1624.6	108.4	86.9	1848.0	91.0	148.2	2212.7	80.4	185.7	2353.5	74.0	101.0	108.9
Lambda-1	405.4	141.5	312.6	634.5	120.1	392.1	820.1	120.0	459.2	1070.3	110.7	568.8	1240.7	88.0	848.5	1558.8	82.7	744.1				554.2
Lhotsky-1	585.4	141.0	142.2	750.4	127.0	107.2	902.9	128.9	159.2	1143.2	121.7	158.7	1288.4	104.7	294.6	1627.2	86.8	504.5	1760.2	83.3	240.4	229.5
Limestone Creek-9																						
Lycium-1	628.9	138.8	139.7	796.9	128.3	27.5	936.4	129.3	116.2	1204.4	121.3	109.0	1401.1	106.6	122.5	1757.8	82.3	562.7	1865.7	83.5	123.3	171.6
Macadama-1	508.8	137.3	287.2	889.3	113.5	300.0	1029.8	114.5	382.8	1373.3	112.3	216.8	1622.4	102.0	41.5	1992.2	82.2	329.1	2112.3	73.9	345.3	271.8
Mackillop-1	605.0	129.5	334.7	893.1	104.5	514.8	1093.1	111.9	382.6	1421.3	103.9	429.3	1568.5	89.3	480.9	1891.6	81.8	449.6	2045.2	68.9	660.3	464.6
Marabooka-2	525.5	138.6	246.9	712.7	122.6	251.7	899.6	124.2	276.9	1196.2	112.2	398.6	1368.8	99.6	368.5	1712.0	78.3	774.6	1781.8	75.3	611.3	418.3
Marengo-1	747.3	125.3	268.3	1033.4	108.8	270.7	1270.8	107.1	321.7	1607.3	100.2	357.4	1799.5	84.4	396.4	2161.2	77.9	339.4	2306.3	69.6	361.3	330.7
Marsilea-1	624.6	138.7	146.0	783.1	121.5	208.7	973.7	121.4	271.0	1241.4	112.6	340.6	1397.3	96.1	445.9	1739.4	81.4	618.1	1773.4	77.9	488.7	359.9
Mawson-1	663.6	142.7	32.7	888.9	125.0	18.8	1110.4	122.2	114.7	1434.1	113.8	111.4	1578.9	101.6	98.8	1893.8	83.3	382.4	2012.4	77.1	289.0	149.7
Mckinlay-3																						
Mcleod-1													1670.0	82.5	584.1	2046.4	78.1	447.0	2142.6	71.2	450.3	493.8
Meeba-1				864.9	108.1	456.2	1098.7	111.5	387.8	1380.0	99.8	596.4	1543.7	86.0	605.5	1872.8	82.2	451.7	2034.1	62.3	992.2	581.6
Meranji-1	587.7	141.7	127.5	1013.1	114.0	162.7	1167.1	122.8	43.6	1426.2	111.9	176.0	1634.6	96.4	199.2	1982.4	81.8	358.0	2105.6	77.3	188.0	179.3
Merrimelia-7	583.4	139.2	177.2	918.3	116.5	196.0	1047.1	123.1	158.1	1317.2	117.8	104.9	1532.7	98.8	228.4	1874.8	83.0	414.4	1981.8	75.7	387.6	238.1
Merrimelia-25													1559.8	93.7	356.4	1881.2	84.1	363.5	1987.3	77.0	322.4	347.4
Minkie-1	727.8	126.4	268.4	960.8	104.9	438.0	1121.5	116.7	239.1	1387.0	115.1	117.6	1555.0	94.5	335.8	1905.8	82.1	422.3	2014.6	77.0	291.8	301.9
Mooliampah-1	361.0	148.0	237.9	585.1	125.3	314.1	763.4	126.3	362.0	1019.4	117.7	405.4	1186.7	100.4	525.8	1513.2	84.5	716.1	1548.2	78.8	673.8	462.1
Moolion-1	713.9	135.9	106.9	1105.5	110.1	165.0	1279.8	115.5	108.3	1579.9	109.2	105.4	1804.1	92.1	159.4	2183.1	81.9	152.1	2323.2	73.8	142.4	134.2
Moomba-27													1720.6	92.5	232.5	2067.3	81.8	273.8	2171.4	68.8	537.2	347.8
Moomba-57	647.0	139.4	110.9	1004.5	108.1	317.4	1199.3	113.6	235.1	1507.8	105.0	309.5	1694.6	90.6	315.1	2011.0	76.1	566.1	2096.2	69.2	593.1	349.6
Moomba North-1	781.9	129.9	150.3	1044.2	107.1	302.1	1222.6	114.8	184.1	1514.0	107.8	216.3	1703.9	92.0	263.2	2029.7	83.9	221.1	2139.1	68.8	570.1	272.5
Moomba South-1							1180.7	119.8	104.3				1686.4	98.3	90.2	2013.4	81.4	343.2	2109.3	67.0	684.6	305.5
Moorari-4																2158.4	80.3	245.2	2285.7	75.9	75.3	160.2
Morney-1	300.4	126.4	695.3	385.4	120.7	626.7	566.4	128.3	510.7	859.0	110.4	790.3	995.4	99.4	748.7	1332.7	86.3	819.0	1472.9	71.9	1084.5	753.6
Mudera-3	574.5	130.4	348.2	744.3	119.8	290.7	921.6	123.1	281.7	1224.7	112.0	375.0	1412.0	94.0	494.6	1763.1	82.3	555.7	1829.3	76.0	529.8	410.8
Munkah-2	447.7	134.1	407.1	696.5	115.7	438.5	865.9	119.4	427.8	1170.7	113.8	373.6	1390.3	96.1	451.9	1766.6	82.1	561.5	1854.4	74.8	562.3	460.4
Munkarie South-1	336.5	149.5	234.4	533.5	130.0	250.3	682.4	130.3	346.2	920.7	117.0	524.4	1084.8	103.4	538.3	1404.9	87.1	715.7	1429.4	79.0	780.2	484.2
Munro-1	419.2	142.8	275.9	556.3	132.9	156.0	717.8	130.0	319.2	958.4	122.2	328.0	1109.8	104.3	483.6	1435.9	84.3	799.2	1459.4	85.7	425.1	398.2
Muteroo-3																						
Naccowlah East-1	497.0	139.4	259.2	694.5	121.2	304.7	836.2	126.3	290.0	1120.2	115.3	379.4	1343.0	95.7	513.5	1699.0	83.2	582.5	1783.4	77.2	517.0	406.6
Naccowlah South-1	409.6	143.4	273.4	649.6	125.2	252.1	808.7	125.4	340.1	1093.1	111.6	518.6	1303.7	96.8	517.3	1653.4	84.4	578.5	1722.6	79.1	483.2	423.3
Naccowlah West-1	389.0	137.0	411.4	633.9	123.7	305.6	813.6	122.4	407.1	1096.3	114.7	421.6	1304.3	94.8	577.2	1661.2	83.2	618.3	1731.9	77.5	550.5	470.3
Naryilco-1																						
Navalla-1							407.9	115.0	992.9	739.6	113.2	824.2	962.3	93.6	955.2	1314.0	80.1	1095.7	1428.8	75.2	966.4	966.9
Nulla-1	561.4	142.5	139.4	958.8	115.6	177.9	1112.2	120.6	152.8	1361.6	112.3	229.3	1627.8	95.1	246.4	1998.7	80.1	410.7	2137.1	75.5	246.3	229.0
Okotoko-1	478.8	134.5	368.8	698.8	110.4	566.4	828.0	120.9	430.8	1149.6	111.1	477.4	1376.9	95.6	482.5	1732.9	83.8	522.8	1825.0	74.9	584.2	490.4
Orientos-2	433.8	141.6	282.4	623.8	120.5	393.5	788.1	121.1	464.8	1053.1	114.0	486.0	1254.3	88.9	807.2							486.8
Packsaddle-4	506.3	138.1	275.4	739.4	116.7	369.3	872.0	120.4	398.0	1173.3	114.4	351.6	1394.0	94.8	488.1	1736.1	78.8	730.0	1848.2	77.4	441.4	436.3
Padulla-1	384.9	147.2	229.1	627.4	134.1	56.8	788.0	134.0	152.2	993.2	120.1	355.4	1098.3	100.1	622.7	1384.6	80.5	1007.2	1433.2	78.0	828.4	464.6
Pallano-1	512.7	136.3	301.7	752.9	117.8	329.9	900.5	120.7	362.3	1222.1	112.7	355.0	1414.6	96.7	411.4	1773.9	77.6	741.3	1828.5	75.8	536.5	434.0
Pandieburra-1																						
Pando South-1																						
Paning-1				918.2	109.4	370.9	1082.6	119.5	209.6	1411.3	109.3	272.1	1666.7	90.6	343.4	2037.1	85.4	152.2	2186.9	75.1	214.1	260.4
Paragilga-1	412.9	141.6	303.6	538.5	122.5	428.4	705.1	126.0	429.0	956.6	120.9	368.6	1107.2	104.1	493.9	1441.3	85.0	766.5	1467.6	80.6	664.1	493.4
Patroclus-1				757.6	115.7	377.1	926.3	117.8	407.8	1314.3	106.6	452.1	1404.2	94.3	493.6	1738.5	79.9	681.1	1788.0	81.5	301.9	452.3
Paxton-1				400.4	143.0	63.7	559.5	142.6	171.6	726.3	140.3	0.0 (R^+)	815.8	117.2	386.8							155.5
Pepita-2	551.1	136.9	251.2	740.5	114.0	434.7	884.3	121.9	349.1	1188.2	111.3	434.0	1423.2	98.2	355.7	1773.6	80.8	609.1	1884.6	75.0	522.0	422.2
Pintari-1																						
Poodrinie-5	627.8	134.3	223.4	812.8	117.3	282.6	936.2	120.0	343.8	1206.2	113.8	338.5	1432.4	100.1	290.3	1790.4	79.8	634.0	1900.3	79.8	269.8	340.3

Table 2. Continued.

	Winton Formation			Mackunda Formation			Allaru Mudstone-Oodnadatta Formation			Bulldog Shale-Wallumbilla Formation			Cadna-owie Formation			Birkhead Formation			Hutton Sandstone			Mean[1]
	Midpoint Depth	Mean Δt_{mtx}[**]	E_A[***]	Midpoint Depth	Mean Δt_{mtx}[**]	E_A[***]	Midpoint Depth	Mean Δt_{mtx}[**]	E_A[***]	Midpoint Depth	Mean Δt_{mtx}[**]	E_A[***]	Midpoint Depth	Mean Δt_{mtx}[**]	E_A[***]	Midpoint Depth	Mean Δt_{mtx}[**]	E_A[***]	Midpoint Depth	Mean Δt_{mtx}[**]	E_A[***]	E_A[***]
Well	(m bgl[*])	(µs/ft)	(m)	(m bgl[*])	(µs/ft)	(m)	(m bgl[*])	(µs/ft)	(m)	(m bgl[*])	(µs/ft)	(m)	(m bgl[*])	(µs/ft)	(m)	(m bgl[*])	(µs/ft)	(m)	(m bgl[*])	(µs/ft)	(m)	(m)
Potiron-1	378.4	135.6	448.3	573.2	117.0	528.9	781.7	119.7	504.2	1109.1	103.8	743.1	1256.6	88.2	824.1	1568.1	86.6	570.0	1748.4	67.6	1020.4	662.7
Putamurdie-1																						
Rheims-1	423.8	145.0	229.5	574.4	127.0	283.7	732.6	127.8	358.3	1019.8	115.9	461.2	1185.8	99.2	562.8	1517.8	87.0	605.7	1550.1	84.3	399.5	414.4
Rho East-1	381.9	144.6	278.7	482.6	122.6	481.9	644.2	130.8	373.0	906.6	117.6	521.1	1071.2	101.4	610.2	1407.4	83.4	865.8	1429.4	80.3	717.6	549.8
Richie-1	280.2	141.2	444.5	425.0	126.7	440.9	630.8	131.4	371.0	916.1	116.9	533.5	1087.1	100.0	637.6	1446.1	82.9	847.2	1496.1	80.4	648.3	560.4
Russel-1	588.1	139.6	165.5	1031.9	100.9	464.9	1225.3	111.8	252.7	1534.7	103.3	334.7	1707.8	92.2	252.1	2106.8	79.0	351.4	2256.1	65.9	593.1	344.9
Snake Hole-1	606.8	143.2	79.6	928.4	118.9	128.2	1145.4	122.9	63.5	1453.9	110.0	207.6	1597.5	97.7	195.8	1929.2	82.3	391.6	2040.6	79.1	163.7	175.7
Spectre-1	814.6	132.4	71.3	1064.4	112.3	153.4	1235.8	115.7	147.8	1552.7	109.6	121.3	1773.3	94.2	128.3	2146.7	81.7	197.5	2278.8	76.6	49.9	124.2
Spencer-4	446.3	145.1	206.0	778.8	121.9	202.6	920.7	124.3	255.0	1192.4	113.2	369.1	1331.7	95.7	522.5	1640.6	83.9	610.8	1743.2	80.9	372.5	362.6
Steward-1	464.4	134.4	384.0	698.5	118.7	361.8	897.7	118.5	418.6	1213.0	107.0	541.2	1358.1	89.8	675.6	1733.4	82.6	572.4	1877.0	72.7	641.3	513.6
Strzelecki-10	457.5	143.3	227.8	744.9	120.6	268.5	923.8	129.5	125.6	1180.6	116.3	286.5	1354.7	99.3	392.2	1719.5	75.1	896.9	1778.4	74.9	631.2	404.1
Strzelecki -27																						
Sturt-6	549.0	143.5	131.9	794.2	120.5	223.3	974.0	128.2	105.2	1206.2	113.0	363.2	1332.7	102.3	322.8	1648.1	83.8	608.1	1745.9	82.5	293.8	292.6
Swan Lake-1													1727.5	86.9	392.9	2089.6	78.4	391.1	2208.3	74.3	232.8	338.9
Taloola-1	563.9	142.5	136.4	782.5	123.3	165.1	950.6	125.4	198.7	1193.2	114.4	333.3	1326.2	101.1	365.9	1649.8	82.7	650.5	1746.1	80.0	415.0	323.5
Tanbar-1																2107.9	80.7	279.2	2262.2	70.2	376.6	327.9
Tanbar North-1													1713.9	95.2	156.6	2074.2	81.2	288.9	2225.0	64.1	710.8	385.5
Tartulla-1																1877.6	84.6	347.2	1972.2	75.3	418.7	382.9
Tennaperra South-1	380.0	144.1	290.7	639.5	120.3	383.3	872.1	120.0	407.5	1115.9	110.0	546.3	1315.2	97.6	481.3	1656.3	80.9	722.0	1692.1	69.0	1004.4	548.0
Three Queens-1	406.7	140.2	336.2	693.2	116.9	410.8	872.2	120.1	404.8	1209.3	110.3	442.1	1410.3	93.7	503.9	1777.4	81.9	560.0	1871.3	75.0	532.5	455.8
Thurakinna-5	712.8	140.4	26.2	883.0	120.9	123.2	1050.2	121.2	200.7	1331.7	112.4	254.6	1487.7	99.5	252.2	1782.2	81.7	561.6	1834.6	77.1	467.5	269.4
Thurra-1	418.7	136.0	400.8	652.0	123.9	282.2	858.7	121.0	396.0	1142.2	113.6	407.4	1314.6	98.6	453.6	1685.3	81.3	676.9	1755.8	77.4	534.0	450.1
Tinchoo-1	655.5	127.7	315.8	864.0	112.9	338.0	1055.3	114.5	359.0	1377.1	110.0	284.2	1593.8	94.3	303.5	1944.7	82.1	383.5	2099.9	70.4	532.1	359.4
Tinga Tingana-1	495.6	153.6	0.0 (R[+])	625.9	134.8	41.3	744.8	142.0	0.0 (R[+])	942.1	132.0	40.0	1086.2	121.1	0.0 (R[+])	1374.9	105.0	0.0 (R[+])	1388.1	95.9	0.0 (R[+])	11.6
Tinpilla-1	312.1	137.2	484.9	473.5	123.6	467.2	664.8	130.2	365.9	949.1	118.3	456.7	1136.3	100.2	582.5	1487.0	78.9	973.6	1547.9	83.8	428.3	537.0
Tirrawarra-13																2047.7	84.3	190.0	2192.6	77.9	73.2	131.6
Tirrawarra-15																2024.8	80.7	359.2	2176.4	74.2	270.3	314.7
Tirrawarra-26																2048.3	78.5	430.4	2208.6	72.1	337.1	383.8
Tirrawarra North-1	678.2	135.2	156.7	1046.5	109.2	246.6	1207.0	121.0	48.5	1513.6	110.3	137.6	1739.8	97.8	50.5	2124.8	80.8	255.5	2267.1	75.4	119.5	145.0
Tirrawarra West-1	640.7	138.9	125.1	997.9	111.2	247.4	1165.6	121.6	76.4	1489.9	111.0	140.7	1716.3	97.0	100.1	2089.0	84.1	155.6	2227.9	74.3	211.8	151.0
Toby-1	281.1	132.9	595.5	371.1	120.0	656.8	563.6	117.0	790.2	916.5	111.0	715.5	1134.3	92.2	828.0	1519.3	80.7	864.2	1638.6	70.8	970.0	774.3
Toolachee-9				754.9	116.2	366.7	933.7	120.3	339.5	1189.4	112.5	396.5	1349.3	96.7	475.9	1680.3	84.6	541.8	1728.6	77.4	558.1	446.4
Toolachee-21	545.3	137.7	242.7	753.9	123.6	186.2	927.6	121.8	308.2	1192.8	111.1	434.0	1359.4	95.2	509.4	1689.4	82.9	602.6	1747.6	77.9	516.4	399.9
Toolachee-39	481.7	147.9	118.6	739.9	115.1	408.6	916.7	121.4	329.4	1207.9	111.3	413.7	1378.8	94.9	500.0	1697.4	79.8	724.0	1752.6	77.8	516.2	430.1
Turban-1	585.4	127.1	397.0	712.5	115.1	437.1	860.3	118.4	457.6	1156.6	113.8	389.1	1382.3	95.4	482.6	1761.3	83.4	513.6	1884.9	76.4	451.3	446.9
Ullenbury-1	465.8	137.4	328.2	777.4	112.2	442.5	1078.1	113.2	367.3	1389.6	104.7	436.4	1552.2	88.6	516.7	1911.7	82.9	383.7	2064.1	69.0	632.3	443.9
Wackett-3	435.4	140.1	309.5	623.1	117.4	469.2	793.3	121.6	447.3	1083.2	115.8	400.6	1282.1	96.7	543.7	1643.3	84.6	581.4	1714.6	75.6	662.2	487.7
Wallawanny-1													1409.3	93.0	528.7	1782.8	85.3	411.9	1830.7	76.2	515.2	485.2
Wancoocha-2	554.1	139.9	194.6	750.4	123.7	188.7	907.4	127.6	186.6	1122.0	118.3	282.6	1263.2	101.8	406.6	1550.2	86.8	582.8	1612.2	74.6	812.0	379.1
Wantana-2	648.9	140.2	94.1	859.0	123.2	90.6	1070.2	119.5	222.1	1401.5	111.4	216.9	1647.8	87.8	446.9	2006.2	79.0	450.8	2130.3	74.1	321.0	263.2
Wareena-1				306.8	109.3	985.2	437.7	119.5	854.7	715.2	115.7	771.3	927.8	92.7	1016.8	1294.4	84.4	936.6	1397.5	72.9	1109.8	945.7
Warnie East-1	522.7	136.8	283.0	610.2	118.4	459.3	800.9	120.6	463.9	1132.9	111.4	484.4	1320.4	96.9	497.8	1667.1	83.2	615.7	1702.6	74.2	741.7	506.5
Watson-1	427.0	142.1	279.5	561.3	121.1	441.7	750.6	117.6	587.4	1043.5	112.2	549.0	1227.3	93.9	681.0	1568.8	82.1	757.9	1603.9	73.6	870.6	592.3
Weena-1																						
Wicho-1	654.5	132.7	225.1	972.5	109.1	323.1	1183.9	111.6	300.7	1458.8	104.1	384.2	1624.6	88.1	460.2	1966.6	83.6	298.1	2119.3	71.3	464.4	350.8
Wills-1	428.2	139.1	333.5	591.2	123.8	345.0	773.1	128.2	308.0	1046.7	118.3	359.9	1215.2	102.0	449.9	1570.5	80.4	828.0	1605.2	80.2	548.9	453.3
Wimma-1	879.9	128.4	80.0	1204.3	111.7	29.3	1370.7	116.3	0.0 (R[+])	1714.3	107.1	36.6	1969.4	89.1	86.1	2357.4	81.4	0.0 (R[+])	2492.8	73.2	0.0 (R[+])	33.1
Wippo-2	527.1	135.3	304.8	644.6	126.7	220.0	842.7	120.2	432.7	1188.1	110.5	458.3	1424.2	94.4	469.9	1805.0	82.0	528.2	1886.8	75.6	491.4	415.1
Wirha-1	496.8	142.8	198.0	647.9	123.8	288.9	848.2	120.1	428.5	1091.4	118.8	299.7	1246.7	101.3	437.5	1559.3	82.3	757.8	1595.5	78.0	662.6	439.0
Witchetty-1	567.3	142.8	126.8	726.3	121.6	262.9	910.3	119.5	380.7	1175.3	111.7	435.0	1339.5	98.2	438.9	1673.8	81.1	694.2	1734.2	77.8	533.1	410.2
Wompi-1	380.4	140.0	365.2	574.2	118.8	484.2	746.0	124.2	432.6	1021.1	112.6	560.3	1215.1	95.5	645.4	1555.5	80.9	819.6	1582.4	74.7	839.0	592.3

Table 2. Continued.

	Winton Formation			Mackunda Formation			Allaru Mudstone-Oodnadatta Formation			Bulldog Shale-Wallumbilla Formation			Cadna-owie Formation			Birkhead Formation			Hutton Sandstone			Mean‡
Well	Midpoint Depth (m bgl*)	Mean Δt_{adj}** (μs/ft)	E_A*** (m)	Midpoint Depth (m bgl*)	Mean Δt_{adj}** (μs/ft)	E_A*** (m)	Midpoint Depth (m bgl*)	Mean Δt_{adj}** (μs/ft)	E_A*** (m)	Midpoint Depth (m bgl*)	Mean Δt_{adj}** (μs/ft)	E_A*** (m)	Midpoint Depth (m bgl*)	Mean Δt_{adj}** (μs/ft)	E_A*** (m)	Midpoint Depth (m bgl*)	Mean Δt_{adj}** (μs/ft)	E_A*** (m)	Midpoint Depth (m bgl*)	Mean Δt_{adj}** (μs/ft)	E_A*** (m)	E_A*** (m)
Wuroopie-1																						
Yanbee-1	651.1	129.9	280.5	933.5	110.1	339.2	1104.8	113.2	340.5	1397.5	106.8	363.4	1618.3	93.0	318.8	1953.6	79.8	467.7	2100.5	71.4	480.6	370.1
Yanda-2	520.4	137.0	280.9	759.5	114.6	402.2	919.8	120.6	346.2	1229.3	111.8	376.2	1448.2	93.1	486.9	1827.0	86.1	333.3	1912.7	77.7	360.6	369.5
Yanta-1	605.6	140.8	125.8	898.9	121.7	88.1	1049.4	126.3	77.5	1303.2	115.9	175.2	1472.2	97.4	332.4	1810.1	83.9	443.0	1972.7	76.3	367.7	229.9
Yumba-1	567.1	141.4	153.4				897.6	121.4	348.8	1177.1	111.3	445.6	1406.0	94.4	487.8	1790.7	83.9	461.0	1869.3	74.8	548.2	407.5

Cooper Basin Stratigraphic Units

	Nappamerri Group			Toolachee Formation			Roseneath Shale			Murteree Shale			Patchawarra Formation			Mean‡‡
Well	Midpoint Depth (m bgl*)	Mean Δt ** (μs/ft)	E_A*** (m)	Midpoint Depth (m bgl*)	Mean Δt ** (μs/ft)	E_A*** (m)	Midpoint Depth (m bgl*)	Mean Δt ** (μs/ft)	E_A*** (m)	Midpoint Depth (m bgl*)	Mean Δt ** (μs/ft)	E_A*** (m)	Midpoint Depth (m bgl*)	Mean Δt ** (μs/ft)	E_A*** (m)	E_A*** (m)
Alkina-1	2379.9	66.8	533.7	2579.0	65.4	1190.0							2633.5	65.1	1190.5	971.4
Alwyn-1																
Amyema-1	1824.1	73.1	678.7	1909.2	75.2	1094.5	2088.2	77.9	600.4	2211.1	74.0	1137.9	2254.1	75.5	845.7	871.5
Andree-1	2521.2	71.3	98.1	2636.9	75.4	354.5				2721.7	75.8	476.0	2753.9	71.5	619.2	386.9
Araburg-1	2196.0	73.6	276.7													276.7
Arrabury-1																
Arrakis-1	2101.7	70.4	577.7	2149.8	73.1	1016.0	2194.7	74.6	723.3	2273.2	73.2	1144.0	2315.0	74.8	828.1	857.8
Atoll-1																
Azolla-1	1775.3	75.1	596.7	1842.6	84.9	406.0	2053.6	79.4	526.5	2191.2	76.2	966.4	2242.5	72.9	1037.7	706.7
Ballera-1	2148.6	65.8	832.8	2280.9	68.1	1275.5							2472.1	69.8	1021.5	1043.2
Baratta-1	1921.5	66.2	1034.5	1988.0	79.6	676.0	2079.4	77.0	672.1	2155.3	76.0	1022.8	2197.4	74.0	1003.1	881.7
Bardoc-1																
Barrolka-1	2347.1	65.0	681.5	2571.1	67.4	1043.2							2622.6	66.3	1118.4	947.7
Baryulah-1	2128.2	70.5	546.2	2250.5	72.5	968.2	2359.5	71.9	740.6	2439.5	68.8	1369.2	2483.3	68.0	1135.0	951.8
Battunga-1	1804.9	78.9	321.8	1918.8	83.2	460.1	1972.1	79.0	637.1	2120.0	78.2	863.6	2183.2	78.0	739.3	604.4
Beanbush-1	2936.2	66.5	0.0 (R*)							3280.2	70.3	395.6	3395.1	70.7	36.6	312.6
Belah-1	1724.3	71.1	913.1	1827.9	78.0	957.4	1952.7	72.8	1089.3	2026.8	70.6	1622.4	2224.5	71.8	1128.0	1142.0
Biala-1																
Big Lake-26	2171.1	66.8	745.7	2304.8	78.9	409.6	2376.2	74.6	536.6	2499.9	74.6	799.5	2558.4	72.7	734.7	645.2
Big Lake-35	2201.6	68.2	623.4	2347.6	71.5	949.7	2419.5	69.8	826.7	2544.0	76.0	632.3	2605.6	72.0	737.2	753.9
Bogala-1				1740.9	73.6	1391.6	1813.1	79.1	793.3				1900.9	76.6	1116.6	1100.5
Boldrewood-1	1774.5	66.9	1130.3	1965.0	68.2	1587.2										1358.8
Bookabourdie-1	2498.3	66.9	412.3										2815.8	72.0	527.2	469.8
Boxwood-1																
Brolga-2	2527.8	69.4	218.8	2668.5	69.3	794.2				2690.5	74.3	632.0	2903.5	71.2	493.7	534.7
Buckinna-1																
Bungee-1	1844.7	75.9	475.2	1930.1	84.1	378.1				2109.3	82.9	464.0	2161.1	79.6	653.0	492.6
Burke-2																
Burley-2	2470.3	67.6	390.2	2701.3	70.1	705.4	2941.9	74.2	0.0 (R*)	3153.5	76.3	0.0 (R*)	3260.0	73.2	0.0 (R*)	219.1
Bycoe-1				1622.5	83.3	750.3	1663.2	87.0	395.6				1723.8	76.6	1298.1	814.7
Carney-1	1806.6	73.3	682.3	1923.9	74.6	1130.0							2062.6	73.0	1212.1	1008.1
Challum-1	2162.3	65.5	836.3										2355.4	71.6	1016.0	926.2
Charo-1																
Childie-1	1794.4	70.6	870.2	1886.0	78.0	903.7				1942.8	73.8	1429.4	1981.9	74.3	1195.6	1099.7
Cooba-1	2427.6	70.5	243.2	2580.7	72.9	605.5				2662.3	71.3	926.3	2999.2	70.8	424.9	550.0
Cook-1	2401.7	73.8	55.8													55.8
Cook North-1	2415.5	67.3	468.2													468.2
Coonavalla-1	1920.9	68.1	906.6										2103.0	68.2	1504.8	1205.7
Cooroo-1				1856.6	75.4	1130.9										1130.9

Table 2. Continued.

	Nappamerri Group			Toolachee Formation			Roseneath Shale			Murteree Shale			Patchawarra Formation			Mean[#]
Well	Midpoint Depth (m bgl*)	Mean Δt ** (µs/ft)	E_A *** (m)	Midpoint Depth (m bgl*)	Mean Δt ** (µs/ft)	E_A *** (m)	Midpoint Depth (m bgl*)	Mean Δt ** (µs/ft)	E_A *** (m)	Midpoint Depth (m bgl*)	Mean Δt ** (µs/ft)	E_A *** (m)	Midpoint Depth (m bgl*)	Mean Δt ** (µs/ft)	E_A *** (m)	E_A *** (m)
Copai-1																
Cowan-3																
Cuddapan-1	2406.7	70.3	276.9													276.9
Curalle-1	1722.0	72.6	816.1													816.1
Daer-1	2268.3	68.7	525.3	2348.3	80.0	280.4										402.8
Daralingie-15	1941.9	75.6	402.8	1999.8	85.1	229.2	2074.0	80.2	455.9	2174.3	77.9	837.6	2215.9	80.8	509.5	487.0
Daralingie-23	1952.2	76.1	356.8				2097.8	79.5	479.1	2196.1	78.7	743.7	2233.9	78.9	624.0	550.9
Darter-1	2412.7	70.3	271.4	2519.4	81.4	0.0 (R*)							2628.2	69.8	867.9	379.8
Della-7	1877.8	71.7	716.9													716.9
Della-10	1863.1	66.8	1052.3	1961.4	79.3	720.8							1981.4	75.4	1119.6	964.2
Denley-1	2504.9	69.7	218.7													218.7
Deparanie-1	2312.0	67.9	527.4	2426.6	71.8	842.4							2437.6	75.6	651.3	673.7
Deramookoo-1																
Dirkala-2																
Doonmulla-1	2466.9	65.0	564.6													564.6
Dullingari-3	2033.6	71.8	557.8	2169.6	77.7	641.2	2317.2	71.6	802.8	2431.5	73.7	946.4	2498.0	73.7	721.3	733.9
Dullingari North-1	2022.5	73.6	448.7	2155.9	77.9	641.2	2290.6	73.1	731.3	2396.0	71.8	1146.8	2444.1	73.2	812.4	756.1
Dunoon-1																
Durham Downs-1	2309.2	68.2	515.5	2501.8	70.9	841.4							2615.4	75.0	516.8	624.6
Echuburra North-1																
Fly Lake-1	2477.4	72.2	82.4							2599.8	82.1	44.1	2801.8	74.7	354.0	442.6
Fly Lake-4	2506.2	72.3	47.8	2637.6	74.8	399.8				2648.6	74.8	628.5	2666.1	75.5	427.9	376.0
Garanjanie-2																
Gidgealpa-20																
Gidgealpa-42																
Gidgee-1																
Gooranie-1	2425.9	66.2	528.3	2623.3	67.8	961.7				2670.8	71.3	916.0	2963.3	71.3	425.0	707.7
Gooranie-2	2462.5	68.6	332.1	2621.8	71.7	657.2				2673.7	74.8	606.1	2958.3	73.5	277.2	468.1
Graham-1				1590.0	87.3	472.7	1700.3	83.8	575.8				1790.9	77.7	1152.5	733.7
Gurra-1																
Haddon Downs-1																
Hammond-1	2527.1	65.3	486.8													486.8
Hooley-1	1533.4	72.6	1004.6													1004.6
Hume-1	1816.3	68.1	1014.7	1897.9	76.9	974.0	2023.1	69.9	1215.6	2091.5	67.3	1849.9	2114.7	76.5	915.7	1194.0
Hydra-1				1633.6	82.4	807.8	1661.3	77.8	1030.2	1728.9	76.9	1368.4	1762.0	74.2	1423.5	1157.5
Ingella-1	2457.9	70.5	213.4													213.4
Innamincka-3	1818.3	71.5	791.0													791.0
Innamincka-4	1926.3	66.2	1023.7	2075.5	72.5	1139.9										1081.8
Jack Lake-2	2374.9	72.2	189.9	2473.8	75.8	484.1	2522.9	75.7	317.4	2600.2	75.3	634.6	2641.3	76.4	392.9	403.8
Jackson-1				1535.4	84.0	780.0	1577.9	85.0	613.6				1668.6	78.9	1195.2	862.9
Jackson South-1				1488.6	83.7	855.1	1546.4	83.4	760.3				1761.1	82.4	857.5	824.3
James-1	2339.5	67.2	548.6													548.6
Jarrar-1																
Johba-1																
Kalladeina-1																
Karmona-2	2079.5	69.8	639.5	2225.0	76.2	703.9							2490.0	71.9	860.3	734.5
Karwin-1				1727.1	81.1	818.9	1928.4	80.2	600.8	2046.7	80.0	783.1	2254.6	76.1	798.3	750.3
Keeto-2	1809.3	78.6	338.5	1874.4	77.2	975.9	2016.5	75.5	837.0	2141.3	74.1	1205.1	2184.2	73.2	1069.8	885.3
Keilor-1	2243.6	68.4	563.3	2451.1	70.8	894.4							2555.2	70.1	920.6	792.8
Kenny-1	2628.4	65.8	353.3													353.3
Kercummurra-1	1645.6	68.0	1190.7	1832.3	68.2	1715.7										1453.2
Kerna-5																

Table 2. Continued.

	Nappamerri Group			Toolachee Formation			Roseneath Shale			Murteree Shale			Patchawarra Formation			Mean[ii]
Well	Midpoint Depth (m bgl*)	Mean Δt ** (µs/ft)	E_A *** (m)	Midpoint Depth (m bgl*)	Mean Δt ** (µs/ft)	E_A *** (m)	Midpoint Depth (m bgl*)	Mean Δt ** (µs/ft)	E_A *** (m)	Midpoint Depth (m bgl*)	Mean Δt ** (µs/ft)	E_A *** (m)	Midpoint Depth (m bgl*)	Mean Δt ** (µs/ft)	E_A *** (m)	E_A *** (m)
Kirby-1	2452.9	65.3	561.1	2718.3	76.2	205.6	2836.4	71.7	282.2	3049.4	71.6	512.5	3174.3	72.0	166.4	345.6
Kirby-2	2411.7	66.8	500.3	2700.9	73.9	407.0	2845.0	70.8	333.5							413.6
Kiwarrick-1				1681.5	83.0	718.0	1632.5	79.6	935.1	1712.2	82.2	918.0	1753.1	77.0	1238.5	952.4
Kobari-1										1580.1	86.2	706.3	1661.4	86.5	673.0	689.7
Koonchera-1																
Kumbarie-1																
Kurunda-1	2177.9	70.2	512.8	2210.5	73.6	916.2										
Kutyo-1				1964.9	77.4	866.2				2276.3	73.6	1106.0	2311.2	77.6	638.3	793.3
Lake Mcmillan-1	2673.6	66.0	290.8	2892.9	64.6	942.2										866.2
Lambda-1										2945.9	67.9	937.0	3069.9	68.1	543.7	678.4
Lhotsky-1																
Limestone Creek-9																
Lycium-1																
Macadama-1	2412.1	68.0	422.2	2644.7	79.8	0.0 (R*)							2140.3	81.2	560.5	560.5
Mackillop-1	2400.6	66.8	514.6	2533.9	63.2	1406.4							3001.2	74.0	198.6	206.9
Marabooka-2	1890.5	66.9	1020.0	1943.4	75.6	1032.7										960.5
Marengo-1	2737.2	65.1	286.4	2962.9	67.5	646.3				1996.7	72.7	1468.4	2162.8	72.9	1116.7	1159.4
Marsilea-1	1864.4	73.9	586.1	1955.1	78.3	808.8	2154.5	75.7	684.5	2278.3	73.8	1088.9	2326.8	75.4	777.9	466.3
Mawson-1	2195.5	70.3	488.8	2244.4	83.5	113.0				2271.1	72.2	1241.2	2302.6	76.0	761.7	789.2
Mckinlay-3																651.1
Mcleod-1	2422.1	68.5	378.4	2657.7	72.2	578.5	2935.7	73.9	26.6	3157.3	72.8	297.1	3243.7	69.1	300.1	362.0
Meeba-1	2384.1	68.9	394.3													394.3
Meranji-1	2333.1	69.3	421.0	2470.9	78.6	271.0				2522.7	74.3	804.2	2813.2	78.0	110.8	401.8
Merrimelia-7	2165.1	70.6	502.5	2227.6	68.4	1309.0										905.8
Merrimelia-25	2199.4	72.0	378.5													199.0
Minkie-1	2221.2	67.7	635.3													635.3
Mooliampah-1				1586.3	82.2	869.0	1658.3	78.6	982.5	1705.5	76.0	1468.6	1757.2	76.7	1258.2	1144.6
Moolion-1	2621.9	67.6	243.1	2813.2	69.2	661.2				2842.9	68.6	981.2	2923.0	76.8	83.3	492.2
Moomba-27	2353.5	67.0	548.2	2517.9	74.6	536.0	2627.3	73.1	392.0	2722.5	72.2	782.2	2781.6	69.8	715.1	594.7
Moomba-57	2264.6	68.1	566.0	2384.6	79.3	298.3	2583.1	74.0	372.6	2755.5	75.7	443.2	2819.1	72.0	518.6	439.7
Moomba North-1	2328.1	69.2	428.3	2496.3	77.2	353.5	2619.2	72.4	449.7	2753.2	74.7	533.4	2811.4	71.5	562.8	409.5
Moomba South-1	2256.6	70.5	419.2	2408.8	77.4	425.6	2524.4	74.8	374.5	2677.6	72.0	849.6	2734.5	69.6	770.7	567.9
Moorari-4	2541.0	68.9	234.3							2710.3	71.9	822.4	2849.2	74.6	309.8	455.5
Morney-1	1818.4	71.4	797.7													797.7
Mudera-3	1947.1	68.9	831.3	2028.0	80.3	577.9				2099.0	72.3	1401.2	2152.7	73.1	1115.1	981.4
Munkah-2	2009.2	69.0	761.7	2115.4	75.0	907.3							2297.9	73.7	922.5	863.8
Munkarie South-1																
Munro-1																
Muteroo-3																
Naccowlah East-1	1851.1	78.2	321.1	1955.5	77.1	900.1	2014.8	79.0	596.8							
Naccowlah South-1	1796.5	75.2	571.9	1844.0	78.6	897.8							2065.5	78.2	841.2	664.8
Naccowlah West-1	1793.2	73.3	700.2													734.9
Naryilco-1																700.2
Navalla-1	1707.5	69.2	1047.5													
Nulla-1	2311.5	70.2	379.6													1047.5
Okotoko-1	1986.1	68.8	796.8	2166.3	71.3	1144.8				2409.3	73.8	960.7	2664.6	70.0	814.7	718.3
Orientos-2													2203.8	72.9	1071.6	1004.4
Packsaddle-4	2032.6	69.2	727.0	2122.5	66.0	1601.2										
Padulla-1																1164.1
Pallano-1																
Pandieburra-1																
Pando South-1																

Table 2. Continued.

	Nappamerri Group			Toolachee Formation			Roseneath Shale			Murteree Shale			Patchawarra Formation			Mean[n]
Well	Midpoint Depth (m bgl*)	Mean Δt ** (µs/ft)	E_A*** (m)	Midpoint Depth (m bgl*)	Mean Δt ** (µs/ft)	E_A*** (m)	Midpoint Depth (m bgl*)	Mean Δt ** (µs/ft)	E_A*** (m)	Midpoint Depth (m bgl*)	Mean Δt ** (µs/ft)	E_A*** (m)	Midpoint Depth (m bgl*)	Mean Δt ** (µs/ft)	E_A*** (m)	E_A*** (m)
Paning-1	2606.3	67.8	240.3										3021.1	71.9	328.7	284.5
Paragilga-1																
Patroclus-1				1858.2	73.0	1319.1	1956.6	76.4	833.4							1076.3
Paxton-1																
Pepita-2	2089.4	67.8	759.5	2229.6	71.6	1055.6										907.6
Pintari-1																
Pondrinie-5	2095.8	68.0	740.6	2204.6	72.4	1016.1										878.4
Potiron-1	2073.5	64.0	1025.2													1025.2
Putamurdie-1																
Rheims-1				1679.1	80.0	954.6	1712.7	75.1	1171.1							1062.9
Rho East-1																
Richie-1				1588.4	86.6	530.4	1633.4	83.2	685.2				1802.9	84.7	654.2	623.2
Russel-1	2619.5	66.8	297.7	2851.4	64.3	1005.3							2878.1	63.5	1052.4	785.1
Snake Hole-1	2250.5	69.7	477.0	2325.8	70.2	1071.8				2394.1	74.9	875.0	2428.9	75.4	677.3	775.3
Spectre-1	2561.4	70.4	118.2	2709.3	72.5	506.7				2759.2	75.2	490.6	3055.8	70.4	397.9	378.3
Spencer-4													1848.2	76.8	1158.4	1158.4
Steward-1	2099.8	79.3	0.0 (R+)													0.0
Strzelecki-10	1848.8	69.4	894.0	1890.8	76.7	1000.0				1984.2	70.0	1714.5	2012.1	72.4	1302.5	1227.8
Strzelecki -27																
Sturt-6																
Swan Lake-1	2409.3	67.2	478.4	2581.7	69.5	870.7				2649.8	73.2	767.5	2956.8	67.4	707.3	705.9
Taloola-1																
Tanbar-1	2636.3	66.4	306.3	2802.6	67.6	799.2										552.7
Tanbar North-1	2575.9	65.2	443.4													443.4
Tartulla-1	2204.8	68.8	578.1	2370.4	78.4	384.7							2525.4	68.7	1043.9	668.9
Tennaperra South-1				1786.5	77.4	1045.2										1045.2
Three Queens-1	2089.9	69.8	628.6	2262.9	73.8	848.2	2427.1	70.7	757.1	2569.7	69.3	1188.9	2665.1	68.1	946.6	873.9
Thurakinna-5	1929.2	74.9	459.1	1966.5	82.9	441.6	2088.0	78.3	569.6	2211.6	76.9	883.1	2259.0	77.1	725.0	615.7
Thurra-1	1839.9	74.6	567.2	1877.9	79.7	779.1	1978.2	76.9	775.7				2068.0	70.8	1356.1	869.5
Tinchoo-1	2461.9	66.9	447.9													447.9
Tinga Tingana-1							1399.3	96.5	0.0 (R+)	1480.9	95.4	0.0 (R+)	1657.7	96.2	0.0 (R+)	0.0
Tinpilla-1				1620.9	81.7	880.2	1677.5	76.3	1122.3				1789.9	74.2	1396.8	1133.1
Tirrawarra-13	2455.8	71.1	180.4							2659.4	73.1	766.9	2682.5	72.6	614.0	520.4
Tirrawarra-15	2446.8	68.6	349.1	2585.3	74.0	517.6				2646.0	73.9	711.8	2865.8	74.9	276.0	463.6
Tirrawarra-26	2470.9	70.7	190.7							2681.2	74.7	612.5	2907.1	70.1	566.0	456.4
Tirrawarra North-1	2535.3	69.6	198.4	2720.8	74.9	306.1				2760.7	74.0	590.2	3007.8	74.4	168.4	241.9
Tirrawarra West-1	2496.0	68.1	335.5	2663.9	71.9	596.2				2700.1	66.4	1318.4	2730.0	72.3	593.3	710.8
Toby-1	1973.7	67.0	930.4	2207.9	76.4	700.0							2253.3	74.3	929.0	853.1
Toolachee-9	1823.9	74.9	560.4	1885.5	82.9	519.7	2062.7	74.9	831.0	2175.0	71.6	1385.3	2208.4	69.9	1278.0	914.9
Toolachee-21	1848.2	74.4	570.3	1910.3	76.9	965.2	2054.5	74.2	889.5	2180.2	72.7	1283.7	2224.2	72.4	1089.6	959.6
Toolachee-39	1829.7	73.0	681.3	2034.1	79.6	629.6	2104.0	77.5	607.4	2251.3	72.8	1200.5	2302.1	73.4	944.0	812.6
Turban-1	2127.2	68.2	696.7													696.7
Ullenbury-1	2452.5	69.8	268.7													268.7
Wackett-3	1801.2	70.0	904.9	1865.4	77.8	936.5										920.7
Wallawanny-1																
Wancoocha-2										1689.8	77.7	1341.4	1714.6	80.8	1012.1	1176.7
Wantana-2	2413.9	65.5	583.4	2518.3	75.6	457.8							2732.7	71.2	667.5	569.5
Wareena-1	1681.2	71.1	951.4	1851.8	72.0	1400.3										1175.8
Warnie East-1	1857.8	70.9	788.6	2026.4	75.8	930.7	2304.3	73.5	686.0	2426.7	71.1	1178.7	2541.2	69.8	951.1	907.0
Watson-1																
Weena-1																
Wicho-1	2491.6	69.2	263.8	2646.2	70.1	754.1										508.9

Table 2. Continued.

	Nappamerri Group			Toolachee Formation			Roseneath Shale			Murteree Shale			Patchawarra Formation			Mean[II]
Well	Midpoint Depth (m bgl*)	Mean Δt ** (µs/ft)	E_A*** (m)	Midpoint Depth (m bgl*)	Mean Δt ** (µs/ft)	E_A*** (m)	Midpoint Depth (m bgl*)	Mean Δt ** (µs/ft)	E_A*** (m)	Midpoint Depth (m bgl*)	Mean Δt ** (µs/ft)	E_A*** (m)	Midpoint Depth (m bgl*)	Mean Δt ** (µs/ft)	E_A*** (m)	E_A*** (m)
Wills-1				1667.9	81.0	886.2	1771.0	73.4	1227.1	1826.8	72.5	1659.3				1257.5
Wimma-1	2889.2	66.3	56.4							3279.4	69.0	511.1	3348.9	67.9	278.9	331.7
Wippo-2	2079.3	69.6	651.3	2290.8	73.0	884.2							2348.3	69.9	1138.0	891.2
Wirha-1				1668.5	82.5	769.5	1715.8	80.0	825.5	1794.1	80.8	960.6	1861.2	80.4	894.9	862.6
Witchetty-1	1816.8	71.6	787.8	1880.1	82.0	594.7	2008.3	75.7	833.1	2095.5	74.3	1228.2	2148.1	74.6	1012.8	891.3
Wompi-1							1742.4	74.2	1199.5	1775.9	72.8	1683.6				1441.5
Wuroopie-1																
Yanbee-1	2420.9	67.7	433.9													433.9
Yanda-2	2059.0	71.7	533.5	2161.4	73.1	1011.4							2342.1	78.1	574.2	706.3
Yanta-1																
Yumba-1	2003.3	71.0	636.9	2081.8	74.0	1019.3										828.1

*m bgl = meters below ground level.

**Δt_{adj} = adjusted interval transit time.

***E_A = apparent exhumation.

[I]Mean = mean of the apparent exhumation values from such of the Eromanga Basin Formations as are present in any given well.

[II]Mean = mean of the apparent exhumation values from such of the Cooper Basin Formations as are present in any given well.

R* = reference well, ie. well used to define normal compaction relationship.

Table 3. Midpoint Depth and Mean Bulk Density Data and Apparent Exhumation Results

Eromanga Basin Stratigraphic Units

	Winton Formation			Mackunda Formation			Allaru Mudstone-Oodnadatta Formation			Bulldog Shale-Wallumbilla Formation			Cadna-owie Formation			Birkhead Formation			Hutton Sandstone			Mean†
Well	Midpoint Depth (m bgl*)	Mean ρ_b** (g/cm³)	E_A*** (m)	Midpoint Depth (m bgl*)	Mean ρ_b** (g/cm³)	E_A*** (m)	Midpoint Depth (m bgl*)	Mean ρ_b** (g/cm³)	E_A*** (m)	Midpoint Depth (m bgl*)	Mean ρ_b** (g/cm³)	E_A*** (m)	Midpoint Depth (m bgl*)	Mean ρ_b** (g/cm³)	E_A*** (m)	Midpoint Depth (m bgl*)	Mean ρ_b** (g/cm³)	E_A*** (m)	Midpoint Depth (m bgl*)	Mean ρ_b** (g/cm³)	E_A*** (m)	E_A*** (m)
Alkina-1													1473.9	2.4	315.1	1841.4	2.4	274.3	1977.4	2.4	452.0	347.1
Alwyn-1	443.4	1.9	189.8	613.4	2.1	154.3	785.9	2.2	659.5	1021.7	2.4	683.7	1154.4	2.4	752.4	1461.8	2.5	905.0	1496.0	2.3	701.9	578.1
Amyema-1													1374.1	2.4	538.8	1700.7	2.5	609.4	1747.5	2.4	749.1	632.4
Andree-1																2115.3	2.5	233.5	2246.4	2.4	257.3	245.4
Araburg-1																						
Arrabury-1																						
Arrakis-1																1860.2	2.5	366.0	1964.6	2.4	420.1	393.0
Atoll-1													1041.7	2.4	819.9	1378.6	2.4	824.4	1421.7	2.4	1054.5	899.6
Azolla-1													1337.6	2.4	530.3	1667.3	2.5	604.1	1705.7	2.4	695.5	609.9
Ballera-1													1514.4	2.5	434.8	1881.3	2.4	312.2	1969.4	2.4	428.9	392.0
Baratta-1	593.0	2.0	358.3	828.0	2.2	304.3	983.0	2.3	684.7	1252.1	2.4	569.7	1427.6	2.4	478.4	1759.2	2.5	635.2	1813.6	2.4	694.5	532.2
Bardoc-1													1346.8	2.4	566.9	1706.6	2.5	590.4	1758.5	2.4	817.5	658.3
Barrolka-1																						
Baryulah-1													1572.8	2.5	417.8	1951.1	2.4	96.2	1990.7	2.4	498.4	337.4
Battunga-1																						
Beanbush-1	990.5	2.0	0.0 (R*)	1220.2	2.3	0.0 (R*)	1376.4	2.2	0.0 (R*)	1717.3	2.4	0.0 (R*)	1971.1	2.5	0.0 (R*)	2348.4	2.5	0.0 (R*)	2522.9	2.4	0.0 (R*)	0.0
Belah-1													1289.8	2.4	615.6	1625.5	2.5	670.9	1661.0	2.3	607.8	631.4
Biala-1	524.6	2.0	406.0	635.8	2.1	139.5	781.3	2.2	654.2	1017.9	2.3	591.6	1158.1	2.4	699.0	1464.5	2.4	631.0	1513.2	2.3	669.5	541.5
Big Lake-26																1952.1	2.5	345.5	2032.7	2.4	496.8	421.2
Big Lake-35	655.1	1.9	4.6													1969.6	2.5	299.0	2053.7	2.4	366.3	223.3
Bogala-1	359.9	1.9	299.8	550.5	2.2	537.4	694.0	2.3	841.8	978.1	2.3	604.4	1195.0	2.4	705.8	1538.8	2.5	835.4	1605.4	2.4	853.8	668.3
Boldrewood-1																						
Bookabourdie-1													1720.1	2.4	181.2	2102.2	2.5	135.7	2231.1	2.4	175.6	164.2
Boxwood-1																						
Brolga-2																						
Buckinna-1	507.4	2.0	512.9	682.4	2.2	230.1	834.5	2.3	714.5				1194.5	2.4	651.8	1520.6	2.5	768.5	1557.5	2.3	639.4	586.2
Bungee-1																						
Burke-2	476.7	2.0	358.5	791.0	2.2	276.0	993.7	2.2	272.0	1293.5	2.3	204.3	1482.0	2.5	476.6							317.4
Burley-2	578.0	1.9	0.0 (R*)	926.7	2.3	501.8	1106.7	2.1	0.0 (R*)	1447.1	2.5	506.3	1687.8	2.5	383.4	2082.2	2.5	164.9	2177.0	2.4	216.9	253.3
Bycoe-1	327.1	2.0	653.1	482.1	2.2	369.3	622.1	2.3	868.0	921.8	2.4	774.3	1135.9	2.4	752.3	1491.7	2.5	774.4	1553.7	2.4	893.8	726.5
Carney-1																						
Challum-1													1489.4	2.5	506.3	1853.3	2.5	407.3	1967.0	2.4	639.9	517.8
Charo-1																1766.5	2.4	412.4	1913.7	2.3	446.7	429.5
Childie-1	443.9	2.0	446.4	699.8	2.2	223.1	889.6	2.3	706.4	1176.7	2.4	594.0	1335.9	2.4	568.6	1659.3	2.5	677.4	1695.8	2.3	605.0	545.8
Cooba-1																						
Cook-1																1920.4	2.5	313.1	2076.1	2.4	510.2	411.7
Cook North-1													1596.7	2.5	389.0	1934.7	2.5	364.4	2067.2	2.5	562.9	438.8
Coonavalla-1																						
Cooroo-1										1183.1	2.4	605.2	1366.0	2.5	574.1	1726.7	2.5	638.0	1781.4	2.4	749.1	
Copai-1				693.9	2.5	1286.1							1285.4	2.5	674.5	1602.3	2.5	669.6	1752.5	2.4	790.4	855.2
Cowan-3																						
Cuddapan-1																						
Curalle-1				350.4	2.4	1306.4	518.9	2.3	1025.4	802.9	2.5	1155.8	939.9	2.5	1094.0	1246.9	2.5	1143.0	1387.8	2.5	1311.9	1172.7
Daer-1																1876.8	2.5	348.8	2046.3	2.4	342.5	345.6
Daralingie-15																						
Daralingie-23																			1863.2	2.4	564.2	564.2
Darter-1																						
Della-7													1353.6	2.5	604.1	1695.6	2.5	699.3	1781.1	2.5	869.2	724.2

Table 3. Continued.

Well	Winton Formation Midpoint Depth (m bgl*)	Winton Formation Mean ρ_b** (g/cm³)	Winton Formation E_A*** (m)	Mackunda Formation Midpoint Depth (m bgl*)	Mackunda Formation Mean ρ_b** (g/cm³)	Mackunda Formation E_A*** (m)	Allaru Mudstone-Oodnadatta Formation Midpoint Depth (m bgl*)	Allaru Mudstone-Oodnadatta Formation Mean ρ_b** (g/cm³)	Allaru Mudstone-Oodnadatta Formation E_A*** (m)	Bulldog Shale-Wallumbilla Formation Midpoint Depth (m bgl*)	Bulldog Shale-Wallumbilla Formation Mean ρ_b** (g/cm³)	Bulldog Shale-Wallumbilla Formation E_A*** (m)	Cadna-owie Formation Midpoint Depth (m bgl*)	Cadna-owie Formation Mean ρ_b** (g/cm³)	Cadna-owie Formation E_A*** (m)	Birkhead Formation Midpoint Depth (m bgl*)	Birkhead Formation Mean ρ_b** (g/cm³)	Birkhead Formation E_A*** (m)	Hutton Sandstone Midpoint Depth (m bgl*)	Hutton Sandstone Mean ρ_b** (g/cm³)	Hutton Sandstone E_A*** (m)	Mean¹ E_A*** (m)
Della-10													1338.4	2.4	585.4	1670.6	2.5	685.4	1755.8	2.4	760.1	676.9
Denley-1																						
Deparanie-1																						
Deramookoo-1																						
Dirkala-2																1627.6	2.4	552.8	1689.0	2.3	626.5	589.7
Doonmulla-1																						
Dullingari-3																						
Dullingari North-1																						
Dunoon-1	391.5	1.9	354.2	565.3	2.1	0.0 (R*)	732.8	2.1	404.7	973.9	2.3	520.0	1109.0	2.4	687.2	1407.1	2.5	828.8	1423.4	2.3	937.6	533.2
Durham Downs-1																						
Etchuburra North-1																						
Fly Lake-1																						
Fly Lake-4													1733.5	2.4	81.5	2087.1	2.5	325.9	2239.4	2.4	381.7	263.0
Garanjanie-2																1629.6	2.4	540.3	1686.9	2.3	481.7	511.0
Gidgealpa-20													1465.8	2.4	438.4	1801.7	2.4	332.7	1869.2	2.3	377.5	382.9
Gidgealpa-42													1464.6	2.4	399.7	1808.7	2.5	531.4	1903.8	2.3	421.1	450.7
Gidgee-1													1125.2	2.4	698.9	1450.1	2.5	939.6	1477.5	2.4	920.8	853.1
Gooranie-1																2046.7	2.5	274.7	2177.8	2.4	325.6	300.1
Gooranie-2																						
Graham-1													1139.5	2.4	764.7	1481.3	2.5	792.4	1542.0	2.4	916.6	824.6
Gurra-1																						
Haddon Downs-1										1118.1	2.5	905.4	1258.6	2.5		1542.8	2.5	782.7	1701.8	2.4	875.7	
Hammond-1															718.7							829.2
Hooley-1													997.1	2.4	914.0	1346.8	2.5	921.4	1424.6	2.4	1121.7	812.0
Hume-1	506.7	2.0	489.5	748.4	2.2	304.6	928.9	2.2	436.4	1194.1	2.1	0.0 (R*)	1377.1	2.4	485.4	1706.1	2.5	643.4	1748.3	2.4	745.4	985.7
Hydra-1													1170.2	2.4	709.2	1497.8	2.5	836.3	1527.8	2.4	884.4	443.5
Ingella-1																1979.0	2.5	262.5	2122.0	2.4	347.3	810.0
Innamincka-3																1525.2	2.5	789.7	1643.3	2.4	894.0	304.9
Innamincka-4													1228.8	2.4	629.6	1595.5	2.3	365.7	1712.4	2.4	850.2	841.8
Jack Lake-2																						
Jackson-1													1055.8	2.4	816.0	1402.2	2.5	848.7	1459.1	2.4	917.2	860.6
Jackson South-1													1035.5	2.4	781.9	1396.9	2.4	775.2	1454.6	2.4	930.9	829.3
James-1													1578.7	2.5	384.0	1912.6	2.5	384.5	2067.0	2.4	487.1	418.5
Jarrar-1													1405.7	2.5	543.6	1774.5	2.5	631.0	1826.3	2.4	771.9	648.8
Johba-1																						
Kalladeina-1	537.4	2.0	434.4	731.2	2.1	14.5	877.5	2.2	379.2	1146.0	2.3	427.3	1314.1	2.4	466.1	1652.8	2.4	469.5	1820.7	2.3	430.3	374.5
Karmona-2																						
Karwin-1													1209.3	2.4	624.5	1563.3	2.4	581.2	1626.2	2.3	701.5	635.7
Keeto-2																						
Keilor-1													1508.6	2.5	441.1	1878.2	2.5	428.1	1986.1	2.5	645.2	504.8
Kenny-1													1753.1	2.5	208.5	2092.5	2.4	0.0 (R*)	2248.5	2.4	181.6	130.1
Kercummurra-1													986.0	2.5	940.5	1351.0	2.5	967.5	1442.6	2.4	1168.0	1025.3
Kerna-5	640.9	2.0	177.4																			177.4
Kirby-1																2010.9	2.5	363.3	2113.9	2.4	291.8	327.5
Kirby-2																						
Kiwarrick-1													1195.3	2.4	711.2	1518.5	2.4	622.0	1567.4	2.3	761.3	698.2
Kobari-1							809.5	2.2	555.8				1172.1	2.4	721.8	1451.6	2.4	697.2	1499.6	2.3	755.1	682.5
Kooncheera-1	518.5	2.1	571.5	696.3	2.2	348.4	849.8	2.3	629.7	1122.8	2.3	474.4	1300.3	2.4	605.5	1609.3	2.5	654.3	1795.3	2.4	744.4	575.4
Kumbarie-1																						
Kurunda-1													1575.6	2.5	400.2	1913.3	2.4	281.2	2024.6	2.3	345.1	342.2
Kutyo-1													1453.6	2.5	487.4	1814.4	2.5	437.5	1869.0	2.4	695.5	540.1

Table 3. Continued.

Well	Winton Formation			Mackunda Formation			Allaru Mudstone-Oodnadatta Formation			Bulldog Shale-Wallumbilla Formation			Cadna-owie Formation			Birkhead Formation			Hutton Sandstone			Mean*
	Midpoint Depth (m bgl*)	Mean ρ_b^{**} (g/cm³)	E_A^{***} (m)	Midpoint Depth (m bgl*)	Mean ρ_b^{**} (g/cm³)	E_A^{***} (m)	Midpoint Depth (m bgl*)	Mean ρ_b^{**} (g/cm³)	E_A^{***} (m)	Midpoint Depth (m bgl*)	Mean ρ_b^{**} (g/cm³)	E_A^{***} (m)	Midpoint Depth (m bgl*)	Mean ρ_b^{**} (g/cm³)	E_A^{***} (m)	Midpoint Depth (m bgl*)	Mean ρ_b^{**} (g/cm³)	E_A^{***} (m)	Midpoint Depth (m bgl*)	Mean ρ_b^{**} (g/cm³)	E_A^{***} (m)	E_A^{***} (m)
Lake Mcmillan-1													1848.0	2.4	43.4	2212.7	2.5	38.5	2353.5	2.4	155.5	79.1
Lambda-1	405.4	2.1	688.1	634.5	2.2	446.3	820.1	2.3	895.2	1070.3	2.4	748.1	1240.7	2.5	755.9	1558.8	2.4	493.6				671.2
Lhotsky-1																						
Limestone Creek-9													1157.7	2.4	694.2							694.2
Lycium-1																						
Macadama-1																						
Mackillop-1																						
Marabooka-2	525.5	2.0	348.5	712.7	2.1	93.8				1196.2	2.3	308.7	1368.8	2.4	515.8	1712.0	2.5	600.8	1781.8	2.4	634.8	417.1
Marengo-1																						
Marsilea-1													1397.3	2.4	513.3	1739.4	2.5	575.6	1773.4	2.4	787.8	625.6
Mawson-1													1578.9	2.4	319.3	1893.8	2.4	322.8	2012.4	2.4	368.6	336.9
Mckinlay-3													1153.0	2.4	688.6	1469.9	2.5	750.2	1506.0	2.3	695.7	711.5
Mcleod-1																						
Meeba-1																						
Meranji-1																1982.4	2.5	315.4	2105.6	2.4	338.1	326.8
Merrimelia-7	583.4	2.0	448.0	918.3	2.2	271.3	1047.1	2.2	382.5	1317.2	2.2	97.8	1532.7	2.4	378.9	1874.8	2.5	388.8	1981.8	2.4	530.2	356.8
Merrimelia-25																						
Minkie-1																						
Mooliampah-1													1186.7	2.4	680.5	1513.2	2.5	762.0	1548.2	2.4	868.8	770.4
Moolion-1																2183.1	2.5	37.3	2323.2	2.4	238.9	138.1
Moomba-27																						
Moomba-57																			2096.2	2.4	314.2	314.2
Moomba North-1																2029.7	2.4	151.2	2139.1	2.3	223.8	187.5
Moomba South-1																2013.4	2.5	335.3	2109.3	2.4	397.4	366.4
Moorari-4																2158.4	2.5	89.0	2285.7	2.4	223.6	156.3
Morney-1										859.0	2.3	768.5	995.4	2.5	935.1	1332.7	2.4	827.5	1472.9	2.4	1103.7	908.7
Mudera-3										1224.7	2.4	494.4	1412.0	2.4	414.7	1763.1	2.5	515.1	1829.3	2.4	638.5	515.6
Munkah-2													1390.3	2.5	546.0	1766.6	2.5	525.1	1854.4	2.4	694.9	588.7
Munkarie South-1	336.5	2.0	481.9	533.5	2.1	236.5	682.4	2.2	731.5	920.7	2.3	715.4	1084.8	2.4	714.2	1404.9	2.4	722.5	1429.4	2.3	819.2	631.6
Munro-1													1109.8	2.4	692.2	1435.9	2.5	857.1	1459.4	2.3	853.3	800.8
Muteroo-3													1365.0	2.5	574.5	1677.3	2.4	540.1				557.3
Naccowlah East-1													1343.0	2.5	659.2	1699.0	2.5	706.5	1783.4	2.5	878.3	748.0
Naccowlah South-1										1093.1	2.4	629.3	1303.7	2.4	607.6	1653.4	2.5	695.9	1722.6	2.4	750.5	670.8
Naccowlah West-1							813.6	2.1	336.9	1096.3	2.4	584.8	1304.3	2.4	615.5	1661.2	2.5	694.9	1731.9	2.4	790.2	604.4
Naryilco-1																						
Navalla-1																						
Nulla-1																1998.7	2.5	286.0	2137.1	2.4	365.7	325.9
Okotoko-1										1149.6	2.4	675.2	1376.9	2.5	572.8	1732.9	2.5	615.5	1825.0	2.4	758.0	655.4
Orientos-2													1254.3	2.5	749.8							749.8
Packsaddle-4													1394.0	2.4	513.9	1736.1	2.5	644.8	1848.2	2.4	632.8	597.1
Padulla-1	384.9	2.2	1248.3	627.4	2.2	559.0	788.0	2.2	658.5	993.2	2.3	454.7	1098.3	2.4	692.0	1384.6	2.4	793.7	1433.2	2.3	884.9	755.9
Pallano-1													1414.6	2.5	564.1	1773.9	2.5	610.2	1828.5	2.4	789.0	654.4
Pandieburra-1																						
Pando South-1																						
Paning-1													1666.7	2.3	0.0 (R*)	2037.1	2.5	216.7	2186.9	2.4	323.3	180.0
Paragilga-1													1107.2	2.4	708.9	1441.3	2.5	871.8	1467.6	2.4	906.1	828.9
Patroclus-1													1404.2	2.5	554.5	1738.5	2.5	595.0	1788.0	2.4	702.5	617.3
Paxton-1	271.4	2.0	519.6	400.4	2.1	129.6	559.5	2.1	639.2	726.3	2.2	622.6	815.8	2.3	866.2							555.4
Pepita-2										1188.2	2.4	516.1	1423.2	2.4	502.4	1773.6	2.5	571.7	1884.6	2.4	632.1	555.6
Pintari-1	499.8	2.0	279.2	759.5	2.2	201.6	919.6	2.3	556.1	1125.8	2.3	478.0	1239.5	2.4	603.3	1541.7	2.3	416.0	1643.0	2.3	607.7	448.8
Pondrinie-5													1432.4	2.4	443.9	1790.4	2.5	528.5	1900.3	2.4	562.8	511.7

Table 3. Continued.

Well	Winton Formation Midpoint Depth (m bgl*)	Winton Formation Mean ρ_b** (g/cm³)	Winton Formation E_A*** (m)	Mackunda Formation Midpoint Depth (m bgl*)	Mackunda Formation Mean ρ_b** (g/cm³)	Mackunda Formation E_A*** (m)	Allaru Mudstone-Oodnadatta Formation Midpoint Depth (m bgl*)	Allaru Mudstone-Oodnadatta Formation Mean ρ_b** (g/cm³)	Allaru Mudstone-Oodnadatta Formation E_A*** (m)	Bulldog Shale-Wallumbilla Formation Midpoint Depth (m bgl*)	Bulldog Shale-Wallumbilla Formation Mean ρ_b** (g/cm³)	Bulldog Shale-Wallumbilla Formation E_A*** (m)	Cadna-owie Formation Midpoint Depth (m bgl*)	Cadna-owie Formation Mean ρ_b** (g/cm³)	Cadna-owie Formation E_A*** (m)	Birkhead Formation Midpoint Depth (m bgl*)	Birkhead Formation Mean ρ_b** (g/cm³)	Birkhead Formation E_A*** (m)	Hutton Sandstone Midpoint Depth (m bgl*)	Hutton Sandstone Mean ρ_b** (g/cm³)	Hutton Sandstone E_A*** (m)	Mean† E_A*** (m)
Potiron-1													1256.6	2.5	740.4	1568.1	2.5	672.4	1748.4	2.5	929.7	780.8
Putamurdie-1																						
Rheims-1													1185.8	2.4	688.4	1517.8	2.5	718.6	1550.1	2.3	705.7	704.2
Rho East-1													1071.2	2.4	796.8	1407.4	2.5	944.4	1429.4	2.3	894.0	878.4
Richie-1	280.2	1.9	478.7	425.0	2.1	317.1	630.8	2.3	867.4	916.1	2.4	801.1	1087.1	2.4	794.0	1446.1	2.5	775.8	1496.1	2.3	837.8	696.0
Russel-1																2106.8	2.5	138.2	2256.1	2.3	0.0 (R*)	69.1
Snake Hole-1													1597.5	2.4	314.5	1929.2	2.5	388.1	2040.6	2.4	362.3	355.0
Spectre-1																2146.7	2.5	153.3	2278.8	2.4	304.0	228.7
Spencer-4													1331.7	2.4	590.7	1640.6	2.4	532.9	1743.2	2.3	551.1	558.2
Steward-1																						
Strzelecki-10				744.9	2.2	246.9	923.8	2.1	131.3	1180.6	2.2	258.1	1354.7	2.4	524.5	1719.5	2.5	522.5	1778.4	2.4	669.2	392.1
Strzelecki -27	531.4	2.0	389.8													1655.1	2.5	634.6	1707.9	2.4	741.0	588.5
Sturt-6																1648.1	2.4	491.7	1745.9	2.3	603.8	547.8
Swan Lake-1													1727.5	2.5	273.7	2089.6	2.5	266.3	2208.3	2.4	398.7	312.9
Taloola-1													1326.2	2.4	549.0	1649.8	2.5	640.6	1746.1	2.4	647.3	612.3
Tanbar-1																						
Tanbar North-1																2074.2	2.5	272.0	2225.0	2.5	442.2	357.1
Tartulla-1																1877.6	2.5	487.0	1972.2	2.4	635.1	561.1
Tennaperra South-1													1315.2	2.4	602.8	1656.3	2.5	672.5	1692.1	2.4	910.2	728.5
Three Queens-1																						
Thurakinna-5													1487.7	2.4	418.5	1782.2	2.4	436.4	1834.6	2.4	569.7	474.9
Thurra-1													1314.6	2.4	600.9	1685.3	2.5	593.7	1755.8	2.4	780.3	658.3
Tinchoo-1																						
Tinga Tingana-1																						
Tinpilla-1	312.1	1.8	109.0	473.5	2.1	359.4	664.8	2.0	85.4	949.1	2.3	626.5	1136.3	2.4	751.0	1487.0	2.5	798.3	1547.9	2.3	821.1	507.3
Tirrawarra-13																2047.7	2.5	295.5	2192.6	2.4	389.5	342.5
Tirrawarra-15																						
Tirrawarra-26																						
Tirrawarra North-1																2124.8	2.5	215.5	2267.1	2.4	244.0	229.7
Tirrawarra West-1																2089.0	2.4	60.1	2227.9	2.4	283.9	172.0
Toby-1										916.5	2.4	963.6	1134.3	2.5	821.5	1519.3	2.5	792.0	1638.6	2.4	954.3	882.9
Toolachee-9													1349.3	2.4	553.9	1680.3	2.5	606.3	1728.6	2.4	697.8	619.3
Toolachee-21													1359.4	2.4	543.8	1689.4	2.5	629.7	1747.6	2.4	647.8	607.1
Toolachee-39																						
Turban-1													1382.3	2.5	547.2	1761.3	2.5	566.3	1884.9	2.4	619.8	577.8
Ullenbury-1													1552.2	2.5	449.8	1911.7	2.4	305.7	2064.1	2.4	465.5	407.0
Wackett-3													1282.1	2.4	609.5	1643.3	2.5	609.2	1714.6	2.4	812.5	677.0
Wallawanny-1													1409.3	2.4	483.2	1782.8	2.5	520.1	1830.7	2.4	724.2	575.8
Wancoocha-2	554.1	2.0	434.0	750.4	2.1	57.9	907.4	2.1	246.6	1122.0	2.3	420.9	1263.2	2.4	610.6	1550.2	2.4	627.9	1612.2	2.4	945.9	477.7
Wantana-2																2006.2	2.5	381.8				381.8
Wareena-1				306.8	2.2	842.6	437.7	2.1	748.8	715.2	2.2	704.4	927.8	2.5	1017.3	1294.4	2.4	780.7	1397.5	2.4	1168.9	877.1
Warnie East-1													1320.4	2.5	612.4	1667.1	2.5	687.9	1702.6	2.4	778.2	692.8
Watson-1													1227.3	2.4	694.1	1568.8	2.5	782.3	1603.9	2.4	926.7	801.1
Weena-1																						
Wicho-1																						
Wills-1	428.2	2.0	540.7	591.2	2.2	352.9	773.1	2.2	682.1	1046.7	2.3	580.0	1215.2	2.5	713.5	1570.5	2.5	666.8	1605.2	2.3	754.2	612.9
Wimma-1													1969.4	2.5	8.4	2357.4	2.5	3.5	2492.8	2.4	4.5	5.4
Wippo-2																						
Wirha-1													1246.7	2.4	622.2	1559.3	2.5	697.9	1595.5	2.4	852.4	724.2
Witchetty-1																						
Wompi-1	380.4	2.0	470.4	574.2	2.2	380.0	746.0	2.3	753.6	1021.1	2.4	751.2	1215.1	2.4	704.7	1555.5	2.5	828.9	1582.4	2.4	958.4	692.5

Table 3. Continued.

Well	Winton Formation Midpoint Depth (m bgl*)	Winton Formation Mean ρ_b** (g/cm³)	Winton Formation E_A*** (m)	Mackunda Formation Midpoint Depth (m bgl*)	Mackunda Formation Mean ρ_b** (g/cm³)	Mackunda Formation E_A*** (m)	Allaru Mudstone-Oodnadatta Formation Midpoint Depth (m bgl*)	Allaru Mudstone-Oodnadatta Formation Mean ρ_b** (g/cm³)	Allaru Mudstone-Oodnadatta Formation E_A*** (m)	Bulldog Shale-Wallumbilla Formation Midpoint Depth (m bgl*)	Bulldog Shale-Wallumbilla Formation Mean ρ_b** (g/cm³)	Bulldog Shale-Wallumbilla Formation E_A*** (m)	Cadna-owie Formation Midpoint Depth (m bgl*)	Cadna-owie Formation Mean ρ_b** (g/cm³)	Cadna-owie Formation E_A*** (m)	Birkhead Formation Midpoint Depth (m bgl*)	Birkhead Formation Mean ρ_b** (g/cm³)	Birkhead Formation E_A*** (m)	Hutton Sandstone Midpoint Depth (m bgl*)	Hutton Sandstone Mean ρ_b** (g/cm³)	Hutton Sandstone E_A*** (m)	Mean† E_A*** (m)
Wuroopie-1																						
Yanbee-1																						
Yanda-2													1448.2	2.5	502.2	1827.0	2.5	509.3	1912.7	2.4	664.4	558.6
Yanta-1													1472.2	2.4	426.1	1810.1	2.5	427.7	1972.7	2.4	449.2	434.3
Yumba-1	567.1	2.1	594.3	751.9	2.3	476.9	897.6	2.4	893.6	1177.1	2.4	663.7	1406.0	2.5	542.1	1790.7	2.5	513.2	1869.3	2.4	681.2	623.6

Cooper Basin Stratigraphic Units

Well	Nappamerri Group Midpoint Depth (m bgl*)	Nappamerri Group Mean ρ_b** (g/cm³)	Nappamerri Group E_A*** (m)	Toolachee Formation Midpoint Depth (m bgl*)	Toolachee Formation Mean ρ_b** (g/cm³)	Toolachee Formation E_A*** (m)	Roseneath Shale Midpoint Depth (m bgl*)	Roseneath Shale Mean ρ_b** (g/cm³)	Roseneath Shale E_A*** (m)	Murteree Shale Midpoint Depth (m bgl*)	Murteree Shale Mean ρ_b** (g/cm³)	Murteree Shale E_A*** (m)	Patchawarra Formation Midpoint Depth (m bgl*)	Patchawarra Formation Mean ρ_b** (g/cm³)	Patchawarra Formation E_A*** (m)	Mean‡ E_A*** (m)
Alkina-1	2379.9	2.5	574.5	2579.0	2.5	653.0							2633.5	2.5	826.2	684.6
Alwyn-1																
Amyema-1	1824.1	2.7	1578.3	1909.2	2.6	1540.8	2088.2	2.7	740.5	2211.1	2.7	1167.8	2254.1	2.6	1352.2	1275.9
Andree-1	2521.2	2.6	765.0	2636.9	2.5	659.9				2721.7	2.7	626.6	2753.9	2.5	687.3	684.7
Araburg-1																
Arrabury-1																
Arrakis-1	2101.7	2.6	1249.7	2149.8	2.5	1059.5	2194.7	2.6	608.9	2273.2	2.6	1041.3	2315.0	2.5	1079.9	1007.8
Atoll-1																
Azolla-1	1775.3	2.6	1466.2	1842.6	2.5	1280.4	2053.6	2.6	648.7	2191.2	2.6	1118.0	2242.5	2.5	1321.5	1167.0
Ballera-1	2148.6	2.5	793.8	2280.9	2.5	1028.7							2472.1	2.4	667.1	829.9
Baratta-1	1921.5	2.7	1601.2	1988.0	2.5	1299.2	2079.4	2.6	668.0	2155.3	2.7	1257.1	2197.4	2.5	1339.4	1233.0
Bardoc-1																
Barrolka-1																
Baryulah-1	2128.2	2.6	1063.6	2250.5	2.6	1365.7	2359.5	2.5	0.0 (R*)	2439.5	2.6	764.9	2483.3	2.4	717.8	782.4
Battunga-1																
Beanbush-1	2936.2	2.5	0.0 (R*)							3280.2	2.6	0.0 (R*)	3395.1	2.6	246.3	246.3
Belah-1	1724.3	2.6	1437.6	1827.9	2.5	1310.0	1952.7	2.6	794.7	2026.8	2.6	1199.8	2224.5	2.5	1279.8	1204.4
Biala-1																
Big Lake-26	2171.1	2.7	1273.5	2304.8	2.4	635.2	2376.2	2.7	576.3	2499.9	2.7	940.2	2558.4	2.6	1040.1	893.1
Big Lake-35	2201.6	2.7	1224.9	2347.6	2.4	675.6	2419.5	2.7	619.9	2544.0	2.7	902.3	2605.6	2.5	947.4	874.0
Bogala-1				1740.9	2.4	1322.0	1813.1	2.5	436.2				1900.9	2.4	1347.3	1035.2
Boldrewood-1																
Bookabourdie-1	2498.3	2.5	348.8										2815.8	2.5	745.4	547.1
Boxwood-1																
Brolga-2																
Buckinna-1																
Bungee-1	1844.7	2.6	1436.4	1930.1	2.4	1048.4				2109.3	2.6	1139.2	2161.1	2.5	1353.8	1244.5
Burke-2																
Burley-2	2470.3	2.6	804.8	2701.3	2.5	433.9	2941.9	2.7	42.5	3153.5	2.7	293.0	3260.0	2.5	304.6	375.8
Bycoe-1				1622.5	2.4	1236.2	1663.2	2.4	196.2				1723.8	2.4	1502.3	978.2
Carney-1																
Challum-1	2162.3	2.6	1201.7										2355.4	2.5	935.7	1068.7
Charo-1																
Childie-1	1794.4	2.7	1696.8	1886.0	2.4	984.5				1942.8	2.7	1395.0	1981.9	2.5	1392.6	1367.2
Cooba-1																
Cook-1	2401.7	2.6	823.2													823.2
Cook North-1	2415.5	2.6	767.4													767.4
Coonavalla-1																
Cooroo-1				1856.6	2.5	1246.9										1246.9

Table 3. Continued.

	Nappamerri Group			Toolachee Formation			Roseneath Shale			Murteree Shale			Patchawarra Formation			Mean[#]
Well	Midpoint Depth (m bgl*)	Mean ρ_b** (g/cm³)	E_A*** (m)	Midpoint Depth (m bgl*)	Mean ρ_b** (g/cm³)	E_A*** (m)	Midpoint Depth (m bgl*)	Mean ρ_b** (g/cm³)	E_A*** (m)	Midpoint Depth (m bgl*)	Mean ρ_b** (g/cm³)	E_A*** (m)	Midpoint Depth (m bgl*)	Mean ρ_b** (g/cm³)	E_A*** (m)	E_A*** (m)
Copai-1																
Cowan-3										2205.4	2.7	1206.4	2247.7	2.6	1347.5	1276.9
Cuddapan-1																
Curalle-1	1722.0	2.6	1499.6													1499.6
Daer-1	2268.3	2.5	641.2	2348.3	2.4	415.7										528.5
Daralingie-15																
Daralingie-23	1952.2	2.6	1318.3				2097.8	2.6	644.1	2196.1	2.6	1047.6	2233.9	2.5	1208.1	1054.5
Darter-1																
Della-7	1877.8	2.7	1608.3													1608.3
Della-10	1863.1	2.6	1509.3	1961.4	2.3	734.0							1981.4	2.5	1335.4	1192.9
Denley-1																
Deparanie-1																
Deramookoo-1																
Dirkala-2				1775.9	2.4	1133.3	1819.2	2.6	667.8	1908.4	2.6	1207.1	1959.5	2.5	1337.5	1086.4
Doonmulla-1																
Dullingari-3	2033.6	2.6	1216.0	2169.6	2.4	784.0	2317.2	2.7	722.0	2431.5	2.7	1021.3	2498.0	2.5	876.5	924.0
Dullingari North-1	2022.5	2.6	1102.9	2155.9	2.5	953.5	2290.6	2.7	633.9	2396.0	2.7	1020.1	2444.1	2.4	592.7	860.7
Dunoon-1																
Durham Downs-1																
Echuburra North-1																
Fly Lake-1	2477.4	2.6	754.5	2589.1	2.5	731.9				2599.8	2.6	600.2	2801.8	2.4	449.6	634.0
Fly Lake-4	2506.2	2.6	741.2	2637.6	2.5	639.1				2648.6	2.6	627.6	2666.1	2.5	795.3	700.8
Garanjanie-2	1753.1	2.5	1019.1	1796.8	2.4	981.7	1837.5	2.6	609.8	1937.8	2.6	1201.0	1982.1	2.5	1437.8	1049.9
Gidgealpa-20																
Gidgealpa-42	2072.0	2.6	1140.5	2121.2	2.5	964.3							2134.7	2.5	1382.4	1162.6
Gidgee-1				1502.1	2.5	1572.4				1517.0	2.6	1603.8	1582.4	2.4	1502.6	1559.6
Gooranie-1	2454.9	2.6	883.1	2623.3	2.5	625.8				2670.8	2.7	730.8	2963.3	2.5	508.7	687.1
Gooranie-2	2462.5	2.6	880.2	2621.8	2.5	541.9				2673.7	2.7	752.7	2958.3	2.5	518.2	673.3
Graham-1				1590.0	2.3	1035.8	1700.3	2.5	612.1				1790.9	2.4	1465.9	1037.9
Gurra-1																
Haddon Downs-1																
Hammond-1			1061.1													1061.1
Hooley-1	1533.4	2.6	1558.0													1558.0
Hume-1	1816.3	2.7	1615.1	1897.9	2.5	1422.5	2023.1	2.7	869.9	2091.5	2.6	1216.1	2114.7	2.3	626.2	1150.0
Hydra-1				1633.6	2.4	1367.3	1661.3	2.6	980.7	1728.9	2.6	1429.5	1762.0	2.5	1704.7	1370.5
Ingella-1	2457.9	2.5	494.3													494.3
Innamincka-3	1818.3	2.6	1419.4													1419.4
Innamincka-4	1926.3	2.5	958.8	2075.5	2.3	433.3										696.0
Jack Lake-2				2473.8	2.5	932.6	2522.9	2.6	56.1	2600.2	2.7	727.7	2641.3	2.5	704.0	605.1
Jackson-1				1535.4	2.4	1403.3	1577.9	2.5	689.3				1668.6	2.4	1538.7	1210.4
Jackson South-1				1488.6	2.5	1609.4	1546.4	2.5	708.6				1761.1	2.4	1373.4	1230.5
James-1	2339.5	2.6	729.9													729.9
Jarrar-1																
Johba-1																
Kalladeina-1																
Karmona-2																
Karwin-1				1727.1	2.5	1370.9	1928.4	2.6	474.9	2046.7	2.5	816.8	2254.6	2.5	1125.5	947.0
Keeto-2																
Keilor-1	2243.6	2.6	1075.2	2451.1	2.5	719.1							2555.2	2.5	787.5	860.6
Kenny-1	2628.4	2.4	99.6													99.6
Kercummurra-1	1645.6	2.6	1604.4	1832.3	2.5	1294.7										1449.5
Kerna-5				2058.9	2.6	1539.7	2284.2	2.7	697.8	2467.3	2.7	991.8	2452.1	2.5	971.7	1050.3

Table 3. Continued.

Well	Nappamerri Group			Toolachee Formation			Roseneath Shale			Murteree Shale			Patchawarra Formation			Mean[‡]
	Midpoint Depth (m bgl[*])	Mean ρ_b[**] (g/cm³)	E_A[***] (m)	Midpoint Depth (m bgl[*])	Mean ρ_b[**] (g/cm³)	E_A[***] (m)	Midpoint Depth (m bgl[*])	Mean ρ_b[**] (g/cm³)	E_A[***] (m)	Midpoint Depth (m bgl[*])	Mean ρ_b[**] (g/cm³)	E_A[***] (m)	Midpoint Depth (m bgl[*])	Mean ρ_b[**] (g/cm³)	E_A[***] (m)	E_A[***] (m)
Kirby-1	2452.9	2.7	993.6	2718.3	2.3	0.0 (R[+])	2836.4	2.7	191.8	3049.4	2.6	0.0 (R[+])	3174.3	2.4	0.0 (R[+])	237.1
Kirby-2																
Kiwarrick-1				1681.5	2.5	1439.5	1632.5	2.6	740.4	1712.2	2.6	1436.9	1753.1	2.5	1607.0	1305.9
Kobari-1										1580.1	2.5	1385.0	1661.4	2.4	1418.8	1401.9
Koonchera-1																
Kumbarie-1																
Kurunda-1	2177.9	2.6	1174.9	2210.5	2.3	197.9				2276.3	2.6	965.6	2311.2	2.5	1031.0	842.4
Kutyo-1				1964.9	2.5	1177.1										1177.1
Lake Mcmillan-1	2673.6	2.6	411.0							2945.9	2.7	458.8	3069.9	2.5	284.4	384.7
Lambda-1																
Lhotsky-1																
Limestone Creek-9																
Lycium-1																
Macadama-1																
Mackillop-1																
Marabooka-2	1890.5	2.7	1598.0	1943.4	2.5	1333.1				1996.7	2.6	1262.4	2162.8	2.5	1214.4	1352.0
Marengo-1																
Marsilea-1	1864.4	2.6	1487.9	1955.1	2.5	1372.4	2154.5	2.7	730.9	2278.3	2.7	1144.4	2326.8	2.5	1039.5	1155.0
Mawson-1	2195.5	2.7	1219.8	2244.4	2.4	615.0				2271.1	2.6	1012.3	2302.6	2.5	1044.8	973.0
Mckinlay-3																
Mcleod-1	2422.1	2.6	806.2	2657.7	2.4	245.1	2935.7	2.7	0.0 (R[+])	3157.3	2.7	234.5	3243.7	2.5	311.8	319.5
Meeba-1																
Meranji-1	2333.1	2.7	1090.2	2470.9	2.4	427.6				2522.7	2.7	835.3	2813.2	2.5	490.4	710.9
Merrimelia-7	2165.1	2.6	1019.0	2227.6	2.6	1194.1										1106.5
Merrimelia-25	2199.4	2.6	1016.6	2262.8	2.4	599.7										808.1
Minkie-1																
Mooliampah-1				1586.3	2.4	1434.4	1658.3	2.6	830.9	1705.5	2.6	1390.6	1757.2	2.4	1472.1	1282.0
Moolion-1	2621.9	2.5	380.5	2813.2	2.5	499.6				2842.9	2.7	489.5	2923.0	2.3	0.0 (R[+])	342.4
Moomba-27							2627.3	2.6	141.5	2722.5	2.7	706.7	2781.6	2.6	935.0	594.4
Moomba-57				2384.6	2.5	857.5	2583.1	2.7	334.0							595.7
Moomba North-1	2328.1	2.7	1220.7	2496.3	2.4	515.9	2619.2	2.7	332.5	2753.2	2.7	702.9	2811.4	2.6	813.0	717.0
Moomba South-1	2256.6	2.7	1148.3	2408.8	2.4	589.2	2524.4	2.7	395.2	2677.6	2.7	734.3	2734.5	2.5	828.7	739.1
Moorari-4	2541.0	2.5	496.2							2710.3	2.7	642.5	2849.2	2.4	391.9	510.2
Morney-1	1818.4	2.6	1405.9													1405.9
Mudera-3	1947.1	2.6	1330.1	2028.0	2.4	970.2				2099.0	2.7	1275.9	2152.7	2.5	1262.7	1209.7
Munkah-2	2009.2	2.6	1361.9	2115.4	2.5	1218.3							2297.9	2.4	973.4	1184.5
Munkarie South-1																
Munro-1																
Muteroo-3																
Naccowlah East-1	1851.1	2.8	1911.7													
Naccowlah South-1	1796.5	2.6	1370.1	1844.0	2.4	1139.2										1911.7
Naccowlah West-1	1793.2	2.8	1905.8													1254.7
Naryilco-1																
Navalla-1																
Nulla-1	2311.5	2.6	1068.1													
Okotoko-1	1986.1	2.7	1410.3	2166.3	2.5	1125.4				2409.3	2.6	734.4	2664.6	2.6	943.2	915.2
Orientos-2													2203.8	2.5	1162.7	1232.8
Packsaddle-4	2032.6	2.6	1292.3	2122.5	2.3	415.7										
Padulla-1																854.0
Pallano-1																
Pandieburra-1																
Pando South-1																

Table 3. Continued.

	Nappamerri Group			Toolachee Formation			Roseneath Shale			Murteree Shale			Patchawarra Formation			Mean[#]
Well	Midpoint Depth (m bgl*)	Mean ρ_b** (g/cm³)	E_A*** (m)	Midpoint Depth (m bgl*)	Mean ρ_b** (g/cm³)	E_A*** (m)	Midpoint Depth (m bgl*)	Mean ρ_b** (g/cm³)	E_A*** (m)	Midpoint Depth (m bgl*)	Mean ρ_b** (g/cm³)	E_A*** (m)	Midpoint Depth (m bgl*)	Mean ρ_b** (g/cm³)	E_A*** (m)	E_A*** (m)
Paning-1	2606.3	2.5	272.8										3021.1	2.4	161.7	217.2
Paragilga-1																
Patroclus-1				1858.2	2.6	1579.2	1956.6	2.7	871.1							1225.2
Paxton-1																
Pepita-2	2089.4	2.7	1305.8	2229.6	2.5	883.1										1094.4
Pintari-1																
Pondrinie-5	2095.8	2.6	1176.7	2204.6	2.5	956.4										1066.6
Potiron-1																
Putamurdie-1																
Rheims-1				1679.1	2.4	1185.9	1712.7	2.6	1049.2							1117.5
Rho East-1																
Richie-1				1588.4	2.4	1265.4	1633.4	2.5	647.3				1802.9	2.5	1478.6	1130.4
Russel-1	2619.5	2.4	0.0 (R*)	2851.4	2.4	0.0 (R*)							2878.1	2.4	99.7	33.3
Snake Hole-1	2250.5	2.7	1194.5	2325.8	2.5	790.4				2394.1	2.6	853.7	2428.9	2.5	998.1	959.2
Spectre-1	2561.4	2.6	696.6	2709.3	2.5	564.9				2759.2	2.7	616.1	3055.8	2.5	427.7	576.3
Spencer-4													1848.2	2.4	1308.4	
Steward-1																
Strzelecki-10	1848.8	2.6	1440.1	1890.8	2.5	1257.2				1984.2	2.7	1352.2	2012.1	2.6	1597.3	1411.7
Strzelecki -27																
Sturt-6																
Swan Lake-1	2409.3	2.7	1024.2	2581.7	2.5	679.7				2649.8	2.7	799.7	2956.8	2.4	236.8	685.1
Taloola-1																
Tanbar-1																
Tanbar North-1	2575.9	2.6	635.7													635.7
Tartulla-1	2204.8	2.7	1209.3	2370.4	2.5	997.8							2525.4	2.6	1165.2	1124.1
Tennaperra South-1				1786.5	2.4	1274.0										1274.0
Three Queens-1																
Thurakinna-5	1929.2	2.6	1398.7	1966.5	2.4	788.3	2088.0	2.6	583.6	2211.6	2.6	1011.7	2259.0	2.5	1277.6	1012.0
Thurra-1	1839.9	2.7	1729.6	1877.9	2.5	1292.6	1978.2	2.5	362.6				2068.0	2.5	1291.0	1169.0
Tinchoo-1																
Tinga Tingana-1																
Tinpilla-1				1620.9	2.4	1437.8	1677.5	2.5	452.2				1789.9	2.4	1412.1	1100.7
Tirrawarra-13	2455.8	2.6	892.6							2659.4	2.7	802.1	2682.5	2.5	890.4	861.7
Tirrawarra-15																
Tirrawarra-26										2681.2	2.7	698.6	2907.1	2.5	580.7	639.6
Tirrawarra North-1	2535.3	2.6	661.2	2720.8	2.5	572.1				2760.7	2.7	622.9	3007.8	2.5	293.2	537.3
Tirrawarra West-1	2496.0	2.6	679.8	2663.9	2.4	397.7				2700.1	2.7	800.7	2730.0	2.5	712.3	647.6
Toby-1	1973.7	2.7	1467.5													1467.5
Toolachee-9	1823.9	2.6	1557.8	1885.5	2.5	1352.4	2062.7	2.6	712.9	2175.0	2.7	1149.4	2208.4	2.6	1487.1	1251.9
Toolachee-21	1848.2	2.7	1536.1	1910.3	2.5	1426.1	2054.5	2.7	814.3	2180.2	2.7	1219.5	2224.2	2.5	1282.5	1255.7
Toolachee-39				2034.1	2.5	1267.6	2104.0	2.7	723.9	2251.3	2.7	1134.9	2302.1	2.5	1197.5	1081.0
Turban-1	2127.2	2.6	1215.5													1215.5
Ullenbury-1	2452.5	2.4	176.0													176.0
Wackett-3	1801.2	2.7	1619.4	1865.4	2.5	1302.2										1461.8
Wallawanny-1																
Wancoocha-2										1689.8	2.6	1446.8	1714.6	2.5	1625.6	1536.2
Wantana-2				2518.3	2.4	489.5										489.5
Wareena-1	1681.2	2.6	1535.5	1851.8	2.6	1803.2										1669.4
Warnie East-1	1857.8	2.7	1542.0	2026.4	2.5	1378.5	2304.3	2.7	680.3	2426.7	2.7	1046.1	2541.2	2.6	1078.8	1145.1
Watson-1																
Weena-1																
Wicho-1																

Table 3. Continued.

	Nappamerri Group			Toolachee Formation			Roseneath Shale			Murteree Shale			Patchawarra Formation			Mean[#]
Well	Midpoint Depth (m bgl*)	Mean ρ_b** (g/cm³)	E_A*** (m)	Midpoint Depth (m bgl*)	Mean ρ_b** (g/cm³)	E_A*** (m)	Midpoint Depth (m bgl*)	Mean ρ_b** (g/cm³)	E_A*** (m)	Midpoint Depth (m bgl*)	Mean ρ_b** (g/cm³)	E_A*** (m)	Midpoint Depth (m bgl*)	Mean ρ_b** (g/cm³)	E_A*** (m)	E_A*** (m)
Wills-1				1667.9	2.5	1490.9	1771.0	2.7	1128.4	1826.8	2.6	1493.8				1371.0
Wimma-1	2889.2	2.5	20.3													20.3
Wippo-2																
Wirha-1				1668.5	2.4	1276.2	1715.8	2.6	1016.3	1794.1	2.6	1469.2	1861.2	2.5	1422.6	1296.1
Witchetty-1																
Wompi-1				1619.4	2.5	1668.0	1742.4	2.6	748.5	1775.9	2.6	1355.1				1263.9
Wuroopie-1																
Yanbee-1																
Yanda-2	2059.0	2.6	1299.4	2161.4	2.6	1268.5							2342.1	2.5	1004.4	1190.8
Yanta-1																
Yumba-1	2003.3	2.7	1496.1	2081.8	2.5	1166.5										1331.3

*m bgl = meters below ground level.

**ρ_b = bulk density.

***E_A = apparent exhumation.

[#]Mean = mean of the apparent exhumation values from such of the Eromanga Basin Formations as are present in any given well.

[##]Mean = mean of the apparent exhumation values from such of the Cooper Basin Formations as are present in any given well.

R* = reference well, ie. well used to define normal compaction relationship.

Table 4. Midpoint Depth and Mean Neutron Porosity Data and Apparent Exhumation Results

	Eromanga Basin Stratigraphic Units																					
	Winton Formation			Mackunda Formation			Allaru Mudstone-Oodnadatta Formation			Bulldog Shale-Wallumbilla Formation			Cadna-owie Formation			Birkhead Formation			Hutton Sandstone			Mean‡
Well	Midpoint Depth (m bgl*)	Mean ϕ_N** (pu)	E_A*** (m)	Midpoint Depth (m bgl*)	Mean ϕ_N** (pu)	E_A*** (m)	Midpoint Depth (m bgl*)	Mean ϕ_N** (pu)	E_A*** (m)	Midpoint Depth (m bgl*)	Mean ϕ_N** (pu)	E_A*** (m)	Midpoint Depth (m bgl*)	Mean ϕ_N** (pu)	E_A*** (m)	Midpoint Depth (m bgl*)	Mean ϕ_N** (pu)	E_A*** (m)	Midpoint Depth (m bgl*)	Mean ϕ_N** (pu)	E_A*** (m)	E_A*** (m)
Alkina-1													1473.9	30.2	407.6	1841.4	22.7	510.6	1977.4	9.0	890.7	603.0
Alwyn-1													1154.4	29.8	746.1				1496.0	18.9	474.7	610.4
Amyema-1													1374.1	29.0	564.4	1700.7	24.6	486.8	1747.5	15.8	503.1	518.1
Andree-1																2115.3	20.7	408.2	2246.4	14.1	154.9	281.5
Araburg-1																						
Arrabury-1																						
Arrakis-1																1860.2	21.0	636.6	1964.6	14.8	375.9	506.2
Atoll-1													1041.7	30.7	813.8	1378.6	28.8	442.4	1421.7	14.8	915.6	724.0
Azolla-1													1337.6	29.0	601.9	1667.3	24.8	503.3	1705.7	17.9	348.1	484.4
Ballera-1													1514.4	25.4	594.3	1881.3	21.7	553.8	1969.4	11.3	687.5	611.9
Baratta-1													1427.6	28.1	552.7	1759.2	18.7	936.4	1813.6	14.4	563.9	684.3
Bardoc-1													1346.8	30.4	524.9	1706.6	23.8	552.2	1758.5	12.9	748.7	608.6
Barrolka-1																						
Baryulah-1													1572.8	27.5	438.7	1951.1	23.4	337.5	1990.7	13.6	457.2	407.8
Battunga-1																						
Beanbush-1																2348.4	19.2	310.2	2522.9	11.7	96.4	203.3
Belah-1													1289.8	28.2	687.3	1625.5	24.6	558.0	1661.0	15.7	599.2	614.5
Biala-1													1158.1	31.4	664.5	1464.5	25.3	660.0	1513.2	19.3	421.6	582.1
Big Lake-26																1952.1	20.4	595.6	2032.7	6.4	1065.1	830.4
Big Lake-35																1969.6	19.1	698.8	2053.7	7.1	983.3	841.1
Bogala-1													1195.0	27.2	827.0	1538.8	20.4	1012.1	1605.4	16.0	624.7	821.3
Boldrewood-1																1401.9						
Bookabourdie-1													1720.1	28.8	225.7	2102.2	18.7	593.3	2231.1	12.7	296.0	371.7
Boxwood-1																						
Brolga-2																						
Buckinna-1													1194.5	31.4	629.9	1520.6	27.1	451.2	1557.5	16.8	600.3	560.4
Bungee-1																						
Burke-2										1293.5	12.5		1482.0	28.3	489.4							489.4
Burley-2													1687.8	23.3	520.4	2082.2	24.1	147.1	2177.0	14.0	229.6	299.0
Bycoe-1	327.1	42.6		482.1	37.6					921.8	33.8		1135.9	30.0	755.6	1491.7	20.5	1047.4	1553.7	18.0	496.9	766.6
Carney-1																						
Challum-1													1489.4	26.0	592.7	1853.3	22.6	510.1	1967.0	10.5	762.9	621.9
Charo-1																1766.5	23.3	536.8	1913.7	16.5	270.4	403.6
Childie-1													1335.9	28.4	629.0	1659.3	23.1	659.0	1695.8	16.8	461.0	583.0
Cooba-1																						
Cook-1																1920.4	19.9	674.1	2076.1	9.7	725.9	700.0
Cook North-1													1596.7	24.3	564.4	1934.7	20.4	620.4	2067.2	9.3	770.8	651.8
Coonavalla-1																						
Cooroo-1													1366.0	28.1	616.8	1726.7	20.5	817.0	1781.4	12.0	813.9	749.3
Copai-1													1285.4	27.4	727.8	1602.3	20.3	959.6	1752.5	13.9	670.5	785.9
Cowan-3																						
Cuddapan-1																						
Curalle-1				350.4	31.6					802.9	27.0		939.9	24.1	1233.8	1246.9	18.5	1473.4	1387.8	8.0	1567.9	1425.1
Daer-1																1876.8	23.4	416.9	2046.3	17.0	90.0	253.4
Daralingie-15																						
Daralingie-23																			1863.2	17.4	235.9	235.9
Darter-1																						
Della-7													1353.6	29.2	572.3	1695.6	16.1	1229.1	1781.1	7.2	1246.8	1016.0

Table 4. Continued.

Well	Winton Formation			Mackunda Formation			Allaru Mudstone-Oodnadatta Formation			Bulldog Shale-Wallumbilla Formation			Cadna-owie Formation			Birkhead Formation			Hutton Sandstone			Mean[1]
	Midpoint Depth (m bgl*)	Mean ϕ_N** (pu)	E_A*** (m)	Midpoint Depth (m bgl*)	Mean ϕ_N** (pu)	E_A*** (m)	Midpoint Depth (m bgl*)	Mean ϕ_N** (pu)	E_A*** (m)	Midpoint Depth (m bgl*)	Mean ϕ_N** (pu)	E_A*** (m)	Midpoint Depth (m bgl*)	Mean ϕ_N** (pu)	E_A*** (m)	Midpoint Depth (m bgl*)	Mean ϕ_N** (pu)	E_A*** (m)	Midpoint Depth (m bgl*)	Mean ϕ_N** (pu)	E_A*** (m)	E_A*** (m)
Della-10													1338.4	28.0	647.8	1670.6	17.6	1121.6	1755.8	9.0	1109.6	959.7
Denley-1																						
Deparanie-1																						
Deramookoo-1																						
Dirkala-2																1627.6	26.8	369.1	1689.0	19.9	183.1	276.1
Doonmulla-1																						
Dullingari-3																						
Dullingari North-1																						
Dunoon-1													1109.0	33.6	608.5	1407.1	23.8		1423.4	16.5	762.1	685.3
Durham Downs-1																						
Etchuburra North-1																						
Fly Lake-1																						
Fly Lake-4													1733.5	31.4		2087.1	19.6	536.7	2239.4	14.6	115.5	326.1
Garanjanie-2																1629.6	26.4	402.1	1686.9	20.0	178.2	290.2
Gidgealpa-20													1465.8	28.9	478.8	1801.7	21.1	687.0	1869.2	15.0	453.5	539.8
Gidgealpa-42													1464.6	30.7	390.1	1808.7	23.4	479.6	1903.8	14.9	427.0	432.2
Gidgee-1													1125.2	32.3	657.0				1477.5	19.1	469.8	563.4
Gooranie-1																2046.7	19.8	555.2	2177.8	15.0	143.3	349.2
Gooranie-2																						
Graham-1													1139.5	29.6	767.1	1481.3	23.0	843.1	1542.0	18.3	475.8	695.3
Gurra-1																						
Haddon Downs-1													1258.6	26.7	791.2	1542.8	22.2	852.9				877.7
Hammond-1																						
Hooley-1													997.1	29.6	911.4	1346.8	22.2	1052.4	1424.6	16.1	792.3	918.7
Hume-1	506.7	41.6		1377.1	35.7					1194.1	31.0		1377.1	25.8	714.2	1706.1	24.4	501.3	1748.3	12.4	804.4	673.3
Hydra-1													1170.2	30.2	708.1	1497.8	26.2	549.0	1527.8	16.9	616.2	624.4
Ingella-1																1979.0	18.9	701.0	2122.0	7.7	861.3	781.1
Innamincka-3																1525.2	21.5	933.5	1643.3	14.9	683.3	808.4
Innamincka-4													1228.8	27.0	803.7	1595.5	18.9	1082.5	1712.4	12.3	849.9	912.1
Jack Lake-2																						
Jackson-1													1055.8	36.4	529.2	1402.2	25.2	732.8	1459.1	21.7	252.9	504.9
Jackson South-1													1035.5	30.6	826.6	1396.9	20.0	1186.1	1454.6	16.9	697.2	903.3
James-1													1578.7	26.3	486.4	1912.6	20.9	591.7	2067.0	9.6	743.9	607.3
Jarrar-1													1405.7	26.5	652.8	1774.5	18.6	938.1	1826.3	10.2	931.1	840.7
Johba-1																						
Kalladeina-1																						
Karmona-2													1434.1	26.0	647.5							647.5
Karwin-1																						
Keeto-2																						
Keilor-1																1878.2	21.1	611.6	1986.1	10.8	717.3	664.5
Kenny-1													1753.1	25.8	337.6	2092.5	18.4	633.0	2248.5	9.6	558.8	509.8
Kercummurra-1													986.0	26.8	1058.6	1351.0	21.9	1073.6	1442.6	13.4	1026.9	1053.0
Kerna-5																						
Kirby-1																2010.9	26.6	0.0 (R*)	2113.9	13.1	379.7	189.9
Kirby-2																						
Kiwarrick-1													1195.3	31.0	648.1	1518.5	24.3	693.5	1567.4	19.7	327.0	556.2
Kobari-1													1172.1	32.4	602.7	1451.6	26.9	537.8	1499.6	21.9	196.6	445.7
Koonchera-1													1300.3	30.2	579.4	1609.3	23.1	705.5	1795.3	13.9	627.5	637.5
Kumbarie-1																						
Kurunda-1																1913.3	22.6	448.2	2024.6	16.0	203.2	325.7
Kutyo-1													1453.6	30.0	435.7	1814.4	18.9	863.9	1869.0	11.3	789.4	696.3

Table 4. Continued.

Well	Winton Formation Midpoint Depth (m bgl*)	Winton Formation Mean ϕ_N** (pu)	Winton Formation E_A*** (m)	Mackunda Formation Midpoint Depth (m bgl*)	Mackunda Formation Mean ϕ_N** (pu)	Mackunda Formation E_A*** (m)	Allaru Mudstone-Oodnadatta Formation Midpoint Depth (m bgl*)	Allaru Mudstone-Oodnadatta Formation Mean ϕ_N** (pu)	Allaru Mudstone-Oodnadatta Formation E_A*** (m)	Bulldog Shale-Wallumbilla Formation Midpoint Depth (m bgl*)	Bulldog Shale-Wallumbilla Formation Mean ϕ_N** (pu)	Bulldog Shale-Wallumbilla Formation E_A*** (m)	Cadna-owie Formation Midpoint Depth (m bgl*)	Cadna-owie Formation Mean ϕ_N** (pu)	Cadna-owie Formation E_A*** (m)	Birkhead Formation Midpoint Depth (m bgl*)	Birkhead Formation Mean ϕ_N** (pu)	Birkhead Formation E_A*** (m)	Hutton Sandstone Midpoint Depth (m bgl*)	Hutton Sandstone Mean ϕ_N** (pu)	Hutton Sandstone E_A*** (m)	Mean† E_A*** (m)
Lake Mcmillan-1																2212.7	20.6	323.0	2353.5	12.7	175.8	249.4
Lambda-1													1240.7	27.6	764.0	1558.8	23.3	743.7				753.8
Lhotsky-1																						
Limestone Creek-9													1157.7	32.7	601.8							601.8
Lycium-1																						
Macadama-1																						
Mackillop-1																						
Marabooka-2													1368.8	28.4	696.8	1712.0	20.2	684.0	1781.8	11.8	585.1	655.3
Marengo-1																						
Marsilea-1													1397.3	26.5	598.0	1739.4	25.4	859.3	1773.4	17.2	832.9	763.4
Mawson-1																						
Mckinlay-3													1153.0	30.8	660.5	1469.9	25.0	381.3	1506.0	17.5	345.9	462.5
Mcleod-1																						248.8
Meeba-1																						
Meranji-1																1982.4	20.7	540.6	2105.6	14.7	239.8	390.2
Merrimelia-7	583.4	42.6		918.3	35.0					1317.2	34.9		1532.7	29.5	379.5	1874.8	22.3	508.6	1981.8	16.6	192.8	360.3
Merrimelia-25																						
Minkie-1																						
Mooliampah-1													1186.7	30.6	672.1	1513.2	24.8	658.4	1548.2	17.4	557.9	629.5
Moolion-1																2183.1	17.8	594.5	2323.2	11.1	346.5	470.5
Moomba-27																						
Moomba-57																			2096.2	6.9	955.1	955.1
Moomba North-1																2029.7	23.4	262.5	2139.1	5.6	1033.6	648.1
Moomba South-1																2013.4	18.6	692.5	2109.3	7.8	865.7	779.1
Moorari-4																2158.4	20.4	397.5	2285.7	13.8	145.7	271.6
Morney-1										859.0	28.9		995.4	28.0	990.3	1332.7	20.4	1215.9	1472.9	10.4	1265.6	1157.3
Mudera-3										1224.7	33.4		1412.0	25.2	708.8	1763.1	19.0	909.9	1829.3	6.2	1290.4	969.7
Munkah-2													1390.3	27.2	632.8	1766.6	21.8	666.7	1854.4	14.0	555.2	618.2
Munkarie South-1	336.5	45.2		1084.8	39.5					920.7	34.2		1084.8	31.8	721.1	1404.9	27.3	547.0	1429.4	15.8	816.9	695.0
Munro-1													1109.8	31.9	690.1				1459.4	19.0	502.2	596.1
Muteroo-3													1365.0	30.6	496.9	1677.3	23.0	646.2				571.5
Naccowlah East-1													1343.0	29.3	580.5	1699.0	21.9	724.0	1783.4	17.9	275.6	526.7
Naccowlah South-1										1093.1	32.6		1303.7	28.7	650.0	1653.4	20.4	894.5	1722.6	16.0	506.3	683.6
Naccowlah West-1										1096.3	31.9		1304.3	27.1	724.1	1661.2	20.6	873.5	1731.9	15.0	592.7	730.1
Naryilco-1																						
Navalla-1																						
Nulla-1																1998.7	20.4	557.0	2137.1	15.7	119.6	338.3
Okotoko-1													1376.9	28.7	576.1	1732.9	23.3	568.1	1825.0	13.8	602.2	582.1
Orientos-2													1254.3	25.7	842.0							842.0
Packsaddle-4													1394.0	27.2	630.4	1736.1	21.4	726.6	1848.2	15.9	395.2	584.1
Padulla-1													1098.3	32.7	660.4				1433.2	15.3	858.6	759.5
Pallano-1													1414.6	21.8	865.3	1773.9	14.4	1302.4	1828.5	7.1	1204.9	1124.2
Pandieburra-1																						
Pando South-1																						
Paning-1													1666.7	34.7	0.0 (R*)	2037.1	23.1	282.6	2186.9	13.1	302.3	150.0
Paragilga-1													1107.2	32.3	672.5	1441.3	27.1	530.1	1467.6	18.0	580.0	594.2
Patroclus-1										1314.3	29.9		1404.2	28.3	566.5	1738.5	23.8	513.6	1788.0	14.4	583.4	554.5
Paxton-1													815.8	38.6	663.7							663.7
Pepita-2													1423.2	30.0	467.6	1773.6	24.1	453.9	1884.6	16.6	290.1	403.9
Pintari-1																						
Pondrinie-5													1432.4	29.7	469.9	1790.4	19.0	879.9	1900.3	16.2	311.7	553.8

Table 4. Continued.

Well	Winton Formation Midpoint Depth (m bgl*)	Winton Formation Mean ϕ_N** (pu)	Winton Formation E_A*** (m)	Mackunda Formation Midpoint Depth (m bgl*)	Mackunda Formation Mean ϕ_N** (pu)	Mackunda Formation E_A*** (m)	Allaru Mudstone-Oodnadatta Formation Midpoint Depth (m bgl*)	Allaru Mudstone-Oodnadatta Formation Mean ϕ_N** (pu)	Allaru Mudstone-Oodnadatta Formation E_A*** (m)	Bulldog Shale-Wallumbilla Formation Midpoint Depth (m bgl*)	Bulldog Shale-Wallumbilla Formation Mean ϕ_N** (pu)	Bulldog Shale-Wallumbilla Formation E_A*** (m)	Cadna-owie Formation Midpoint Depth (m bgl*)	Cadna-owie Formation Mean ϕ_N** (pu)	Cadna-owie Formation E_A*** (m)	Birkhead Formation Midpoint Depth (m bgl*)	Birkhead Formation Mean ϕ_N** (pu)	Birkhead Formation E_A*** (m)	Hutton Sandstone Midpoint Depth (m bgl*)	Hutton Sandstone Mean ϕ_N** (pu)	Hutton Sandstone E_A*** (m)	Mean[‡] E_A*** (m)
Potiron-1													1256.6	25.8	834.5	1568.1	21.5	889.7	1748.4	8.4	1171.8	965.3
Putamurdie-1																						
Rheims-1													1185.8	30.3	687.8	1517.8	27.0	457.8	1550.1	18.3	469.6	538.4
Rho East-1													1071.2	31.3	756.8	1407.4	27.5	526.9	1429.4	16.8	730.4	671.4
Richie-1	280.2	42.9		1087.1	38.7					916.1	33.2		1087.1	30.0	801.6	1446.1	23.3	852.0	1496.1	18.1	541.3	731.7
Russel-1																2106.8	16.3	798.3	2256.1	5.0	969.9	884.1
Snake Hole-1													1597.5	29.5	316.6	1929.2	19.4	712.3	2040.6	15.0	282.5	437.0
Spectre-1																2146.7	19.3	499.2	2278.8	14.8	58.4	278.9
Spencer-4													1331.7	32.0	461.0	1640.6	25.1	505.7	1743.2	17.3	365.0	443.9
Steward-1																						
Strzelecki-10										1180.6	9.9		1354.7	29.9	538.7	1719.5	16.6	1162.7	1778.4	10.6	937.7	879.7
Strzelecki -27																1655.1	22.5	718.0	1707.9	11.2	956.1	837.0
Sturt-6																1648.1	21.8	786.1	1745.9	18.3	273.1	529.6
Swan Lake-1																2089.6	18.6	619.7	2208.3	11.3	444.3	532.0
Taloola-1													1326.2	31.8	477.5	1649.8	24.5	547.6	1746.1	17.6	337.9	454.3
Tanbar-1																						
Tanbar North-1																						
Tartulla-1																						
Tennaperra South-1													1315.2	28.5	646.7	1656.3	22.4	722.0	1692.1	12.1	891.1	753.2
Three Queens-1																						
Thurakinna-5													1487.7	30.2	390.4	1782.2	18.9	896.3	1834.6	13.9	586.7	624.5
Thurra-1													1314.6	31.0	525.2	1685.3	21.9	735.9	1755.8	14.8	584.8	615.3
Tinchoo-1																						
Tinga Tingana-1																						
Tinpilla-1	312.1	42.1		1136.3	36.7					949.1	32.6		1136.3	29.0	801.5	1487.0	19.1	1173.9	1547.9	17.1	582.5	852.6
Tirrawarra-13																2047.7	19.5	579.8	2192.6	14.7	153.9	366.8
Tirrawarra-15																						
Tirrawarra-26																						
Tirrawarra North-1																2124.8	19.9	473.7	2267.1	14.2	128.9	331.7
Tirrawarra West-1																2089.0	20.7	433.8	2227.9	13.5	229.6	331.7
Toby-1													1134.3	26.0	946.9	1519.3	17.7	1265.9	1638.6	10.1	1124.7	1112.5
Toolachee-9													1349.3	27.3	669.4	1680.3	22.5	689.8	1728.6	14.0	679.0	679.4
Toolachee-21													1359.4	28.9	581.6	1689.4	21.5	763.4	1747.6	15.2	553.0	632.7
Toolachee-39																						
Turban-1													1382.3	27.4	631.4	1761.3	19.6	861.7	1884.9	15.4	399.5	630.9
Ullenbury-1													1552.2	24.3	611.3	1911.7	19.0	758.4	2064.1	7.6	925.4	765.0
Wackett-3													1282.1	27.9	706.3	1643.3	20.2	927.6	1714.6	14.0	692.4	775.4
Wallawanny-1													1409.3	26.5	649.8	1782.8	18.8	911.5	1830.7	12.9	681.3	747.5
Wancoocha-2													1263.2	31.5	553.0	1550.2	26.7	450.6	1612.2	14.0	803.0	602.2
Wantana-2																2006.2	21.8	427.7				427.7
Wareena-1				306.8	34.6					715.2	31.8		927.8	26.2	1141.2	1294.4	24.3	914.4	1397.5	13.1	1095.3	1050.3
Warnie East-1													1320.4	27.0	711.8	1667.1	19.6	956.9	1702.6	11.4	943.9	870.9
Watson-1													1227.3	27.3	792.5	1568.8	23.0	752.7	1603.9	15.1	704.4	749.9
Weena-1																						
Wicho-1																						
Wills-1													1215.2	30.4	657.4	1570.5	19.4	1068.4	1605.2	14.6	747.6	824.4
Wimma-1													1969.4	28.3	0.0 (R*)	2357.4	22.6	0.0 (R*)	2492.8	13.1	0.0 (R*)	0.0
Wippo-2																						
Wirha-1													1246.7	28.4	721.3	1559.3	21.1	927.9	1595.5	14.3	783.9	811.0
Witchetty-1																						
Wompi-1																						

Table 4. Continued.

Well	Winton Formation			Mackunda Formation			Allaru Mudstone-Oodnadatta Formation			Bulldog Shale-Wallumbilla Formation			Cadna-owie Formation			Birkhead Formation			Hutton Sandstone			Mean[1]
	Midpoint Depth (m bgl*)	Mean ϕ_N** (pu)	E_A*** (m)	Midpoint Depth (m bgl*)	Mean ϕ_N** (pu)	E_A*** (m)	Midpoint Depth (m bgl*)	Mean ϕ_N** (pu)	E_A*** (m)	Midpoint Depth (m bgl*)	Mean ϕ_N** (pu)	E_A*** (m)	Midpoint Depth (m bgl*)	Mean ϕ_N** (pu)	E_A*** (m)	Midpoint Depth (m bgl*)	Mean ϕ_N** (pu)	E_A*** (m)	Midpoint Depth (m bgl*)	Mean ϕ_N** (pu)	E_A*** (m)	E_A*** (m)
Wuroopie-1																						
Yanbee-1																						
Yanda-2													1448.2	24.8	690.5	1827.0	19.2	833.1	1912.7	14.5	455.9	659.9
Yanta-1													1472.2	30.8	377.9	1810.1	22.5	556.6	1972.7	16.0	261.1	398.5
Yumba-1	567.1	48.2		1406.0	38.9					1177.1	33.8		1406.0	31.5	413.4	1790.7	28.5	55.9	1869.3	20.0	0.0 (R*)	156.5

Cooper Basin Stratigraphic Units

Well	Nappamerri Group			Toolachee Formation			Roseneath Shale			Murteree Shale			Patchawarra Formation			Mean[2]
	Midpoint Depth (m bgl*)	Mean ϕ_N** (pu)	E_A*** (m)	Midpoint Depth (m bgl*)	Mean ϕ_N** (pu)	E_A*** (m)	Midpoint Depth (m bgl*)	Mean ϕ_N** (pu)	E_A*** (m)	Midpoint Depth (m bgl*)	Mean ϕ_N** (pu)	E_A*** (m)	Midpoint Depth (m bgl*)	Mean ϕ_N** (pu)	E_A*** (m)	E_A*** (m)
Alkina-1	2379.9	15.2	481.2	2579.0	3.8	692.6							2633.5	9.1	888.8	687.6
Alwyn-1																
Amyema-1	1824.1	19.2	720.6	1909.2	20.2	599.4	2088.2	23.7	1153.3	2211.1	23.1	869.8	2254.1	20.2	555.4	779.7
Andree-1	2521.2	13.6	472.2	2636.9	12.3	241.2				2721.7	23.1	351.6	2753.9	15.0	389.3	363.5
Araburg-1																
Arrabury-1																
Arrakis-1	2101.7	18.1	528.9	2149.8	12.2	729.3	2194.7	23.4	1103.7	2273.2	23.1	806.8	2315.0	17.5	665.4	766.8
Atoll-1																
Azolla-1	1775.3	19.9	712.3	1842.6	23.4	517.0	2053.6	22.5	1389.6	2191.2	21.8	1040.7	2242.5	17.2	759.4	883.8
Ballera-1	2148.6	14.7	756.8	2280.9	20.4	216.6							2472.1	8.5	1086.6	686.6
Baratta-1	1921.5	17.4	765.3	1988.0	22.1	429.8	2079.4	22.7	1336.9	2155.3	22.7	974.0	2197.4	16.0	879.5	877.1
Bardoc-1																
Barrolka-1																
Baryulah-1	2128.2	15.3	726.8	2250.5	18.2	350.4	2359.5	20.5	1411.3	2439.5	17.2	1322.9	2483.3	11.8	862.1	934.7
Battunga-1																
Beanbush-1	2936.2	14.3	0.0 (R*)							3280.2	21.4	0.0 (R*)				0.0
Belah-1	1724.3	16.6	1032.3	1827.9	19.9	694.0	1952.7	21.8	1603.7	2026.8	18.6	1574.7	2224.5	14.1	977.3	1176.4
Biala-1																
Big Lake-26	2171.1	15.8	648.7	2304.8	11.7	598.9	2376.2	21.8	1183.4	2499.9	21.8	734.8	2558.4	13.4	685.0	770.2
Big Lake-35	2201.6	15.8	618.2	2347.6	13.2	485.5	2419.5	21.7	1149.8	2544.0	22.5	603.8	2605.6	11.9	737.3	718.9
Bogala-1				1740.9	16.6	934.2	1813.1	23.2	1511.5				1900.9	14.6	1266.9	1237.5
Boldrewood-1																
Bookabourdie-1	2498.3	13.2	528.1										2815.8	17.6	158.5	343.3
Boxwood-1																
Brolga-2																
Buckinna-1																
Bungee-1	1844.7	21.2	545.2	1930.1	19.5	612.9				2109.3	25.0	749.4	2161.1	20.2	649.9	639.4
Burke-2																
Burley-2	2470.3	13.6	520.7	2701.3	9.6	302.9	2941.9	19.5	989.5	3153.5	18.4	467.5	3260.0	9.6	230.8	502.3
Bycoe-1				1622.5	23.6	725.5	1663.2	29.6	625.8				1723.8	18.5	1197.2	849.5
Carney-1																
Challum-1													2355.4	4.2	1480.1	1480.1
Charo-1																
Childie-1	1794.4	17.6	878.8							1942.8	23.9	1044.9	1981.9	17.6	991.5	971.7
Cooba-1																
Cook-1	2401.7	15.1	471.4													471.4
Cook North-1	2415.5	13.5	584.8													584.8
Coonavalla-1																
Cooroo-1				1856.6	16.9	807.7										807.7

Table 4. Continued.

	Nappamerri Group			Toolachee Formation			Roseneath Shale			Murteree Shale			Patchawarra Formation			Mean[#]
Well	Midpoint Depth (m bgl*)	Mean ϕ_N** (pu)	E_A*** (m)	Midpoint Depth (m bgl*)	Mean ϕ_N** (pu)	E_A*** (m)	Midpoint Depth (m bgl*)	Mean ϕ_N** (pu)	E_A*** (m)	Midpoint Depth (m bgl*)	Mean ϕ_N** (pu)	E_A*** (m)	Midpoint Depth (m bgl*)	Mean ϕ_N** (pu)	E_A*** (m)	E_A*** (m)
Copai-1																
Cowan-3										2205.4	22.1	984.7	2247.7	17.4	742.8	863.8
Cuddapan-1																
Curalle-1	1722.0	22.9	534.0													534.0
Daer-1	2268.3	9.0	1084.8	2348.3	20.3	154.7										619.7
Daralingie-15																
Daralingie-23	1952.2	20.8	464.7				2097.8	25.1	930.4	2196.1	24.1	758.3	2233.9	21.0	523.1	669.1
Darter-1																
Della-7	1877.8	18.0	764.2													764.2
Della-10	1863.1	16.1	925.9	1961.4	8.1	1108.6							1981.4	12.5	1324.3	1119.6
Denley-1																
Deparanie-1																
Deramookoo-1																
Dirkala-2							1819.2	23.8	1409.6	1908.4	26.5	771.9	1959.5	24.3	589.3	923.6
Doonmulla-1																
Dullingari-3																
Dullingari North-1	2022.5	16.5	735.2	2155.9	18.5	431.1	2290.6	22.2	1196.1	2396.0	22.7	732.5	2444.1	14.2	751.7	769.3
Dunoon-1																
Durham Downs-1																
Echuburra North-1																
Fly Lake-1																
Fly Lake-4	2506.2	14.3	432.1	2637.6	10.5	322.1				2648.6	19.9	803.8	2666.1	16.4	387.5	486.4
Garanjanie-2	1753.1	16.2	1028.8	1796.8	17.3	845.1	1837.5	22.4	1617.9	1937.8	25.7	833.4	1982.1	22.4	686.7	1002.4
Gidgealpa-20																
Gidgealpa-42	2072.0	19.7	437.1	2121.2	13.6	693.0							2134.7	17.3	858.0	662.7
Gidgee-1				1502.1	22.0	923.5				1517.0	25.7	1261.0	1582.4	20.2	1230.2	1138.2
Gooranie-1	2425.9	14.6	485.9	2623.3	11.5	289.5				2670.8	24.7	215.3	2963.3	15.8	130.9	280.4
Gooranie-2	2462.5	14.9	429.2	2621.8	15.3	113.8				2673.7	24.0	297.2	2958.3	16.2	104.7	236.2
Graham-1				1590.0	27.2	592.2	1700.3	27.7	894.2				1790.9	12.9	1484.6	990.3
Gurra-1																
Haddon Downs-1																
Hammond-1																
Hooley-1	1533.4	17.1	1182.0													1182.0
Hume-1	1816.3	17.0	906.0	1897.9	20.5	595.6	2023.1	21.2	1627.4	2091.5	16.4	1768.0	2114.7	22.1	572.6	1093.9
Hydra-1				1633.6	19.6	902.9	1661.3	22.7	1746.2	1728.9	21.1	1584.4	1762.0	17.6	1215.2	1362.2
Ingella-1	2457.9	12.3	637.3													637.3
Innamincka-3	1818.3	15.1	1053.5													1053.5
Innamincka-4	1926.3	14.9	962.9	2075.5	15.0	677.3										820.1
Jack Lake-2				2473.8	13.3	354.5	2522.9	22.9	853.7	2600.2	22.4	554.5	2641.3	17.0	376.2	534.7
Jackson-1				1535.4	29.4	542.9	1577.9	34.0	0.0 (R*)				1668.6	18.3	1261.3	601.4
Jackson South-1				1488.6	28.4	639.4	1546.4	26.8	1195.8				1761.1	13.9	1450.3	1095.1
James-1	2339.5	14.0	622.3													622.3
Jarrar-1																
Johba-1																
Kalladeina-1																
Karmona-2																
Karwin-1																
Keeto-2																
Keilor-1	2243.6	14.8	648.8	2451.1	19.3	97.7							2555.2	16.5	488.8	411.8
Kenny-1	2628.4	11.6	523.8													523.8
Kercummurra-1	1645.6	15.4	1202.4	1832.3	10.5	1127.3										1164.9
Kerna-5				2058.9	15.9	651.5	2284.2	22.9	1094.6	2467.3	21.8	759.8	2452.1	17.6	523.6	757.4

Table 4. Continued.

	Nappamerri Group			Toolachee Formation			Roseneath Shale			Murteree Shale			Patchawarra Formation			Mean[#]
Well	Midpoint Depth (m bgl*)	Mean ϕ_N** (pu)	E_A*** (m)	Midpoint Depth (m bgl*)	Mean ϕ_N** (pu)	E_A*** (m)	Midpoint Depth (m bgl*)	Mean ϕ_N** (pu)	E_A*** (m)	Midpoint Depth (m bgl*)	Mean ϕ_N** (pu)	E_A*** (m)	Midpoint Depth (m bgl*)	Mean ϕ_N** (pu)	E_A*** (m)	E_A*** (m)
Kirby-1	2425.9	20.7	0.0 (R*)	2718.3	15.7	0.0 (R*)	2836.4	26.2	0.0 (R*)	3032.6	22.5	110.7	3174.3	13.0	96.3	41.4
Kirby-2																
Kiwarrick-1				1681.5	18.1	926.7	1632.5	22.9	1737.5	1712.2	25.6	1070.6	1753.1	19.6	1095.6	1207.6
Kobari-1										1580.1	28.9	814.4	1661.4	25.8	787.9	801.1
Koonchera-1																
Kumbarie-1																
Kurunda-1	2177.9	18.3	436.4	2210.5	23.5	145.2				2276.3	24.3	660.5	2311.2	21.2	434.0	419.0
Kutyo-1				1964.9	24.3	353.3										353.3
Lake Mcmillan-1	2673.6	13.8	299.1	2892.9	8.8	147.3				2945.9	24.2	0.0 (R*)	3069.9	15.2	59.9	126.6
Lambda-1																
Lhotsky-1																
Limestone Creek-9																
Lycium-1																
Macadama-1																
Mackillop-1																
Marabooka-2	1890.5	18.1	462.5							1996.7	23.2	460.3	2162.8	12.5	173.6	
Marengo-1																532.7
Marsilea-1	1864.4	18.5	743.9	1955.1	18.9	505.8				2278.3	21.6	1069.4	2326.8	16.6	1137.5	864.2
Mawson-1																
Mckinlay-3																
Mcleod-1	2422.1	14.9	320.2	2657.7	6.4	484.0				3157.3	18.5	553.1	3243.7	10.7	552.1	477.4
Meeba-1																
Meranji-1	2333.1	16.0	470.5	2470.9	13.4	354.5				2522.7	23.3	533.9	2813.2	16.2	250.2	402.3
Merrimelia-7	2165.1	17.0	557.3													557.3
Merrimelia-25	2199.4	18.2	424.3													424.3
Minkie-1																
Mooliampah-1				1586.3	23.4	773.1	1658.3	24.4	1480.1	1705.5	22.9	1395.2	1757.2	22.4	911.2	1139.9
Moolion-1	2621.9	11.6	525.8	2813.2	7.9	267.6				2842.9	22.2	344.2	2923.0	16.4	127.8	316.3
Moomba-27							2627.3	22.3	846.4	2722.5	20.7	629.6				738.0
Moomba-57				2384.6	15.0	368.3	2583.1	21.5	1027.4							679.8
Moomba North-1	2328.1	14.3	611.2	2496.3	12.4	377.7	2619.2	21.0	1063.8	2753.2	19.2	782.4	2811.4	11.7	541.4	675.3
Moomba South-1	2256.6	17.5	427.6	2408.8	13.4	418.3	2524.4	21.4	1103.4	2677.6	20.4	716.2	2734.5	10.9	673.3	667.8
Moorari-4	2541.0	13.1	490.5							2710.3	22.6	428.5	2849.2	12.9	429.3	449.4
Morney-1	1818.4	21.4	551.4													551.4
Mudera-3	1947.1	14.6	964.4	2028.0	21.3	431.2				2099.0	24.1	860.5	2152.7	13.5	1085.2	835.3
Munkah-2	2009.2	16.2	771.7	2115.4	21.1	349.8							2297.9	9.5	1198.9	773.5
Munkarie South-1																
Munro-1																
Muteroo-3																
Naccowlah East-1	1851.1	24.4	281.2													281.2
Naccowlah South-1	1796.5	21.0	606.1	1844.0	16.4	842.1										724.1
Naccowlah West-1																
Naryilco-1																
Navalla-1																
Nulla-1	2311.5	16.3	468.5							2409.3	23.9	576.8	2664.6	12.6	630.7	558.6
Okotoko-1	1986.1	16.7	762.2	2166.3	13.1	672.8							2203.8	14.2	991.8	808.9
Orientos-2																
Packsaddle-4	2032.6	15.1	838.2	2122.5	8.7	923.1										880.6
Padulla-1																
Pallano-1																
Pandieburra-1																
Pando South-1																

Table 4. Continued.

	Nappamerri Group			Toolachee Formation			Roseneath Shale			Murteree Shale			Patchawarra Formation			Mean[‡]
Well	Midpoint Depth (m bgl*)	Mean ϕ_N** (pu)	E_A*** (m)	Midpoint Depth (m bgl*)	Mean ϕ_N** (pu)	E_A*** (m)	Midpoint Depth (m bgl*)	Mean ϕ_N** (pu)	E_A*** (m)	Midpoint Depth (m bgl*)	Mean ϕ_N** (pu)	E_A*** (m)	Midpoint Depth (m bgl*)	Mean ϕ_N** (pu)	E_A*** (m)	E_A*** (m)
Paning-1	2606.3	15.6	222.1										3021.1	16.9	0.0 (R+)	111.1
Paragilga-1																
Patroclus-1				1858.2	22.0	566.1	1956.6	19.7	1933.2							1249.7
Paxton-1																
Pepita-2	2089.4	18.4	521.6	2229.6	16.0	473.2										497.4
Pintari-1																
Pondrinie-5	2095.8	15.3	756.6	2204.6	13.2	630.4										693.5
Potiron-1																
Putamurdie-1																
Rheims-1				1679.1	22.0	745.2	1712.7	23.4	1576.1							1160.6
Rho East-1																
Richie-1							1633.4	27.9	940.9				1802.9	26.2	624.6	782.8
Russel-1	2619.5	12.7	445.0	2851.4	3.9	416.8							2878.1	7.6	741.3	534.3
Snake Hole-1	2250.5	15.9	559.4	2325.8	11.0	609.2				2394.1	22.5	754.8	2428.9	18.5	489.1	482.5
Spectre-1	2561.4	13.9	405.1	2709.3	11.2	217.8				2759.2	23.0	331.3	3055.8	14.3	130.7	271.2
Spencer-4																
Steward-1																
Strzelecki-10	1848.8	18.4	760.4	1890.8	22.6	504.4				1984.2	25.0	875.8	2012.1	19.1	867.7	752.1
Strzelecki -27																
Sturt-6																
Swan Lake-1	2409.3	14.5	511.7	2581.7	12.2	300.4				2649.8	22.8	466.0	2956.8	4.0	890.7	542.2
Taloola-1																
Tanbar-1																
Tanbar North-1																
Tartulla-1																
Tennaperra South-1				1786.5	19.1	772.5										772.5
Three Queens-1																
Thuraltinna-5	1929.2	19.5	596.6				2088.0	23.0	1275.4	2211.6	23.5	815.4	2259.0	19.6	585.7	818.3
Thurra-1	1839.9	23.0	407.9	1877.9	24.7	420.7	1978.2	24.4	1150.2				2068.0	10.0	1392.8	842.9
Tinchoo-1																
Tinga Tingana-1																
Tinpilla-1				1620.9	19.8	907.7	1677.5	26.2	1162.6				1789.9	12.2	1532.0	1200.8
Tirrawarra-13	2455.8	14.6	453.2							2659.4	22.7	459.3	2682.5	15.1	456.6	456.4
Tirrawarra-15																
Tirrawarra-26										2681.2	23.1	400.7	2907.1	14.5	269.2	334.9
Tirrawarra North-1	2535.3	15.1	333.9	2720.8	13.3	109.0				2760.7	23.7	245.4	3007.8	16.3	52.6	185.2
Tirrawarra West-1	2496.0	14.0	464.4	2663.9	12.3	214.9				2700.1	23.4	346.8	2730.0	14.6	436.0	365.5
Toby-1																
Toolachee-9	1823.9	17.9	828.0	1885.5	22.7	504.2	2062.7	23.4	1235.0	2175.0	22.5	976.3	2208.4	16.1	861.2	880.9
Toolachee-21	1848.2	18.2	780.8	1910.3	22.0	516.2	2054.5	22.4	1404.2	2180.2	22.8	931.4	2224.2	16.4	830.0	892.5
Toolachee-39				2034.1	19.5	508.5	2104.0	23.3	1208.2	2251.3	22.6	880.3	2302.1	14.0	905.8	875.7
Turban-1	2127.2	17.1	587.0	2263.9	25.4	0.0 (R+)							2273.3	28.6	0.0 (R+)	195.7
Ullenbury-1	2452.5	20.1	21.0													21.0
Wackett-3	1801.2	18.4	807.0	1865.4	22.6	529.6										668.3
Wallawanny-1																
Wancoocha-2										1689.8	25.7	1082.8	1714.6	22.8	927.8	1005.3
Wantana-2																
Wareena-1	1681.2	16.2	1104.6	1851.8	22.2	565.0										834.8
Warnie East-1	1857.8	16.3	917.1	2026.4	18.9	540.9	2304.3	20.0	1538.8	2426.7	18.2	1218.1	2541.2	6.4	1154.0	1073.8
Watson-1																
Weena-1																
Wicho-1																

Table 4. Continued.

	Nappamerri Group			Toolachee Formation			Roseneath Shale			Murteree Shale			Patchawarra Formation			Mean‡‡
Well	Midpoint Depth (m bgl*)	Mean ϕ_N** (pu)	E_A*** (m)	Midpoint Depth (m bgl*)	Mean ϕ_N** (pu)	E_A*** (m)	Midpoint Depth (m bgl*)	Mean ϕ_N** (pu)	E_A*** (m)	Midpoint Depth (m bgl*)	Mean ϕ_N** (pu)	E_A*** (m)	Midpoint Depth (m bgl*)	Mean ϕ_N** (pu)	E_A*** (m)	E_A*** (m)
Wills-1				1667.9	22.4	739.2	1771.0	23.6	1491.8	1826.8	22.9	1275.4				1168.8
Wimma-1	2889.2	14.1	59.0							3279.4	19.9	177.7				118.4
Wippo-2																
Wirha-1				1668.5	21.7	770.1	1715.8	23.4	1582.4	1794.1	22.7	1325.8	1861.2	17.1	1145.9	1206.0
Witchetty-1																
Wompi-1																
Wuroopie-1																
Yanbee-1																
Yanda-2	2059.0	15.6	775.4	2161.4	19.3	390.2							2342.1	11.2	1041.1	735.6
Yanta-1																
Yumba-1	2003.3	21.6	351.1	2081.8	26.3	142.4										246.7

*m bgl = meters below ground level.

**ϕ_N = neutron porosity.

***E_A = apparent exhumation.

‡Mean = mean of the apparent exhumation values from such of the Eromanga Basin Formations as are present in any given well.

‡‡Mean = mean of the apparent exhumation values from such of the Cooper Basin Formations as are present in any given well.

R* = reference well, ie. well used to define normal compaction relationship.

Table 5. Midpoint Depth and Mean Log Data for Toolachee and Patchawarra Formations Including Coals

	Toolachee Formation					Patchawarra Formation				
Well	Midpoint Depth (m bgl*)	Mean Δt ** (µs/ft)	Mean Δt_{adj}*** (µs/ft)	Mean ρ_b+ (g/cm³)	Mean ϕ_N++ (pu)	Midpoint Depth (m bgl*)	Mean Δt ** (µs/ft)	Mean Δt_{adj}*** (µs/ft)	Mean ρ_b+ (g/cm³)	Mean ϕ_N++ (pu)
Alkina-1	2569.4	93.3	91.6	2.0	24.4	2617.9	66.8	65.4	2.5	8.7
Alwyn-1										
Amyema-1	1948.0	82.3	76.1	2.4	22.8	2302.5	77.1	74.7	2.4	18.6
Andree-1	2656.8	76.5	82.4	2.4	17.7	2903.7	78.1	85.1	2.3	17.7
Araburg-1										
Arrabury-1	2635.2	95.1								
Arrakis-1	2135.3	86.6	88.9	2.2	25.0	2331.1	81.8	81.7	2.4	22.4
Atoll-1										
Azolla-1	1889.2	89.7	88.7	2.3	27.0	2291.6	75.6	78.0	2.5	19.7
Ballera-1	2312.0	79.9	84.1	2.1	19.6	2433.6	76.5	74.6	2.2	14.7
Baratta-1	2022.8	80.0	81.2	2.4	20.6	2211.2	75.7	73.5	2.5	16.8
Bardoc-1	1806.8	89.4	90.0	2.2	26.2					
Barrolka-1	2583.6	80.2	77.3			2636.5	81.5	79.1		
Baryulah-1	2282.4	76.5	77.6	2.4	18.9	2490.1	69.2	61.9	2.4	12.4
Battunga-1	1886.6	99.9	98.4			2324.0	80.6	82.9		
Beanbush-1	3227.8	109.3	112.1	1.7	35.1	3414.6	82.1	88.9	2.2	24.6
Belah-1	1819.7	84.8	85.7	2.3	24.4	2156.2	74.6	83.2	2.5	16.8
Biala-1										
Big Lake-26	2286.4	76.3	80.7	2.4	15.9	2678.2	76.6	78.5	2.4	15.9
Big Lake-35	2326.1	74.6	82.3	2.5	16.4	2730.6	76.2	84.2	2.5	15.4
Bogala-1	1749.7	80.3	73.4	2.3	20.1	1912.9	80.1	93.7	2.3	17.8
Boldrewood-1	1956.1	78.1	78.6							
Bookabourdie-1	2667.0	87.5	88.8	2.1	22.6	2766.1	75.4	87.1	2.4	18.3
Boxwood-1						1820.3	92.8			
Brolga-2	2658.8	83.0	88.1			2807.3	81.9	93.3		
Buckinna-1										
Bungee-1	1915.3	91.8	97.1	2.2	27.1	2296.0	82.2	90.1	2.4	23.2
Burke-2										
Burley-2	2746.3	75.1	74.3	2.4	11.9	3377.5	72.7	78.6	2.5	10.9
Bycoe-1	1622.5	83.2				1713.9	84.7	80.8	2.3	23.6
Carney-1	1890.2	79.1	72.2			2024.0	74.8	83.2		
Challum-1	2309.5	74.4	68.7	2.6	19.4	2358.5	74.1	70.2	2.5	9.6
Charo-1										
Childie-1	1862.6	83.1	87.9	2.4	22.3	2023.3	79.0	76.7	2.4	17.4
Cooba-1	2561.3	80.7	70.8			2870.3	80.0	84.9		
Cook-1										
Cook North-1										
Coonavalla-1	2057.9	107.8	109.6			2113.2	81.0	82.3		
Cooroo-1	1852.0	79.1	93.4	2.4	20.0					
Copai-1										
Cowan-3	2046.9	87.6				2267.5	79.4		2.5	19.3
Cuddapan-1										
Curalle-1										
Daer-1	2348.3	78.5		2.4						
Daralingie-15	1992.8	94.4	119.7			2259.9	84.2	77.3		
Daralingie-23						2259.2	78.8	77.5	2.4	21.6
Darter-1	2506.2	94.7	86.8			2581.6	88.0	99.2		
Della-7	1946.6	86.9	78.0	2.4	19.2					
Della-10	1946.1	82.7	85.9	2.3	16.0	1999.5	79.9	73.9	2.4	13.4
Denley-1										
Deparanie-1	2417.9	81.2	76.9			2440.3	81.4	80.5		
Deramookoo-1										
Dirkala-2	1762.0	84.3		2.4	20.7	2014.6	88.7		2.3	27.6
Doonmulla-1										
Dullingari-3	2207.1	83.4	86.1	2.3		2614.7	77.3	78.1		
Dullingari North-1	2191.2	80.0	83.1	2.3	19.4	2573.7	75.6	73.9	2.3	12.6
Dunoon-1										
Durham Downs-1	2522.9	74.2	74.3			2597.5	78.3	78.3		
Echuburra North-1										
Fly Lake-1	2575.8	84.6	87.5	2.2		2721.2	83.1	93.1	2.3	
Fly Lake-4	2625.7	82.4	79.2	2.3	20.9	2757.4	84.6	89.2	2.3	22.9
Garanjanie-2	1795.1	87.3		2.3	23.6	2056.8	85.7		2.3	24.1
Gidgealpa-20										
Gidgealpa-42	2104.3	84.4		2.3	19.0	2162.4	85.0		2.3	21.2
Gidgee-1	1502.1	80.0				1560.0	86.0		2.3	24.3
Gooranie-1	2609.7	76.9	77.1	2.4	18.0	2854.8	78.9	88.0	2.3	19.6
Gooranie-2	2615.3	80.2	87.9	2.3	20.6	2849.0	81.8	89.3	2.3	21.9
Graham-1	1631.9	83.4	79.5	2.4	23.7	1792.8	86.5	94.0	2.2	23.7
Gurra-1										
Haddon Downs-1										
Hammond-1										
Hooley-1										
Hume-1	1923.4	80.5	78.2	2.4	22.2	2114.7	77.4	75.5	2.3	22.1
Hydra-1	1595.5	85.1	75.3	2.4	24.6	1760.3	75.6	71.5	2.5	19.1
Ingella-1										
Innamincka-3										
Innamincka-4	2078.0	78.7								
Jack Lake-2	2467.8	79.7	79.6	2.3	20.2	2833.7	79.4	88.1	2.3	19.5
Jackson-1	1535.0	86.3	101.8	2.3	31.0	1645.6	87.5	93.8	2.2	28.4
Jackson South-1	1504.9	87.1	83.9	2.3	27.5	1670.7	91.5	96.5	2.2	21.3
James-1										
Jarrar-1	1912.0	88.9	81.5	2.2	23.0					
Johba-1										
Kalladeina-1										

Table 5. Continued.

	Toolachee Formation					Patchawarra Formation				
Well	Midpoint Depth (m bgl*)	Mean Δt ** (µs/ft)	Mean Δt_{adj}*** (µs/ft)	Mean ρ_b+ (g/cm³)	Mean ϕ_N++ (pu)	Midpoint Depth (m bgl*)	Mean Δt ** (µs/ft)	Mean Δt_{adj}*** (µs/ft)	Mean ρ_b+ (g/cm³)	Mean ϕ_N++ (pu)
Karmona-2	2251.6	76.6	74.4			2411.6	72.7	78.2		
Karwin-1	1790.5	87.0	78.8	2.3		2291.5	78.0	86.5	2.3	
Keeto-2	1905.9	88.3	82.6			2221.5	75.4	77.3		
Keilor-1	2482.4	75.0	67.4	2.4	18.2	2636.1	79.9	69.3	2.3	20.0
Kenny-1										
Kercummurra-1	1809.3	74.2	75.7	2.5	16.2					
Kerna-5	2130.2	78.9		2.5	21.6	2497.2	75.4		2.4	13.8
Kirby-1	2687.9	78.6	79.7			3424.4	74.3			
Kirby-2	2709.8	77.4	78.6	2.4	23.4			73.9	2.4	11.7
Kiwarrick-1	1664.5	82.7	86.1	2.4	23.5	1773.6	78.6	86.9	2.5	21.2
Kobari-1						1661.4	86.1			
Koonchera-1										
Kumbaric-1						1478.1	89.9			
Kurunda-1	2219.8	81.6	84.9	2.3	20.4			87.4	2.4	22.4
Kutyo-1	1944.1	78.6	75.1	2.5	23.9	3033.1	86.2			
Lake Mcmillan-1	2881.1	100.2	69.3	1.8	29.9			90.0	2.2	23.7
Lambda-1										
Lhotsky-1										
Limestone Creek-9						2082.4	88.9			
Lycium-1						2883.5	73.2	90.5		
Macadama-1	2661.1	81.4	82.4					75.5		
Mackillop-1	2538.7	73.9	94.1			2093.0	75.7			
Marabooka-2	1959.5	83.1	82.8	2.3	21.1			75.2	2.4	14.6
Marengo-1	2943.9	71.9	71.8			2380.1	75.5			
Marsilea-1	2012.0	81.8	78.3	2.4	21.6	2393.0	80.3	79.5	2.4	16.3
Mawson-1	2228.8	80.3	95.9	2.3	20.9			88.4	2.4	22.4
Mckinlay-3						3379.3	71.9			
Mcleod-1	2713.0	77.0	85.7	2.4	14.8			71.9	2.6	12.1
Meeba-1						2733.0	77.9			
Meranji-1	2448.0	80.2	87.3	2.4	16.7			85.4	2.4	18.0
Merrimelia-7	2227.6	70.8	68.4	2.6	17.0					
Merrimelia-25	2276.7	80.7	82.5	2.4	12.7					
Minkie-1	2796.7	91.4								
Mooliampah-1	1605.5	85.7	85.5	2.3	24.3					
Moolion-1						1745.1	81.7	94.1	2.2	19.2
Moomba-27	2495.4	82.3	83.6			2898.7	79.6	76.0	2.4	14.3
Moomba-57	2408.2	75.7	85.1	2.4	17.1	2861.0	75.3	73.3		
Moomba North-1	2481.4	77.8	74.4	2.4	16.0	2924.6	73.4	77.9	2.5	12.5
Moomba South-1	2375.7	79.7	88.3	2.3	19.9	2887.0	72.1	79.2	2.5	12.8
Moorari-4	2678.9	91.7	73.7	2.2	28.6	2828.0	71.7	105.2	2.3	21.5
Morney-1						2800.5	84.6			
Mudera-3	2046.9	84.1	89.0	2.3	23.0					
Munkah-2	2148.7	77.7	76.4	2.4	20.2	2217.6	74.4	84.5	2.3	14.5
Munkarie South-1						2258.7	75.0			
Munro-1										
Muteroo-3										
Naccowlah East-1	1934.0	80.4	76.9							
Naccowlah South-1	1836.3	81.7	79.1	2.4	19.1	2067.9	81.3			
Naccowlah West-1	1796.8	92.6								
Naryilco-1										
Navalla-1										
Nulla-1	2377.4	88.3	93.9	2.2	25.7					
Okotoko-1	2138.8	74.3	72.5	2.5	18.2	2549.0	80.3	77.7	2.4	17.6
Orientos-2						2225.3	74.3			
Packsaddle-4	2122.5	66.8		2.3						
Padulla-1										
Pallano-1	1898.6	76.5	83.2	2.5	12.4					
Pandieburra-1										
Pando South-1										
Paning-1	2873.1	97.6	98.6	2.0	36.4					
Paragilga-1						2966.3	82.6			
Patroclus-1	1892.8	85.2	80.1	2.4	24.0					
Paxton-1										
Pepita-2	2229.6	71.7	71.6	2.5	16.0					
Pintari-1										
Pondrinie-5	2204.6	76.1	58.8	2.5	13.2	1743.0	77.6			
Potiron-1										
Putamurdie-1										
Rheims-1	1633.0	83.9	90.2	2.4	24.4					
Rho East-1										
Richie-1	1574.1	89.6	86.9	2.3	27.2	1731.3	91.0	95.1	2.2	26.1
Russel-1	2841.4	74.0	76.1	2.3	12.5	2878.1	63.5	63.5	2.4	7.6
Snake Hole-1	2334.6	77.1	73.0	2.4	16.4	2505.9	84.3	82.7	2.3	20.8
Spectre-1	2688.8	77.9	73.8	2.4	18.9	2936.3	76.2	82.6	2.4	18.0
Spencer-4						1848.2	77.6	82.7	2.4	18.7
Steward-1										
Strzelecki-10	1923.0	81.8	79.9	2.4	20.7	2059.7	67.2	67.5	2.5	14.0
Strzelecki -27										
Sturt-6						1878.2	106.1	67.4	2.0	36.9
Swan Lake-1	2556.8	75.7	72.5	2.4	14.9	2818.3	75.7	77.7	2.4	17.3
Taloola-1						1866.7	95.1	89.4	2.2	33.4
Tanbar-1	2802.6	67.6								
Tanbar North-1										
Tartulla-1	2395.3	75.9	89.4	2.5		2511.9	85.0	85.2	2.3	
Tennaperra South-1	1778.1	82.5	64.4	2.4	21.1					
Three Queens-1	2294.9	81.1	83.6			2754.2	69.1	68.6		
Thurakinna-5						2320.1	78.6	84.2	2.4	21.0
Thurra-1	1994.6	91.9	82.4	2.5	21.6	2036.2	74.9	72.0	2.5	15.2

Table 5. Continued.

	Toolachee Formation					Patchawarra Formation				
Well	Midpoint Depth (m bgl*)	Mean Δt ** (µs/ft)	Mean Δt_{adj}*** (µs/ft)	Mean ρ_b+ (g/cm³)	Mean ϕ_N++ (pu)	Midpoint Depth (m bgl*)	Mean Δt ** (µs/ft)	Mean Δt_{adj}*** (µs/ft)	Mean ρ_b+ (g/cm³)	Mean ϕ_N++ (pu)
Tinchoo-1	1912.3	79.0				2682.5	71.5	76.7		
Tinga Tingana-1	2670.4	75.2				1583.0	101.2	103.2		
Tinpilla-1						1757.9	79.8	81.3	2.4	18.5
Tirrawarra-13	1632.8	82.4	72.9	2.4	20.1	2774.6	79.8	76.5	2.4	16.9
Tirrawarra-15	2616.3	81.0	65.3			2779.3	80.7	91.0		
Tirrawarra-26	2594.3	79.7	90.7	2.4	19.9	2810.1	78.4	82.2	2.4	18.6
Tirrawarra North-1	2633.6	79.6	81.3	2.4	19.5	2907.5	79.3	93.6	2.4	21.5
Tirrawarra West-1	2703.4	78.6	83.1	2.3	20.3	2855.4	77.3	82.1	2.4	18.0
Toby-1	2654.1	81.9	83.5			2242.0	70.7	75.5		
Toolachee-9	2194.1	80.1	71.8	2.4	22.9	2272.1	75.0	78.7	2.5	16.8
Toolachee-21	1940.8	82.2	82.3	2.4	22.6	2259.5	75.6	76.2	2.5	18.3
Toolachee-39	1957.0	81.9	81.7	2.4	23.3	2389.3	74.5	77.0	2.4	19.9
Turban-1	1960.8	82.3	65.8	2.4	25.4	2293.8	85.0	60.9	2.3	28.7
Ullenbury-1	2263.9	76.3								
Wackett-3										
Wallawanny-1	1851.3	84.0								
Wancoocha-2						1724.7	83.9	83.4	2.4	20.1
Wantana-2						2659.4	72.5	80.3		
Wareena-1	2531.1	78.6	69.4	2.6	22.2					
Warnie East-1	1851.8	72.1	85.2	2.4	21.3	2509.7	68.3	77.7	2.5	8.9
Watson-1	2119.7	85.2								
Weena-1						1408.9	103.7			
Wicho-1										
Wills-1	2645.5	70.1	80.8	2.5	27.5					
Wimma-1	1672.9	88.7	106.8	2.1	29.8	3457.5	81.8	81.8		25.7
Wippo-2	3211.8	102.6	75.6			2394.9	73.1	77.0		
Wirha-1	2256.1	75.5	80.6	2.3	25.1	1861.2	77.3			
Witchetty-1	1923.8	81.4	81.2			2148.1	74.4			
Wompi-1	1652.6	90.9	81.4	2.2		1783.6	73.4	102.6	2.5	
Wuroopie-1	1659.0	98.0				1923.2	77.7			
Yanbee-1										
Yanda-2	2169.6	76.4	69.8	2.4	17.7	2312.0	78.6	78.2	2.4	15.6
Yanta-1										
Yumba-1	2098.9	77.2	81.9	2.4	23.7	2137.0	70.6	72.5	2.5	17.1

*m bgl = meters below ground level.
**Δt = interval transit time.
***Δt_{adj} = adjusted interval transit time.
ρ_b+ = bulk density.
ϕ_N++ = neutron porosity.

APPENDIX B: PRESENT AND MAXIMUM BURIAL-DEPTHS FOR HUTTON SANDSTONE AND PATCHAWARRA FORMATION

Table 1. Maximum Burial-Depth Results for Hutton Sandstone and Patchawarra Formation

Well	Present Burial Depth (B_P) for Base of Hutton Sandstone (m)	Maximum Burial Depth (B_T) for Base of Hutton Sandstone (m)	Present Burial Depth (B_P) for Base of Patchawarra Formation (m)	Maximum Burial Depth (B_T) for Base of Patchawarra Formation (m)
Alkina-1	2069.6	2598.7	2646.0	3175.1
Alwyn-1	1554.6	1907.7		
Amyema-1	1782.8	2149.2	2364.7	2731.1
Andree-1	2349.7	2516.6	3080.9	3247.8
Araburg-1	2026.0	2486.9		
Arrabury-1	2267.4	2510.7		
Arrakis-1	2043.2	2296.3	2368.1	2621.2
Atoll-1	1456.3	2033.7		
Azolla-1	1751.2	2108.2	2357.8	2714.8
Ballera-1	2030.0	2467.5	2510.4	2947.9
Baratta-1	1863.9	2293.5	2267.4	2697.0
Bardoc-1	1788.9	2257.5		
Barrolka-1	2137.9	2593.8	2662.4	3118.4
Baryulah-1	2013.3	2379.6	2534.2	2900.5
Battunga-1	1770.3	2072.5	2494.5	2796.7
Beanbush-1	2640.4	2640.4	3536.8	3536.8
Belah-1	1685.8	2120.1	2268.6	2702.9
Biala-1	1559.4	1896.5		
Big Lake-26	2096.2	2679.4	2846.6	3429.8
Big Lake-35	2116.5	2450.5	2888.3	3222.3
Bogala-1	1644.2	2222.5	1998.7	2577.0
Boldrewood-1	1574.0	2392.6		
Bookabourdie-1	2294.8	2495.9	2850.8	3051.9
Boxwood-1	1670.0	2071.4	1853.2	2254.6
Brolga-2	2411.6	2671.8	2918.5	3178.7
Buckinna-1	1614.4	2048.8		
Bungee-1	1788.0	2066.0	2457.1	2735.0
Burke-2				
Burley-2	2242.4	2627.7	3564.9	3950.2
Bycoe-1	1590.8	2199.8	1756.3	2365.3
Carney-1	1743.6	2229.1	2105.4	2590.9
Challum-1	2033.0	2421.8	2372.0	2760.8
Charo-1	2030.2	2324.3		
Childie-1	1760.5	2171.4	2080.9	2491.7
Cooba-1	2265.5	2428.4	3060.1	3223.0
Cook-1	2189.2	2538.9		
Cook North-1	2153.9	2568.8		
Coonavalla-1	1727.6	2405.7	2156.8	2834.8
Cooroo-1	1810.5	2263.5		
Copai-1	1858.1	2389.1		
Cowan-3	1961.1	2255.5	2307.3	2601.8
Cuddapan-1	2158.3	2597.5		
Curalle-1	1487.6	2484.0		
Daer-1	2171.1	2376.4		
Daralingie-15	1908.8	2337.2	2322.4	2750.8
Daralingie-23	1914.8	2191.4	2299.4	2576.1
Darter-1	2265.2	2420.3	2644.4	2799.4
Della-7	1832.4	2541.2		
Della-10	1807.8	2365.5	2025.1	2582.8
Denley-1	2248.2	2686.0		
Deparanie-1	2173.9	2401.8	2436.6	2664.5
Deramookoo-1	2310.8	2499.9		
Dirkala-2	1738.6	2096.0	2095.5	2453.0
Doonmulla-1	2229.9	2586.4		
Dullingari-3	1914.1	2427.7	2769.4	3283.0
Dullingari North-1	1908.4		2724.3	
Dunoon-1	1437.9	1831.8		
Durham Downs-1	2140.6	2668.8	2627.1	3155.2
Echuburra North-1	1776.4	2360.9		
Fly Lake-1	2394.9	2537.8	2839.0	2981.9
Fly Lake-4	2406.1	2710.9	2862.7	3167.5
Garanjanie-2	1733.1	1999.1	2150.7	2416.7
Gidgealpa-20	1907.9	2253.4		
Gidgealpa-42	2062.6	2328.7	2197.6	2463.8
Gidgee-1	1503.9	1918.7	1589.9	2004.7
Gooranie-1	2266.8	2471.4	3030.9	3235.6
Gooranie-2	2276.9	2522.2	3016.9	3262.3
Graham-1	1579.0	2182.4	1869.8	2473.2
Gurra-1				
Haddon Downs-1	1826.1	2403.6		

Table 1. Continued.

Well	Present Burial Depth (B_P) for Base of Base of Hutton Sandstone (m)	Maximum Burial Depth (B_T) for Base of Base of Hutton Sandstone (m)	Present Burial Depth (B_P) for Base of Patchawarra Formation (m)	Maximum Burial Depth (B_T) for Base of Patchawarra Formation (m)
Hammond-1	2249.7	2648.1		
Hooley-1	1478.9	2236.2		
Hume-1	1780.9	2230.6	2122.0	2571.6
Hydra-1	1548.4	2082.3	1780.7	2314.5
Ingella-1	2220.5	2721.7		
Innamincka-3	1721.8	2388.4		
Innamincka-4	1791.2	2457.3		
Jack Lake-2	2212.5	2349.5	3051.0	3188.0
Jackson-1	1492.6	2267.1	1701.7	2476.2
Jackson South-1	1479.9	2112.6	1778.6	2411.3
James-1	2175.5	2546.7		
Jarrar-1	1857.3	2315.4		
Johba-1	1763.6	2260.8		
Kalladeina-1	1951.9	2176.2		
Karmona-2	1953.8	2400.3	2571.9	3018.5
Karwin-1	1659.8	2202.0	2557.4	3099.6
Keeto-2	1766.0	2098.8	2273.5	2606.3
Keilor-1	2058.9	2484.2	2735.6	3160.8
Kenny-1	2362.5	2603.8		
Kercummurra-1	1503.9	2305.9		
Kerna-5	1901.3	2239.1	2559.1	2896.8
Kirby-1	2204.0	2577.0	3765.2	4138.2
Kirby-2	2177.5	2592.4		
Kiwarrick-1	1629.2	2070.4	1810.5	2251.7
Kobari-1	1510.9	1896.8	1743.5	2129.4
Koonchera-1	1943.9	2354.6		
Kumbarie-1			1521.0	1749.2
Kurunda-1	2111.4	2357.4	2523.7	2769.8
Kutyo-1	1894.1	2299.5		
Lake Mcmillan-1	2447.2	2572.3	3109.6	3234.7
Lambda-1				
Lhotsky-1	1870.6	2137.8		
Limestone Creek-9				
Lycium-1	1953.5	2203.9	2176.6	2427.0
Macadama-1	2195.9	2531.8	3062.5	3398.3
Mackillop-1	2154.9	2601.1		
Marabooka-2	1833.5	2234.7	2182.8	2584.0
Marengo-1	2402.9	2756.7		
Marsilea-1	1798.4	2206.6	2452.2	2860.4
Mawson-1	2108.8	2323.8	2503.5	2718.5
Mckinlay-3	1522.7	1967.6		
Mcleod-1	2173.8	2691.1	3560.1	4077.4
Meeba-1	2140.8	2578.8		
Meranji-1	2192.7	2402.5	2929.4	3139.2
Merrimelia-7	2048.4	2275.9		
Merrimelia-25	2141.5	2491.1		
Minkie-1	2109.3	2404.3		
Mooliampah-1	1567.1	2080.7	1770.7	2284.3
Moolion-1	2415.8	2595.0	2949.2	3128.4
Moomba-27	2250.0	2585.1	2974.2	3309.3
Moomba-57	2179.3	2503.5	3055.9	3380.1
Moomba North-1	2220.7	2566.2	2990.9	3336.4
Moomba South-1	2183.5	2633.0	2996.7	3446.2
Moorari-4	2195.2	2394.9	2873.4	3073.1
Morney-1	1563.0	2386.7		
Mudera-3	1877.6	2330.2	2313.7	2766.4
Munkah-2	1922.7	2357.8	2322.0	2757.1
Munkarie South-1	1444.1	1978.6		
Munro-1	1476.5	1903.3		
Muteroo-3	1763.9	2149.3		
Naccowlah East-1	1806.0	2220.5	2253.4	2668.0
Naccowlah South-1	1767.3	2225.5		
Naccowlah West-1	1783.1	2265.8		
Naryilco-1	1388.7	1851.0		
Navalla-1	1507.9	2479.6		
Nulla-1	2197.9	2427.7	2685.3	2915.1
Okotoko-1	1883.8	2400.7	2261.9	2778.8
Orientos-2				
Packsaddle-4	1928.8	2386.2		
Padulla-1	1476.8	1873.3		
Pallano-1	1858.1	2311.2		
Pandieburra-1	2058.6	2539.0		
Pando South-1	1691.6	2002.5		

Table 1. Continued.

Well	Present Burial Depth (B_P) for Base of Base of Hutton Sandstone (m)	Maximum Burial Depth (B_T) for Base of Base of Hutton Sandstone (m)	Present Burial Depth (B_P) for Base of Patchawarra Formation (m)	Maximum Burial Depth (B_T) for Base of Patchawarra Formation (m)
Paning-1	2316.1	2569.4	3032.1	3285.4
Paragilga-1	1487.5	1955.5		
Patroclus-1	1822.4	2216.3		
Paxton-1				
Pepita-2	1962.4	2393.4		
Pintari-1	1715.1	2013.5	1763.0	2061.3
Pondrinie-5	1971.0	2323.8		
Potiron-1	1888.2	2574.9		
Putamurdie-1	1824.9	2367.1		
Rheims-1	1579.5	2054.0		
Rho East-1	1443.5	2018.6		
Richie-1	1529.0	2133.9	1814.9	2419.8
Russel-1	2353.7	2691.0	2891.6	3229.0
Snake Hole-1	2140.9	2327.8	2606.7	2793.6
Spectre-1	2382.3	2528.5	3108.4	3254.6
Spencer-4	1818.9	2175.3	1877.4	2233.8
Steward-1	1970.3	2484.0		
Strzelecki-10	1816.3	2250.5	2032.4	2466.6
Strzelecki -27	1741.9	2124.8		
Sturt-6	1826.8	2140.5	1897.2	2210.9
Swan Lake-1	2270.5	2621.5	2969.7	3320.7
Taloola-1	1831.3	2196.0	1876.4	2241.2
Tanbar-1	2493.0	2881.8		
Tanbar North-1	2327.8	2952.9		
Tartulla-1	2032.1	2537.9	2571.0	3076.8
Tennaperra South-1	1717.0	2235.8		
Three Queens-1	1923.6	2400.3	2902.0	3378.7
Thurakinna-5	1875.4	2163.0	2402.1	2689.7
Thurra-1	1806.3	2280.1	2085.5	2559.2
Tinchoo-1	2169.0	2576.8	2686.5	3094.3
Tinga Tingana-1	1397.8	1431.0	1677.3	1710.6
Tinpilla-1	1581.1	2177.4	1829.0	2425.3
Tirrawarra-13	2324.6	2630.6	2884.5	3190.5
Tirrawarra-15	2306.1	2585.4	2909.6	3188.9
Tirrawarra-26	2357.9	2707.0	2934.6	3283.7
Tirrawarra North-1	2350.9	2536.2	3047.4	3232.6
Tirrawarra West-1	2317.1	2485.8	3005.0	3173.7
Toby-1	1709.0	2514.6	2267.4	3073.0
Toolachee-9	1781.8	2227.1	2342.0	2787.3
Toolachee-21	1786.9	2183.8	2310.8	2707.8
Toolachee-39	1757.8	2194.5	2494.5	2931.2
Turban-1	1964.0	2421.0	2317.5	2774.5
Ullenbury-1	2169.6	2622.5		
Wackett-3	1756.7	2239.5		
Wallawanny-1	1858.1	2381.4		
Wancoocha-2	1648.2	2056.6	1745.4	2153.9
Wantana-2	2236.0	2542.3	2769.4	3075.7
Wareena-1	1466.9	2338.1		
Warnie East-1	1713.0	2254.5	2576.2	3117.7
Watson-1	1651.7	2264.7		
Weena-1			1520.0	1520.0
Wicho-1	2226.3	2586.8		
Wills-1	1623.1	2103.8		
Wimma-1	2605.9	2605.9	3608.0	3608.0
Wippo-2	1928.3	2369.4	2473.0	2914.0
Wirha-1	1621.0	2090.1	1904.5	2373.6
Witchetty-1	1769.4	2187.8	2175.7	2594.1
Wompi-1	1599.9	2188.3	1790.4	2378.8
Wuroopie-1	1603.3	2047.1	1959.9	2403.7
Yanbee-1	2209.0	2564.3		
Yanda-2	1969.7	2351.7	2433.0	2815.0
Yanta-1	2089.4	2365.0		
Yumba-1	1909.9	2322.2	2140.3	2552.7

REFERENCES

Apak, S.N., Stuart, W.J. and Lemon, N.M. 1993. Structural-stratigraphic development of the Gidgealpa-Merrimelia-Innamincka Trend with implications for petroleum trap styles, Cooper Basin, Australia. *Australian Petroleum Exploration Association Journal* **33**, 94-104.

Armagnac, C., Bucci, J., Kendall, C.G.St.C. and Lerche, I. 1985. *Estimating the thickness of sediment removed at an unconformity using vitrinite reflectance data. In:* Naeser, N.D. (ed): Society of Economist Paleontologists and Mineralogists Special Publication.

Armagnac, C., Bucci, J., Kendall, C.G.St.C. and Lerche, I. 1989. *Estimating the thickness of sediment removed at an unconformity using vitrinite reflectance data. In:* Naeser, N.D. and McCulloh, T.H. (eds): *Thermal History of Sedimentary Basins-Methods and Case Histories*. New York, Springer Verlag, 217-238.

Arne, D.C. 1992. Evidence from Apatite Fission-Track Analysis for Regional Cretaceous Cooling in the Ouachita Mountain Fold Belt and Arkoma Basin of Arkansas. *American Association of Petroleum Geologists Bulletin* **76**, 392-402.

Asquith, G. B. 1990. *Log Evaluation of Shaly Sandstones: A Practical Guide.* Continuing Education, Course Note Series **31**. American Association of Petroleum Geologists. Tulsa, Oklahoma, USA, pp. 59.

Athy, L.F. 1930. Density, porosity and compaction of sedimentary rocks. *American Association of Petroleum Geologists Bulletin* **14**, 1-24.

Baldwin, B. and Butler, C.O. 1985. Compaction Curves. *American Association of Petroleum Geologists Bulletin* **69**, 622-626.

Battersby, D.G. 1976. Cooper Basin oil and gas fields. *In*: Leslie, R.B., Evans, H.J. and Knight, C.L. (eds): Economic geology of Australia and Papua New Guinea. 3. Petroleum. *Australasian Institute of Mining and Metallurgy, Monograph Series* **7**, 321-368.

Beardsmore, G.R. and O'Sullivan, P.B. 1995. Uplift and erosion on the Ashmore platform, North west shelf: conflicting evidence from maturation indicators. *Australian Petroleum Exploration Association Journal* **35**, 333-343.

BEICIP, MATOIL, 1990. *A quantitative model of hydrocarbon generation for the personal computer.* Release No. 2: Paris, Bureau d'Etudes Industrielles et de Coopération de l'Institut Français du Pétrole.

Bowering, O.J.W. 1982. Hydrodynamics and hydrocarbon migration. A model for the Eromanga Basin. *Australian Petroleum Exploration Association Journal* **22**, 227-236.

Bray, R.J., Green, P.F. and Duddy, I.R. 1992. Thermal history reconstruction using apatite fission track analysis and vitrinite reflectance: a case study from the UK East Midlands and the Southern North Sea. *In:* Hardman, R.F.P.(ed): *Exploration Britain: Into the next decade.* Geological Society, London, Special Publication **67**, 3-25.

Brodie, J. and White, N. 1995. The link between sedimentary basin inversion and igneous underplating. *Basin Inversion.* Geological Society, London, Special Publication **88**, 21-38.

Brown, R. W. 1991. Backstacking apatite fission track "stratigraphy": A method for resolving the erosional and isostatic rebound components of tectonic uplift histories. *Geology* **19**, 74-77.

Bulat, J. and Stoker, S.J. 1987. Uplift determination from interval velocity studies, UK southern North Sea. *In:* Brooks, J. and Glennie, K. (eds): *Petroleum Geology of North West Europe.* Graham & Trotman, London, 293-305.

Burnham, A.K. 1989. A simple model of petroleum formation and cracking. Lawrence Livermore Laboratory report UCID 21665, March 1989.

Burnham, A.K. and Sweeney, J.J. 1989. A chemical Kinetic model of vitrinite maturation and reflectance. *Geochimica et Cosmochimica Acta* **53**, 2649-2657.

Bustin, R.M. 1989. Diagenesis of kerogen. *In:* Hutcheon, I.E. (ed): *Short course in burial diagenesis.* Mineralogical Association of Canada, short course handbook **15**, 1-38.

Callen, R.A. and Tedford, R.A. 1976. New Cainozoic rock units and depositional environments, Lake Frome area, South Australia. *Royal Society of South Australia Transactions* **100**, 125-167.

Cande, S.C. and Mutter, J.C. 1982. A revised identification of the oldest sea-floor spreading anomalies between Australia and Antarctica. *Earth and Planetary Science Letters* **58**, 151-160.

Cao, S., Lerche, I. and Hermanrud, C. 1988. Formation temperature estimation by inversion of borehole measurements. *Geophysics* **53**, 979-988.

Castelli, A., Chiaramonte, M.A., Beltrame, P.L., Carniti, R., Del Bianco, A. and Stroppa, F. 1990. Thermal degradation of kerogen by hydrous pyrolisis: a kinetic study. *In*: Durand, B. and Behar, F. (eds): *Advances in Organic Geochemistry 1989*, Pergamon Press, Oxford, **16** (1-3), 75-82.

Chadwick, R.A. 1985. Permian, Mesozoic and Cenozoic structural evolution of England and Wales in relation to the principles of extension and inversion tectonics. *In*: Whittaker, A. (ed): *Atlas of Onshore Sedimentary Basins in England and Wales: Post-Carboniferous Tectonics and Stratigraphy*. Blackie, Glasgow, 9-25.

Channon, G.J. and Wood, G.R. 1989. Stratigraphy and hydrocarbon prospectivity of Triassic sediments in the northern Cooper Basin. *Department of Mines and Energy South Australia*. Confidential envelope, 8126 (unpublished).

Cloetingh, S., McQueen, H. and Lambeck, K. 1985. On a tectonic mechanism for regional sealevel variations. *Earth and Planetary Science Letters* **75**, 157-166.

Coventry, R.J., Stephenson, P.J. and Webb, A.B. 1985. Chronology of landscape and soil development in the upper Flinders Range area, Queensland, based on isotopic dating of Cainozoic basalts. *Australian Journal of Earth Science* **32**, 433-447.

Crook, K.A.W. and Belbin, L. 1978. The southwest Pacific area during the last 90 million years. *Geological Society of Australia Journal* **25**, 23-40.

Desbrandes, R. 1985. *Encyclopedia of well logging*. Institut Français du pétrole publications. Translated from the French by G.Brace. Graham and Trotman, London, UK, pp. 584.

Dow, W.G. 1977. Kerogen studies and geological interpretations. *Journal of Geochemical Exploration* **7**, 79-99.

Dutton, S.P. 1993. Influence of provenance and burial history on diagenesis of Lower Cretaceous Frontier formation sandstones, Green River Basin, Wyoming. *Journal of Sedimentary Petrology* **63**, 665-667.

Dutton, S.P. and Diggs, T.N. 1992. Evolution of Porosity and Permeability in the Lower Cretaceous Travis Peak Formation, East Texas. *American Association of Petroleum Geologists Bulletin* **76**, 252-269.

Eadington, P.J., Hamilton, P.J., and Green, P. 1989. Hydrocarbon fluid history in relation to diagenesis in the Hutton Sandstone, south-west Queensland. *In:* O'neil, B.J. (ed): *The Cooper and Eromanga Basins Australia.* Petroleum Exploration Society of Australia, Society of Petroleum Engineers and the Australian Society of Exploration Geophysicists, 601-618.

Elliott, L.G. 1993. Post-Carboniferous tectonic evolution of eastern Australia. *Australian Petroleum Exploration Association Journal* **33**, 215-236.

Elliott, P. 1985. Burley-2. Well completion report compiled for Delhi Petroleum Pty Ltd.

England, P. and Molnar, P. 1990. Surface uplift, uplift of rocks, and exhumation of rocks. *Geology* **18**, 1173-1177.

Espitalié, J., Ungerer, P., Irwin, I. and Marquis, F. 1988. Primary cracking of kerogens Experimenting and modelling C1, C2-C5, C6-C15 and C15+ classes of hydrocarbons formed. *In:* Matavelli, L. and Novelli, L. (eds): *Advances in Organic Geochemistry 1987*, Pergamon Press, Oxford, **13** (4-6), 893-899.

Etheridge, M., McQueen, H. and Lambeck, K. 1991. The Role of Intraplate Stress in Tertiary (and Mesozoic) Deformation of the Australian Continent and Its Margins: A key Factor in the Petroleum Trap Formation. *Exploration Geophysics* **22**, 123-128.

Falvey, D.A. and Deighton, I. 1982. Recent advances in burial and thermal geohistory analysis. *Australian Petroleum Exploration Association Journal* **22**, 65-81.

Fang, H. and Jianyu, C. 1992. The cause and mechanisms of vitrinite reflectance anomalies. *Journal of Petroleum Geology* **15**, 419-434.

Finlayson, D.M., Leven, J.H. and Etheridge, M.A. 1988. Structural Styles and Basin Evolution in Eromanga Region, Eastern Australia. *American Association of Petroleum Geologists Bulletin* **72**, 33-48.

Forbes, P.L., Ungener, P.M., Kuhfuss, A.B., Riis, F., and Eggen, S. 1991. Compositional modelling of petroleum generation and expulsion: Trial application to a local mass balance in the Smørbukk Sør Field, Haltenbanken area, Norway. *American Association of Petroleum Geologists Bulletin* **75**, 873-893.

Foster, D.A., Murphy, J.M. and Gleadow, A.J.W. 1994. Middle Tertiary hydrothermal activity and uplift of the northern Flinders Ranges, South Australia: Insights from apatite fission-track thermochronology. *Australian Journal of Earth Sciences* **41**, 11-17.

Gallagher, K. 1987. Thermal conductivity and heat flow in the southern Cooper Basin. *Proceedings of the 5th Australian Society of Exploration Geophysics Conference*, 62-65.

Gallagher, K. 1988. The subsidence history and thermal state of the Eromanga and Cooper Basins. Ph.D. dissertation, Australian National University, Canberra, Australia.

Gallagher, K. 1990. Permian-Cretaceous subsidence history along the Eromanga-Brisbane Geoscience Transect. *In*: Finlayson, D.M. (ed): *The Eromanga-Brisbane Geoscience transect: a guide to basin development across the Phanerozoic Australia in southern Queensland.* Bureau of Mineral Resources, Geology and Geophysics Bulletin **232**, 133-151.

Gallagher, K., Dumitru, T.A., and Gleadow, J.W. 1994. Constraints on the vertical motion of eastern Australia during the Mesozoic. *Basin Research* **6**, 77-94.

Gallagher, K. and Lambeck, K. 1989. Subsidence, sedimentation and sea-level changes in the Eromanga Basin, Australia. *Basin Research* **2**, 115-131.

Gatehouse, C.G. 1986. The geology of the Warburton Basin in South Australia. *Australian Journal of Earth Sciences* **33**, 161-180.

Geotrack International 1988. R.A.C.E. project. Technical note No. 14. Apatite fission track thermal history analysis of samples from four Queensland Eromanga basin wells: Jackson-1, Watson-1, Pepita-1 and Morney-1 (Unpublished GEOTRACK Report No 115 for ESSO Australia Ltd), 1-32.

Gleadow, A.J.W., Duddy, I.R., Green, P.F., and Lovering, J.F. 1986. Confined fission track lengths in apatite: a diagnostic tool for thermal history analysis. *Contributions to Mineralogy and Petrology* **94**, 405-415.

Gleadow, A.J.W., Duddy, I.R., Green, P.F., and Lovering, J.F. 1987. Assessment of hydrocarbon resource potential in Australian sedimentary basins: development of fission track techniques. End of Grant Technical Report, NERDDC Project No. 720 (Unpublished annual report).

Gleadow, A.J.W., Duddy, I.R., Green, P.F., and Lovering, J.F. 1988. Assessment of hydrocarbon resource potential in Australian sedimentary basins: development of fission track techniques. End of Grant Technical Report, NERDDC Project No. 720 (Unpublished annual report), 1-116.

Gleadow, A.J.W., Duddy, I.R., Green, P.F., and Lovering, J.F. 1989. Assessment of hydrocarbon resource potential in Australian sedimentary basins: development of fission track techniques. End of Grant Technical Report, NERDDP Project No. 1046 (Unpublished annual report), 1-54.

Gleadow, A.J.W., Duddy, I.R. and Lovering, J.F. 1983. Fission track analysis: a new tool for the evaluation of thermal histories and hydrocarbon potential. *Australian Petroleum Exploration Association Journal* **23**, 93-102.

Goetz, J.F., Dupal, L. and Bowler, J. 1979. An investigation into discrepancies between sonic log and seismic check shot velocities. *Australian Petroleum Exploration Association Journal* **19**, 131-141.

Gravestock, D.I., Callen, R.A., Alexander, E.M. and Hill, A.J. 1995. Strzelecki South Australia. *In*: Fairburn, W.A. (ed): Explanatory Notes-1:250,000 Geological Series. *Geological Survey of South Australia and Department of Mines and Energy South Australia*, pp. 45.

Green, P.F., Duddy, I.R., Bray, R.J. 1995. Applications of Thermal History Reconstruction in inverted basins. *In:* Buchanan, J.G. and Buchanan, P.G. (eds): *Basin Inversion.* Geological Society, London, Special Publication **88**, 149-165.

Green, P.F., Duddy, I.R., Gleadow, A.J.W., Hegarty, K.A., Laslett, G.M., Lovering, J.F. 1989. Thermal annealing of fission tracks in apatite: 4-quantitative modelling techniques and extension to geologic time scales. *Chemical Geology (Isotope Geoscience Section)* **79**, 155-182.

Green, P.F., Duddy, I.R., Gleadow, A.J.W., Tingate, P.R., and Laslett, G.M. 1986. Thermal annealing of fission tracks in apatite. 1. A qualitative description. *Chemical Geology (Isotope Geoscience Section)* **59**, 237-253.

Hallam, A. 1984. Pre-Quaternary sea-level changes. Annual Review *Earth and Planetary Science* **12**, 205-243.

Hansen, S. 1996. A compaction trend for Cretaceous and Tertiary shales on the Norwegian Shelf based on sonic transit times. *Petroleum Geoscience* **2**, 159-166.

Haq, B. U., Hardenbol, J. and Vail, P.R. 1987. Chronology of fluctuating sea levels since the Triassic. *Science* **235**, 1156-1167.

Harland, W.B., Armstrong, R.L., Cox, A.V., Craig, L.E., Smith, A.G. and Smith, D.G. 1989. *A Geological Time Scale.* Cambridge University Press, Cambridge, pp. 263.

Hawkins, P.J., Almond, C.S., Carmichael, D.C., Smith, R.J. and Williams, L.J. 1989. Kerogen characterisation and organic and mineral diagenesis of potential source rocks in Jurassic units, southern Eromanga Basin, Queensland. *In*: O'Neil, B.J. (ed): *The Cooper and Eromanga Basins, Australia.* Proceedings of the Cooper and Eromanga Basins Conference, Adelaide, 1989. Petroleum Exploration Society of Australia, Society of Petroleum Engineers, Australian Society of Exploration Geophysicists (South Australia Branches), 583-599.

Heath, R.S. 1989. Exploration in the Cooper Basin. *Australian Petroleum Exploration Association Journal* **29**, 366-378.

Heath, R.S., McIntyre, S. and Gibbins, N. 1989. A Permian origin for Jurassic reservoired oil in the Eromanga Basin. *In*: O'Neil, B.J. (ed): *The Cooper and Eromanga Basins, Australia.* Proceedings of the Cooper and Eromanga Basins Conference, Adelaide, 1989. Petroleum Exploration Society of Australia, Society of Petroleum Engineers, Australian Society of Exploration Geophysicists (South Australia Branches), 405-416.

Hellinger, S. J. and Sclater, J.G. 1983. Some comments on two-layer extensional models for the evolution of sedimentary basins. *Journal of Geophysical Research* **B88**, 8251-8269.

Hillis, R.R. 1991. Chalk porosity and Tertiary uplift, Western Approaches Trough, SW UK and NW French continental shelves. *Journal of the Geological Society*, London **148**, 669-679.

Hillis, R.R. 1992a. Evidence for Pliocene erosion at Ashmore Reef (Timor Sea) from the sonic velocities of Neogene limestone formations. *Exploration Geophysics* **23**, 489-495.

Hillis, R.R. 1992b. A two-layer lithospheric compressional model for the Tertiary uplift of the southern United Kingdom. *Geophysical Research Letters* **19**, 573-576.

Hillis, R.R. 1993. Quantifying erosion in sedimentary basins from sonic velocities in shales and sandstones. *Exploration Geophysics* **24**, 561-566.

Hillis, R.R. 1995a. Quantification of Tertiary Exhumation in the United Kingdom Southern North Sea Using Sonic Velocity Data. *American Association of Petroleum Geologists Bulletin* **79**, 130-152.

Hillis, R.R. 1995b. Regional Tertiary Exhumation in and around the United Kingdom. *Basin Inversion.* Geological Society, London, Special Publication **88**, 167-190.

Hillis, R.R., Macklin, T.A. and Siffleet, P. 1995. Regional depth-conversion of mapped seismic two-way-times in the Cooper-Eromanga Basins. *Exploration Geophysics* **26**, 412-418.

Hillis, R.R., Thomson, K., and Underhill, J.R. 1994. Quantification of Tertiary erosion in the Inner Moray Firth using sonic velocity data from the Chalk and Kimmeridge Clay. *Marine and Petroleum Geology* **11**, 283-293.

Hollister, L.S. and Crawford, M.L. 1981. *Fluid inclusions: applications to petrology.* Mineralogical Association of Canada, Short Course Handbook 6.

Horváth, F., Dövényi, P., Szalay, A. and Royden, L.H. 1988. Subsidence, Thermal and Maturation History of the Great Hungarian Plain. *In:* Royden, L.H.and Horváth, F. (eds): *The Pannonian basin-a study in basin evolution.* American Association of Petroleum Geologists Bulletin Memoir **45**, 355-372.

Houseknecht, D.W. 1987. Assessing the Relative Importance of Compaction Processes and Cementation to Reduction of Porosity in Sandstones. *American Association of Petroleum Geologists Bulletin* **71**, 633-642.

Hsu, K., Burridge, R. and Walsh, J. 1990. P-wave and S-wave drifts in a slow formation. *Society of Exploration Geophysics*, 62nd Annual International Meeting, Expanded Abstracts, 185-188.

Hunt, J. 1979. *Petroleum geochemistry and geology.* W.H. Freeman and Co., San Francisco, pp. 617.

Hunt, J.W., Heath, R. and McKenzie, P.E. 1989. Thermal maturity and other geological controls on the distribution and composition of Cooper Basin hydrocarbons. *In*: O'Neil, B.J. (ed): *The Cooper and Eromanga Basins, Australia.* Proceedings of the Cooper and Eromanga Basins Conference, Adelaide, 1989. Petroleum Exploration Society of Australia, Society of Petroleum Engineers, Australian Society of Exploration Geophysicists (South Australia Branches), 509-524.

Hurford, A.J., and Green, P.F. 1983. The zeta age calibration of fission track dating. *Isotope Geoscience* **1**, 285-317.

Hutton, A.C., and Cook, A.C. 1980. Influence of alginite on the reflectance of vitrinite from Joadja, NSW, and some other coals and oil shales containing alginite. *Fuel* **59**, 711-714.

Issler, D.R. 1984. Calculation of organic maturation levels for offshore eastern Canada-implications for general application of Lopatin's method. *Canadian Journal of Earth Sciences* **21**, 477-488.

Issler, D.R. 1992. A New Approach to Shale Compaction and Stratigraphic Restoration, Beaufort-Mackenzie Basin and Mackenzie Corridor, Northern Canada. *American Association of Petroleum Geologists Bulletin* **76**, 1170-1189.

Jankowsky, W. 1962. Diagenesis and oil accumulation as aids in the analysis of the structural history of the north-western German Basin: *Zeitschrift der Deutscher Geologischer Gesellschaft* **114**, 452-460.

Japsen, P. 1993. Influence of Lithology and Neogene Uplift on Seismic Velocities in Denmark: Implications for Depth Conversion of Maps. *American Association of Petroleum Geologists Bulletin* **77**, 194-211.

Jenkins, C.C. 1989. Geochemical correlation of source rocks and crude oils from the Cooper and Eromanga Basins. *In*: O'Neil, B.J. (ed): *The Cooper and Eromanga Basins, Australia.* Proceedings of the Cooper and Eromanga Basins Conference, Adelaide, 1989. Petroleum Exploration Society of Australia, Society of Petroleum Engineers, Australian Society of Exploration Geophysicists (South Australia Branches), 525-540.

Jensen, L.N. and Schmidt, B.J. 1992. Late Tertiary uplift and erosion in the Skagerrak area: magnitude and consequences. *Norsk Geologisk Tidsskrift* **72**, 275-279.

Jensen, L.N. and Schmidt, B.J. 1993. Neogene uplift and erosion offshore south Norway; Magnitudes and consequences for hydrocarbon exploration in the Farsund Basin. *In:* Spencer, A.M. (ed): *Generation, accumulation and production of Europe's hydrocarbons.* European Association of Petroleum Geoscientists, Statoil, Stavanger, Norway, Special Publication **3**, 79-88.

Jones, J.G. and Veevers, J.J. 1982. A Cainozoic history of Australia's Southeast Highlands. *Geological Society of Australia Journal* **29**, 1-12.

Kalkreuth, W. and McMechan, M.E. 1984. Regional pattern of thermal maturation as determined from coal-rank studies. Rocky Mountain Foothills anf Front Ranges north of Grand Cache. Alberta-implications for petroleum exploration. *Bulletin of Canadian Petroleum Geology* **32**, 249-271.

Kantsler, A.J., Cook, A.C. and Smith, G.C. 1978a. Rank variation, calculated palaeotemperature in understanding oil, gas occurence. *The oil and gas journal* November 1978, 196-205.

Kantsler, A.J., Cook, A.C. and Zwigulis, M. 1986. Organic maturation in the Eromanga Basin. *In:* Gravestock, D.I., Moore, P.S. and Pitt, G.M. (eds): *Contributions to the geology and hydrocarbon potential of the Eromanga Basin.* Geological Society of Australia, Special publication **12**, 305-322.

Kantsler, A.J., Prudence, T.J.C., Cook, A.C. and Zwigulis, M. 1983. Hydrocarbon habitat of the Cooper/Eromanga Basin, Australia. *Australian Petroleum Exploration Association Journal* **23**, 75-92.

Kantsler, A.J., Smith, G.C. and Cook, A.C. 1978b. Lateral and vertical rank variation: implications for hydrocarbon exploration. *Australian Petroleum Exploration Association Journal* **18**, 143-156.

Katz, B.J., Pfeiffer, R.N. and Schunk, D.J. 1988. Interpretation of discontinuous vitrinite reflectance profiles. *American Association of Petroleum Geologists Bulletin* **72**, 926-931.

Khorasani, G.K. and Michelsen, J.K. 1994. The effects of overpressure, lithology, chemistry and heating rate on vitrinite reflectance evolution, and its relationship with oil generation. *Australian Petroleum Exploration Association Journal* **34**, (1), 418-435.

Kuang, K.S. 1985. History and style of Cooper-Eromanga Basin structures. *Exploration Geophysics* **16**, 245-248.

Kusznir, N.J., Karner, G.D. and Egan, S. 1987. Geometric, thermal and isostatic consequences of detachments in continental lithosphere extension and basin formation. *In*: Beaumont, C. and Tankard, A.J. (eds): *Sedimentary Basins and Basin-Forming Mechanisms*. Canadian Society of Petroleum Geologists Memoir **12**, 185-203.

Lang, W.H. 1978. The determination of prior depth of burial (uplift and erosion) using interval transit time. *Society of Professional Well Log Analysts*, Transactions of the Nineteenth Annual Logging Symposium. June 13-16, paper B.

Larter, S. 1988. Some pragmatic perspectives in source rock geochemistry. *Marine and Petroleum Geology* **5**, 249-271.

Liu, G. and Roaldset, E. 1994. A new decompaction model and its application to the northern North Sea. *First Break* **12** (2), 81-87.

Lopatin, N.V. 1971. Temperature and geologic time as factors in coalification (in Russian). *Izvestiya Akademiya Nauk SSSR, Seriya Geologicheskaya* **3**, 95-106. English translation by Bostick, N.H., 1972, Illinois State Geological Society.

Magara, K. 1976. Thickness of Removed Sedimentary Rocks, Paleopore Pressure, and Paleotemperature, Southwestern Part of Western Canada Basin. *American Association of Petroleum Geologists Bulletin* **60**, 554-565.

Marie, J.P.P. 1975. Rotliegendes stratigraphy and diagenesis. *In:* Woodland, A.W.(ed). *Petroleum and the continental shelf of north-west Europe*. Geology **1**, 205-211. Applied Science Publishers, London.

McKenzie, D.1978. Some remarks on the development of sedimentary basins. *Earth and Planetary Science Letters* **40**, 25-32.

McKirdy, D.M. 1982. Aspects of the source rock and petroleum geochemistry of the Eromanga Basin. *In*: Moore, P.J. and Mount, T.J. (compilers): *Eromanga Basin Symposium*. Summary papers. Adelaide, Geological Society of Australia and Petroleum Exploration Society of Australia.

Menpes, R.J. and Hillis, R.R. 1995. Quantification of Tertiary exhumation from sonic velocity data, Celtic Sea/South -Western Approaches. *Basin Inversion.* Geological Society, London, Special Publication **88**, 191-207.

Michaelsen, B.H. and McKirdy, D.M. 1989. Organic facies and petroleum geochemistry of the lacustrine Murta Member (Mooga Formation) in the Eromanga Basin, Australia. *In*: O'Neil, B.J. (ed): *The Cooper and Eromanga Basins, Australia.* Proceedings of the Cooper and Eromanga Basins Conference, Adelaide, 1989. Petroleum Exploration Society of Australia, Society of Petroleum Engineers, Australian Society of Exploration Geophysicists (South Australia Branches), 541-558.

Middleton, M.F. 1979. Heat flow in the Moomba, Big Lake and Toolachee gas fields of the Cooper Basin and implications for hydrocarbon maturation. *Australian Society of Exploration Geophysicists Bulletin* **10**, 149-155.

Middleton, M.F. 1980. A model of intracratonic basin formation, entailing deep crustal metamorphism. *Geophysical Journal of the Royal Astronomical Society* **62**, 1-14.

Middleton, M.F. 1982. Tectonic history from vitrinite reflectance. *Geophysical Journal of the Royal Astronomical Society* **62**, 121-132.

Middleton, M.F. 1983. Coal rank trends in Eastern Australian Permian coal basins. CSIRO Investigation Report 141, Unpublished.

Middleton, M.F. 1989. A model for the formation of intracratonic sag basins. *Geophysical Journal International* **99**, 665-676.

Middleton, M.F. and Hunt, J. 1989. Influence of tectonics on Permian coal-rank patterns in Australia. *International Journal of Coal Geology* **13**, 391-411.

Mielnik, V. 1984. Tirrawarra North-1. Well completion report compiled for Delhi Petroleum Pty Ltd.

MINCOM Pty Ltd 1989. *GEOLOG* Version: 5. Brisbane, Australia.

Mitrovica, J.X., Beaumont, C. and Jarvis, J.T. 1989. Tilting of continental interiors by the dynamical effects of subduction. *Tectonics* **8**, 1079-1094.

Moore, P.S. 1986. An exploration overview of the Eromanga Basin. *In:* Gravestock, D.I., Moore, P.S. and Pitt, G.M. (eds): *Contributions to the geology and hydrocarbon potential of the Eromanga Basin.* Geological Society of Australia, Special publication **12**, 1-8.

Moore, P.S. and Pitt, G.M. 1984. Cretaceous of the Eromanga Basin - implications for hydrocarbon exploration. *Australian Petroleum Exploration Association Journal* **24**, 358-376.

Morrow, D.W. and Issler, D.R. 1993. Calculation of Vitrinite Reflectance from Thermal Histories: A Comparison of Some Methods. *American Association of Petroleum Geologists Bulletin* **77**, 610-624.

Morton, J. 1987. Post Cretaceous structure of the Cooper Basin region and its relevance to petroleum migration and entrapment. *South Australian Department of Mines and Energy.* Unpublished report of the Rept. Book 839, pp. 4.

Murrell,S.A.F. 1986. Mechanics of tectogenesis in plate collision zones. *In*: Coward, M.P. and Ries, A.C. (eds): *Collision Tectonics.* Geological Society, London, Special Publication **19**, 95-111.

Naeser, C. W., and Faul, H. 1969. Fission track annealing in apatite and sphene. *Journal of Geophysical Research* **74**, 705-10.

Naeser, N.D., Naeser, C.W., and McCulloh, T.H. 1990. Thermal history of rocks in southern San Joaquin Valley, California: evidence from fission track analysis. *American Association of Petroleum Geologists Bulletin* **74**, 13-29.

Nelson, A.W. 1985. Tectonics of the Jackson-Naccowlah area, Cooper-Eromanga Basins, southwest Queensland, and their implications for hydrocarbon accumulation. *Australian Petroleum Exploration Association Journal* **25**, 85-94.

Nyland, B., Jensen, L.N., Skagen, J., Skarpnes, O. and Vorren, T. 1992. Tertiary uplift and erosion in the Barents Sea: magnitude, timing and consequences. *In:* Larsen, R.M., Brekke, H., Larsen, B.T. and Talleraas, E. (eds). *Structural and tectonic modelling and its application to petroleum geology.* Norwegian Petroleum Society, Special Publication **1**, 153-162.

Ollier, C.D. 1982. The Great Escarpment of eastern Australia: tectonic and geomorphic significance. *Geological Society of Australia Journal* **29**, 13-24.

Passmore, V.L. 1989. Petroleum accumulation of the Eromanga Basin: A comparison with other Australian Mesozoic accumulations. *In*: O'Neil, B.J. (ed): *The Cooper and Eromanga Basins, Australia.* Proceedings of the Cooper and Eromanga Basins Conference, Adelaide, 1989. Petroleum Exploration Society of Australia, Society of Petroleum Engineers, Australian Society of Exploration Geophysicists (South Australia Branches), 371-389.

Perrier, R. and Quiblier, J. 1974. Thickness Changes in Sedimentary Layers During Compaction History; Methods for Quantitative Evaluation. *American Association of Petroleum Geologists Bulletin* **58**, 507-520.

Petroleum Management Associates Pty. Ltd. (PMA) 1986. *A detailed analysis of the Cooper and Eromanga Basins*, pp. 149.

Pitt, G.M. 1982. Geothermal gradients in the Eromanga-Cooper Basin region. *In:* Moore, P.S. and Mount, T.J. (eds): *Eromanga Basin Symposium.* Geological Society of Australia and Petroleum Exploration Society of Australia. Adelaide, 262-283.

Pitt, G.M. 1986. Geothermal gradients, geothermal histories and the timing of thermal maturation in the Eromanga-Cooper Basins. *In:* Gravestock, D.I., Moore, P.S. and Pitt, G.M. (eds): *Contributions to the geology and hydrocarbon potential of the Eromanga Basin.* Geological Society of Australia, Special publication **12**, 323-351.

Platte River Associates Inc. 1995. BasinMod 1-D® for Windows™. *Basin Modelling System, Document Version 5.* Denver Co, USA.

Powell, C.M. 1984. Uluru and Adelaidean regimes; Late Devonian and Early Carboniferous. *In*: Veevers, J.J. (ed): *Phanerozoic earth history of Australia.* Oxford, England, Clarendon Press, 329-339.

Powell, T.G. and McKirdy, D.M. 1976. Geochemical character of crude oils from Australia and Papua New Guinea. *In*: Leslie, R.B., Evans, H.J., and Knight, C.L. (eds): *Economic geology of Australia and Papua New Guinea, 3, Petroleum.* Australasian Institute of Mining and Mettalurgy, Monograph **7**, 18-29.

Powis, G.D. 1989. Revision of Triassic stratigraphy at the Cooper Basin to Eromanga Basin transition. *In*: O'Neil, B.J. (ed): *The Cooper and Eromanga Basins, Australia.* Proceedings of the Cooper and Eromanga Basins Conference, Adelaide, 1989. Petroleum Exploration Society of Australia, Society of Petroleum Engineers, Australian Society of Exploration Geophysicists (South Australia Branches), 265-277.

Price, L.C. and Barker, C.E. 1985. Suppression of vitrinite reflectance in amorphous rich kerogen - a major unrecognized problem. *Journal of Petroleum Geology* **8**, 59-84.

Pryor, W.A. 1973. Permeability-porosity patterns and variations in some Holocene sand bodies. *American Association of Petroleum Geologists Bulletin* **57**, 162-189.

Quigley, T.M., Mackenzie, A.S. and Gray, J.R. 1987. Kinetic theory of petroleum generation. *In:* Doligez, B. (ed): *Migration of Hydrocarbons in Sedimentary Basins*, Technip, 649-666.

Raiga-Clemenceau, J., Martin, J.P. and Nicoletis, S. 1988. The Concept of Acoustic Formation Factor for More Accurate Porosity Determination from Sonic Transit Time Data. *The Log Analyst* January-February, 54-59.

Raymer, L.L., Hunt, E.R. and Gardner, J.S. 1980. An improved sonic transit time-to-porosity transform. *Society of Professional Well Log Analysts Twenty-First Annual Logging Symposium.* July 8-11, 1980, Paper P.

Rider, M.H. 1991. *The Geological Interpretation of Well Logs.* Whittles Publishing, Caithness, U.K., pp. 175.

Rieke III, H.H. and Chilingarian, G.V. 1974. *Compaction of Argillaceous Sediments.* Elsevier, Amsterdam, pp. 424.

Riis, F. and Jensen, L.N. 1992. Introduction: measuring uplift and erosion-proposal for a terminology. *In*: Jensen, L.N., Riis, F. and Boyd, R. (eds): *Post-cretaceous uplift and sedimentation along the western Fennoscandian Shield.* Scandinavian University Press, Oslo, Stockholm. Norsk Geologisk Tidsskrift **72**, 223-228.

Robinson, S. 1982. Jackson-1. Well completion report compiled for Delhi Petroleum Pty Ltd.

Rodgers, J., Wehr, F.L. and Hunt, J.W. 1991. Tertiary Uplift Estimation from Velocity Data in the Eromanga Basin. *Exploration Geophysics* **22**, 321-324.

Roedder, E. (ed) 1984. Fluid inclusions. *Reviews in Mineralogy* **12**. Mineralogical Society of America, Washington.

Rubey, W.W. and Hubbert, M.K. 1959. Role of fluid pressure in mechanics of thrust faulting. *Bulletin of the Geological Society of America* **70**, 167-206.

Russell, N.J. and Baillie, P.W. 1989. Vitrinite palaeothermometry of offshore exploration wells, Tasmania, Australia. *Australian Petroleum Exploration Association Journal* **29**, 130-156.

Russell, N.J. and Bone, Y. 1989. Palaeogeothermometry of the Cooper and Eromanga Basins, South Australia. *In:* O'neil, B.J. (ed): *The Cooper and Eromanga Basins Australia.* Petroleum Exploration Society of Australia, Society of Petroleum Engineers and the Australian Society of Exploration Geophysicists, 559-582.

Russell, M. and Gurnis, M. 1994. The planform of epeirogeny: vertical motions of Australia during the Cretaceous. *Basin Research* **6**, 63-76.

Sandiford, M. and Powell, R. 1990. Some isostatic and thermal consequences of the vertical strain geometry in convergent orogens. *Earth and Planetary Science Letters* **98**, 154-165.

Santos Ltd. 1991. Patchawarra Trough, summary of stratigraphy, structuring and maturation history. File report edited by M. Zwigulis.

Santos Ltd. 1992. Eromanga Basin Mesozoic Palynostratigraphy. File report edited by G. Wood and M. Zwigulis.

Sarmiento, R. 1961. Geological Factors Influencing Porosity Estimates from Velocity Logs. *American Association of Petroleum Geologists Bulletin* **45**, 633-644.

Saxby, J. 1982. A reassessment of the range of kerogen maturities in which hydrocarbons are generated. *Journal of Petroleum Geology* **5**, 117-128.

Schlumberger 1974. *Well Evaluation Conference North Sea.* Services Techniques Schlumberger, France.

Schlumberger 1987. *Log Interpretation Principles/Applications.* Schlumberger Educational Services, USA.

Schlumberger 1989. *Log Interpretation Principles/Applications.* Schlumberger Educational Services, Houston, Texas.

Schneider, F., Bouteca, M. and Vasseur, G. 1994. Validity of the Porosity/effective-stress concept in sedimentary basin modelling. *First Break* **12**, 321-326.

Schulz-Rojahn, J.P. 1993. Calcite-cemented zones in the Eromanga Basin: Clues to petroleum migration and entrapment? *Australian Petroleum Exploration Association Journal* **33**, 63-76.

Sclater, J.G. and Christie, P.A.F. 1980. Continental stretching: an explanation of the post-mid- Cretaceous subsidence of the Central North Sea Basin. *Journal of Geophysical Research* **B85**, 3711-3739.

Selley, R.C. 1978. Porosity Gradients in the North Sea oil-bearing sandstones. *Journal of Geological Society* **135**, 119-132.

Senior, B.R., Mond, A. and Harrison, P.L. 1978. Geology of the Eromanga Basin. *Bureau of Mineral Resources Bulletin* **167**, pp. 102.

Serra, O. 1984. *Fundamentals of well-log interpretation. 1. The acquisition of logging data.* Developments in Petroleum Science, 15A. Elsevier, Amsterdam, The Netherlands, pp. 423.

Shaw, R.D. 1990. Development of the Tasman Sea and easternmost Australian continental margin - a review. *In*: Finlayson, D.M. (ed): *The Eromanga-Brisbane Geoscience transect: a guide to basin development across the Phanerozoic Australia in southern Queensland.* Bureau of Mineral Resources, Geology and Geophysics Bulletin **232**, 53-66.

Shaw, R.D. 1991. Tertiary structuring in Southwest Queensland: Implications for Petroleum Exploration. *Exploration Geophysics* **22**, 339-344.

Sheriff, R.E. 1980. *Seismic Stratigraphy.* Int. Human Resources Dev. Corp., Boston.

Shibaoka, M. and Bennett, A.J.R. 1977. Patterns of diagenesis in some Australian sedimentary basins. *Australian Petroleum Exploration Association Journal* **17**, 58-63.

Shibaoka, M., Bennett, A.J.R. and Gould, K.W. 1973. Diagenesis of organic matter and occurence of hydrocarbons in some Australian sedimentary basins. *Australian Petroleum Exploration Association Journal* **13**, 73-80.

Skagen, J.I. 1992. Methodology applied to uplift and erosion. *In*: Jensen, L.N., Riis, F. and Boyd, R. (eds): *Post-cretaceous uplift and sedimentation along the western Fennoscandian Shield.* Scandinavian University Press, Oslo, Stockholm. Norsk Geologisk Tidsskrift **72**, 307-311.

Smith, L. and Chapman, D.S. 1983. On the Thermal Effects of Groundwater Flow. Regional Scale Systems. *Journal of Geophysical Research* **88**, 593-608.

Smith, G.C. and Cook, A.C. 1980. Coalification paths of exinite, vitrinite, and intertinite. *Fuel* **59**, 641-646.

Sprigg, R.C. 1958. Petroleum prospects of western parts of Great Australian Artesian Basin. *American Association of Petroleum Geologists Bulletin* **42**, 2465-2491.

Sprigg, R.C. 1961. On the structural evolution of the Great Artesian Basin. *Australian Petroleum Exploration Association Journal* **1**, 37-56.

Stanmore, P.J. 1989. Case studies of stratigraphic and fault traps in the Cooper Basin, Australia. *In*: O'Neil, B.J. (ed): *The Cooper and Eromanga Basins, Australia.* Proceedings of the Cooper and Eromanga Basins Conference, Adelaide, 1989. Petroleum Exploration Society of Australia, Society of Petroleum Engineers, Australian Society of Exploration Geophysicists (South Australia Branches), 361-369.

Stanmore, P.J. and Johnstone, E.M. 1988. The search for stratigraphic traps in the southern Patchawarra Trough, South Australia. *Australian Petroleum Exploration Association Journal* **28**, 156-166.

Stuart, W.J. 1976. The genesis of Permian and Lower Triassic reservoir sandstones during phases of southern Cooper Basin Development. *Australian Petroleum Exploration Association Journal* **16**, 37-47.

Stuart, W.J., Kennedy, S. and Thomas, A.D. 1988. Influence of strucutral growth and other factors on the configuration of fluvial sandstones, Permian Cooper Basin. *Australian Petroleum Exploration Association Journal* **28**, 255-265.

Stuart, W.J., Tingate, P.R., Schulz-Rojahn, J.P., Hamilton, N.J., Ping, L. and Michaelsen, B. 1993. The influence of thermal history and fluid migration on porosity and permeability in Permian sandstones: Southern Cooper Basin. National Centre for Petroleum Geology and Geophysics. State energy research advisory committee, volume I, unpublished report.

Suggate, R.P. and Lowery, J.H. 1982. The influence of moisture content on vitrinite reflectance and the assessment of maturation of coal. *New Zealand Journal of Geology and Geophysics* **25**, 227-231.

Suzuki, N., Matsubayashi, H. and Waples, D.W. 1993. A simpler kinetic model of vitrinite reflectance. *American Association of Petroleum Geologists Bulletin* **77**, 1502-1508.

Sweeney, J.J. and Burnham, A.K. 1990. Evaluation of a Simple Model of Vitrinite Reflectance Based on Chemical Kinetics. *American Association of Petroleum Geologists Bulletin* **74**, 1559-1570.

Sweeney, J.J., Burnham, A.K. and Braun, R.L. 1987. A Model of Hydrocarbon Generation from Type I Kerogen: Application to Uinta Basin, Utah. *American Association of Petroleum Geologists Bulletin* **71**, 967-985.

Thornton, R.C.N. 1979. Regional stratigraphic analysis of the Gidgealpa Group, southern Cooper Basin, Australia. *South Australia Geological Survey Bulletin* **49**, pp. 140.

Till, R. 1974. *Statistical Methods for the Earth Scientist.* Macmillan, London, pp. 154.

Tingate, P.R., Alexander, E.M., Michaelsen, B.H., Duddy, I.R. and Griffiths, C.M. 1996. Tectonic events affecting the thermal history of the western margin of the Eromanga Basin. 13th Australian Geological Convention, *Geological Society of Australia Abstracts* **41**, 442.

Tissot, B. and Espitalié, J. 1975. L'évolution thermique de la matière organique des sédiments: applications d'une simulation mathématique. *Rev. IFP* **30**, 743-777.

Tissot, B.P., Pelet, R. and Ungerer, P. 1987. Thermal History of Sedimentary Basins, Maturation Indices, and Kinetics of Oil and Gas Generation. *American Association of Petroleum Geologists Bulletin* **71**, 1445-1466.

Tissot, B. and Welte, D.H. 1978. *Petroleum formation and occurence.* Springer-Verlag, New York, pp. 538.

Toupin, D.D. 1993. The effect of groundwater flow patterns in evolving intracratonic sedimentary basins on heat flow and petroleum generation. M.Sc dissertation, University of New Hampshire, USA.

Ungerer, P. 1993. Modelling to petroleum generation and expulsion-an update to recent reviews. *In*: Dore, A.G., *et al.*, (eds): *Basin Modelling: Advances and Applications.* Amsterdam, Elsevier, 219-232.

Ungerer, P., Burrus, J., Doligez, B., Chénet, P.Y. and Bessis, F. 1990. Basin Evaluation by Integrated Two-Dimensional Modelling of Heat Transfer, Fluid Flow, Hydrocarbon Generation and Migration. *American Association of Petroleum Geologists Bulletin* **74**, 309-335.

Valceva, S.P. 1979. Reflectance of macerals from bright brown coal, Pernik basin. *Fuel* **58**, 55-58.

Veevers, J.J. 1984. *Phanerozoic earth history of Australia.* Clarendon Press Oxford, pp. 418.

Veevers, J.J. 1986. Breakup of Australia and Antarctica estimated as mid-Cretaceous (95 ± 5 Ma) from magnetic and seismic data at the continental margin. *Earth and Planetary Science Letters* **77**, 91-99.

Vincent, P.W., Mortimore, I.R. and McKirdy, D.M. 1985. Hydrocarbon generation, migration and entrapment in the Jackson-Naccowlah area, ATP 259P, southwestern Queensland. *Australian Petroleum Exploration Association Journal* **25**, 62-85.

Vine, R.R. 1976. Eromanga Basin. In: Leslie, R.B., Evans, H.J. and Knight, C.L. (eds): Economic geology of Australia and Papua New Guinea 3. Petroleum. *Australasian Institute of Mining and Metallurgy, Monograph Series* **7**, 306-309.

Waples, D.W. 1980. Time and Temperature in Petroleum Formation: Application of Lopatin's Method to Petroleum Exploration. *American Association of Petroleum Geologists Bulletin* **64**, 916-926.

Waples, D.W. 1994. Maturity Modeling: Thermal Indicators, Hydrocarbon Generation, and Oil Cracking. *In*: Magoon, L.B. and Dow, W.G. (eds): *The Petroleum System-From Source to Trap*. American Association of Petroleum Geologists Memoir **60**, 285-306.

Waples, D.W., Kamata, H., and Suizu, M. 1992a. The Art of Maturity Modeling. Part 1: Finding a Satisfactory Geologic Model. *American Association of Petroleum Geologists Bulletin* **76**, 31-46.

Waples, D.W., Suizu, M., Kamata, H. 1992b. The Art of Maturity Modeling. Part 2: Alternative Models and Sensitivity Analysis. *American Association of Petroleum Geologists Bulletin* **76**, 47-66.

Wecker, H.R.B. 1989. The Eromanga Basin. *Australian Petroleum Exploration Association Journal* **29**, 379-397.

Wellman, P. 1987. Eastern Highlands of Australia; their uplift and erosion. *Bureau of Mineral Resources Journal of Australian Geology and Geophysics* **10**, 277-286.

Wells, P.E. 1990. Porosities and seismic velocities of mudstones from Wairarapa and oil wells of North Island, New Zealand, and their use in determining burial history. *New Zealand Journal of Geology and Geophysics* **33**, 29-39.

Wenger, L.M. and Baker, D.R. 1987. Variations in vitrinite reflectance with organic facies-examples from Pennsylvanian cyclothems of the Midcontinent, USA. *Organic Geochemistry* **11**, 411-416.

White, R. and McKenzie, D. 1989. Magmatism at rift zones: the generation of volcanic continental margins and flood basalts. *Journal of Geophysical Research* **B94**, 76885-7729.

Williams, T. and Moriarty, K. 1986. Hydrocarbon flushing in the Eromanga Basin fact or fallacy? *In:* Gravestock, D.I., Moore, P.S. and Pitt, G.M. (eds): *Contributions to the geology and hydrocarbon potential of the Eromanga Basin.* Geological Society of Australia, Special publication **12**, 377-384.

Wiltshire, M.J. 1982a. Late Triassic and Early Jurassic sedimentation in the Great Artesian Basin. *In*: Moore, P.S. and Mount, T.J. (eds): *Eromanga Basin Symposium Summary Papers.* Petroleum Exploration Society of Australia and Geological Society of Australia, Adelaide, 58-67.

Wiltshire, M.J. 1982b. Revision of Eromanga Basin limits. *In*: Moore, P.S. and Mount, T.J. (eds): *Eromanga Basin Symposium Summary Papers.* Petroleum Exploration Society of Australia and Geological Society of Australia, Adelaide, 68-75.

Wood, D.A. 1988. Relationship Between Thermal Maturity Indices Calculated Using Arrhenius Equation and Lopatin Method. *American Association of Petroleum Geologists Bulletin* **72**, 115-134.

Wopfner, H. 1960. On some structural developments in the central part of the Great Artesian Australian Basin. *Transactions Royal Society South Auustralia* **83**, 179-193.

Wopfner, H., Callen, R.A. and Harris, W.K. 1974. The lower Tertiary Eyre Formation of the southwestern Great Artesian Basin. *Geological Society of Australia Journal* **21**, 17-52.

Wyllie, M.R.J., Gregory, A.R. and Gardner, L.W. 1956. Theory of propagation of elastic waves in a fluid saturated porous solid. *Journal of the Acoustical Society of America* **28**, 168-191.

Yew, C.C. and Mills, A.A. 1989. The occurence and search for Permian oil in the Cooper Basin, Australia. *In*: O'Neil, B.J. (ed): *The Cooper and Eromanga Basins, Australia.* Proceedings of the Cooper and Eromanga Basins Conference, Adelaide, 1989. Petroleum Exploration Society of Australia, Society of Petroleum Engineers, Australian Society of Exploration Geophysicists (South Australia Branches), 339-360.

Zwigulis, M. 1983. Permian Geology of the Cooper Basin in Queensland. Proceedings of the Symposium on the Permian Geology of Queensland, July 14-16, Brisbane. *Geological Society of Australia Queensland Division*, 43-49.